AD_____

Award Number: DAMD17-03-1-0773

TITLE: Mouse Models for Bone Research to Assess Military Stress Fracture Risk

PRINCIPAL INVESTIGATOR: Leah R. Donahue, Ph.D.

CONTRACTING ORGANIZATION: Jackson Laboratory
Bar Harbor, ME 04609-1500

REPORT DATE: April 2005

TYPE OF REPORT: Final

PREPARED FOR: U.S. Army Medical Research and Materiel Command
Fort Detrick, Maryland 21702-5012

REPORT DOCUMENTATION PAGE

Form Approved
OMB No. 074-0188

1. AGENCY USE ONLY	2. REPORT DATE	3. REPORT TYPE AND DATES COVERED
	April 2005	Final(30 Sep 2003 - 31 Mar 2005)

4. TITLE AND SUBTITLE
Mouse Models for Bone Research to Assess Military Stress Fracture Risk

5. FUNDING NUMBERS
DAMD17-03-1-0773

6. AUTHOR(S)

Leah R. Donahue, Ph.D.

7. PERFORMING ORGANIZATION NAME(S) AND ADDRESS(ES)

Jackson Laboratory
Bar Harbor, ME 04609-1500

E-Mail: lrd@jax.org

8. PERFORMING ORGANIZATION REPORT NUMBER

9. SPONSORING / MONITORING AGENCY NAME(S) AND ADDRESS(ES)
U.S. Army Medical Research and Materiel Command
Fort Detrick, Maryland 21702-5012

10. SPONSORING / MONITORING AGENCY REPORT NUMBER

11. SUPPLEMENTARY NOTES

Original contains color plates: ALL DTIC reproductions will be in black and white

12a. DISTRIBUTION / AVAILABILITY STATEMENT
Approved for Public Release; Distribution Unlimited

12b. DISTRIBUTION CODE

13. ABSTRACT (Maximum 200 Words)

Researchers at The Jackson Laboratory identified a strong correlation between lean body mass and bone mineral content in some but not all inbred strains of mice. Research projects reported herein, with Dr. Donahue as Principal Investigator, capitalize on the newly established Mouse Phenome Project to expand the publicly available Mouse Phenome Database and analytical tools for bone morphology and associated phenotypes in target strains (Dr. Bogue, Part I); extend the on-going research defining heritable muscle/bone relationships (Drs. Donahue, Beamer, Rosen, and Bouxsein, Part II); and initiate genetic analyses to establish characteristics of muscle/bone relationships based on systematic diallele crosses among strains defined in Dr. Donahue's investigations (Dr. Churchill, Part III). The data and conclusions presented in this report provide insight into the etiology and heritability of bone strength, and thus benefit readiness and retention of U.S. Armed Forces by establishing a means to identify male and female recruits at high risk for fracturing during basic training and in combat situations.

14. SUBJECT TERMS
bone, strength, density, muscle, mouse, genetic, heritable, diallele, database, phenome, fracture

15. NUMBER OF PAGES
240

16. PRICE CODE

17. SECURITY CLASSIFICATION OF REPORT	18. SECURITY CLASSIFICATION OF THIS PAGE	19. SECURITY CLASSIFICATION OF ABSTRACT	20. LIMITATION OF ABSTRACT
Unclassified	Unclassified	Unclassified	Unlimited

Table of Contents

Final Report: Mouse Models to Assess Military Stress Fracture Risk

INTRODUCTION:

Researchers at The Jackson Laboratory have identified a strong correlation between lean body mass and bone mineral content in some but not all inbred strains of mice. Research projects in this application, with Dr. Donahue as Principal Investigator, will capitalize on the newly established Mouse Phenome Project to expand the publicly available Mouse Phenome Database and analytical tools for bone morphology and associated phenotypes in target strains (Dr. Bogue, Part I); extend the on-going research defining heritable muscle and bone relationships (Drs. Donahue, Beamer, Rosen, and Bouxsein, Part II); and initiate genetic analyses to establish characteristics of muscle/bone relationships based on systematic diallele crosses among strains defined in Dr. Donahue's investigations (Dr. Churchill, Part III). In the context of military significance, the proposed genetics-based research will provide insight into the etiology of stress fractures and thus benefit readiness and retention of U.S. Armed Forces by establishing a means to identify recruits at high risk for stress fracturing during basic training and in combat situations.

BODY:

Part I: Mouse Phenome Database:

The Statement of Work has not changed for this component of the study. We had three aims involving the organization of activities relating to strain availability, endpoint data curation and posting on the Mouse Phenome Database (MPD) website, and data analyses. The results of these aims are discussed in detail.

Aim 1. Coordinate and facilitate phenotyping efforts to generate quantitative, reproducible, comprehensive data on bone and body composition traits outlined in Parts II and III – We provided a framework that assured genetic and environmental continuity for each component of this project. We helped maximize data quality by using pedigreed, genetically stable inbred strains for testing and generating F1 hybrids for the diallele cross (Part III). Mice were from the JAX production facility; animals were of high-health status, and environmental variables were minimized through routine JAX animal care procedures. Detailed records are maintained by the Mouse Phenome Project and made available to investigators requesting them.

Aim 2. Provide assistance for data structuring and review; curate and annotate data and accompanying documentation; make data publicly available; provide long-term data storage – We defined a structure for endpoint data generated from Parts II and III that provides uniformity with other MPD data sets. These data have been entered in the MPD and have been assigned unique accession numbers. We are compiling documentation for this work so that detailed procedures can be publicly accessed through the MPD Protocol Directory. Documentation includes environmental conditions and biological parameters. Data and associated information are being standardized and annotated with controlled ontologies to enable linkage and integration with other community databases and to provide critical relationships for optimal searching and for maximizing database functions and computational methods. Distinct MPD project web pages were created and accessioned for each dataset generated in Parts II and III (see Part I Appendix for example). Complete documentation, per-animal

data, and strain (by sex) summary statistics (currently registered as 'private') will be made public through the MPD web interface. Multiple downloading options are provided. Web pages and content are reviewed by MPD staff and principal investigators prior to public release of the data. As the primary, public repository for these studies, the Mouse Phenome Project will protect and maintain the data indefinitely through other funding mechanisms.

Aim 3. Develop and improve MPD user analysis tools and perform global, high-level analyses using existing MPD data and the newly generated dataset – We have developed and improved web-based searching, retrievals, and analysis methods for MPD users by expanding our user analysis package and adding more visualization options (see below and Part I Appendix). In addition, advanced query capabilities (see Find Mouse Models below) and tools for building user-specified custom datasets are publicly available now. Developing and implementing new web-based tools and collecting and posting strain data are consistent with the mission of The Mouse Phenome Project to help conserve community resources (and funding dollars) and strive to maximize the value of strain characterization data.

Global MPD Analysis
We ran a series of analyses involving data generated from Parts II and III and phenotypic data from other MPD Collaborations. Existing MPD data were used to validate Parts II and III data sets and to search for compelling relationships that may indicate genetic co-determination between bone phenotypes. The MPD provides a unique and effective way to formulate and test hypotheses and to confirm preliminary observations. The success and conclusiveness of this strategy, however, is totally dependent on the data content of the MPD at the time of the analysis; over time with more data in the database, this strategy will be quite powerful. MPD analysis tools were used also to compare and validate commonly used tomography methodologies (pQCT versus microQT) lean body mass, % fat, and bone mineral content and density. Validations for bone mineral density across four projects are presented in Part I Appendix.

We also searched across the MPD for compelling correlations to other data. Preliminary analyses identified some interesting correlations between bone phenotypes and activity levels, drinking preference (calcium-containing solutions), red cell distribution width, and HDL cholesterol levels. It should be stressed that these preliminary observations require follow-up work to determine biological significance.

Diallele-Cross Analysis Tools
MPD user analysis tools and viewing options are under development for the special type of data generated in Part III for the 8-way diallele cross. The new tools are slated for public release simultaneous to making the data fully public. Previews of these data and applications are in Part I Appendix.

Find Mouse Models
New mouse models with biological phenotypes relevant to human disease are needed for many areas of biomedical research. Among other applications, new models will be used to help improve bone fracture risk assessment and to better understand osteoporosis, other bone-related diseases, and normal bone biology. In addition to validating previously identified QTL, new models will be important for finding new genes

for variation in bone composition, geometry, and other biomechanical properties contributing to bone strength.

New mouse models may be identified through the systematic characterization of inbred and F1 hybrid strains for bone phenotypes. Comprehensive surveys of bone parameters are requisite to knowledgeably choosing optimal strains for many applications. Strains may be chosen for second-tier (more refined) phenotyping to help deconstruct complex bone phenotypes. Quantitative phenotypic data and parallel SNP data can be used for *in silico* QTL analysis.

For illustration, we have identified mouse models using analysis tools we have developed for MPD users. MPD data sets were used to find suitable strains based on a set of user criteria involving BMD, femur geometry, strength, and relevant biological factors (see Part I Appendix). These tools are publicly available for MPD users.

MPD SNP Interface
Software for multivariate analysis and haplotype association predictions are still in the development stage. We expect the high-quality data generated for Parts II and III to provide excellent test data sets for modeling and software development. As a requisite to haplotype map construction, we have collected over two million community SNPs for all 30 strains used in these projects. These SNPs are publicly available through the MPD interface, and more SNPs will be collected as they are made available.

Part II: Decomposition of Skeletal Mineral and Lean Body Mass for Mouse Genetic Models:

Stress fractures are a major barrier to combat readiness in the military. Animal models are needed to dissect the complex relationships between genetic components and environmental factors that underlie stress fractures. Bone mineral density (BMD) and body composition data from 28 genetically diverse inbred strains of mice were previously collected as part of the Mouse Phenome Project. Data on adult body weight, BMD, and lean body mass (LBM) show wide variability and gender specificity. By refining the phenotypes of femur geometry and muscle mass in a subset of these strains, and by assessing femoral strength, we have identified a number of special crosses of inbred strains that could be used to study the genetic regulation of bone strength. Bone strength is a critical issue for the military because strong bones resist fracture when placed under repetitive loading such as associated with strenuous training.

Our Statement of Work has not changed and encompasses three Aims utilizing 10 of the original 28 inbred strains characterized for the Mouse Phenome Project. The first Aim is an in-depth analyses of males and females from 10 of the original 28 strains to further characterize skeletal phenotypes that may be related to LBM via a response to muscle loading. The second Aim is acquisition of new data on serum biomarkers related to bone and body composition. Finally, the third Aim is to complete data collection and analyses for strains that have less than 10 mice per group in the Mouse Phenome Database (MPD) on bone mineral density and body composition. Data from all 3 specific aims will be contributed to the MPD and made accessible to investigators worldwide.

Methods for Part II Specific Aims.

Source of mice: All inbred mouse strains utilized for the studies reported herein were obtained from the Animal Resources colonies of The Jackson Laboratory, Bar Harbor, Maine. The mice were received into our research colony at 4 weeks of age, and housed in groups of 3-4 of the same sex on sterilized White Pine shavings. Animal were provided free access to acidified water (pH 2.5 with HCl to retard bacterial growth) and NIH31 diet containing 6% fat, 17% protein, plus vitamin and mineral fortification (Purina Mills International, Brentwood, MO). The full composition of this open formula diet is available at www.labdiet.com/indexlabdiethome.htm.

Group 1. At 16 weeks of age, when mice have generally acquired their adult skeletal mass, females and males from the inbred strains under investigation were necropsied, whole body weights recorded, and tissue samples collected. Whole blood samples were allowed to clot on ice for 3-4 hours, then serum was harvested by centrifugation and stored at –20 C for subsequent assays of thyroxine (T4), osteocalcin (Oc), and Insulin-like Growth Factor-1 (IGF-I), as described below. Following blood sample collection, rear limbs of these mice were skinned and carefully separated from the pelvic bones. One leg was stored frozen at –20 C for subsequent determination of biomechanical properties using the MTS Q/1 testing instrument as described below. The remaining freshly dissected limb with muscle mass intact was immediately placed in the Stratec SA Plus pQCT densitometer and three scans obtained at 1 mm intervals at the mid point of the diaphysis. This permitted obtaining data on the entire cross-sectional area of the mid-thigh muscle as well as the cross-sectional area of the mid-femoral diaphysis associated with the muscle area. Following the mid-thigh densitometry scanning, the quadriceps muscle was carefully dissected and weighed on a Mettler H-30 balance (accurate to 0.1 mg) that is routinely calibrated with known standard weights. Finally, these femurs were dissected free of remaining muscle and connective tissue,

measured for length by digital calipers (Stoelting, Wood Dale, IL) and placed in 95% EtOH until whole femoral total volumetric bone mineral density (vBMD) could be assessed with the Stratec SA Plus pQCT densitometer and mid diaphyseal cortical thickness dimensions obtained by mCT40 scan as described below.

Group 2. A small sub-set of mice was collected to complete missing data points from the 28 inbred strain set destined for the Mouse Phenome Database (See Table 13). These mice were also obtained from the Animal Resources colonies of The Jackson Laboratory, and subjected to the same husbandry conditions described above. At 16 weeks of age, these mice were were necropsied for trunk blood samples, followed by determination of whole body composition data (lean, fat, bone mineral) using the PIXImus dual energy X-ray densitometer (DXA) as describe below.

Cross-sectional muscle area and volumetric bone mineral density measurements by pQCT: Mid-thigh cross-sectional area (muscle plus bone) was determined at the mid diaphysis per instructions with the SA Plus 5.50 software (Stratec SA Plus Research Unit, White Plains, NY). The mid-diaphysis cross-sectional area was also determined and subtracted from the mid-thigh area to obtain the estimated cross-sectional muscle area. The small area occupied by deep tissue vessels, nerves, and surrounding fat could not be discriminated sufficiently by the SA Plus to quantify and use as a correction factor for the cross-sectional muscle area.

Volumetric BMD data were measured on the entire left femur from each female and male mouse. Isolated femur length was measured with digital calipers (Stoelting, Wood Dale, IL), and then measured for density using the Stratec SA Plus densitometer. The bone scans were analyzed with two different outer threshold settings to separate bone from soft tissue. An outer (and inner) threshold of 710 mg/cm^3 was used to determine cortical bone areas and surfaces. This threshold was selected to yield area values consistent with histomorphometrically-derived values. To determine mineral content, a second analysis was carried out with an outer threshold setting of 220 mg/cm^3. This lower threshold was selected so that mineral from most partial voxels (0.07 mm) would be included in the analysis. Density values were calculated from the analyzed areas and associated mineral contents. Precision of the SA Plus for repeated measurement of a single femur was found to be 1.2%. Isolated femurs were scanned at 7 locations at 2 mm intervals, beginning 1.0 mm from the distal ends of the epiphyseal condyles. Due to variation in femur lengths, the femoral head could not be scanned at the same location for each bone, and thus was not included in final data. Total volumetric mineral density (vBMD) values were calculated by dividing the total mineral content by the total bone volume (bone and marrow) and expressed as mg/mm^3. Midshaft values were determined from the midpoint slice, typically slice 4. We found that correlation between total and cortical vBMD values at the mid diaphysis was very high and nearly identical for females (r = 0.923) and males (r = 0.929, Beamer, unpublished data). Therefore, mid-diaphyseal total vBMD, which captures all mineral (subcortical and cortical) as well as all volume (subcortical, cortical, and marrow) was used for subsequent data analyses.

DEXA scanning by PIXImus: The PIXImus densitometer (GE-Lunar, Madison, WI) was used to assess whole body areal (a)BMD and body composition at 16 weeks of age. This methodology has been validated in small animals (Nagy and Clair 2000; Nagy, Prince et al. 2001). PIXImus scanning of mice for BMC and % fat is both accurate and precise although body size must be considered when comparing inbred strains. To obtain the PIXImus scans, mice were killed by decapitation to obtain blood samples devoid of effects from excess handling stress or serum dilution with euthanasia injection

vehicle. Next, mice were placed ventral side down with each limb and tail positioned away from the body. Full body scans were obtained and X-ray absorptiometry data gathered and processed with manufacturer supplied software (Lunar PIXImus 2,vers. 2.1). The head area was specifically excluded from all analyses by the PIXImus software.

Biomechanical measurements: Frozen rear limbs were thawed in 0.85% NaCl, then femurs were dissected free of all muscle and connective tissue, measured for length, plus M/L and A/P dimensions at the mid-diaphysis with digital calipers and subjected to three point bending tests for biomechanical properties using a MTS Systems 'Qtest/1L instrument (Eden Prairie, MN). Femurs were placed condyles down and centered on stationary supports 6 mm apart. Force was applied at 0.05 mm/sec to obtain the force displacement relationship using the 100 g load cell for each bone. Force displacement curves were generated for each femur. Data were analyzed using the manufacturer's supplied TestWorks software (vers. 4).

MicroCT 40 Femoral Cross-Sectional Geometry: Femurs from female and male mice were scanned using Microcomputed Tomography (μCT40, Scanco Medical AG, Bassersdorf, Switzerland) to evaluate cross-sectional geometry at the femoral mid-shaft. The femurs were scanned at low resolution, energy level of 55KeV, and intensity of 145 μA. Eighteen slices were measured at the mid-point of each femur, with an isotropic pixel size of 12 μm and slice thickness of 12 μm, and used to compute the average total cross-sectional area (mm^2), bone area (mm^2), marrow area (mm^2), and cortical thickness (μm).

Serum measurements: Serum thyroxine (T4), osteocalcin (Oc), and Insulin-like Growth Factor-I (IGF-I) were chosen as factors likely to be important to one or more of the bone strength components that are the focus of our investigations. Serum T4 was measured in duplicate 9 ml volumes at The Jackson Laboratory using the Beckman CX5 Clinical Chemistry Analyzer, with data expressed as ng/ml. Serum Oc was measured in duplicate 25 ml volumes using the mouse specific assay developed by Dr. Caren Gundberg in her laboratory (Yale University, New Haven, CT), with data expressed as ng/ml. Serum IGF-I levels were measured in duplicate 25 ml volumes using kits obtained from ALPCO (Windham, NH). Values are normalized to a standard C57BL/6J serum pool that is run on each assay to avoid interassay variation; data presented as "adjusted IGF-I."

Statistical assessments: Part II, Specific Aim 1: Ten of the original 28 strains (see Aim 2) were identified to further characterize skeletal phenotypes. Within gender these strains have similar lean body mass but marked differences in bone mineral content. Males and females from the following strains were used: 129S1/SvImJ, BALB/cJ, C3H/HeJ, C57BL/6J, C58/J, FVB/NJ, NZB/BINJ, PERA/EiJ, SJL/J, and SWR/J. The following phenotypes were measured on 10 inbred strains of mice: peak load, work to failure, load at yield, stiffness, μCT cortical thickness, femur length, A/P diameter, M/L diameter, whole body weight, isolated quad weight, mid-shaft vBMD, pQCT final muscle area, cortical thickness, periosteal circumference (PERI C), endosteal circumference (ENDO C), total density, cortical density, and trabecular density. Estimated elastic modulus and estimated ultimate strength were calculated from contributing measured parameters. The formula for calculating estimated ultimate strength is: $s = FLc / 4I$ {F = peak load (N); L = length between supports (mm); c = radius of M/L dimension (mm); I = moment of inertia M/L dimension (mm^4); units are ($GPa=(N/mm^2/10^6)$}. The formula for calculating

estimated elastic modulus is: $E = K(L^3/48I)$; (K = stiffness (n/mm); L = distance between supports (mm); I = moment of inertia M/L dimension (mm^4); units are $MPa=(N/mm^2/10^4)$. We ran t-tests to test the sex difference in each phenotype within each inbred strain. We calculated the mean ± standard error of the phenotypes for each inbred strain by male and female, separately. We performed correlation analysis, cluster analysis and multiple regression analysis using the sex-specific strain means of all phenotypes. All the analyses were conducted using MATLAB software (Mathworks, Natic, MA).

We calculated the Pearson product-moment correlation coefficient of strain means between two phenotypes as a surrogate for estimating genetic correlations. Employing strain means in correlations reduces the numerator of the phenotypic correlation by (n-1)/n times the within-strain covariance (where n is the number of animals measured for each inbred strain) and has an analogous effect on the variances used to calculate the denominator of the correlation ratio. Under condition of high heritabilities, estimates from the two methods will be similar. Significant correlations between traits were reported based on Family-wised error rate. However, bearing in mind that correlations of strain means are never free of environmental sources of variation and covariation.

We used Ward's hierarchical agglomerative method (Ward 1963) to conduct cluster analysis of the phenotypes. We use one minus the absolute value of Pearson's correlation as a measure of 'distance' between strain mean phenotypes. Ward's method uses an analysis of variance approach to evaluate the distances between clusters. Ward's method initializes with each phenotype as a cluster by itself. At each step, the two closest clusters are merged to form a new cluster. This merging is repeated until only one cluster remains. The smaller the increase in the total within-group sum of squares as a result of joining two clusters, the closer they are. The within-group sum of squares of a cluster is defined as the sum of the squares of the distance between all phenotypes in the cluster and the centroid of the cluster. The resulting dendrogram was used to identify groups of correlated traits. Same method was applied to identify groups of correlated strains.

We conducted multiple regression analysis to evaluate the relationship between a dependent variable energy to break with one or more independent variables including mid shaft vBMD, total vBMD, cortical vBMD, cortical thickness, femur length, whole body weight, PERI C, M/L Diam, A/P Diam, isolated quad weight, and pQCT final muscle area. We repeat the analysis for other 5 dependent variables including stiffness, load at yield, peak load, estimated ultimate strength, and estimated elastic modulus. Sex effect was controlled in each regression model. Sex by independent variable interaction was also examined by adding a cross-product term of sex and independent variable into each regression model.

Part II, Specific Aim 2: Male and female mice from the following 28 strains were used for statistical analyses: 129S1/SvImJ, A/J, AKR/J, BALB/cJ, BTBR T^+ *tf/tf*/J, BUB/BnJ, C3H/HEJ, C57BL/6J, C57L/J, C58/J, CAST/EiJ, CZECHII/EiJ, DBA/2J, FVB/NJ, JF1/MsJ, MOLF/EiJ, MSM/MsJ, NOD/LtJ, NZB/BINJ, NZW/LacJ, PERA/EiJ, PL/J, PWK/PhJ, SJL/J, SM/J, SPRET/EiJ, SWR/J, and WSB/EiJ. Eleven phenotypes were measured on 28 inbred strains of mice: body weight, lean mass, fat mass, Area BMD, BMC, Spine BMD, osteocalcin (OC), T4, adjusted IGF-1, %fat, and %lean. We ran Student's t-test to determine the sex difference in each phenotype within each inbred strain. There were significant differences between the sexes in most of the phenotypes; therefore, we analyzed the data separately by gender. We calculated the mean ± standard error of the mean for all phenotypes for each inbred strain. The covariance between two phenotypes arises from both genetic (between strain) and environmental

(within strain) causes. Therefore, we calculated the Pearson product-moment correlation coefficient between phenotypes as a surrogate for estimating genetic correlation. Significant correlations between traits were reported based on Family-wised error rate. We conducted multiple regression analysis of the association between body composition measurements (body weight, %fat and %lean) and areal bone density (aBMD) for the whole body and for the spine, and for the association between the serum markers (OC, T4 and ADJ IGF-1) and bone density in the inbred mice. Strain and sex were included in all multiple regression analysis. Basic statistics, t-test, multivariate analysis, and matrices for correlations were generated in MATLAB software (Mathworks, Natic, MA).

RESULTS

Aim 1: To further characterize skeletal phenotypes that may be related to lean body mass (LBM) via a response to muscle loading. Four sets of measurements have been taken; they include pQCT, μCT, and bone strength assessments.

A. Measure volumetric femur density and geometry by pQCT.

Part II: Table 1. Strain means derived from pQCT measurement of male and female mice at 16 wks of age.

Female data	mid shaft vBMD (mg/mm3)			Cortical thickness (mm)			Periosteal circum (mm)			Endosteal circum (mm)			Cortical vBMD (mg/mm3)		
Strains	MEAN	SD	N	MEAN	SD	N	MEAN	SD	N	MEAN	SD	N	MEAN	SD	N
129S1/SvImJ	0.766	0.007	10	0.2258	0.0042	10	4.608	0.052	10	3.188	0.056	10	1.1953	0.0085	10
BALB/cJ	0.807	0.006	10	0.2446	0.0031	10	4.755	0.039	10	3.218	0.023	10	1.1919	0.0071	10
C3H/HeJ	1.005	0.009	9	0.3144	0.0027	9	4.555	0.027	9	2.580	0.018	9	1.2320	0.0084	9
C57BL/6J	0.631	0.005	10	0.1919	0.0013	9	4.954	0.039	9	3.748	0.034	9	1.0828	0.0080	9
C58/J	0.689	0.012	10	0.2068	0.0034	9	4.721	0.051	9	3.421	0.053	9	1.1498	0.0166	9
FVB/NJ	0.693	0.010	11	0.2135	0.0014	11	4.835	0.047	11	3.493	0.052	11	1.1436	0.0073	11
NZB/BINJ	0.782	0.007	11	0.2356	0.0041	11	4.621	0.026	11	3.140	0.026	11	1.1744	0.0027	11
PWK/PhJ	0.716	0.008	12	0.1934	0.0024	12	4.004	0.027	12	2.788	0.029	12	1.0678	0.0080	12
SJL/J	0.727	0.015	7	0.2288	0.0044	8	4.743	0.036	8	3.306	0.054	8	1.1600	0.0135	8
SWR/J	0.663	0.005	9	0.1876	0.0032	9	4.176	0.031	9	2.997	0.033	9	1.1049	0.0091	9
Male data															
Strains	MEAN	SD	N	MEAN	SD	N	MEAN	SD	N	MEAN	SD	N	MEAN	SD	N
129S1/SvImJ	0.788	0.010	14	0.2311	0.0040	14	4.737	0.047	13	3.274	0.040	13	1.1965	0.0086	13
BALB/cJ	0.829	0.010	10	0.2554	0.0052	10	5.039	0.057	10	3.435	0.058	10	1.1637	0.0034	10
C3H/HeJ	0.967	0.009	10	0.3389	0.0047	11	5.049	0.030	11	2.920	0.035	11	1.2204	0.0050	11
C57BL/6J	0.619	0.010	12	0.2076	0.0025	12	5.627	0.079	12	4.323	0.081	12	1.0800	0.0057	12
C58/J	0.673	0.005	10	0.2057	0.0025	10	4.976	0.067	10	3.682	0.066	10	1.1220	0.0045	10
FVB/NJ	0.639	0.006	9	0.2013	0.0028	9	5.131	0.018	9	3.867	0.032	9	1.0948	0.0045	9
NZB/BINJ	0.780	0.010	13	0.2453	0.0036	13	4.998	0.038	13	3.456	0.031	13	1.1728	0.0052	13
PWK/PhJ	0.712	0.012	11	0.1859	0.0073	10	3.936	0.063	10	2.767	0.061	10	1.0640	0.0052	10
SJL/J	0.688	0.008	11	0.2325	0.0026	11	5.028	0.043	11	3.567	0.046	11	1.1137	0.0066	11
SWR/J	0.704	0.009	10	0.2035	0.0025	10	4.504	0.029	10	3.225	0.039	10	1.1059	0.0043	10

An ANOVA was performed for each phenotype presented in Table 1 to determine if strain differences were significant; all traits had a significant $p<0.0001$ for within sex comparisons. In addition, body weight was found to be a covariant in females for cortical thickness and periosteal and endosteal circumferences, but not for mid shaft vBMD or cortical vBMD. In males, body weight was a covariant for periosteal and endosteal circumferences and for cortical vBMD, but not for mid shaft vBMD or cortical thickness.

In addition to strain differences, the data in Table 1 clearly show sex differences for all traits for some strains:

- mid shaft vBMD differs for C3H/HeJ, FVB/NJ, SJL/J, & SWR/J ($p<0.02$)
- cortical thickness differs for C3H/HeJ, C67BL/6J, FVB/NJ, & SWR/J ($p<0.0009$)
- periosteal and endosteal circumferences differ for all strains except 129S1/SvImJ & PWK/PhJ
- cortical vBMD differs for BALB/cJ, FVB/NJ, & SJL/J ($p<0.002$).

We conclude from these data that bone traits, even at a specific site such as femoral mid shaft, vary independently of one another between sexes and among strains. Consequently, in a heterogeneous human population, predicting a high or low value for a particular bone trait based on the value of another bone trait, even within a specific site, is not reliable and would require additional confirmation.

B. Measure femoral trabecular bone by μCT 40 imaging.

We have utilized the Research SA Plus pQCT densitometer to assess trabecular bone quantity rather than the μCT 40 as originally proposed. The reasons for this change are time, labor efficiency, and agreement of SA Plus and μCT40 data for this phenotype. With the advanced SA Plus software and enhanced precision, we are able to acquire accurate and reliable trabecular bone data in much less time than with the μCT 40. The trabecular data in Table 2 below represents the low density compartment within the endosteum of the entire femur. Consequently, we have made the μCT available for measurement of cortical thickness and polar moment of inertia (MOI) that are required to adjust the bone strength data acquired from the MTS (Materials Testing System) for differences in bone size. These measures are thought to be essential for better interpretation of bone strength data.

Part II: Table 2. Strain means derived from pQCT measurement of male and female mice at 16 weeks of age.

Female data	Total vBMD (mg/cm3)			Cortical vBMD (mg/cm3)			Trabecular vBMD (mg/cm3)		
Strains	MEAN	SD	N	MEAN	SD	N	MEAN	SD	N
129S1/SvImJ	0.7076	0.0110	10	1.1953	0.0085	10	0.1091	0.0070	10
BALB/cJ	0.7059	0.0075	10	1.1919	0.0071	10	0.0902	0.0058	10
C3H/HeJ	0.8314	0.0031	9	1.2320	0.0084	9	0.1105	0.0087	9
C57BL/6J	0.5661	0.0062	9	1.0828	0.0080	9	0.0739	0.0029	9
C58/J	0.6039	0.0178	9	1.1498	0.0166	9	0.0482	0.0082	9
FVB/NJ	0.6799	0.0087	11	1.1436	0.0073	11	0.0777	0.0041	11
NZB/BINJ	0.7238	0.0093	11	1.1744	0.0027	11	0.0993	0.0046	11
PWK/Ph	0.6409	0.0127	12	1.0678	0.0080	12	0.1206	0.0059	12
SJL/J	0.7267	0.0116	8	1.1600	0.0135	8	0.0808	0.0053	8
SWR/J	0.6515	0.0096	9	1.1049	0.0091	9	0.0926	0.0098	9
Male data									
Strains	MEAN	SD	N	MEAN	SD	N	MEAN	SD	N
129S1/SvImJ	0.6945	0.0126	14	1.1965	0.0086	13	0.1087	0.0066	14
BALB/cJ	0.6884	0.0096	10	1.1637	0.0034	10	0.1248	0.0035	10
C3H/HeJ	0.8027	0.0076	11	1.2204	0.0050	11	0.1123	0.0055	11
C57BL/6J	0.6061	0.0093	12	1.0800	0.0057	12	0.0985	0.0051	12
C58/J	0.5696	0.0074	10	1.1220	0.0045	10	0.0768	0.0037	10
FVB/NJ	0.6169	0.0081	9	1.0948	0.0045	9	0.0898	0.0037	9
NZB/BINJ	0.6948	0.0110	13	1.1728	0.0052	13	0.0900	0.0060	13
PWK/Ph	0.6031	0.0117	10	1.0640	0.0052	10	0.0932	0.0073	10
SJL/J	0.6923	0.0097	11	1.1137	0.0066	11	0.1010	0.0055	11
SWR/J	0.6223	0.0082	10	1.1059	0.0043	10	0.1124	0.0041	10

For all 3 density measures – total vBMD, cortical vBMD, and trabecular vBMD - data were collected for the entire femur. ANOVA illustrated that for both males and females, there was a highly significant difference ($p<0.001$) among strains for all three density phenotypes. Only cortical vBMD in males was found to have body weight as a significant covariate. When sex differences were analyzed, we found that there was no consistency among traits. For example, the following strains showed sex differences for total vBMD, but not for cortical vBMD: C3H/HeJ, C57BL/6J, PWK/PhJ, and SWR/J. Strains with no sex differences in cortical vBMD but with sex differences in trabecular vBMD include: C57BL/6J, C58/J, and PWK/PhJ. Sex differences for both cortical and trabecular vBMD were found for: BALB/cJ, FVB/NJ, and SJL/J.

These data clearly show that the two bone compartments, cortical vBMD and trabecular vBMD, have independent genetic regulation. These data further illustrate the complex nature of the bone density phenotype and emphasize the probability that the genetic regulation of its components will also be complex. Consequently, these genetic analyses would be difficult or impossible to accomplish in a heterogeneous human population, but can be approached with appropriate mouse models.

C. Measure site specific muscle mass of femur.

In addition to measurement of muscle area by pQCT, we also dissected the quadriceps muscle from one femur and recorded wet weight. The correlation between cross-sectional muscle area via pQCT and the weight of the isolated quadriceps muscle was highly significant for both females ($r=.74$, $p < 0.0001$) and males ($r=.86$, $p < 0.0001$).

SWR/J, C57BL/6J, SJL/J, and 129S1/SvImJ strain females were originally selected for similar lean body mass as measured by PIXImus. These strains had isolated quadriceps weights that ranged from highest (210mg for C57BL/6J) to next to

lowest (150mg for SWR/J), with a similar range in the area of the muscle mass (see Table 3). The same is true for males from strains selected for similar lean body mass - BALB/cJ, C3H/HeJ, FVB/NJ, NZB/BINJ, C58/J. Consequently, there appears to be no clear relationship between PIXImus lean body mass and thigh muscle area or relationship between PIXImus lean and quadriceps weight. Thus, the stratification of lean body mass seen in the original DEXA data from 28 strains was not repeated in the pQCT or weighed muscle data for the subset of strains selected for this study.

As a consequence, we have chosen to consider our data without a selection bias, that is, we looked for relationships between muscle mass and bone strength in the entire population of males and females from all strains without regard to their original selection criteria of similar lean body mass and variable bone mineral content. Once relationships between bone phenotypes, muscle mass, and bone strength were found, we evaluated individual strains for appropriate genetic models.

Part II: Table 3. Strain means for body weight, muscle mass, and femoral geometry derived from scale, pQCT, and caliper measurements of male and female mice at 16 wks of age.

Female data	whole body wt (g)			isolated quadriceps wt (g)			pQCT final muscle area (mm2)			femur lgth (mm)			A/P Diam (mm)			M/L Diam (mm)		
Strains	MEAN	SD	N	MEAN	SD	N	MEAN	SD	N	MEAN	SD	N	MEAN	SD	N	MEAN	SD	N
129S1/SvImJ	20.14	0.63	10	0.1694	0.0102	10	63.52	2.01	10	15.64	0.12	10	1.2300	0.015	10	1.445	0.029	10
BALB/cJ	23.90	0.55	10	0.1796	0.0053	10	65.57	2.53	10	15.65	0.16	10	1.2610	0.061	10	1.725	0.075	10
C3H/HeJ	22.15	0.58	9	0.1482	0.0092	9	69.22	2.58	9	15.08	0.09	9	1.1078	0.029	9	1.453	0.025	9
C57BL/6J	21.93	0.68	8	0.2096	0.0127	10	64.03	2.42	8	15.51	0.13	10	1.2240	0.022	10	1.694	0.057	10
C58/J	21.18	0.53	10	0.1594	0.0051	10	54.65	1.18	10	15.44	0.10	10	1.2070	0.023	10	1.577	0.034	10
FVB/NJ	22.67	0.64	11	0.1811	0.0062	11	69.68	1.60	11	15.08	0.12	11	1.1564	0.048	11	1.529	0.047	11
NZB/BINJ	26.96	1.03	10	0.1749	0.0111	11	76.33	2.25	10	16.50	0.14	11	1.2391	0.017	11	1.597	0.028	11
PWK/Ph	15.14	0.22	11	0.1165	0.0053	12	44.81	1.79	12	14.07	0.10	12	1.0775	0.008	12	1.298	0.019	12
SJL/J	20.00	0.63	8	0.1669	0.0126	8	66.34	4.87	8	14.44	0.07	8	1.1563	0.023	8	1.660	0.028	8
SWR/J	17.79	0.47	9	0.1485	0.0060	9	54.83	2.08	9	14.36	0.12	9	1.1067	0.010	9	1.319	0.023	9
Male data																		
Strains	MEAN	SD	N	MEAN	SD	N	MEAN	SD	N	MEAN	SD	N	MEAN	SD	N	MEAN	SD	N
129S1/SvImJ	26.09	0.67	15	0.2318	0.0156	15	69.64	3.87	15	15.72	0.10	15	1.2100	0.011	15	1.573	0.021	15
BALB/cJ	28.67	0.84	10	0.2639	0.0090	10	81.73	2.39	10	15.76	0.12	10	1.2540	0.048	10	2.003	0.064	10
C3H/HeJ	32.00	0.59	11	0.2264	0.0153	11	78.00	3.31	10	15.59	0.05	11	1.2618	0.014	11	1.726	0.028	11
C57BL/6J	30.10	0.50	12	0.2777	0.0146	12	88.73	3.86	12	16.21	0.06	12	1.3708	0.026	12	2.048	0.032	12
C58/J	30.63	1.43	10	0.2049	0.0070	10	72.24	2.25	10	15.38	0.12	10	1.2350	0.026	10	1.704	0.022	10
FVB/NJ	28.08	0.38	9	0.2405	0.0059	9	84.10	3.18	9	15.50	0.10	9	1.3200	0.012	9	1.763	0.025	9
NZB/BINJ	32.16	0.65	13	0.2406	0.0048	13	97.01	4.02	12	16.72	0.09	13	1.3408	0.019	13	1.795	0.034	13
PWK/Ph	16.43	0.64	11	0.1254	0.0050	11	48.05	2.94	11	13.87	0.17	10	1.0018	0.045	11	1.205	0.052	11
SJL/J	26.03	0.62	11	0.2159	0.0074	11	69.53	2.35	11	14.54	0.09	11	1.2173	0.017	11	1.809	0.020	11
SWR/J	23.55	0.51	10	0.2221	0.0070	10	78.88	1.53	10	14.86	0.05	10	1.1510	0.007	10	1.493	0.013	10

ANOVA demonstrated that there are significant differences ($p < 0.0001$) among strains for each of the muscle and femur dimensional phenotypes shown in Table 3. In addition, many traits also displayed significant differences between the sexes ('p' values not shown).

Of particular interest for the goals of this research project are the relationships between muscle and bone geometric phenotypes that may provide important insights into stress fracture risk. For example, we found a significant correlation in both males and females between either isolated quadriceps weight or cross sectional muscle area and femur size as measured by length and mid shaft diameters as shown below.

Part II: Table 4: Correlation of muscle measurements and femur geometric measurements in males and females at 16 weeks of age (r values shown, p<.0001).

	Femur lgth.	A/P Diam.	M/L Diam.
Females			
Quadriceps Wt. (g)	0.63	0.73	0.79
Muscle Area (mm^2)	0.7	0.65	0.65
Males			
Quadriceps Wt. (g)	0.8	0.88	0.89
Muscle Area (mm^2)	0.88	0.9	0.75

Note that for both muscle phenotypes, females have lower correlations overall with femoral dimensions than do males. These findings suggest that in males the bone geometry may be more responsive to stimulation by muscle mass than in females.

D. Measurement of femoral strength by three point bending tests.
Shown below are five measurements of bone mechanical behavior chosen to represent different bone strength properties. The first three - peak load, stiffness, and work to failure - represent bone biomechanical properties that are not adjusted for bone size. Estimated ultimate strength and estimated elastic modulus are biomechanical properties that have been adjusted for the geometry of the femur using moment of inertia (MOI) about the M/L axis (derived from μCT) and M/L diameter (measured with a digital caliper). The formula for calculating estimated ultimate strength is: $s = FLc / 4I$ {F = peak load (N); L = length between supports (mm); c = radius of M/L dimension (mm); I = moment of inertia M/L dimension (mm^4); units are ($GPa=(N/mm^2/10^6)$}. The formula for calculating estimated elastic modulus is: $E = K(L^3/48I)$; (K = stiffness (n/mm); L = distance between supports (mm); I = moment of inertia M/L dimension (mm^4); units are $MPa=(N/mm^2/10^4)$.

Part II: Table 5. Strain means of biomechanical properties derived from three point bending tests of femurs from females and males at 16 weeks of age.

Female data	Peak Load (N)			Stiffness (N/mm)			Work to Faiure (N*mm)			Estimated Ultimate Strengh (Mpa)			Estimated Elastic Modulus (GPa)		
Strains	MEAN	SD	N	MEAN	SD	N	MEAN	SD	N	MEAN	SD	N	MEAN	SD	N
129S1/SvImJ	23.74	1.26	10	188.62	8.96	10	3.36	0.52	10	253.59	13.32	10	4.23	0.11	10
BALB/cJ	30.28	0.69	10	197.60	3.92	10	5.22	0.39	10	329.32	15.95	10	4.42	0.14	10
C3H/HeJ	39.74	0.90	9	222.63	7.60	9	6.97	0.51	9	408.78	19.82	9	5.30	0.29	9
C57BL/6J	20.93	0.86	10	148.30	4.93	10	8.48	0.51	9	216.93	11.56	10	3.29	0.07	10
C58/J	23.99	0.66	10	160.27	5.99	10	5.07	0.35	10	268.83	13.01	10	3.70	0.20	10
FVB/NJ	26.86	0.61	11	170.83	5.96	11	6.12	0.30	11	256.51	8.72	10	3.56	0.16	10
NZB/BINJ	30.76	0.88	11	184.02	6.57	11	7.89	0.57	11	331.26	8.49	11	4.12	0.11	11
PWK/Ph	18.99	0.70	12	127.37	5.76	12	3.51	0.34	12	280.82	11.89	12	4.99	0.22	12
SJL/J	26.34	1.12	8	168.41	7.64	8	6.16	0.78	8	310.04	18.58	8	4.35	0.21	8
SWR/J	21.60	0.42	9	133.74	7.13	9	4.78	0.40	9	308.23	18.62	9	5.06	0.31	9
Male data															
Strains	MEAN	SD	N	MEAN	SD	N	MEAN	SD	N	MEAN	SD	N	MEAN	SD	N
129S1/SvImJ	28.04	1.03	15	196.86	6.44	14	5.18	0.52	15	278.17	9.90	15	3.74	0.30	15
BALB/cJ	32.18	0.54	10	185.35	6.83	10	5.59	0.27	10	310.75	15.67	10	3.62	0.18	10
C3H/HeJ	45.19	1.27	11	243.26	8.42	11	8.35	0.60	11	359.41	14.06	10	4.03	0.26	10
C57BL/6J	26.25	0.70	12	160.58	4.57	12	5.91	0.62	12	206.22	8.99	12	2.18	0.10	12
C58/J	23.63	0.89	10	150.94	5.47	10	5.45	0.48	10	225.01	10.77	10	3.04	0.09	10
FVB/NJ	24.18	0.71	9	150.13	5.72	9	6.12	0.87	9	210.92	11.15	9	2.62	0.11	9
NZB/BINJ	37.11	0.95	13	211.08	4.47	13	9.29	0.96	13	303.62	7.06	13	3.23	0.09	13
PWK/Ph	18.62	0.82	11	128.37	5.22	11	3.68	0.34	11	267.51	14.60	11	5.63	0.25	11
SJL/J	28.30	0.63	11	168.98	6.54	11	8.88	0.71	11	301.70	13.84	11	3.44	0.15	11
SWR/J	24.09	1.05	10	132.75	10.89	10	6.37	0.81	10	324.60	12.80	10	3.79	0.30	10

ANOVA of the five biomechanical properties revealed significant strain differences and gender differences for some traits in most strains. As predicted by biomechanical principles, the correlation between peak load and stiffness was significant for the nine strains taken together for both males (r=.95) and females (r=.90). And, as expected, the correlation between peak load and work to failure was very low among strains in females (r=.41). But, what was not predicted, was the better correlation between peak load and work to failure in males (r=.71). When females from individual strains were examined for correlation between peak load and stiffness, all strains but two, SJL/J (r=.40) and SWR/J (r=-.01), had significant correlation values. However, in males, the correlation between peak load and stiffness was significant (r>.66) in only three strains, 129S1/SvImJ, FVB/NJ, and PWK/PhJ. These data suggest that some inbred strains of mice have biomechanical properties of the femur that are uniquely regulated such that the expected correlation between peak load and stiffness does not hold true. It is these 5 strains that could prove to be most useful for genetic analyses of bone mechanical traits.

Careful inspection of our data revealed that the C3H/HeJ strain was frequently an outlier in scattergrams (See Appendix) for nearly all phenotypes considered. Consequently, the C3H/HeJ strain skewed the data when regression analyses or correlational analyses were done for both males and females. For this reason, we have set aside the C3H/HeJ strain from further consideration as an appropriate strain for predicting relationships among bone phenotypes and strength. In addition, because such an outlier would make interpretation of potential F2 data very confusing, we have eliminated C3H/HeJ as a possible strain to be used as a genetic model.

Relationships between BMD, bone geometry, muscle mass, and bone strength

Together these data have been used to answer several questions about the relationship between BMD, bone geometry, muscle mass, and bone strength. Since our comparisons are based on only 9 inbred strains, the level of significance ($p<0.05$) requires that $r>0.91$. However, for discussion purposes, we consider $r > 0.5$ as suggestive and worthy of further investigation.

1. *Is muscle mass a good predictor of BMD?* We have chosen the quadriceps muscle, the cross-sectional muscle area, and the vBMD from the cross-section of the associated femur as measurements to be evaluated. In both male and female mice from 9 strains, the values for isolated quadriceps weight and the area of the muscle as measured by pQCT were correlated females: r=0.74; males: r=0.86 (Table 6 below). However, in females, there was no correlation ($r<0.5$) between isolated quadriceps weight and any density phenotype; whereas, the correlation between muscle area and total BMD was r=0.53, and the correlation between muscle area and cortical femoral density was r=0.63. In males, the best correlation between muscle measurements and density phenotypes was r=0.40 between isolated quadriceps weight and cortical density. These data suggest that the relationship between muscle area and BMD are likely to be sex specific, wherein muscle area predicts BMD better for females than for males. Curiously, isolated quadriceps weight, although correlated with muscle area, does not predict BMD in either males or females.

Part II: Table 6. Correlation Tables of Bone and Muscle Phenotypes

Based on 9 Female Strains means	femur lgth (mm)	A/P Dim (mm)	M/L Dim (mm)	whole body wt (g)	isolated quadriceps wt (g)	mid shaft BMD (mg/cm3)	pQCT final muscle area (mm2)	Cortical thickness (mm)	Periosteal circum (mm)	Total density (mg/cm3)	Cortical Density (mg/cm3)
Femur Lgth	1.00	0.90	0.56	0.89	0.63	0.44	0.70	0.57	0.59	0.15	0.60
A/P Dim	0.90	1.00	0.76	0.81	0.73	0.46	0.65	0.66	0.74	0.14	0.69
M/L Dim	0.56	0.76	1.00	0.73	0.79	0.21	0.65	0.57	0.88	0.07	0.44
Whole Body Wt	0.89	0.81	0.73	1.00	0.71	0.41	0.88	0.66	0.70	0.30	0.61
Isolated Quad Wt	0.63	0.73	0.79	0.71	1.00	-0.08	0.74	0.29	0.91	-0.08	0.31
Mid Shaft vBMD	0.44	0.46	0.21	0.41	-0.08	1.00	0.38	0.89	0.01	0.79	0.77
pQCT Final Muscle Area	0.70	0.65	0.65	0.88	0.74	0.38	1.00	0.68	0.70	0.53	0.63
Cortical Thickness	0.57	0.66	0.57	0.66	0.29	0.89	0.68	1.00	0.43	0.78	0.90
Periosteal circum (mm)	0.59	0.74	0.88	0.70	0.91	0.01	0.70	0.43	1.00	-0.03	0.45
Total Density (mg/cm3)	0.15	0.14	0.07	0.30	-0.08	0.79	0.53	0.78	-0.03	1.00	0.69
Cortical Density (mg/cm3)	0.60	0.69	0.44	0.61	0.31	0.77	0.63	0.90	0.45	0.69	1.00
Based on 9 Male Strains means											
Femur Lgth	1.00	0.87	0.70	0.87	0.80	0.20	0.88	0.52	0.72	0.29	0.56
A/P Dim	0.87	1.00	0.87	0.92	0.88	-0.16	0.90	0.38	0.94	0.18	0.28
M/L Dim	0.70	0.87	1.00	0.83	0.89	-0.04	0.75	0.54	0.94	0.26	0.24
Whole Body Wt	0.87	0.92	0.83	1.00	0.80	0.01	0.85	0.49	0.85	0.18	0.46
Isolated Quad Wt	0.80	0.88	0.89	0.80	1.00	0.05	0.86	0.51	0.87	0.33	0.40
Mid Shaft vBMD	0.20	-0.16	-0.04	0.01	0.05	1.00	0.02	0.77	-0.29	0.72	0.80
pQCT Final Muscle Area	0.88	0.90	0.75	0.85	0.86	0.02	1.00	0.43	0.76	0.24	0.34
Cortical Thickness	0.52	0.38	0.54	0.49	0.51	0.77	0.43	1.00	0.32	0.87	0.81
Periosteal circum (mm)	0.72	0.94	0.94	0.85	0.87	-0.29	0.76	0.32	1.00	0.10	0.14
Total Density (mg/cm3)	0.29	0.18	0.26	0.18	0.33	0.72	0.24	0.87	0.10	1.00	0.73
Cortical Density (mg/cm3)	0.56	0.28	0.24	0.46	0.40	0.80	0.34	0.81	0.14	0.73	1.00

2. *Is muscle mass a good predictor of femur geometry?* Next we assessed the relationships between muscle area and bone geometric phenotypes including length, anterior/posterior and medio/lateral diameters, and periosteal circumference of the femur at the mid diaphysis. In both males and females the regression coefficients ranged between r=0.65 and r=0.88 (Table 6 above). Similar relationships were found for the weight of the quadriceps muscle and the bone geometric phenotypes. One possible sex difference was found whereby the correlation between muscle area and cortical thickness was r=0.67 in females and only r=0.43 in males. Isolated quadriceps weight and cortical thickness were not correlated in either sex. These data suggest that the

muscle mass and the overall size of the femur as indicated by length and mid shaft diameters are likely to be correlated in both males and females. Coupled with interpretation from the relationship between muscle mass and BMD, we would conclude that muscle has a more profound effect on femur geometry than on femoral BMD in both sexes.

Part II: Table 7. Bone and muscle phenotypes as predictors of bone strength (highlighted values are significant, $p<0.05$).

Predictor	Peak Load	Stiffness	Work to Failure
Mid shaft vBMD (mg/mm3)	0.006	0.002	0.784
Total density (mg/mm3)	0.002	0.002	0.513
Cortical Density (mg/mm3)	0.000	0.000	0.659
Cortical thickness (mm)	0.000	0.000	0.226
Femur lgth (mm)	0.002	0.001	0.087
Whole body wt (g)	0.001	0.004	0.014
Periosteal circumference (mm)	0.052	0.053	0.044
M/L Diam (mm)	0.009	0.029	0.037
A/P Diam (mm)	0.008	0.008	0.064
Isolated quadriceps wt (g)	0.020	0.034	0.041
pQCT final muscle area (mm2)	0.001	0.011	0.009

1. *Is muscle mass a good predictor of femoral bone strength?* Bone strength can be measured in different ways depending on the bone property of interest. Peak load is the maximum force the bone can withstand before it breaks; the stiffness indicates how much the bone will deform as a force is applied, and the work to failure is the amount of energy required to cause the bone to fracture, often called toughness of bone. The predictors of these bone strength measures were determined by regression analyses of strain means for males and females from 9 inbred strains. Results are shown in Table 7 above with significant predictors ($p<0.05$) highlighted in yellow; male and female data are combined, since no overall sex effect was found. It is clear that quadriceps weight, muscle area, and whole body weight strongly predicted all three strength measures.

2. *Is vBMD a good predictor of femoral bone strength?* We found that vBMD at the midshaft of the femur, and total and cortical vBMD of the entire femur predicted peak load and stiffness, but not work to failure (Table 7).

3. *Is bone geometry a good predictor of femoral bone strength?* We found M/L diameter to be the best geometric predictor of the 3 measures of femoral strength. Femur length and A/P diameter both predicted peak load and stiffness but not work to failure. In contrast, periosteal circumference was a stronger predictor of work to failure than of peak load or stiffness.

Overall, we found that relationships between muscle mass, vBMD, and bone geometry were clearly all important determinants of femur strength. However the relative effect each phenotype has on strength depends on the biomechanical measure made. These data illustrate that bone strength is a complex phenotype with many interrelated regulatory factors.

These data suggest that to predict which recruits would be better suited for rigorous training without suffering a fracture, it would be informative to measure the cross sectional area of the muscle at mid thigh with QCT, since this phenotype strongly predicts peak load, stiffness and work to failure. With this one QCT scan, data for M/L

diameter, mid shaft vBMD and cortical thickness (predictors of peak load and stiffness), plus periosteal circumference (work to failure predictor) would be available for additional consideration.

In addition to peak load, stiffness, and work to failure, we also calculated two size adjusted strength measures: estimated ultimate strength and estimated elastic modulus. The predictors of these measures are shown in Table 8 below.

Part II: Table 8. Bone and muscle phenotypes as predictors of size adjusted measures of femoral bone strength (highlighted values are significant, $p<0.05$).

Predictor	Estimated Ultimate Strength	Estimated Elastic Modulus
Mid shaft vBMD (mg/mm3)	0.002	0.139
Total density (mg/mm3)	0.004	0.470
Cortical Density (mg/mm3)	0.088	0.758
Cortical thickness (mm)	0.022	0.678
Femur lgth (mm)	0.798	0.007
Whole body wt (g)	0.847	0.000
Periosteal circumference (mm)	0.140	0.000
M/L Diam (mm)	0.668	0.000
A/P Diam (mm)	0.378	0.000
Isolated quadriceps wt (g)	0.529	0.000
pQCT final muscle area (mm2)	0.872	0.001

As expected, density was a significant predictor of the estimated ultimate strength, but surprisingly density was not associated with estimated elastic modulus.

Proposed Genetic Models

We have focused our recommendations for genetic models on measures that could be readily obtained in both mice and humans. Apart from body weight, all of the chosen contributing phenotypes could be acquired from a single QCT measurement of the mid thigh. Comparable measurements can be been made in experimental mice using a pQCT instrument. This enables translation of research findings to practical clinical applications, including the screening of recruits. We have proposed genetic models for three strength phenotypes as described below.

As shown in Table 7, regression analyses of predictors and strength measures using males and females from nine strains revealed that stiffness and peak load were predicted by the same bone phenotypes. They include: body weight, femur length, and 5 measures from the center of the femoral diaphysis (A/P & M/L diameter, total vBMD, cortical thickness, muscle area). We examined the individual strain means of peak load and stiffness predictors as shown in Table 9 below (SD and group sizes are included for each phenotype in original Tables 1-4 presented above and are eliminated here for clarity). The strains with the lowest values for each phenotype are highlighted in yellow.

Part II: Table 9. Strain means for predictors of peak load and stiffness in males and females.

Strains	Peak Load (N)	Stiffness (N/mm)	whole body wt (g)	femur lgth (mm)	A/P Dim (mm)	M/L Dim (mm)	mid shaft BMD (mg/mm3)	Cortical thickness (mm)	pQCT final muscle area (mm2)
Females									
129S1/SvImJ	23.74	188.62	20.14	15.64	1.23	1.45	766.49	0.23	63.52
BALB/cJ	30.28	197.60	23.90	15.65	1.26	1.73	806.74	0.24	65.57
C57BL/6J	20.93	148.30	21.93	15.51	1.22	1.69	631.39	0.19	64.03
C58/J	23.99	160.27	21.18	15.44	1.21	1.58	688.88	0.21	54.65
FVB/NJ	26.86	170.83	22.67	15.08	1.16	1.53	693.11	0.21	69.68
NZB/BINJ	30.76	184.02	26.96	16.50	1.24	1.60	781.95	0.24	76.33
PWK/Ph	18.99	127.37	15.14	14.07	1.08	1.30	715.58	0.19	44.81
SJL/J	26.34	168.41	20.00	14.44	1.16	1.66	726.87	0.23	66.34
SWR/J	21.60	133.74	17.79	14.36	1.11	1.32	663.02	0.19	54.83
Males									
129S1/SvImJ	28.04	196.86	26.09	15.72	1.21	1.57	787.54	0.23	69.64
BALB/cJ	32.18	185.35	28.67	15.76	1.25	2.00	829.35	0.26	81.73
C57BL/6J	26.25	160.58	30.10	16.21	1.37	2.05	619.17	0.21	88.73
C58/J	23.63	150.94	30.63	15.38	1.24	1.70	673.15	0.21	72.24
FVB/NJ	24.18	150.13	28.08	15.50	1.32	1.76	639.23	0.20	84.10
NZB/BINJ	37.11	211.08	32.16	16.72	1.34	1.80	780.41	0.25	97.01
PWK/Ph	18.62	128.37	16.43	13.87	1.00	1.20	711.57	0.19	48.05
SJL/J	28.30	168.98	26.03	14.54	1.22	1.81	687.66	0.23	69.53
SWR/J	24.09	132.75	23.55	14.86	1.15	1.49	703.88	0.20	78.88

An appropriate model to determine the genetic regulation of peak load and stiffness would include one strain with low values for peak load and stiffness coupled with low values for predictors of these strength measures, mated to a strain with high values for the strength measures and high values for predictors. Using the data in Table 9 above, we would propose to use SWR/J females as the low strength/predictors strain crossed to BALB/cJ males as the high strength/predictors strain. F2 progeny would segregate alleles of regulatory genes for strength/predictor phenotypes randomly, making it possible to perform genetic analyses for any/all of the strength/predictor phenotypes.

Similar reasoning has been used to determine a genetic model for work to failure, i.e., the amount of energy it takes to cause the bone to fracture. Predictors of work to failure are the same for males and females and include whole body weight, M/L diameter, periosteal circumference, and muscle area. It is interesting to note that vBMD is not indicated to be a predictor of work to failure. Strain with the lowest means highlighted in yellow are shown in Table 10.

Part II: Table 10. Strain means for predictors of work failure in males and females.

Strains	Work to Failure (N*mm)	M/L Dim (mm)	whole body wt (g)	pQCT final muscle area (mm2)	Periosteal circum (mm)
Females					
129S1/SvImJ	3.36	1.45	20.14	63.52	4.61
BALB/cJ	5.22	1.73	23.90	65.57	4.76
C57BL/6J	8.48	1.69	21.93	64.03	4.95
C58/J	5.07	1.58	21.18	54.65	4.72
FVB/NJ	6.12	1.53	22.67	69.68	4.84
NZB/BINJ	7.89	1.60	26.96	76.33	4.62
PWK/Ph	3.51	1.30	15.14	44.81	4.00
SJL/J	6.16	1.66	20.00	66.34	4.74
SWR/J	4.78	1.32	17.79	54.83	4.18
Males					
129S1/SvImJ	5.18	1.57	26.09	69.64	4.74
BALB/cJ	5.59	2.00	28.67	81.73	5.04
C57BL/6J	5.91	2.05	30.10	88.73	5.63
C58/J	5.45	1.70	30.63	72.24	4.98
FVB/NJ	6.12	1.76	28.08	84.10	5.13
NZB/BINJ	9.29	1.80	32.16	97.01	5.00
PWK/Ph	3.68	1.20	16.43	48.05	3.94
SJL/J	8.88	1.81	26.03	69.53	5.03
SWR/J	6.37	1.49	23.55	78.88	4.50

Again, a strain with low work to failure and low predictors would be crossed with a strain that has high work to failure and high predictors. It is interesting to note that within an inbred strain, C57BL/6J for example, females have a high work to failure, whereas males have a low work to failure; values for predictors vary consistently for sex within the C57BL/6J strain. These sex differences dictate choice of high and low strain, but it is not predetermined that the female strain should necessarily be either the low or high strength strain. Since the data shown in **Table 10** offers only one high work to failure/high predictors strain, NZB/BINJ males, we would propose to use a low work to failure/low predictors strain from the female set - 129S1/SvImJ or SWR/J – mated to NZB/BINJ, high work to failure/high predictors males. Since 129S1/SvImJ has low work to failure and low predictors in both males and females, the analyses of F2 progeny would be simplified by choosing this strain as the low strength/low predictors strain.

Estimated ultimate strength is a calculated parameter that is corrected for bone size using peak load, moment of inertia (from μCT), and M/L diameter. Interestingly, the predictors for ultimate strength are more related to bone density than to femur geometry and include mid shaft vBMD and total density of the entire femur. The reason for this may be that all other predictors have been accounted for in the calculation of the trait itself. **Table 11** below shows strain means for predictors of estimated ultimate strength;

as before, the lowest values are highlighted in yellow (SD and n's are presented in Tables 1-4 above).

Part II: Table 11. Strain means for predictors of estimated ultimate strength

Strains	Estimated Ultimate Strengh (Mpa)	mid shaft BMD (mg/mm3)	Cortical thickness (mm)	Total density (mg/cm3)
Females				
129S1/SvImJ	253.60	766.49	0.23	0.71
BALB/cJ	329.30	806.74	0.24	0.71
C57BL/6J	216.90	631.39	0.19	0.57
C58/J	268.80	688.88	0.21	0.60
FVB/NJ	256.50	693.11	0.21	0.68
NZB/BINJ	331.30	781.95	0.24	0.72
PWK/Ph	279.00	715.58	0.19	0.64
SJL/J	310.00	726.87	0.23	0.73
SWR/J	308.20	663.02	0.19	0.65
Males				
129S1/SvImJ	278.20	787.54	0.23	0.69
BALB/cJ	310.80	829.35	0.26	0.69
C57BL/6J	206.20	619.17	0.21	0.61
C58/J	225.00	673.15	0.21	0.57
FVB/NJ	210.90	639.23	0.20	0.62
NZB/BINJ	303.60	780.41	0.25	0.69
PWK/Ph	267.50	711.57	0.19	0.60
SJL/J	301.70	687.66	0.23	0.69
SWR/J	324.60	703.88	0.20	0.62

There are several suitable genetic models for estimated ultimate strength. Females with low values for ultimate strength and for predictors are: C57BL/6J, C58/J, FVB/BINJ, and PWK/Ph. Males from C57BL/6J, C58/J, and FVB/BINJ also have low values for ultimate strength and its predictors. Having consistency between sexes within a strain would simplify genetic analyses of F2s as previously mentioned. Similarly, both females and males from the BALB/cJ and NZB/BINJ strains have high values for ultimate strength and its predictors, making these strains good high value choice. Considering the reproductive performance and potential genetic polymorphisms to use for mapping genes related to strength, we would propose using the C57BL/6J and BALB/cJ strains for genetic analyses. If potential regulatory genes on the X Chromosome were to be evaluated, then reciprocal matings could be made, that is, C57BL/6J would be used as the female in one cross and the male in the reciprocal cross. Using reciprocal crosses is also critical if maternal or paternal effects are to be evaluated. Parental effects are discussed in Part III, Dr. Churchill's section of this report.

Estimated elastic modulus is a calculated parameter that is corrected for bone size using stiffness, moment of inertia (from μCT), and M/L diameter. Strain means for EM and its predictors are shown in **Table 12** below (SD and n's are presented in Tables

1-4). Although the femur geometry and muscle phenotypes that are predictors of EM have highly significant p values when the entire population of mice is considered together, it is clear that within an individual strain, the relationship between EM and its predictors is not as strong. The only instance where EM and all of its predictors are either high or low is for BALB/cJ females where all are high. In both PWK/Ph and SWR/J males and females, all of the predictors are relatively low while EM is in the high class. It is quite possible that this strength phenotype is so complex that a clear genetic model is not available using these 9 strains of mice.

Part II: Table 12. Strain means for predictors of estimated elastic modulus in males and females.

Strains	Elastic Modulus (GPa)	femur lgth (mm)	whole body wt (g)	Periosteal circum (mm)	M/L Dim (mm)	A/P Dim (mm)	isolated quad wt (g)	pQCT final muscle area (mm2)
Females								
129S1/SvImJ	4.23	15.64	20.14	4.61	1.45	1.23	0.17	63.52
BALB/cJ	4.42	15.65	23.90	4.76	1.73	1.26	0.18	65.57
C57BL/6J	3.25	15.51	21.93	4.95	1.69	1.22	0.21	64.03
C58/J	3.74	15.44	21.18	4.72	1.58	1.21	0.16	54.65
FVB/NJ	3.56	15.08	22.67	4.84	1.53	1.16	0.18	69.68
NZB/BINJ	4.05	16.50	26.96	4.62	1.60	1.24	0.17	76.33
PWK/Ph	4.90	14.07	15.14	4.00	1.30	1.08	0.12	44.81
SJL/J	4.35	14.44	20.00	4.74	1.66	1.16	0.17	66.34
SWR/J	5.01	14.36	17.79	4.18	1.32	1.11	0.15	54.83
Males								
129S1/SvImJ	3.93	15.72	26.09	4.74	1.57	1.21	0.23	69.64
BALB/cJ	3.62	15.76	28.67	5.04	2.00	1.25	0.26	81.73
C57BL/6J	2.35	16.21	30.10	5.63	2.05	1.37	0.28	88.73
C58/J	3.04	15.38	30.63	4.98	1.70	1.24	0.20	72.24
FVB/NJ	2.62	15.50	28.08	5.13	1.76	1.32	0.24	84.10
NZB/BINJ	3.22	16.72	32.16	5.00	1.80	1.34	0.24	97.01
PWK/Ph	5.67	13.87	16.43	3.94	1.20	1.00	0.13	48.05
SJL/J	3.66	14.54	26.03	5.03	1.81	1.22	0.22	69.53
SWR/J	3.79	14.86	23.55	4.50	1.49	1.15	0.22	78.88

Aim 2: To acquire new data on serum biomarkers related to bone density and body composition.

A. Measure serum IGF-I, an important growth factor for bone (Table 14).
B. Measure T4, thyroxine, a marker of overall metabolic activity (Table 14).
C. Measure osteocalcin, a marker of bone formation (Table 14).

The data for DEXA measurement of areal BMD (aBMD) and body compartments in males and females of 28 strains that were used to generate the original application are presented below in **Table 13** for comparative purposes. As discussed in our proposal, there are significant differences in all phenotypes among inbred strains, providing

potential models for genetic analyses. New data for serum biomarkers are presented in **Table 14.**

Part II: Tables 13 A&B: DEXA measurement of areal BMD (aBMD) and body compartments in males (Table 13A) and females (Table 13B) of 28 strains.

		Body WT (g)		%Fat		%Lean		aBMD (g/cm^2)		SPINE BMD L2-L5 (g/mm^2)	
28 male strains	N	MEAN	SEM	MEAN	SEM	MEAN	SEM	MEAN	SEM	MEAN	SEM
129S1/SvImJ	10	23.80	0.87	21.15	1.05	78.80	1.04	0.052	0.00070	0.084	0.0022
A/J	10	23.23	0.72	24.07	1.13	75.91	1.13	0.041	0.00026	0.061	0.0022
AKR/J	10	32.27	0.84	28.78	1.20	71.23	1.21	0.052	0.00062	0.083	0.0036
BALB/cJ	10	25.08	0.33	16.65	0.93	83.38	0.93	0.048	0.00033	0.073	0.0026
BTBR+Ttf/tf	10	27.04	0.84	15.51	0.84	84.42	0.82	0.051	0.00043	0.079	0.0019
BUB/BnJ	10	25.13	0.77	14.12	1.12	85.88	1.12	0.049	0.00046	0.068	0.0018
C3H/HeJ	10	26.25	0.89	23.60	1.01	76.41	1.01	0.052	0.00049	0.083	0.0026
C57BL/6J	10	25.99	0.48	16.66	1.23	83.32	1.21	0.047	0.00033	0.070	0.0025
C57L/J	10	25.35	0.52	19.52	1.69	80.51	1.67	0.048	0.00049	0.064	0.0026
C58/J	10	25.59	1.08	21.21	1.34	78.85	1.34	0.045	0.00083	0.062	0.0026
CAST/EiJ	10	13.51	0.34	14.30	0.57	85.72	0.63	0.039	0.00038	0.057	0.0012
CZECHII/EiJ	12	13.39	0.45	13.91	0.60	86.11	0.58	0.040	0.00051	0.056	0.0016
DBA/2J	10	25.76	0.86	23.85	1.30	76.10	1.32	0.045	0.00050	0.062	0.0025
FVB/NJ	10	23.19	0.47	14.53	1.09	85.49	1.11	0.048	0.00057	0.071	0.0031
JF1/Ms	10	20.38	0.56	35.17	2.30	63.90	1.76	0.041	0.00027	0.060	0.0019
MOLF/EiJ	8	12.69	0.25	13.76	1.12	86.21	1.15	0.039	0.00046	0.053	0.0024
MSM/Ms	9	11.94	0.32	15.12	0.65	85.04	0.64	0.041	0.00072	0.066	0.0023
NOD/LtJ	10	25.75	0.70	14.72	0.60	85.20	0.60	0.049	0.00067	0.073	0.0022
NZB/B1NJ	10	24.58	0.60	16.26	1.55	83.71	1.55	0.047	0.00031	0.068	0.0020
NZW/LacJ	10	26.97	0.88	18.25	1.62	81.78	1.59	0.051	0.00063	0.081	0.0013
PERA/EiJ	10	21.30	0.63	18.38	0.79	81.65	0.80	0.048	0.00059	0.072	0.0013
PL/J	11	21.32	0.69	19.72	0.67	80.14	0.67	0.044	0.00042	0.072	0.0031
PWK/PhJ	9	18.10	0.87	19.44	1.88	80.50	1.89	0.041	0.00053	0.061	0.0016
SJL/J	10	22.13	0.47	16.10	0.98	83.97	0.99	0.051	0.00057	0.076	0.0019
SM/J	10	23.01	0.53	20.06	0.70	79.93	0.67	0.044	0.00065	0.059	0.0028
SPRET/EiJ	10	14.47	0.62	23.10	1.45	77.04	1.42	0.043	0.00036	0.072	0.0011
SWR/J	10	20.26	0.34	11.95	0.78	87.97	0.74	0.045	0.00029	0.075	0.0017
WSB/EiJ	10	13.47	0.30	14.94	0.67	85.19	0.68	0.039	0.00046	0.057	0.0021

		Body WT (g)		%Fat		%Lean		aBMD (g/cm^2)		SPINE BMD L2-L5 (g/mm^2)	
28 female strains	N	MEAN	SEM	MEAN	SEM	MEAN	SEM	MEAN	SEM	MEAN	SEM
129S1/SvImJ	10	16.30	0.34	16.08	0.48	83.98	0.50	0.049	0.00057	0.094	0.0026
A/J	10	18.97	0.60	22.14	1.50	77.94	1.50	0.041	0.00041	0.065	0.0027
AKR/J	10	30.32	1.12	31.50	1.49	68.55	1.47	0.053	0.00062	0.090	0.0048
BALB/cJ	10	19.50	0.63	22.31	1.22	77.74	1.24	0.046	0.00065	0.074	0.0016
BTBR T$^+$ tf/tf	8	23.81	0.64	16.03	0.62	83.93	0.68	0.054	0.00087	0.095	0.0034
BUB/BnJ	10	21.93	0.45	15.42	0.70	84.56	0.71	0.048	0.00029	0.075	0.0024
C3H/HeJ	10	20.39	0.66	23.26	1.02	76.67	1.02	0.050	0.00047	0.081	0.0016
C57BL/6J	10	16.91	0.48	15.24	0.90	84.81	0.89	0.044	0.00047	0.071	0.0013
C57L/J	10	18.21	0.31	15.73	1.17	84.34	1.17	0.050	0.00051	0.085	0.0031
C58/J	10	19.49	0.80	13.41	1.33	86.55	1.31	0.045	0.00035	0.069	0.0021
CAST/EiJ	10	11.66	0.23	13.96	0.57	86.17	0.53	0.040	0.00034	0.064	0.0013
CZECHII/EiJ	12	10.49	0.22	15.52	0.89	84.32	0.93	0.039	0.00064	0.059	0.0024
DBA/2J	10	19.76	0.57	22.49	1.38	77.48	1.39	0.044	0.00029	0.066	0.0016
FVB/NJ	10	19.72	0.43	20.82	0.99	79.18	1.01	0.047	0.00037	0.076	0.0023
JF1/Ms	11	13.87	0.38	21.66	1.41	78.34	1.43	0.043	0.00077	0.075	0.0026
MOLF/EiJ	10	10.39	0.19	13.20	0.34	86.71	0.38	0.040	0.00047	0.060	0.0023
MSM/Ms	11	8.94	0.19	15.90	0.84	84.12	0.86	0.040	0.00085	0.070	0.0013
NOD/LtJ	10	20.86	0.32	13.84	1.00	86.10	1.03	0.047	0.00040	0.080	0.0026
NZB/B1NJ	10	20.29	0.47	17.82	1.15	82.10	1.12	0.049	0.00058	0.091	0.0030
NZW/LacJ	10	24.57	0.66	28.41	1.52	71.58	1.56	0.050	0.00067	0.089	0.0026
PERA/EiJ	10	18.12	0.35	27.16	1.00	72.85	1.04	0.044	0.00073	0.057	0.0021
PL/J	10	15.97	0.41	19.56	1.07	80.33	1.03	0.044	0.00056	0.069	0.0013
PWK/PhJ	13	12.24	0.28	13.60	0.36	86.63	0.31	0.043	0.00070	0.076	0.0027
SJL/J	10	16.18	0.39	17.68	0.73	82.25	0.72	0.049	0.00057	0.079	0.0020
SM/J	10	15.40	0.44	21.84	1.06	78.16	1.05	0.038	0.00054	0.053	0.0023
SPRET/EiJ	10	11.37	0.62	19.30	1.03	80.68	1.05	0.047	0.00082	0.089	0.0023
SWR/J	10	16.43	0.30	15.30	0.43	84.69	0.42	0.044	0.00021	0.071	0.0011
WSB/EiJ	10	11.24	0.23	13.80	0.72	86.38	0.70	0.038	0.00046	0.057	0.0016

Part II: Table 14. Serum biomarkers for 28 strains in males and females.

	OC (ng/ml)			T4 (ng/ml)			Adj. IGF-1					OC (ng/ml)			T4 (ng/ml)			Adj. IGF-1		
28 female strains	MEAN	SEM	N	MEAN	SEM	N	MEAN	SEM	N	28 male strains	MEAN	SEM	N	MEAN	SEM	N	MEAN	SEM	N
129S1/SvImJ	84.00	5.74	10	3.88	0.31	10	91.14	2.78	10	129S1/SvImJ	82.89	10.98	9	4.61	0.20	9	109.22	2.90	9
A/J	47.70	1.75	10	4.90	0.20	10	106.44	5.59	10	A/J	46.60	2.68	10	4.36	0.16	10	103.36	3.50	10
AKR/J	40.30	3.45	10	3.55	0.11	10	114.60	4.12	10	AKR/J	52.50	5.95	4	3.93	0.29	4	68.43	17.12	7
BALB/cJ	51.00	2.88	10	7.92	0.23	10	107.44	2.96	10	BALB/cJ	27.80	1.92	10	7.87	0.37	10	118.24	3.52	10
BTBR T$^+$ tf/tf	74.75	2.83	8	4.30	0.15	8	161.71	4.02	8	BTBR+Ttf/tf	49.40	3.92	10	5.16	0.17	10	135.69	3.35	10
BUB/BnJ	40.60	2.67	10	6.64	0.45	10	108.88	3.20	10	BUB/BnJ	33.33	6.94	6	7.50	0.88	6	108.35	6.61	6
C3H/HeJ	58.00	2.29	10	9.74	0.77	10	127.38	5.49	10	C3H/HeJ	55.50	7.87	10	9.00	0.33	10	122.83	3.16	10
C57BL/6J	59.40	3.03	10	7.18	0.68	10	83.45	2.07	10	C57BL/6J	60.30	3.35	10	6.40	0.23	10	87.38	1.22	10
C57L/J	42.10	1.83	10	5.27	0.24	9	113.26	3.30	10	C57L/J	40.14	7.69	7	5.76	0.23	7	94.74	5.64	8
C58/J	70.60	4.71	10	5.69	0.27	10	111.09	3.30	10	C58/J	31.00	3.31	10	3.77	0.14	9	80.30	3.11	10
CAST/EiJ	57.30	5.64	10	3.59	0.38	10	119.92	4.32	10	CAST/EiJ	61.13	5.46	8	3.08	0.32	8	138.25	4.82	8
CZECHII/EiJ	69.13	6.66	8	5.51	0.33	7	80.23	4.90	8	CZECHII/EiJ	39.67	3.57	9	5.91	0.36	8	88.47	1.46	9
DBA/2J	54.40	2.75	10	6.64	0.40	10	82.87	3.77	10	DBA/2J	50.90	5.13	10	5.72	0.38	10	88.44	3.33	10
FVB/NJ	41.70	2.17	10	3.14	0.18	9	85.75	2.18	10	FVB/NJ	32.60	3.20	10	2.96	0.19	10	95.13	2.98	10
JF1/Ms	40.56	2.61	9	5.48	0.30	9	131.29	4.21	9	JF1/Ms	30.60	1.64	10	3.63	0.33	10	119.41	3.16	10
MOLF/EiJ	86.70	3.58	10	3.56	0.15	9	101.42	2.91	10	MOLF/EiJ	43.13	5.14	8	4.21	0.43	7	93.40	6.68	8
MSM/Ms	49.63	5.33	8	4.74	0.32	5	95.63	7.60	8	MSM/Ms	54.14	4.98	7	3.77	0.50	6	110.06	4.52	7
NOD/LtJ	41.20	4.45	10	4.50	0.48	10	126.56	4.55	10	NOD/LtJ	45.88	5.71	8	3.68	0.56	9	132.63	6.72	9
NZB/B1NJ	75.40	3.78	10	5.59	0.26	10	110.14	4.05	10	NZB/B1NJ	42.90	5.26	10	4.50	0.27	10	107.22	5.77	10
NZW/LacJ	58.10	3.20	10	4.97	0.27	10	105.11	3.58	10	NZW/LacJ	42.10	2.66	10	4.15	0.25	10	114.72	2.24	10
PERA/EiJ	49.63	4.61	8	4.38	0.20	8	133.49	3.80	8	PERA/EiJ	44.78	6.70	9	2.61	0.26	9	119.10	6.24	9
PL/J	52.00	5.02	10	5.43	0.25	10	98.22	3.96	10	PL/J	53.17	3.32	6	6.40	0.24	6	92.76	7.41	7
PWK/PhJ	83.00	7.01	7	4.13	0.24	7	120.60	4.07	7	PWK/PhJ	67.33	13.09	9	4.66	0.57	9	122.56	7.88	9
SJL/J	49.40	3.21	10	3.85	0.25	10	81.51	3.64	10	SJL/J	54.30	4.53	10	3.73	0.52	10	88.53	3.85	10
SM/J	45.60	4.48	10	--	--	0	54.32	3.59	10	SM/J	50.78	7.17	9	--	--	0	60.54	7.44	10
SPRET/EiJ	34.70	2.54	10	4.03	0.49	8	124.88	5.29	10	SPRET/EiJ	39.40	1.78	10	4.17	0.29	7	126.37	4.94	10
SWR/J	36.67	2.97	9	6.87	0.18	10	105.78	2.88	10	SWR/J	39.78	8.36	9	5.00	0.35	9	94.97	2.69	9
WSB/EiJ	56.70	3.23	10	2.59	0.12	10	84.01	3.01	10	WSB/EiJ	42.50	5.19	8	2.91	0.31	7	83.44	2.79	8

Part II: Table 15. Sex comparisons within strains for body composition, aBMD, and serum biomarkers. Significant p values ($p<0.05$) are highlighted in yellow.

Strains	Body WT (g)	%Fat	%Lean	aBMD (g/cm^2)	SPINE BMD L2-L5 (g/mm^2)	OC (ng/ml)	T4 (ng/ml)	Adj. IGF-1
129S1/SvImJ	0.0000	0.0004	0.0003	0.0030	0.0097	0.9274	0.0726	0.0003
A/J	0.0003	0.3174	0.2942	0.9514	0.2731	0.7351	0.0517	0.6458
AKR/J	0.1795	0.1720	0.1770	0.8139	0.2544	0.0893	0.1531	0.0075
BALB/cJ	0.0000	0.0017	0.0018	0.0155	0.7354	0.0000	0.9098	0.0305
BTBR T+ tf/tf	0.0100	0.6445	0.6641	0.0242	0.0004	0.0001	0.0021	0.0001
BUB/BnJ	0.0021	0.3386	0.3317	0.0682	0.0392	0.2683	0.3493	0.9364
C3H/HeJ	0.0000	0.8157	0.8578	0.0565	0.5712	0.7640	0.3892	0.4816
C57BL/6J	0.0000	0.0812	0.0767	0.0181	0.0001	0.7749	0.1662	0.0090
C57L/J	0.0003	0.0006	0.0007	0.8439	0.0577	0.0000	0.0000	0.0000
C58/J	0.0000	0.3629	0.3350	0.0000	0.5700	0.8442	0.2889	0.1189
CAST/EiJ	0.0003	0.6771	0.5953	0.0461	0.0009	0.6384	0.3295	0.0120
CZECHII/EiJ	0.0000	0.1464	0.1173	0.5400	0.2487	0.0011	0.4364	0.1105
DBA/2J	0.0000	0.4816	0.4828	0.0367	0.2302	0.5551	0.1115	0.2832
FVB/NJ	0.0000	0.0005	0.0005	0.4565	0.1956	0.0300	0.4955	0.0204
JF1/MsJ	0.0000	0.0001	0.0000	0.0329	0.0002	0.0042	0.0007	0.0354
MOLF/EiJ	0.0000	0.6024	0.6597	0.2816	0.0660	0.0000	0.1343	0.2532
MSM/MsJ	0.0000	0.4910	0.4245	0.5095	0.0653	0.5502	0.1515	0.1400
NOD/LtJ	0.0000	0.4586	0.4625	0.0623	0.0688	0.5213	0.2783	0.4566
NZB/B1NJ	0.0000	0.4284	0.4140	0.0164	0.0000	0.0001	0.0097	0.6838
NZW/LacJ	0.0427	0.0002	0.0002	0.0949	0.0135	0.0012	0.0401	0.0353
PERA/EiJ	0.0003	0.0000	0.0000	0.0001	0.0000	0.5699	0.0001	0.0758
PL/J	0.0000	0.8995	0.8753	0.7165	0.3543	0.8706	0.0230	0.4922
PWK/PhJ	0.0000	0.0016	0.0010	0.0917	0.0003	0.3487	0.4566	0.8429
SJL/J	0.0000	0.2135	0.1773	0.0215	0.2668	0.3890	0.8372	0.2015
SM/J	0.0000	0.1786	0.1733	0.0000	0.1481	0.5397		0.4613
SPRET/EiJ	0.0023	0.0462	0.0540	0.0003	0.0000	0.1476	0.8078	0.8393
SWR/J	0.0000	0.0014	0.0011	0.0037	0.0556	0.7305	0.0002	0.0143
WSB/EiJ	0.0000	0.2630	0.2369	0.2189	0.7967	0.0278	0.2803	0.8931

As would be expected, body weight is the trait with the greatest frequency of sexual dimorphism, whereas traits associated with body composition (%fat, %lean) are similar between sexes in 18 of the 28 strains. Sex differences for whole body BMD (aBMD) and BMD of the lumbar spine are not congruent, consequently predicting sex differences in one density phenotype based on sex differences in the other is unreliable. Inspection of serum data shows that four strains, BTBR, C57L/J, JF1/MsJ, and NZW/LacJ have sex effects for all three serum markers.

Inspection of serum data shows a wide range of values for all three biomakers among strains. To determine if serum markers might be used to predict aBMD or body composition traits, we have done a regression analyses and results are presented in **Table 16** below. Significant correlations are highlighted in yellow, r=.5 or better. It is clear that, at least in mice, serum markers cannot be used to predict aBMD, either whole body or at the lumbar spine, or body composition compartments. It is important to note that in this population of 28 strains of male and female mice, body weight is significantly correlated with both whole body aBMD and BMD of the lumbar spine, and that the correlation is stronger in males than in females. This is true also in human populations.

Part II: Table 16. Regression analyses of serum biomarkers, aBMD, and body composition.

females	Body WT (g)	%Fat	%Lean	aBMD (g/cm^2)	SPINE BMD L2-L5 (g/mm^2)	OC (ng/ml)	T4 (ng/ml)	Adj. IGF-1
Body WT (g)	1.00	0.57	-0.57	0.75	0.52	-0.19	0.21	0.28
%Fat	0.57	1.00	-1.00	0.31	0.16	-0.37	0.12	0.06
%Lean	-0.57	-1.00	1.00	-0.31	-0.16	0.37	-0.13	-0.06
Area BMD (g/cm^2)	0.75	0.31	-0.31	1.00	0.90	-0.06	0.14	0.48
SPINE BMD (g/mm^2)	0.52	0.16	-0.16	0.90	1.00	0.06	0.01	0.46
OC (ng/ml)	-0.19	-0.37	0.37	-0.06	0.06	1.00	-0.11	0.03
T4 (ng/ml)	0.21	0.12	-0.13	0.14	0.01	-0.11	1.00	0.04
Adj. IGF-1	0.28	0.06	-0.06	0.48	0.46	0.03	0.04	1.00
males	Body WT (g)	%Fat	%Lean	Area BMD (g/cm^2)	SPINE BMD L2-L5 (g/mm^2)	OC (ng/ml)	T4 (ng/ml)	Adj. IGF-1
Body WT (g)	1.00	0.32	-0.32	0.82	0.62	-0.02	0.32	-0.14
%Fat	0.32	1.00	-1.00	0.08	0.10	0.02	0.00	-0.07
%Lean	-0.32	-1.00	1.00	-0.07	-0.09	-0.02	0.00	0.06
Area BMD (g/cm^2)	0.82	0.08	-0.07	1.00	0.89	0.13	0.27	0.07
SPINE BMD (g/mm^2)	0.62	0.10	-0.09	0.89	1.00	0.23	0.23	0.20
OC (ng/ml)	-0.02	0.02	-0.02	0.13	0.23	1.00	-0.01	0.08
T4 (ng/ml)	0.32	0.00	0.00	0.27	0.23	-0.01	1.00	0.02
Adj. IGF-1	-0.14	-0.07	0.06	0.07	0.20	0.08	0.02	1.00

Aim 3: To complete data collection and analyses for strains with less than 10 mice per group for bone mineral density and body composition phenotypes and to contribute these data to The Mouse Phenome Database (MPD).

Thirty eight mice were needed to bring the 28 strains in our original data set up to 10 males and 10 females per group. These mice were collected and data is shown in Table 17 below. However, these data have not been added to the original data set submitted to MPD. When the range of values for individual traits within strains of the original MPD data set were compared to the range of values in these new data, we found that values for the new data were outside the original range by a considerable amount for some traits. For example, four new CZECHII/Ei females were added to the four in the original data set. The whole body aBMD of the original four ranged from .0359 to .0381g/cm^2 with a mean of .0372g/cm^2. The aBMD for the four newly added CZECHII/Ei females ranged from .0401 to .0422g/cm^2 with a mean of .0412g/cm^2, nearly 10% higher than the mean of the original set. This is most likely a technical issue and not a true biological change. During the time between the two collections, we changed not only our laboratory space, but also our DEXA technician. We have determined that the statistical limitations associated with smaller group size are preferable to those associated with a larger range of values for individual traits and will not submitted these additional data to MPD. However, they are presented below in Table 17.

Part II: Table 17: DEXA measurements for additional males and females at 16 weeks of age.

Strain	Sex	PIXI whole body BMD (g/cm2)	PIXI whole body BMC (grams)	PIXI Lean (grams)	PIXI Fat (grams)	PIXI Total (grams)	PIXI % Fat	Spine BMD (L2-L5) (g/cm2)	BMD skull (g/cm2)
BTBR/T+ tf/tf	F	0.0525	0.524	18.6	3.4	21.9	15.4	0.0840	0.1390
BTBR/T+ tf/tf	F	0.0549	0.528	18.9	3.7	22.6	16.5	0.0930	0.1410
BUB/Bnj	M	0.0493	0.509	18.5	3.0	21.5	13.9	0.0801	0.1142
BUB/Bnj	M	0.0494	0.494	21.4	5.5	26.9	20.3	0.0720	0.1150
Cast/Ei	M	0.0432	0.310	12.6	2.2	14.8	15.0	0.0529	0.0979
Cast/Ei	M	0.0394	0.273	10.1	2.2	12.3	17.9	0.0573	0.0892
Czech II/Ei	F	0.0418	0.302	8.2	1.5	9.7	15.4	0.0724	0.0989
Czech II/Ei	F	0.0422	0.268	10.4	1.9	12.3	15.6	0.0684	0.0976
Czech II/Ei	F	0.0408	0.312	8.9	1.7	10.6	15.8	0.0690	0.0936
Czech II/Ei	F	0.0401	0.279	8.5	1.4	10.0	14.5	0.0666	0.0987
Czech II/Ei	M	0.0407	0.307	10.7	1.7	12.4	13.8	0.0628	0.0929
Czech II/Ei	M	0.0408	0.305	13.3	2.4	15.7	15.1	0.0570	0.1016
Czech II/Ei	M	0.0425	0.304	12.9	2.6	15.4	16.6	0.0638	0.0987
JF1/Ms	F	0.0486	0.317	12.2	4.5	16.7	27.0	0.0882	0.1126
JF1/Ms	F	0.0465	0.284	11.2	4.2	15.3	27.2	0.0767	0.1118
Molf/Ei	M	0.0404	0.279	12.4	2.3	14.7	16.0	0.0477	0.1226
Molf/Ei	M	0.0386	0.237	10.7	1.8	12.4	14.6	0.0550	0.0909
MSM/Ms	F	0.0357	0.249	7.5	1.6	9.0	17.5	0.0670	0.0926
MSM/Ms	F	0.0423	0.291	6.9	1.5	8.4	18.2	0.0791	0.0954
MSM/Ms	F	0.0431	0.298	6.8	1.4	8.2	17.0	0.0719	0.0935
MSM/Ms	M	0.0448	0.320	9.0	1.3	10.3	12.4	0.0765	0.0910
MSM/Ms	M	0.0429	0.334	9.3	1.6	10.8	14.5	0.0733	0.0918
Pera/Ei	F	0.0450	0.321	14.2	5.5	19.8	27.9	0.0481	0.1186
Pera/Ei	F	0.0451	0.316	14.4	6.6	21.2	31.4	0.0676	0.1176
Pera/Ei	F	0.0456	0.331	12.6	5.2	17.9	29.2	0.0549	0.1300
Pera/Ei	F	0.0472	0.345	13.3	6.6	19.9	33.3	0.0620	0.1126
PL/J	M	0.0454	0.384	15.2	3.7	19.0	19.5	0.0873	0.1112
PL/J	M	0.0451	0.371	16.6	4.9	21.5	22.6	0.0786	0.1057
PWK/Ph	F	0.0413	0.332	10.1	1.4	11.5	12.1	0.0758	0.1107
PWK/Ph	F	0.0417	0.325	9.2	1.7	10.9	15.8	0.0722	0.1062
PWK/Ph	F	0.0440	0.344	8.9	1.4	10.3	14.1	0.0866	0.1044
PWK/Ph	F	0.0470	0.411	10.2	1.7	11.8	14.0	0.0903	0.1083
PWK/Ph	F	0.0475	0.420	9.8	1.8	11.6	15.9	0.0892	0.1074
PWK/Ph	F	0.0466	0.403	10.5	1.8	12.2	14.4	0.0894	0.1128
WSB/Ei	M	0.0421	0.363	11.4	1.9	13.3	14.5	0.0730	0.1047
WSB/Ei	M	0.0403	0.315	9.5	1.8	11.3	16.0	0.0606	0.1072
WSB/Ei	M	0.0442	0.361	12.9	2.3	15.2	14.9	0.0678	0.1068
WSB/Ei	M	0.0433	0.373	12.0	2.0	14.0	14.2	0.0610	0.1092

Part III: Diallele Cross for Skeletal/Body Composition

We have carried out a diallel cross among 8 inbred strains: PWK, C57BL/6J, SJL/J, 129S1/SvImJ, C3H/HeJ, C58/J, NZB/BINJ, and BALB/cJ. These strains correspond to 8 of the 10 strains chosen for Project Part II. The purpose of the study is to investigate the role of genetic and maternal effects on body mass and bone mineral content in the context of hybrid (outbred) individuals, representing a more normal genetic state than the standard, fully inbred, strains of mice. The data generated by this study will provide a basis for identifying new mouse models for bone related phenotypes and for selecting lines for further genetic mapping studies. We were particularly interested in the role of sex and sex-by-genotype interactions in the determination of lean body mass and bone mineral content.

Statistical Methods for Part III:

Eight parental inbred strains used to generate the 8 x 8 diallel cross are 129, B6, BALB, C3H, C58, SJL, NZB, and PWK. From this design, 8 parental types, 27 F1 crosses (no pups of BALB x PWK) and 28 reciprocal F1's were produces. A total of 626 mice were used in this study. Litters were standardized to 10 young at birth; 5 males and 5 females where possible. Phenotypes of male and female mice from each family measured in the diallel cross includes aBMD, Body Weight, Fat Mass, Lean Mass, %Fat, vBMD, skullBMD, Ear length, and Quad Weight. Comparison of the traits of the 8 parental strains (inbred data only) by the general linear models (GLM) indicated significant strain effect on most of the traits, except for %Fat (SAS institute 1990). GLM procedures also indicated sex or sex by strain interaction for most of the phenotypes (data not shown). As a consequence, we analyzed the diallel data for each sex separately throughout the study. We calculated the mean ± standard error of the phenotypes for each cross by sex. Results of selected phenotypes were summarized in Tables 2A to 2D. Marginal mean of female and male parental strains was calculated using the mean of all F1 hybrid who had that same parental strains. For example, aBMD of F1 hybrid produced from B6×129, B6×BALB, B6×C3H, B6×C58, B6×SJL, B6×NZB, and B6×PWK was pooled together to calculate the mean of aBMD. This mean value is the female parent marginal mean of B6. Scattor plot of parental marginal means versus inbred means in the 8 x 8 diallel cross was plotted in Figure 1 with results below. We conducted two-sample t test for overall comparison of the traits of inbred (8 groups pooled) and hybrids of the diallel cross (55 groups pooled). Results are presented in table 3 below.

We used the MIXED procedure with method=REML in SAS according to the model of Cockerham and Weir (Cockerham and Weir 1977) to estimate the source of genetic variation for the 8 x 8 diallel data without cross within lines (excluding diagonal). Based on the model of Cockerham and Weir (Cockerham and Weir 1977), the phenotype of *k*th offspring of the cross between parent i as sire and parent j as dam can be written as $Y_{ijk} = \mu + N_i + N_j + T_{ij} + P_i + M_j + K_{ij} + W_{k(ij)}$

N_i is the general combining abilities (GCA) of parent i; $T_{ij} = T_{ji}$ is the specific combining abilities (SCA) of $i \times j$ matings; ; P_i and M_j are the parental and maternal extranuclear contributions (reciprocal GCAs which include environmental and genetic effect specific to sperm and variations caused by nuclear genes that affect only the parental function, and maternal environmental effects, genetic and nongenetic cytoplasmic effects, and variations caused by nuclear genes that affect only the maternal

function), respectively, of sire i and dam j; K_{ij} is the specific interactions between the maternal and paternal genotypes (reciprocal SCAs); and $W_{k(ij)}$ is the effect individual k (within family effects). We assume that the effects are independent and normally distributed, with mean zero and respective variances σ_N^2, σ_T^2, σ_P^2, σ_M^2, σ_K^2, and σ_W^2.

We calculated the Pearson product-moment correlation coefficient of cross means between two phenotypes and used Ward's hierarchical agglomerative method (Ward 1963) to conduct cluster analysis of the phenotypes. We use one minus the absolute value of Pearson's correlation as a measure of 'distance' between strain mean phenotypes. Ward's method uses an analysis of variance approach to evaluate the distances between clusters. Ward's method initializes with each phenotype as a cluster by itself. At each step, the two closest clusters are merged to form a new cluster. This merging is repeated until only one cluster remains. The smaller the increase in the total within-group sum of squares as a result of joining two clusters, the closer they are. The within-group sum of squares of a cluster is defined as the sum of the squares of the distance between all phenotypes in the cluster and the centroid of the cluster. The resulting dendrogram was used to identify groups of correlated traits.

Partial correlation of lean mass and % fat with aBMD, vBMD and skullBMD after adjusting for Body Weight were calculated using cross mean values. We also calculated partial R-square of lean mass and %Fat in the regression model of BMD measurements where lean mass and %Fat were the only predictors. Same approach was used to calculate partial R-square of body weight and %Fat in the regression model of BMD measurements.

Results:

A full diallel consists of 64 genetically distinct types of mice, including the parental lines and crosses in both directions. We were able to generate 5 female and 5 male mice for 63 of these combinations (Table 1). We note the failure to produce live pups from the BALBxPWK cross is an interesting result that will be followed separately. The total number of mice surveyed is 625.

Part III: Table 1. 8x8 Diallel cross progeny (female + male)

Sire → Dam ↓	129	B6	BALB	C3H	C58	NZB	PWK	SJL
129	5 + 5	5 + 5	5 + 5	5 + 5	5 + 5	5 + 5	5 + 5	5 + 5
B6	5 + 5	5 + 5	5 + 5	5 + 5	5 + 4	5 + 5	5 + 5	5 + 5
BALB	5 + 5	5 + 5	5 + 5	5 + 5	5 + 5	5 + 5	0 + 0	5 + 5
C3H	5 + 5	5 + 5	5 + 5	5 + 5	4 + 5	5 + 5	5 + 5	5 + 5
C58	5 + 5	5 + 5	4 + 5	5 + 5	5 + 5	3 + 5	5 + 5	5 + 5
NZB	5 + 5	5 + 5	5 + 5	5 + 5	5 + 5	6 + 5	5 + 5	5 + 5
PWK	5 + 5	5 + 5	5 + 5	5 + 5	5 + 5	5 + 5	6 + 5	5 + 5
SJL	5 + 5	5 + 5	5 + 5	5 + 5	5 + 5	5 + 5	5 + 4	5 + 5

For each animal in the study population we obtained PIXImus data providing key information on body composition and bone mineral content. We also collected ear length and quad weight data as additional measures of body size and muscle mass. Formatted and error checked data (aBMD, body weight, fat mass, lean mass, %fat, vBMD, skullBMD, ear length and quad weight) will be submitted to the Mouse Phenome

Database (MPD). Summary data (mean and SE) for areal BMD by PIXImus (aBMD), volumetric BMD by pQCT for the femur (vBMD), lean mass and percent fat are provided in Tables 2A-D. In addition, we have collected and archived serum, femurs and skulls for later analyses of blood chemistries, mid-femoral bone structure, mineral, and strength assessments.

Part III: Table 2A. Mean (standard errors) of aBMD of eight parents (diagonal), their F1s (above diagonal) and reciprocals (below diagonal) in 8x8 diallel cross.

	129	B6	BALB	C3H	C58	NZB	PWK	SJL
Female								
129	0.0538 (0.00118)	0.0558 (0.00154)	0.0536 (0.0008)	0.0588 (0.00053)	0.0548 (0.00085)	0.0631 (0.00025)	0.0565 (0.00047)	0.0598 (0.00082)
B6	0.0535 (0.00066)	0.0465 (0.00075)	0.0518 (0.00065)	0.053 (0.00055)	0.0495 (0.00071)	0.054 (0.00075)	0.0486 (0.0008)	0.0517 (0.00063)
BALB	0.0552 (0.0016)	0.0514 (0.00072)	0.054 (0.00081)	0.055 (0.00046)	0.0525 (0.00155)	0.0559 (0.00037)	- -	0.0561 (0.00048)
C3H	0.062 (0.0013)	0.0563 (0.00048)	0.0566 (0.0003)	0.0556 (0.0004)	0.0557 (0.00072)	0.0586 (0.00039)	0.0526 (0.00087)	0.0611 (0.00084)
C58	0.0534 (0.00124)	0.0482 (0.00082)	0.053 (0.001)	0.0562 (0.00067)	0.0489 (0.00044)	0.0539 (0.00033)	0.0471 (0.00085)	0.0519 (0.00043)
NZB	0.0594 (0.00053)	0.0546 (0.00053)	0.0548 (0.00053)	0.0602 (0.00063)	0.0561 (0.00127)	0.0556 (0.00114)	0.0503 (0.0011)	0.0616 (0.0009)
PWK	0.0517 (0.00059)	0.0479 (0.00066)	0.0468 (0.00062)	0.0532 (0.00037)	0.0482 (0.00051)	0.0503 (0.00066)	0.0456 (0.00058)	0.0516 (0.00029)
SJL	0.0534 (0.00142)	0.0559 (0.00069)	0.0559 (0.00067)	0.0582 (0.00064)	0.0547 (0.00014)	0.0595 (0.00086)	0.0507 (0.00144)	0.0532 (0.00059)
Male								
129	0.0508 (0.00088)	0.0548 (0.00062)	0.0559 (0.00092)	0.0569 (0.00041)	0.0555 (0.00035)	0.0602 (0.00092)	0.0521 (0.00075)	0.0579 (0.00097)
B6	0.0564 (0.00132)	0.0491 (0.00117)	0.0521 (0.00074)	0.0547 (0.00014)	0.0496 (0.00067)	0.0544 (0.00103)	0.0508 (0.00064)	0.0577 (0.00088)
BALB	0.0525 (0.00064)	0.0537 (0.00107)	0.0519 (0.00039)	0.0563 (0.00051)	0.0515 (0.00043)	0.0548 (0.00077)	- -	0.0574 (0.00067)
C3H	0.0593 (0.00104)	0.0567 (0.00109)	0.0565 (0.0009)	0.0555 (0.00066)	0.0556 (0.00058)	0.0625 (0.00076)	0.0543 (0.00072)	0.0593 (0.00066)
C58	0.0557 (0.00122)	0.0508 (0.00078)	0.053 (0.00105)	0.0577 (0.00064)	0.0491 (0.00057)	0.054 (0.00055)	0.0496 (0.00095)	0.0544 (0.00059)
NZB	0.0594 (0.00101)	0.0569 (0.00053)	0.0559 (0.00099)	0.0607 (0.00042)	0.0547 (0.00072)	0.0539 (0.00151)	0.0524 (0.00045)	0.0609 (0.001)
PWK	0.0525 (0.00076)	0.0525 (0.00118)	0.0494 (0.00067)	0.0536 (0.00189)	0.0497 (0.00084)	0.0512 (0.00044)	0.0419 (0.0005)	0.0535 (0.00132)

Part III: Table 2B. Mean (standard errors) of vBMD of eight parents (diagonal), their F1s (above diagonal) and reciprocals (below diagonal) in 8x8 diallel cross.

	129	B6	BALB	C3H	C58	NZB	PWK	SJL
Female								
129	0.101 (0.0065)	0.095 (0.0038)	0.093 (0.0035)	0.111 (0.0048)	0.096 (0.0022)	0.115 (0.0029)	0.11 (0.0038)	0.113 (0.0059)
B6	0.101 (0.0058)	0.082 (0.0053)	0.092 (0.005)	0.09 (0.0034)	0.076 (0.0029)	0.091 (0.0029)	0.081 (0.0034)	0.083 (0.004)
BALB	0.116 (0.0086)	0.082 (0.0053)	0.091 (0.0044)	0.098 (0.004)	0.093 (0.0009)	0.107 (0.0025)	- -	0.102 (0.0041)
C3H	0.119 (0.0044)	0.095 (0.0039)	0.091 (0.0033)	0.096 (0.0048)	0.092 (0.0044)	0.1 (0.0066)	0.102 (0.0043)	0.106 (0.0037)
C58	0.104 (0.0048)	0.074 (0.0025)	0.097 (0.0026)	0.097 (0.0057)	0.072 (0.003)	0.091 (0.0032)	0.077 (0.0021)	0.088 (0.003)
NZB	0.116 (0.0027)	0.102 (0.0022)	0.109 (0.0026)	0.092 (0.0036)	0.097 (0.0042)	0.098 (0.0037)	0.095 (0.0059)	0.109 (0.0036)
PWK	0.092 (0.0051)	0.082 (0.0026)	0.073 (0.0017)	0.088 (0.0034)	0.077 (0.0015)	0.085 (0.0042)	0.075 (0.0021)	0.083 (0.0023)
SJL	0.09	0.098	0.103	0.106	0.099	0.122	0.083	0.081
Male								
129	0.084 (0.0054)	0.078 (0.0073)	0.096 (0.0058)	0.089 (0.003)	0.093 (0.0033)	0.085 (0.0043)	0.094 (0.0039)	0.094 (0.0038)
B6	0.096 (0.0049)	0.066 (0.0061)	0.067 (0.0033)	0.07 (0.0032)	0.072 (0.002)	0.075 (0.0076)	0.069 (0.0052)	0.084 (0.0065)
BALB	0.08 (0.0068)	0.08 (0.006)	0.087 (0.0029)	0.079 (0.0028)	0.074 (0.0061)	0.079 (0.0033)	- -	0.08 (0.0023)
C3H	0.088 (0.0074)	0.082 (0.0087)	0.081 (0.0049)	0.082 (0.0038)	0.072 (0.0046)	0.094 (0.0053)	0.07 (0.0055)	0.091 (0.003)
C58	0.085 (0.0044)	0.074 (0.0071)	0.079 (0.0052)	0.081 (0.0046)	0.067 (0.0032)	0.069 (0.0046)	0.078 (0.0024)	0.089 (0.0042)
NZB	0.098 (0.004)	0.08 (0.0048)	0.082 (0.0048)	0.079 (0.0047)	0.076 (0.0048)	0.079 (0.0078)	0.075 (0.0056)	0.104 (0.0083)
PWK	0.079 (0.0016)	0.073 (0.0049)	0.055 (0.004)	0.083 (0.0026)	0.08 (0.003)	0.064 (0.0048)	0.059 (0.0025)	0.076 (0.0028)
SJL	0.096	0.092	0.094	0.096	0.076	0.105	0.087	0.082

Part III: Table 2C. Mean (standard errors) of lean mass of eight parents (diagonal), their F1s (above diagonal) and reciprocals (below diagonal) in 8x8 diallel cross.

	129	B6	BALB	C3H	C58	NZB	PWK	SJL
Female								
129	15.13 (1.025)	19.28 (1.041)	14.78 (1.026)	16.26 (1.007)	18.41 (1.043)	21.77 (1.033)	14.43 (1.035)	15.6 (1.032)
B6	16.84 (1.016)	16.12 (1.018)	17.76 (1.018)	17.48 (1.023)	16.25 (1.026)	20.15 (1.019)	14.05 (1.046)	16.49 (1.043)
BALB	15.04 (1.03)	17.92 (1.009)	18.14 (1.03)	16.67 (1.028)	18.76 (1.059)	19.85 (1.026)	- -	17.4 (1.022)
C3H	17.67 (1.055)	18.21 (1.026)	19.08 (1.029)	16.26 (1.035)	17.93 (1.02)	21.16 (1.018)	14.59 (1.012)	16.93 (1.012)
C58	16.92 (1.019)	16.31 (1.028)	18.28 (1.03)	18.34 (1.04)	17.28 (1.03)	19.3 (1.025)	12.63 (1.043)	14.66 (1.029)
NZB	18.93 (1.019)	21.78 (1.023)	18.72 (1.016)	21.8 (1.025)	20.73 (1.009)	19.82 (1.042)	16.09 (1.03)	19.41 (1.03)
PWK	13.82 (1.013)	14.4 (1.039)	13.53 (1.021)	15.76 (1.046)	13.35 (1.052)	15.53 (1.012)	11.66 (1.037)	13.13 (1.018)
SJL	14.66 (1.025)	17.97 (1.021)	16.44 (1.024)	16.31 (1.006)	16.05 (1.007)	17.67 (1.019)	12.54 (1.054)	15.02 (1.019)
Male								
129	18.12 (1.025)	23.37 (1.027)	24.31 (1.04)	21.93 (1.022)	23.68 (1.015)	27.71 (1.033)	18.59 (1.01)	21.7 (1.028)
B6	24.05 (1.042)	23.23 (1.034)	23.07 (1.014)	24.71 (1.007)	23.64 (1.023)	27.78 (1.022)	22.2 (1.057)	23.87 (1.016)
BALB	20.21 (1.035)	25.4 (1.038)	24.01 (1.015)	24.44 (1.007)	25.52 (1.032)	27.01 (1.035)	- -	24.99 (1.011)
C3H	23.07 (1.028)	26.14 (1.035)	26.84 (1.013)	20.29 (1.02)	25.15 (1.02)	31.11 (1.013)	21.53 (1.025)	24.15 (1.012)
C58	24.55 (1.038)	23.34 (1.014)	23.77 (1.061)	25.15 (1.031)	22.47 (1.019)	27.3 (1.027)	18.19 (1.032)	20.41 (1.016)
NZB	25.62 (1.028)	28.12 (1.027)	27.47 (1.023)	29.9 (1.029)	27.41 (1.016)	22.98 (1.069)	23.36 (1.023)	26.08 (1.027)
PWK	17.71 (1.028)	19.79 (1.043)	21.71 (1.031)	21.01 (1.051)	18.58 (1.032)	23.29 (1.017)	14.09 (1.031)	16.6 (1.027)

Part III: Table 2D. Means and standard errors for the 63 groups of the diallel on the %Fat

	129	B6	BALB	C3H	C58	NZB	PWK	SJL
Female								
129	20.52 (1.078)	22.31 (1.043)	20.05 (1.043)	20.94 (1.037)	17.58 (1.068)	22.77 (1.092)	14.78 (1.019)	25.34 (1.176)
B6	15.87 (1.057)	15.89 (1.058)	16.43 (1.012)	22.41 (1.054)	14.47 (1.053)	27.3 (1.074)	14.53 (1.048)	18.27 (1.088)
BALB	17.25 (1.074)	21.15 (1.088)	23.35 (1.062)	21.16 (1.035)	14.83 (1.144)	19.42 (1.026)	- -	21.1 (1.073)
C3H	18.8 (1.079)	21.13 (1.066)	27.76 (1.07)	25.15 (1.088)	19.58 (1.091)	28.58 (1.112)	14.62 (1.042)	22.88 (1.104)
C58	14 (1.048)	13.84 (1.059)	15.57 (1.045)	19.05 (1.151)	19.42 (1.156)	17.82 (1.108)	14.64 (1.031)	18.02 (1.058)
NZB	23.54 (1.094)	27.1 (1.089)	22.47 (1.067)	33.18 (1.043)	21.95 (1.092)	26.01 (1.149)	13.52 (1.015)	30.78 (1.074)
PWK	15.72 (1.039)	15.77 (1.052)	17.66 (1.029)	17.16 (1.07)	13.23 (1.042)	12.8 (1.065)	19.77 (1.042)	18.36 (1.058)
SJL	26.49 (1.141)	23.97 (1.089)	18.04 (1.068)	18.48 (1.102)	17.32 (1.042)	17.68 (1.074)	18.21 (1.107)	17.49 (1.063)
Male								
129	24.05 (1.094)	28.38 (1.088)	16.8 (1.166)	31.45 (1.063)	25.33 (1.034)	34.87 (1.013)	17.89 (1.063)	18.96 (1.223)
B6	15.02 (1.118)	17.13 (1.091)	26.04 (1.04)	31.72 (1.027)	23.03 (1.13)	20.35 (1.293)	23.46 (1.189)	22.23 (1.054)
BALB	20.89 (1.117)	22.71 (1.175)	15.55 (1.126)	25.93 (1.035)	25.68 (1.06)	27.54 (1.059)	- -	17.21 (1.092)
C3H	27.93 (1.099)	22.2 (1.093)	26.79 (1.041)	21.41 (1.07)	29.74 (1.04)	26.15 (1.044)	25.77 (1.07)	16.57 (1.091)
C58	27.55 (1.047)	19.68 (1.093)	19.7 (1.136)	25.66 (1.088)	30.85 (1.098)	35.39 (1.031)	15.5 (1.129)	20.64 (1.048)
NZB	27.98 (1.084)	19.85 (1.077)	19.49 (1.167)	28.03 (1.015)	25.3 (1.042)	21 (1.16)	23.25 (1.061)	16.78 (1.163)
PWK	22.19 (1.098)	20.8 (1.133)	25.79 (1.086)	26.77 (1.058)	19.82 (1.101)	34.1 (1.061)	21.83 (1.085)	19.78 (1.073)
SJL	15.95 (1.178)	15.28 (1.054)	16.37 (1.073)	16.5 (1.182)	26.09 (1.071)	20.8 (1.083)	15.91 (1.05)	17.45 (1.053)

F1 hybrid animals provide an alternative to fully inbred animal models for human bone characteristics. They are qualitatively different from inbreds, being generally healthier and more vigorous. Our results show that hybrid animals differ substantially from their parents in several keys traits (Table 3).

Part III: Table 3. Overall Inbred vs. Hybrid comparison

	aBMD	Body Weight[†] (g)	Fat mass[†] (g)	Lean mass[†] (g)	%Fat[†]	vBMD	skullBMD[†]	Ear length (mm)	Quad Weight[†] (gm)
Male									
Inbred	0.051**	25.99**	5.38**	20.32**	20.71	0.076*	0.12	13.61**	0.21**
Hybrid	0.055	31.01	6.99	23.62	22.55	0.082	0.12	14.50	0.25
Female									
Inbred	0.052**	20.39	4.23	15.97	20.77	0.087**	0.12	13.42**	0.17**
Hybrid	0.054	21.03	4.01	16.81	19.08	0.096	0.13	14.23	0.18

[†] Geometric mean was presented
Note. * and ** indicate the difference between inbred and hybrid is significant at 0.01 and 0.0025 level based on two-tailed t test

Male hybrid mice are generally larger with greater lean mass and higher fat percentage. Although female hybrid did not show significant increases in body size, both male and female mice have significantly higher bone density as assessed in the whole skeleton (aBMD) and the vertebral component (vBMD). We examined the effects of hybrid vigor on a strain by strain basis by plotting the mean values of all hybrids that shared a common parent against the parental values for aBMD, vBMD, lean mass and percent fat (Figure 1).

Part III: Figure 1: Scatterplot of mean trait values for hybrid mice versus the parental trait values. Red points indicate mean values of hybrids that share a common mother and blue points indicate mean values across hybrids that share a common father. Data are shown for aBMD, vBMD, lean mass and percent fat. Panels on the left are female mice and panels on the right are male values. A reference line indicates the expected locations of point in the absence of hybrid vigor.

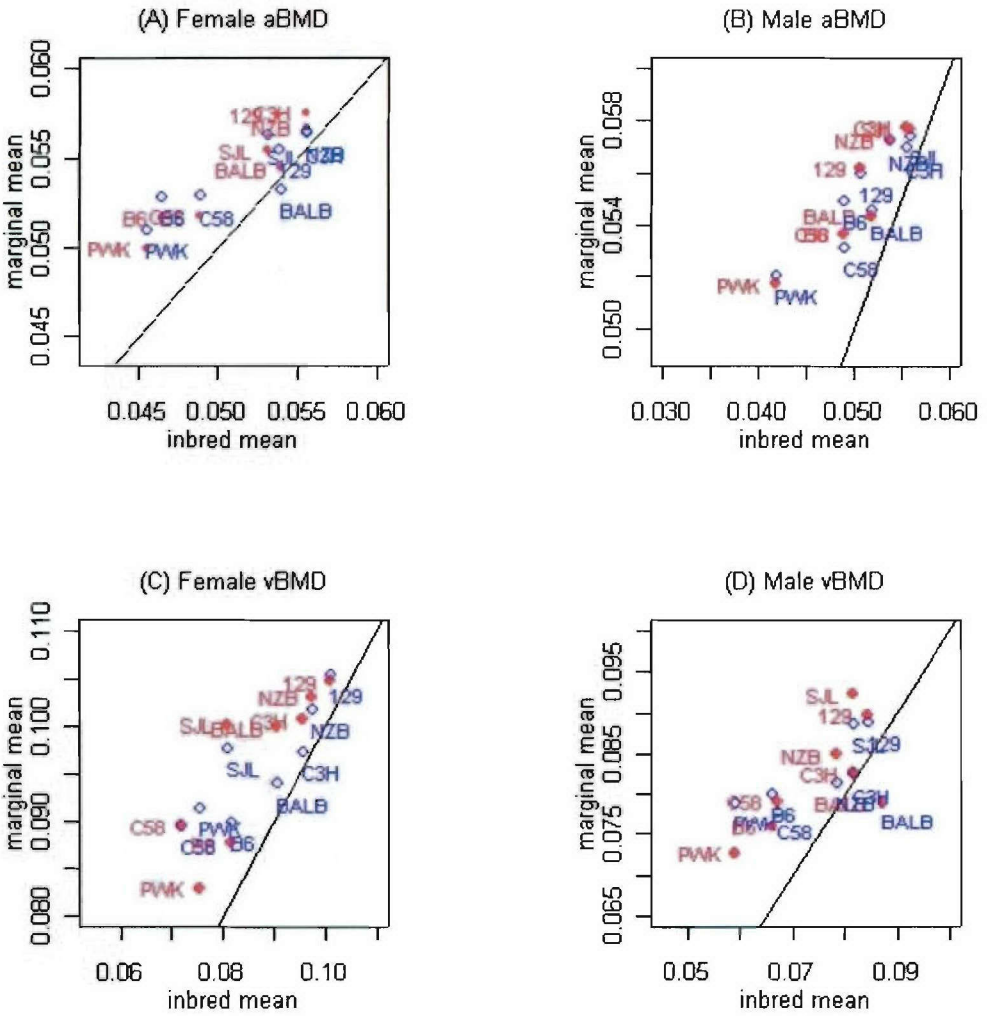

Figure 1A. – Parental marginal means versus inbred means in the 8 x 8 diallel cross. Marginal mean of female and male parental strains was calculated using the mean of all F1 hybrid who had that same parental strains. Red and blue open circles correspond to female and male parent marginal means. (A) Female aBMD. (B) Male aBMD. (C) Female vBMD. (D) Male vBMD.

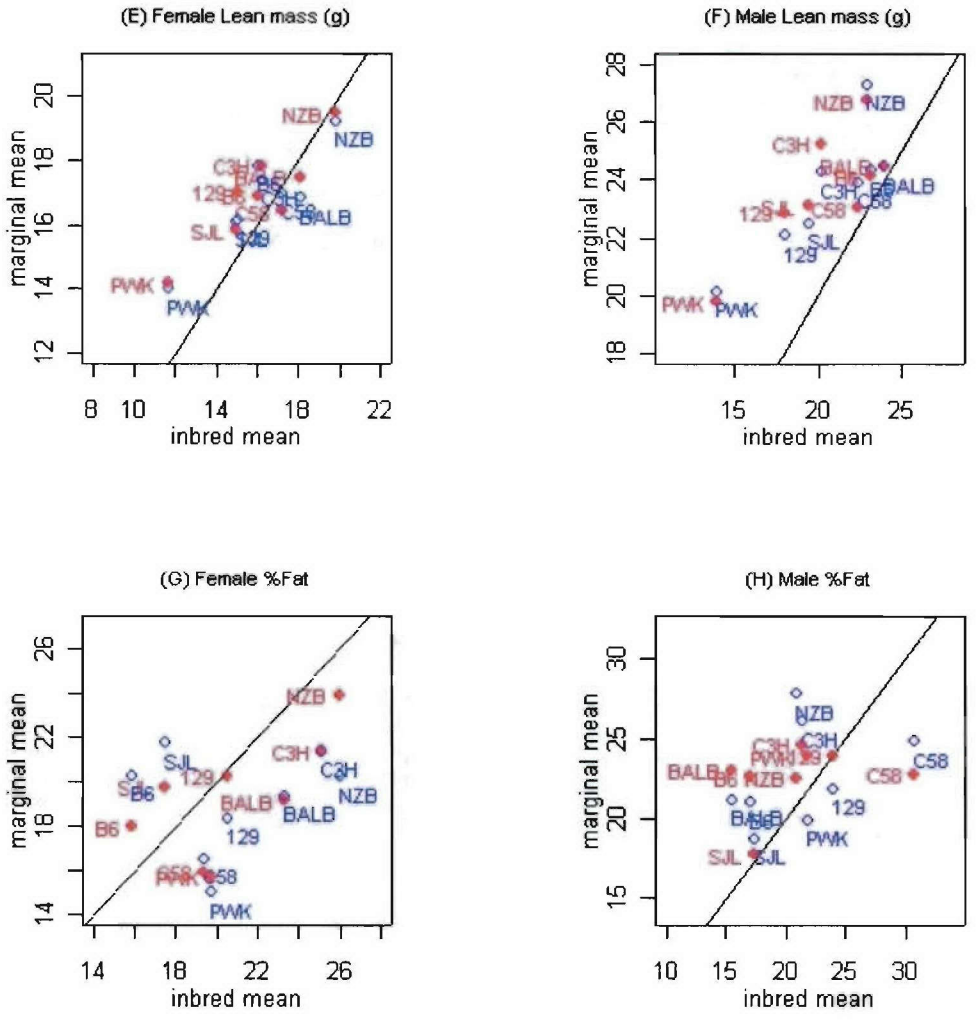

Figure 1B. – Parental marginal means versus inbred means in the 8 x 8 diallel cross. Marginal mean of female and male parental strains was calculated using the mean of all F1 hybrid who had that same parental strains. Red and blue open circles correspond to female and male parent marginal means. (E) Female lean mass (g). (F) Male lean mass (g) (G) Female %Fat. (H) Male %Fat.

Hybrid mice show uniform increases in both areal and vertebral bone density in both sexes, however the increase is most dramatic for offspring of low bone density strains PWK, C57BL/6J and C58. Increased lean mass is apparent only in male hybrid mice and absent for females. There are no trends apparent in the percentage of fat in hybrid mice.

The diallele cross was used to estimate heritability of a trait, as well as to decompose the observed variation into genetic and environmental components. The genetic component can be further general (GCA) and specific combining (SCA) abilities (Table 4).

Part III: Table 4. Source of genetic variation[1]

Source	aBMD	Body Weight[2]	Fat Mass[2]	Lean Mass[2]	%Fat[2]	vBMD	skullBMD[2]	Ear Length	Quad Weight[2]
GCA	1.55**	0.31**	0.13**	1.26**	1.19**	0.54**	0.38**	1.87**	1.07**
SCA	0.17	0.02	0.05	0.10	0.10	0.07	0.06	0.20*	0.33**
RSCA	0.22**	0.16**	0.04	0.13**	0.29**	0.50**	0.06	0.15	0.09*
RGCA	0.048	0.037	0.022	0.044	0.030	0.13	0.03	0.05	0.01

Note: GCA: General combining Abilities. SCA: Specific Combining Abilities. RGCA: Reciprocal GCA. RSCA: Reciprocal SCA

[1]The causal components of genetic variance associated with the Cockerham-Weir model (1977) were analyzed using PROC MIXED procedure with REML method in SAS. All values were standardized within-family variance parameter estimates. Footnote symbols for rows 1 to 5 (Standardized to within-family variation). * P<0.05, ** P<0.01

[2] Trait data was log-transformed

Across the board significance of GCA indicates heritability of all traits under investigation here, offspring tend to be like their parents. The SCA provides an alternative assessment of hybrid vigor. Several traits, including BMDs and lean mass, show differences between reciprocal crosses (AxB vs BxA) indicating that maternal effects can influence these parameters.

Trait correlations are summarized separately for female and male mice in Table 5.

Part III: Table 5. Unadjusted correlation of traits

		aBMD	Body Weight	Fat Mass	Lean Mass	%Fat	vBMD	skullBMD	Ear Length
Female									
	aBMD								
	Body Weight	0.671							
	Fat Mass	0.673	0.923						
	Lean Mass	0.613	0.961	0.783					
	%Fat	0.598	0.753	0.948	0.547				
	vBMD	0.838	0.424	0.381	0.426	0.302			
	skullBMD	0.859	0.731	0.725	0.663	0.637	0.637		
	Ear Length	0.484	0.399	0.296	0.431	0.178	0.553	0.351	
	Quad Weight	0.554	0.881	0.674	0.948	0.427	0.377	0.556	0.482
Male									
	aBMD								
	Body Weight	0.519							
	Fat Mass	0.255	0.866						
	Lean Mass	0.627	0.935	0.635					
	%Fat	-0.004	0.593	0.917	0.275				
	vBMD	0.711	0.007	-0.261	0.192	-0.424			
	skullBMD	0.667	0.417	0.445	0.336	0.382	0.467		
	Ear Length	0.478	0.535	0.311	0.6	0.073	0.43	0.27	
	Quad Weight	0.582	0.751	0.371	0.905	-0.003	0.203	0.076	0.547

Body Weight, Fat Mass, Lean Mass, %Fat, skullBMD and Quad Weight are log-transformed.

These tables indicate the most important result to come out of this experiment. We find that the relationship of body composition and bone density is strikingly different between the sexes. In female mice, both lean mass and percent fat show very strong, positive correlations with bone density. In contrast, male mice, show strong correlation of lean mass with aBMD but only weak (non-significant) positive correlation between lean mass and vBMD.

The percentage of fat in male mice shows no correlation with aBMD and a significant negative correlation with vBMD. These relationships are corroborated by multiple regression analyses summarized in Tables 6 and 7. Lastly the correlative relationships among traits studied here are summarized graphically in Figure 2.

Part III: Figure 2. Correlative relationships among traits.

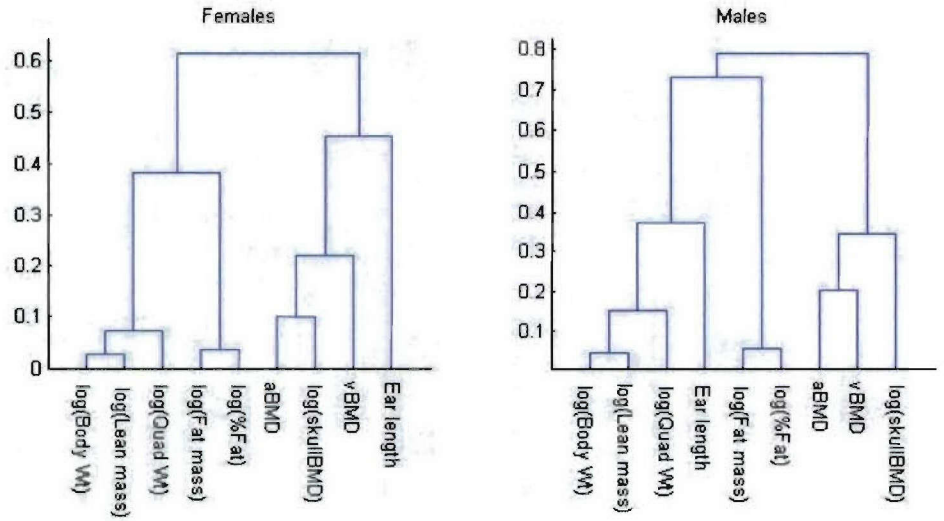

In summary, phenotypic characterization of F1 animals has lead to new insights into the mode and mechanisms of inheritance that determine the heritability of bone parameters. Although inheritance of these is largely additive (offspring are similar to parents), there is a hybrid vigor that affects bone density and (in males) lean body mass. Significant maternal affects are observed for lean body mass and bone density. Most importantly, we have observed striking differences in the relation of body composition to both whole body and verterbral bone density between male and female mice suggesting that prognostic variables for fracture in military recruits should use different criteria for the two sexes.

KEY RESEARCH ACCOMPLISHMENTS:

Part I: Mouse Phenome Database:

• This comprehensive survey across inbred strains enables us and other investigators worldwide to explore the relationships of bone strength to size, shape, and material content, to body composition, and to other phenotypes cataloged in the MPD.

• These studies have produced valuable data (to be freely accessed) and new analysis tools that will benefit the research community by providing an opportunity to assess strain background (genotype) effects and gender specificity for many bone and body composition phenotypes.

• MPD tools will help identify critical mouse models for studying genetic influences on bone strength and geometry using the comprehensive strain characteristics data from Parts II and III.

Part II: Decomposition of Skeletal Mineral and Lean Body Mass for Mouse Genetic Models:

• Data included in this report show that inbred strains of mice have a wide range of values for measures of muscle mass, femur geometry, BMD, and biomechanical properties that can be utilized as tools to understand the genetic, morphologic, and physiological relationships among these phenotypes.

• Gender differences were identified for nearly every phenotype measured; this consideration needs to be incorporated into every recommendation of suitable training regimens for new recruits.

• Mouse models for genetic analyses of bone strength phenotypes and associated femur geometry have been developed and are recommended in this report.

Part III: Diallele Cross for Skeletal/Body Composition:

• We have developed and tested new analytic methods for the analysis and interpretation of diallele cross data. These results have been published and further details may be found in Tsaih et al. (2005; Appendix Part III).

REPORTABLE OUTCOMES:

Part I: Mouse Phenome Database:

The data generated from this study will be accessible to investigators worldwide. Three new MPD Projects have been created and accessioned and will be made public pending final review and publication of significant findings in appropriate journals. Data from Part II is housed in the Donahue projects, and the diallele data from Part III is in the Churchill project.

• Donahue L Bone mineral density, body composition, and craniofacial characterization. *Accession MPD:115.*
30 Strains, 22 Measurements

• Donahue L, Beamer WG, Bogue M, Churchill GA Models of skeletal geometry and bone strength. *Accession MPD:172.*

10 Strains, 26 Measurements

• Churchill GA Bone characteristics and body composition of an 8-way diallele cross. *Accession MPD:171.*
8 Inbred strains and 55 F1 Hybrids, 9 Measurements

Part II: Decomposition of Skeletal Mineral and Lean Body Mass for Mouse Genetic Models:

• An abstract entitled, "Using Inbred Mouse Strains to Identify Models for Determining Genetic Regulation of Bone Strength," L.R. Donahue, C.J. Rosen, G.A. Churchill, S-W Tsaih, M.L. Bouxsein, L. Horton, A.R. Sears & W.G. Beamer, The Jackson Laboratory, Bar Harbor, ME, has been submitted to a meeting in Bethesda, MD, May 2-3, 2005, entitled, "Bone Quality: What Is It and How Can We Measure It?"

• A Presentation was made to the Scientific Staff at The Jackson Laboratory by Dr. Donahue, March 17, 2004, entitled, "Skeletal Plasticity." Data from this project was used for this presentation focused on bone strength.

• Drs. Leah Rae Donahue and Wesley Beamer have trained a new research assistant with support from this grant. Amy Sears has continued to be employed by our Bone Biology Research Program beyond the termination of this funding.

• The Bone Biology Research Program at The Jackson Laboratory has acquired three new instruments with support from this award. Purchase would not have been possible without these funds. The first is the SA Plus pQCT bone densitometer that provides volumetric bone data from isolated specimens. Our laboratory previously had an older XCT 960M unit with nearly 11 years of steady usage. The SA Plus has provided us with more accurate data at a faster rate than the 960M unit and has greatly enhanced the studies described here. The second is a Faxitron Cabinet X-ray that provides 2-D film data for morphology and is also equipped with a digital camera for immediate computerized access to images. This instrument provides high resolution films of whole body and selected extremities and permits acquisition of additional measures of limbs and muscle mass about the femur, as well as provides a permanent record of the skeleton. The third is a Materials Testing System that provides measures of biomechanical strength. This instrument was used to obtain all of the strength measures presented in this report.

Part III: Diallele Cross for Skeletal/Body Composition:

• A paper has been submitted to *Mammalian Genome* entitled, "Quantitative Trait Mapping in a Diallel Cross of Recombinant Inbred Lines." Shirng-Wern Tsaih, Lu Lu, David C. Airey, Robert W. Williams, Gary A. Churchill.

CONCLUSIONS:

Part I: Mouse Phenome Database:

These DAMD-supported projects contain a wealth of bone phenotype data and information, enabling investigators to access this data from their own desktop computers for analysis and comparison to their own data, with the goal of accelerating the research pace and maximizing community resources. The value of these data sets will increase over time as the MPD is more densely populated with phenotypic data and SNPs.

Part II: Decomposition of Skeletal Mineral and Lean Body Mass for Mouse Genetic Models:

1. Our original hypothesis that total lean body mass by DEXA would predict muscle mass at a specific skeletal site has proven to be incorrect. That is, when we compared the lean body mass of 29 inbred strains to the femur muscle area or quadriceps weight of the selected subset of 10 strains, we did not find a similar rank ordering of strains. Consequently, body composition data by DEXA is not useful for understanding the relationship between lean mass and bone phenotypes in mice.

2. We found strain variability for nearly all traits, offering opportunities for genetic analyses of many phenotypes related to bone geometry, density, and strength. This variation represents strain specific allelic differences that regulate bone traits leading to a wide range of normal values.

3. In addition to strain differences, we found gender effects for nearly all phenotypes considered. It is critically important to recognize these gender differences when selecting models for genetic analyses, and particularly important when translating results from animal models to human populations.

4. Bone strength is a complex phenotype with sex specificity for most contributing traits. Each biomechanical property assesses a different aspect of femur strength and many are predicted by different sets of femur characteristics. Consequently, genetic analyses of these individual properties, capitalizing on differences among inbred strains, would be expected to reveal different regulatory genes. A high priority phenotype for genetic analysis of bone strength would be muscle area, since it strongly predicted peak load, stiffness, and work to failure. Our original concept was that lean body mass would be related to site specific muscle mass and would predict bone strength. Even though the first relationship between lean body mass and site specific muscle mass was not well correlated, it is clear that muscle mass and biomechanical measures of bone strength are related.

We propose that the muscle area/femoral bone strength relationships described above would hold for the tibia, a frequent site for stress fractures. Thus, we would suggest that to predict which recruits would be better suited for rigorous training, it would be informative to measure the cross sectional area of the proximal tibia and associated muscle with QCT to assess fracture risk.

5. Genetic models: After careful consideration of all the data reported herein, we would recommend genetic analyses for biomechanical properties utilizing the following inbred strain combinations:
Peak load & stiffness: Female SWR/J (low strain) x Male BALB/cJ (high strain)
Work to failure: Female 129S1/SvIm (low strain) x Male NZB/BINJ (high strain)
If analyses for potential genes on the X Chromosome are to be considered, then reciprocal crosses would be required. Once these regulatory genes are identified in mouse, it is possible to predict the chromosomal location of their human homologues. Potential clinical application would follow.

6. It is clear that, at least in mice, serum markers cannot be used to predict aBMD, either whole body or at the lumbar spine, or body composition compartments.

7. A survey of the relationship between bone strength and femur geometric and densitometric phenotypes on ten week old females from 29 inbred strains has recently been published in Bone (Wergedal, et. al, 2005:36, 111-122). The mice for these studies and densitometry data were collected at The Jackson Laboratory in collaboration with Dr. Wesley Beamer who is a Co-PI on this award. These studies were completed approximately 5 years ago and supported an NIH application for bone size awarded to Dr. Wergedal (AR46204). Subsequently, bone strength measures were performed in Dr. Wergedal's lab and combined with the size data to form the basis of the publication in Bone cited above.

Comparison of result from Dr. Wergedal's paper with data collected for this report are limited due to the difference in strains and gender selected, to phenotypes measured, and to the difference in age between females in the two data sets. Seven of ten strains are included in both data sets; the Wergedal females are 10 weeks of age (no males are included); females in our study are 16 week old adults. Even though statistical comparisons are affected by developmental age and by the number of strains compared, we examined the two data sets for trends. We compared the two data sets for correlations between body weight, femur length, and periosteal circumference with each of 3 measures of bone strength: peak load, stiffness, and work to failure. Overall, trends in these correlations were similar for the two data sets, but the absolute r values were lower in the Wergedal paper than in this report. When we compared numbers for peak load in the 7 common strains, we found large differences (50-100%) in absolute values. Variation could be attributed to age differences, sample handling and storage, or mechanical testing equipment and methodology. Together these studies demonstrate the differences among inbred strains that can be manipulated for genetic analyses. However, they also illustrate the need for attention to important issues of age, gender, methodology, and a common vocabulary prior to meta analyses of such data sets.

Part III: Diallele Cross for Skeletal/Body Composition

1. Phenotypic characterization of F1 animals has lead to new insights into the mode and mechanisms of inheritance that determine the heritability of bone parameters. Although inheritance of these is largely additive (offspring are similar to parents), there is a hybrid vigor that affects bone density and (in males) lean body mass.

2. Significant maternal affects are observed for lean body mass and bone density. Most importantly, we have observed striking differences in the relation of body composition to both whole body and verterbral bone density between male and female mice suggesting that prognostic variables for fracture in military recruits should use different criteria for the two sexes.

REFERENCES:

Cockerham, C. C. and B. S. Weir (1977). "Quadratic analyses of reciprocal crosses." Biometrics **33**: 187-203.

Nagy, T. R. and A. L. Clair (2000). "Precision and accuracy of dual-energy x-ray absorptiometry for determining in vivo body composition of mice." Obesity Research **8**(5): 397.

Nagy, T. R., C. W. Prince, et al. (2001). "Validation of peripheral dual-energy x-ray absorptiometry for the measurement of bone mineral in intact and excised long bones of rats." J Bone Miner Res **16**(9): 1682-1687.

Ward, J. (1963). "Hierarchical grouping to optimize an objective function." JI Amer Stat Assoc **58**: 236-244.

BIBLIOGRAPHY

Manuscript:
Submitted to *Mammalian Genome*, "Quantitative Trait Mapping in a Diallel Cross of Recombinant Inbred Lines." Shirng-Wern Tsaih, Lu Lu, David C. Airey, Robert W. Williams, Gary A. Churchill.

Abstract:
"Using Inbred Mouse Strains to Identify Models for Determining Genetic Regulation of Bone Strength," L.R. Donahue, C.J. Rosen, G.A. Churchill, S-W Tsaih, M.L. Bouxsein, L. Horton, A.R. Sears & W.G. Beamer, The Jackson Laboratory, Bar Harbor, ME, Plenary Poster to be presented at a meeting in Bethesda, MD, May 2-3, 2005, entitled, "Bone Quality:What Is It and How Can We Measure It?"

Database Contributions:
The data generated from this study will be accessible to investigators worldwide. Three new MPD Projects have been created and accessioned and will be made public pending final review and publication of significant findings in appropriate journals. Data from Part II is housed in the Donahue projects, and the diallele data from Part III is in the Churchill project.

- Donahue L Bone mineral density, body composition, and craniofacial characterization. *Accession MPD:115.*
30 Strains, 22 Measurements
- Donahue L, Beamer WG, Bogue M, Churchill GA Models of skeletal geometry and bone strength. *Accession MPD:172.*
10 Strains, 26 Measurements
- Churchill GA Bone characteristics and body composition of an 8-way diallele cross. *Accession MPD:171.*
8 Inbred strains and 55 F1 Hybrids, 9 Measurements

PERSONNEL

Wesley G. Beamer, Senior Staff Scientist, Co-PI
Molly A. Bogue, Associate Research Scientist, Co-PI
Mary Bouxsein, Assistant Professor, Harvard Medical School, Boston, Co-PI
Gary A. Churchill, Senior Staff Scientist, Co-PI
Harold F. Coombs, III, Research Assistant I
Leah Rae Donahue, Senior Research Scientist, PI
Lindsay G. Horton, Research Assistant I
Julie M. Hurd, Laboratory Technician IV
Renhua Li, Associate Research Scientist, Data Analyst
Greg W. MacKenzie, Research Assistant I
Clifford J. Rosen, Adjunct Staff Scientist, Co-PI
Amy R. Sears, Research Assistant I

APPENDICES:

Part I: Mouse Phenome Database:

Donahue & Beamer Project (Part II) Examples

- pp. 1A-2 thru 1A-17
- Previews, data not public
- Illustrates MPD organization, data formats, selected analysis tools, and viewing/downloading options.
- Important Note: All analysis tools shown in this example can be used in the Churchill Project as well as across multiple MPD projects. See p. 1A-17 for details.

Data Validation Example

pp. 1A-18

- BMD measurements from four different projects

Churchill Project (Part III) Examples

- pp. 1A-19 thru 1A-22
- Previews, data not public
- Shows the new MPD Diallele Cross Analysis tools.

Find Mouse Models – Criteria Fit Tool

- pp. 1A-23
- Tool is publicly available
- Donahue and Beamer data used for this example is not yet publicly available
- Example demonstrates power of this query tool

Part II: Decomposition of Skeletal Mineral and Lean Body Mass for Mouse Genetic Models:

Appendix Part II:

Table 1: Strain means for 10 selected strains
Table 2: Sex effect within strains for 10 selected strains
Table 3: Correlation of traits for 9 strains (without C3H/HeJ)
Table 4: Regression of predictors for 9 strains (without C3H/HeJ)
Table 5: Correlation of predictors for 9 strains (without C3H/HeJ)
Scatter Plots 1: Examples of comparisons with C3H/HeJ
Scatter Plots 2: Examples of comparisons without C3H/HeJ
Table 6: Strain means for 28 strains
Table 7: Sex effect within strains, 28 strains
Table 8: Correlation of traits, 28 strains
Abstract 1: Entitled, "Using Inbred Mouse Strains to Identify Models for Determining Genetic Regulation of Bone Strength," Plenary Poster for "Bone Quality: What Is It and How Can We Measure It?" meeting in Bethesda, MD, May 2-3, 2005.
Presentation 1: "Skeletal Plasticity," presented to the Scientific Staff at The Jackson Laboratory by Dr. Donahue, March 17, 2004.

Part III: Diallele Cross for Skeletal/Body Composition

Appendix Part III:

Paper submitted to *Mammalian Genome* entitled, "Quantitative Trait Mapping in a Diallel Cross of Recombinant Inbred Lines." Shirng-Wern Tsaih, Lu Lu, David C. Airey, Robert W. Williams, Gary A. Churchill.

APPENDICES

Part I: Mouse Phenome Database: **1A-1**

Donahue & Beamer Project (Part II) Examples
- pp. 1A-2 thru 1A-17
- Previews, data not public
- Illustrates MPD organization, data formats, selected analysis tools, and viewing/downloading options.
- Important Note: All analysis tools shown in this example can be used in the Churchill Project as well as across multiple MPD projects. See p. 1A-17 for details.

Data Validation Example
- pp. 1A-18
- BMD measurements from four different projects

Churchill Project (Part III) Examples
- pp. 1A-19 thru 1A-22
- Previews, data not public
- Shows the new MPD Diallele Cross Analysis tools.

Find Mouse Models – Criteria Fit Tool
- pp. 1A-23
- Tool is publicly available
- Donahue and Beamer data used for this example is not yet publicly available
- Example demonstrates power of this query tool

Measurement names and descriptions are carefully annotated to provide consistency with other MPD data. Units are standardized (NIST).

Project: Donahue L - Models of skeletal geometry and bone strength

Preview - the following is not visible to the public...

MPD:172 **Donahue2** (2004)

- Participants, publications, funding
- Protocols and animal documentation
- Strains, sexes, ages, animal notes
- Tools for displaying and analyzing data
- View or download the submitted data set
- Notes pertaining to the data set

Get more info about specific measurements and view summary data-- graphic or tabular . . .

Measurements Units & abbreviations Click on a measurement description for summary, and to compare strains	Short name	Flag	Click for correlations
body weight			
whole body weight (with head) [g]	bw		
bone mineral density and content			
femur			
ensity of whole left femur [mg/mm³]	femur_BMD		
ensity of cortical shell of whole left femur [mg/mm³]	femur_cortical_BMD		
neral density of right femur (1-mm thick cross section at mid-ysis) [mg/mm³]	femur_shaft_BMD		
bone mineral content of right femur (cross section at mid-diaphysis) [mg]	femur_shaft_BMC		
bone strength			
femur			
maximum load on load-displacement curve [n]	femur_peak_load		
displacement at peak load [mm]	femur_peak_extension		
load at specimen failure (break point) [n]	femur_break_load		
load at 95% break load [n]	femur_yield_load		
area under load-displacement curve to break point [n mm]	femur_break_energy		
area under load-displacement curve to peak load [n mm]	femur_peak_energy		
slope of force-displacement curve in linear region [n/mm]	femur_stiffness		
estimated elastic modulus [Mpa]	elastic_modulus		
estimated ultimate strength [Gpa]	ultimate_strength		
body measurements (miscellaneous)			
leg			
length of right femur (condyles to rostral tip of greater trochanter) [mm]	femur_length		
anterior to posterior width of right femur (mid-diaphysis) [mm]	femur_width_AP		
medial to lateral width of right femur (mid-diaphysis) [mm]	femur_width_ML		
area of right femur (cross section at mid-diaphysis) [mm²]	femur_area		

cortical thickness of right femur pQCT (periosteal to endosteal surface at mid-diaphysis) [mm]	femur_thickness_R1	
cortical thickness of right femur uCT (periosteal to endosteal surface at mid-diaphysis) [mm]	femur_thickness_R2	
cortical thickness of left femur pQCT (periosteal to endosteal surface at mid-diaphysis) [mm]	femur_thickness_L	
periosteal (outer) circumference of left femur (mid-diaphysis) [mm]	femur_out	
endosteal (inner) circumference of left femur (mid-diaphysis) [mm]	femur_in	
area of muscle and bone of right femur (cross section at mid-diaphysis) [mm^2]	thigh_area	
thigh area minus femur area (cross section at mid-diaphysis) [mm^2]	thigh_muscle_area	
weight of isolated right quadriceps muscle [g]	quadricep_wt	

Flag selected entries now
Flag all measurements in project Help

Strains, sexes, ages

Mouse strains N = 10	MPD priority strains: 129S1/SvImJ BALB/cJ C3H/HeJ C57BL/6J C58/J FVB/NJ NZB/BINJ PWK/PhJ SJL/J SWR/J Other strains: Strain details Number of animals tested, by strain and sex
Sex	both

Project protocols: not available

Animal documentation: not available

Displaying & analyzing the data:

View / download data set

- Graph all strains - single measurement - vertical
- Graph all strains - multiple measurements - horizontal NEW!
- List outliers
- Individual strains
- Pairwise strain comparisons List format Graph format
- Sex differences
- Bar graph of selected strains and measurements
- Scatterplot comparison of two measurements
- Ratio or difference for any two measurements
- Correlated measurements
  this project vs. all MPD within project in matrix format in list format
- MPD priority strains set coverage
- Measurements ranked by # flaggings NEW!

MENU OF TOOLS AND DISPLAYS

Summary of available project files and documents

- MPD data set mpd172.dat

MPD measurement: femur_peak_load

Category	Description	Short name	Units	Project
bone strength, femur	**maximum load on load-displacement curve**	femur_peak_load	n	Donahue2 (pending)

MPD 17206

Female	10 strains tested	**Male**	10 strains tested
Low	19.0 n	Low	18.6 n
Mean	26.3 n SD=6.08	Mean	28.8 n SD=7.68
Median	25.1 n	Median	27.1 n
High	39.7 n	High	45.2 n

- Graph all strains - vertical
- Graph all strains - horizontal NEW!
- List strain values
- List outliers
- Download
- Sex differences
- Correlations
- Scatterplots
- Bar graphs
- Compute ratio or difference
- Flag this measurement Help

MENU OF OPTIONS get summary graph . . .

Select another measurement to display:

Go

Mouse Phenome Database Your flagged measurements

Home Quick start Contents Tools Downloads Preferences About MPD Search:

Graph all strains (measurement: femur_peak_load)

Category	Description	Short name	Units	Project
bone strength, femur	**maximum load on load-displacement curve**	femur_peak_load	n	Donahue2 (pending)

MPD 17206

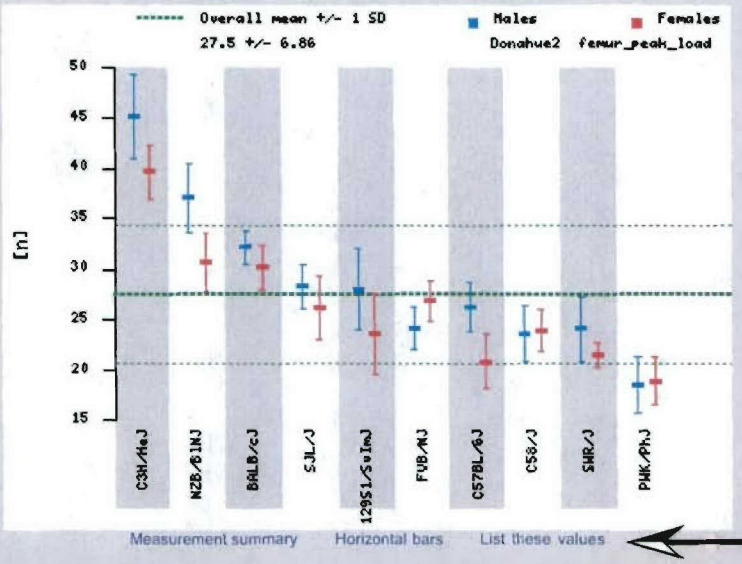

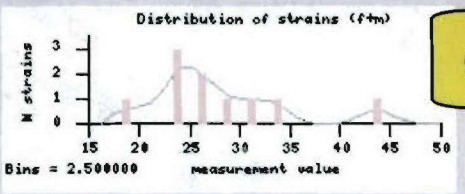

get statistical data . . .

Ordering: magnitude Sex: females, males

Error bars: 1 standard deviation Tick marks: thick Overall mean ± 1 SD bands? yes

Log transform? no Color mode: color Result file format: PNG Go

Select another measurement to display: Go

DISPLAY OPTIONS
for error bars, log transform, data ordering, and other format options

The Jackson Laboratory

ploticus 2.31 http://ploticus.sourceforge.net (GPL)

Mouse Phenome Database Your flagged measurements

Home Quick start Contents Tools Downloads Preferences About MPD Search

List all strains (measurement: femur_peak_load)

Category	Description	Short name	Units	Project
bone strength, femur	**maximum load on load-displacement curve**	femur_peak_load	n	Donahue2 (pending)

MPD 17206

Listing options, links and color code e

Find correlated measurements . . .

Female N strains: 10 Overall mean:26.3 Median:25.1

Strain	Sex	Mean	Standard Deviation	Standard Error	Coef. of Variation	Range	Z score	N mice	# Missing Obs.	Per-animal data
C3H/HeJ	f	**39.7**	2.69	0.896	0.0676	35.2 - 42.8	2.20	9	0	Per-animal data
NZB/BINJ	f	**30.8**	2.92	0.881	0.0950	26.7 - 37.4	0.74	11	0	Per-animal data
BALB/cJ	f	**30.3**	2.18	0.690	0.0721	25.5 - 32.9	0.65	10	0	Per-animal data
FVB/NJ	f	**26.9**	2.02	0.610	0.0754	23.6 - 29.7	0.10	11	0	Per-animal data
SJL/J	f	**26.3**	3.17	1.12	0.121	22.0 - 32.0	0.00	8	0	Per-animal data
C58/J	f	**24.0**	2.08	0.658	0.0867	21.4 - 27.2	-0.38	10	0	Per-animal data
129S1/SvImJ	f	**23.7**	4.01	1.27	0.169	18.2 - 30.9	-0.43	10	0	Per-animal data
SWR/J	f	**21.6**	1.25	0.417	0.0579	20.5 - 24.2	-0.78	9	0	Per-animal data
C57BL/6J	f	**20.9**	2.71	0.856	0.129	17.9 - 25.2	-0.89	10	0	Per-animal data
PWK/PhJ	f	**19.0**	2.41	0.697	0.127	15.3 - 22.7	-1.20	12	0	Per-animal data

Male N strains: 10 Overall mean:28.8 Median:27.1 SD:7.68

Strain	Sex	Mean	Standard Deviation	Standard Error	Coef. of Variation	Range	Z score	N mice	# Missing Obs.	Per-animal data
C3H/HeJ	m	**45.2**	4.22	1.27	0.0934	36.9 - 50.8	2.14	11	0	Per-animal data
NZB/BINJ	m	**37.1**	3.42	0.947	0.0920	31.0 - 43.1	1.09	13	0	Per-animal data
BALB/cJ	m	**32.2**	1.68	0.532	0.0523	29.9 - 35.2	0.45	10	0	Per-animal data
SJL/J	m	**28.3**	2.10	0.634	0.0742	25.8 - 31.1	-0.06	11	0	Per-animal data
129S1/SvImJ	m	**28.0**	4.00	1.03	0.143	23.4 - 36.4	-0.10	15	0	Per-animal data
C57BL/6J	m	**26.3**	2.42	0.698	0.0921	21.7 - 29.9	-0.32	12	0	Per-animal data
FVB/NJ	m	**24.2**	2.13	0.710	0.0882	21.6 - 27.5	-0.59	9	0	Per-animal data
SWR/J	m	**24.1**	3.30	1.04	0.137	19.8 - 29.7	-0.61	10	0	Per-animal data
C58/J	m	**23.6**	2.79	0.883	0.118	19.4 - 28.2	-0.67	10	0	Per-animal data
PWK/PhJ	m	**18.6**	2.74	0.826	0.147	13.0 - 22.2	-1.32	11	0	Per-animal data

Yellow = high end outlier Blue = low end outlier

An outlier is any measurement mean more than 1 SD away from the overall mean.

Terse list Measurment summary Download Graph strains Explanation of statistics

Listing options: Male & female, separately | Magnitude order | Go

Select another measurement to display:

CONTENT & SORTING OPTIONS

The Jackson Laboratory

Mouse Phenome Database Your flagged measurements

Home Quick start Contents Tools Downloads Preferences About MPD Search:

Measurement correlations

MPD measurements correlated with measurement femur_peak_load

Category	Description	Short name	Units	Project
bone strength, femur	maximum load on load-displacement curve	femur_peak_load	n	Donahue2 (pending)

Show best 20 | positive & negative | correlations of 0.50 or higher | having at least 10 strains in common. Go

Show only projects: Albers1, Crabbe1, Deschepper1, Dietrich1

Omit projects: Albers1, Crabbe1, Deschepper1, Dietrich1

Omit: body weight measurement pairs, body composition measurement pairs, bone mineral density & content pairs

= move mouse pointer over yellow dots to see descriptions (browser dependent)
= click on blue dots to see MPD correlations for measurement 2

Positive correlations

Measurement 1	Measurement 2	Sex	Best correlation	N strains	Scatterplot	Method	Linear Pearson	Spearman
femur_peak_load	femur_break_load Donahue2 (pending)	m	0.99	10	Plot	0	0.99	0.96
femur_peak_load	femur_break_load Donahue2 (pending)	f	0.99	10	Plot	0	0.99	0.98
femur_peak_load	femur_thickness_R2 Donahue2 (pending)	m	0.96	10	Plot	2	0.96	0.88
femur_peak_load	femur_thickness_R2 Donahue2 (pending)	f	0.96	10	Plot	2	0.96	0.91
femur_peak_load	femur_thickness_L Donahue2 (pending)	f	0.95	10	Plot	2	0.95	0.88
femur_peak_load	femur_thickness_R1 Donahue2 (pending)	f	0.95	10	Plot	2	0.95	0.89
femur_peak_load	femur_stiffness Donahue2 (pending)	m	0.95	10	Plot	0	0.95	0.93
femur_peak_load	femur_thickness_L Donahue2 (pending)	m	0.95	10	Plot	2	0.95	0.94
femur_peak_load	femur_thickness_R1 Donahue2 (pending)	m	0.94	10	Plot	2	0.93	0.90
femur_peak_load	femur_peak_energy Donahue2 (pending)	m	0.94	10	Plot	3	0.93	0.85
femur_peak_load	femur_yield_load Donahue2 (pending)	f	0.93	10	Plot	0	0.93	0.85
femur_peak_load	femur_stiffness Donahue2 (pending)	f	0.92	10	Plot	1	0.91	0.84
femur_peak_load	femur_shaft_BMC Donahue2 (pending)	m	0.92	10	Plot	1	0.90	0.93
femur_peak_load	femur_shaft_BMD Donahue2 (pending)	f	0.90	10	Plot	0	0.90	0.75
femur_peak_load	femur_BMD Donahue2 (pending)	m	0.90	10	Plot	0	0.90	0.89
femur_peak_load	femur_yield_load Donahue2 (pending)	m	0.90	10	Plot	0	0.90	0.88
femur_peak_load	femur_cortical_BMD Donahue2 (pending)	f	0.89	10	Plot	1	0.86	0.80
femur_peak_load	femur_shaft_BMC Donahue2 (pending)	f	0.88	10	Plot	1	0.86	0.88
femur_peak_load	femur_cortical_BMD Donahue2 (pending)	m	0.85	10	Plot	3	0.83	0.72
femur_peak_load	femur_BMD Donahue2 (pending)	f	0.85	10	Plot	0	0.85	0.75

view scatterplots of interest . . .

The Jackson

Part I
1A-8

Scatterplot of two measurements

	Project	Category	Description	Units	Links
Measurement 1: femur_peak_load	Donahue2	bone strength, femur	**maximum load on load-displacement curve**	n	
Measurement 2: femur_thickness_L	Donahue2	body measurements (miscellaneous), leg	**cortical thickness of left femur pQCT (periosteal to endosteal surface at mid-diaphysis)**	mm	

Select other measurements

Showing all strains common to both measurements

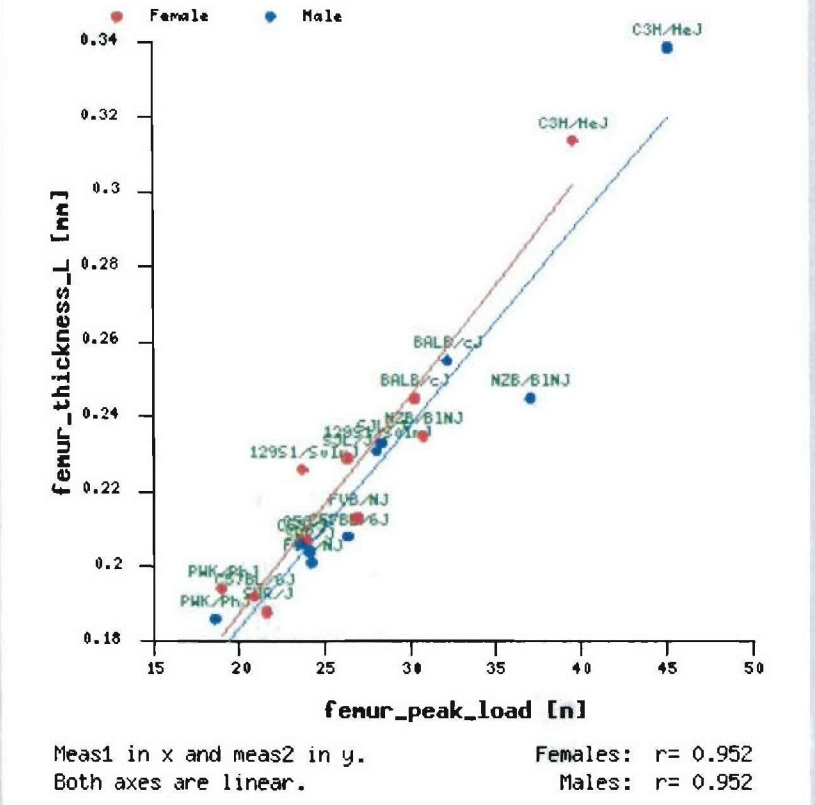

Mean values:

Strain & sex	femur_peak_load	femur_thickness_L
129S1/SvImJ f	23.7	0.226
129S1/SvImJ m	28.0	0.231
BALB/cJ f	30.3	0.245
BALB/cJ m	32.2	0.255
C3H/HeJ f	39.7	0.314
C3H/HeJ m	45.2	0.339
C57BL/6J f	20.9	0.192
C57BL/6J m	26.3	0.208
C58/J f	24.0	0.207
C58/J m	23.6	0.206
FVB/NJ f	26.9	0.213
FVB/NJ m	24.2	0.201
NZB/BINJ f	30.8	0.235
NZB/BINJ m	37.1	0.245
PWK/PhJ f	19.0	0.194
PWK/PhJ m	18.6	0.186
SJL/J f	26.3	0.229
SJL/J m	28.3	0.233
SWR/J f	21.6	0.188
SWR/J m	24.1	0.204

Plot parameters

Generate scatterplot

Data points are	strain sex means	More info
Sex	Female (red), male (blue)	
Show strain names?	yes	(not avail with indiv. animal plots)
Error bars	none	(not avail with indiv. animal plots)
Log transform	none	(not avail with indiv. animal plots)
Overall size	normal	
Data point size	normal	

These correlations are compelling. Omitting C3H/HeJ (high-end outlier) and re-running the analysis would help confirm the relationship . . .

Options for omitting and highlighting strains have been truncated.

Mouse Phenome Database Your flagged measurements

Home Quick start Contents Tools Downloads Preferences About MPD Search

Scatterplot of two measurements

	Project	Category	Description	Units	Links
Measurement 1: femur_peak_load	Donahue2	bone strength, femur	maximum load on load-displacement curve	n	
Measurement 2: femur_thickness_L	Donahue2	body measurements (miscellaneous), leg	cortical thickness of left femur pQCT (periosteal to endosteal surface at mid-diaphysis)	mm	

Select other measurements

Omitting selected strains

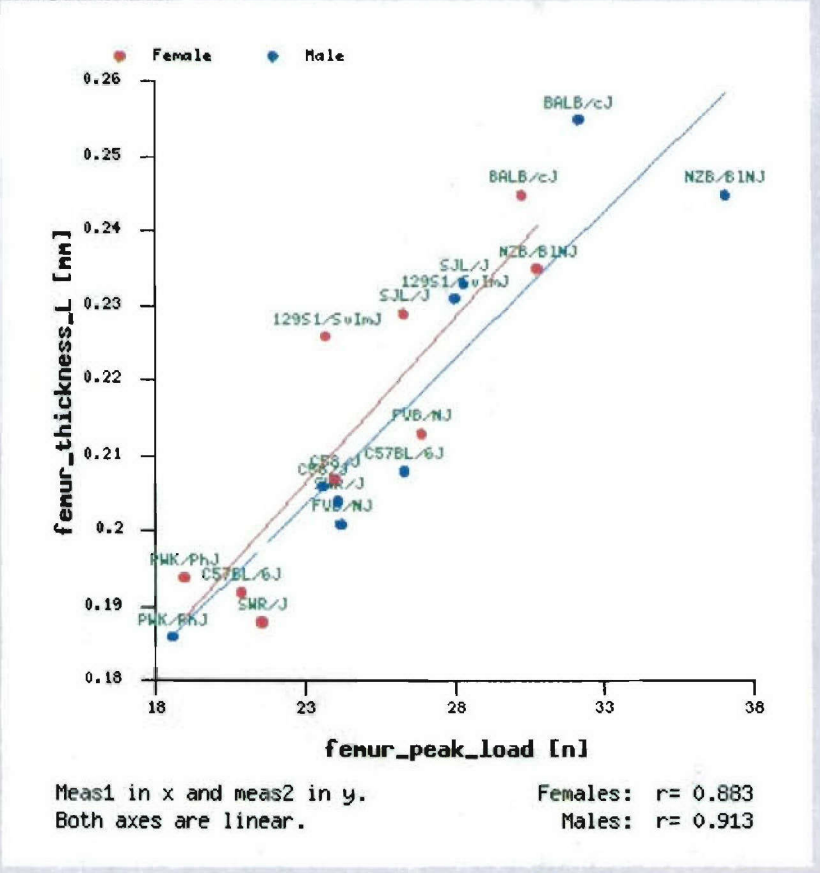

Mean values:

Strain & sex	femur_peak_load	femur_thickness_L	
129S1/SvImJ f	23.7	0.226	
129S1/SvImJ m	28.0	0.231	
BALB/cJ f	30.3	0.245	
BALB/cJ m	32.2	0.255	
C3H/HeJ f	39.7	0.314	(omitted)
C3H/HeJ m	45.2	0.339	(omitted)
C57BL/6J f	20.9	0.192	
C57BL/6J m	26.3	0.208	
C58/J f	24.0	0.207	
C58/J m	23.6	0.206	
FVB/NJ f	26.9	0.213	
FVB/NJ m	24.2	0.201	
NZB/BINJ f	30.8	0.235	
NZB/BINJ m	37.1	0.245	
PWK/PhJ f	19.0	0.184	
PWK/PhJ m	18.6	0.186	
SJL/J f	26.3	0.229	
SJL/J m	28.3	0.233	
SWR/J f	21.6	0.188	
SWR/J m	24.1	0.204	

Plot parameters

Generate scatterplot

Data points are: strain sex means (More info)

Sex: Female (red), male (blue)

Show strain names? yes (not avail with indiv. animal plots)

Error bars: none (not avail with indiv. animal plots)

Log transform: none (not avail with indiv. animal plots)

Overall size: normal

Data point size: normal

Axis ranges (enter 2 values, eg. ...): X axis: Y axis:

Strains can be omitted from or highlighted in the scatterplot. After omitting C3H/HeJ, regression analysis is re-computed for user customization. The results still show significant Pearson correlations without C3H/HeJ, so we can proceed on the assumption that the original correlation is valid, confirming other studies that showed cortical thickness is highly correlated to peak load.

Scatterplot of two measurements

	Project	Category	Description	Units	Links
Measurement 1: femur_peak_load	Donahue2	bone strength, femur	**maximum load on load-displacement curve**	n	
Measurement 2: femur_thickness_L	Donahue2	body measurements (miscellaneous), leg	**cortical thickness of left femur pQCT (periosteal to endosteal surface at mid-diaphysis)**	mm	

Select other measurements

Showing all strains common to both measurements

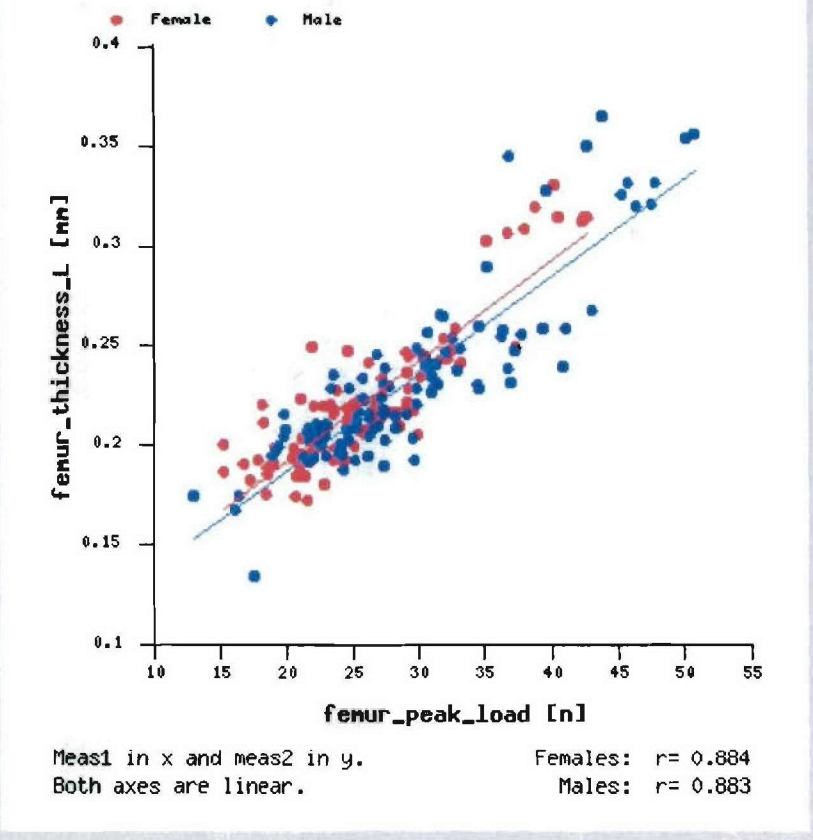

Plot parameters

Per-animal data can be checked to make sure correlations are consistent across all individuals in the population tested. Correlation coefficients are re-computed for individual mice. Strains can be highlighted . . .

Overall size normal

Data point size normal

Scatterplot of two measurements

	Project	Category	Description	Units	Links
Measurement 1: femur_peak_load	Donahue2	bone strength, femur	**maximum load on load-displacement curve**	n	
			cortical thickness of left mur pQCT (periosteal to dosteal surface at mid-physis)	mm	

ents

Highlighting C3H/HeJ.

Because no strains have been omitted, the correlation coefficient has not changed from the previous scatterplot.

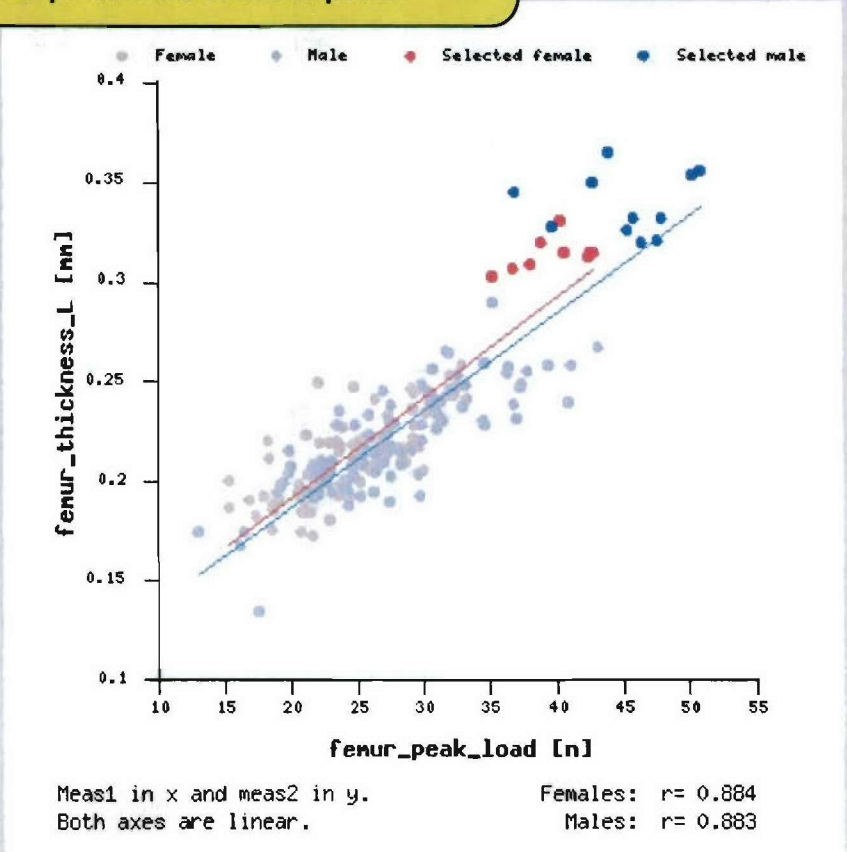

Meas1 in x and meas2 in y.
Both axes are linear.

Females: r= 0.884
Males: r= 0.883

Plot parameters

Generate scatterplot

Data points are: individual animals More

Se

Show strain names

Search for other interesting correlations . . .

that particular measurement.

The more intense the color, the higher the correlation coefficient. Red-based cells indicate positive correlations; blue are negative. Clicking on a cell will produce a scatterplot. Clicking on a blue dot will find more correlations to that measurement. Compare to males . . .

Show: all cells | Go

Within each cell, show: correlation coefficient | correlation method: linear pe

Display measurments in: category order

View a matrix of scatterplot thumbnails NEW!

Female				1	2	3	4	5	6	7	8	9	10	11	12	13	14	15	16	17	18	19	20
area of right femur (cross section at mid-diaphysis)	Donahue2	femur_area	1.		.14	.26	.07	.76	.56	.91	.92	.70	.63	.32	-.06	-.06	.57	.33	-.78	-.24	.17	.21	.40
cortical thickness of left femur pQCT (periosteal to endosteal surface at mid-diaphysis)	Donahue2	femur_thickness_L	2.	.14		.99	.99	-.53	.26	.14	.17	.42	.85	.87	.98	.89	.25	.64	.42	.82	.94	.95	.91
cortical thickness of right femur pQCT (periosteal to endosteal surface at mid-diaphysis)	Donahue2	femur_thickness_R1	3.	.26	.99		.97	-.43	.32	.28	.28	.50	.91	.88	.99	.96	.32	.65	.32	.78	.93	.96	.93
cortical thickness of right femur uCT (periosteal to endosteal surface at mid-diaphysis)	Donahue2	femur_thickness_R2	4.	.07	.99	.97		-.57	.23	.06	.11	.40	.80	.83	.97	.88	.25	.67	.46	.65	.95	.96	.98
endosteal (inner) circumference of left femur (mid-diaphysis)	Donahue2	femur_in	5.	.76	-.53	-.43	-.57		.31	.60	.74	.30	-.02	-.30	-.69	-.65	.33	-.16		-.77	-.47	-.42	-.25
length of right femur (condyles to rostral tip of greater trochanter)	Donahue2	femur_length	6.	.56	.26	.32	.23	.31		.54	.56	.87	.52	.50	.17	.10	.42	.57	.47	.00	.39	.37	.54
medial to lateral width of right femur (mid-diaphysis)	Donahue2	femur_width_ML	7.	.91	.14	.28	.06	.66	.54		.87	.69	.61	.28	-.02	-.07	.56	.32	-.63	-.11	.16	.24	.36
periosteal (outer) circumference of left femur (mid-diaphysis)	Donahue2	femur_out	8.	.89	.17	.28	.11	.74	.56	.87		.69	.65	.33	.03	-.05	.59	.33	-.77	-.25	.20	.27	.43
whole body weight (with head)	Donahue2	bw	9.	.70	.42	.50	.40	.30	.87	.69	.69		.71	.57	.28	.28	.67	.83	-.43	.23	.60	.61	.64
bone mineral content of right femur (cross section at mid-diaphysis)	Donahue2	femur_shaft_BMC	10.	.63	.85	.91	.80	.02	.52	.61	.65	.71		.96	.73	.87	.46	.66	-.08	.52	.82	.86	.93
bone mineral density of cortical shell of whole left femur	Donahue2	femur_cortical_BMD	11.	.32	.87	.88	.83	-.30	.50	.28	.33	.57	.86		.82	.82	.10	.60	.20	.65	.88	.86	.98
bone mineral density of right femur (1-mm thick cross section at mid-diaphysis)	Donahue2	femur_shaft_BMD	12.	.06	.98	.96	.97	-.69	.17	-.02	-.03	.28	.73	.82		.92	.11	.56	.56	.87	.90	.90	.95
bone mineral density of whole left femur	Donahue2	femur_BMD	13.	.08	.89	.96	.93	-.66	.10	-.07	-.05	.28	.67	.82	.92		.06	.56	.57	.84	.87	.85	.91
area under load-displacement curve to break point	Donahue2	femur_break_energy	14.	.57	.25	.32	.26	.33	.42	.56	.59	.67	.46	.10	.11	.06		.66	-.38	.13	.31	.41	.25
area under load-displacement curve to peak load	Donahue2	femur_peak_energy	15.	.33	.64	.65	.67	-.16	.57	.32	.33	.83	.66	.60	.56	.56	.66		-.01	.61	.82	.83	.66
estimated elastic modulus	Donahue2	elastic_modulus	16.	-.78	.42	.32	.46		-.47	-.83	-.77	-.43	-.08	.20	.56	.57	-.38	-.01		.74	.33	.30	.13
estimated ultimate strength	Donahue2	ultimate_strength	17.	-.24	.82	.78	.85	-.77	.00	-.11	-.25	.23	.52	.65	.87	.84	.43	.61	.74		.82	.83	.82
load at specimen failure (break point)	Donahue2	femur_break_load	18.	.17	.94	.93	.95	-.47	.39	.16	.20	.60	.82	.88	.90	.87	.31	.82	.33	.82		.96	.91
maximum load on load-displacement curve	Donahue2	femur_peak_load	19.	.24	.95	.95	.96	-.42	.37	.24	.27	.61	.86	.86	.90	.85	.41	.83	.30	.83	.96		.91
slope of force-displacement curve in linear region	Donahue2	femur_stiffness	20.	.40	.91	.93	.88	-.25	.54	.36	.43	.64	.93	.96	.93	.90	.25	.66	.13	.82	.91	.91	

The correlation patterns are similar for males and females but there are some interesting differences. We can select specific measurements to compare side-by side . . .

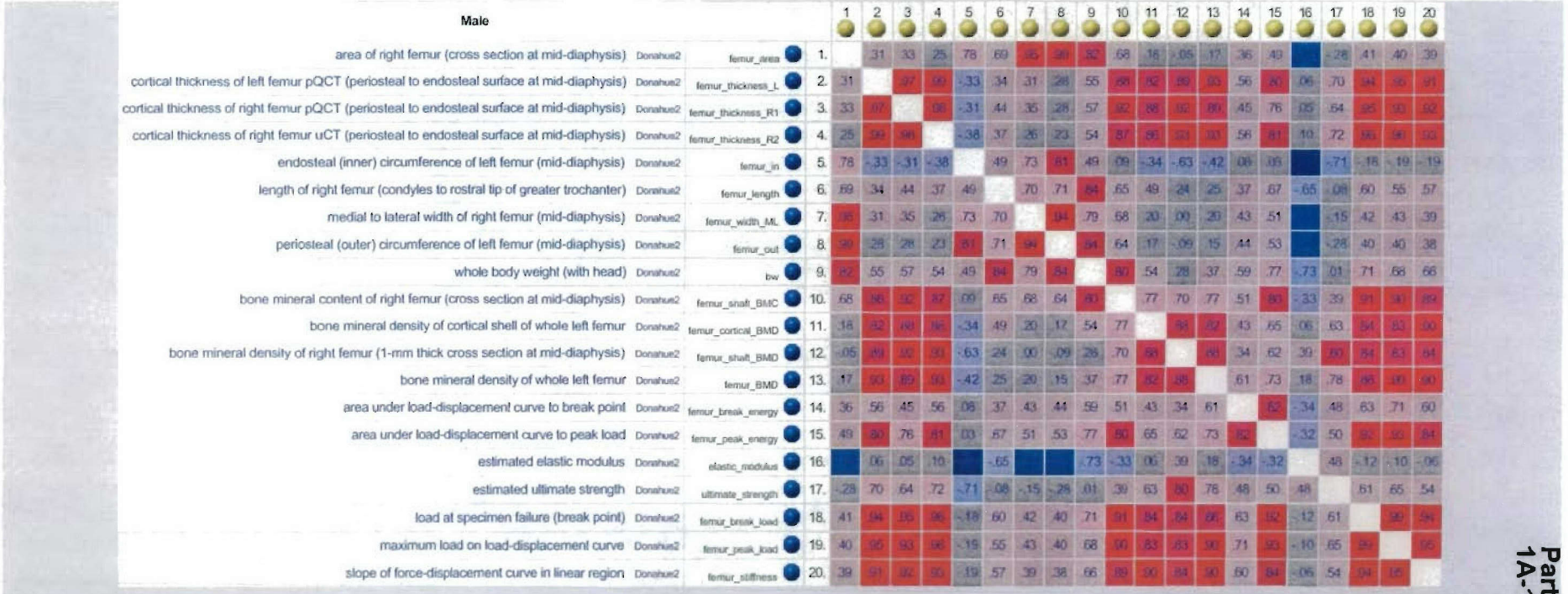

This application aligns bar graphs by strain and sex for quick comparisons across selected measurements. This tool helps identify strains with complex phenotypes. Outlier strains for single measurements can be found . . .

Horizontal bar display of several measurements

Select other measurements

Move mouse over a measurement to see longer description,
or click to see measurement summary pages or strain profile pages.
Error bars are 1 SD. More graph settings available at bottom of page.

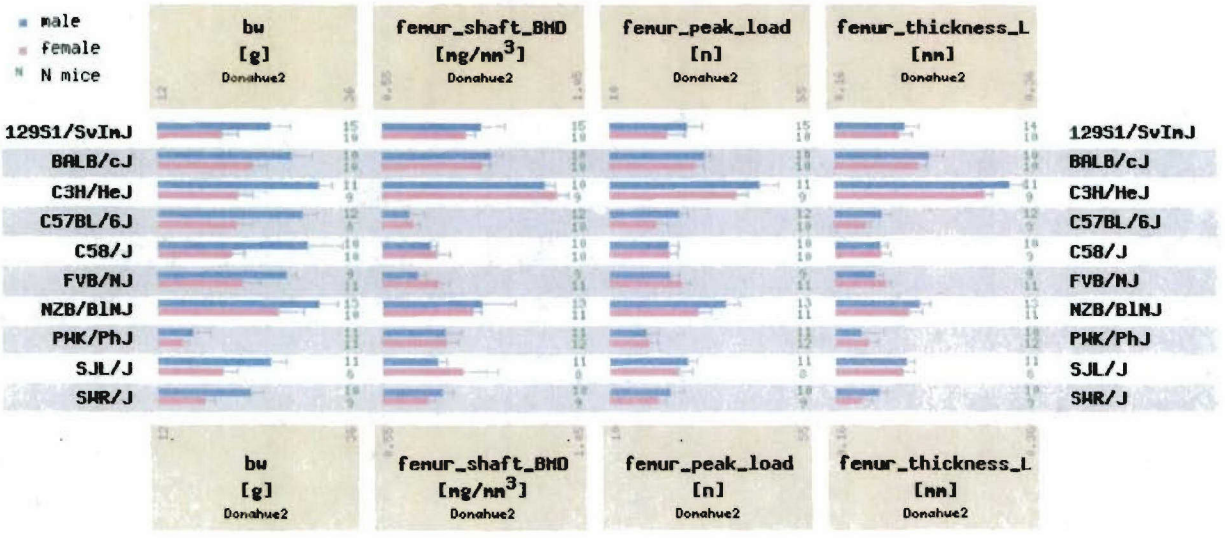

Sexes: both females and males ⇕ Show N mice (in green) for all ⇕

Highlight the following strains: 129S1/SvImJ
BALB/cJ
C3H/HeJ
C57BL/6J

Set a fixed X range for all panels:

Result file format: png ⇕ Go

C3H/HeJ has already been identified as a model for bone strength and formation, usually found as a high-end outlier for bone phenotypes. This study has identified an interesting strain at the other end of the spectrum for bone phenotypes.

We can further compare C3H/HeJ and PWK/PhJ . . .

All outliers from project Donahue2

Outliers will have a Z score greater than 2.0 or less than -2.0 in linear space.
Male only Order: project order Go

Yellow = high end outlier Blue = low end outlier relative to all strains tested by project

All outliers for project Donahue2

Category	Measurement		Strain	Sex	Mean	Units	SD	N mice	Z score relative to all strains tested by project
body weight	whole body weight (with head)	bw	PWK/PhJ	male	16.4	g	2.12	11	-2.31
bone mineral density and content femur	bone mineral density of whole left femur	femur_BMD	C3H/HeJ	male	0.803	mg/mm^3	0.0250	11	2.10
bone mineral density and content femur	bone mineral density of right femur (1-mm thick cross section at mid-diaphysis)	femur_shaft_BMD	C3H/HeJ	male	0.966	mg/mm^3	0.0288	10	2.11
bone strength femur	maximum load on load-displacement curve	femur_peak_load	C3H/HeJ	male	45.2	n	4.22	11	2.14
bone strength femur	load at specimen failure (break point)	femur_break_load	C3H/HeJ	male	44.5	n	4.44	11	2.17
bone strength femur	estimated elastic modulus	elastic_modulus	PWK/PhJ	male	5.63	Mpa	0.837	11	2.20
body measurements (miscellaneous) leg	anterior to posterior width of right femur (mid-diaphysis)	femur_width_AP	PWK/PhJ	male	1.00	mm	0.148	11	-2.22
body measurements (miscellaneous) leg	medial to lateral width of right femur (mid-diaphysis)	femur_width_ML	PWK/PhJ	male	1.20	mm	0.174	11	-2.07
body measurements (miscellaneous) leg	area of right femur (cross section at mid-diaphysis)	femur_area	PWK/PhJ	male	1.46	mm^2	0.217	11	-2.06
body measurements (miscellaneous) leg	cortical thickness of right femur pQCT (periosteal to endosteal surface at mid-diaphysis)	femur_thickness_R1	C3H/HeJ	male	0.340	mm	0.0165	10	2.25
body measurements (miscellaneous) leg	cortical thickness of right femur uCT (periosteal to endosteal surface at mid-diaphysis)	femur_thickness_R2	C3H/HeJ	male	0.378	mm	0.00990	11	2.42
body measurements (miscellaneous) leg	cortical thickness of left femur pQCT (periosteal to endosteal surface at mid-diaphysis)	femur_thickness_L	C3H/HeJ	male	0.339	mm	0.0156	11	2.47
body measurements (miscellaneous) leg	periosteal (outer) circumference of left femur (mid-diaphysis)	femur_out	PWK/PhJ	male	3.94	mm	0.198	10	-2.17
body measurements (miscellaneous) leg	area of muscle and bone of right femur (cross section at mid-diaphysis)	thigh_area	PWK/PhJ	male	49.5	mm^2	9.91	11	-2.18
body measurements (miscellaneous) leg	thigh area minus femur area (cross section at mid-diaphysis)	thigh_muscle_area	PWK/PhJ	male	48.1	mm^2	9.76	11	-2.16
body measurements (miscellaneous) leg	weight of isolated right quadriceps muscle	quadriceps_wt	PWK/PhJ	male	0.126	g	0.0165	11	-2.41

Click on category names or project symbols to see more data for the strain.

[N rows = 16]

Pairwise comparison of strains, projectDonahue2

Strains will be compared using measurement Z scores.

Select 2 - 8 strains to compare:
(Help)

--- involved strains:
129S1/SvImJ
BALB/cJ
C3H/HeJ
C57BL/6J
C58/J
FVB/NJ
NZB/BINJ
PWK/PhJ
SJL/J
SWR/J

Select one strain to compare all others against:
C3H/HeJ
C57BL/6J
PWK/PhJ

Measurements in project Donahue2

Log transform? no

Compare strains

Pair comparions in list format:
- C57BL/6J vs. C3H/HeJ
- C57BL/6J vs. PWK/PhJ

All measurements in project Donahue2

Move mouse over a bar to see measurement description. Click on bar to see measurement summary.

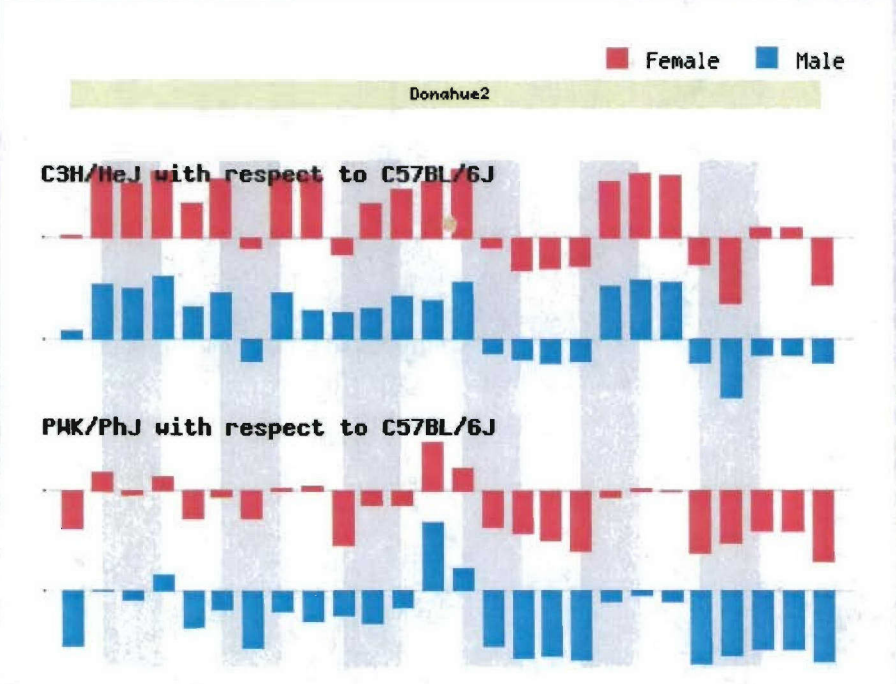

The bars represent differences between strain Z-scores.
Z score differences of less than ± 0.05 are marked with a green pip.

Zooming and popup labels may not work on older browsers (client-side imagemaps support required).

C3H/HeJ and PWK/PhJ are compared against C57BL/6J, which is also a powerful model for certain bone phenotypes. PWK/PhJ brings in novel alleles not seen in the more common lab strains. See the Diallele Cross data (Part III) for clues about the dominance of PWK alleles. Another place to find out more about a strain is by accessing accumulated MPD profile data . . .

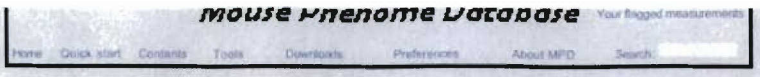

Donahue2: measurements involving C3H/HeJ

Outliers will have a Z score greater than 2.0 or less than -2.0 in linear space

Strain: C3H/HeJ | Female and Male | Order: alphabetical | Go

Yellow = high end outlier Blue = low end outlier relative to all strains tested by project

Donahue2: measurements for C3H/HeJ

Category	Measurement		Sex	Mean	Units	SD	N mice	Z score relative to all strains tested by project
body measurements (miscellaneous) kg	anterior to posterior width of right femur (mid-diaphysis) Donahue2 (pending)	femur_width_AP	female	1.11	mm	0.0870	9	-1.08
			male	1.26		0.0479	11	0.24
body measurements (miscellaneous) kg	area of muscle and bone of right femur (cross section at mid-diaphysis) Donahue2 (pending)	thigh_area	male	80.3	mm^2	10.5	10	0.10
			female	71.1		7.78	9	0.68
body measurements (miscellaneous) kg	area of right femur (cross section at mid-diaphysis) Donahue2 (pending)	femur_area	male	2.33	mm^2	0.247	10	0.41
			female	1.82		0.145	9	-0.33
body measurements (miscellaneous) kg	cortical thickness of left femur pQCT (periosteal to endosteal surface at mid-diaphysis) Donahue2 (pending)	femur_thickness_L	male	0.339	mm	0.0156	11	2.47
			female	0.314		0.00809	9	2.42
body measurements (miscellaneous) kg	cortical thickness of right femur pQCT (periosteal to endosteal surface at mid-diaphysis) Donahue2 (pending)	femur_thickness_R1	male	0.340	mm	0.0165	10	2.25
			female	0.315		0.0104	9	2.27
body measurements (miscellaneous) kg	cortical thickness of right femur uCT (periosteal to endosteal surface at mid-diaphysis) Donahue2 (pending)	femur_thickness_R2	male	0.378	mm	0.00990	11	2.42
			female	0.365		0.0163	9	2.54
body measurements (miscellaneous) kg	endosteal (inner) circumference of left femur (mid-diaphysis) Donahue2 (pending)	femur_in	female	2.58	mm	0.0559	9	-1.79
			male	2.92		0.117	11	-1.18
body measurements (miscellaneous) kg	length of right femur (condyles to rostral tip of greater trochanter) Donahue2 (pending)	femur_length	male	15.6	mm	0.161	11	0.22
			female	15.1		0.277	9	-0.12
body measurements (miscellaneous) kg	medial to lateral width of right femur (mid-diaphysis) Donahue2 (pending)	femur_width_ML	male	1.73	mm	0.0919	11	0.08
			female	1.45		0.0740	9	-0.54
body measurements (miscellaneous) kg	periosteal (outer) circumference of left femur (mid-diaphysis) Donahue2 (pending)	femur_out	female	4.55	mm	0.0834	9	-0.16
			male	5.05		0.0987	11	0.33
body measurements (miscellaneous) kg	thigh area minus femur area (cross section at mid-diaphysis) Donahue2 (pending)	thigh_muscle_area	male	78.0	mm^2	10.5	10	0.09
			female	69.2		7.73	9	0.69
body measurements (miscellaneous) kg	weight of isolated right quadriceps muscle Donahue2 (pending)	quadriceps_wt	female	0.148	g	0.0276	9	-0.69
			male	0.226		0.0506	11	0.03
body weight			male	32.0		1.95	11	0.98

MPD strain profiles show a Z-score bar for each measurement to indicate where C3H/HeJ is a high-end outlier (blue), low-end (red), or very close to the overall strain mean (green). Measurements can be sorted by category and users can set the stringency for outliers.
******end of Donahue project******

ALL ANALYSES SHOWN FOR THIS EXAMPLE ARE ACTUAL. THE SAME TOOLS ILLUSTRATED HERE CAN BE USED ON A SET OF USER-SPECIFIED MEASUREMENTS. MEASUREMENTS OF INTEREST ARE FLAGGED AND MANAGED IN A USER'S OWN 'SHOPPING CART' ACCESSED FROM THE HEADER OF EACH MPD WEBPAGE.

DATA VALIDATION:
BMD MEASUREMENTS FROM 4 MPD PROJECTS

Comparing new data to relevant existing MPD data is an effective (and quick) way of validating the new data sets. These matrices represent BMD comparisons from Parts II and III of this study along with data generated from 2 other projects that each analyzed over 30 strains. The high correlations (red) indicate consistency between measurement (project) pairs.

Correlations matrix

Click on a cell to see more information about a correlation, or to do a scatterplot. Cells containing a dash (-) have less than 5 strains in common. Move mouse pointer over yellow dots to see measurement descriptions (browser dependent). Click on blue dots to see all MPD measurements that are correlated with that particular measurement.

Select measurements

Show: all cells — Go

Within each cell, show: correlation coefficient — correlation method: linear pearson

Display measurments in: project order

View a matrix of scatterplot thumbnails NEW!

Female				1	2	3	4
whole body bone mineral density (without head)	Churchill1	body_BMD	1.		.92	.95	.89
whole body bone mineral density	Donahue1	body_BMD	2.	.92		.89	.93
bone mineral density (BMD) after 8 wks on atherogenic diet	Naggert1	BMD_8	3.	.95	.89		.94
bone mineral density	Tordoff3	BMD	4.	.89	.93	.94	

Male				1	2	3	4
whole body bone mineral density (without head)	Churchill1	body_BMD	1.		.92	.95	.97
whole body bone mineral density	Donahue1	body_BMD	2.	.92		.90	.91
bone mineral density (BMD) after 8 wks on atherogenic diet	Naggert1	BMD_8	3.	.95	.90		.97
bone mineral density	Tordoff3	BMD	4.	.97	.91	.97	

DIALLELE CROSS (Part III)
The Churchill project has all the capabilities and tools as shown for the Donahue project in the first example. This is a view of thumbnail scatterplots for all pairwise combinations of measurements.

Showing females and males. Display females only Display males only

Hold down your control key while clicking, to deploy in a new window. Click on a plot thumbnail to see a full-sized scatterplot. Move mouse pointer over a measurement name to see full description, or move mouse pointer over a scatterplot to see correlation coefficients (browser-dependent).

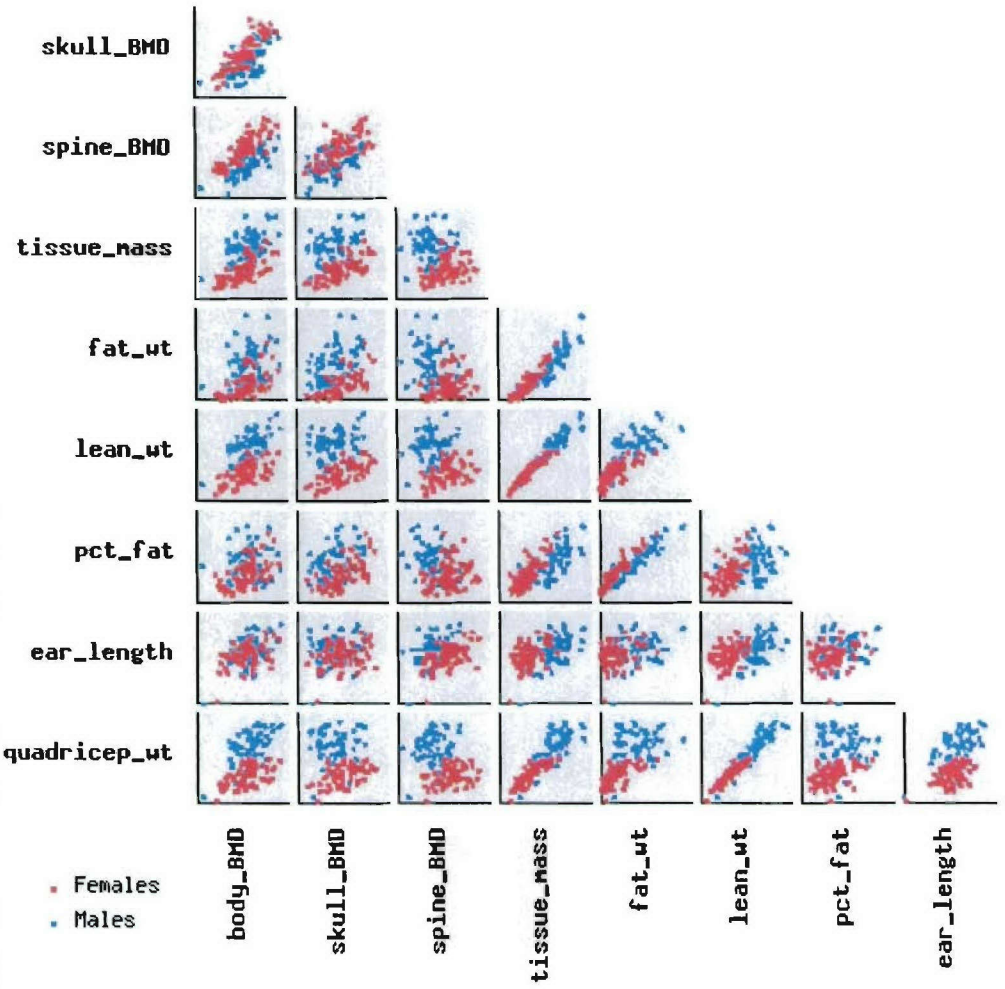

Measurements appearing in the above display:

body_BMD	whole body bone mineral density (without head)	Churchill1
skull_BMD	skull bone mineral density	Churchill1
spine_BMD	spine bone mineral density	Churchill1
tissue_mass	calculated total tissue mass	Churchill1
fat_wt	calculated weight of fat tissue	Churchill1
lean_wt	calculated weight of lean tissue	Churchill1
pct_fat	percent fat	Churchill1
ear_length	length of ear	Churchill1
quadricep_wt	weight of isolated quadracep muscle	Churchill1

This is a preview of the diallele analysis tools we have developed for this project. This representation of diallele data helps sort and visualize the data for reciprocal crosses. Data from F1 offspring are shown by Z-score bars. F1 females are in the table just below; F1 males are on the next page. Circles were added for illustration purposes (see next page).

Diallele cross analysis

Category	Description	Short name	Units	Project
body composition	**percent fat**	pct_fat	%	Churchill1 (pending) (F1 8-way cross strains)

MPD 17107

Select another Churchill1 measurement

Show: Z score bars | Matrix size: normal | Go

Move your pointer over a bar to see details. Click on a bar to see raw data.

Females

This data format helps detect sex-specific, maternal and paternal effects, and dominant strain alleles.

Some interesting results have been circled with color-coding to indicate pairs.

The first example in green shows female F1 data from a reciprocal cross (SJLxPWK and PWKxSJL) with very diverse phenotypes.

The second example in blue shows a reciprocal cross (NZBxC3; C3xNZB) that gave very similar results in their female offspring.

The third example in red shows large sex differences between F1s of the same reciprocal cross (PWxNZB). Note the dominant effects of the PWK alleles. The female allele is particularly strong in female but not male offspring.

We can switch to strain means and standard deviations in a similar format (matrix sizes can be matched for ease of cross-referencing) . . .

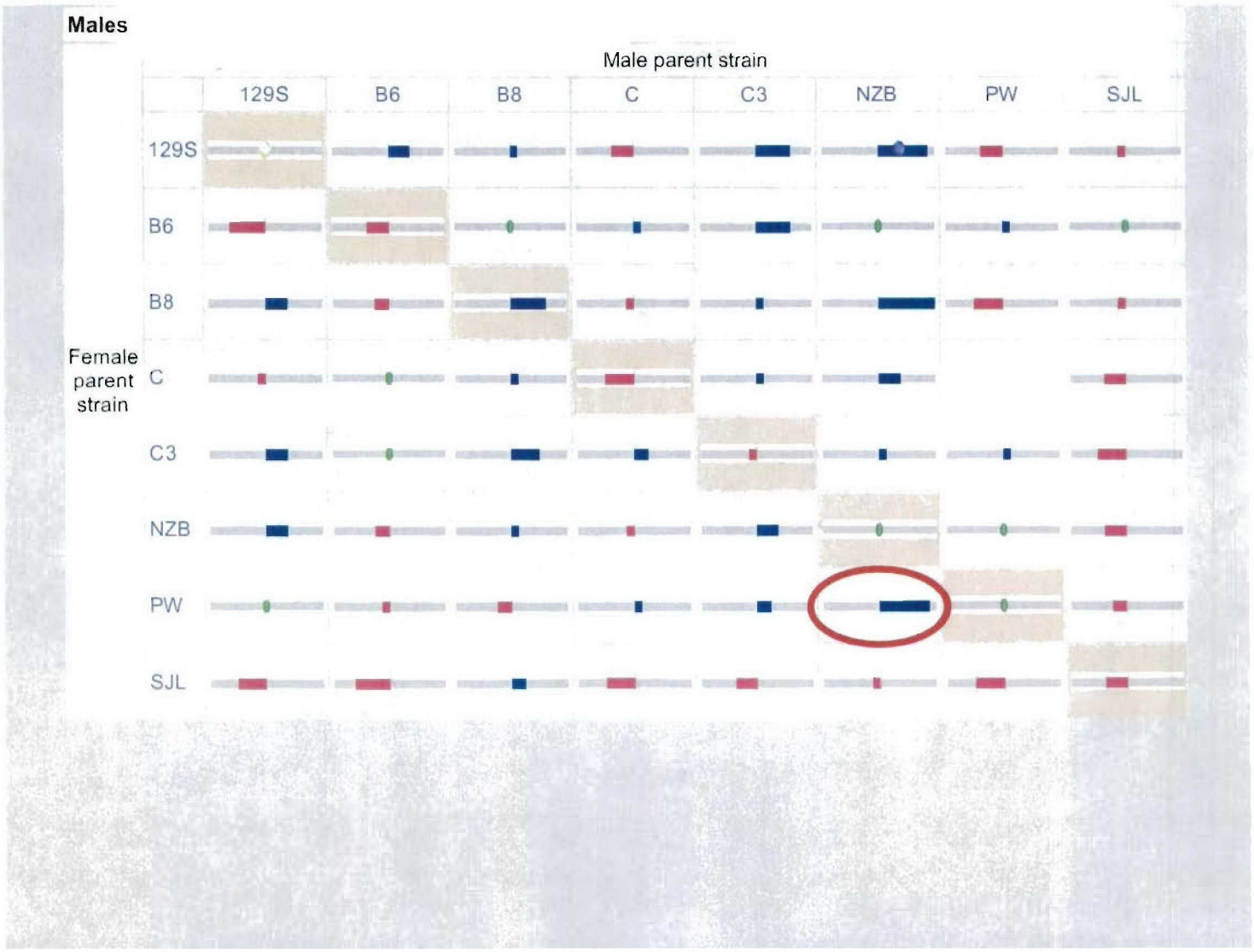

Diallele cross analysis

Category	Description	Short name	Units	Project
body composition	**percent fat**	pct_fat	%	Churchill1 (pending) (F1 8-way cross strains)

MPD 17107

Select another Churchill1 measurement

Show: Strain means and SD Matrix size: compact Go

Move your pointer over a bar to see details. Click on a bar to see raw data.

Females

Female parent strain	Male parent strain: 129S	B6	B8	C	C3	NZB	PW	SJL	Mean
129S	20.8 ±3.16	22.4 ±2.12	17.7 ±2.76	20.1 ±1.83	21 ±1.67	23.1 ±3.99	14.8 ±0.61	21.6 ±1.19	20.2 ±2.72
B6	15.9 ±1.9	16 ±2.07	14.5 ±1.64	16.4 ±0.428	22.5 ±2.75	27.6 ±3.91	14.6 ±1.56	18.6 ±3.65	18.3 ±4.58
B8	14.1 ±1.52	13.9 ±1.7	20.3 ±6.56	15.6 ±1.53	19.7 ±5.92	18.2 ±4.3	14.7 ±0.953	18.1 ±2.29	16.8 ±2.56
C	17.4 ±2.72	21.5 ±3.69	15.3 ±4.57	23.5 ±3.21	21.2 ±1.66	19.4 ±1.1		21.3 ±3.4	19.9 ±2.79
C3	19 ±3.18	21.3 ±3.31	19.9 ±3.95	28 ±4.44	25.5 ±4.48	29.2 ±6.91	14.7 ±1.33	23.3 ±5.2	22.6 ±4.87
NZB	23.9 ±4.68	27.5 ±5.24	22.1 ±3.5	22.7 ±3.16	33.3 ±3.09	27.3 ±8.9	13.5 ±0.416	31.1 ±5.12	25.2 ±6.15
PW	15.8 ±1.35	15.8 ±1.81	13.3 ±1.25	17.7 ±1.12	17.3 ±2.75	12.9 ±1.86	19.8 ±2.03	18.5 ±2.46	16.4 ±2.42
SJL	27.4 ±7.27	24.3 ±4.68	17.4 ±1.62	18.2 ±2.73	18.8 ±3.82	17.9 ±3.08	18.6 ±4.46	17.6 ±2.29	20.0 ±3.72
Mean	19.3 ±4.53	20.3 ±4.70	17.6 ±3.08	20.3 ±4.21	22.4 ±5.04	22.0 ±5.77	15.8 ±2.38	21.3 ±4.46	

Males

Female parent strain	Male parent strain: 129S	B6	B8	C	C3	NZB	PW	SJL	Mean
129S	24.5 ±4.75	28.8 ±5.24	25.4 ±1.91	17.7 ±6.17	31.7 ±4.29	34.9 ±1.03	18 ±2.61	20.6 ±9.45	25.2 ±6.31
B6	15.4 ±4.2	17.4 ±3.66	23.7 ±6.24	26.1 ±2.43	31.8 ±1.93	23.1 ±12.7	24.8 ±8.71	22.3 ±2.58	23.1 ±5.08
B8	27.7 ±2.92	19.9 ±3.51	31.4 ±6.4	20.4 ±5.97	26 ±5.04	35.4 ±2.43	16 ±4.63	20.7 ±2.18	24.7 ±6.58
C	21.4 ±4.79	23.8 ±7.59	25.9 ±3.3	16 ±4.4	26 ±2.07	27.7 ±3.42		17.5 ±3.42	22.6 ±4.49
C3	28.5 ±6.52	22.5 ±4.19	29.8 ±2.49	26.9 ±2.42	21.6 ±3.17	26.2 ±2.5	26 ±3.78	16.8 ±3.25	24.8 ±4.24
NZB	28.4 ±4.91	20.1 ±3.25	25.4 ±2.41	20.5 ±8.19	28 ±0.913	21.9 ±7.34	23.4 ±3.12	17.6 ±6.05	23.2 ±3.87
PW	22.6 ±4.3	21.5 ±6.13	20.2 ±4.21	26.1 ±4.91	26.9 ±3.26	34.3 ±4.43	22.2 ±4.45	19.9 ±2.75	24.2 ±4.80
SJL	16.9 ±7.16	15.4 ±1.79	26.3 ±3.97	16.5 ±2.6	17.4 ±5.9	21.1 ±3.67	16 ±1.69	17.5 ±2.04	18.4 ±3.63
Mean	23.2 ±5.09	21.2 ±4.09	26.0 ±3.45	21.3 ±4.52	26.2 ±4.84	28.1 ±6.03	20.9 ±4.20	19.1 ±2.01	

******end of Churchill project******

MOUSE MODELS: BONE PHENOTYPES

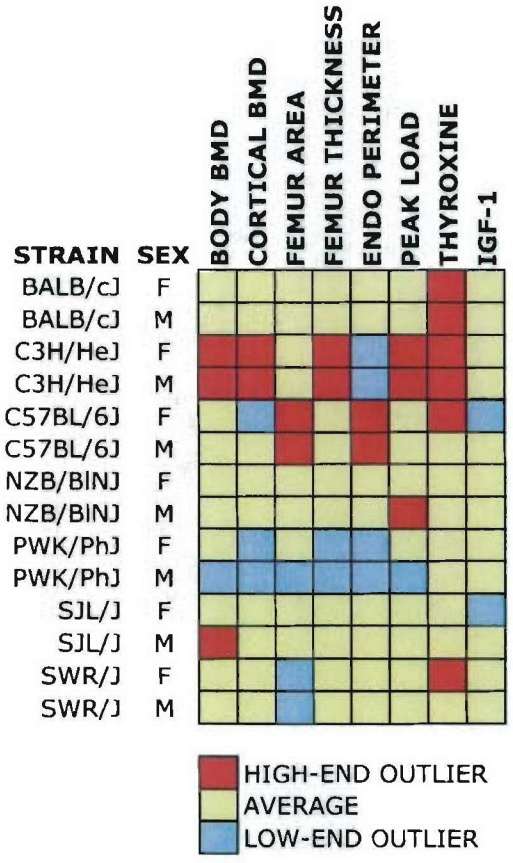

These strains were identified using the 'Find Mouse Models - Criteria Fit Tool' available on the MPD website. Data from both Donahue projects were selected for this application. Users must first carefully choose the best measurements for their application and apply criteria for each. This table simplifies the query results which are tabular Z-scores and other statistics with relevant links to protocols and supplementary measurement descriptions. The Find Mouse Models tools assists in idendifying strains having specific complex phenotypes. Optimal control strains can be identified as well.

APPENDICES

Part II: Decomposition of Skeletal Mineral and Lean Body Mass for Mouse Genetic Models:

Table 1: Strain means for 10 selected strains
Table 2: Sex effect within strains for 10 selected strains
Table 3: Correlation of traits for 9 strains (without C3H/HeJ)
Table 4: Regression of predictors for 9 strains (without C3H/HeJ)
Table 5: Correlation of predictors for 9 strains (without C3H/HeJ)
Scatter Plots 1: Examples of comparisons with C3H/HeJ
Scatter Plots 2: Examples of comparisons without C3H/HeJ
Table 6: Strain means for 28 strains
Table 7: Sex effect within strains, 28 strains
Table 8: Correlation of traits, 28 strains
Abstract 1: Entitled, "Using Inbred Mouse Strains to Identify Models for Determining Genetic Regulation of Bone Strength," Plenary Poster for "Bone Quality: What Is It and How Can We Measure It?" meeting in Bethesda, MD, May 2-3, 2005.
Presentation 1: "Skeletal Plasticity," presented to the Scientific Staff at The Jackson Laboratory by Dr. Donahue, March 17, 2004.

Table 1. Strain Means																		
Female data	**Peak Load**			**Load At Break**			**Energy To Yield**			**Work to Failure**			**Load At Yield**			**Stiffness**		
Strains	**MEAN**	**SD**	**N**	**MEAN**	**SD**	**N**	**MEAN**	**SD**	**N**	**MEAN**	**SD**	**N**	**MEAN**	**SD**	**N**	**MEAN**	**SD**	**N**
129S1/SvImJ	23.741	1.26	10	23.004	1.03	10	0.5731	0.055	10	3.3623	0.52	10	14.1	0.77	10	188.62	8.959	10
BALB/cJ	30.278	0.69	10	29.097	0.86	10	0.7136	0.029	10	5.2174	0.39	10	16.355	0.48	10	197.6	3.92	10
C3H/HeJ	39.737	0.9	9	38.366	0.77	9	1.3577	0.054	9	6.9697	0.51	9	23.519	0.65	9	222.63	7.604	9
C57BL/6J	20.93	0.86	10	17.078	1.37	10	0.381	0.053	10	8.4788	0.51	9	10.264	0.75	10	148.3	4.927	10
C58/J	23.992	0.66	10	22.255	0.95	10	0.609	0.072	10	5.0701	0.35	10	13.063	0.81	10	160.27	5.989	10
FVB/NJ	26.857	0.61	11	25.971	0.8	11	0.5396	0.054	10	6.1175	0.3	11	12.277	0.47	10	170.83	5.962	11
NZB/BINJ	30.756	0.88	11	29.754	0.86	11	0.60009	0.038	11	7.8919	0.57	11	14.228	0.48	11	184.02	6.572	11
PWK/Ph	18.991	0.7	12	17.706	0.84	12	0.49483	0.038	12	3.5058	0.34	12	11.015	0.53	12	127.37	5.764	12
SJL/J	26.344	1.12	8	23.052	1.36	8	0.47387	0.032	8	6.1565	0.78	8	12.326	0.23	8	168.41	7.641	8
SWR/J	21.601	0.42	9	19.838	0.55	9	0.37367	0.032	9	4.7831	0.4	9	9.2822	0.27	9	133.74	7.132	9
Male data																		
Strains	**MEAN**	**SD**	**N**	**MEAN**	**SD**	**N**	**MEAN**	**SD**	**N**	**MEAN**	**SD**	**N**	**MEAN**	**SD**	**N**	**MEAN**	**SD**	**N**
129S1/SvImJ	28.037	1.03	15	26.579	1.12	15	0.63327	0.052	15	5.1794	0.52	15	15.292	0.48	14	196.86	6.444	14
BALB/cJ	32.184	0.54	10	31.633	0.6	10	0.88644	0.047	9	5.5907	0.27	10	17.428	0.49	9	185.35	6.835	10
C3H/HeJ	45.193	1.27	11	44.512	1.34	11	1.279	0.073	11	8.3476	0.6	11	23.692	0.84	11	243.26	8.419	11
C57BL/6J	26.252	0.7	12	25.154	1.19	12	1.1092	0.132	12	5.9122	0.62	12	17.463	0.93	12	160.58	4.57	12
C58/J	23.632	0.89	10	22.789	0.93	10	0.6423	0.051	10	5.4547	0.48	10	13.064	0.51	10	150.94	5.467	10
FVB/NJ	24.18	0.71	9	23.282	0.84	9	0.48778	0.044	9	6.1194	0.87	9	11.178	0.43	9	150.13	5.717	9
NZB/BINJ	37.112	0.95	13	35.602	1.14	13	0.87515	0.064	13	9.2942	0.96	13	18.005	0.58	13	211.08	4.47	13
PWK/Ph	18.615	0.82	11	16.646	1.41	11	0.47391	0.056	11	3.6821	0.34	11	10.788	0.77	11	128.37	5.216	11
SJL/J	28.302	0.63	11	23.578	1.56	11	0.58664	0.072	11	8.8785	0.71	11	13.352	0.63	11	168.98	6.542	11
SWR/J	24.086	1.05	10	23.225	1.09	10	0.4369	0.067	10	6.3683	0.81	10	10.149	0.51	10	132.75	10.89	10

Part II
Table 1

Table 1. Strain

Female data	µCT CRT Thickness			femur lgth			A/P Diam			M/L Diam			whole body wt			isolated quad wt		
Strains	**MEAN**	**SD**	**N**	**MEAN**	**SD**	**N**	**MEAN**	**SD**	**N**	**MEAN**	**SD**	**N**	**MEAN**	**SD**	**N**	**MEAN**	**SD**	**N**
129S1/SvImJ	0.2396	0	10	15.644	0.12	10	1.23	0.015	10	1.445	0.029	10	20.142	0.63	10	0.16941	0.0102	10
BALB/cJ	0.2665	0	10	15.652	0.16	10	1.261	0.061	10	1.725	0.075	10	23.901	0.55	10	0.17958	0.0053	10
C3H/HeJ	0.36511	0.01	9	15.077	0.09	9	1.1078	0.029	9	1.4533	0.025	9	22.152	0.58	9	0.14824	0.0092	9
C57BL/6J	0.2026	0	10	15.506	0.13	10	1.224	0.022	10	1.694	0.057	10	21.925	0.68	8	0.20964	0.0127	10
C58/J	0.2247	0	10	15.444	0.1	10	1.207	0.023	10	1.577	0.034	10	21.177	0.53	10	0.15942	0.0051	10
FVB/NJ	0.2331	0	10	15.077	0.12	11	1.1564	0.048	11	1.5291	0.047	11	22.666	0.64	11	0.18105	0.0062	11
NZB/BINJ	0.25873	0.01	11	16.502	0.14	11	1.2391	0.017	11	1.5973	0.028	11	26.956	1.03	10	0.1749	0.0111	11
PWK/Ph	0.20858	0	12	14.066	0.1	12	1.0775	0.008	12	1.2975	0.019	12	15.14	0.22	11	0.11645	0.0053	12
SJL/J	0.24125	0	8	14.443	0.07	8	1.1563	0.023	8	1.66	0.028	8	19.995	0.63	8	0.1669	0.0126	8
SWR/J	0.20911	0	9	14.361	0.12	9	1.1067	0.01	9	1.3189	0.023	9	17.794	0.47	9	0.14846	0.006	9
Male data																		
Strains	**MEAN**	**SD**	**N**	**MEAN**	**SD**	**N**	**MEAN**	**SD**	**N**	**MEAN**	**SD**	**N**	**MEAN**	**SD**	**N**	**MEAN**	**SD**	**N**
129S1/SvImJ	0.258	0.01	14	15.715	0.1	15	1.21	0.011	15	1.5727	0.021	15	26.085	0.67	15	0.23177	0.0156	15
BALB/cJ	0.2835	0	10	15.76	0.12	10	1.254	0.048	10	2.003	0.064	10	28.668	0.84	10	0.26391	0.009	10
C3H/HeJ	0.37755	0	11	15.594	0.05	11	1.2618	0.014	11	1.7264	0.028	11	32.003	0.59	11	0.22639	0.0153	11
C57BL/6J	0.221	0	12	16.214	0.06	12	1.3708	0.026	12	2.0475	0.032	12	30.102	0.5	12	0.27766	0.0146	12
C58/J	0.2281	0	10	15.381	0.12	10	1.235	0.026	10	1.704	0.022	10	30.625	1.43	10	0.20494	0.007	10
FVB/NJ	0.21922	0	9	15.5	0.1	9	1.32	0.012	9	1.7633	0.025	9	28.08	0.38	9	0.24047	0.0059	9
NZB/BINJ	0.28392	0	13	16.721	0.09	13	1.3408	0.019	13	1.7954	0.034	13	32.155	0.65	13	0.24056	0.0048	13
PWK/Ph	0.208	0	11	13.865	0.17	10	1.0018	0.045	11	1.2045	0.052	11	16.429	0.64	11	0.1254	0.005	11
SJL/J	0.248	0	11	14.54	0.09	11	1.2173	0.017	11	1.8091	0.02	11	26.031	0.62	11	0.21585	0.0074	11
SWR/J	0.2236	0	10	14.856	0.05	10	1.151	0.007	10	1.493	0.013	10	23.548	0.51	10	0.22214	0.007	10

Table 1. Strain																		
Female data	**mid shaft vBMD**			**pQCT final muscle area**			**Cortical thickness**			**Peri-osteal circum**			**End-osteal circum**			**Total vBMD**		
Strains	**MEAN**	**SD**	**N**	**MEAN**	**SD**	**N**	**MEAN**	**SD**	**N**	**MEAN**	**SD**	**N**	**MEAN**	**SD**	**N**	**MEAN**	**SD**	**N**
129S1/SvImJ	766.49	7.096	10	63.517	2.01	10	0.22583	0.0042	10	4.6077	0.052	10	3.1883	0.056	10	0.7076	0.011	10
BALB/cJ	806.74	5.999	10	65.571	2.53	10	0.24457	0.0031	10	4.7552	0.039	10	3.2184	0.023	10	0.70591	0.0075	10
C3H/HeJ	1005.2	8.569	9	69.221	2.58	9	0.31437	0.0027	9	4.5548	0.027	9	2.5801	0.018	9	0.83135	0.0031	9
C57BL/6J	631.39	4.775	10	64.028	2.42	8	0.19189	0.0013	9	4.9539	0.039	9	3.7477	0.034	9	0.56612	0.0062	9
C58/J	688.88	11.68	10	54.645	1.18	10	0.20678	0.0034	9	4.7211	0.051	9	3.4214	0.053	9	0.58965	0.0121	8
FVB/NJ	693.11	9.716	11	69.676	1.6	11	0.21345	0.0014	11	4.835	0.047	11	3.4929	0.052	11	0.67986	0.0087	11
NZB/BINJ	781.95	6.897	11	76.325	2.25	10	0.23555	0.0041	11	4.6205	0.026	11	3.1402	0.026	11	0.72384	0.0093	11
PWK/Ph	715.58	8.27	12	44.813	1.79	12	0.19344	0.0024	12	4.0041	0.027	12	2.7883	0.029	12	0.6409	0.0127	12
SJL/J	726.87	15.07	7	66.344	4.87	8	0.22875	0.0044	8	4.743	0.036	8	3.3059	0.054	8	0.72669	0.0116	8
SWR/J	663.02	5.266	9	54.827	2.08	9	0.18756	0.0032	9	4.1759	0.031	9	2.9969	0.033	9	0.65148	0.0096	9
Male data																		
Strains	**MEAN**	**SD**	**N**	**MEAN**	**SD**	**N**	**MEAN**	**SD**	**N**	**MEAN**	**SD**	**N**	**MEAN**	**SD**	**N**	**MEAN**	**SD**	**N**
129S1/SvImJ	787.54	10.41	14	69.643	3.87	15	0.23112	0.004	14	4.7366	0.047	13	3.2735	0.04	13	0.69453	0.0126	14
BALB/cJ	829.35	9.798	10	81.725	2.39	10	0.25537	0.0052	10	5.039	0.057	10	3.4345	0.058	10	0.68838	0.0096	10
C3H/HeJ	966.89	9.332	10	78	3.31	10	0.33885	0.0047	11	5.0493	0.03	11	2.9203	0.035	11	0.80268	0.0076	11
C57BL/6J	619.17	10.03	12	88.726	3.86	12	0.20758	0.0025	12	5.6274	0.079	12	4.3232	0.081	12	0.60609	0.0093	12
C58/J	673.15	5.12	10	72.236	2.25	10	0.20573	0.0025	10	4.9759	0.067	10	3.6821	0.066	10	0.56961	0.0074	10
FVB/NJ	639.23	6.366	9	84.104	3.18	9	0.20126	0.0028	9	5.1314	0.018	9	3.8665	0.032	9	0.61691	0.0081	9
NZB/BINJ	780.41	9.708	13	97.005	4.02	12	0.24533	0.0036	13	4.9979	0.038	13	3.4562	0.031	13	0.6948	0.011	13
PWK/Ph	711.57	12.46	11	48.054	2.94	11	0.19163	0.0051	9	3.9355	0.063	10	2.767	0.061	10	0.60311	0.0117	10
SJL/J	687.66	8.227	11	69.525	2.35	11	0.23252	0.0026	11	5.0279	0.043	11	3.567	0.046	11	0.69225	0.0097	11
SWR/J	703.88	8.819	10	78.875	1.53	10	0.20353	0.0025	10	4.5044	0.029	10	3.2252	0.039	10	0.62225	0.0082	10

Table 1. Strain												
Female data	**Cortical vBMD**			**Tra-becular vBMD**			**Estimated Elastic modulus**			**Estimated Ultimate Strengh**		
Strains	**MEAN**	**SD**	**N**	**MEAN**	**SD**	**N**	**MEAN**	**SD**	**N**	**MEAN**	**SD**	**N**
129S1/SvImJ	1.1953	0.0085	10	0.10905	0.007	10	4.233	0.11	10	253.59	13.32	10
BALB/cJ	1.1919	0.0071	10	0.09021	0.0058	10	4.42	0.14	10	329.32	15.95	10
C3H/HeJ	1.232	0.0084	9	0.11053	0.0087	9	5.3011	0.29	9	408.78	19.82	9
C57BL/6J	1.0828	0.008	9	0.0739	0.0029	9	3.2899	0.07	10	216.93	11.56	10
C58/J	1.1498	0.0166	9	0.04815	0.0082	9	3.7036	0.2	10	268.83	13.01	10
FVB/NJ	1.1436	0.0073	11	0.07773	0.0041	11	3.5578	0.16	10	256.51	8.719	10
NZB/BINJ	1.1744	0.0027	11	0.09931	0.0046	11	4.1221	0.11	11	331.26	8.491	11
PWK/Ph	1.0678	0.008	12	0.12064	0.0059	12	4.9896	0.22	12	280.82	11.89	12
SJL/J	1.16	0.0135	8	0.08075	0.0053	8	4.3513	0.21	8	310.04	18.58	8
SWR/J	1.1049	0.0091	9	0.0926	0.0098	9	5.064	0.31	9	308.23	18.62	9
Male data												
Strains	**MEAN**	**SD**	**N**	**MEAN**	**SD**	**N**	**MEAN**	**SD**	**N**	**MEAN**	**SD**	**N**
129S1/SvImJ	1.1965	0.0086	13	0.1087	0.0066	14	4.0103	0.15	14	278.17	9.9	15
BALB/cJ	1.1637	0.0034	10	0.1248	0.0035	10	3.6209	0.18	10	310.75	15.67	10
C3H/HeJ	1.2204	0.005	11	0.11226	0.0055	11	4.034	0.26	10	359.41	14.06	10
C57BL/6J	1.08	0.0057	12	0.09851	0.0051	12	2.1783	0.1	12	206.22	8.993	12
C58/J	1.122	0.0045	10	0.07676	0.0037	10	3.035	0.09	10	225.01	10.77	10
FVB/NJ	1.0948	0.0045	9	0.08984	0.0037	9	2.6193	0.11	9	210.92	11.15	9
NZB/BINJ	1.1728	0.0052	13	0.09004	0.006	13	3.2335	0.09	13	303.62	7.062	13
PWK/Ph	1.064	0.0052	10	0.09323	0.0073	10	5.6325	0.25	11	267.51	14.6	11
SJL/J	1.1137	0.0066	11	0.10099	0.0055	11	3.4436	0.15	11	301.7	13.84	11
SWR/J	1.1059	0.0043	10	0.11236	0.0041	10	3.788	0.3	10	324.6	12.8	10

Table 2. P-value of Sex Effect within each strain

Strains	Peak Load	Load At Break	Energy To Yield	Work to Failure	Load At Yield	Stiffness	µCT CRT Thickness	femur lgth	A/P Diam	M/L Diam	whole body wt
129S1/SvImJ	0.01488	0.03704	0.45085	0.02776	0.73864	0.45097	0.01521	0.66499	0.28771	0.00128	0.00000
BALB/cJ	0.04223	0.02707	0.09462	0.44010	0.11875	0.13753	0.00337	0.58943	0.92897	0.01132	0.00016
C3H/HeJ	0.00356	0.00146	0.41755	0.10544	0.87704	0.09177	0.04982	0.00009	0.00009	0.00000	0.00000
C57BL/6J	0.00010	0.00024	0.00012	0.00679	0.00001	0.08307	0.00019	0.00003	0.00041	0.00001	0.00000
C58/J	0.74883	0.69193	0.71004	0.52652	0.99917	0.26534	0.43516	0.69167	0.43334	0.00533	0.00001
FVB/NJ	0.00985	0.03327	0.28769	0.99816	0.15205	0.02378	0.00197	0.01739	0.00722	0.00066	0.00000
NZB/BINJ	0.00008	0.00063	0.00187	0.24578	0.00007	0.00206	0.00149	0.19238	0.00072	0.00021	0.00022
PWK/Ph	0.72900	0.51716	0.75813	0.71796	0.80735	0.89949	0.91879	0.30099	0.09580	0.09837	0.07221
SJL/J	0.12189	0.81151	0.22116	0.02064	0.20292	0.95586	0.14650	0.44711	0.04107	0.00036	0.00000
SWR/J	0.04943	0.01600	0.42524	0.10968	0.16692	0.94154	0.00472	0.00147	0.00212	0.00000	0.00000
All 10 strains	0.00398	0.00455	0.00808	0.01981	0.01534	0.28463	0.05354	0.01510	0.00033	0.00000	0.00000

	p<0.05	p<0.005

Strains	isolated quad wt	mid shaft vBMD	pQCT final muscle area	Cortical thickness	PERI C	ENDO C	Total vBMD	Cortical vBMD	Trab vBMD	Estimated Elastic modulus	Estimated Ultimate Strengh
129S1/SvImJ	0.00680	0.14002	0.23700	0.37687	0.08072	0.21670	0.46675	0.92427	0.97184	0.21166	0.14449
BALB/cJ	0.00000	0.06466	0.00020	0.08940	0.00066	0.00294	0.16570	0.00215	0.00008	0.00231	0.41707
C3H/HeJ	0.00062	0.00801	0.05499	0.00046	0.00000	0.00000	0.00455	0.23071	0.86392	0.00498	0.05460
C57BL/6J	0.00262	0.31479	0.00014	0.00008	0.00000	0.00001	0.00366	0.77288	0.00117	0.00000	0.46653
C58/J	0.00005	0.23331	0.00000	0.80726	0.00844	0.00765	0.08237	0.10840	0.00413	0.00785	0.01831
FVB/NJ	0.00000	0.00034	0.00044	0.00063	0.00004	0.00002	0.00006	0.00004	0.04792	0.00024	0.00465
NZB/BINJ	0.00001	0.90190	0.00040	0.08327	0.00000	0.00000	0.06145	0.79987	0.24813	0.00000	0.01929
PWK/Ph	0.23512	0.78789	0.34746	0.30437	0.29754	0.74422	0.04382	0.70621	0.00750	0.06675	0.48399
SJL/J	0.00244	0.02421	0.52974	0.44394	0.00015	0.00186	0.03526	0.00381	0.02059	0.00215	0.71749
SWR/J	0.00000	0.00124	0.00000	0.00094	0.00000	0.00040	0.03235	0.91529	0.07069	0.00894	0.47106
All 10 strains	0.00000	0.70762	0.00000	0.12551	0.00000	0.00000	0.04246	0.10149	0.00655	0.00000	0.06558

Part II
Table 2

Table 3: Correlation of Traits

Based on 9 Female Strains means	Peak Load	Load At Break	Energy To Yield	Work to Failure	Load At Yield	Stiffness	µCT CRT Thickness	femur lgth	A/P Diam	M/L Diam	whole body wt	isolated quad wt	mid shaft vBMD	pQCT final muscle area	Cortical thickness	PERI C	ENDO C	Total vBMD	Cortical vBMD	Trab vBMD	Estimated Elastic modulus	Estimated Ultimate Strengh
Peak Load	1.00	0.97	0.70	0.35	0.79	0.85	0.94	0.64	0.63	0.61	0.85	0.40	0.71	0.81	0.89	0.49	0.14	0.67	0.80	-0.13	-0.19	0.60
Load At Break	0.97	1.00	0.78	0.18	0.82	0.84	0.94	0.63	0.57	0.45	0.79	0.27	0.78	0.73	0.88	0.36	0.00	0.71	0.82	-0.02	-0.10	0.61
Energy To Yield	0.70	0.78	1.00	-0.19	0.95	0.77	0.82	0.55	0.59	0.36	0.52	0.04	0.82	0.29	0.79	0.25	-0.09	0.42	0.75	-0.03	-0.08	0.40
Work to Failure	0.35	0.18	-0.19	1.00	-0.08	0.12	0.08	0.47	0.40	0.66	0.67	0.74	-0.23	0.65	0.08	0.62	0.65	-0.14	-0.06	-0.41	-0.62	-0.07
Load At Yield	0.79	0.82	0.95	-0.08	1.00	0.91	0.91	0.64	0.73	0.51	0.62	0.22	0.89	0.48	0.92	0.38	0.00	0.56	0.86	0.03	-0.12	0.41
Stiffness	0.85	0.84	0.77	0.12	0.91	1.00	0.91	0.72	0.82	0.61	0.75	0.51	0.77	0.75	0.93	0.61	0.24	0.63	0.94	-0.06	-0.31	0.28
µCT CRT Thickness	0.94	0.94	0.82	0.08	0.91	0.91	1.00	0.58	0.63	0.51	0.69	0.24	0.90	0.67	0.98	0.36	-0.06	0.79	0.89	0.08	-0.01	0.63
femur lgth	0.64	0.63	0.55	0.47	0.64	0.72	0.58	1.00	0.90	0.56	0.89	0.63	0.44	0.70	0.57	0.59	0.39	0.15	0.60	-0.18	-0.54	0.05
A/P Diam	0.63	0.57	0.59	0.40	0.73	0.82	0.63	0.90	1.00	0.76	0.81	0.73	0.46	0.65	0.66	0.74	0.51	0.14	0.69	-0.29	-0.56	0.01
M/L Diam	0.61	0.45	0.36	0.66	0.51	0.61	0.51	0.56	0.76	1.00	0.73	0.79	0.21	0.65	0.57	0.88	0.71	0.07	0.44	-0.54	-0.64	0.04
whole body wt	0.85	0.79	0.52	0.67	0.62	0.75	0.69	0.89	0.81	0.73	1.00	0.71	0.41	0.88	0.66	0.70	0.47	0.30	0.61	-0.31	-0.57	0.23
isolated quad wt	0.40	0.27	0.04	0.74	0.22	0.51	0.24	0.63	0.73	0.79	0.71	1.00	-0.08	0.74	0.29	0.91	0.87	-0.08	0.31	-0.46	-0.79	-0.32
mid shaft vBMD	0.71	0.78	0.82	-0.23	0.89	0.77	0.90	0.44	0.46	0.21	0.41	-0.08	1.00	0.38	0.89	0.01	-0.40	0.79	0.77	0.43	0.28	0.64
pQCT final muscle area	0.81	0.73	0.29	0.65	0.48	0.75	0.67	0.70	0.65	0.65	0.88	0.74	0.38	1.00	0.68	0.70	0.47	0.53	0.63	-0.15	-0.50	0.19
Cortical thickness	0.89	0.88	0.79	0.08	0.92	0.93	0.98	0.57	0.66	0.57	0.66	0.29	0.89	0.68	1.00	0.43	0.01	0.78	0.90	0.08	-0.07	0.54
PERI C	0.49	0.36	0.25	0.62	0.38	0.61	0.36	0.59	0.74	0.88	0.70	0.91	0.01	0.70	0.43	1.00	0.91	-0.03	0.45	-0.64	-0.87	-0.30
ENDO C	0.14	0.00	-0.09	0.65	0.00	0.24	-0.06	0.39	0.51	0.71	0.47	0.87	-0.40	0.47	0.01	0.91	1.00	-0.39	0.08	-0.74	-0.93	-0.58
Total vBMD	0.67	0.71	0.42	-0.14	0.56	0.63	0.79	0.15	0.14	0.07	0.30	-0.08	0.79	0.53	0.78	-0.03	-0.39	1.00	0.69	0.46	0.36	0.67
Cortical vBMD	0.80	0.82	0.75	-0.06	0.86	0.94	0.89	0.60	0.69	0.44	0.61	0.31	0.77	0.63	0.90	0.45	0.08	0.69	1.00	-0.08	-0.13	0.40
Trab vBMD	-0.13	-0.02	-0.03	-0.41	0.03	-0.06	0.08	-0.18	-0.29	-0.54	-0.31	-0.46	0.43	-0.15	0.08	-0.64	-0.74	0.46	-0.08	1.00	0.66	0.25
Estimated Elastic modulus	-0.19	-0.10	-0.08	-0.62	-0.12	-0.31	-0.01	-0.54	-0.56	-0.64	-0.57	-0.79	0.28	-0.50	-0.07	-0.87	-0.93	0.36	-0.13	0.66	1.00	0.61
Estimated Ultimate Strengh	0.60	0.61	0.40	-0.07	0.41	0.28	0.63	0.05	0.01	0.04	0.23	-0.32	0.64	0.19	0.54	-0.30	-0.58	0.67	0.40	0.25	0.61	1.00

Significance threshold of correlation: r>=0.924
(p<0.05, based on 1000 permutation tests)

Based on 9 Male Strains means	Peak Load	Load At Break	Energy To Yield	Work to Failure	Load At Yield	Stiffness	µCT CRT Thickness	femur lgth	A/P Diam	M/L Diam	whole body wt	isolated quad wt	mid shaft vBMD	pQCT final muscle area	Cortical thickness	PERI C	ENDO C	Total vBMD	Cortical vBMD	Trab vBMD	Estimated Elastic modulus	Estimated Ultimate Strengh
Peak Load	1.00	0.97	0.58	0.71	0.80	0.91	0.93	0.75	0.62	0.61	0.69	0.63	0.59	0.72	0.90	0.47	0.20	0.77	0.75	0.27	-0.36	0.43
Load At Break	0.97	1.00	0.61	0.59	0.81	0.88	0.90	0.84	0.66	0.62	0.73	0.69	0.60	0.78	0.85	0.48	0.23	0.67	0.76	0.28	-0.40	0.36
Energy To Yield	0.58	0.61	1.00	0.21	0.92	0.55	0.44	0.74	0.68	0.77	0.64	0.67	0.11	0.60	0.47	0.71	0.60	0.20	0.23	0.13	-0.52	-0.19
Work to Failure	0.71	0.59	0.21	1.00	0.33	0.52	0.51	0.39	0.52	0.44	0.53	0.39	0.06	0.60	0.52	0.43	0.28	0.54	0.30	-0.07	-0.44	0.35
Load At Yield	0.80	0.81	0.92	0.33	1.00	0.83	0.73	0.80	0.64	0.72	0.67	0.65	0.42	0.58	0.74	0.61	0.40	0.51	0.57	0.21	-0.40	0.04
Stiffness	0.91	0.88	0.55	0.52	0.83	1.00	0.90	0.73	0.55	0.50	0.61	0.53	0.63	0.52	0.87	0.41	0.14	0.80	0.87	0.20	-0.25	0.28
µCT CRT Thickness	0.93	0.90	0.44	0.51	0.73	0.90	1.00	0.58	0.37	0.46	0.51	0.46	0.82	0.46	0.98	0.25	-0.06	0.84	0.87	0.41	-0.10	0.57
femur lgth	0.75	0.84	0.74	0.39	0.80	0.73	0.58	1.00	0.87	0.70	0.87	0.80	0.20	0.88	0.52	0.72	0.58	0.29	0.56	0.00	-0.69	-0.15
A/P Diam	0.62	0.66	0.68	0.52	0.64	0.55	0.37	0.87	1.00	0.87	0.92	0.88	-0.16	0.90	0.38	0.94	0.86	0.18	0.28	-0.11	-0.93	-0.35
M/L Diam	0.61	0.62	0.77	0.44	0.72	0.50	0.46	0.70	0.87	1.00	0.83	0.89	-0.04	0.75	0.54	0.94	0.82	0.26	0.24	0.17	-0.83	-0.19
whole body wt	0.69	0.73	0.64	0.53	0.67	0.61	0.51	0.87	0.92	0.83	1.00	0.80	0.01	0.85	0.49	0.85	0.74	0.18	0.46	-0.17	-0.86	-0.22
isolated quad wt	0.63	0.69	0.67	0.39	0.65	0.53	0.46	0.80	0.88	0.89	0.80	1.00	0.05	0.86	0.51	0.87	0.75	0.33	0.40	0.35	-0.82	-0.09
mid shaft vBMD	0.59	0.60	0.11	0.06	0.42	0.63	0.82	0.20	-0.16	-0.04	0.01	0.05	1.00	0.02	0.77	-0.29	-0.56	0.72	0.80	0.56	0.43	0.72
pQCT final muscle area	0.72	0.78	0.60	0.60	0.58	0.52	0.46	0.88	0.90	0.75	0.85	0.86	0.02	1.00	0.43	0.76	0.65	0.24	0.34	0.05	-0.80	-0.04
Cortical thickness	0.90	0.85	0.47	0.52	0.74	0.87	0.98	0.52	0.38	0.54	0.49	0.51	0.77	0.43	1.00	0.32	0.01	0.87	0.81	0.50	-0.13	0.56
PERI C	0.47	0.48	0.71	0.43	0.61	0.41	0.25	0.72	0.94	0.94	0.85	0.87	-0.29	0.76	0.32	1.00	0.95	0.10	0.14	-0.05	-0.95	-0.42
ENDO C	0.20	0.23	0.60	0.28	0.40	0.14	-0.06	0.58	0.86	0.82	0.74	0.75	-0.56	0.65	0.01	0.95	1.00	-0.19	-0.13	-0.21	-0.95	-0.63
Total vBMD	0.77	0.67	0.20	0.54	0.51	0.80	0.84	0.29	0.18	0.26	0.18	0.33	0.72	0.24	0.87	0.10	-0.19	1.00	0.73	0.56	0.08	0.66
Cortical vBMD	0.75	0.76	0.23	0.30	0.57	0.87	0.87	0.56	0.28	0.24	0.46	0.40	0.80	0.34	0.81	0.14	-0.13	0.73	1.00	0.33	-0.05	0.45
Trab vBMD	0.27	0.28	0.13	-0.07	0.21	0.20	0.41	0.00	-0.11	0.17	-0.17	0.35	0.56	0.05	0.50	-0.05	-0.21	0.56	0.33	1.00	0.19	0.62
Estimated Elastic modulus	-0.36	-0.40	-0.52	-0.44	-0.40	-0.25	-0.10	-0.69	-0.93	-0.83	-0.86	-0.82	0.43	-0.80	-0.13	-0.95	-0.95	0.08	-0.05	0.19	1.00	0.47
Estimated Ultimate Strengh	0.43	0.36	-0.19	0.35	0.04	0.28	0.57	-0.15	-0.35	-0.19	-0.22	-0.09	0.72	-0.04	0.56	-0.42	-0.63	0.66	0.45	0.62	0.47	1.00

Significance threshold of correlation: r>=0.918
(p<0.05, based on 1000 permutation tests)

Part II
Table 3

Table 4: Regression analysis of 6 response variables

(A) (N=18, after excluding C3H)

Y = SEX + Xi

	SEX as ADD COV	Y=Work to Failure		*Y=Stiffness*		Y=Load.at.Yield		*Y=Peak Load*		Y=Estimated Ultimate Strength		*Y=Estimated Elastic modulus*	
	Predictor (Xi)	beta	pval	*beta*	*pval*	beta	pval	*beta*	*pval*	beta	pval	*beta*	*pval*
1	mid shaft BMD	-0.002	0.784	0.281	0.002	0.025	0.012	0.047	0.006	0.449	0.002	0.005	0.139
2	Total vBMD	5.571	0.513	343.470	0.002	25.639	0.033	62.454	0.002	512.190	0.004	2.849	0.470
3	Cortical vBMD	4.471	0.659	519.320	0.000	39.870	0.003	79.923	0.000	394.330	0.088	-1.446	0.758
4	Cortical thickness	25.466	0.226	1103.100	0.000	100.320	0.000	198.460	0.000	1078.600	0.022	-4.137	0.678
5	femur lgth	0.915	0.087	23.284	0.001	2.372	0.001	4.076	0.002	-3.431	0.798	-0.619	0.007
6	whole body wt	0.249	0.014	4.240	0.004	0.420	0.005	0.860	0.001	-0.516	0.847	-0.151	0.000
7	PERI C	2.196	0.044	31.621	0.053	3.608	0.027	5.755	0.052	-39.649	0.140	-1.899	0.000
8	M/L Diam	4.187	0.037	64.939	0.029	8.133	0.005	13.559	0.009	-22.096	0.668	-2.961	0.000
9	A/P Diam	8.927	0.064	180.920	0.008	19.591	0.004	32.445	0.008	-106.090	0.378	-7.478	0.000
10	isolated quad wt	24.717	0.041	379.600	0.034	39.010	0.032	74.329	0.020	-193.710	0.529	-18.620	0.000
11	pQCT final muscle area	0.090	0.009	1.321	0.011	0.123	0.022	0.298	0.001	0.149	0.872	-0.049	0.001

p<0.05

(B)

Y = SEX + Xi + Sex*Xi

	SEX as INT COV	Y=Y=Work to Failure		*Y=Stiffness*		Y=Load.at.Yield		*Y=Peak Load*		Y=Estimated Ultimate Strength		*Y=Estimated Elastic modulus*	
	Predictor (Xi)	beta	pval	*beta*	*pval*	beta	pval	*beta*	*pval*	beta	pval	*beta*	*pval*
1	mid shaft BMD	-0.01	0.54	0.32	0.02	0.03	0.03	0.05	0.06	0.43	0.05	0.00	0.56
	sex*V1	0.01	0.57	-0.07	0.67	-0.02	0.40	-0.01	0.85	0.03	0.92	0.00	0.65
2	Total density	-4.32	0.69	261.05	0.04	21.01	0.17	47.14	0.04	443.59	0.05	3.76	0.48
	sex*V2	23.84	0.17	198.70	0.29	11.17	0.63	36.91	0.28	165.38	0.61	-2.21	0.79
3	Cortical vBMD	-2.44	0.86	493.98	0.00	40.63	0.02	70.76	0.01	337.12	0.30	-1.68	0.80
	sex*V3	14.30	0.49	52.43	0.70	-1.58	0.95	18.95	0.60	118.36	0.79	0.49	0.96
4	Cortical thickness	7.00	0.82	1093.20	0.00	97.24	0.00	175.56	0.00	1012.00	0.14	-2.15	0.89
	sex*V4	34.44	0.41	18.50	0.95	5.74	0.89	42.70	0.43	124.14	0.89	-3.71	0.86
5	femur lgth	1.07	0.19	22.63	0.02	1.80	0.06	3.36	0.06	2.32	0.91	-0.42	0.18
	sex*V5	-0.27	0.80	1.17	0.92	1.02	0.39	1.28	0.57	-10.35	0.71	-0.35	0.40
6	whole body wt	0.34	0.04	5.31	0.03	0.39	0.10	1.01	0.01	2.59	0.58	-0.10	0.09
	sex*V6	-0.14	0.47	-1.64	0.55	0.04	0.89	-0.23	0.60	-4.74	0.41	-0.08	0.27
7	PERI C	3.51	0.07	47.34	0.11	2.70	0.34	6.47	0.22	-37.31	0.44	-1.70	0.00
	sex*V7	-1.90	0.40	-22.70	0.51	1.31	0.70	-1.04	0.87	-3.38	0.95	-0.29	0.53
8	M/L Diam	7.46	0.05	95.46	0.10	7.18	0.17	16.04	0.10	9.94	0.92	-2.49	0.06
	sex*V8	-4.45	0.30	-41.46	0.52	1.30	0.82	-3.37	0.76	-43.51	0.72	-0.64	0.66
9	A/P Diam	11.02	0.26	313.03	0.02	25.17	0.05	40.36	0.09	5.13	0.98	-5.33	0.06
	sex*V9	-2.76	0.80	-174.66	0.21	-7.37	0.59	-10.46	0.69	-147.03	0.61	-2.84	0.36
10	isolated quad wt	50.57	0.03	482.15	0.17	18.83	0.58	64.67	0.29	-491.03	0.43	-18.81	0.02
	sex*V10	-34.67	0.18	-137.55	0.73	27.07	0.49	12.95	0.85	398.80	0.58	0.25	0.98
11	pQCT final muscle area	0.12	0.04	1.93	0.04	0.11	0.24	0.35	0.02	0.78	0.65	-0.03	0.18
	sex*V11	-0.05	0.49	-0.88	0.39	0.02	0.88	-0.08	0.62	-0.92	0.66	-0.02	0.39

None of the interaction is significant at 0.05 level

Part II
Table 4

Table 5: Correlation of 11 predictors

Based on 9 Female Strains means	mid shaft vBMD	Total vBMD	Cortical vBMD	Cortical thickness	femur lgth	whole body wt	PERI C	M/L Diam	A/P Diam	isolated quad wt	pQCT final muscle area
1 mid shaft vBMD	1.00	0.79	0.77	0.89	0.44	0.41	0.01	0.21	0.46	-0.08	0.38
2 Total vBMD	0.79	1.00	0.69	0.78	0.15	0.30	-0.03	0.07	0.14	-0.08	0.53
3 Cortical vBMD	0.77	0.69	1.00	0.90	0.60	0.61	0.45	0.44	0.69	0.31	0.63
4 Cortical thickness	0.89	0.78	0.90	1.00	0.57	0.66	0.43	0.57	0.66	0.29	0.68
5 femur lgth	0.44	0.15	0.60	0.57	1.00	0.89	0.59	0.56	0.90	0.63	0.70
6 whole body wt	0.41	0.30	0.61	0.66	0.89	1.00	0.70	0.73	0.81	0.71	0.88
7 PERI C	0.01	-0.03	0.45	0.43	0.59	0.70	1.00	0.88	0.74	0.91	0.70
8 M/L Diam	0.21	0.07	0.44	0.57	0.56	0.73	0.88	1.00	0.76	0.79	0.65
9 A/P Diam	0.46	0.14	0.69	0.66	0.90	0.81	0.74	0.76	1.00	0.73	0.65
10 isolated quad wt	-0.08	-0.08	0.31	0.29	0.63	0.71	0.91	0.79	0.73	1.00	0.74
11 pQCT final muscle area	0.38	0.53	0.63	0.68	0.70	0.88	0.70	0.65	0.65	0.74	1.00

Significance threshold r = 0.89
Suggestive threshold r = 0.72

Based on 9 Male Strains means	mid shaft vBMD	Total vBMD	Cortical vBMD	Cortical thickness	femur lgth	whole body wt	PERI C	M/L Diam	A/P Diam	isolated quad wt	pQCT final muscle area
1 mid shaft vBMD	1.00	0.72	0.80	0.77	0.20	0.01	-0.29	-0.04	-0.16	0.05	0.02
2 Total vBMD	0.72	1.00	0.73	0.87	0.29	0.18	0.10	0.26	0.18	0.33	0.24
3 Cortical vBMD	0.80	0.73	1.00	0.81	0.56	0.46	0.14	0.24	0.28	0.40	0.34
4 Cortical thickness	0.77	0.87	0.81	1.00	0.52	0.49	0.32	0.54	0.38	0.51	0.43
5 femur lgth	0.20	0.29	0.56	0.52	1.00	0.87	0.72	0.70	0.87	0.80	0.88
6 whole body wt	0.01	0.18	0.46	0.49	0.87	1.00	0.85	0.83	0.92	0.80	0.85
7 PERI C	-0.29	0.10	0.14	0.32	0.72	0.85	1.00	0.94	0.94	0.87	0.76
8 M/L Diam	-0.04	0.26	0.24	0.54	0.70	0.83	0.94	1.00	0.87	0.89	0.75
9 A/P Diam	-0.16	0.18	0.28	0.38	0.87	0.92	0.94	0.87	1.00	0.88	0.90
10 isolated quad wt	0.05	0.33	0.40	0.51	0.80	0.80	0.87	0.89	0.88	1.00	0.86
11 pQCT final muscle area	0.02	0.24	0.34	0.43	0.88	0.85	0.76	0.75	0.90	0.86	1.00

Significance threshold r = 0.89
Suggestive threshold r = 0.72

Part II
Table 5

Scatter plots of strain means (by sex)

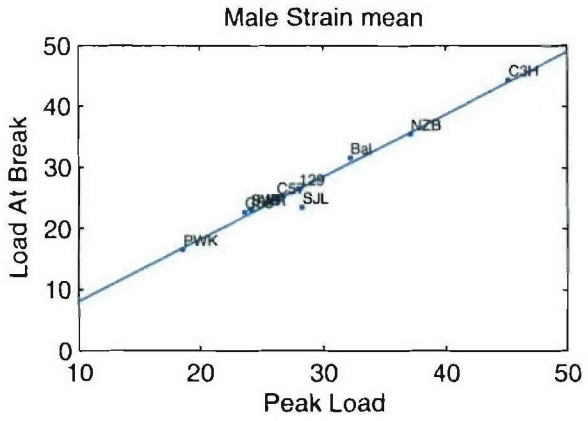
Male Strain mean
Load At Break
Peak Load
C3H
NZB
Bal
129
SJL
PWK

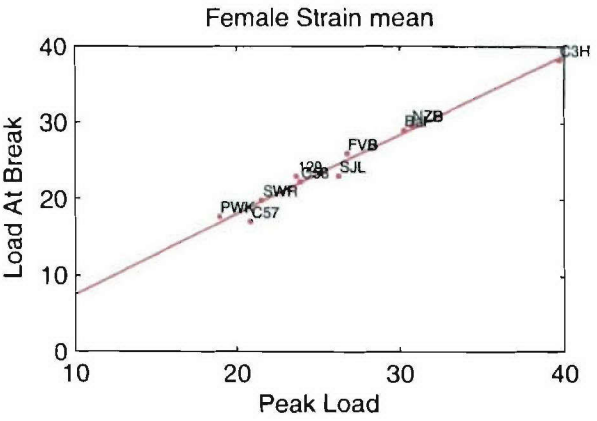
Female Strain mean
Load At Break
Peak Load
C3H
NZB
FVB
SJL
SWR
PWK
C57

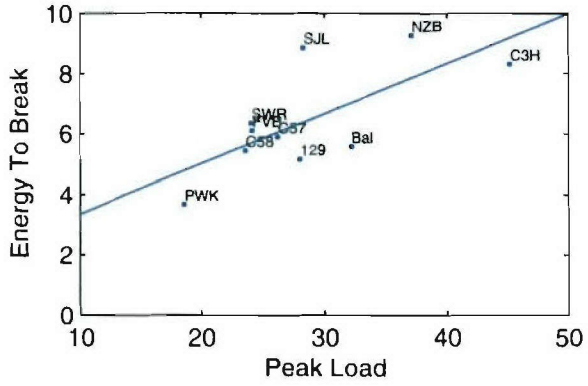
Energy To Break
Peak Load
SJL
NZB
C3H
SWR
C57
C58
129
Bal
PWK

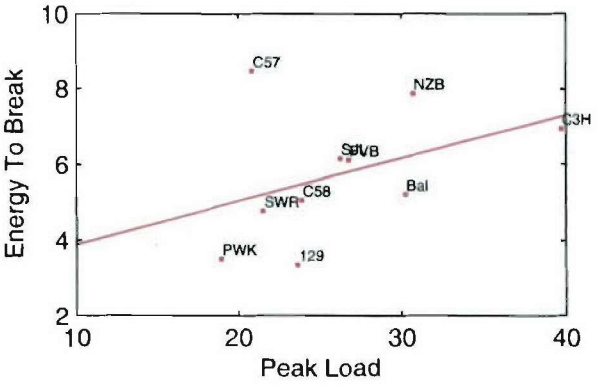
Energy To Break
Peak Load
C57
NZB
C3H
FVB
Bal
C58
SWR
PWK
129

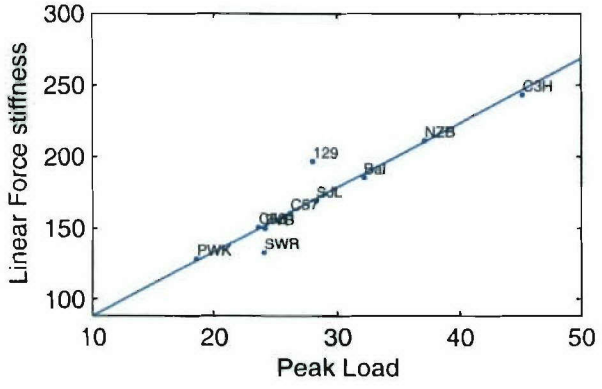
Linear Force stiffness
Peak Load
C3H
NZB
129
Bal
SJL
C57
PWK
SWR

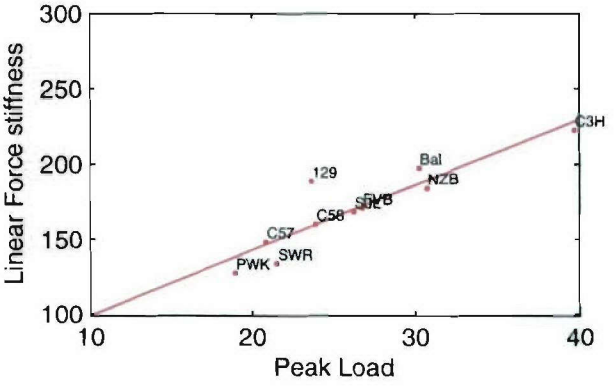
Linear Force stiffness
Peak Load
C3H
129
Bal
NZB
C58
C57
PWK
SWR

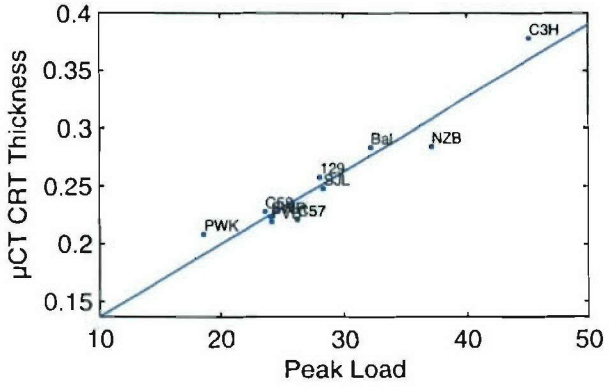
µCT CRT Thickness
Peak Load
C3H
Bal
NZB
129
SJL
PWK

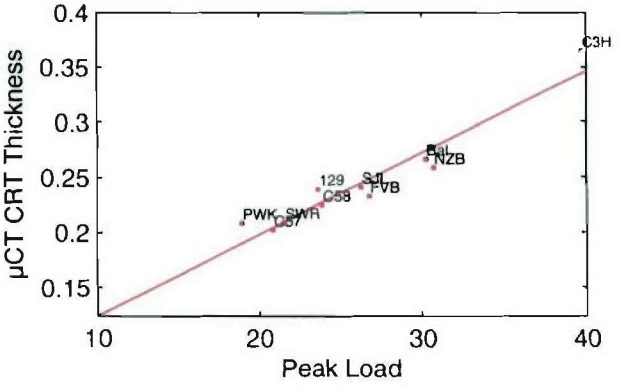
µCT CRT Thickness
Peak Load
C3H
NZB
129
SJL
FVB
C58
PWK
SWR
C57

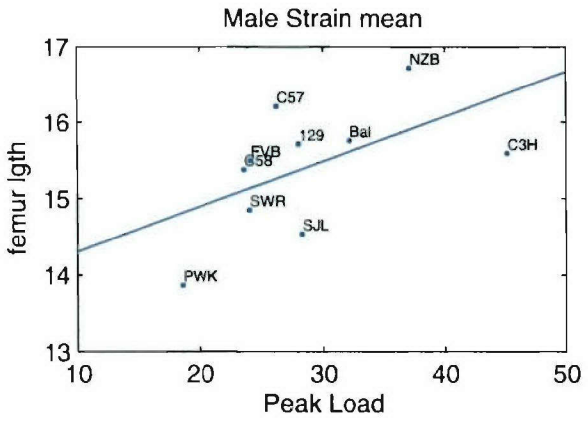
Male Strain mean
femur lgth
Peak Load
NZB
C57
129
Bal
C3H
FVB
SWR
SJL
PWK

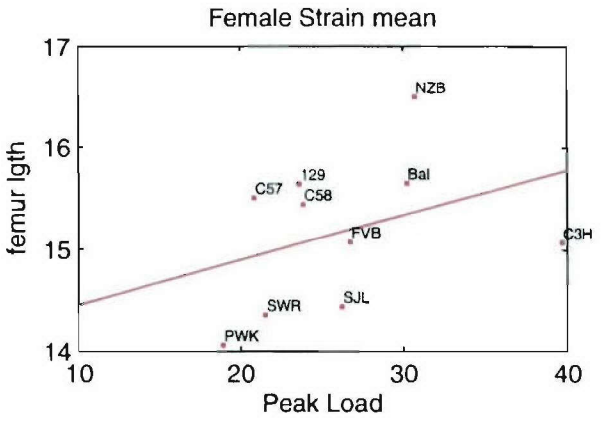
Female Strain mean
femur lgth
Peak Load
NZB
C57
129
Bal
C58
FVB
C3H
SWR
SJL
PWK

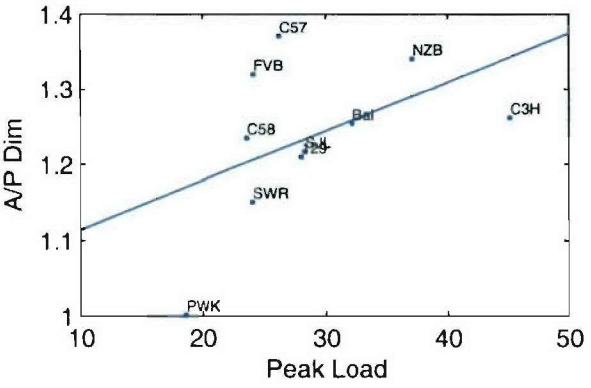
A/P Dim
Peak Load
C57
NZB
FVB
Bal
C3H
C58
SWR
PWK

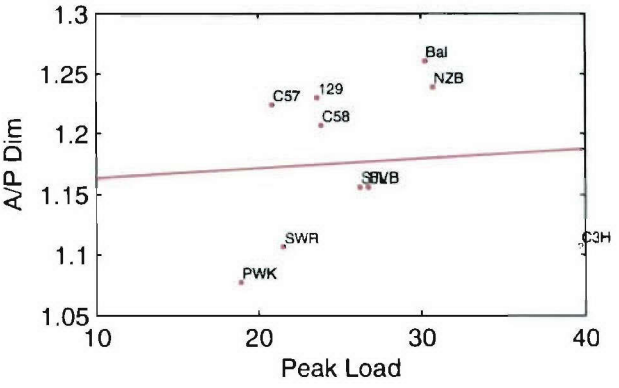
A/P Dim
Peak Load
Bal
NZB
C57
129
C58
C3H
SWR
PWK

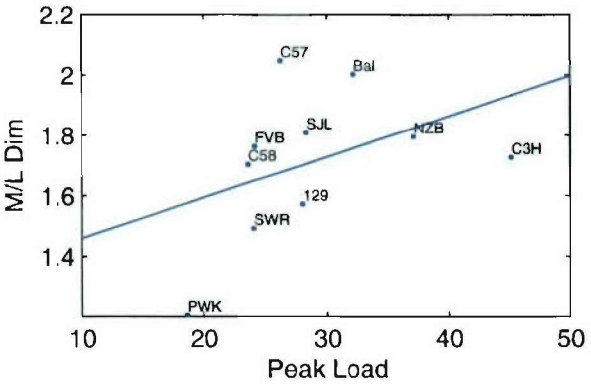
M/L Dim
Peak Load
C57
Bal
SJL
FVB
NZB
C3H
C58
129
SWR
PWK

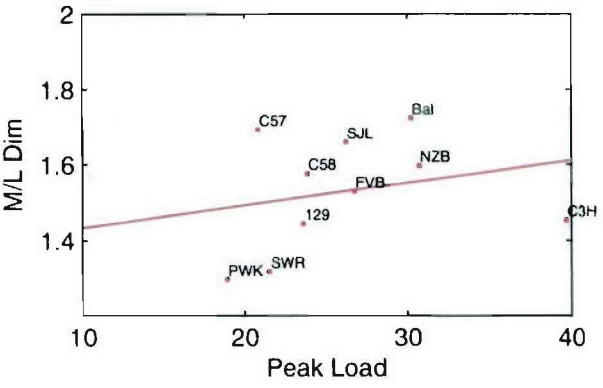
M/L Dim
Peak Load
C57
Bal
SJL
NZB
C58
FVB
129
C3H
PWK
SWR

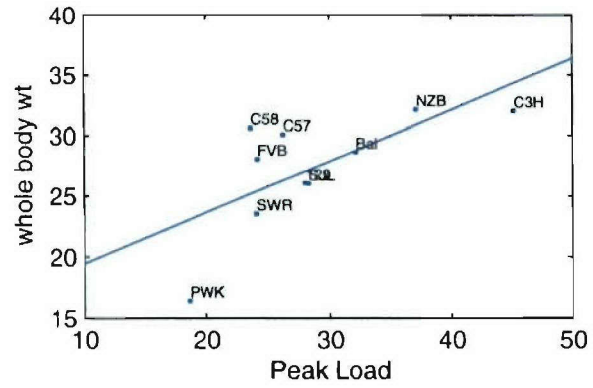
whole body wt
Peak Load
NZB
C3H
C58
C57
FVB
Bal
SWR
PWK

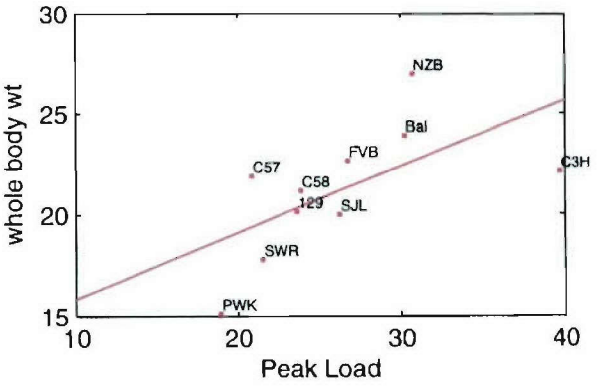
whole body wt
Peak Load
NZB
Bal
FVB
C57
C3H
C58
129
SJL
SWR
PWK

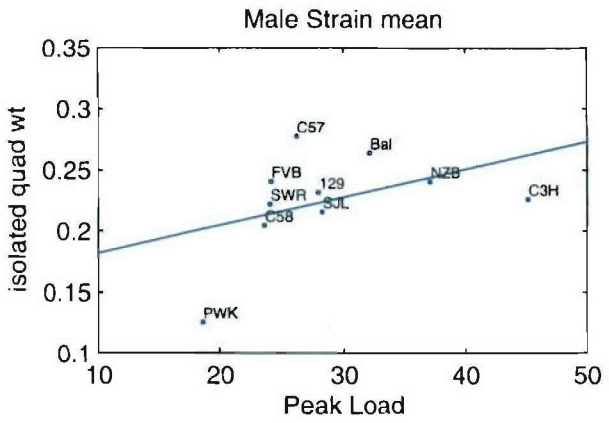
Male Strain mean
isolated quad wt
Peak Load
C57
Bal
FVB
NZB
SWR
129
C3H
SJL
C58
PWK

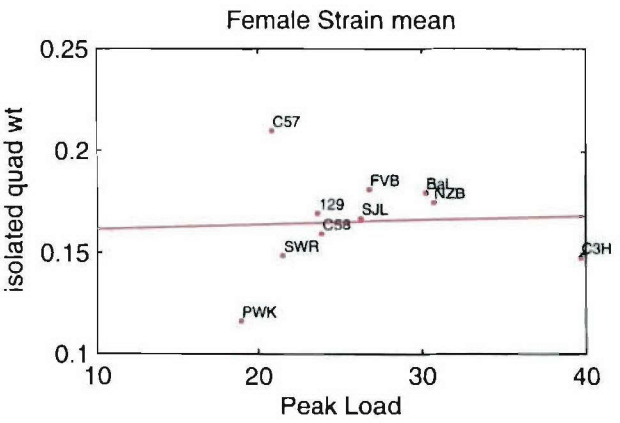
Female Strain mean
isolated quad wt
Peak Load
C57
FVB
Bal
NZB
129
SJL
C58
SWR
C3H
PWK

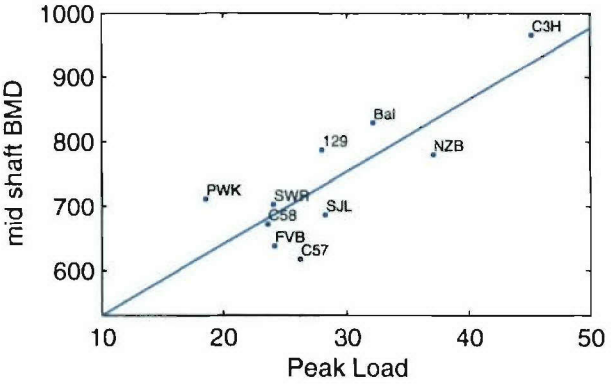
mid shaft BMD
Peak Load
C3H
Bal
129
NZB
PWK
SWR
SJL
C58
FVB
C57

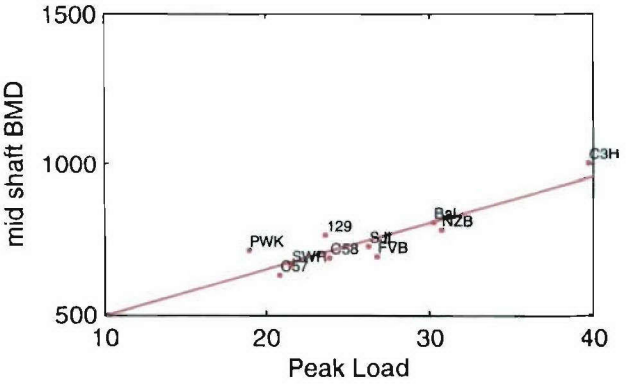
mid shaft BMD
Peak Load
C3H
Bal
NZB
129
PWK
SJL
C58
FVB
SWR
C57

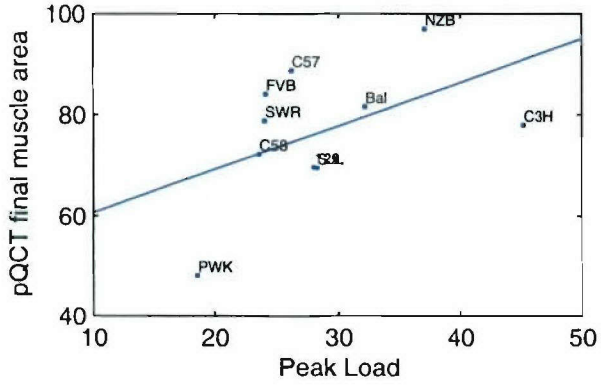
pQCT final muscle area
Peak Load
NZB
C57
FVB
SWR
Bal
C3H
C58
PWK

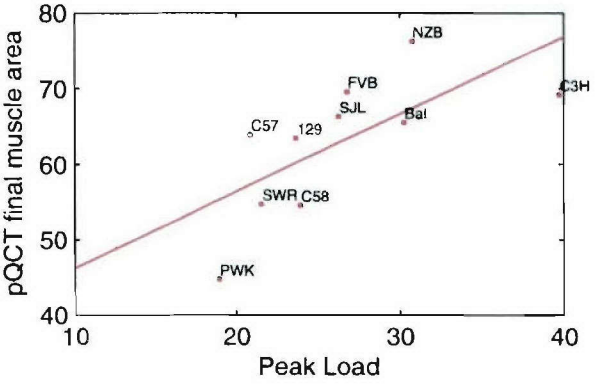
pQCT final muscle area
Peak Load
NZB
FVB
C3H
SJL
C57
129
Bal
SWR
C58
PWK

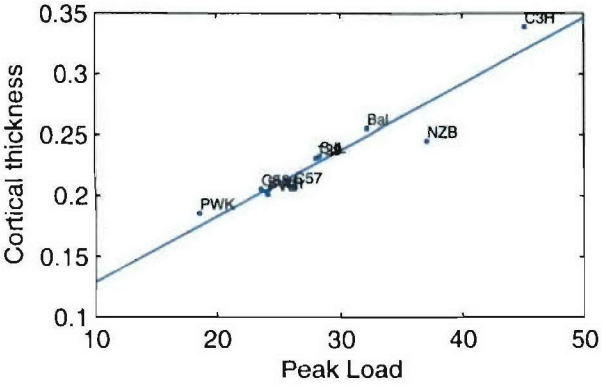
Cortical thickness
Peak Load
C3H
Bal
NZB
PWK

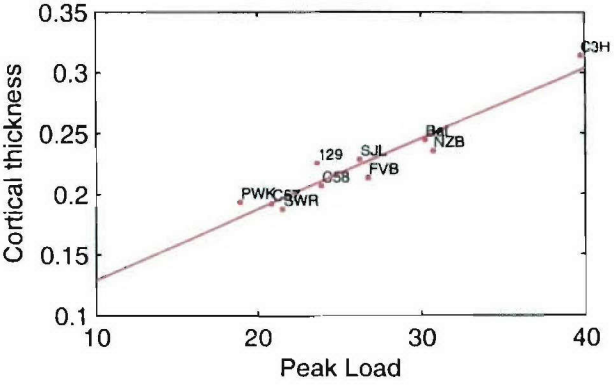
Cortical thickness
Peak Load
C3H
129
SJL
Bal
NZB
FVB
C58
PWK
C57
SWR

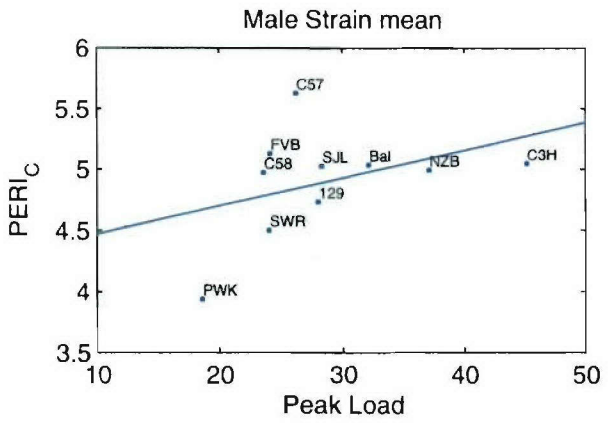
Male Strain mean
PERI$_C$
Peak Load
C57
FVB
C58
SJL
Bal
NZB
C3H
129
SWR
PWK

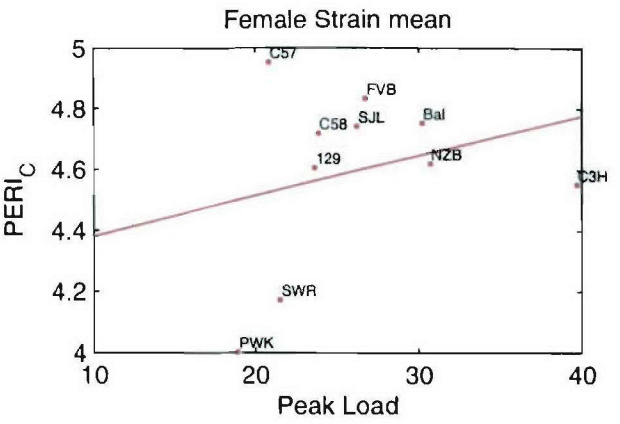
Female Strain mean
PERI$_C$
Peak Load
C57
FVB
C58
SJL
Bal
129
NZB
C3H
SWR
PWK

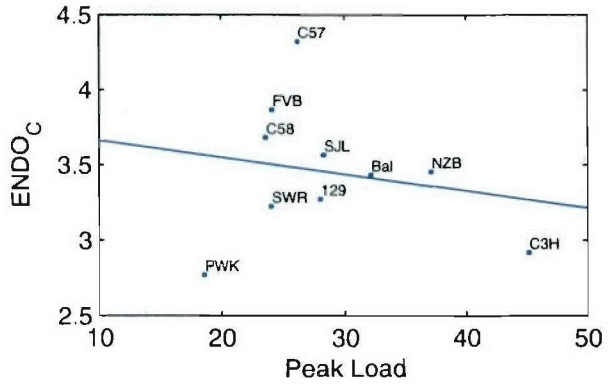
ENDO$_C$
Peak Load
C57
FVB
C58
SJL
Bal
NZB
SWR
129
C3H
PWK

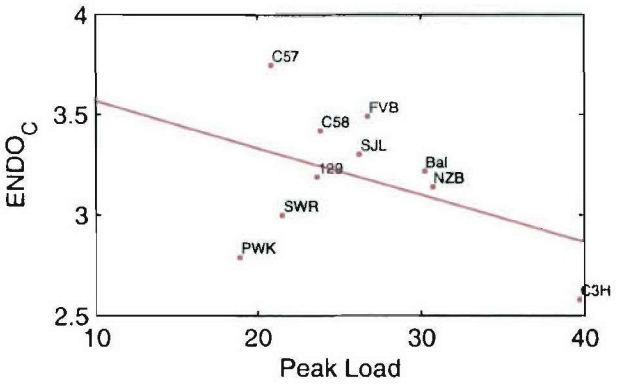
ENDO$_C$
Peak Load
C57
C58
FVB
SJL
129
Bal
NZB
SWR
PWK
C3H

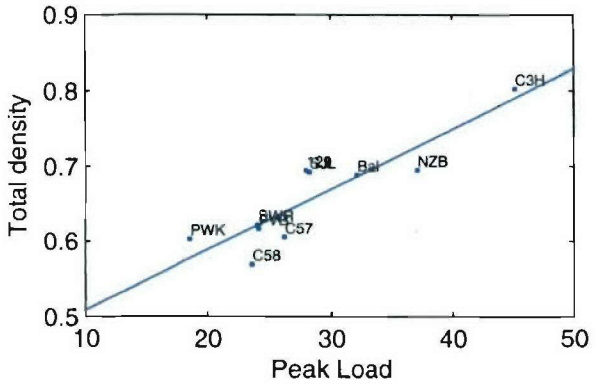
Total density
Peak Load
C3H
Bal
NZB
PWK
C57
C58

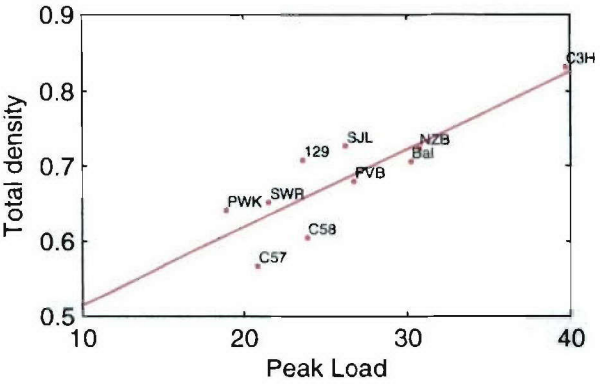
Total density
Peak Load
C3H
129
SJL
NZB
Bal
FVB
PWK
SWR
C58
C57

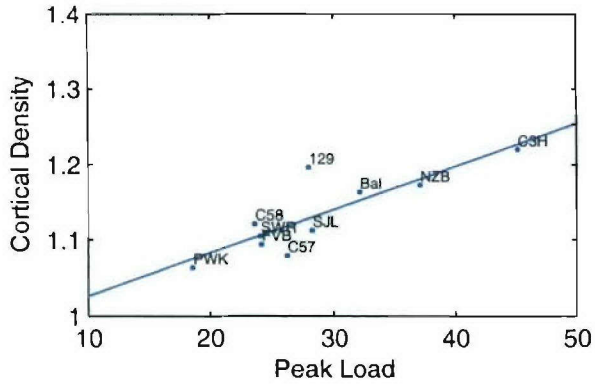
Cortical Density
Peak Load
129
C3H
Bal
NZB
C58
SJL
PWK
C57

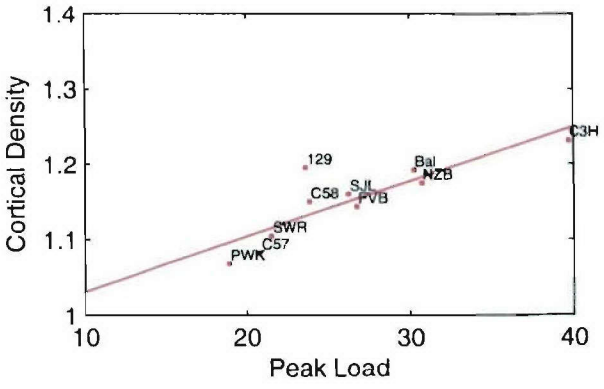
Cortical Density
Peak Load
129
Bal
NZB
C58
SJL
FVB
C3H
SWR
C57
PWK

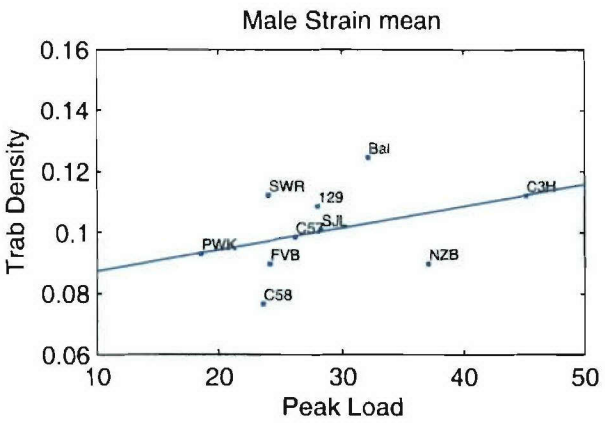
Male Strain mean
Trab Density
Peak Load
0.16
0.14
0.12
0.1
0.08
0.06
10
20
30
40
50
Bal
SWR
129
C3H
SJL
C57
PWK
FVB
NZB
C58

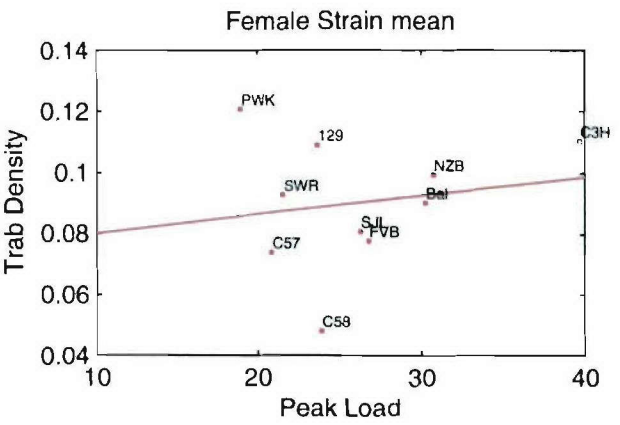
Female Strain mean
Trab Density
Peak Load
0.14
0.12
0.1
0.08
0.06
0.04
10
20
30
40
PWK
129
C3H
NZB
SWR
Bal
SJL
FVB
C57
C58

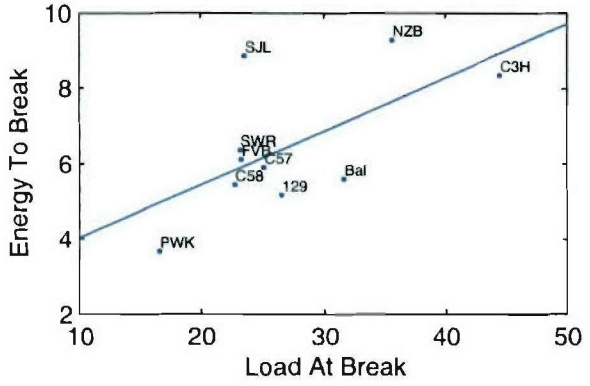
Energy To Break
Load At Break
10
8
6
4
2
10
20
30
40
50
NZB
SJL
C3H
SWR
FVB
C57
C58
Bal
129
PWK

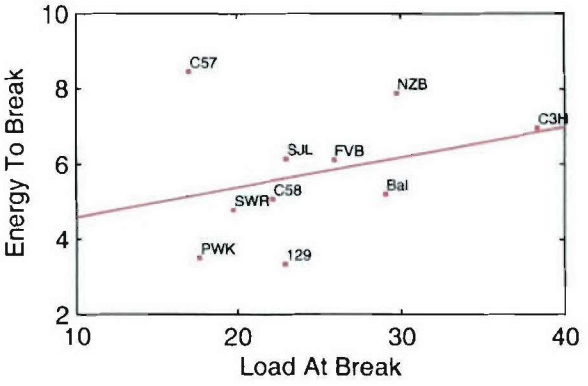
Energy To Break
Load At Break
10
8
6
4
2
10
20
30
40
C57
NZB
C3H
SJL
FVB
Bal
SWR
C58
PWK
129

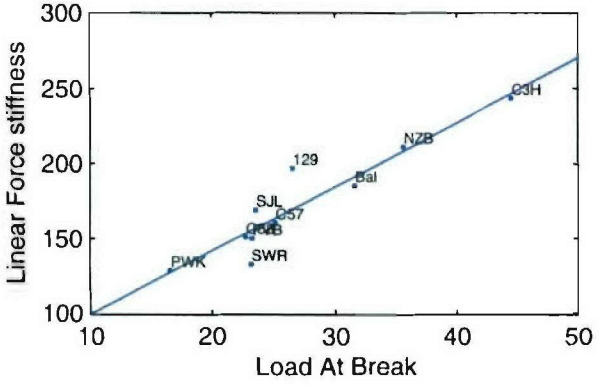
Linear Force stiffness
Load At Break
300
250
200
150
100
10
20
30
40
50
C3H
NZB
129
Bal
SJL
C57
PWK
SWR

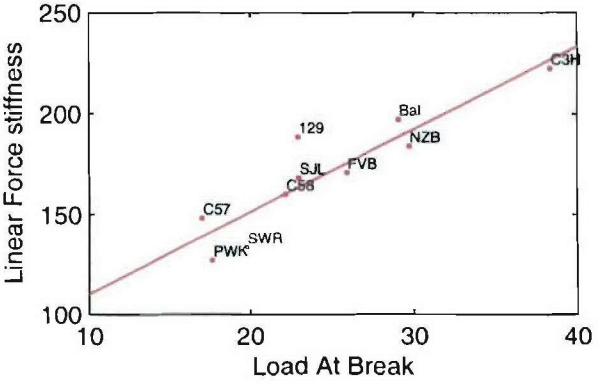
Linear Force stiffness
Load At Break
250
200
150
100
10
20
30
40
C3H
Bal
129
NZB
SJL
FVB
C58
C57
PWK
SWR

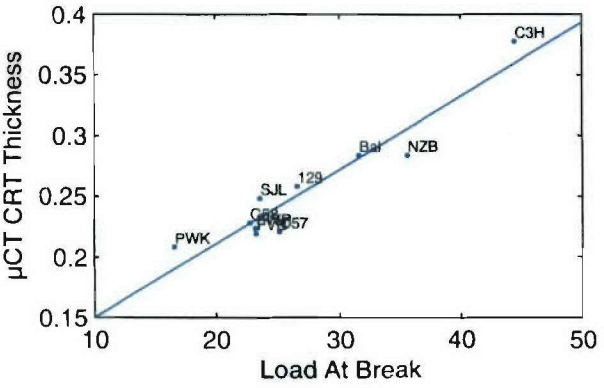
µCT CRT Thickness
Load At Break
0.4
0.35
0.3
0.25
0.2
0.15
10
20
30
40
50
C3H
Bal
NZB
129
SJL
PWK
C57

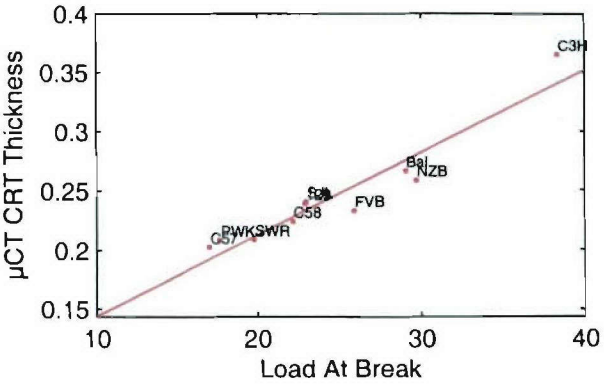
µCT CRT Thickness
Load At Break
0.4
0.35
0.3
0.25
0.2
0.15
10
20
30
40
C3H
Bal
NZB
FVB
C58
PWK
SWR
C57

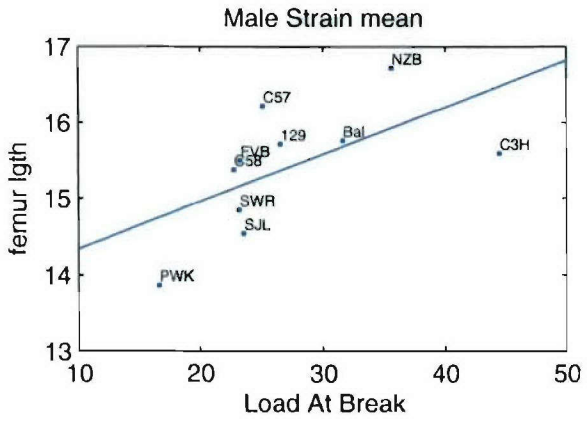
Male Strain mean
femur lgth
Load At Break
NZB
C57
129
Bal
C3H
FVB
C58
SWR
SJL
PWK

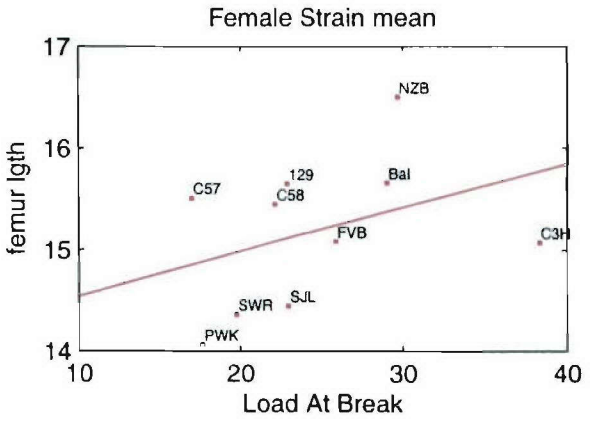
Female Strain mean
femur lgth
Load At Break
NZB
C57
129
Bal
C58
FVB
C3H
SWR
SJL
PWK

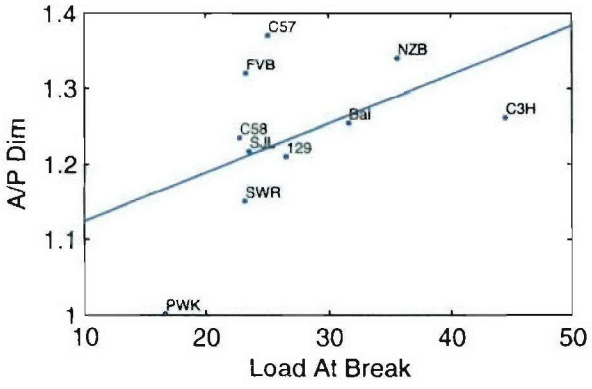
A/P Dim
Load At Break
C57
NZB
FVB
C3H
Bal
C58
SJL
129
SWR
PWK

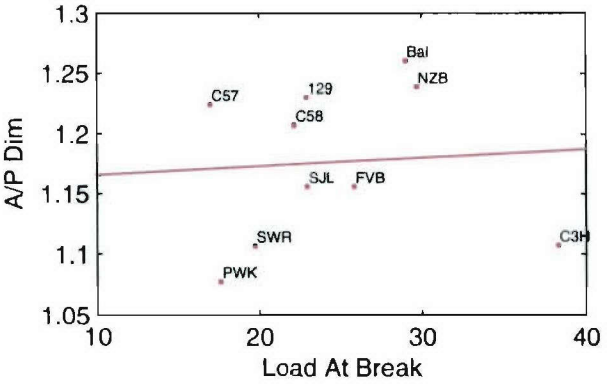
A/P Dim
Load At Break
Bal
NZB
C57
129
C58
SJL
FVB
SWR
C3H
PWK

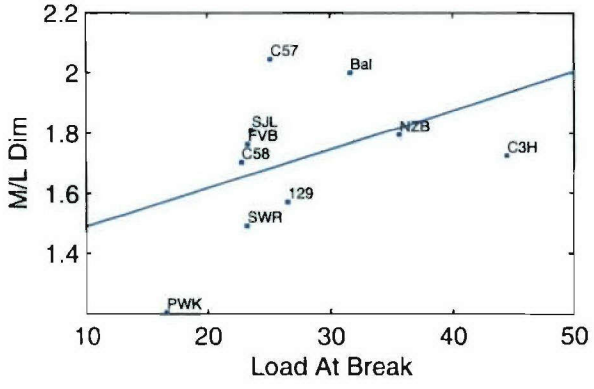
M/L Dim
Load At Break
C57
Bal
SJL
FVB
NZB
C3H
C58
129
SWR
PWK

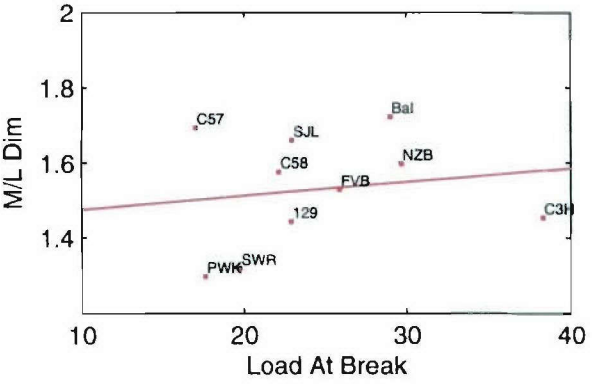
M/L Dim
Load At Break
C57
Bal
SJL
NZB
C58
FVB
129
C3H
PWK
SWR

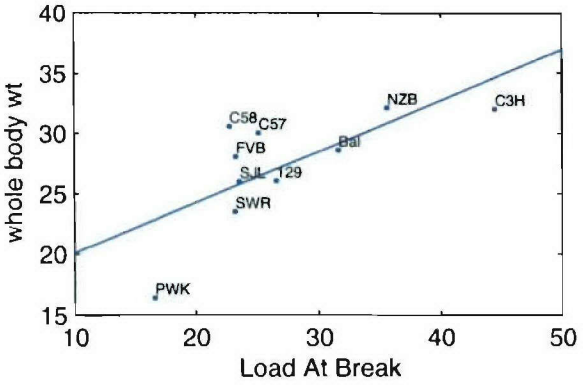
whole body wt
Load At Break
NZB
C3H
C58
C57
FVB
Bal
SJL
129
SWR
PWK

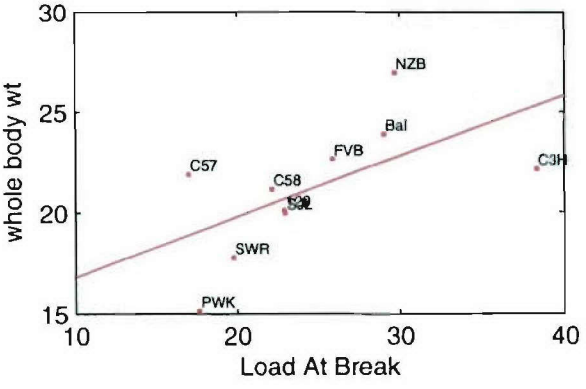
whole body wt
Load At Break
NZB
Bal
FVB
C57
C3H
C58
SWR
PWK

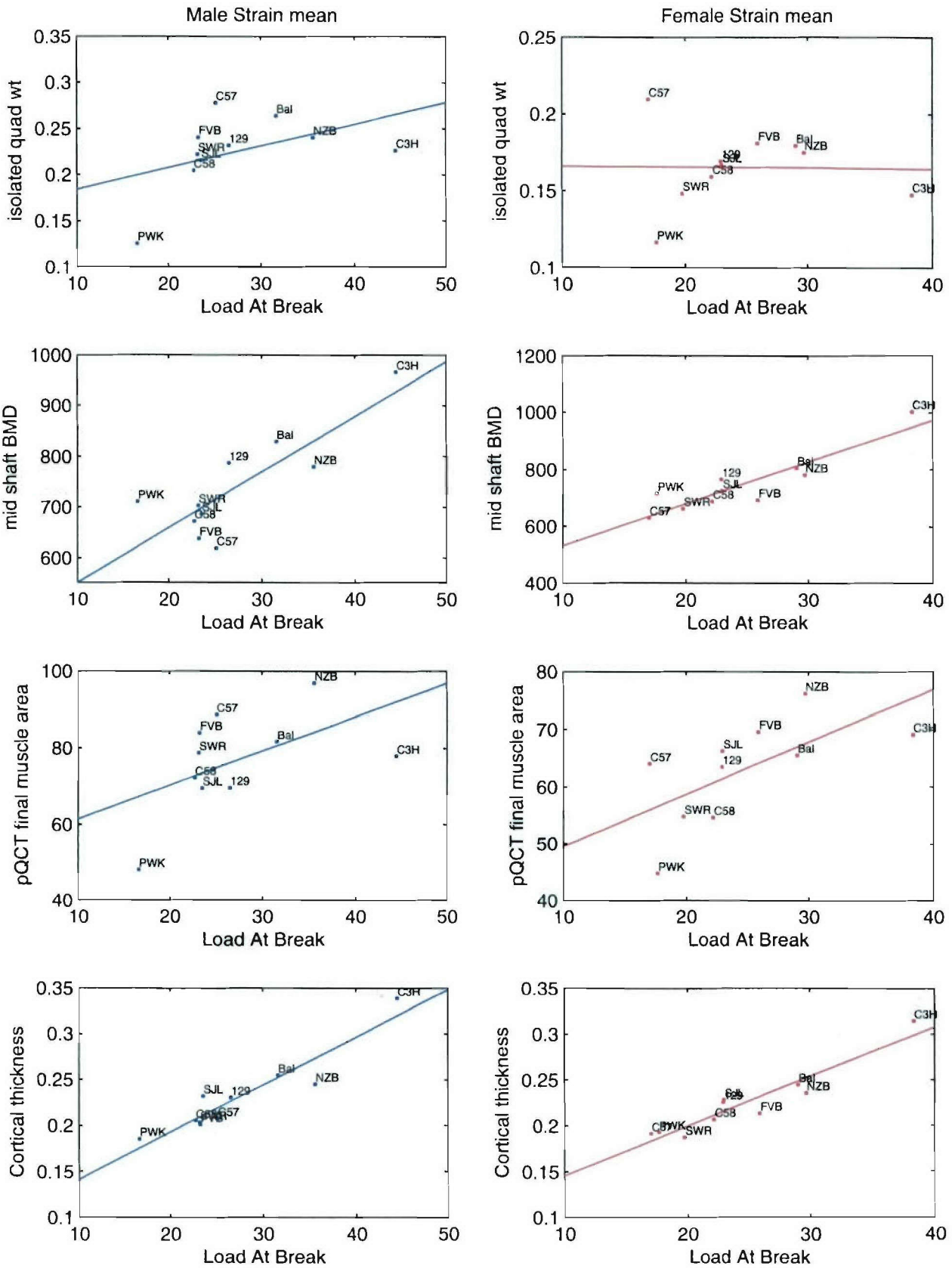
Male Strain mean
Female Strain mean
isolated quad wt
mid shaft BMD
pQCT final muscle area
Cortical thickness
Load At Break
C57
Bal
FVB
129
NZB
C3H
SWR
C58
SJL
PWK

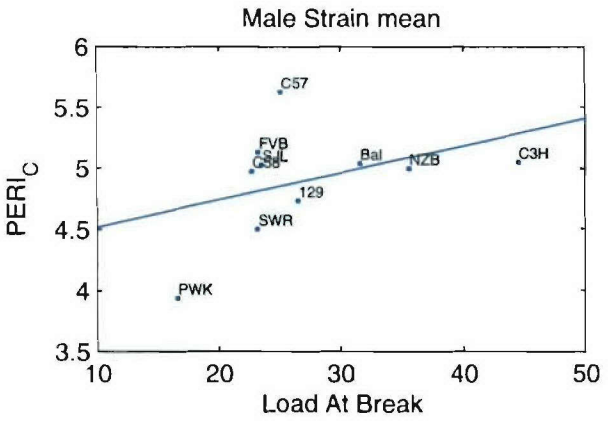
Male Strain mean
PERI_C
Load At Break
C57
FVB
SJL
C58
Bal
NZB
C3H
129
SWR
PWK

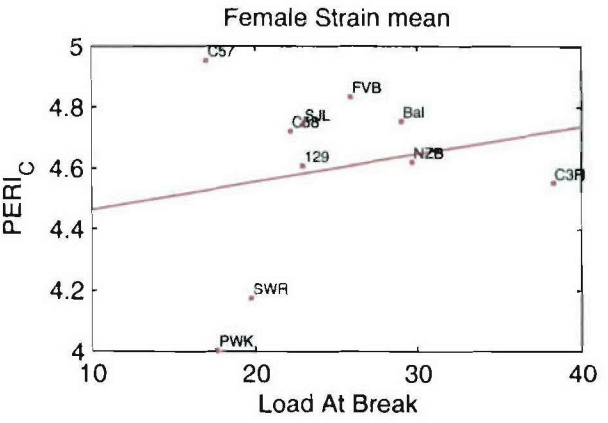
Female Strain mean
PERI_C
Load At Break
C57
FVB
SJL
C58
Bal
129
NZB
C3H
SWR
PWK

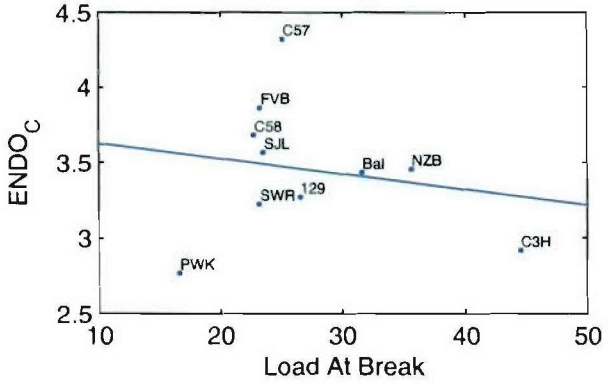
ENDO_C
Load At Break
C57
FVB
C58
SJL
Bal
NZB
SWR
129
C3H
PWK

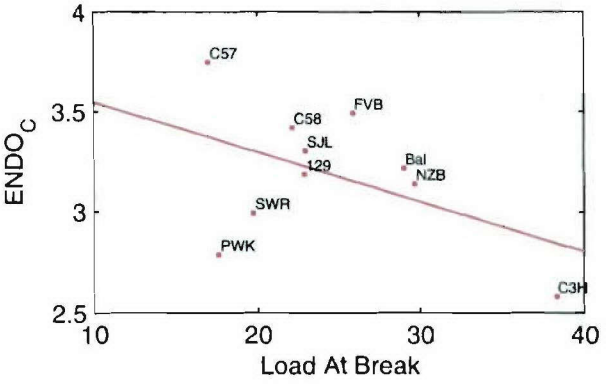
ENDO_C
Load At Break
C57
C58
FVB
SJL
129
Bal
NZB
SWR
PWK
C3H

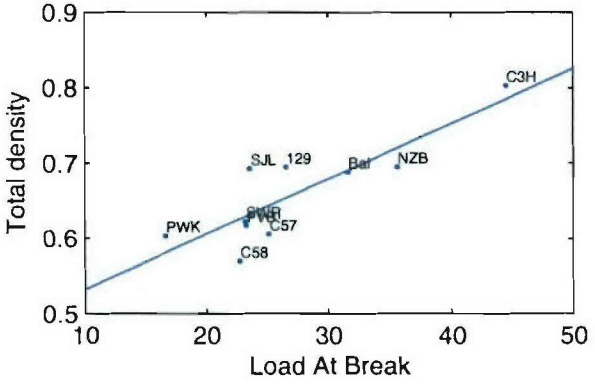
Total density
Load At Break
C3H
SJL
129
Bal
NZB
PWK
SWR
C57
C58

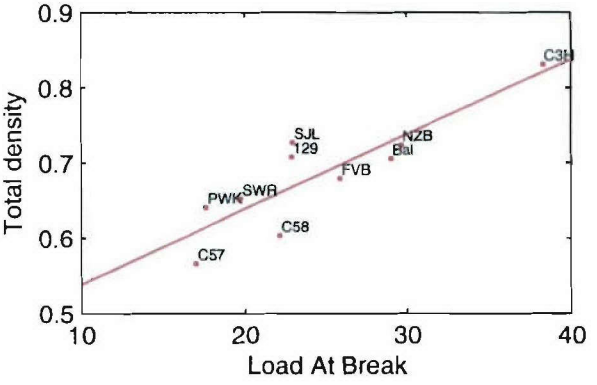
Total density
Load At Break
C3H
SJL
129
NZB
Bal
FVB
PWK
SWR
C58
C57

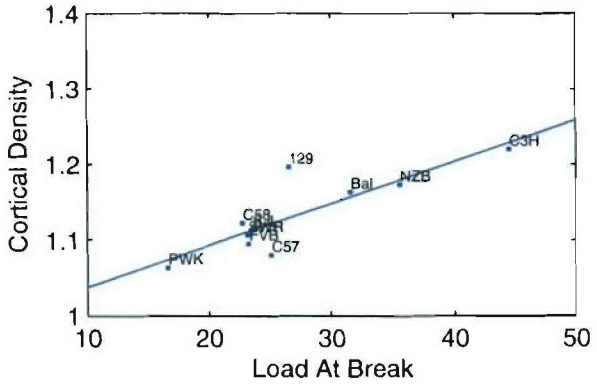
Cortical Density
Load At Break
129
C3H
Bal
NZB
C58
FVB
SWR
PWK
C57

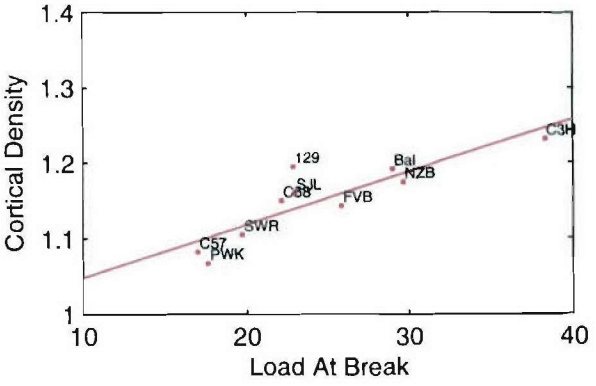
Cortical Density
Load At Break
129
C3H
Bal
NZB
SJL
C58
FVB
SWR
C57
PWK

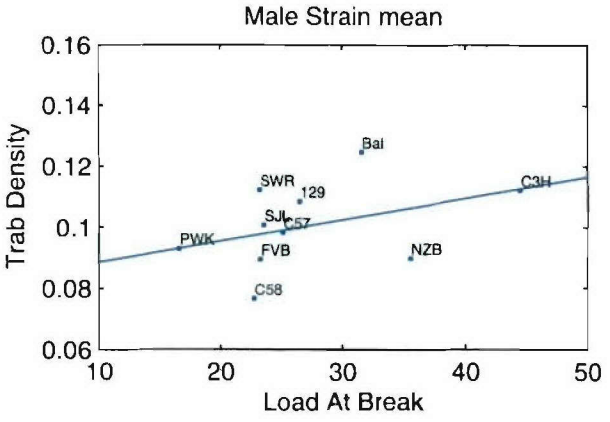
Male Strain mean
Trab Density
Load At Break
Bal
SWR
129
C3H
SJL
C57
PWK
FVB
NZB
C58

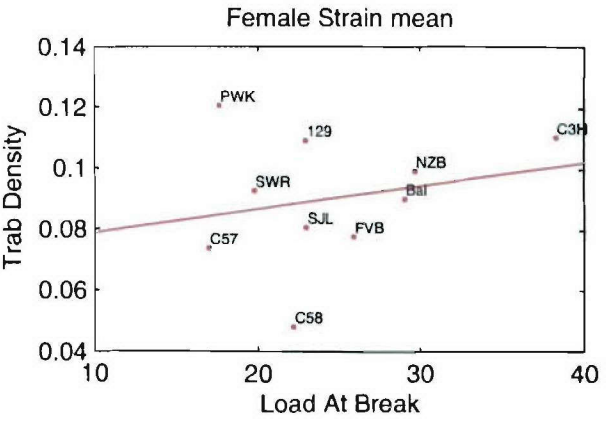
Female Strain mean
Trab Density
Load At Break
PWK
129
C3H
NZB
SWR
Bal
SJL
FVB
C57
C58

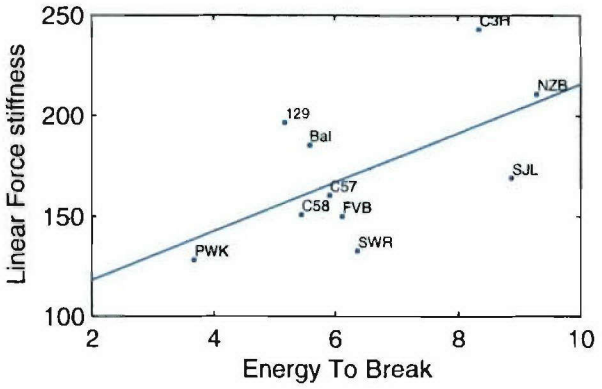
Linear Force stiffness
Energy To Break
C3H
NZB
129
Bal
SJL
C57
C58
FVB
PWK
SWR

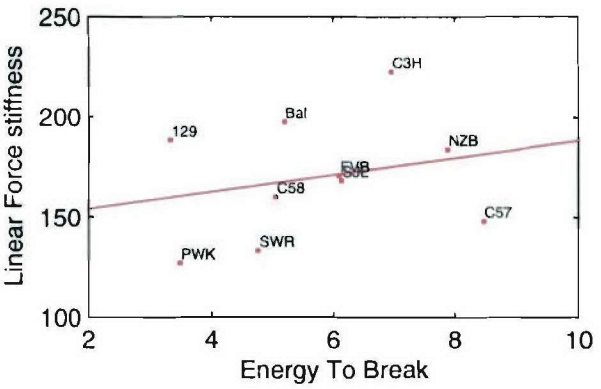
Linear Force stiffness
Energy To Break
C3H
Bal
129
NZB
C58
C57
PWK
SWR

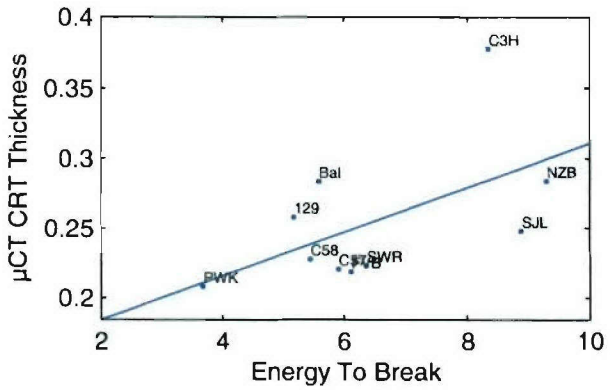
µCT CRT Thickness
Energy To Break
C3H
Bal
NZB
129
SJL
C58
SWR
PWK

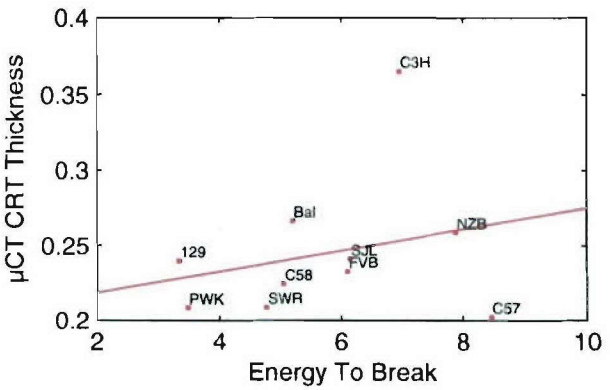
µCT CRT Thickness
Energy To Break
C3H
Bal
NZB
129
SJL
FVB
C58
PWK
SWR
C57

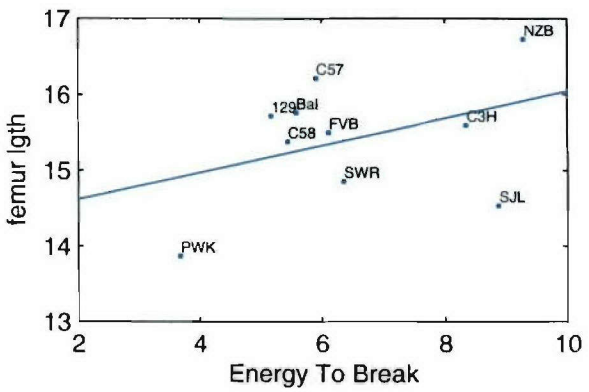
femur lgth
Energy To Break
NZB
C57
Bal
C58
FVB
C3H
SWR
SJL
PWK

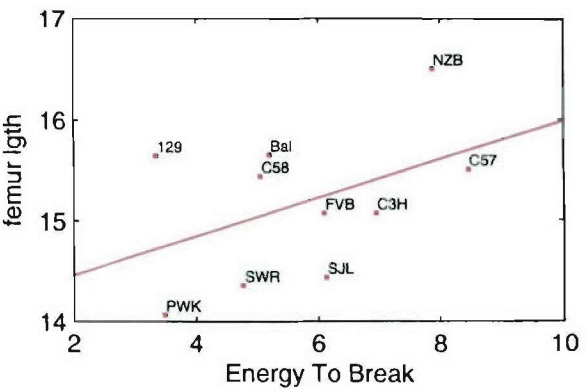
femur lgth
Energy To Break
NZB
129
Bal
C58
C57
FVB
C3H
SWR
SJL
PWK

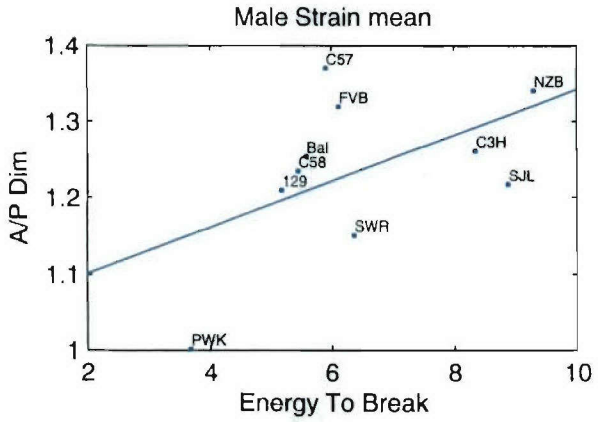
Male Strain mean
A/P Dim
Energy To Break
C57
NZB
FVB
Bal
C3H
C58
SJL
129
SWR
PWK

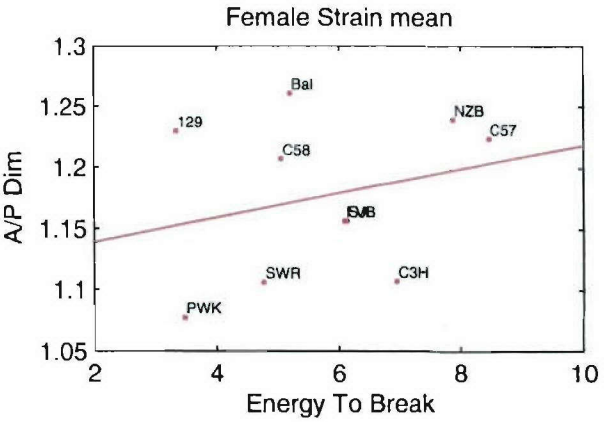
Female Strain mean
A/P Dim
Energy To Break
Bal
NZB
129
C57
C58
SWR
C3H
PWK

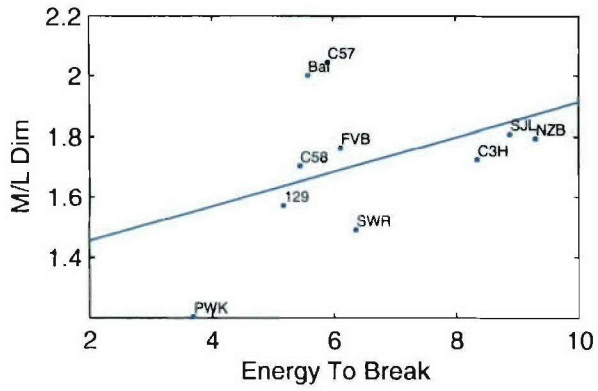
M/L Dim
Energy To Break
C57
Bal
FVB
SJL
NZB
C58
C3H
129
SWR
PWK

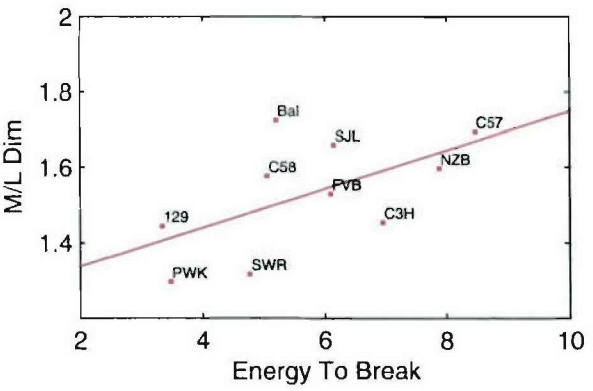
M/L Dim
Energy To Break
Bal
SJL
C57
C58
NZB
FVB
C3H
129
PWK
SWR

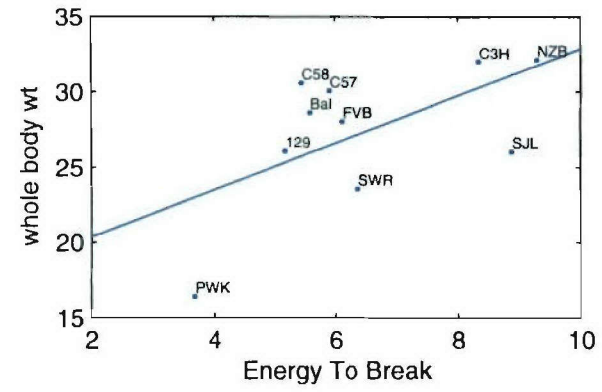
whole body wt
Energy To Break
C3H
NZB
C58
C57
Bal
FVB
129
SJL
SWR
PWK

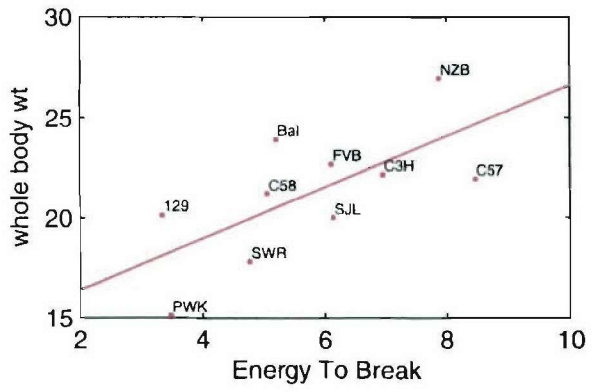
whole body wt
Energy To Break
NZB
Bal
FVB
C3H
C57
C58
129
SJL
SWR
PWK

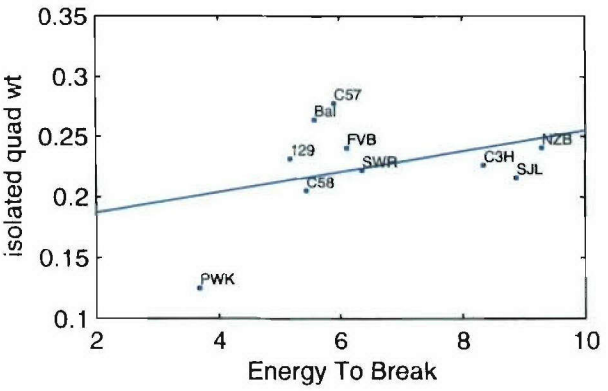
isolated quad wt
Energy To Break
C57
Bal
FVB
NZB
129
SWR
C3H
SJL
C58
PWK

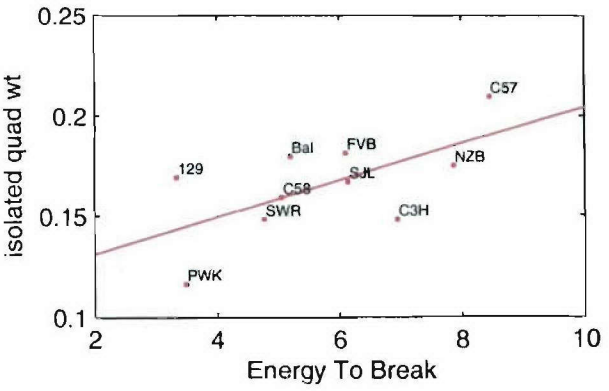
isolated quad wt
Energy To Break
C57
Bal
FVB
129
NZB
SJL
C58
SWR
C3H
PWK

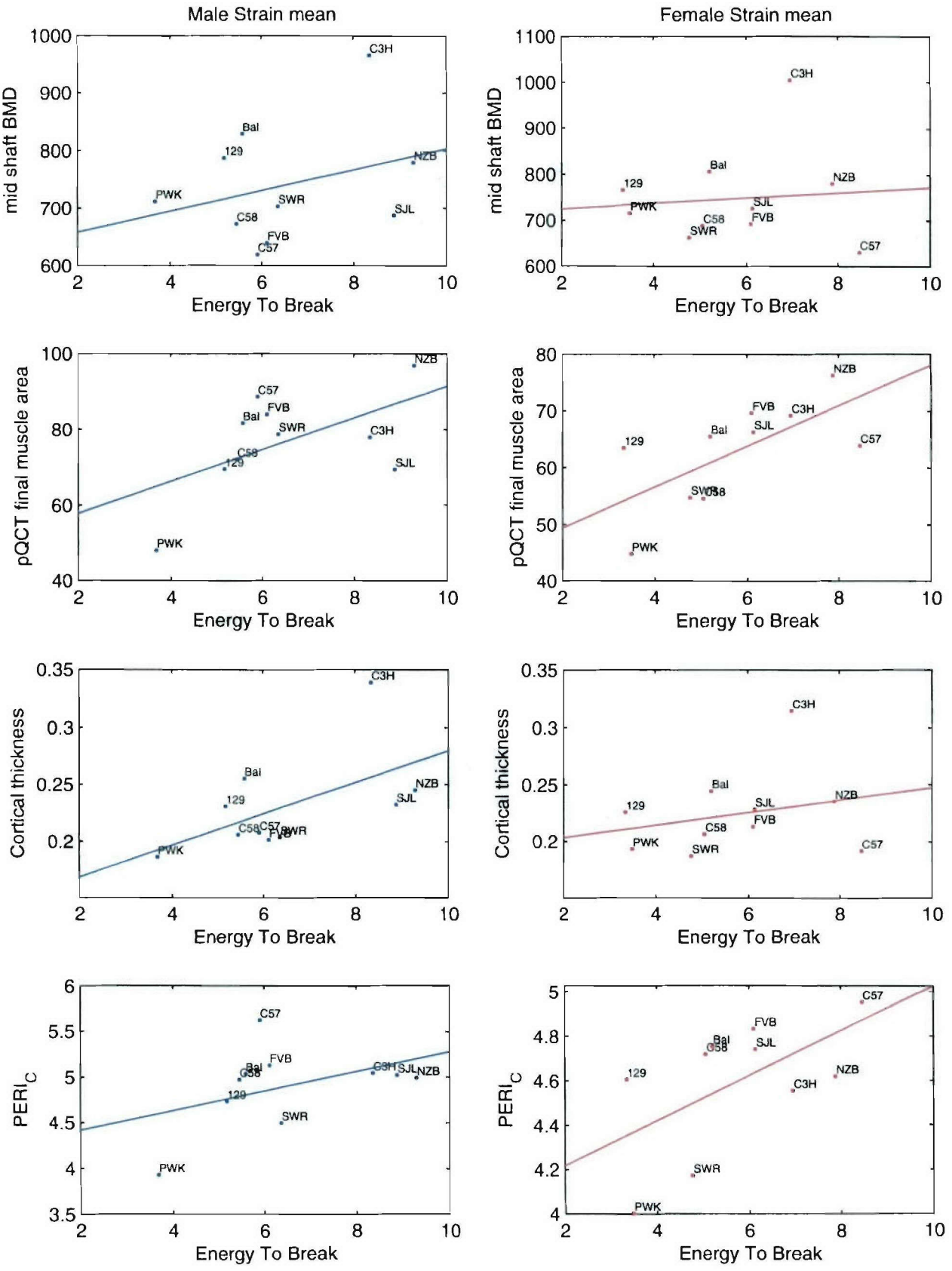
Male Strain mean
Female Strain mean
mid shaft BMD
pQCT final muscle area
Cortical thickness
PERI_C
Energy To Break
C3H
Bal
129
NZB
PWK
SWR
SJL
C58
FVB
C57

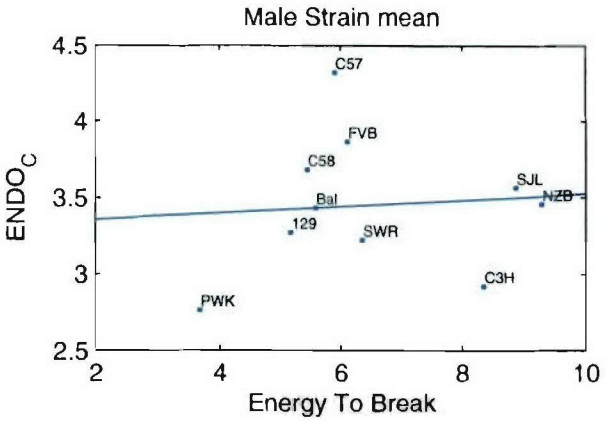
Male Strain mean
ENDO$_C$
Energy To Break
C57
FVB
C58
SJL
Bal
NZB
129
SWR
C3H
PWK

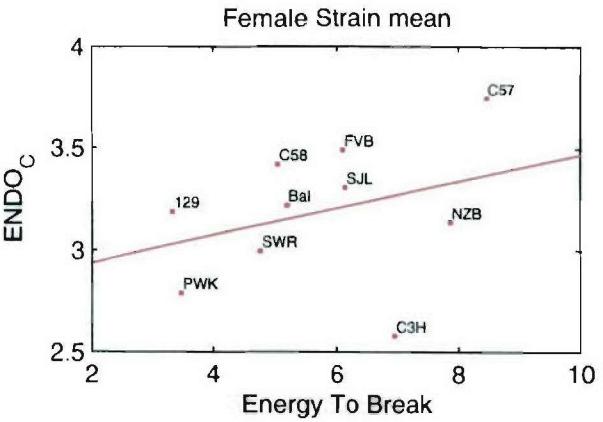
Female Strain mean
ENDO$_C$
Energy To Break
C57
C58
FVB
SJL
129
Bal
NZB
SWR
PWK
C3H

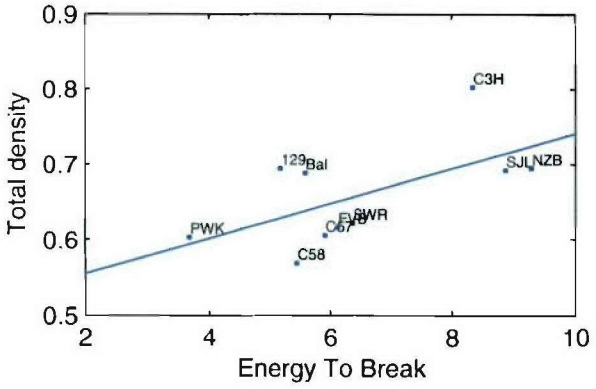
Total density
Energy To Break
C3H
129
Bal
SJL
NZB
PWK
SWR
FVB
C57
C58

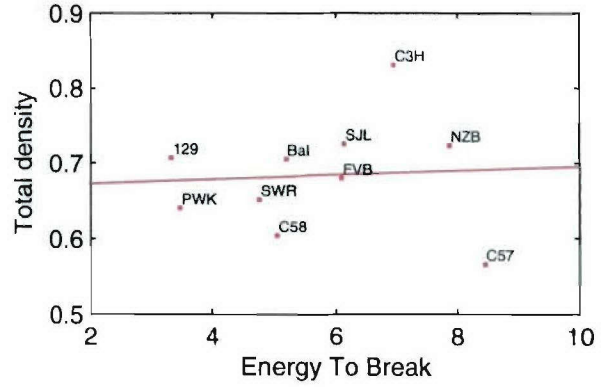
Total density
Energy To Break
C3H
129
Bal
SJL
NZB
FVB
PWK
SWR
C58
C57

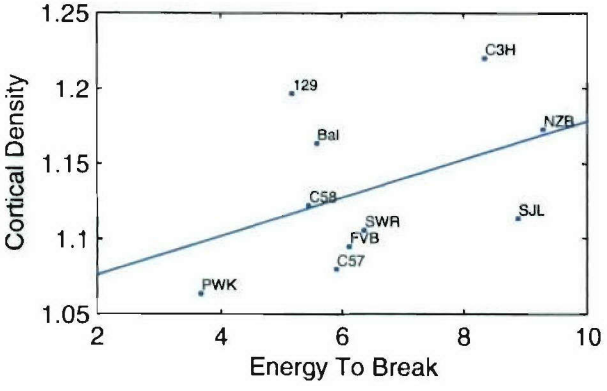
Cortical Density
Energy To Break
C3H
129
NZB
Bal
C58
SWR
SJL
FVB
C57
PWK

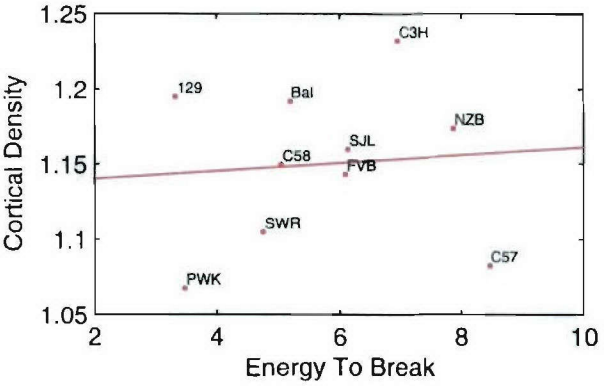
Cortical Density
Energy To Break
C3H
129
Bal
NZB
SJL
C58
FVB
SWR
C57
PWK

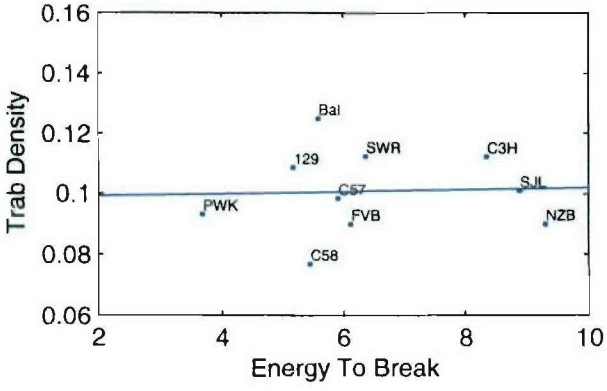
Trab Density
Energy To Break
Bal
129
SWR
C3H
SJL
C57
PWK
FVB
NZB
C58

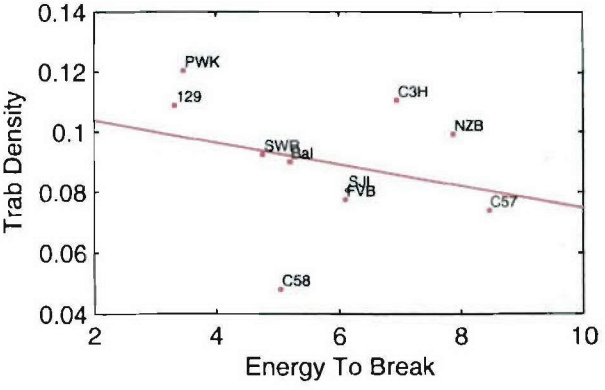
Trab Density
Energy To Break
PWK
129
C3H
NZB
SWR
Bal
SJL
FVB
C57
C58

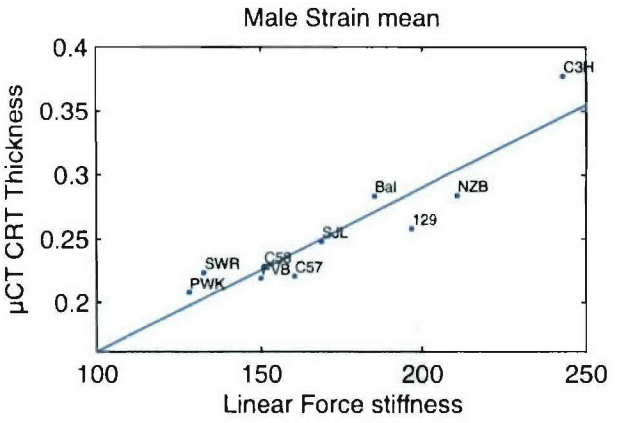
Male Strain mean
µCT CRT Thickness
Linear Force stiffness
C3H
Bal
NZB
129
SJL
SWR
C58
FVB
C57
PWK

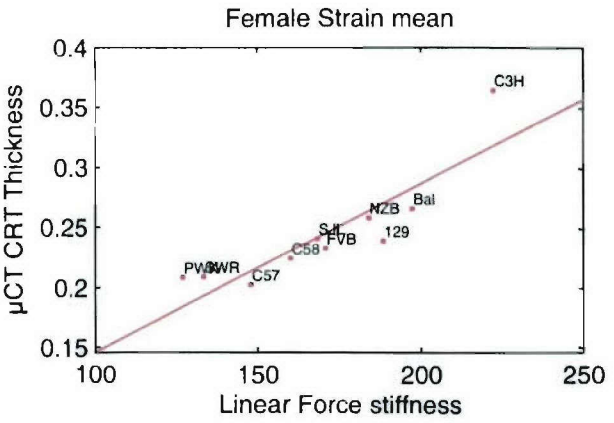
Female Strain mean
µCT CRT Thickness
Linear Force stiffness
C3H
NZB
Bal
SJL
FVB
129
C58
C57
SWR
PWK

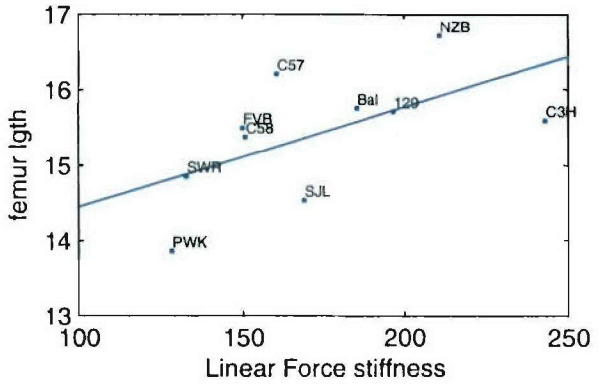
femur lgth
Linear Force stiffness
NZB
C57
Bal
129
C3H
FVB
C58
SWR
SJL
PWK

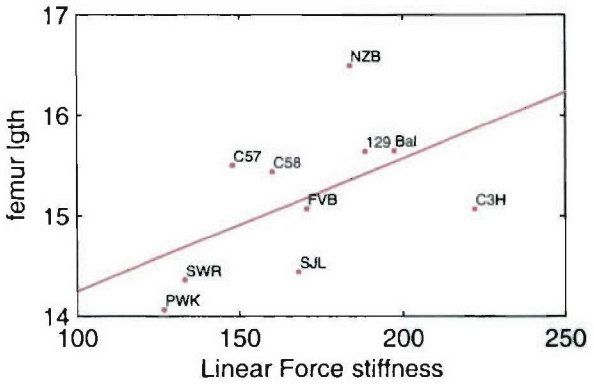
femur lgth
Linear Force stiffness
NZB
129
Bal
C57
C58
FVB
C3H
SWR
SJL
PWK

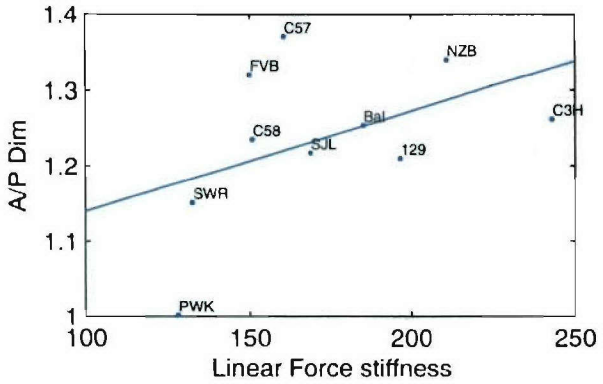
A/P Dim
Linear Force stiffness
C57
NZB
FVB
C3H
Bal
C58
SJL
129
SWR
PWK

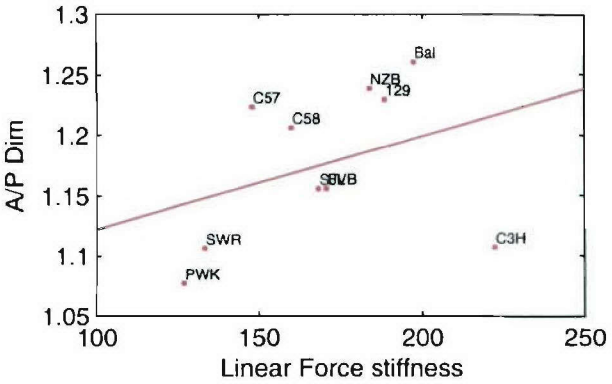
A/P Dim
Linear Force stiffness
Bal
NZB
129
C57
C58
FVB
SWR
C3H
PWK

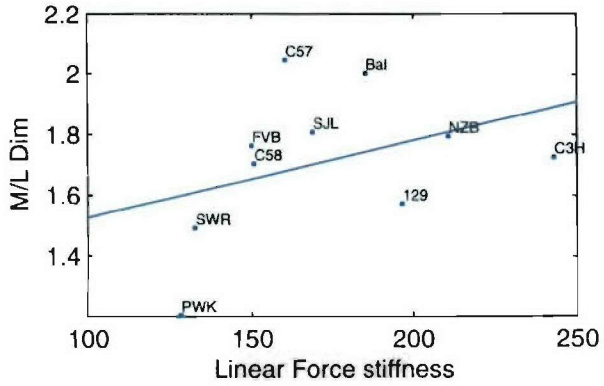
M/L Dim
Linear Force stiffness
C57
Bal
SJL
FVB
NZB
C3H
C58
129
SWR
PWK

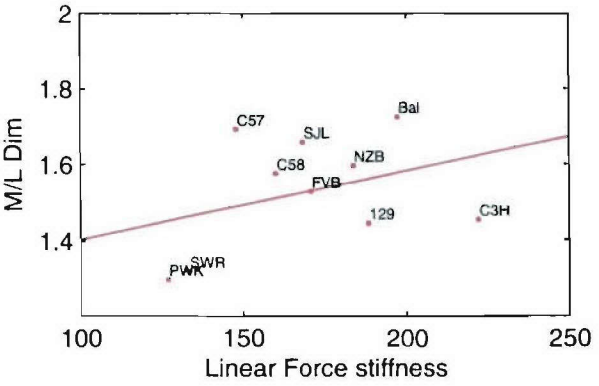
M/L Dim
Linear Force stiffness
C57
Bal
SJL
C58
NZB
FVB
129
C3H
SWR
PWK

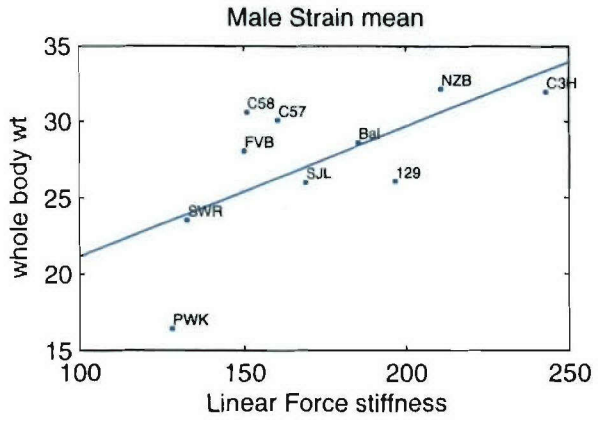
Male Strain mean
whole body wt
Linear Force stiffness
NZB
C3H
C58
C57
FVB
Bal
SJL
129
SWR
PWK

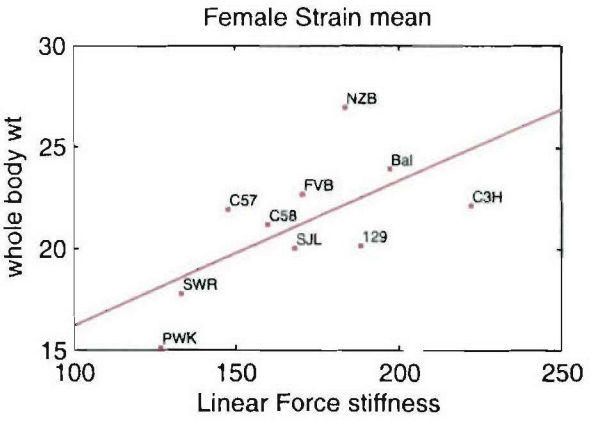
Female Strain mean
whole body wt
Linear Force stiffness
NZB
Bal
FVB
C57
C3H
C58
SJL
129
SWR
PWK

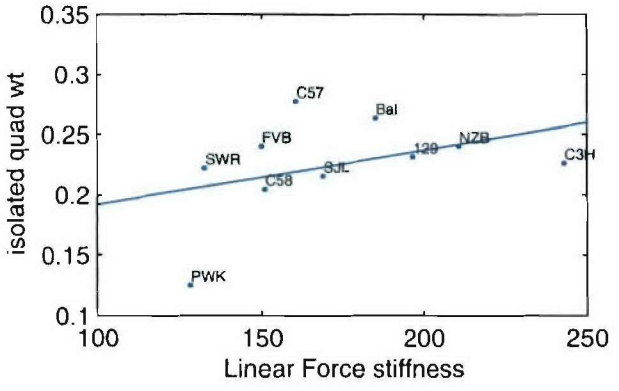
isolated quad wt
Linear Force stiffness
C57
Bal
FVB
SWR
129
NZB
C3H
SJL
C58
PWK

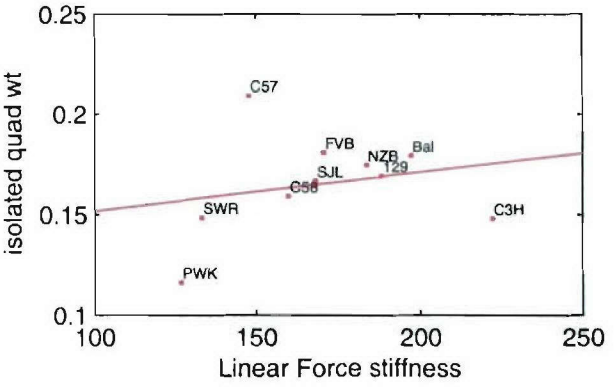
isolated quad wt
Linear Force stiffness
C57
FVB
Bal
NZB
SJL
129
C58
SWR
C3H
PWK

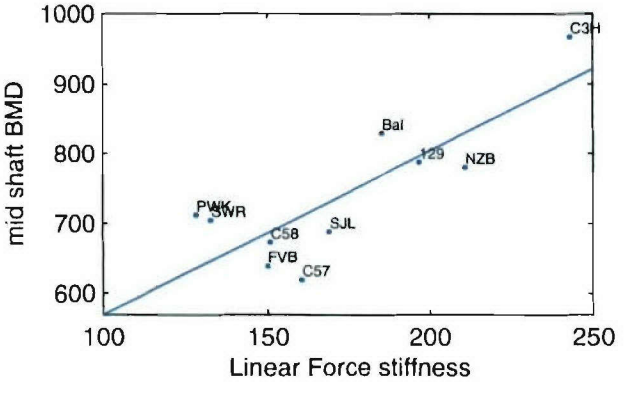
mid shaft BMD
Linear Force stiffness
C3H
Bal
129
NZB
PWK
SWR
SJL
C58
FVB
C57

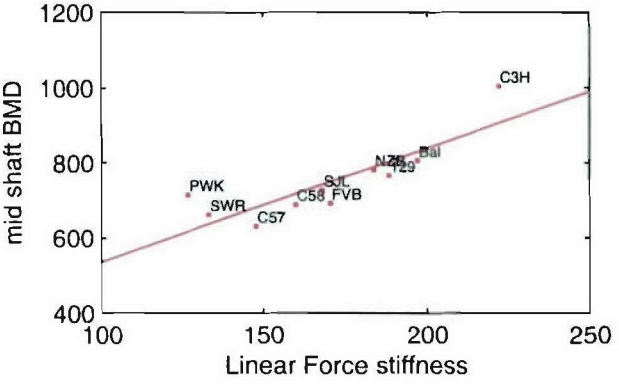
mid shaft BMD
Linear Force stiffness
C3H
PWK
SWR
C57
SJL
C58
FVB
NZB
129
Bal

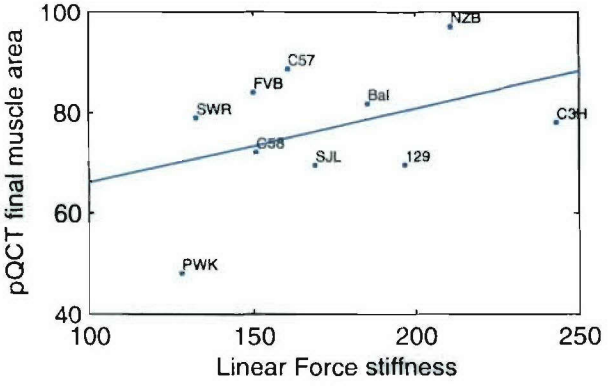
pQCT final muscle area
Linear Force stiffness
NZB
C57
FVB
SWR
Bal
C3H
C58
SJL
129
PWK

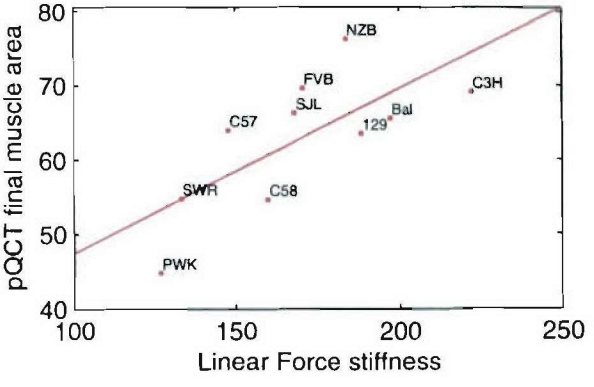
pQCT final muscle area
Linear Force stiffness
NZB
FVB
C3H
SJL
C57
Bal
129
SWR
C58
PWK

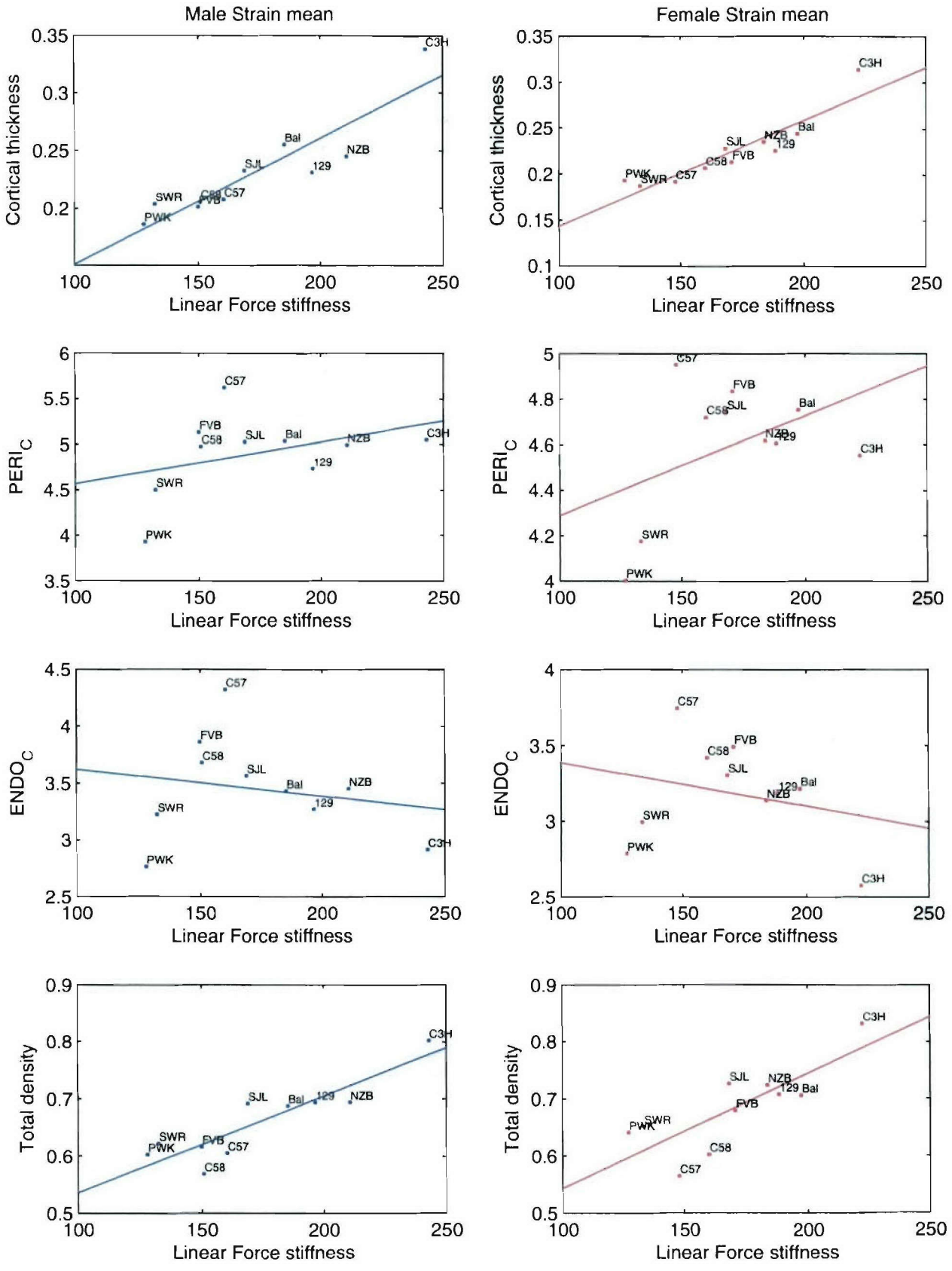
Male Strain mean
Female Strain mean
Cortical thickness
Linear Force stiffness
PERI_C
ENDO_C
Total density
C3H
Bal
NZB
SJL
129
SWR
C58
FVB
C57
PWK

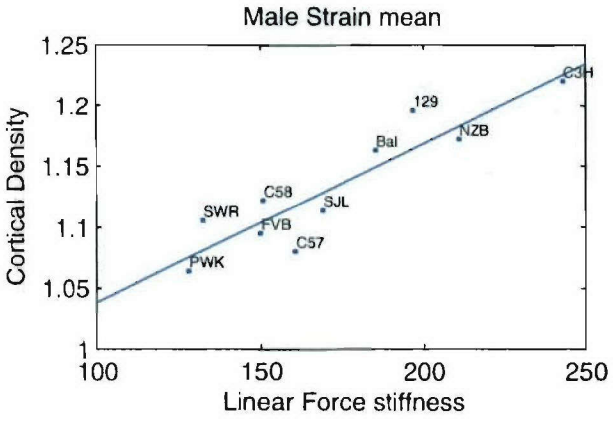
Male Strain mean
Cortical Density
Linear Force stiffness
C3H
129
NZB
Bal
C58
SWR
SJL
FVB
C57
PWK

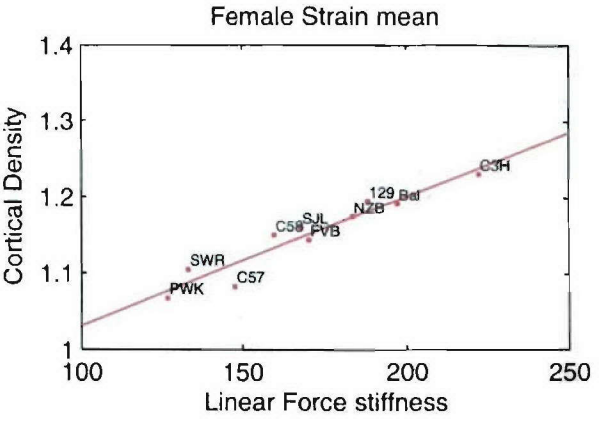
Female Strain mean
Cortical Density
Linear Force stiffness
C3H
129
Bal
NZB
SJL
C58
FVB
SWR
C57
PWK

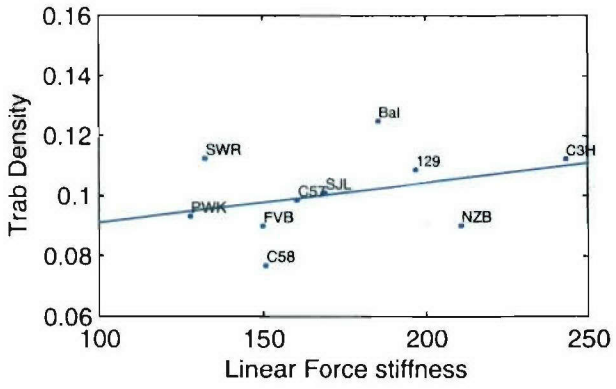
Trab Density
Linear Force stiffness
Bal
SWR
129
C3H
SJL
C57
PWK
FVB
NZB
C58

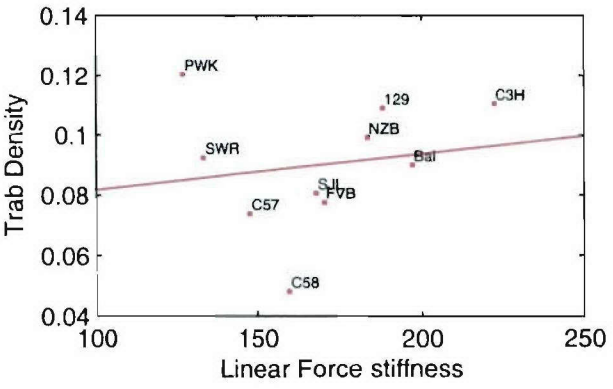
Trab Density
Linear Force stiffness
PWK
129
C3H
NZB
SWR
Bal
SJL
FVB
C57
C58

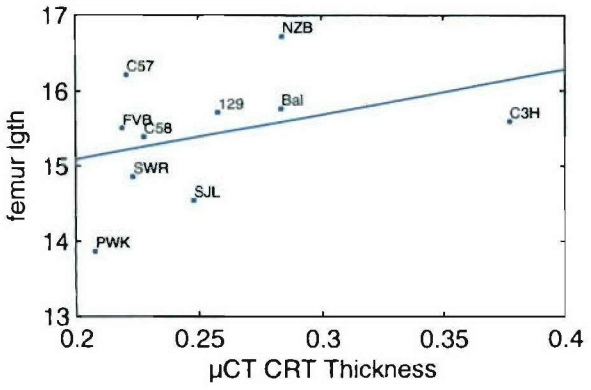
femur lgth
μCT CRT Thickness
NZB
C57
129
Bal
FVB
C58
C3H
SWR
SJL
PWK

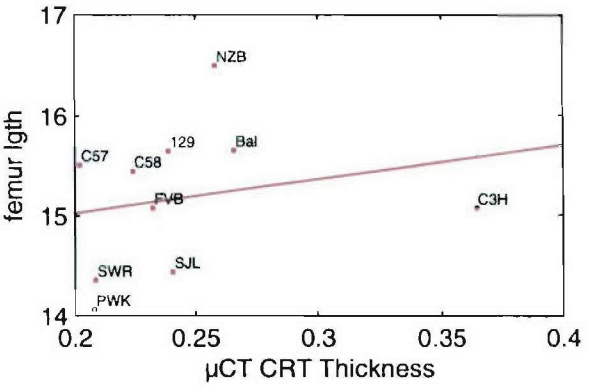
femur lgth
μCT CRT Thickness
NZB
129
Bal
C57
C58
FVB
C3H
SWR
SJL
PWK

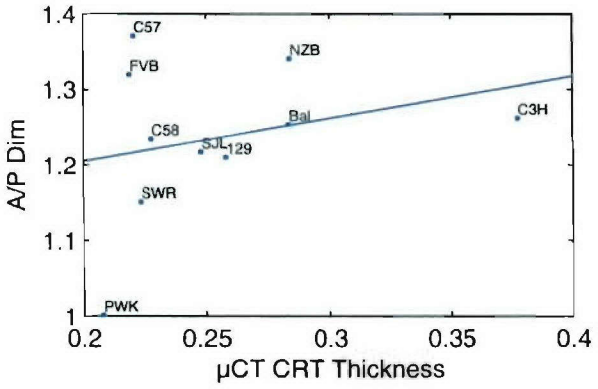
A/P Dim
μCT CRT Thickness
C57
NZB
FVB
C58
Bal
C3H
SJL
129
SWR
PWK

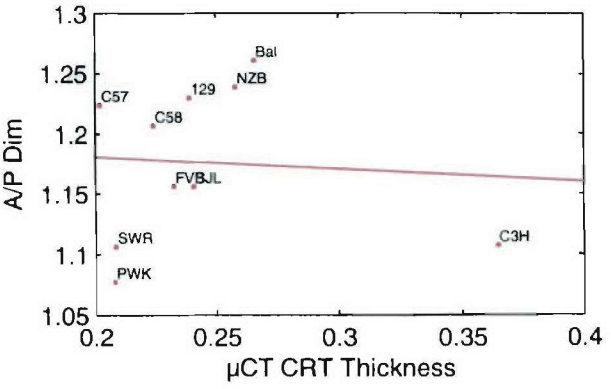
A/P Dim
μCT CRT Thickness
Bal
C57
129
NZB
C58
FVBJL
SWR
C3H
PWK

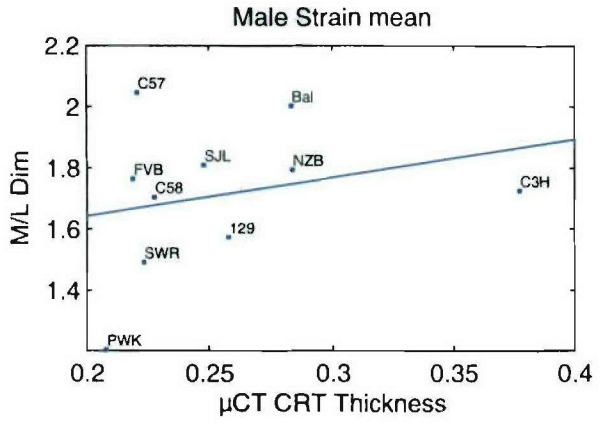
Male Strain mean
M/L Dim
µCT CRT Thickness
C57
Bal
SJL
NZB
FVB
C58
C3H
129
SWR
PWK

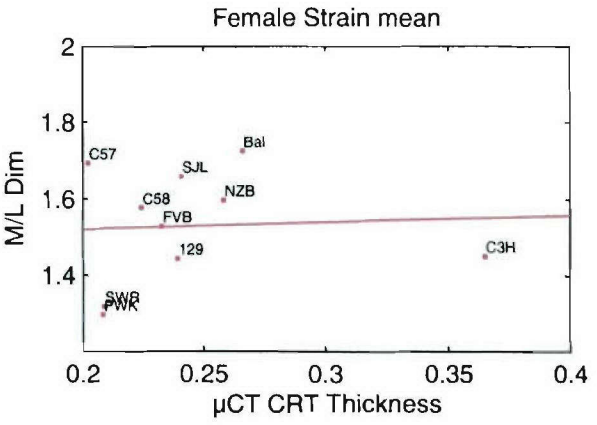
Female Strain mean
M/L Dim
µCT CRT Thickness
Bal
C57
SJL
NZB
C58
FVB
C3H
129
SWR
PWK

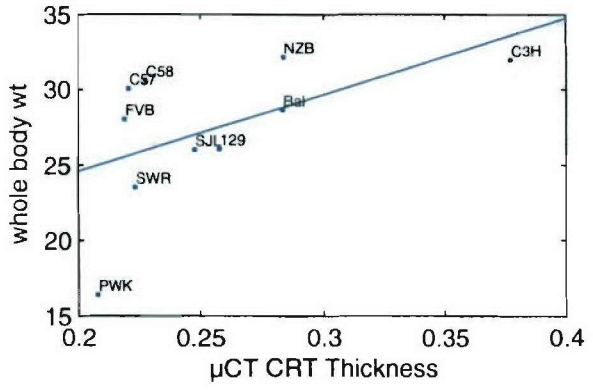
whole body wt
µCT CRT Thickness
NZB
C3H
C58
C57
FVB
Bal
SJL
129
SWR
PWK

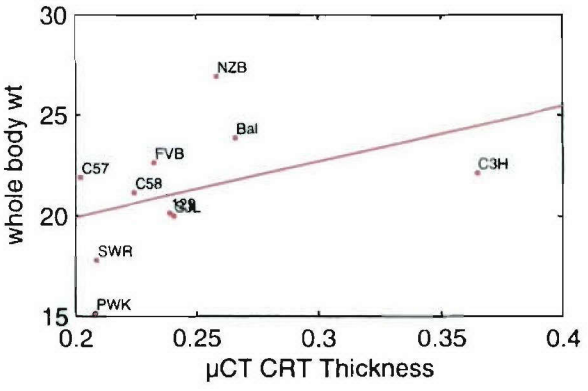
whole body wt
µCT CRT Thickness
NZB
Bal
FVB
C57
C3H
C58
SWR
PWK

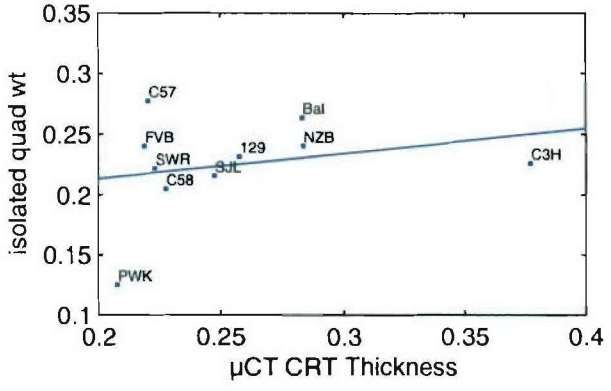
isolated quad wt
µCT CRT Thickness
C57
Bal
FVB
129
NZB
SWR
SJL
C3H
C58
PWK

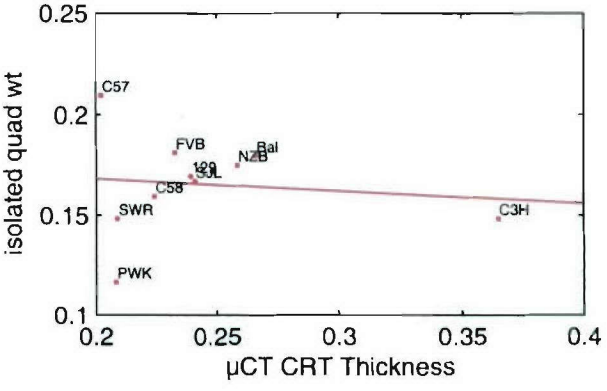
isolated quad wt
µCT CRT Thickness
C57
FVB
Bal
NZB
C58
SWR
C3H
PWK

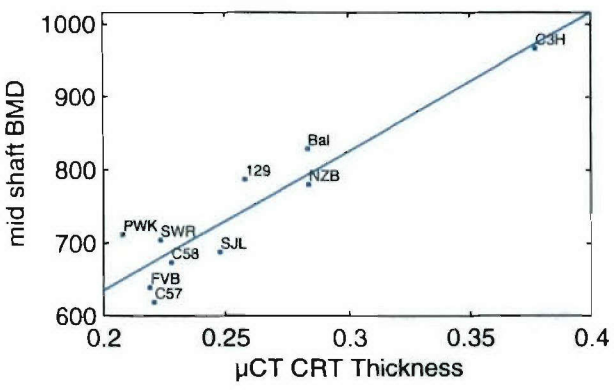
mid shaft BMD
µCT CRT Thickness
C3H
Bal
129
NZB
PWK
SWR
SJL
C58
FVB
C57

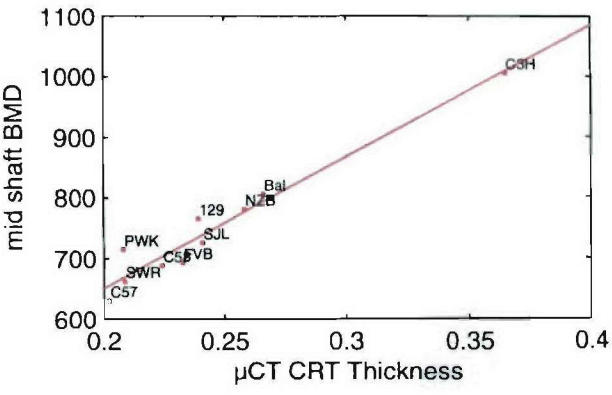
mid shaft BMD
µCT CRT Thickness
C3H
Bal
NZB
129
PWK
SJL
C58
FVB
SWR
C57

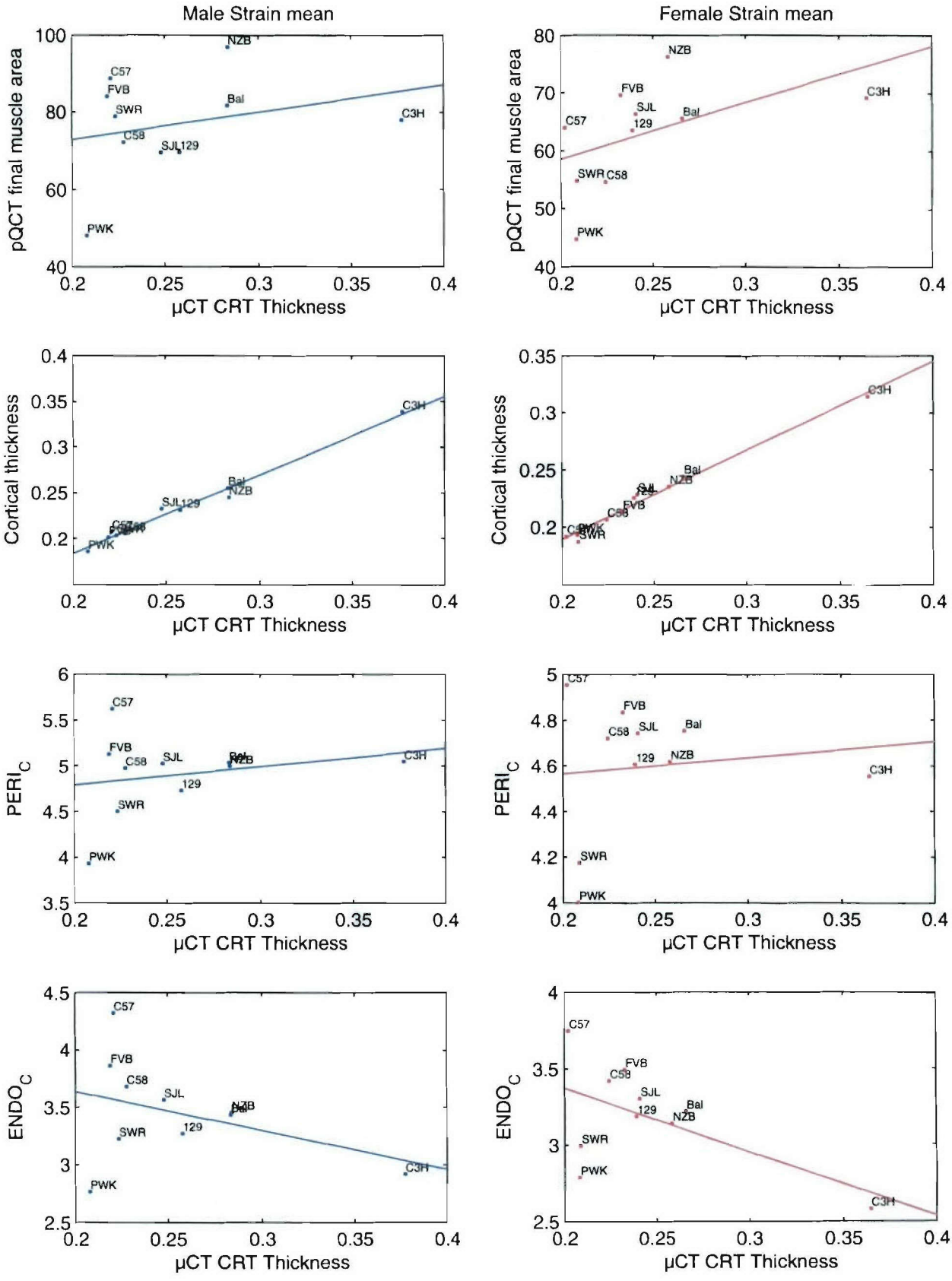
Male Strain mean
Female Strain mean
pQCT final muscle area
Cortical thickness
PERI_C
ENDO_C
μCT CRT Thickness
NZB
C57
FVB
SWR
Bal
C3H
C58
SJL
129
PWK

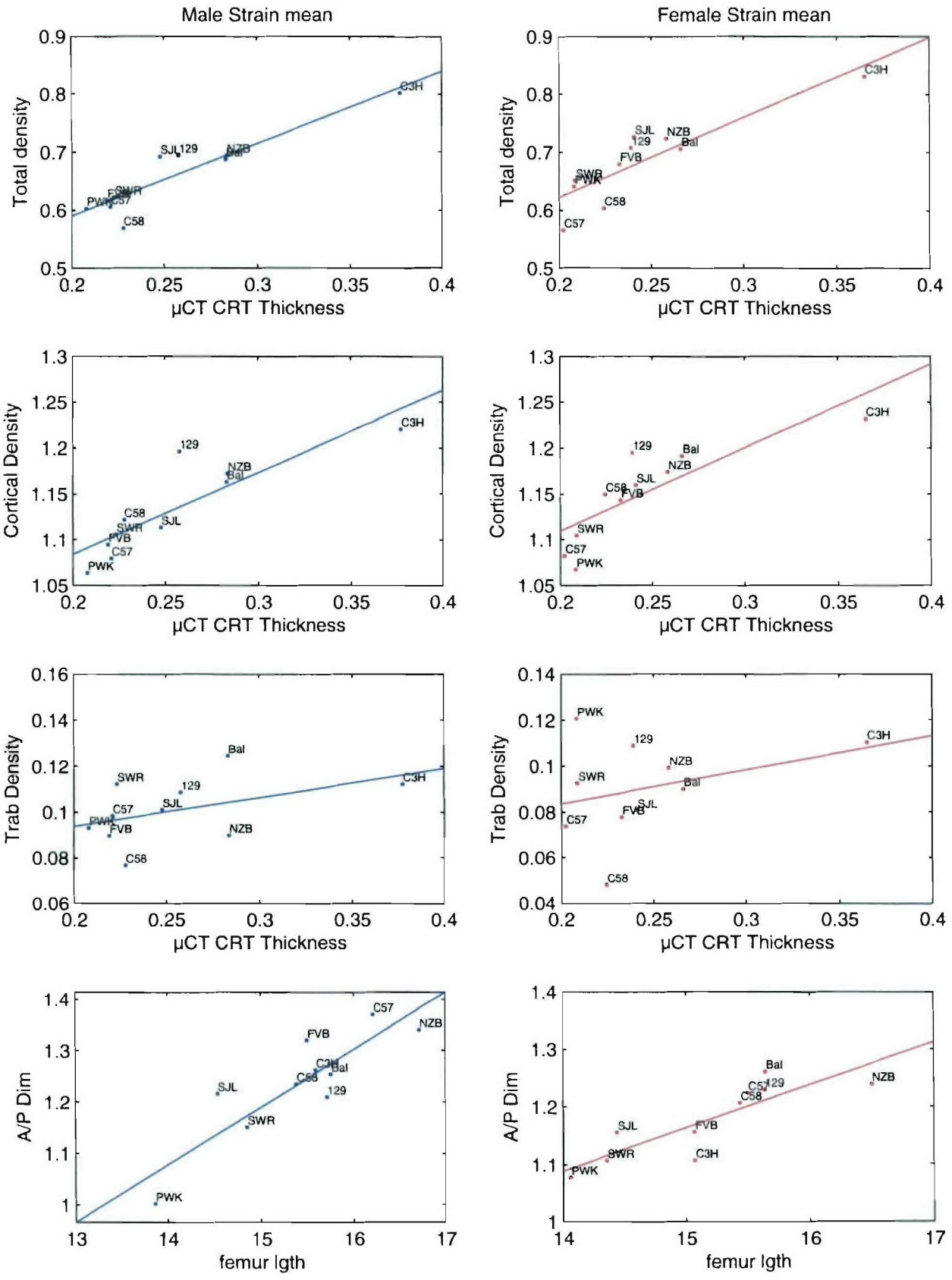
Male Strain mean
Female Strain mean
Total density
Cortical Density
Trab Density
A/P Dim
µCT CRT Thickness
femur lgth
C3H
129
NZB
Bal
SJL
SWR
FVB
PWK
C57
C58

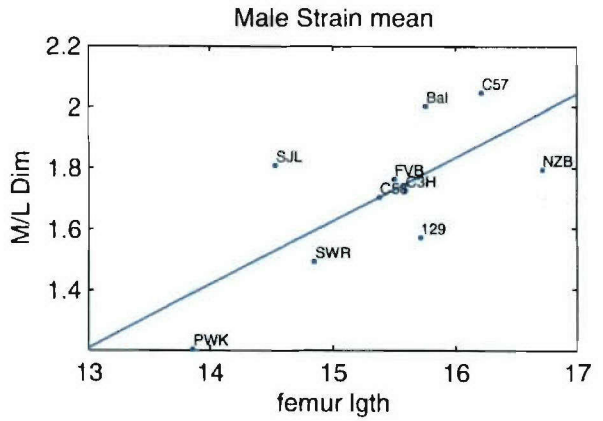
Male Strain mean
M/L Dim
femur lgth
2.2
2
1.8
1.6
1.4
13
14
15
16
17
C57
Bal
SJL
NZB
FVB
C3H
129
SWR
PWK

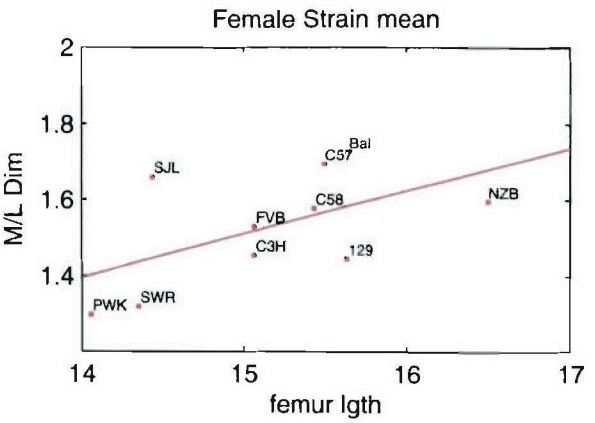
Female Strain mean
M/L Dim
femur lgth
2
1.8
1.6
1.4
14
15
16
17
Bal
C57
SJL
NZB
C58
FVB
C3H
129
PWK
SWR

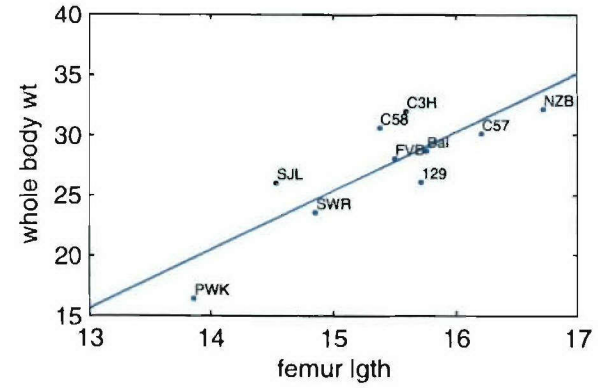
whole body wt
femur lgth
40
35
30
25
20
15
13
14
15
16
17
C3H
C58
NZB
C57
FVB
Bal
SJL
129
SWR
PWK

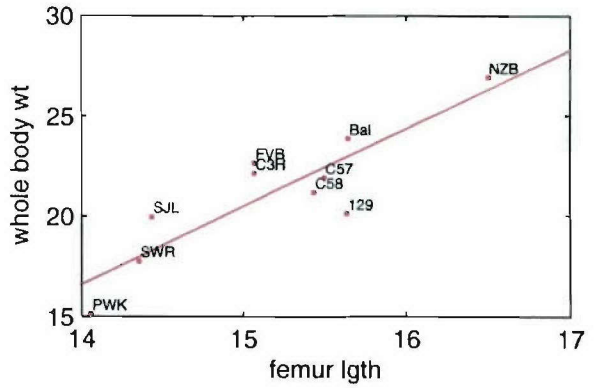
whole body wt
femur lgth
30
25
20
15
14
15
16
17
NZB
Bal
FVB
C3H
C57
C58
SJL
129
SWR
PWK

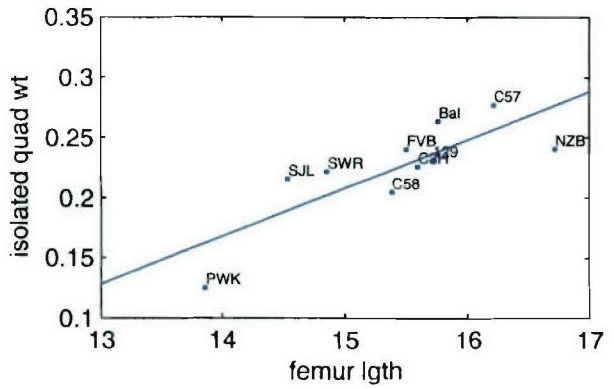
isolated quad wt
femur lgth
0.35
0.3
0.25
0.2
0.15
0.1
13
14
15
16
17
C57
Bal
FVB
NZB
SJL
SWR
C58
PWK

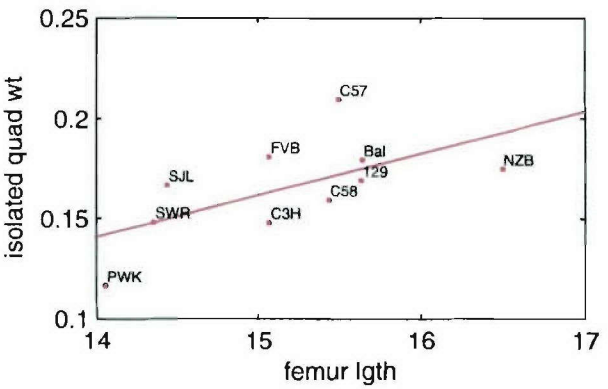
isolated quad wt
femur lgth
0.25
0.2
0.15
0.1
14
15
16
17
C57
FVB
Bal
NZB
129
SJL
C58
SWR
C3H
PWK

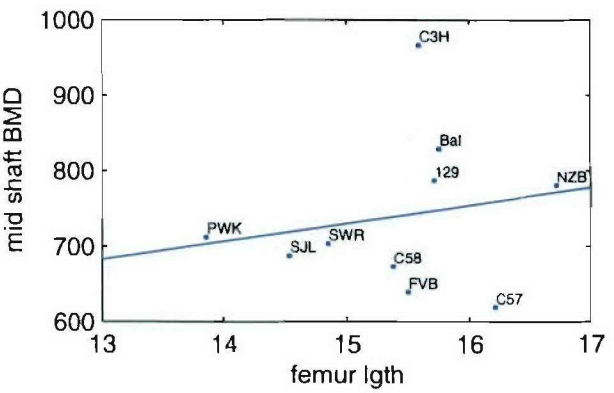
mid shaft BMD
femur lgth
1000
900
800
700
600
13
14
15
16
17
C3H
Bal
129
NZB
PWK
SJL
SWR
C58
FVB
C57

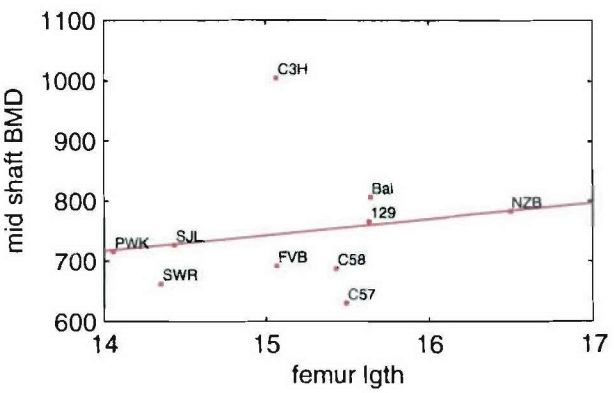
mid shaft BMD
femur lgth
1100
1000
900
800
700
600
14
15
16
17
C3H
Bal
129
NZB
PWK
SJL
FVB
C58
SWR
C57

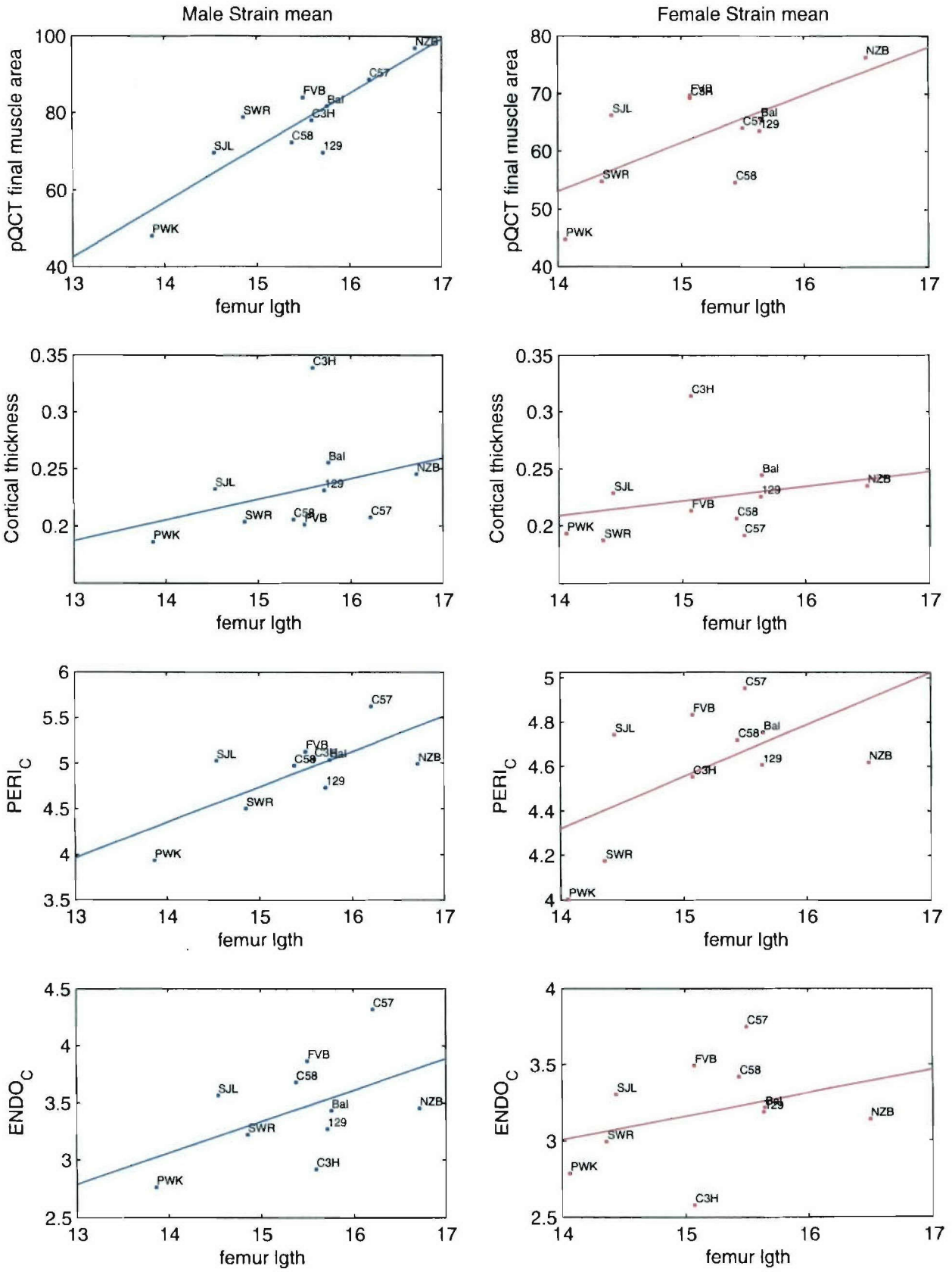
Male Strain mean
Female Strain mean
pQCT final muscle area
Cortical thickness
PERI_C
ENDO_C
femur lgth
NZB
C57
FVB
Bal
C3H
SWR
SJL
C58
129
PWK

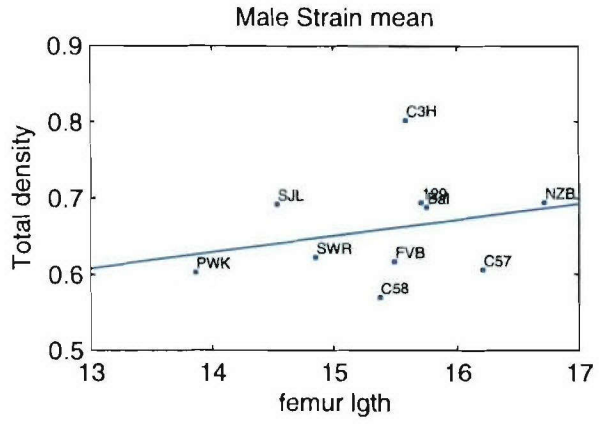
Male Strain mean
Total density
femur lgth
C3H
SJL
129
Bal
NZB
PWK
SWR
FVB
C57
C58

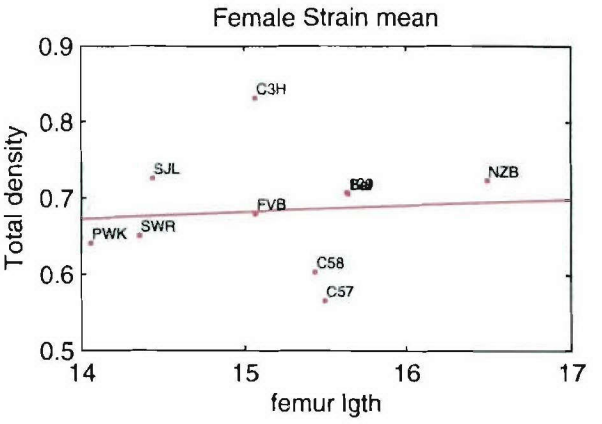
Female Strain mean
Total density
femur lgth
C3H
SJL
NZB
FVB
PWK
SWR
C58
C57

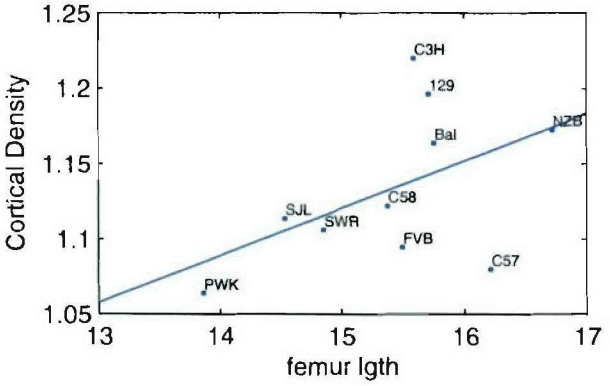
Cortical Density
femur lgth
C3H
129
Bal
NZB
SJL
C58
SWR
FVB
C57
PWK

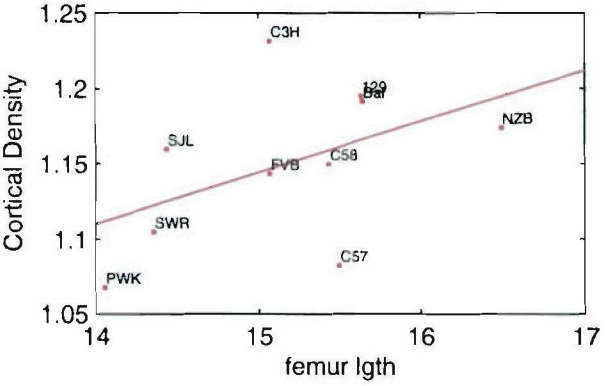
Cortical Density
femur lgth
C3H
129
Bal
NZB
SJL
FVB
C58
SWR
C57
PWK

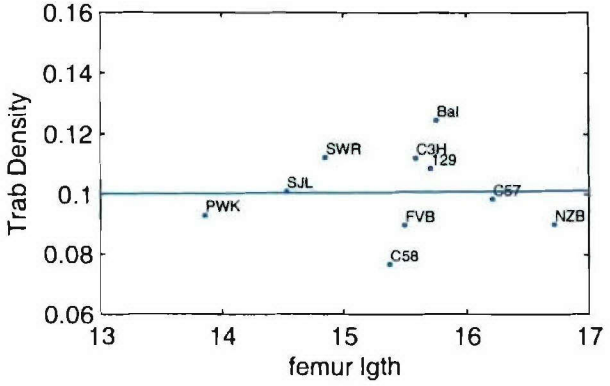
Trab Density
femur lgth
Bal
SWR
C3H
129
SJL
C57
PWK
FVB
NZB
C58

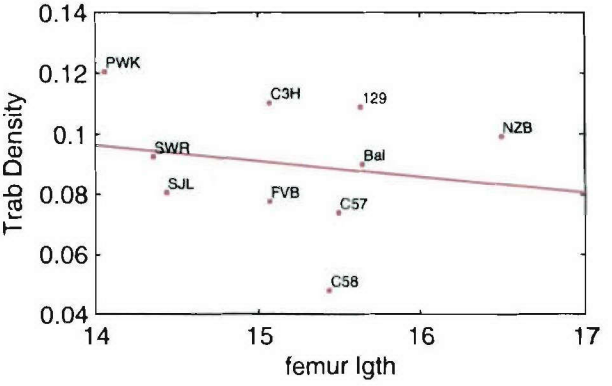
Trab Density
femur lgth
PWK
C3H
129
NZB
SWR
Bal
SJL
FVB
C57
C58

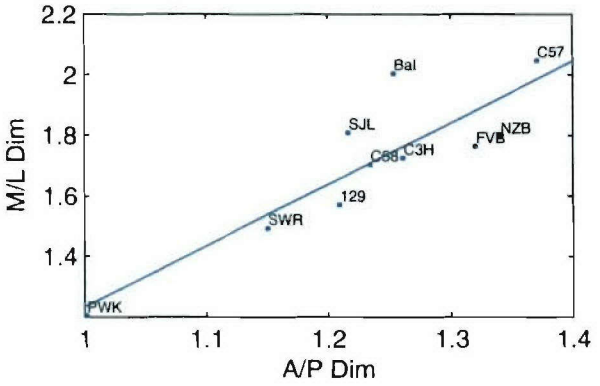
M/L Dim
A/P Dim
C57
Bal
SJL
NZB
FVB
C58
C3H
129
SWR
PWK

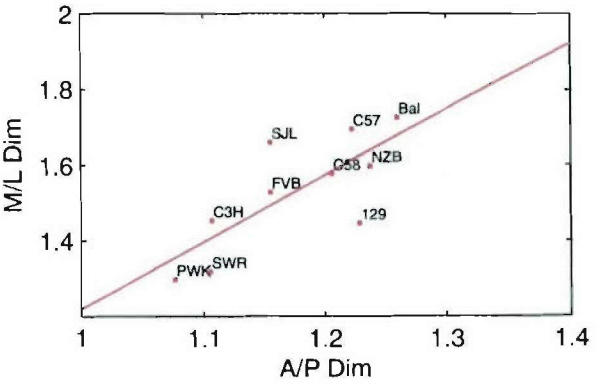
M/L Dim
A/P Dim
C57
Bal
SJL
C58
NZB
FVB
C3H
129
PWK
SWR

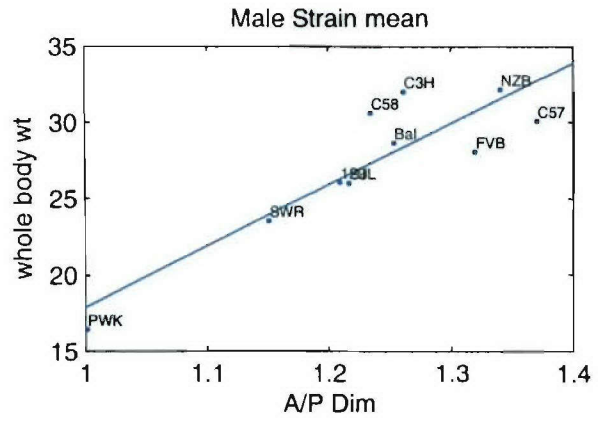
Male Strain mean
whole body wt
A/P Dim
C3H
NZB
C58
C57
Bal
FVB
SJL
SWR
PWK

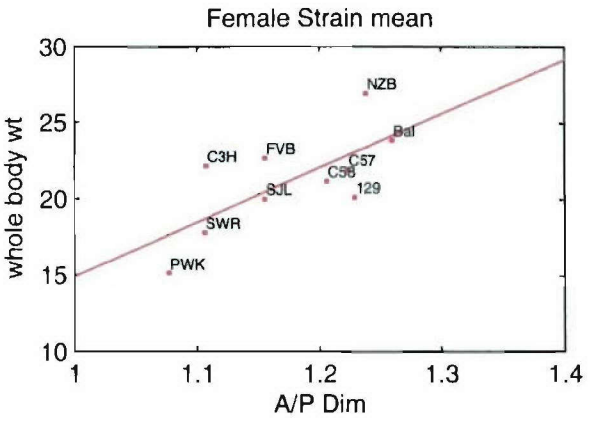
Female Strain mean
whole body wt
A/P Dim
NZB
Bal
C3H
FVB
C57
C58
SJL
129
SWR
PWK

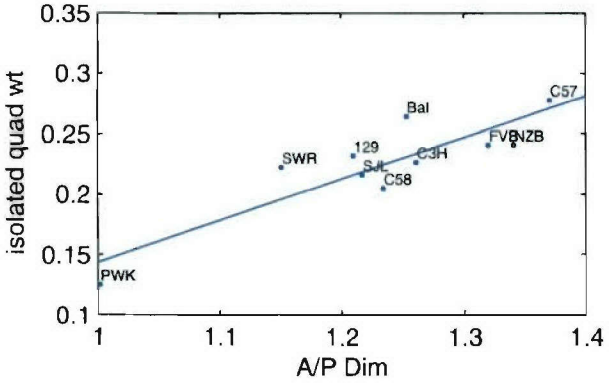
isolated quad wt
A/P Dim
C57
Bal
SWR
129
C3H
FVB
NZB
SJL
C58
PWK

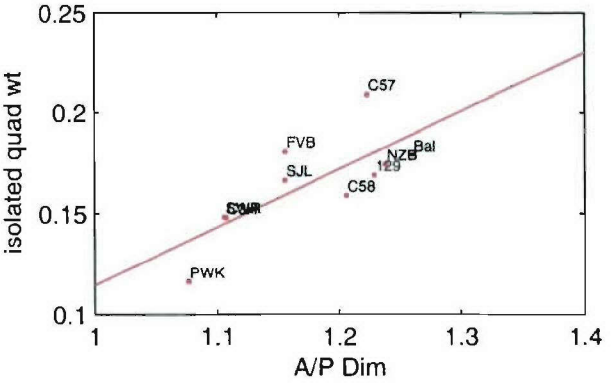
isolated quad wt
A/P Dim
C57
FVB
Bal
NZB
SJL
129
C58
PWK

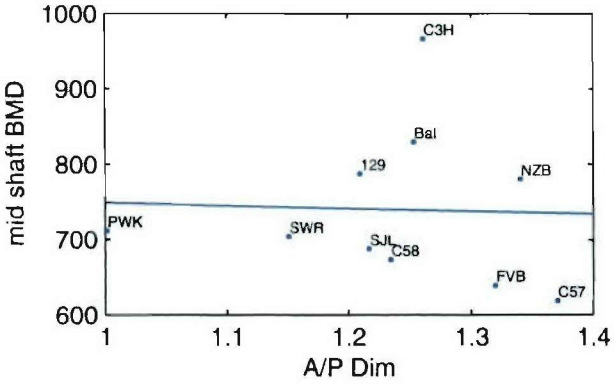
mid shaft BMD
A/P Dim
C3H
Bal
129
NZB
PWK
SWR
SJL
C58
FVB
C57

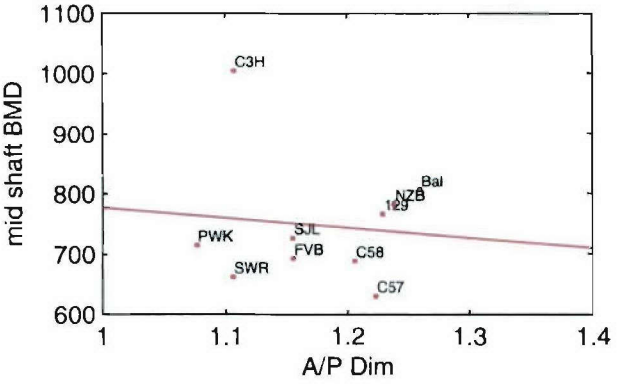
mid shaft BMD
A/P Dim
C3H
Bal
NZB
129
PWK
SJL
FVB
C58
SWR
C57

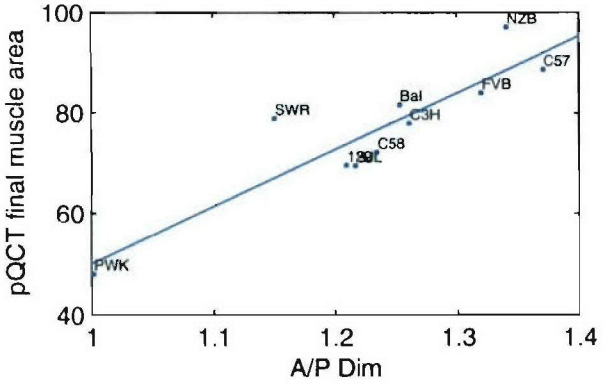
pQCT final muscle area
A/P Dim
NZB
C57
FVB
Bal
SWR
C3H
C58
PWK

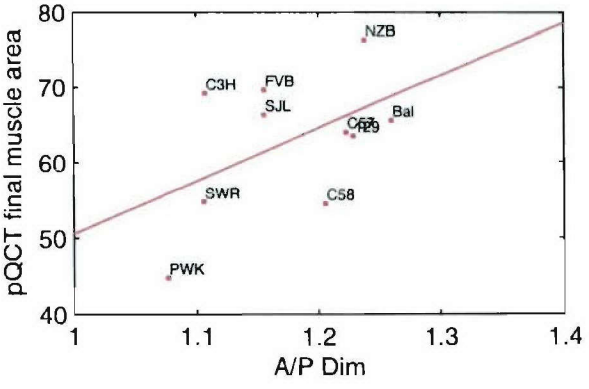
pQCT final muscle area
A/P Dim
NZB
C3H
FVB
SJL
Bal
C57
129
SWR
C58
PWK

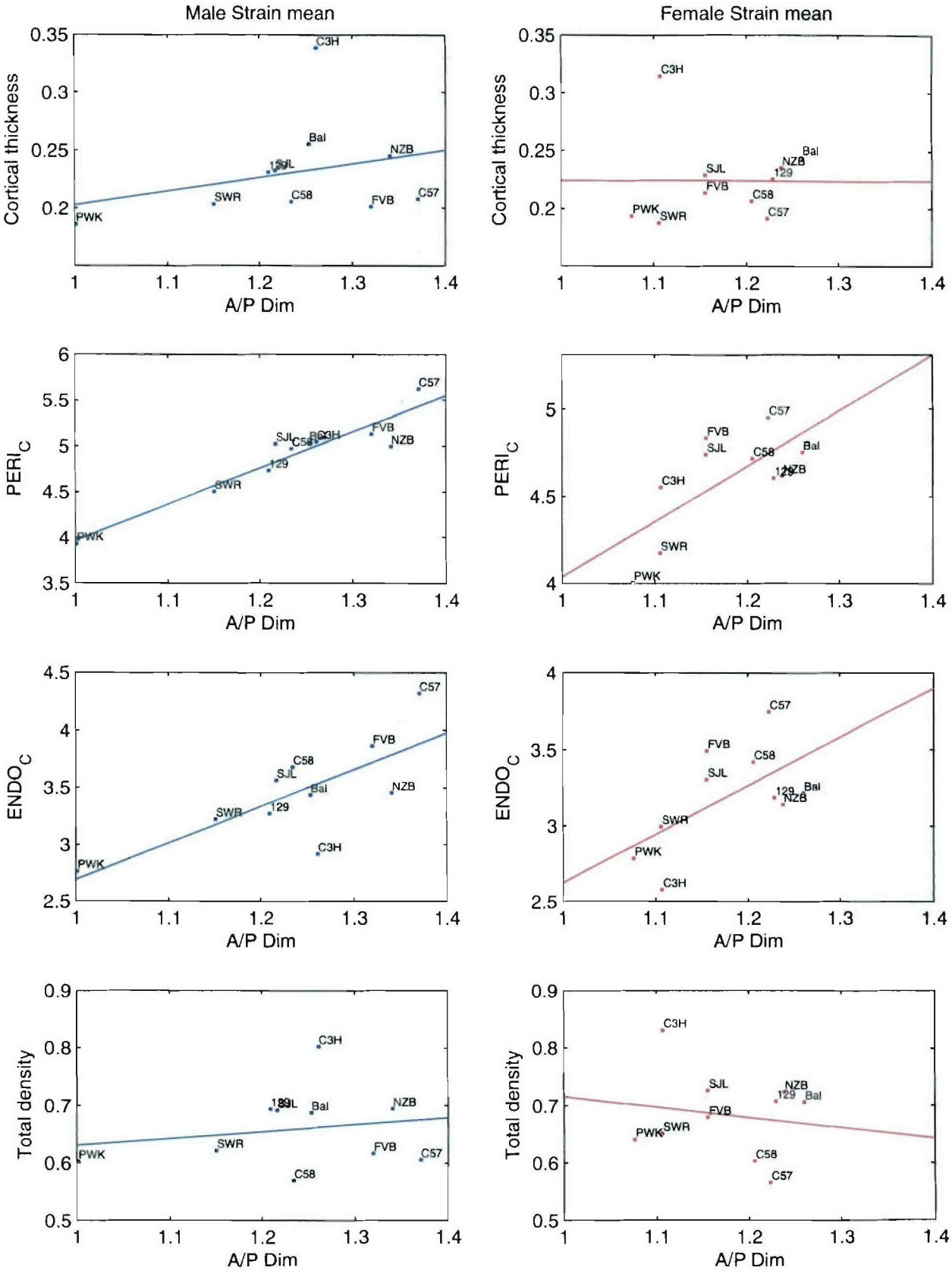
Male Strain mean
Female Strain mean
Cortical thickness
PERI_C
ENDO_C
Total density
A/P Dim
C3H
Bal
NZB
SJL
129
SWR
C58
FVB
C57
PWK

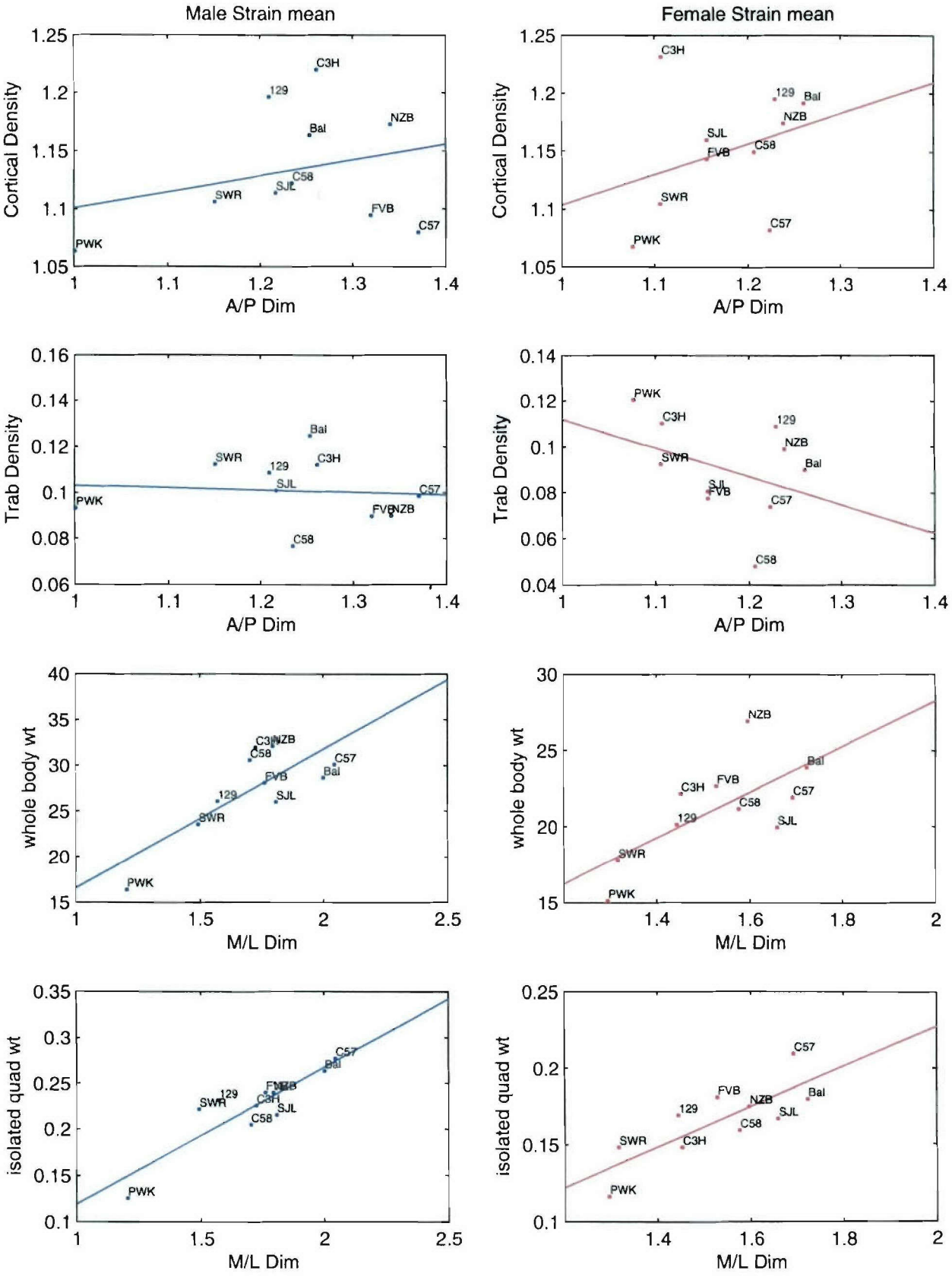
Male Strain mean
Female Strain mean
Cortical Density
Trab Density
whole body wt
isolated quad wt
A/P Dim
M/L Dim
C3H
129
Bal
NZB
SJL
C58
FVB
SWR
C57
PWK

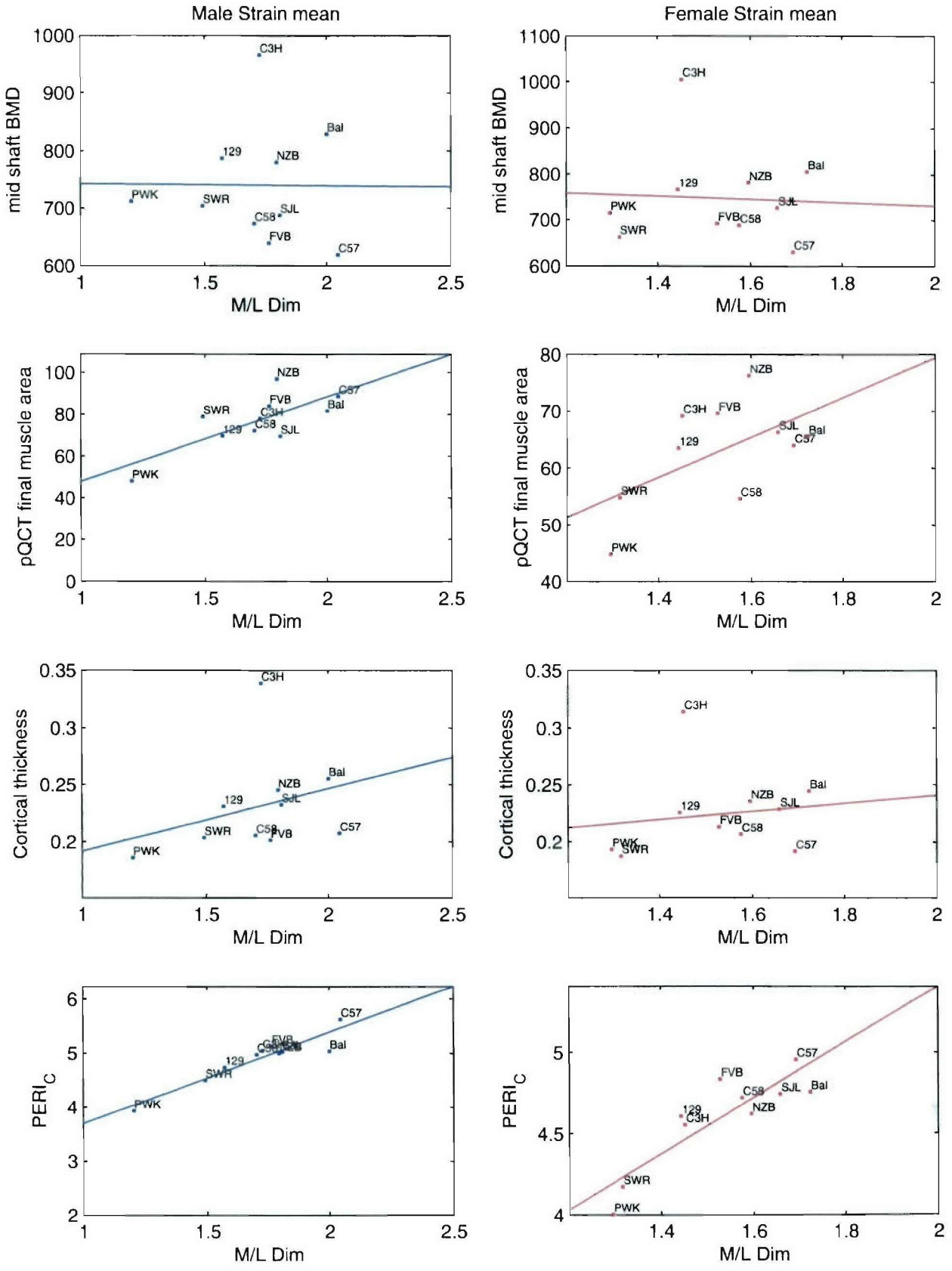
Male Strain mean
Female Strain mean
mid shaft BMD
pQCT final muscle area
Cortical thickness
PERI_C
M/L Dim
C3H
Bal
129
NZB
PWK
SWR
C58
SJL
FVB
C57

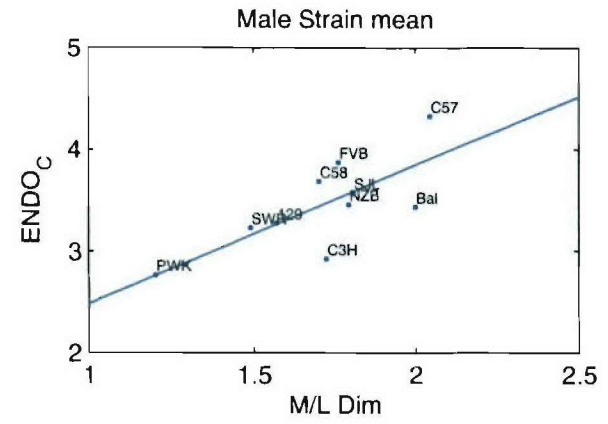
Male Strain mean
ENDO$_C$
M/L Dim
C57
FVB
C58
SJL
NZB
Bal
129
SWR
C3H
PWK

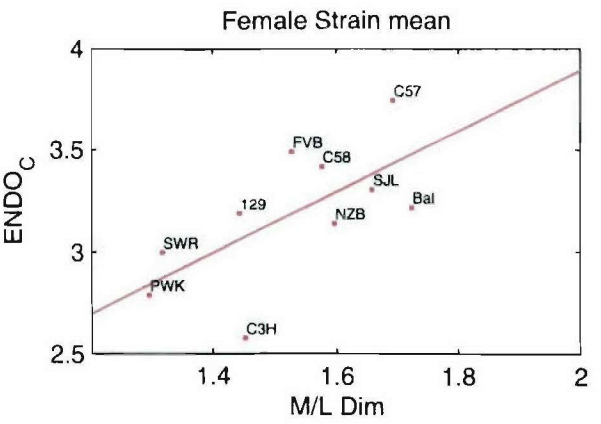
Female Strain mean
ENDO$_C$
M/L Dim
C57
FVB
C58
SJL
Bal
129
NZB
SWR
PWK
C3H

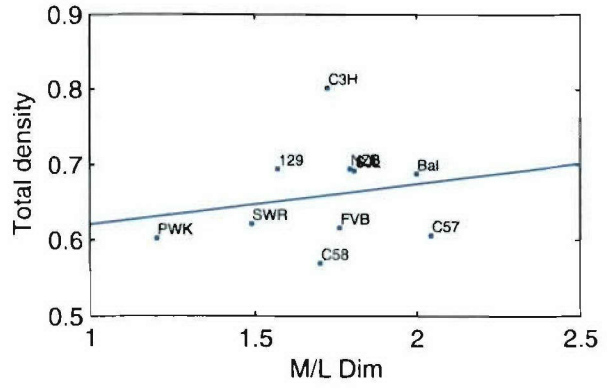
Total density
M/L Dim
C3H
129
Bal
PWK
SWR
FVB
C57
C58

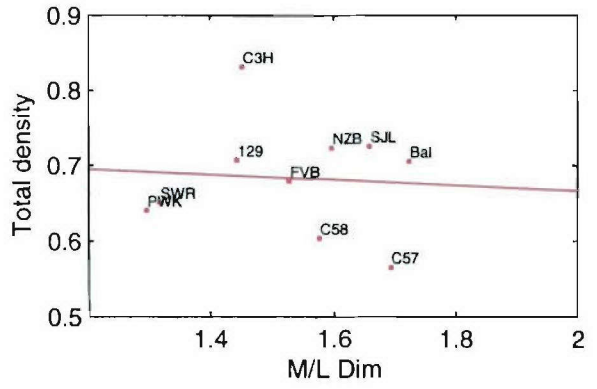
Total density
M/L Dim
C3H
129
NZB
SJL
Bal
FVB
SWR
PWK
C58
C57

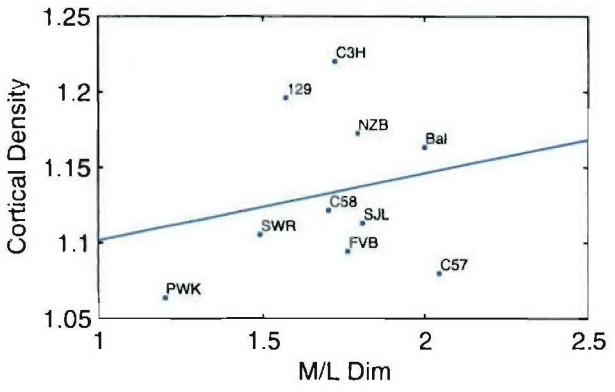
Cortical Density
M/L Dim
C3H
129
NZB
Bal
C58
SJL
SWR
FVB
C57
PWK

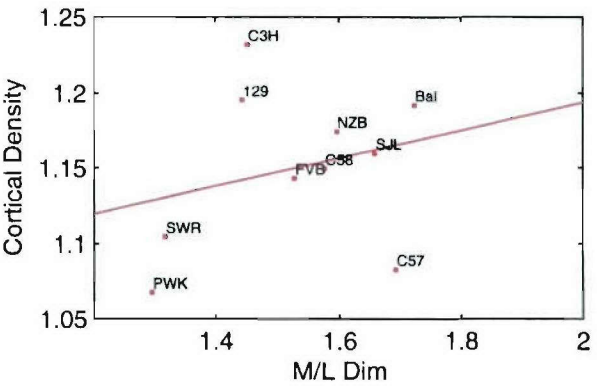
Cortical Density
M/L Dim
C3H
129
Bal
NZB
SJL
C58
FVB
SWR
C57
PWK

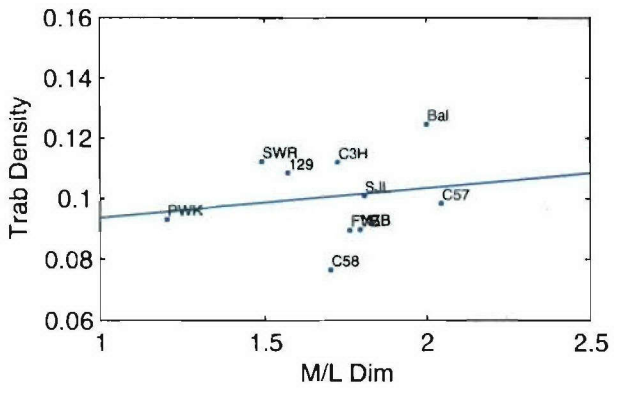
Trab Density
M/L Dim
Bal
SWR
129
C3H
SJL
C57
PWK
C58

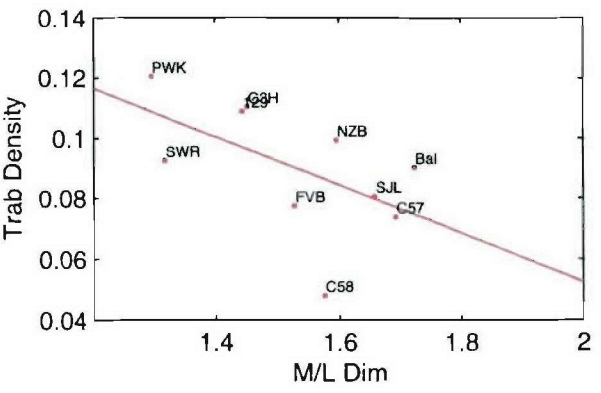
Trab Density
M/L Dim
PWK
C3H
129
NZB
SWR
Bal
SJL
FVB
C57
C58

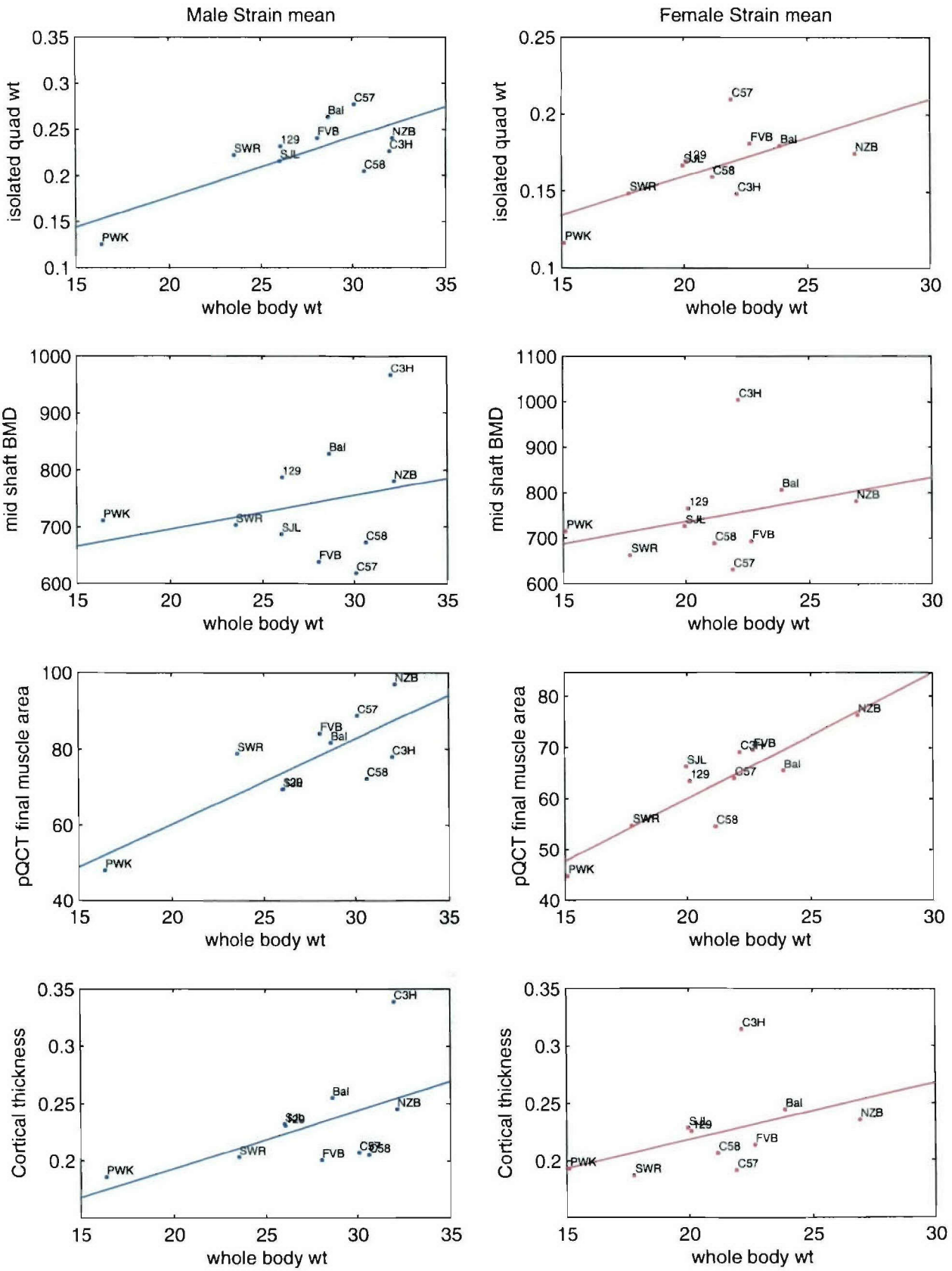
Male Strain mean
Female Strain mean
isolated quad wt
mid shaft BMD
pQCT final muscle area
Cortical thickness
whole body wt
PWK
SWR
129
SJL
Bal
FVB
NZB
C3H
C57
C58

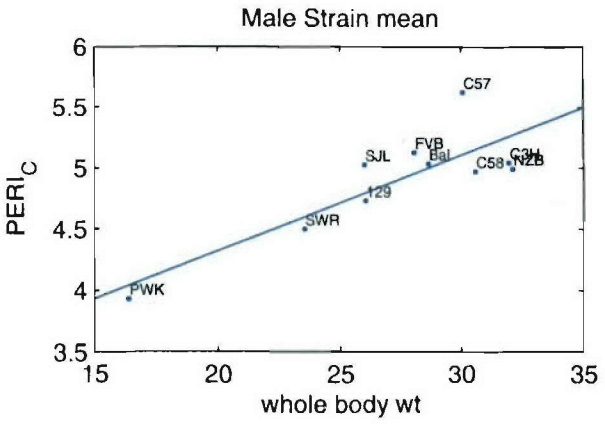
Male Strain mean
PERI_C
whole body wt
C57
FVB
SJL
Bal
C58
C3H
NZB
129
SWR
PWK

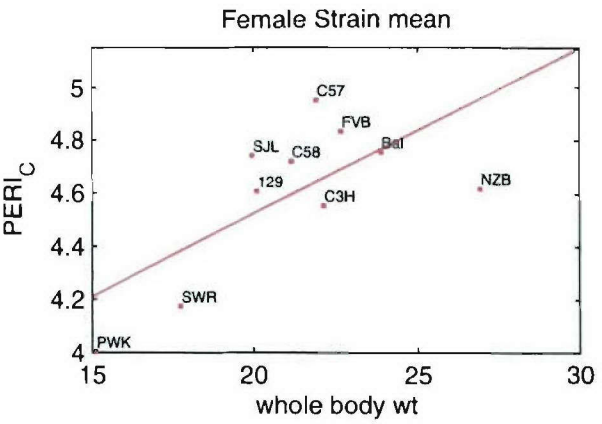
Female Strain mean
PERI_C
whole body wt
C57
FVB
SJL
C58
Bal
129
NZB
C3H
SWR
PWK

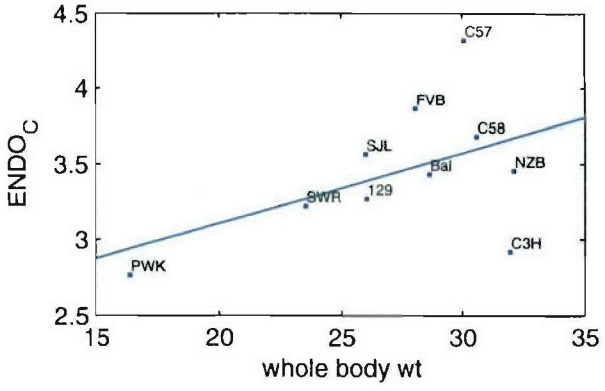
ENDO_C
whole body wt
C57
FVB
C58
SJL
Bal
NZB
SWR
129
C3H
PWK

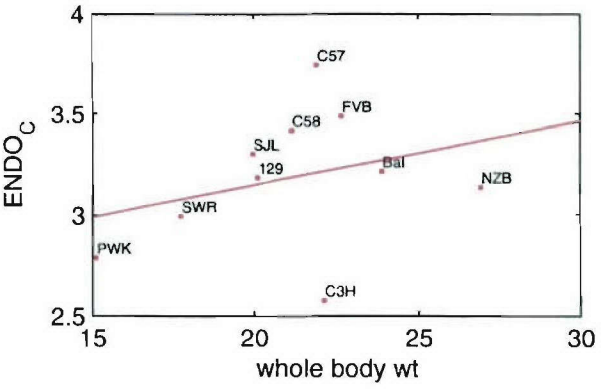
ENDO_C
whole body wt
C57
FVB
C58
SJL
129
Bal
NZB
SWR
PWK
C3H

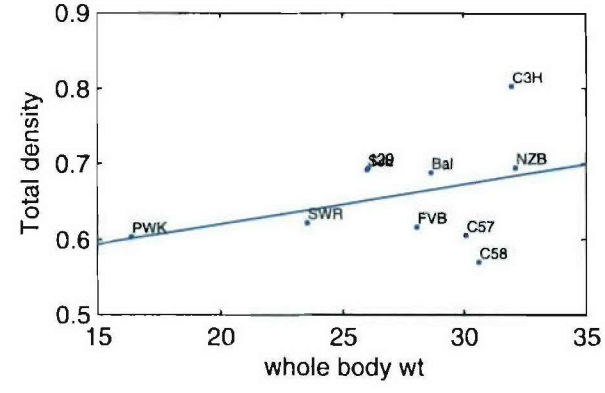
Total density
whole body wt
C3H
Bal
NZB
PWK
SWR
FVB
C57
C58

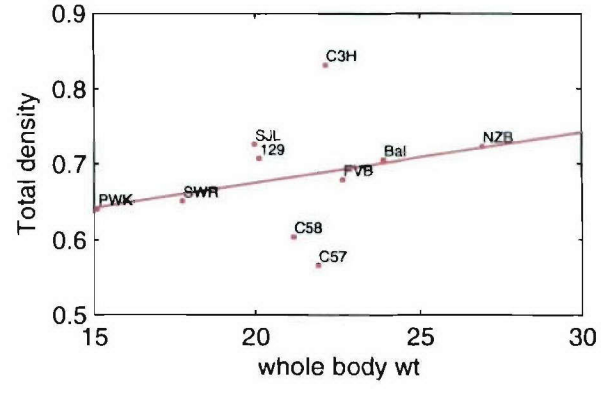
Total density
whole body wt
C3H
SJL
129
Bal
NZB
FVB
PWK
SWR
C58
C57

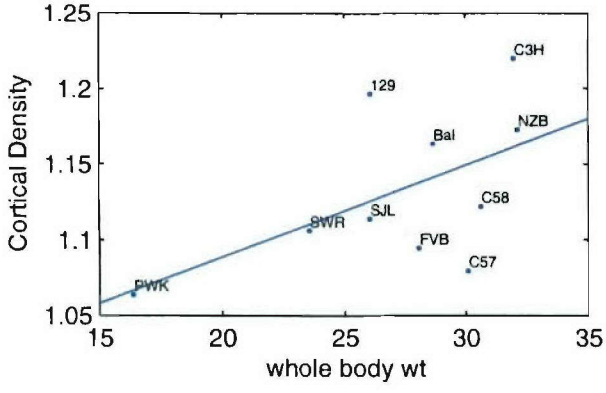
Cortical Density
whole body wt
C3H
129
NZB
Bal
C58
SWR
SJL
FVB
C57
PWK

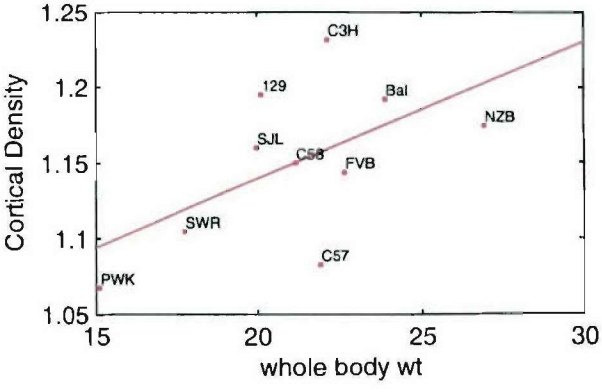
Cortical Density
whole body wt
C3H
129
Bal
NZB
SJL
C58
FVB
SWR
C57
PWK

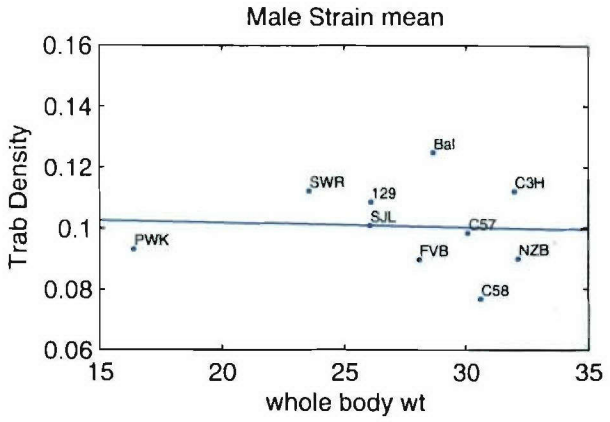
Male Strain mean
Trab Density
whole body wt
0.16
0.14
0.12
0.1
0.08
0.06
15
20
25
30
35
Bal
SWR
129
C3H
SJL
C57
PWK
FVB
NZB
C58

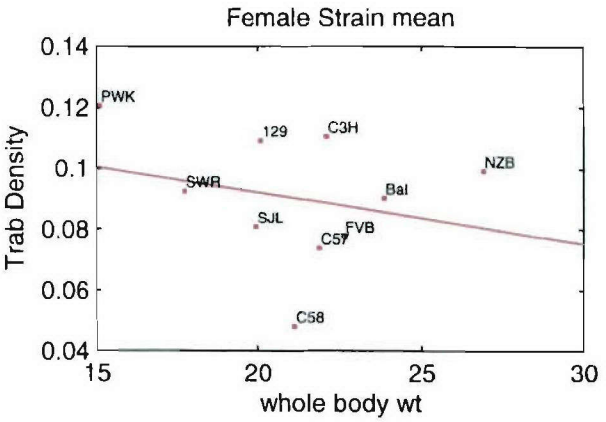
Female Strain mean
Trab Density
whole body wt
0.14
0.12
0.1
0.08
0.06
0.04
15
20
25
30
PWK
129
C3H
NZB
SWR
Bal
SJL
FVB
C57
C58

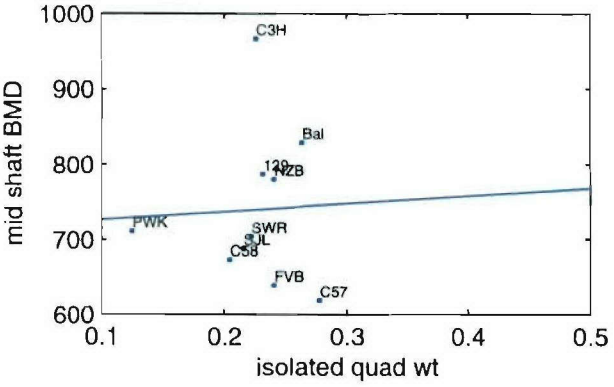
mid shaft BMD
isolated quad wt
1000
900
800
700
600
0.1
0.2
0.3
0.4
0.5
C3H
Bal
129
NZB
PWK
SWR
SJL
C58
FVB
C57

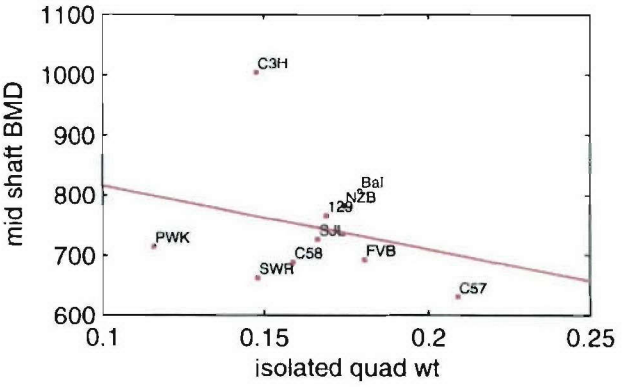
mid shaft BMD
isolated quad wt
1100
1000
900
800
700
600
0.1
0.15
0.2
0.25
C3H
Bal
NZB
129
PWK
SJL
C58
FVB
SWR
C57

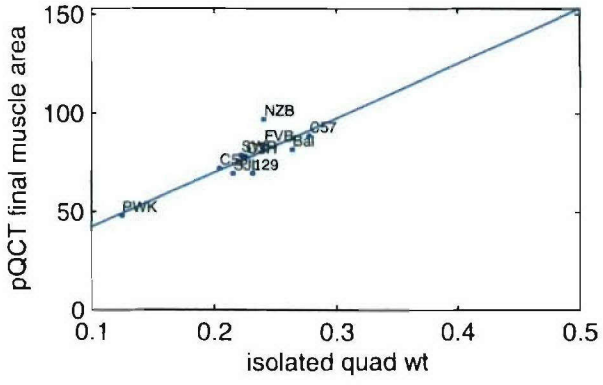
pQCT final muscle area
isolated quad wt
150
100
50
0
0.1
0.2
0.3
0.4
0.5
NZB
C57
FVB
Bal
129
PWK

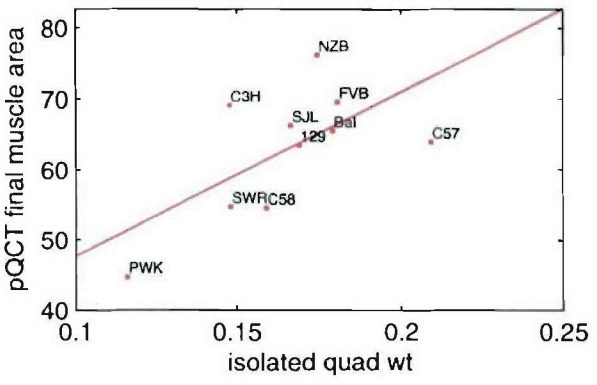
pQCT final muscle area
isolated quad wt
80
70
60
50
40
0.1
0.15
0.2
0.25
NZB
C3H
FVB
SJL
Bal
129
C57
SWR
C58
PWK

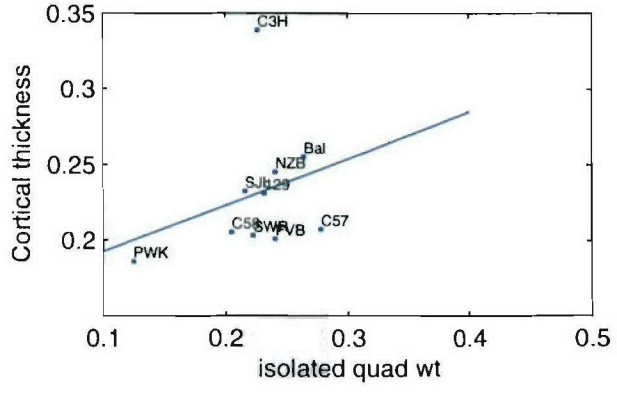
Cortical thickness
isolated quad wt
0.35
0.3
0.25
0.2
0.1
0.2
0.3
0.4
0.5
C3H
Bal
NZB
SJL
129
C58
SWR
FVB
C57
PWK

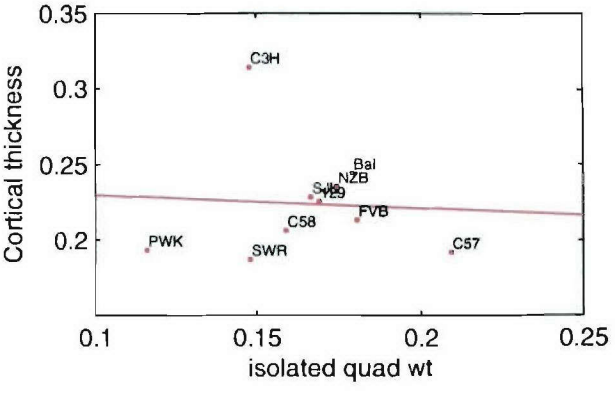
Cortical thickness
isolated quad wt
0.35
0.3
0.25
0.2
0.1
0.15
0.2
0.25
C3H
Bal
NZB
129
FVB
C58
PWK
SWR
C57

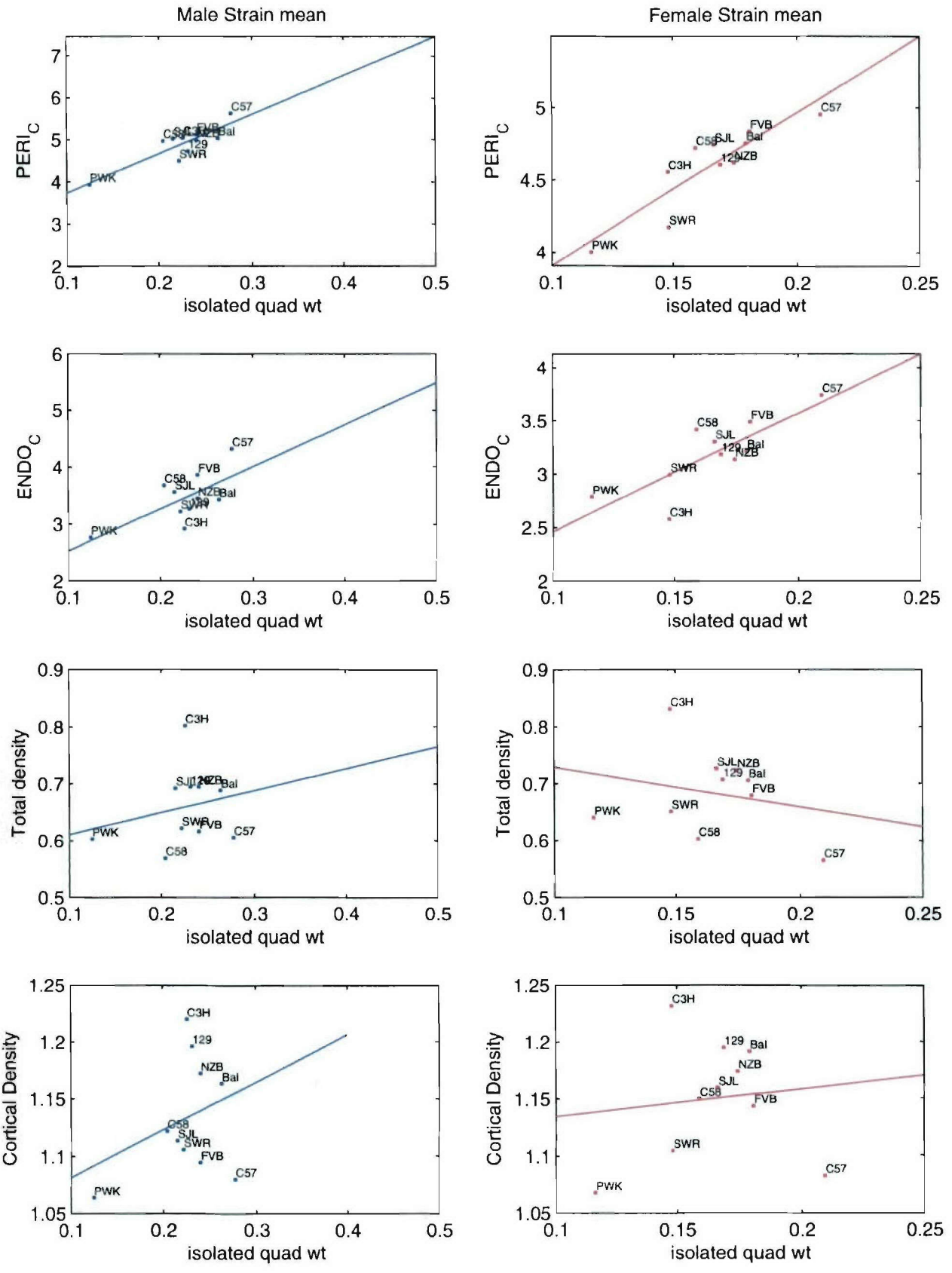
Male Strain mean
Female Strain mean
PERI_C
ENDO_C
Total density
Cortical Density
isolated quad wt
C57
C58
FVB
SJL
Bal
129
NZB
C3H
SWR
PWK

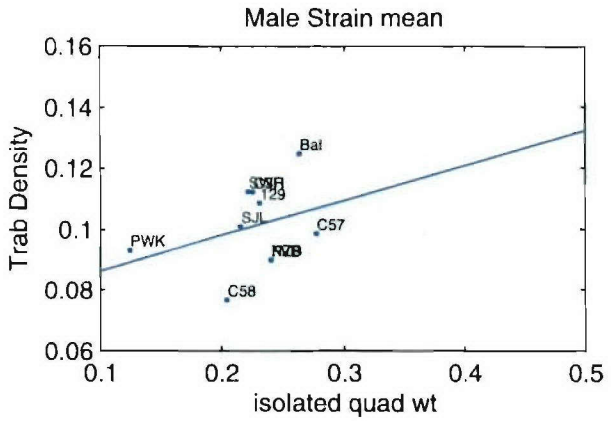
Male Strain mean
Trab Density
isolated quad wt
Bal
129
SJL
C57
PWK
C58

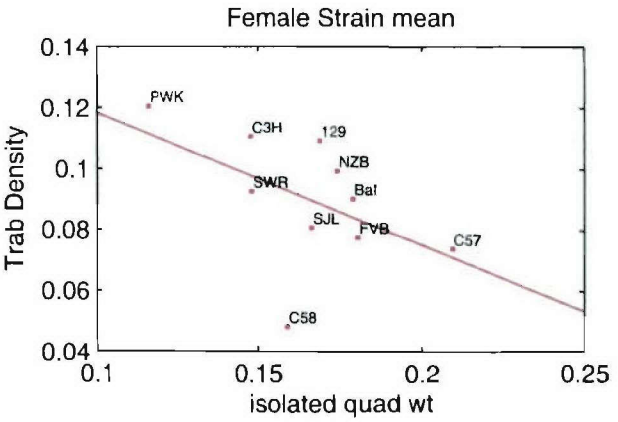
Female Strain mean
Trab Density
isolated quad wt
PWK
C3H
129
NZB
SWR
Bal
SJL
FVB
C57
C58

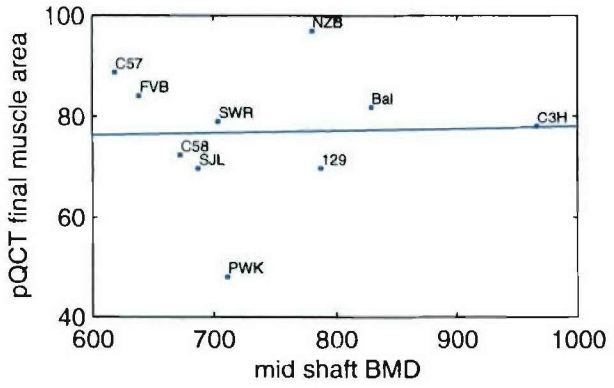
pQCT final muscle area
mid shaft BMD
NZB
C57
FVB
SWR
Bal
C3H
C58
SJL
129
PWK

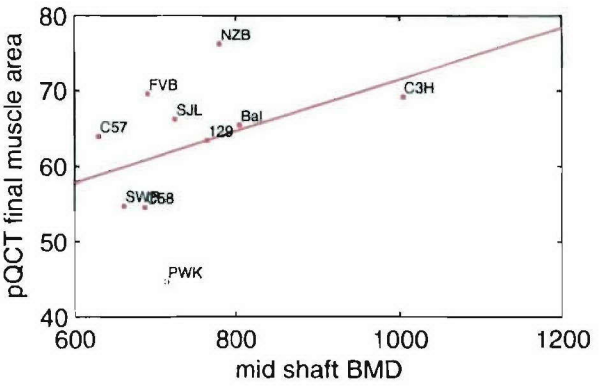
pQCT final muscle area
mid shaft BMD
NZB
FVB
C3H
SJL
Bal
C57
129
PWK

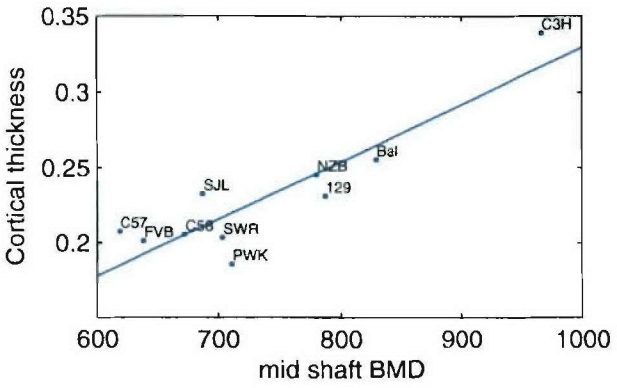
Cortical thickness
mid shaft BMD
C3H
Bal
NZB
SJL
129
C57
FVB
SWR
PWK

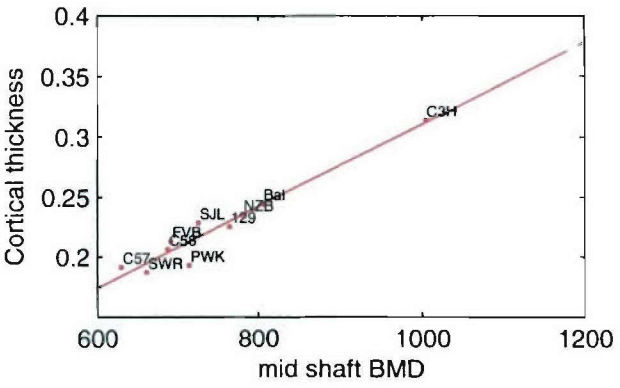
Cortical thickness
mid shaft BMD
C3H
Bal
SJL
NZB
129
FVB
C57
SWR
PWK

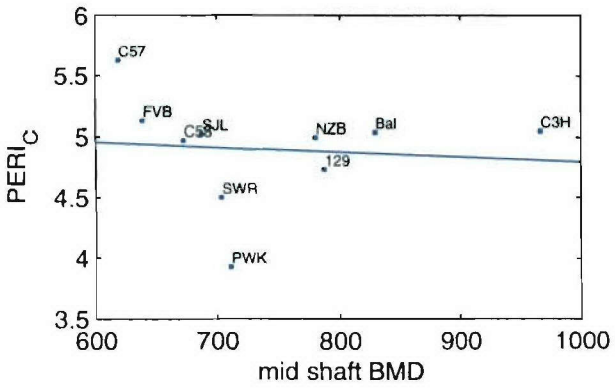
PERI_C
mid shaft BMD
C57
FVB
SJL
NZB
Bal
C3H
129
SWR
PWK

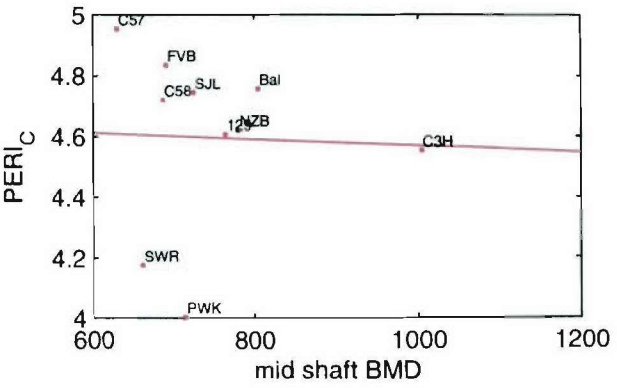
PERI_C
mid shaft BMD
C57
FVB
SJL
Bal
NZB
C3H
SWR
PWK

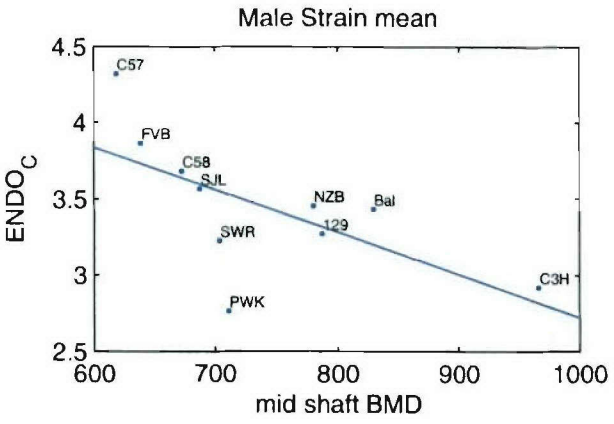
Male Strain mean
ENDO$_C$
mid shaft BMD
C57
FVB
C58
SJL
NZB
Bal
SWR
129
C3H
PWK

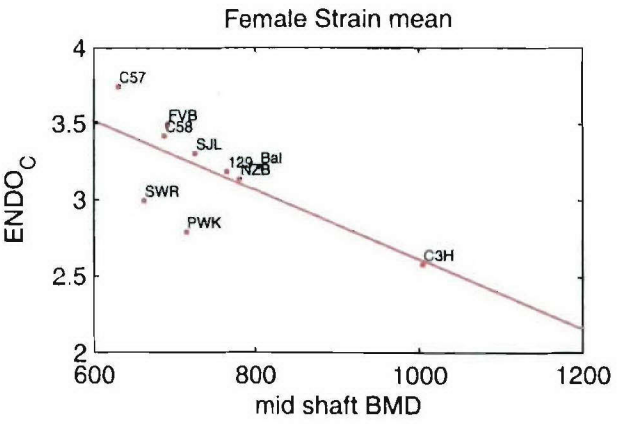
Female Strain mean
ENDO$_C$
mid shaft BMD
C57
FVB
C58
SJL
129
Bal
NZB
SWR
PWK
C3H

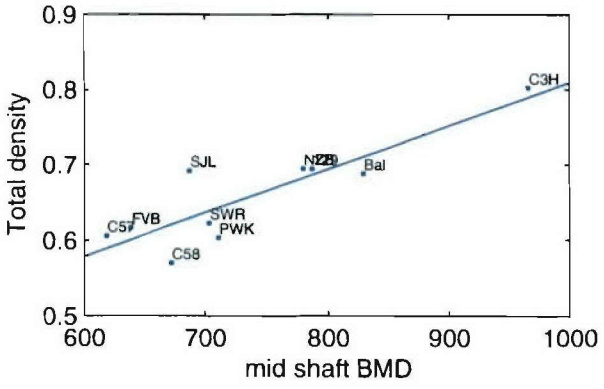
Total density
mid shaft BMD
C3H
SJL
NZB
Bal
C57
FVB
SWR
PWK
C58

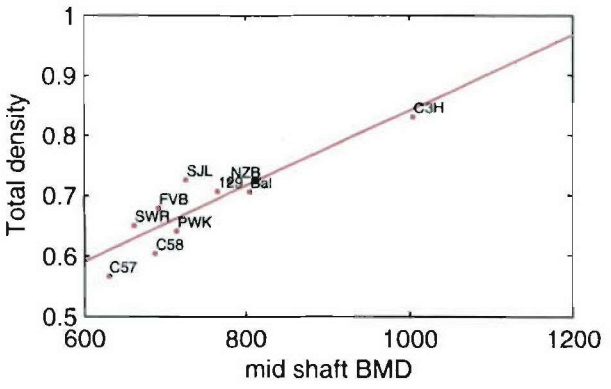
Total density
mid shaft BMD
C3H
SJL
NZB
129
Bal
FVB
SWR
PWK
C58
C57

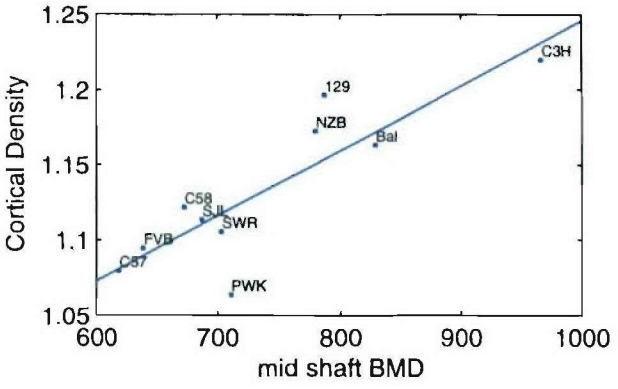
Cortical Density
mid shaft BMD
C3H
129
NZB
Bal
C58
SJL
SWR
FVB
C57
PWK

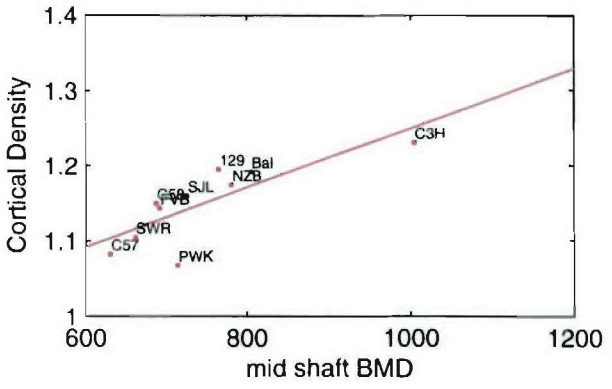
Cortical Density
mid shaft BMD
C3H
129
Bal
NZB
SJL
SWR
C57
PWK

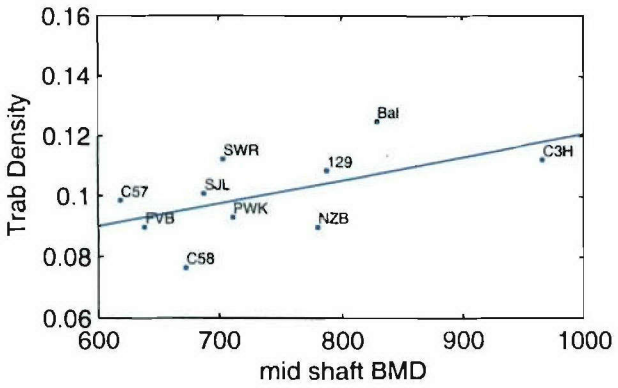
Trab Density
mid shaft BMD
Bal
SWR
129
C3H
C57
SJL
PWK
FVB
NZB
C58

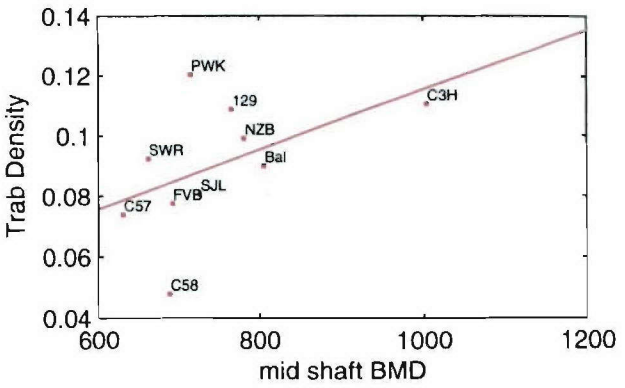
Trab Density
mid shaft BMD
PWK
129
C3H
NZB
SWR
Bal
SJL
C57
FVB
C58

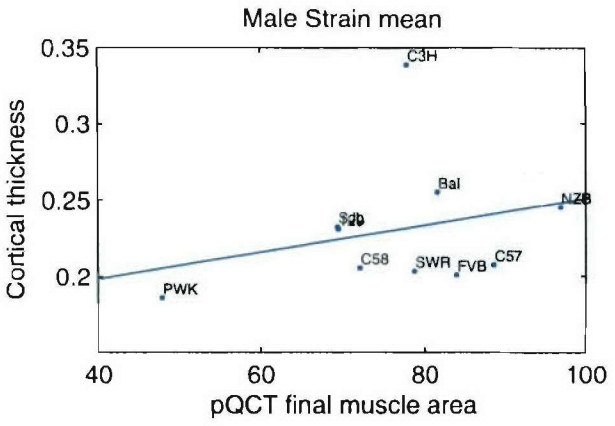
Male Strain mean
Cortical thickness
pQCT final muscle area
C3H
Bal
NZB
C58
SWR
FVB
C57
PWK

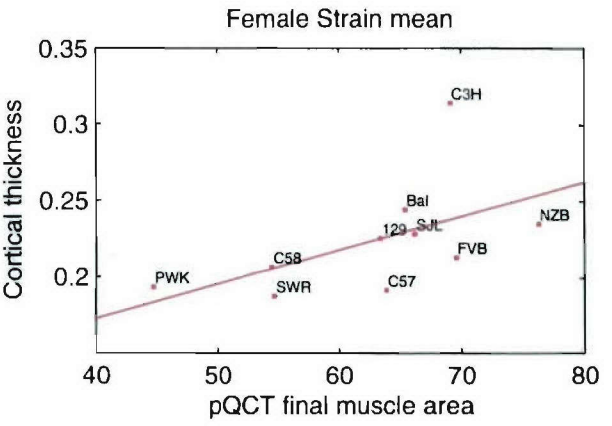
Female Strain mean
Cortical thickness
pQCT final muscle area
C3H
Bal
NZB
129
SJL
FVB
C58
PWK
SWR
C57

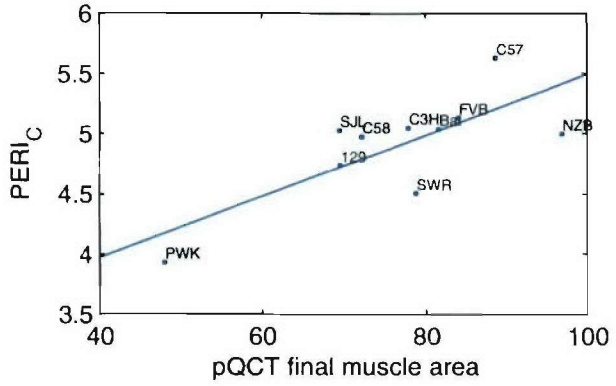
PERI_C
pQCT final muscle area
C57
SJL
C58
C3H
Bal
FVB
NZB
129
SWR
PWK

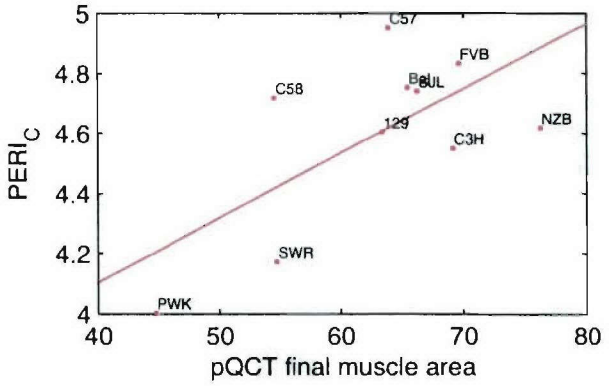
PERI_C
pQCT final muscle area
C57
FVB
C58
Bal
SJL
129
NZB
C3H
SWR
PWK

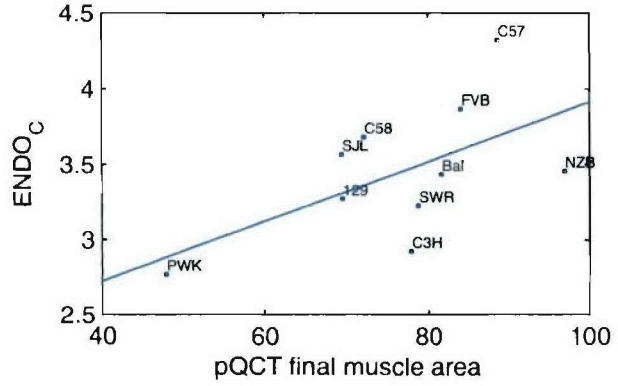
ENDO_C
pQCT final muscle area
C57
FVB
C58
SJL
Bal
NZB
129
SWR
C3H
PWK

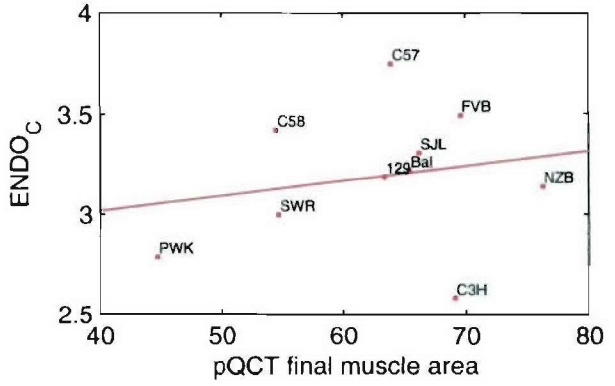
ENDO_C
pQCT final muscle area
C57
C58
FVB
SJL
129
Bal
NZB
SWR
PWK
C3H

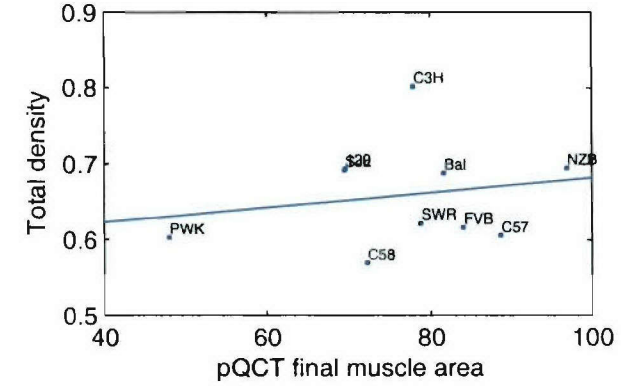
Total density
pQCT final muscle area
C3H
Bal
NZB
SWR
FVB
C57
PWK
C58

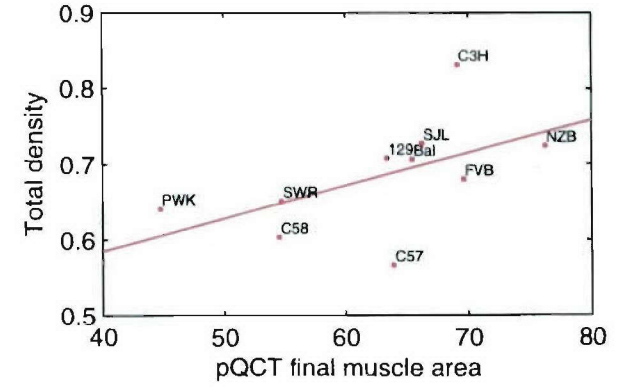
Total density
pQCT final muscle area
C3H
SJL
129
Bal
NZB
FVB
PWK
SWR
C58
C57

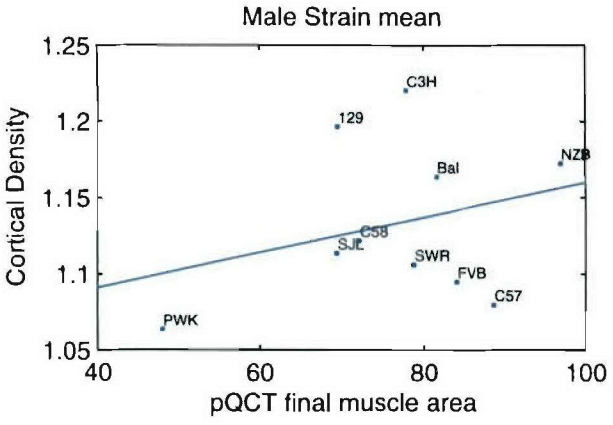
Male Strain mean
Cortical Density
pQCT final muscle area
C3H
129
Bal
NZB
C58
SJL
SWR
FVB
C57
PWK

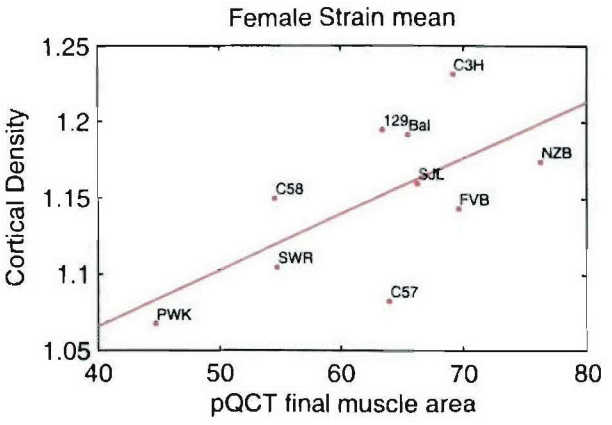
Female Strain mean
Cortical Density
pQCT final muscle area
C3H
129
Bal
NZB
SJL
C58
FVB
SWR
C57
PWK

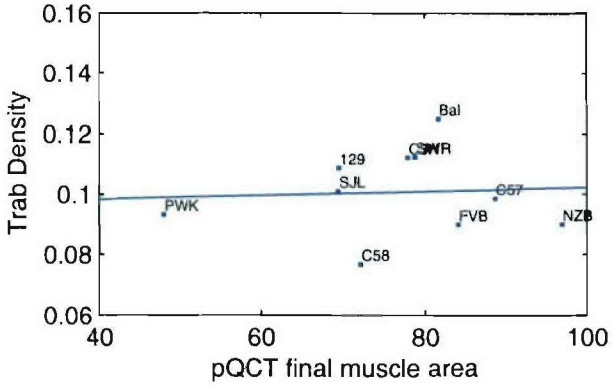
Trab Density
pQCT final muscle area
Bal
129
SJL
C57
PWK
FVB
NZB
C58

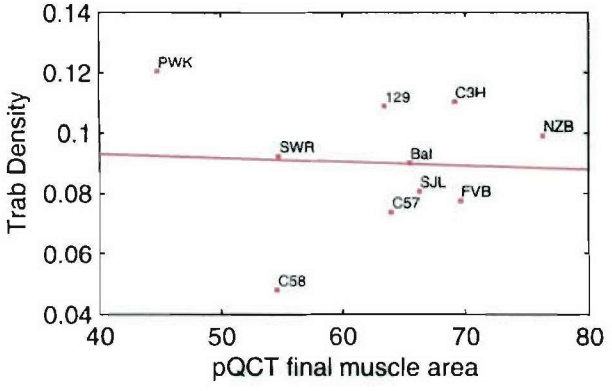
Trab Density
pQCT final muscle area
PWK
129
C3H
NZB
SWR
Bal
SJL
FVB
C57
C58

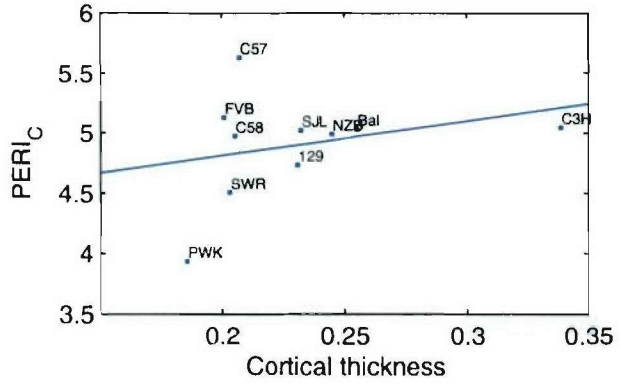
PERI_C
Cortical thickness
C57
FVB
C58
SJL
NZB
Bal
C3H
129
SWR
PWK

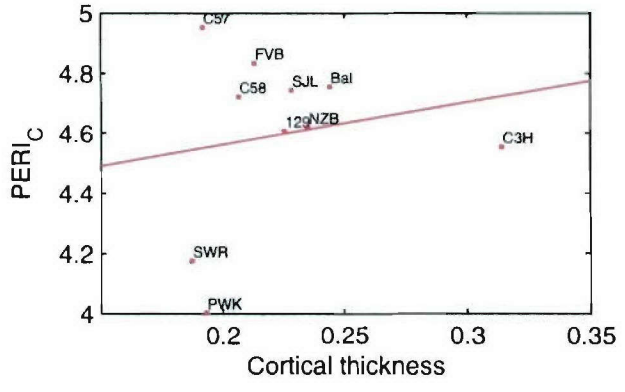
PERI_C
Cortical thickness
C57
FVB
C58
SJL
Bal
129
NZB
C3H
SWR
PWK

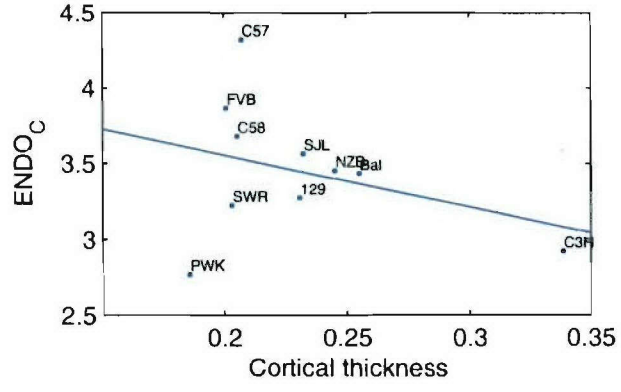
ENDO_C
Cortical thickness
C57
FVB
C58
SJL
NZB
Bal
SWR
129
C3H
PWK

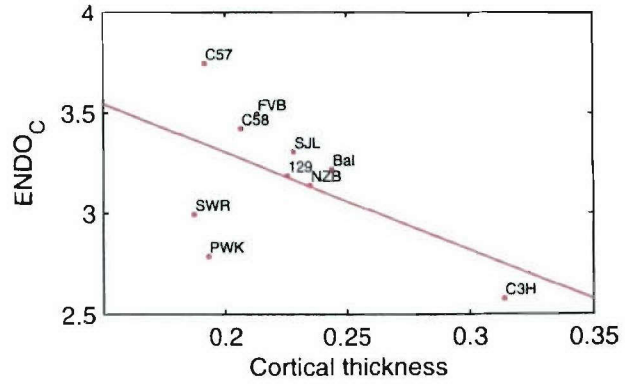
ENDO_C
Cortical thickness
C57
FVB
C58
SJL
129
Bal
NZB
SWR
PWK
C3H

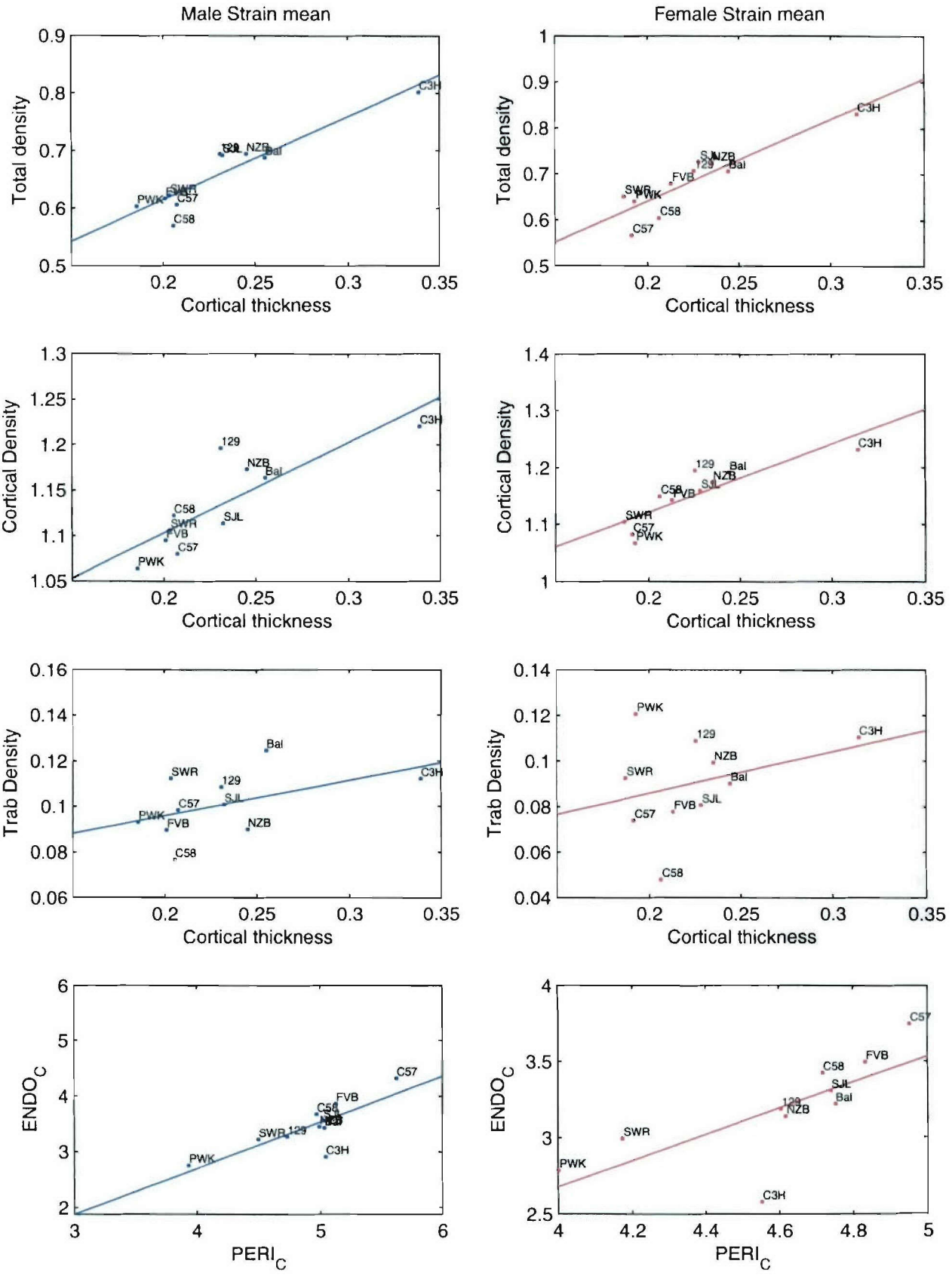
Male Strain mean
Female Strain mean
Total density
Cortical thickness
Cortical Density
Trab Density
ENDO_C
PERI_C
C3H
NZB
Bal
129
SJL
FVB
SWR
PWK
C57
C58

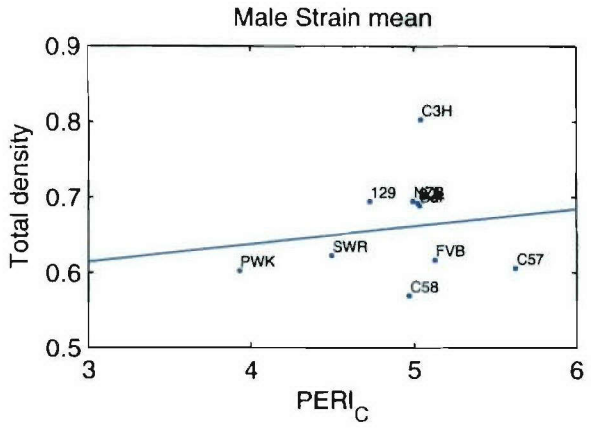
Male Strain mean
Total density
PERI_C
C3H
129
PWK
SWR
FVB
C57
C58

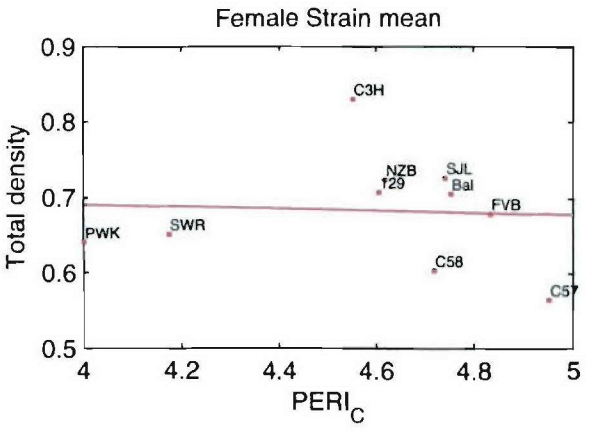
Female Strain mean
Total density
PERI_C
C3H
NZB
SJL
129
Bal
FVB
PWK
SWR
C58
C57

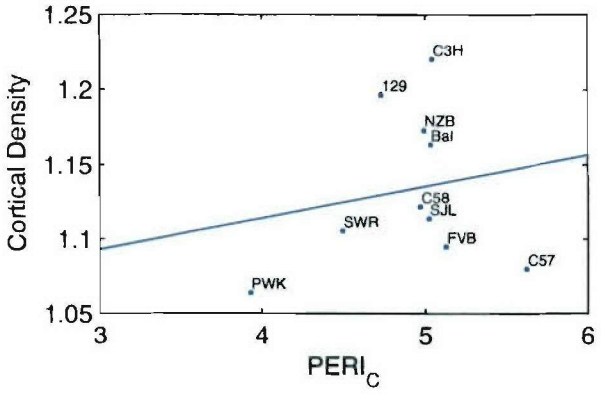
Cortical Density
PERI_C
C3H
129
NZB
Bal
C58
SJL
SWR
FVB
C57
PWK

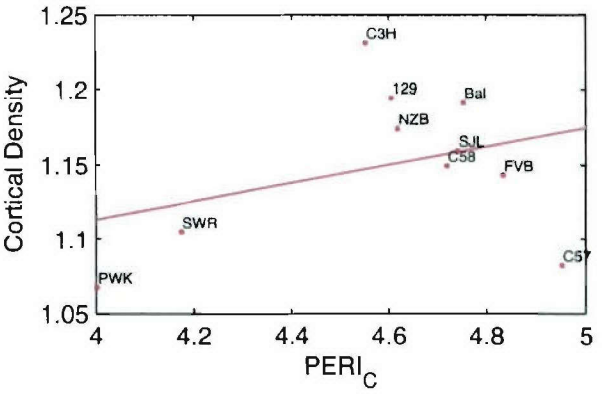
Cortical Density
PERI_C
C3H
129
Bal
NZB
SJL
C58
FVB
SWR
C57
PWK

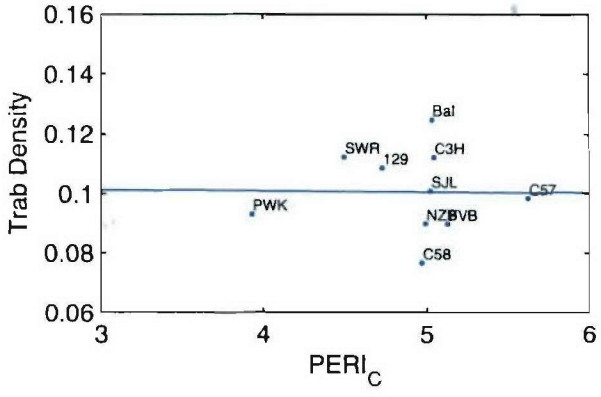
Trab Density
PERI_C
Bal
SWR
129
C3H
SJL
C57
PWK
NZB
FVB
C58

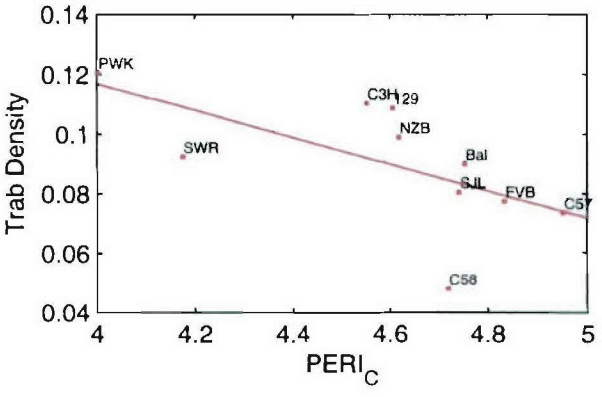
Trab Density
PERI_C
PWK
C3H
129
NZB
SWR
Bal
SJL
FVB
C57
C58

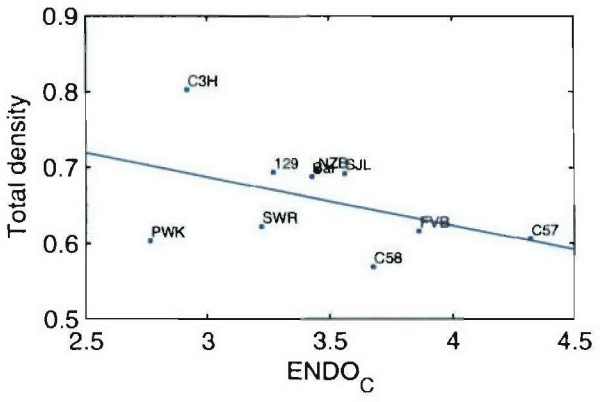
Total density
ENDO_C
C3H
129
NZB
SJL
PWK
SWR
FVB
C57
C58

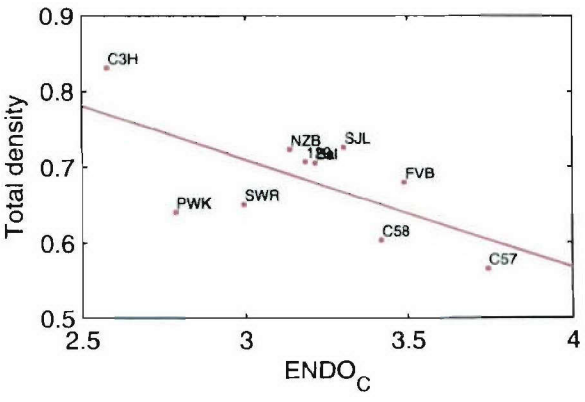
Total density
ENDO_C
C3H
NZB
SJL
FVB
PWK
SWR
C58
C57

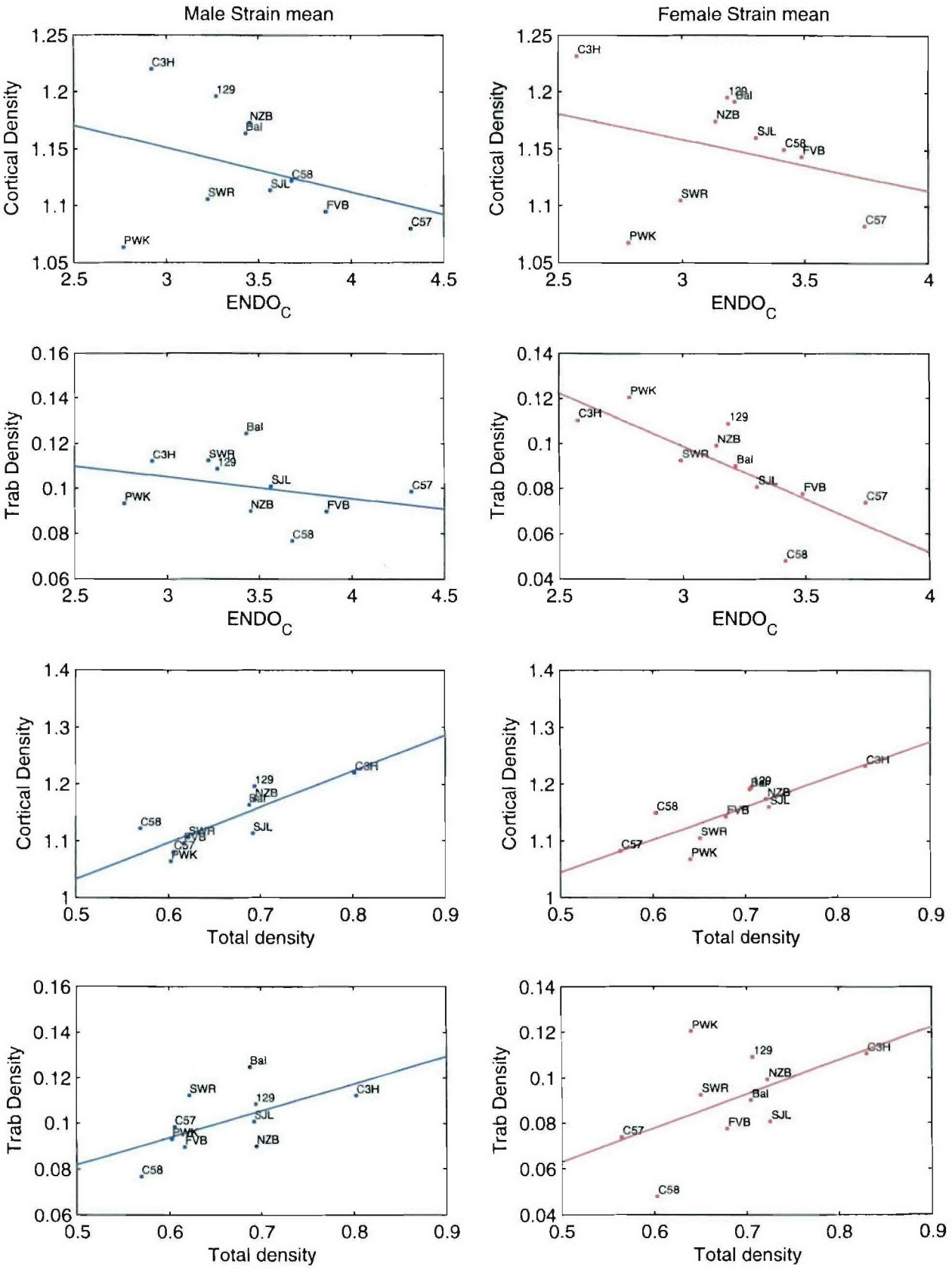
Male Strain mean
Female Strain mean
Cortical Density
Trab Density
Total density
ENDO_C
C3H
129
NZB
Bal
SJL
C58
FVB
SWR
C57
PWK

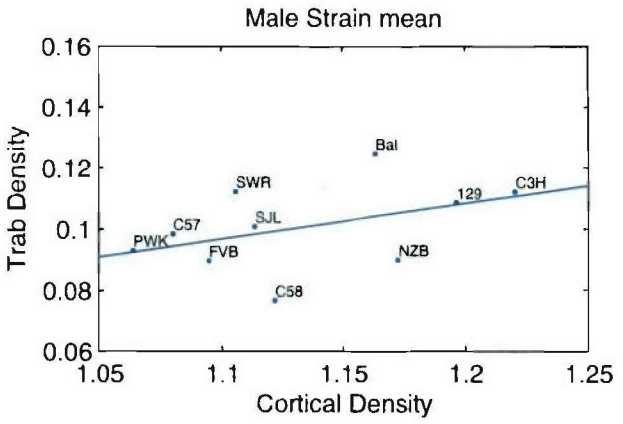
Male Strain mean
Trab Density
Cortical Density
0.16
0.14
0.12
0.1
0.08
0.06
1.05
1.1
1.15
1.2
1.25
Bal
SWR
129
C3H
C57
SJL
PWK
FVB
NZB
C58

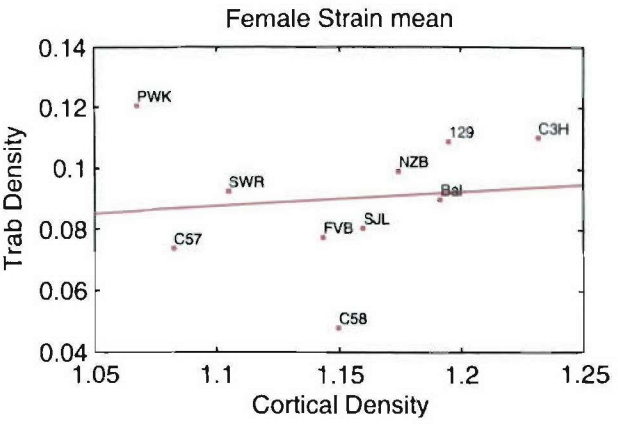
Female Strain mean
Trab Density
Cortical Density
0.14
0.12
0.1
0.08
0.06
0.04
1.05
1.1
1.15
1.2
1.25
PWK
129
C3H
NZB
SWR
Bal
C57
FVB
SJL
C58

Scatter plots of strain means

Exclude C3H/HeJ

(Jan-10-2005)

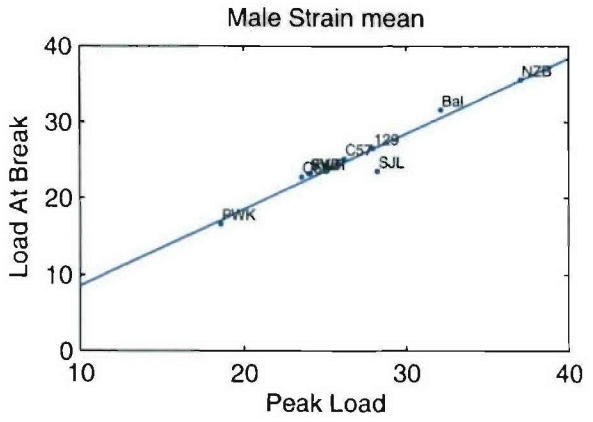
Male Strain mean
Load At Break
Peak Load
NZB
Bal
129
C57
SJL
PWK

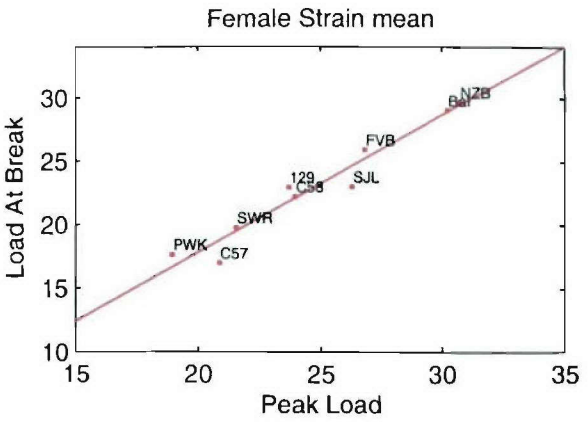
Female Strain mean
Load At Break
Peak Load
NZB
Bal
FVB
129
SJL
SWR
PWK
C57

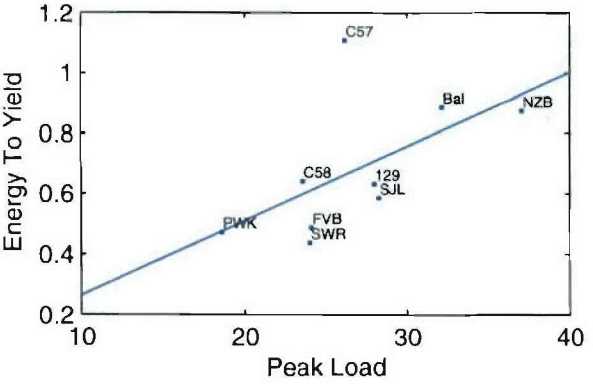
Energy To Yield
Peak Load
C57
Bal
NZB
C58
129
SJL
PWK
FVB
SWR

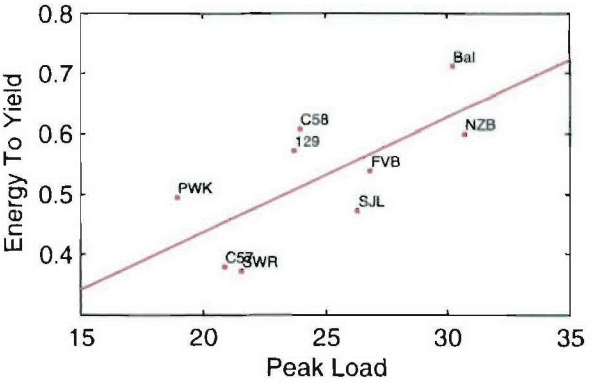
Energy To Yield
Peak Load
Bal
C58
129
NZB
FVB
PWK
SJL
SWR

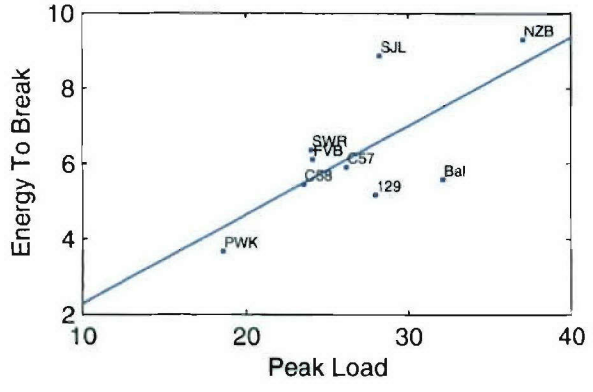
Energy To Break
Peak Load
NZB
SJL
SWR
FVB
C57
C58
Bal
129
PWK

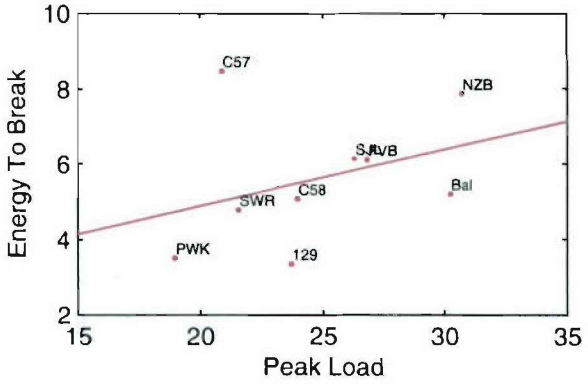
Energy To Break
Peak Load
C57
NZB
SJL
FVB
SWR
C58
Bal
PWK
129

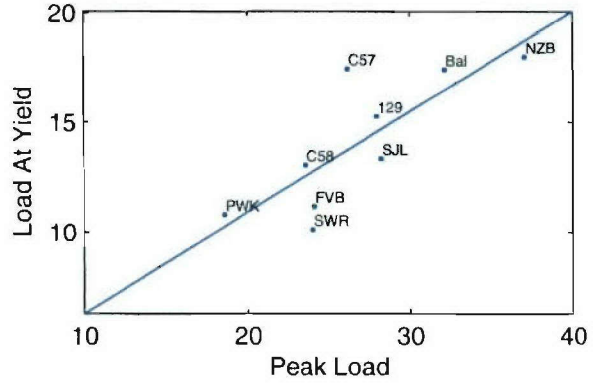
Load At Yield
Peak Load
C57
Bal
NZB
129
C58
SJL
PWK
FVB
SWR

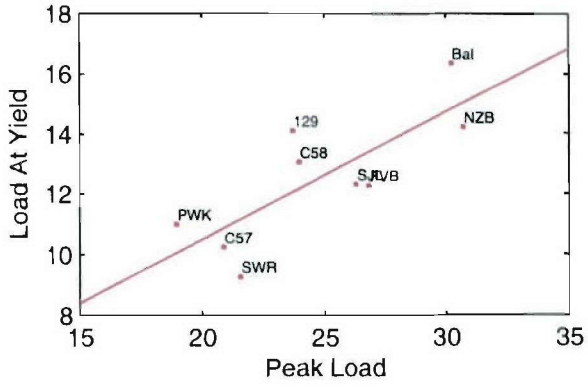
Load At Yield
Peak Load
Bal
129
NZB
C58
SJL
FVB
PWK
C57
SWR

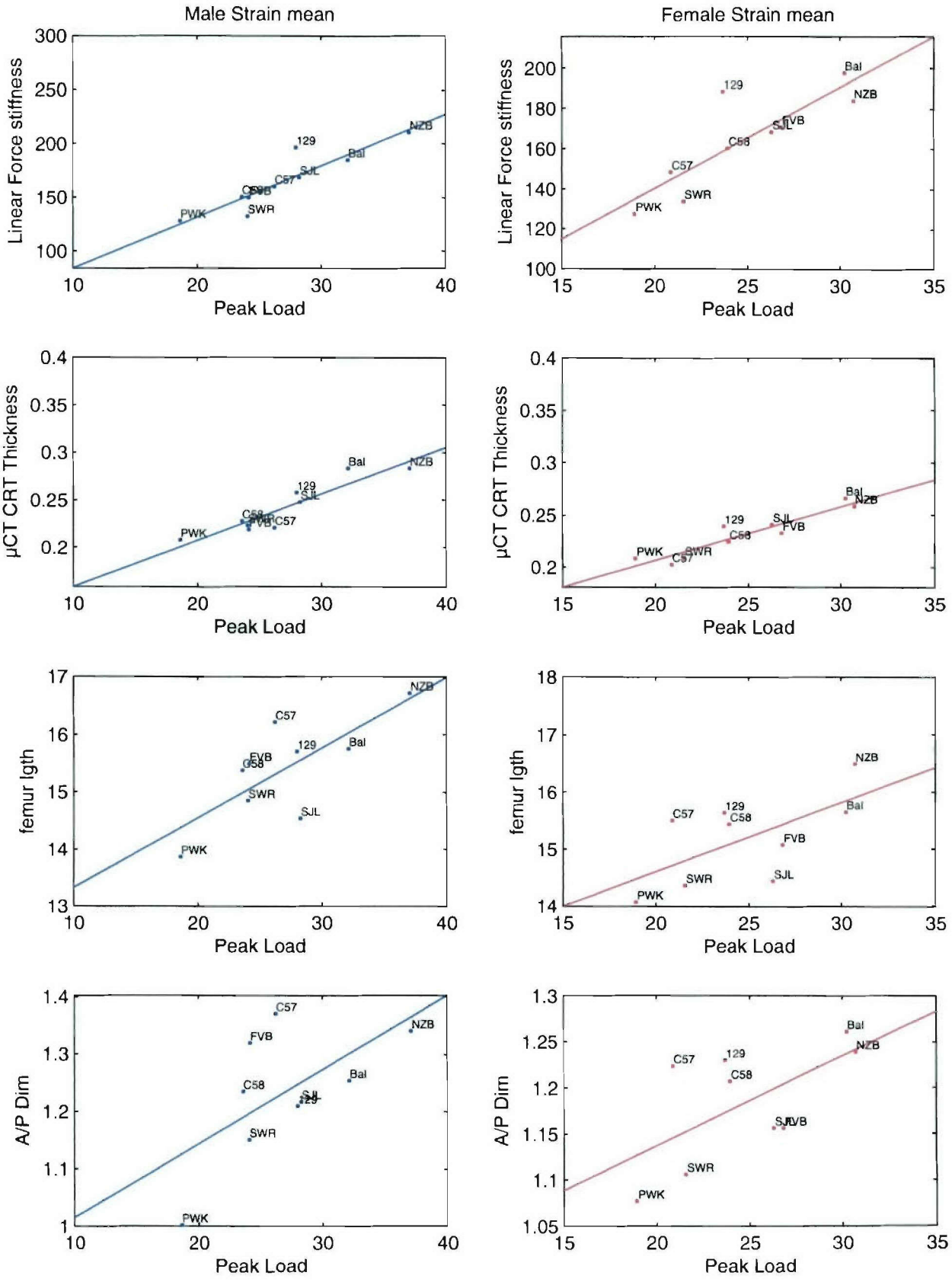
Male Strain mean
Female Strain mean
Linear Force stiffness
µCT CRT Thickness
femur lgth
A/P Dim
Peak Load
PWK
SWR
C57
C58
129
SJL
FVB
Bal
NZB

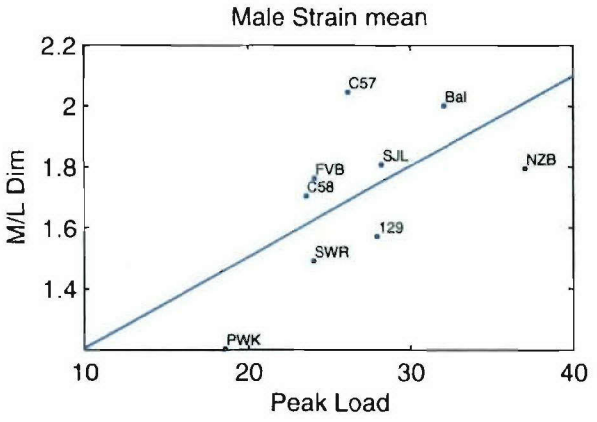
Male Strain mean
M/L Dim
Peak Load
C57
Bal
SJL
NZB
FVB
C58
129
SWR
PWK

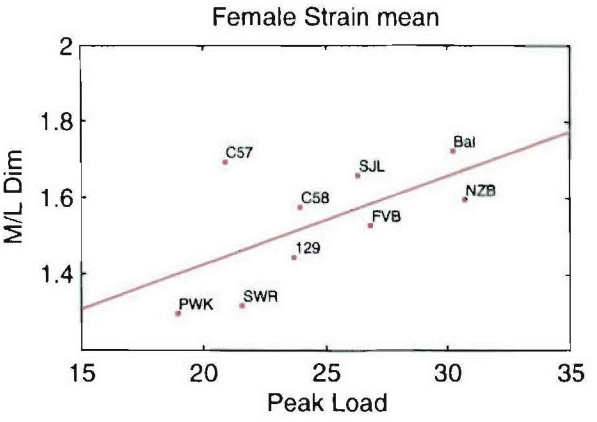
Female Strain mean
M/L Dim
Peak Load
C57
Bal
SJL
C58
NZB
FVB
129
PWK
SWR

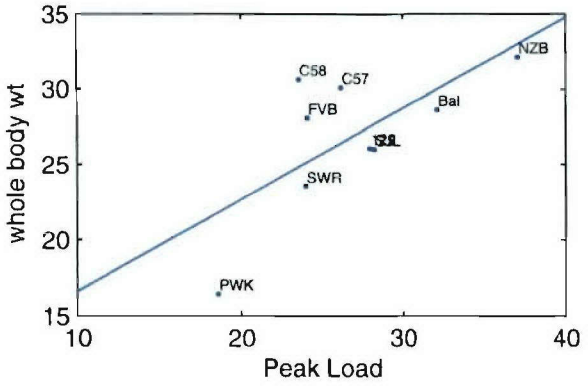
whole body wt
Peak Load
NZB
C58
C57
FVB
Bal
SWR
PWK

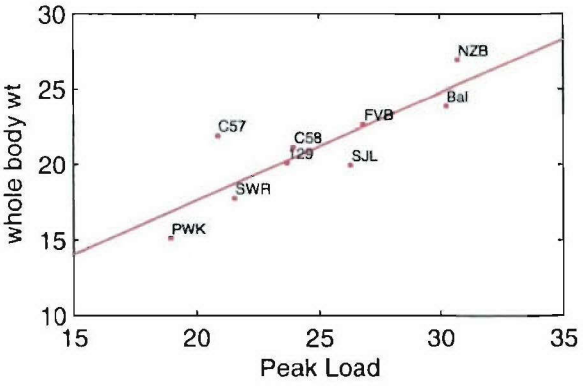
whole body wt
Peak Load
NZB
Bal
FVB
C57
C58
129
SJL
SWR
PWK

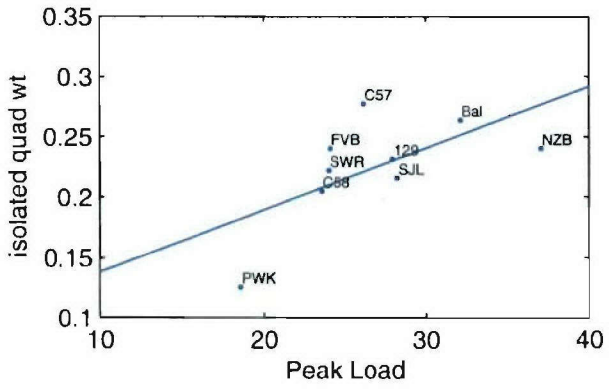
isolated quad wt
Peak Load
C57
Bal
FVB
NZB
129
SWR
SJL
C58
PWK

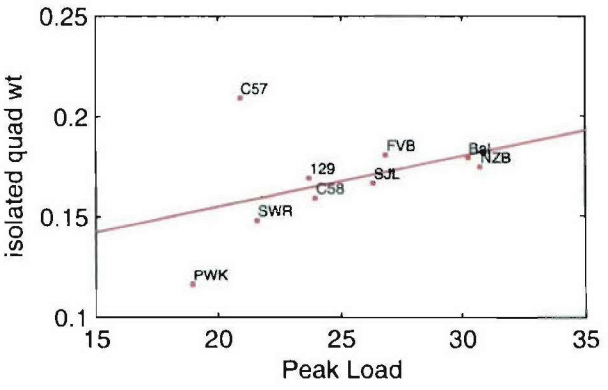
isolated quad wt
Peak Load
C57
FVB
Bal
NZB
129
SJL
C58
SWR
PWK

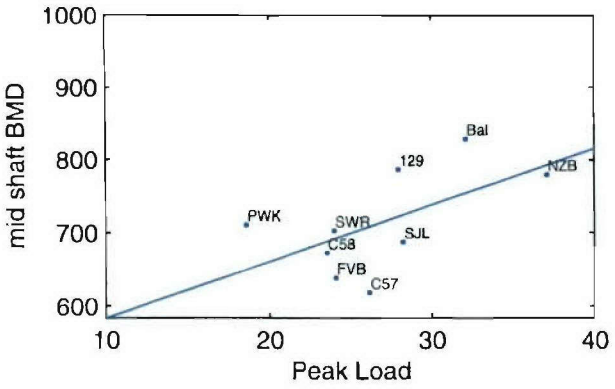
mid shaft BMD
Peak Load
Bal
129
NZB
PWK
SWR
SJL
C58
FVB
C57

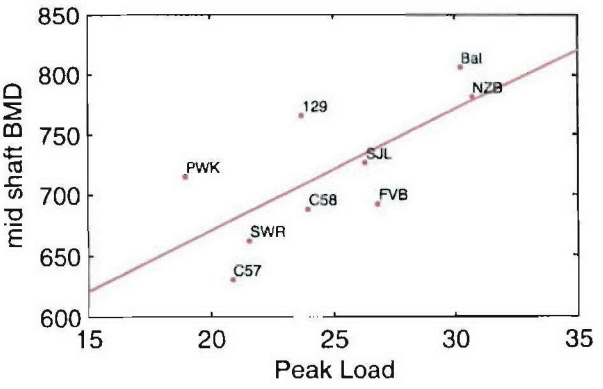
mid shaft BMD
Peak Load
Bal
NZB
129
PWK
SJL
C58
FVB
SWR
C57

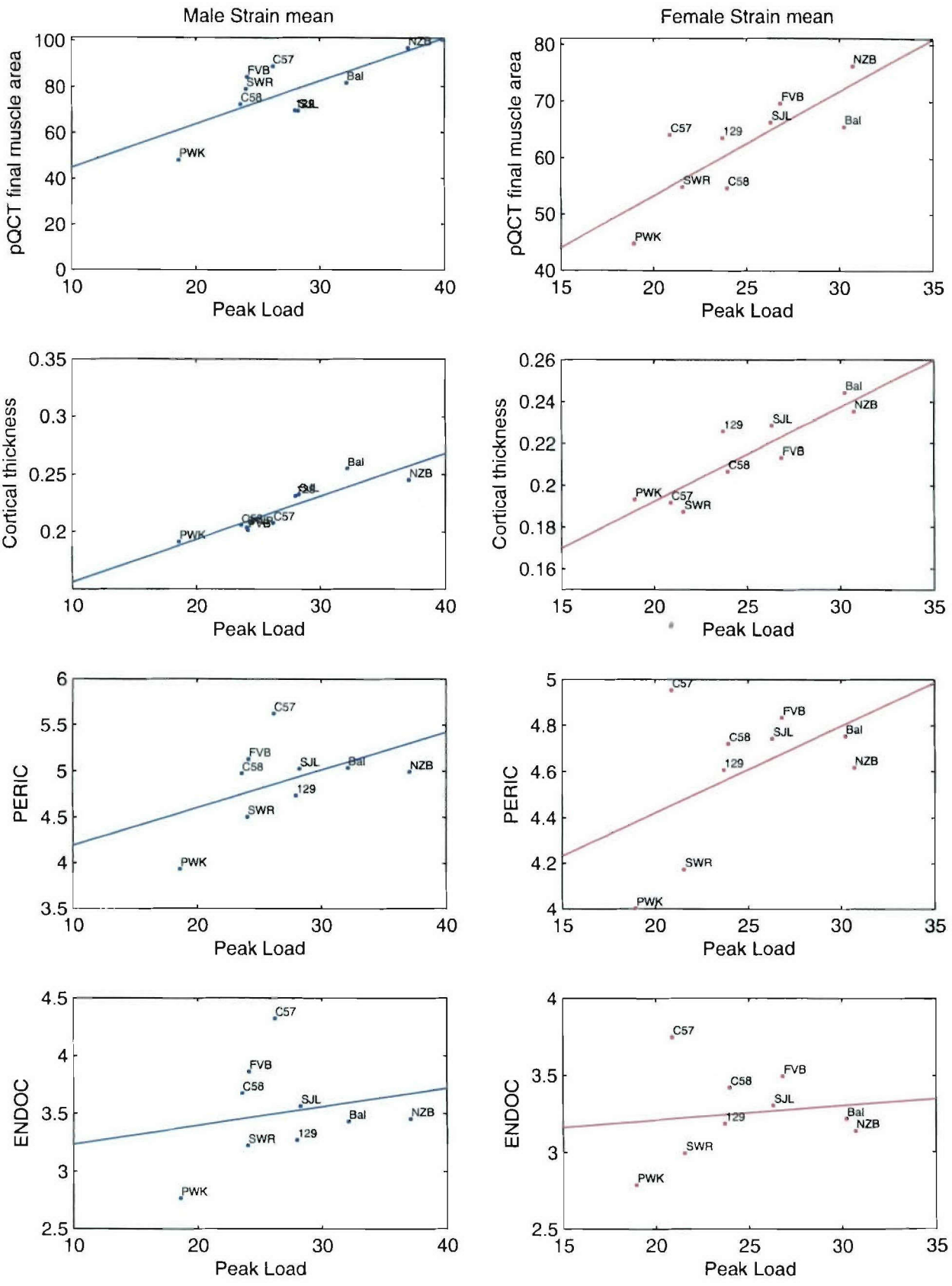
Male Strain mean
Female Strain mean
pQCT final muscle area
Cortical thickness
PERIC
ENDOC
Peak Load
C57
FVB
SWR
C58
Bal
NZB
PWK
SJL
129

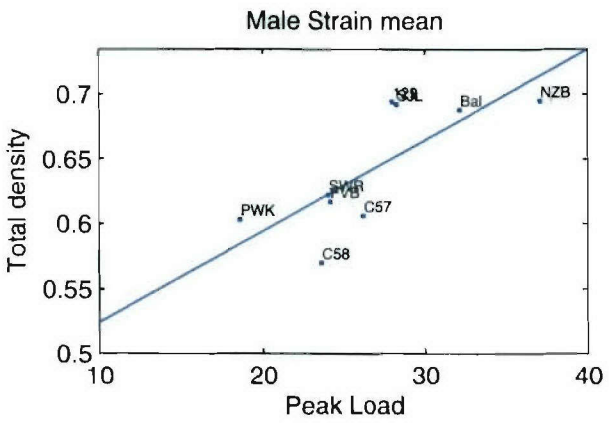
Male Strain mean
Total density
Peak Load
PWK
SWR
FVB
C57
C58
Bal
NZB

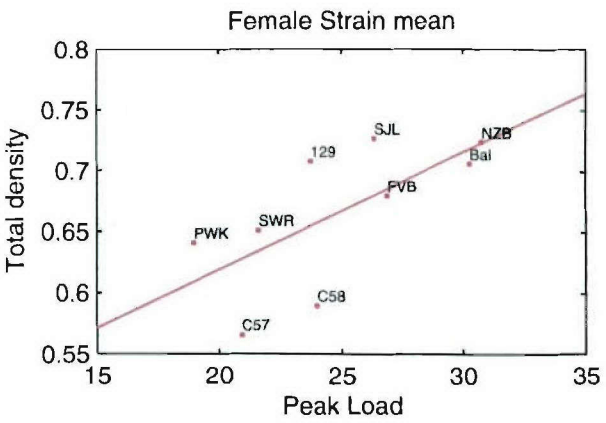
Female Strain mean
Total density
Peak Load
SJL
NZB
129
Bal
FVB
PWK
SWR
C58
C57

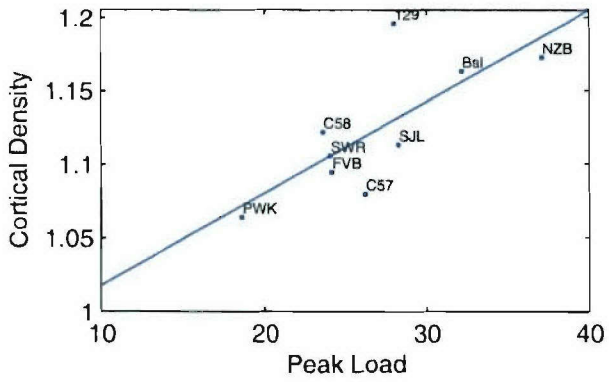
Cortical Density
Peak Load
Bal
NZB
C58
SJL
SWR
FVB
C57
PWK

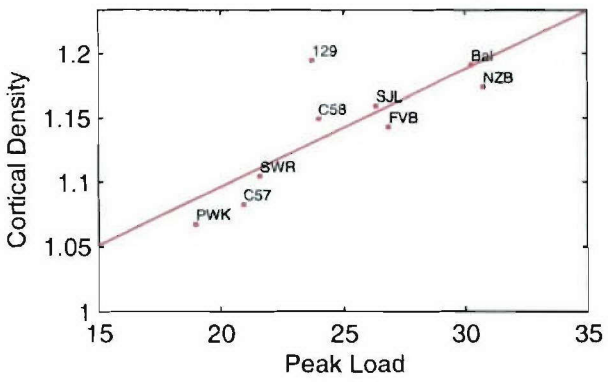
Cortical Density
Peak Load
129
Bal
NZB
SJL
C58
FVB
SWR
C57
PWK

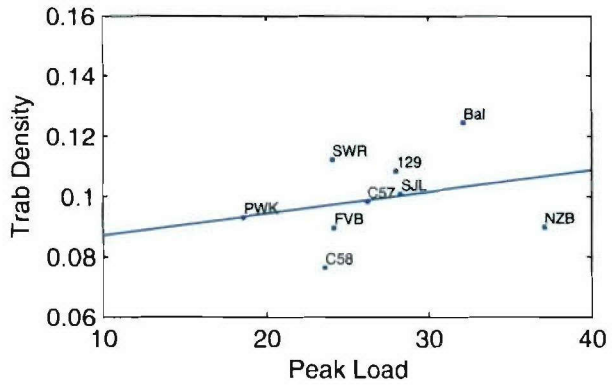
Trab Density
Peak Load
Bal
SWR
129
SJL
C57
PWK
FVB
NZB
C58

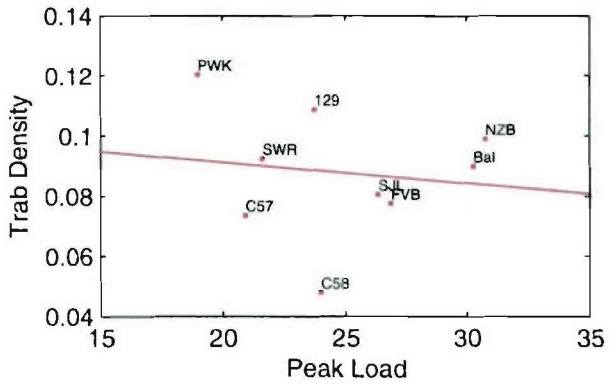
Trab Density
Peak Load
PWK
129
NZB
SWR
Bal
SJL
FVB
C57
C58

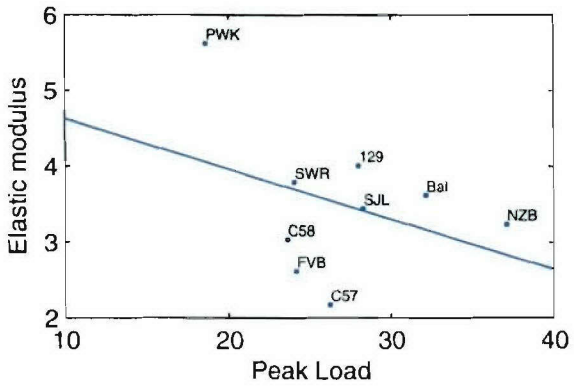
Elastic modulus
Peak Load
PWK
129
SWR
Bal
SJL
NZB
C58
FVB
C57

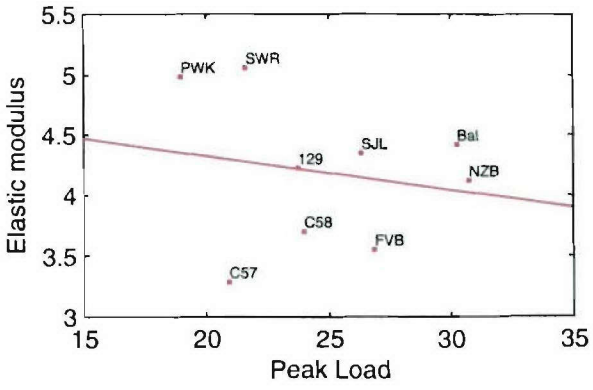
Elastic modulus
Peak Load
PWK
SWR
SJL
Bal
129
NZB
C58
FVB
C57

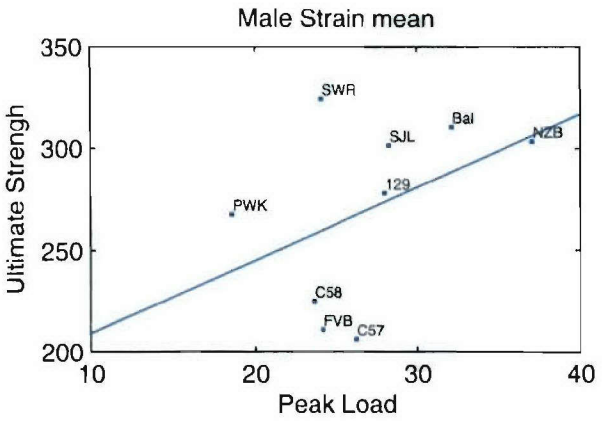
Male Strain mean
Ultimate Strengh
Peak Load
SWR
Bal
SJL
NZB
129
PWK
C58
FVB
C57

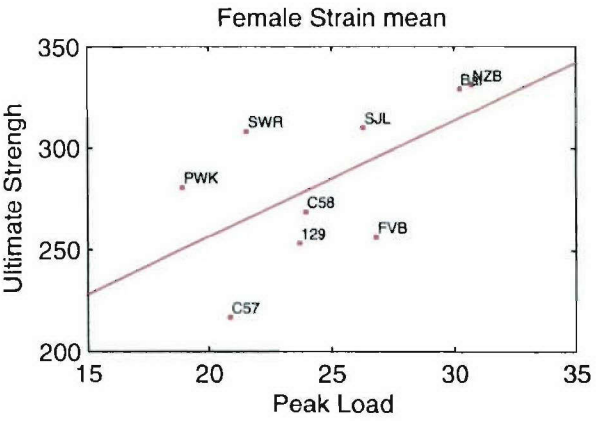
Female Strain mean
Ultimate Strengh
Peak Load
NZB
Bal
SWR
SJL
PWK
C58
129
FVB
C57

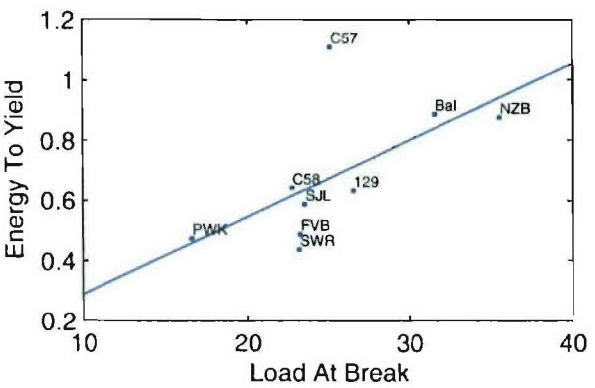
Energy To Yield
Load At Break
C57
Bal
NZB
C58
SJL
129
PWK
FVB
SWR

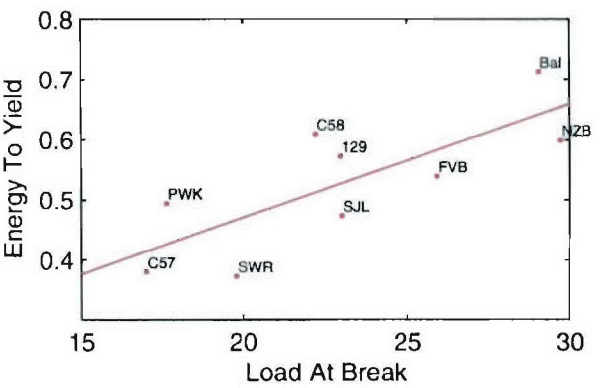
Energy To Yield
Load At Break
Bal
C58
NZB
129
FVB
PWK
SJL
C57
SWR

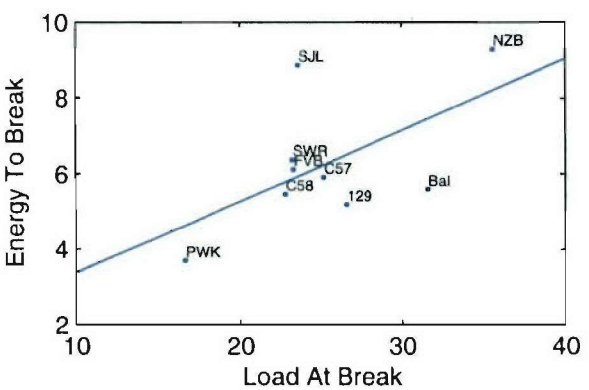
Energy To Break
Load At Break
NZB
SJL
SWR
FVB
C57
C58
Bal
129
PWK

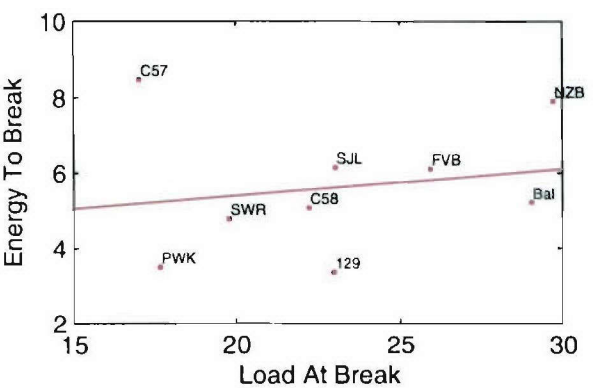
Energy To Break
Load At Break
C57
NZB
SJL
FVB
SWR
C58
Bal
PWK
129

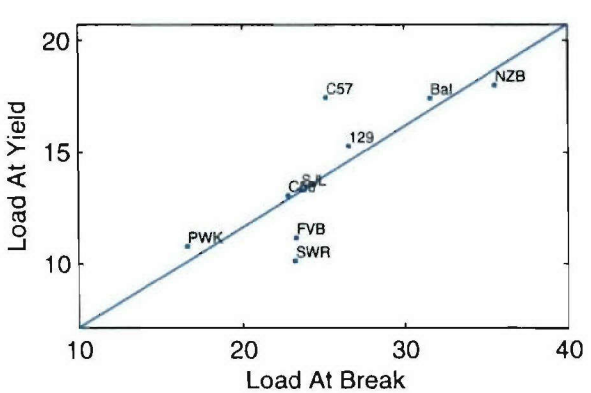
Load At Yield
Load At Break
C57
Bal
NZB
129
SJL
C58
PWK
FVB
SWR

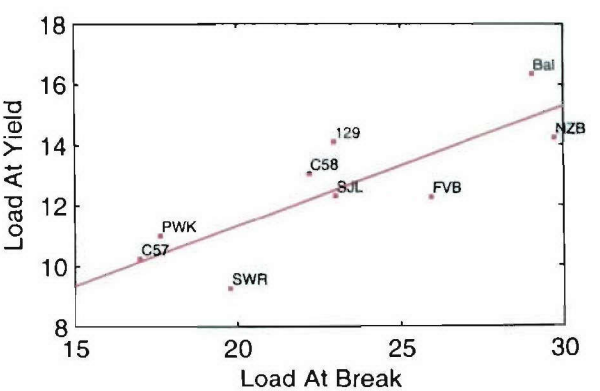
Load At Yield
Load At Break
Bal
129
NZB
C58
SJL
FVB
PWK
C57
SWR

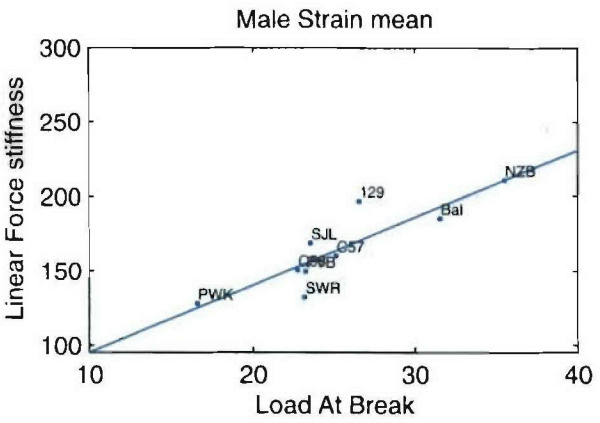
Male Strain mean
Linear Force stiffness
Load At Break
300
250
200
150
100
10
20
30
40
NZB
129
Bal
SJL
C57
PWK
SWR

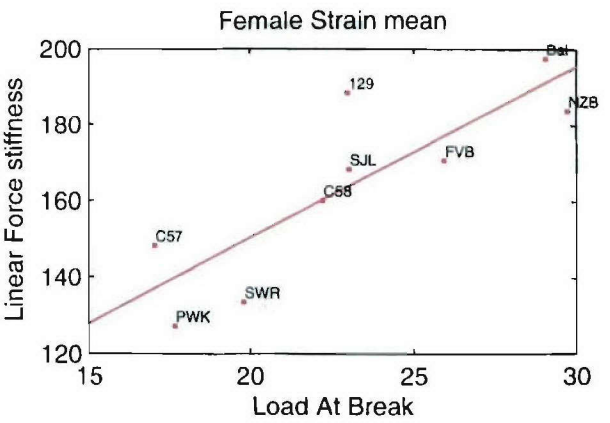
Female Strain mean
Linear Force stiffness
Load At Break
200
180
160
140
120
15
20
25
30
Bal
129
NZB
SJL
FVB
C58
C57
SWR
PWK

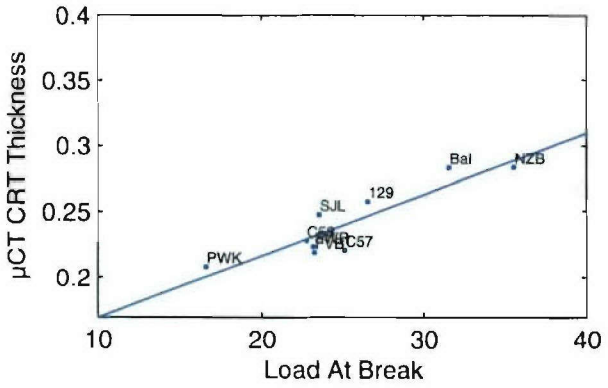
µCT CRT Thickness
Load At Break
0.4
0.35
0.3
0.25
0.2
10
20
30
40
Bal
NZB
SJL
129
PWK
C57

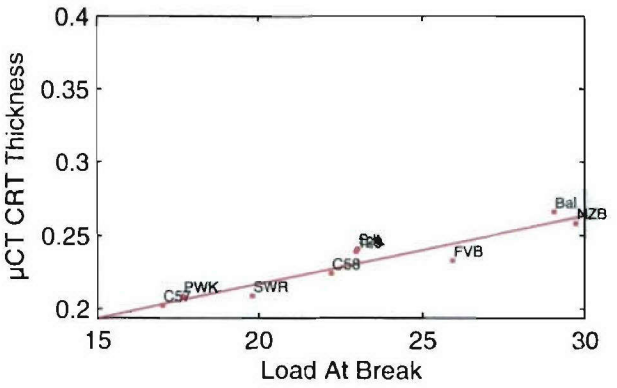
µCT CRT Thickness
Load At Break
0.4
0.35
0.3
0.25
0.2
15
20
25
30
Bal
NZB
C58
FVB
PWK
SWR
C57

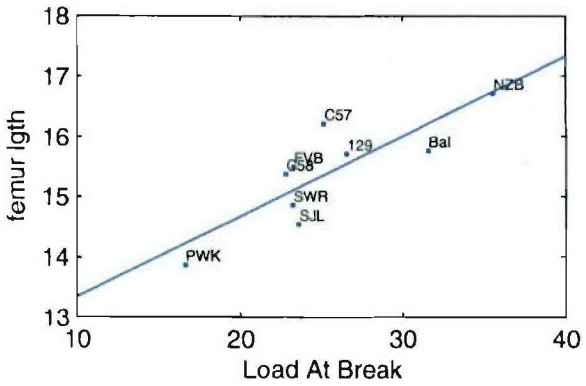
femur lgth
Load At Break
18
17
16
15
14
13
10
20
30
40
NZB
C57
129
Bal
FVB
SWR
SJL
PWK

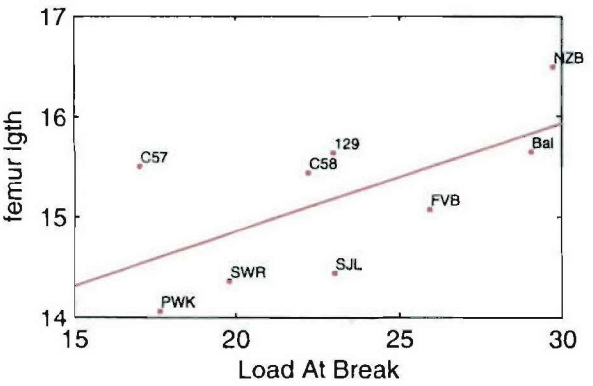
femur lgth
Load At Break
17
16
15
14
15
20
25
30
NZB
C57
129
C58
Bal
FVB
SWR
SJL
PWK

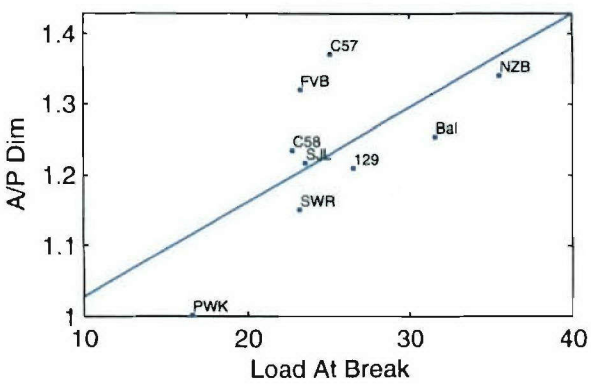
A/P Dim
Load At Break
1.4
1.3
1.2
1.1
1
10
20
30
40
C57
NZB
FVB
Bal
C58
SJL
129
SWR
PWK

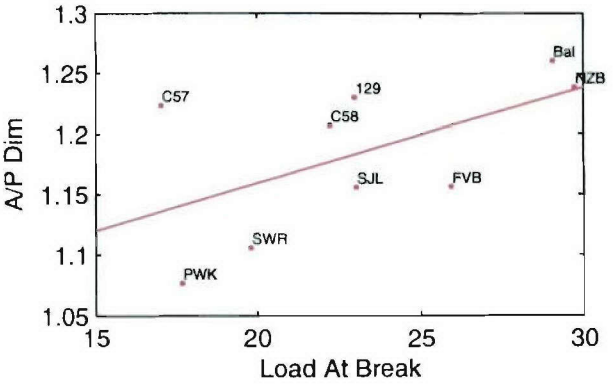
A/P Dim
Load At Break
1.3
1.25
1.2
1.15
1.1
1.05
15
20
25
30
Bal
C57
129
NZB
C58
SJL
FVB
SWR
PWK

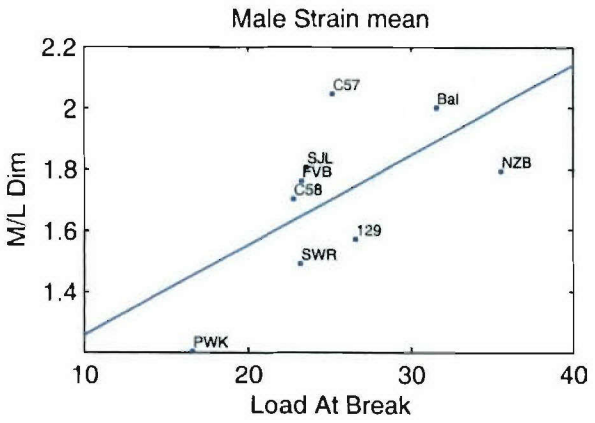
Male Strain mean
M/L Dim
Load At Break
C57
Bal
SJL
FVB
NZB
C58
129
SWR
PWK

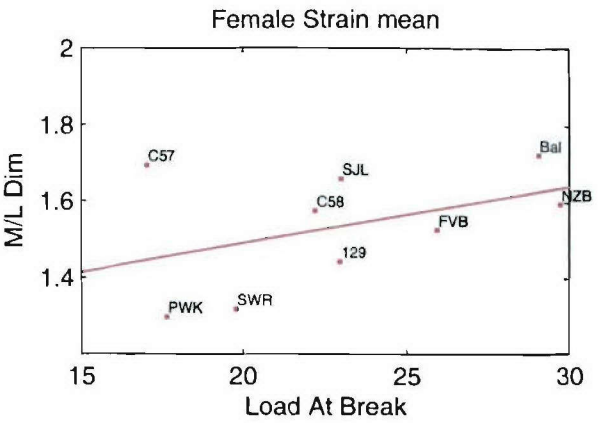
Female Strain mean
M/L Dim
Load At Break
C57
Bal
SJL
C58
NZB
FVB
129
PWK
SWR

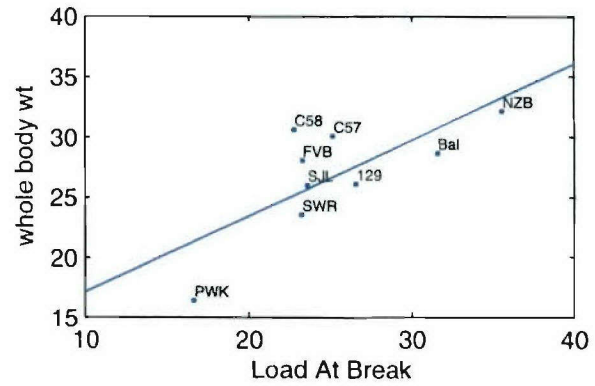
whole body wt
Load At Break
C58
C57
NZB
FVB
Bal
SJL
129
SWR
PWK

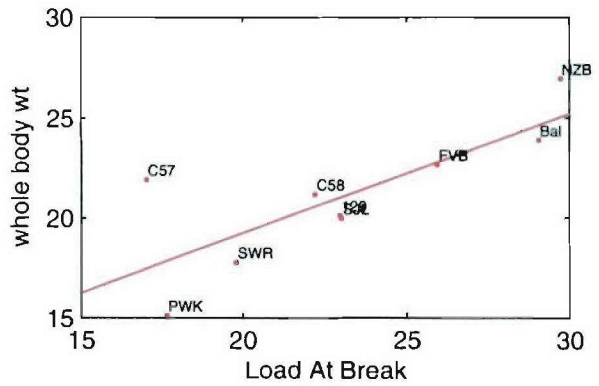
whole body wt
Load At Break
NZB
Bal
FVB
C57
C58
SWR
PWK

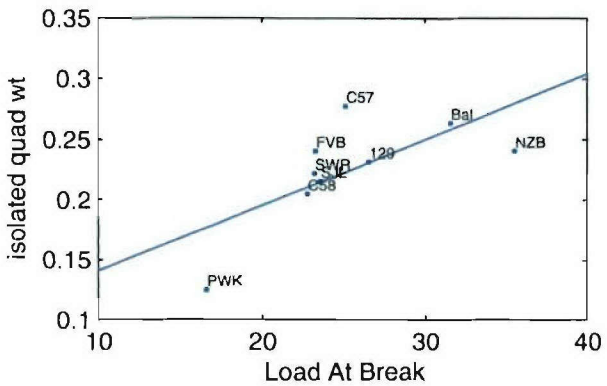
isolated quad wt
Load At Break
C57
Bal
FVB
NZB
SWR
129
C58
PWK

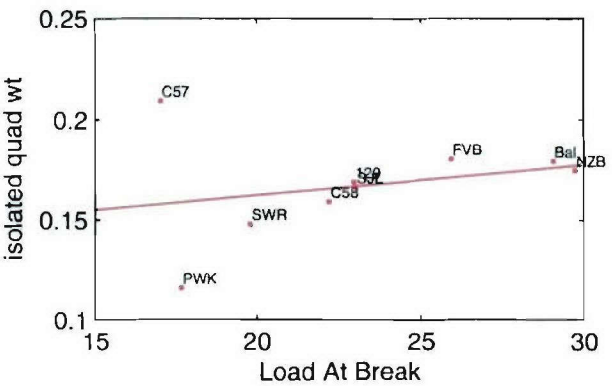
isolated quad wt
Load At Break
C57
FVB
Bal
NZB
C58
SWR
PWK

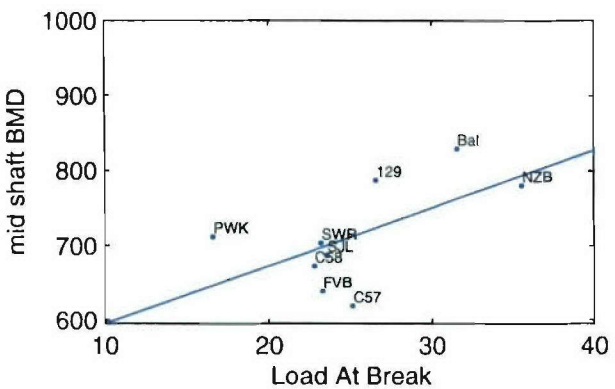
mid shaft BMD
Load At Break
Bal
129
NZB
PWK
SWR
C58
FVB
C57

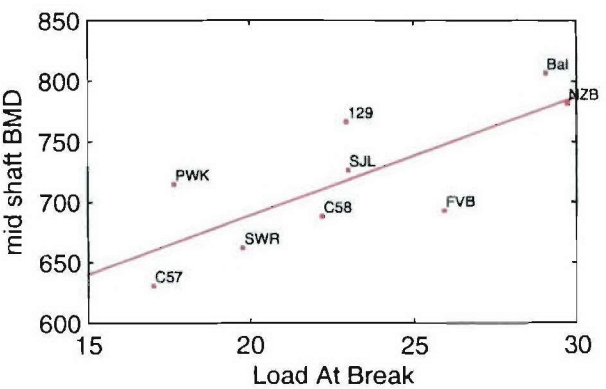
mid shaft BMD
Load At Break
Bal
NZB
129
PWK
SJL
C58
FVB
SWR
C57

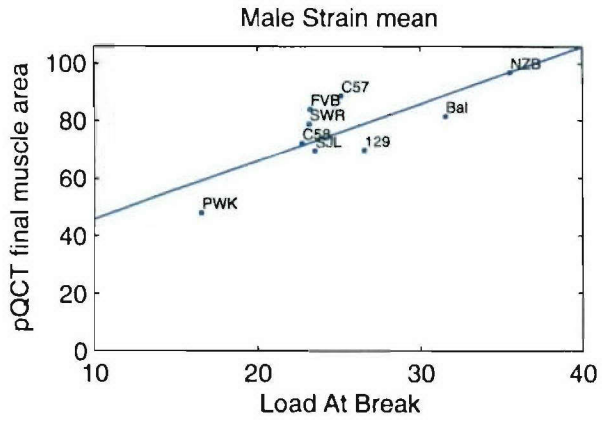
Male Strain mean
pQCT final muscle area
Load At Break
NZB
C57
FVB
SWR
Bal
129
PWK
SJL

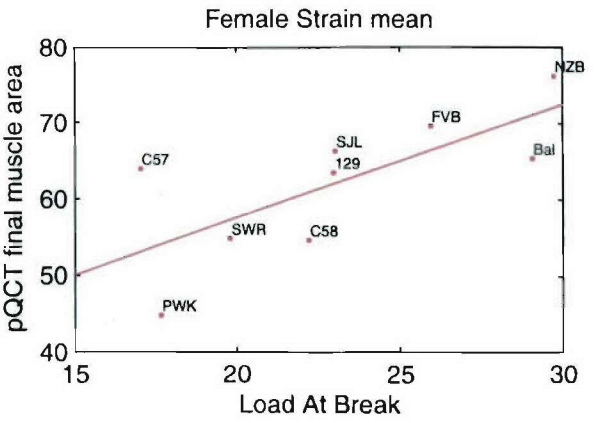
Female Strain mean
pQCT final muscle area
Load At Break
NZB
FVB
SJL
Bal
C57
129
SWR
C58
PWK

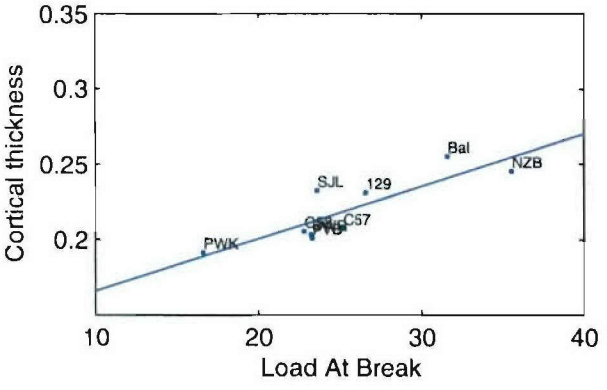
Cortical thickness
Load At Break
Bal
NZB
SJL
129
C57
PWK

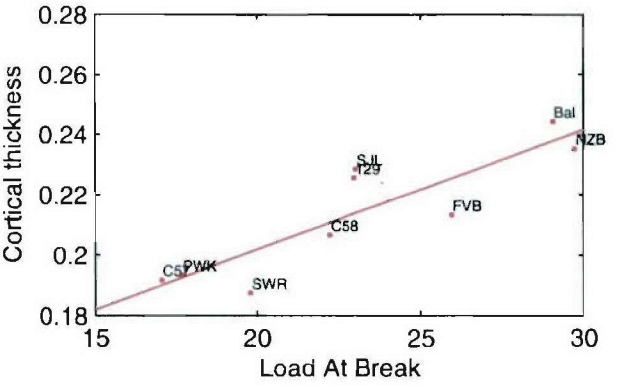
Cortical thickness
Load At Break
Bal
NZB
SJL
129
FVB
C58
PWK
SWR

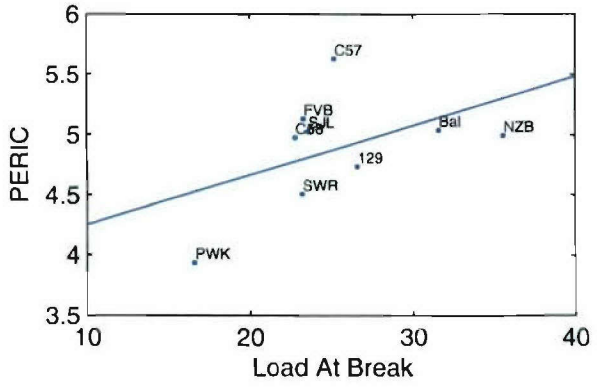
PERIC
Load At Break
C57
FVB
SJL
Bal
NZB
129
SWR
PWK

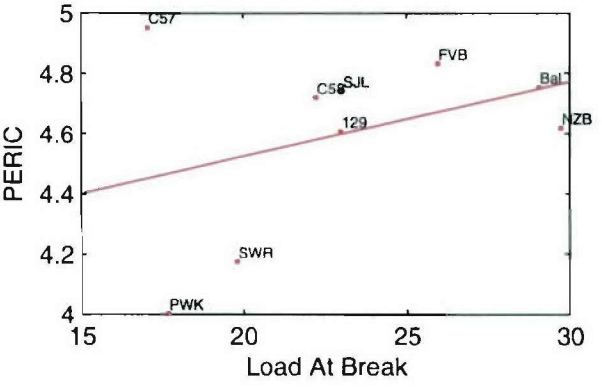
PERIC
Load At Break
C57
FVB
C58
SJL
Bal
129
NZB
SWR
PWK

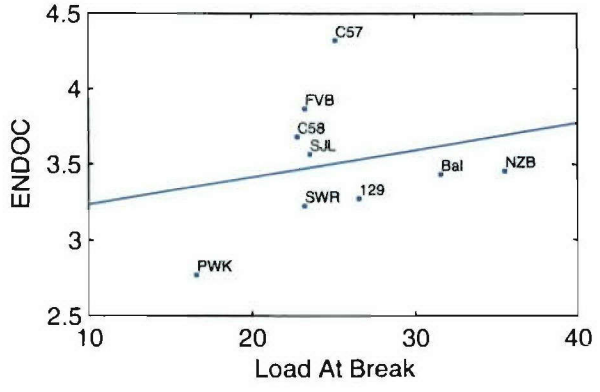
ENDOC
Load At Break
C57
FVB
C58
SJL
Bal
NZB
SWR
129
PWK

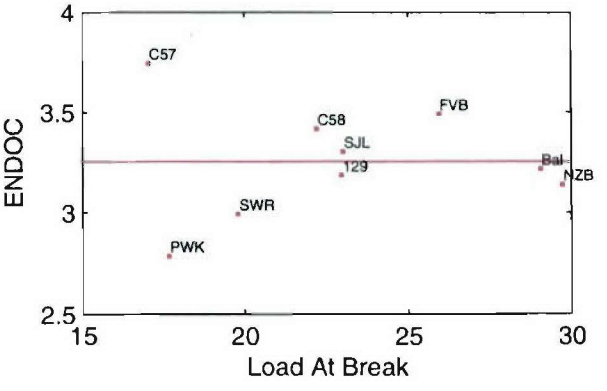
ENDOC
Load At Break
C57
FVB
C58
SJL
129
Bal
NZB
SWR
PWK

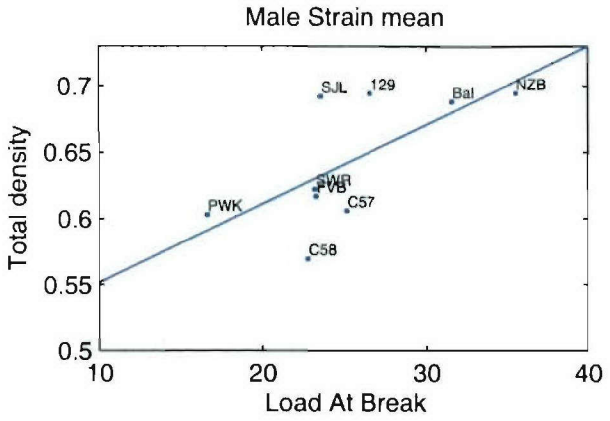
Male Strain mean
Total density
Load At Break
SJL
129
Bal
NZB
PWK
SWR
FVB
C57
C58

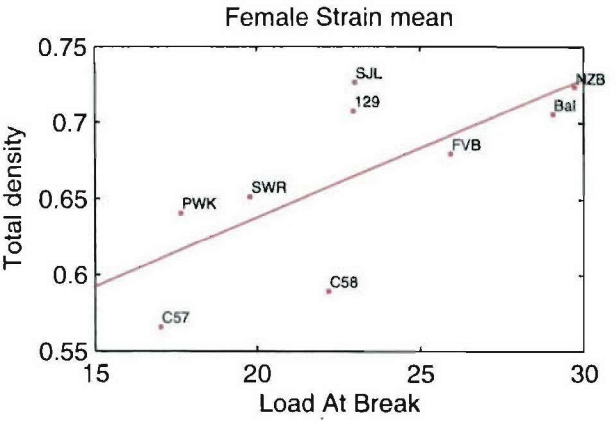
Female Strain mean
Total density
Load At Break
SJL
129
NZB
Bal
FVB
PWK
SWR
C58
C57

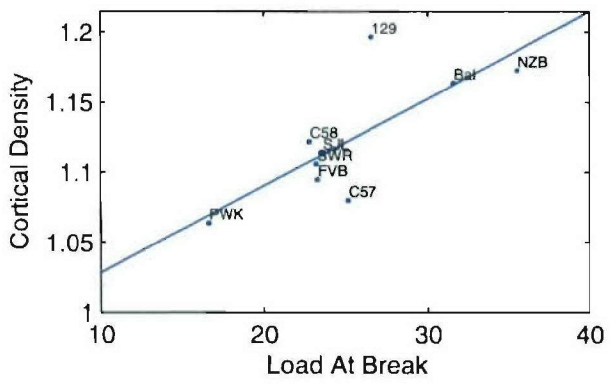
Cortical Density
Load At Break
129
Bal
NZB
C58
SWR
FVB
C57
PWK

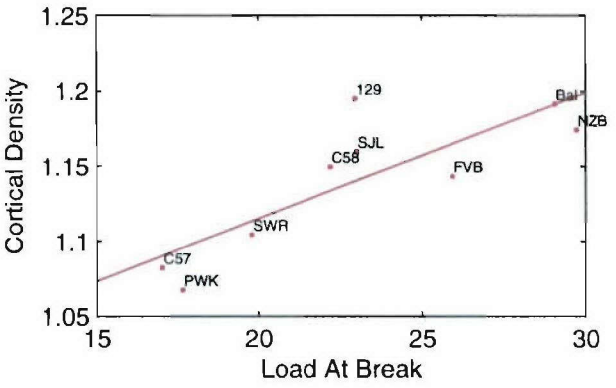
Cortical Density
Load At Break
129
Bal
NZB
SJL
C58
FVB
SWR
C57
PWK

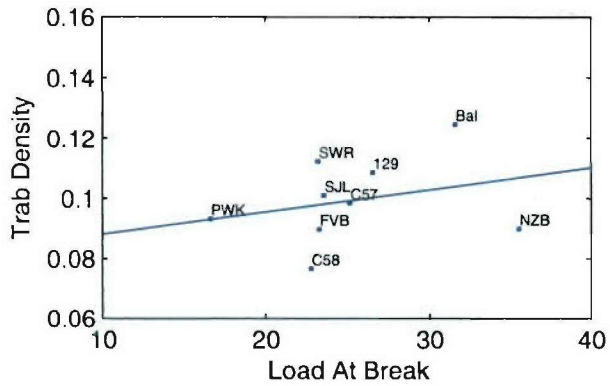
Trab Density
Load At Break
Bal
SWR
129
SJL
C57
PWK
FVB
NZB
C58

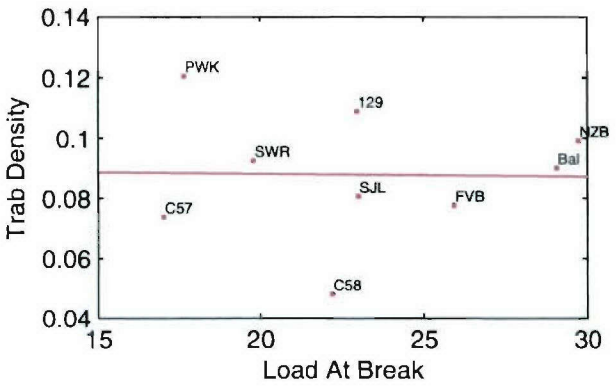
Trab Density
Load At Break
PWK
129
NZB
SWR
Bal
SJL
FVB
C57
C58

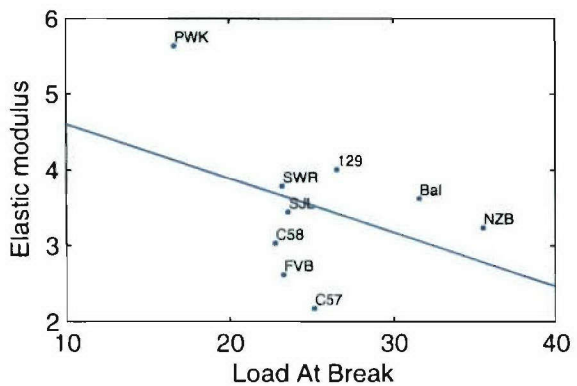
Elastic modulus
Load At Break
PWK
129
SWR
Bal
SJL
NZB
C58
FVB
C57

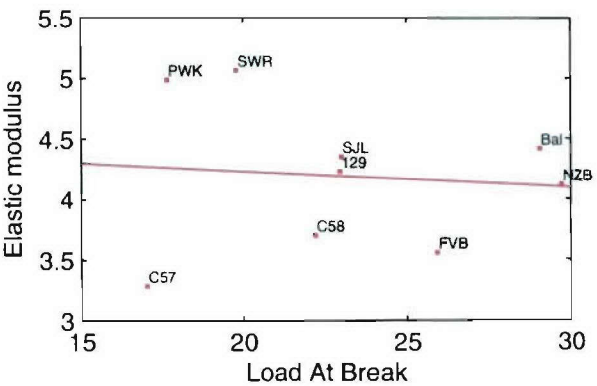
Elastic modulus
Load At Break
PWK
SWR
SJL
129
Bal
NZB
C58
FVB
C57

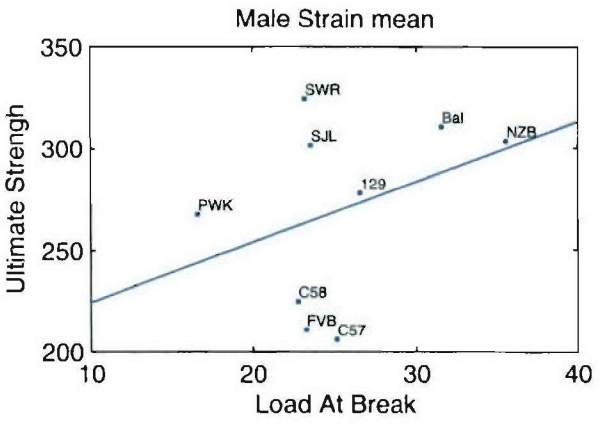
Male Strain mean
Ultimate Strengh
Load At Break
SWR
Bal
NZB
SJL
129
PWK
C58
FVB
C57

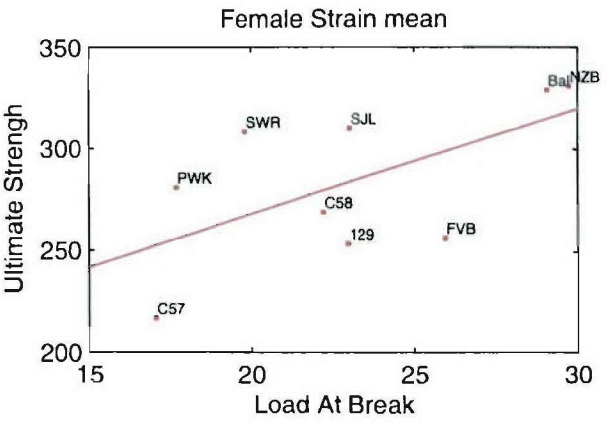
Female Strain mean
Ultimate Strengh
Load At Break
Bal
NZB
SWR
SJL
PWK
C58
129
FVB
C57

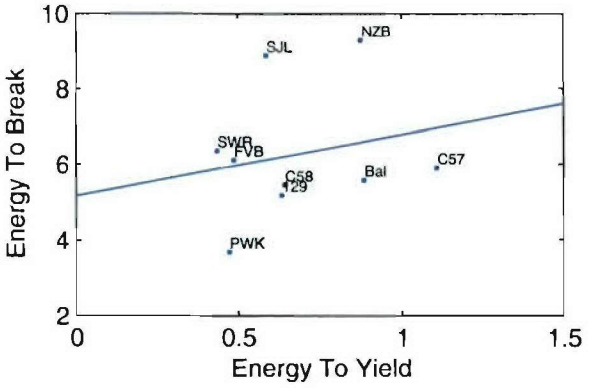
Energy To Break
Energy To Yield
NZB
SJL
SWR
FVB
C58
129
Bal
C57
PWK

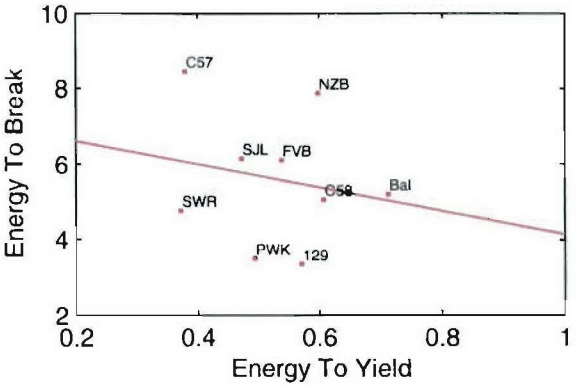
Energy To Break
Energy To Yield
C57
NZB
SJL
FVB
C58
Bal
SWR
PWK
129

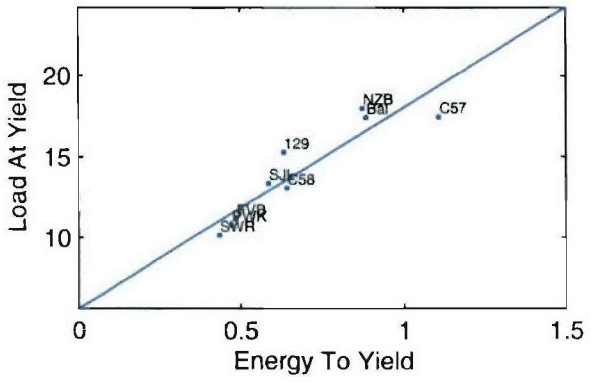
Load At Yield
Energy To Yield
NZB
Bal
C57
129
SJL
C58
FVB
PWK
SWR

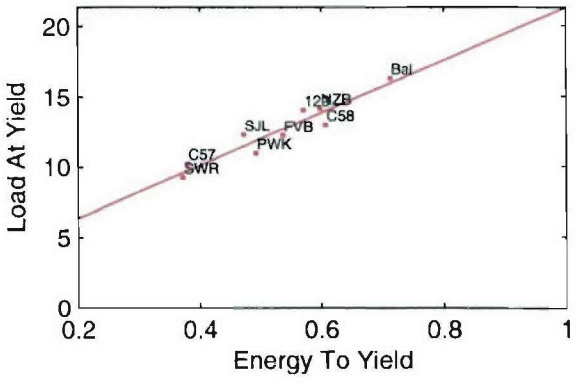
Load At Yield
Energy To Yield
Bal
129
NZB
C58
SJL
FVB
PWK
C57
SWR

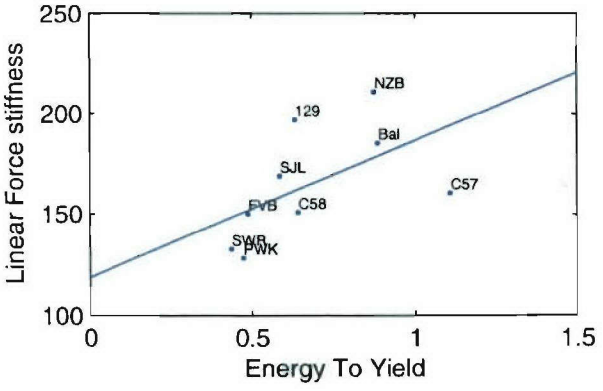
Linear Force stiffness
Energy To Yield
NZB
129
Bal
SJL
C57
FVB
C58
SWR
PWK

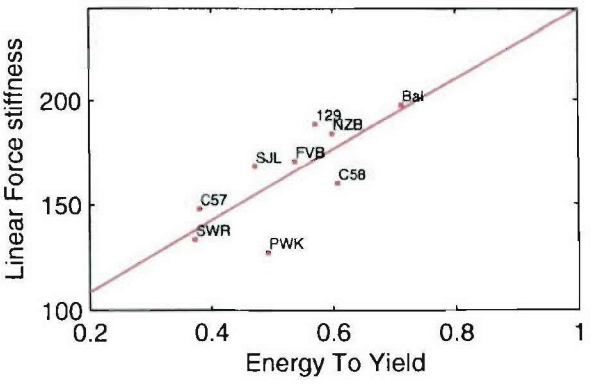
Linear Force stiffness
Energy To Yield
Bal
129
NZB
SJL
FVB
C58
C57
SWR
PWK

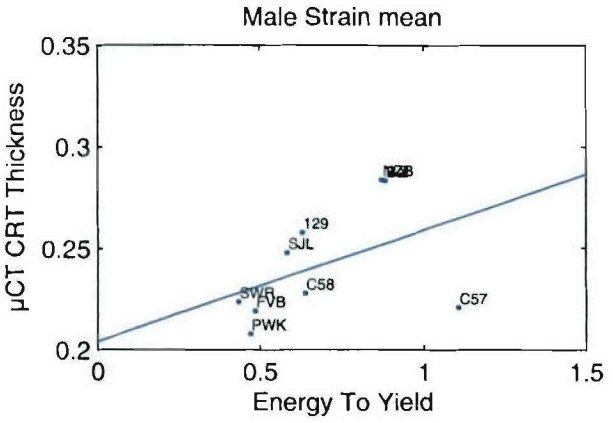
Male Strain mean
µCT CRT Thickness
Energy To Yield
0.35
0.3
0.25
0.2
0
0.5
1
1.5
129
SJL
C58
SWR
FVB
PWK
C57

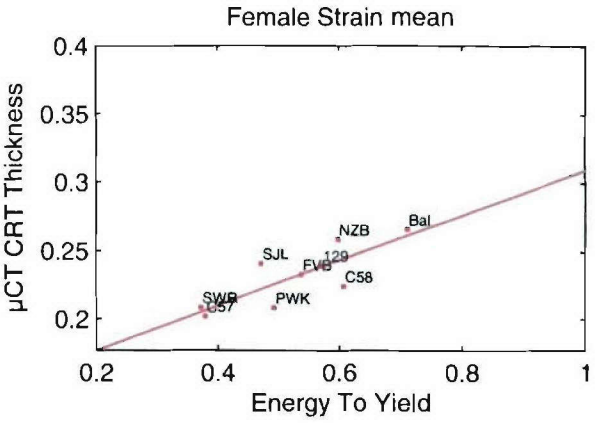
Female Strain mean
µCT CRT Thickness
Energy To Yield
0.4
0.35
0.3
0.25
0.2
0.2
0.4
0.6
0.8
1
NZB
Bal
SJL
129
FVB
C58
SWR
C57
PWK

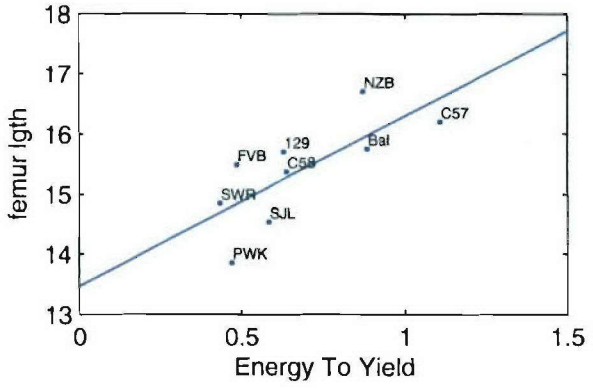
femur lgth
Energy To Yield
18
17
16
15
14
13
0
0.5
1
1.5
NZB
C57
FVB
129
Bal
C58
SWR
SJL
PWK

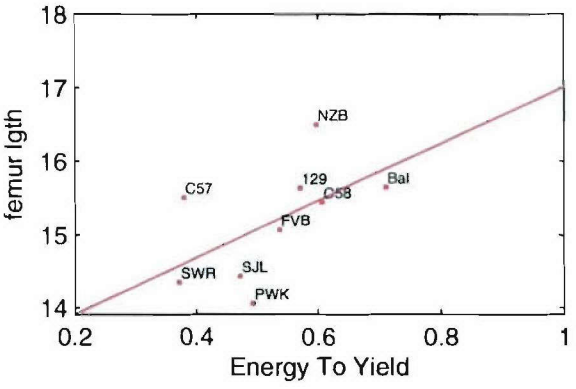
femur lgth
Energy To Yield
18
17
16
15
14
0.2
0.4
0.6
0.8
1
NZB
C57
129
Bal
C58
FVB
SWR
SJL
PWK

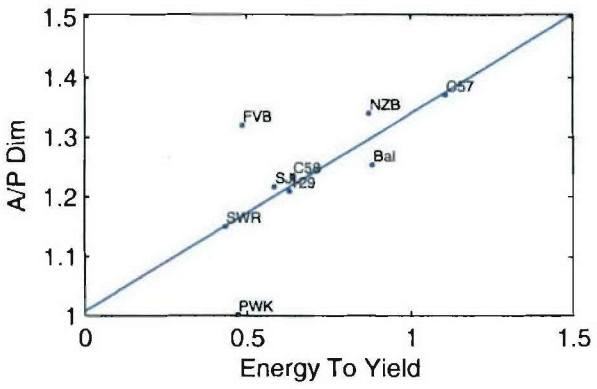
A/P Dim
Energy To Yield
1.5
1.4
1.3
1.2
1.1
1
0
0.5
1
1.5
C57
NZB
FVB
Bal
C58
SJL
129
SWR
PWK

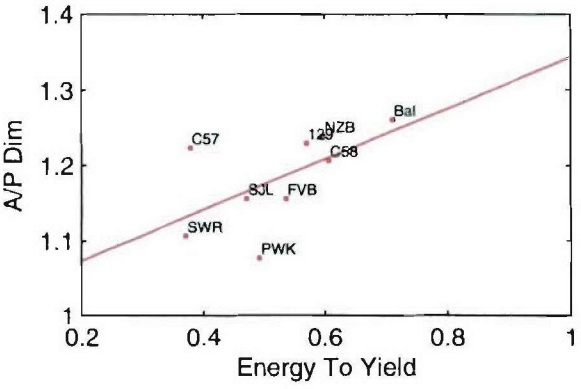
A/P Dim
Energy To Yield
1.4
1.3
1.2
1.1
1
0.2
0.4
0.6
0.8
1
Bal
C57
NZB
129
C58
SJL
FVB
SWR
PWK

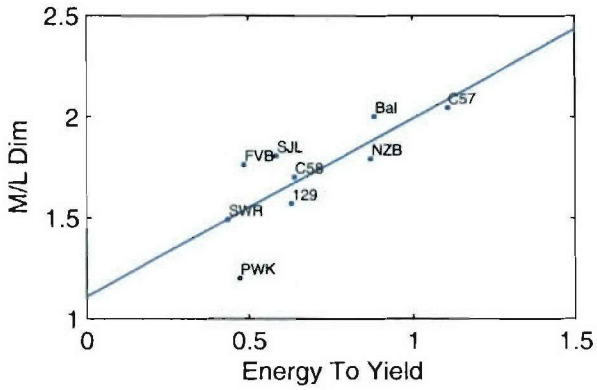
M/L Dim
Energy To Yield
2.5
2
1.5
1
0
0.5
1
1.5
Bal
C57
FVB
SJL
NZB
C58
129
SWR
PWK

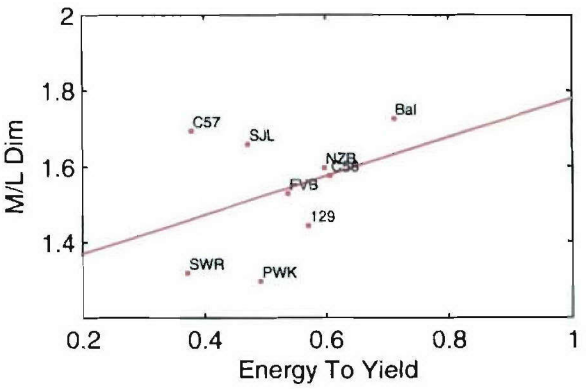
M/L Dim
Energy To Yield
2
1.8
1.6
1.4
0.2
0.4
0.6
0.8
1
Bal
C57
SJL
NZB
C58
FVB
129
SWR
PWK

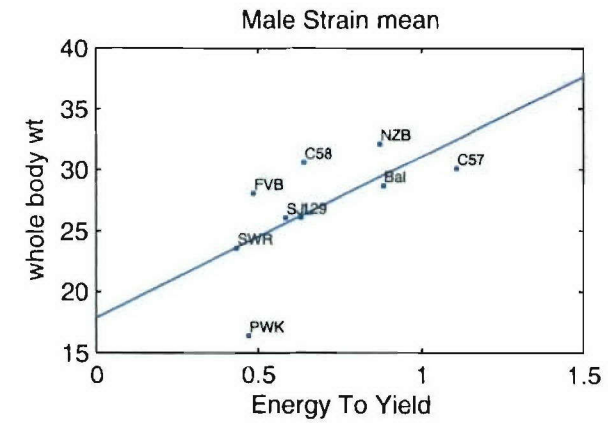
Male Strain mean
whole body wt
Energy To Yield
NZB
C58
C57
FVB
Bal
SJL
129
SWR
PWK

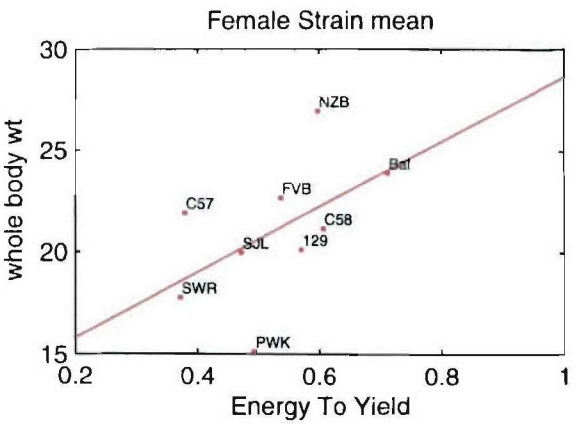
Female Strain mean
whole body wt
Energy To Yield
NZB
Bal
FVB
C57
C58
SJL
129
SWR
PWK

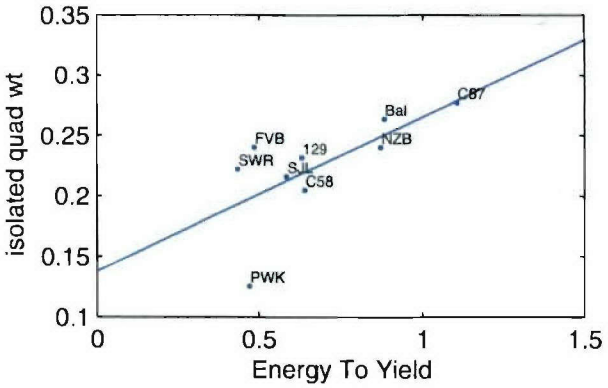
isolated quad wt
Energy To Yield
Bal
C57
FVB
NZB
129
SWR
SJL
C58
PWK

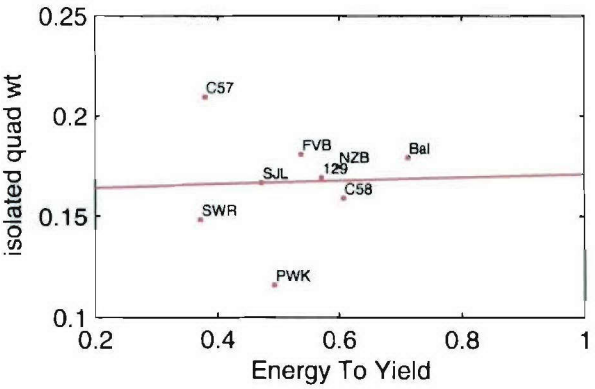
isolated quad wt
Energy To Yield
C57
FVB
NZB
Bal
SJL
129
C58
SWR
PWK

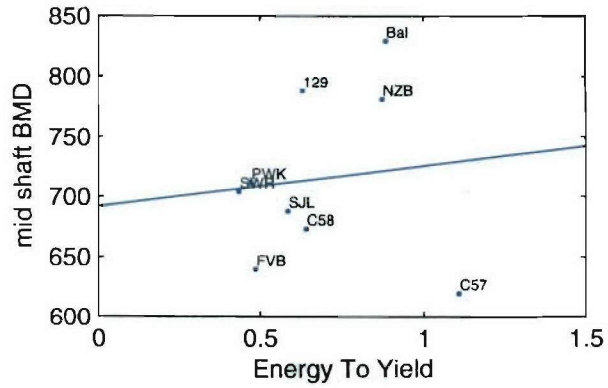
mid shaft BMD
Energy To Yield
Bal
129
NZB
PWK
SWR
SJL
C58
FVB
C57

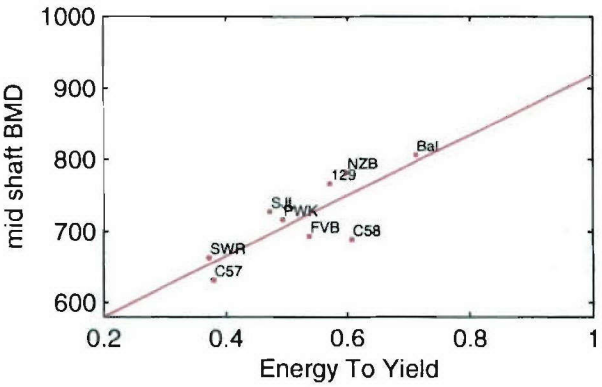
mid shaft BMD
Energy To Yield
Bal
NZB
129
SJL
PWK
FVB
C58
SWR
C57

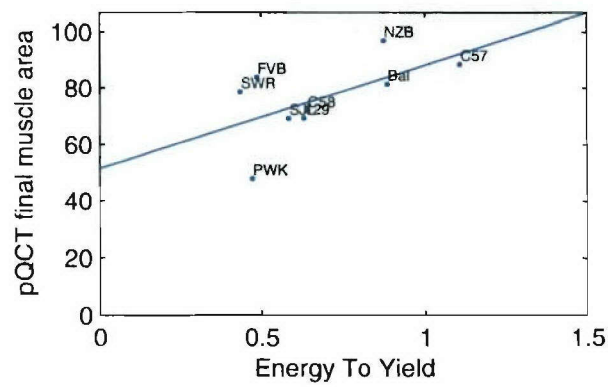
pQCT final muscle area
Energy To Yield
NZB
FVB
SWR
Bal
C57
C58
SJL
129
PWK

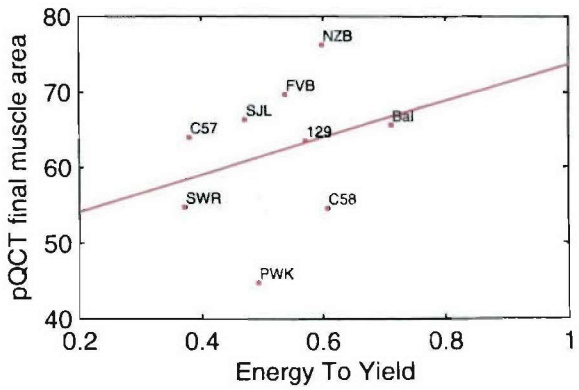
pQCT final muscle area
Energy To Yield
NZB
FVB
SJL
C57
Bal
129
SWR
C58
PWK

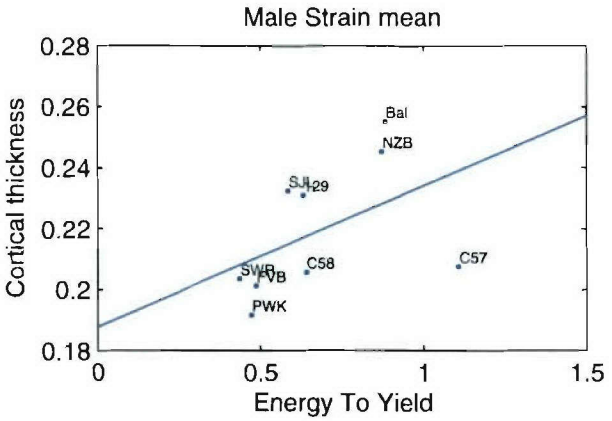
Male Strain mean
Cortical thickness
Energy To Yield
Bal
NZB
SJL
129
C57
SWR
FVB
C58
PWK

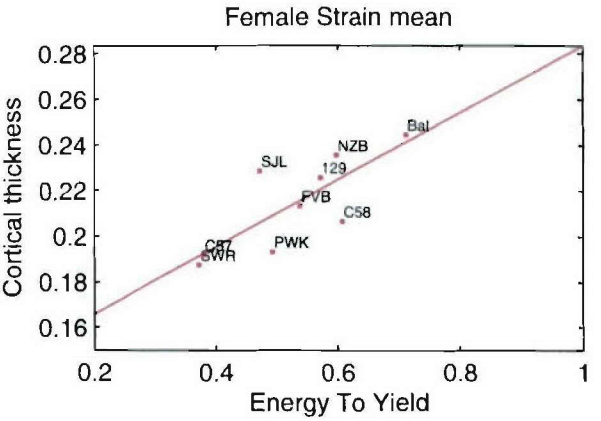
Female Strain mean
Cortical thickness
Energy To Yield
Bal
NZB
SJL
129
FVB
C58
PWK
SWR

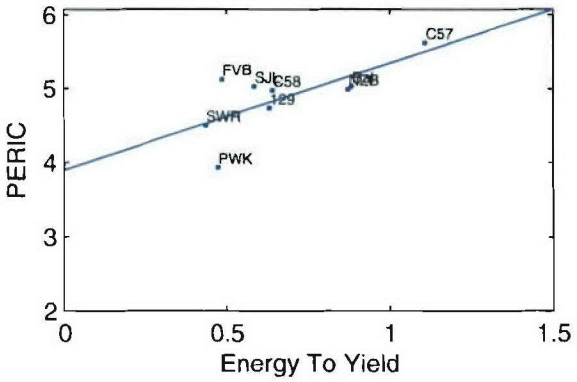
PERIC
Energy To Yield
C57
FVB
SJL
C58
129
SWR
PWK

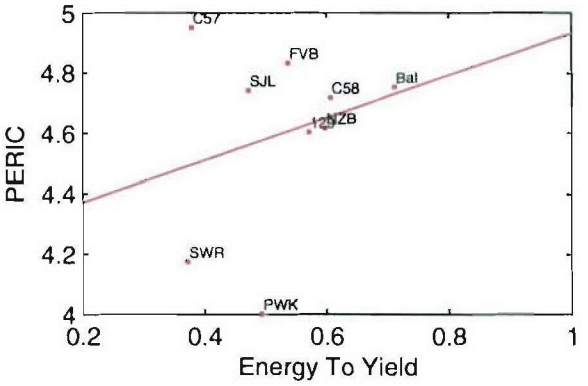
PERIC
Energy To Yield
C57
FVB
SJL
C58
Bal
NZB
SWR
PWK

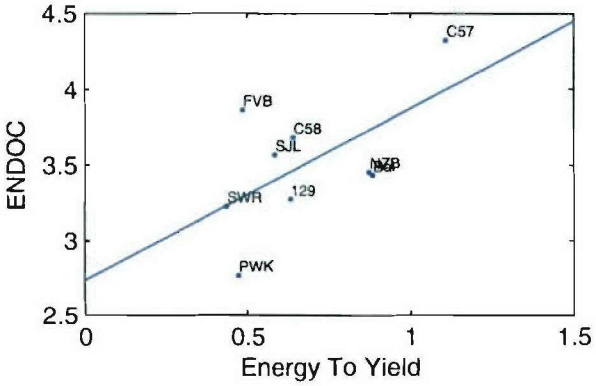
ENDOC
Energy To Yield
C57
FVB
C58
SJL
SWR
129
PWK

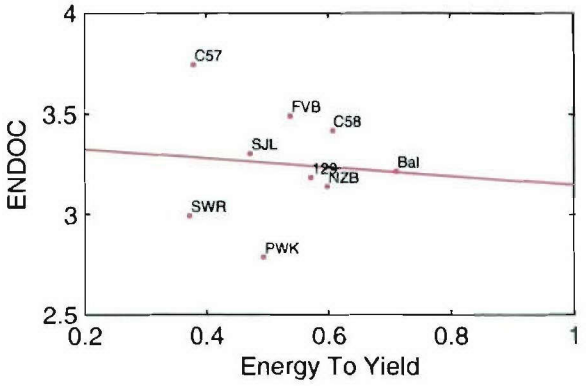
ENDOC
Energy To Yield
C57
FVB
C58
SJL
Bal
NZB
SWR
PWK

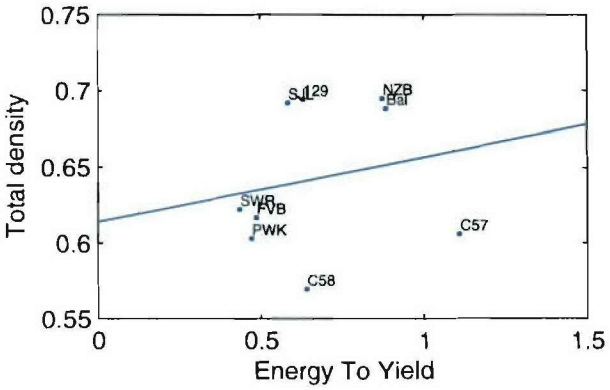
Total density
Energy To Yield
SJL
129
NZB
Bal
SWR
FVB
PWK
C57
C58

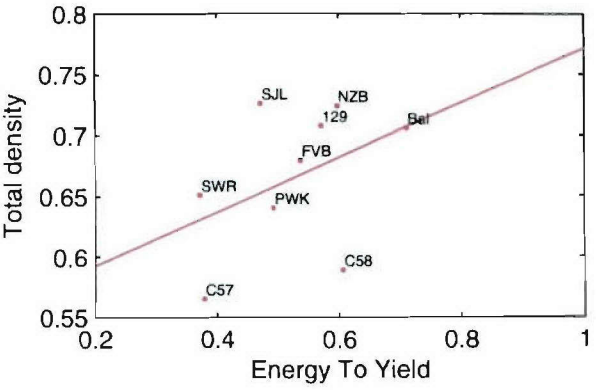
Total density
Energy To Yield
SJL
NZB
129
Bal
FVB
SWR
PWK
C58
C57

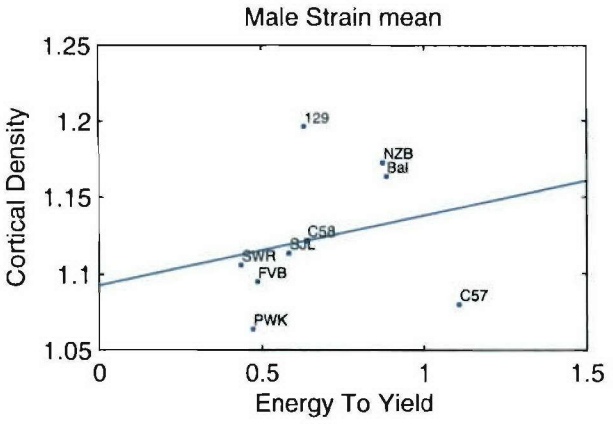
Male Strain mean
Cortical Density
Energy To Yield
129
NZB
Bal
C58
SJL
SWR
FVB
C57
PWK

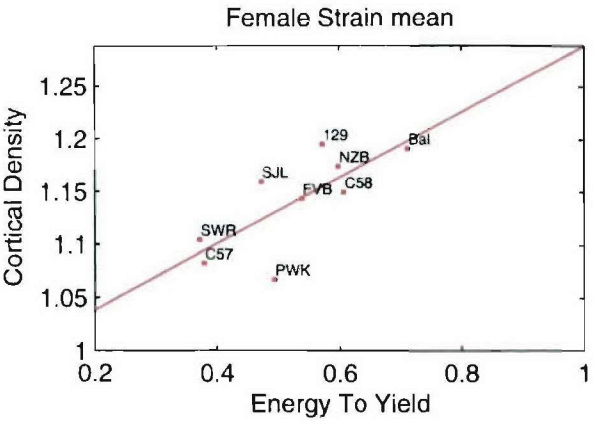
Female Strain mean
Cortical Density
Energy To Yield
129
Bal
NZB
SJL
FVB
C58
SWR
C57
PWK

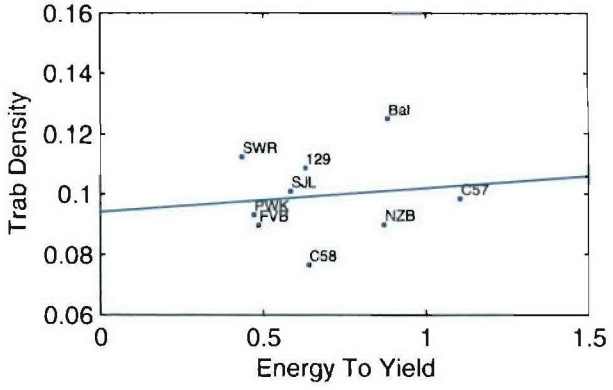
Trab Density
Energy To Yield
Bal
SWR
129
SJL
C57
PWK
FVB
NZB
C58

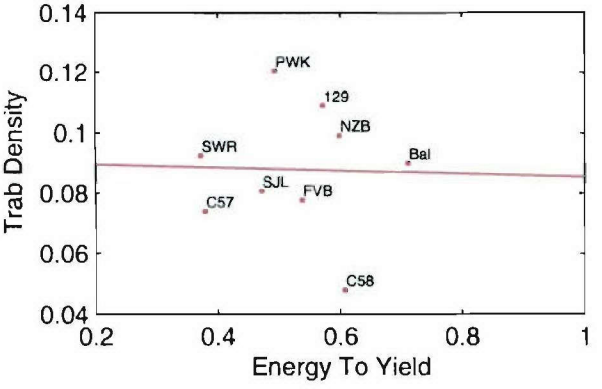
Trab Density
Energy To Yield
PWK
129
NZB
SWR
Bal
SJL
FVB
C57
C58

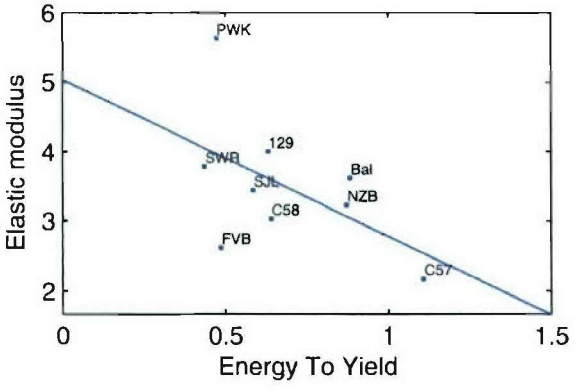
Elastic modulus
Energy To Yield
PWK
129
SWR
Bal
SJL
NZB
C58
FVB
C57

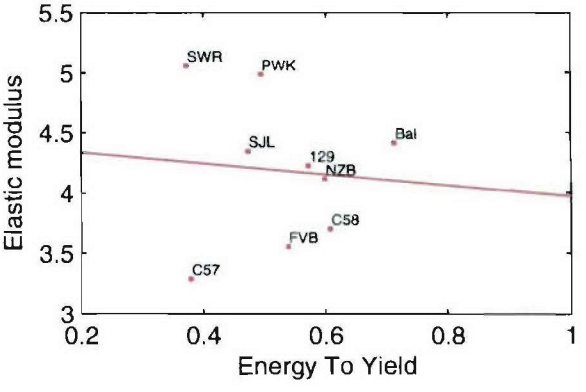
Elastic modulus
Energy To Yield
SWR
PWK
SJL
Bal
129
NZB
C58
FVB
C57

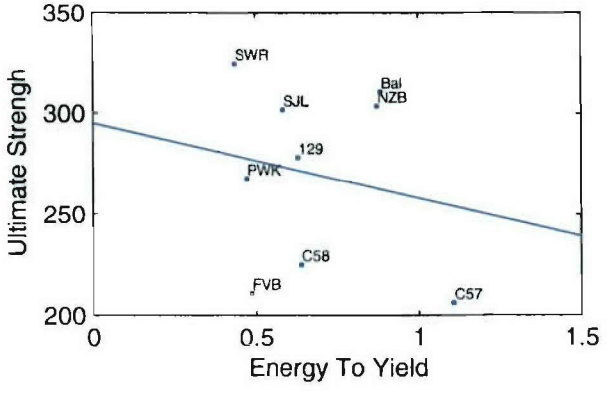
Ultimate Strengh
Energy To Yield
SWR
Bal
SJL
NZB
129
PWK
C58
FVB
C57

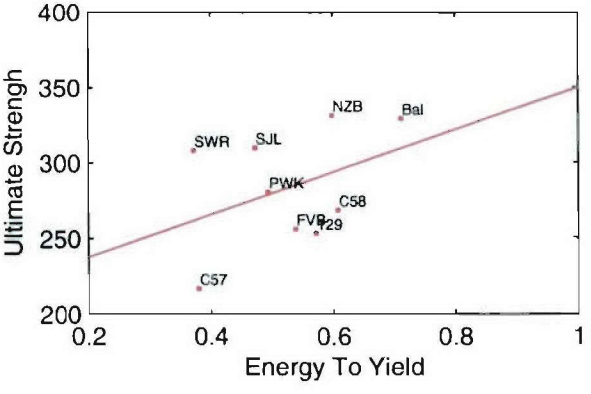
Ultimate Strengh
Energy To Yield
NZB
Bal
SWR
SJL
PWK
C58
FVB
129
C57

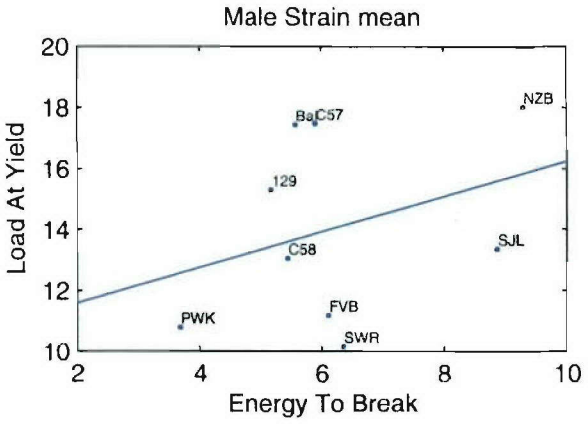
Male Strain mean
Load At Yield
Energy To Break
NZB
Bal
C57
129
SJL
C58
FVB
PWK
SWR

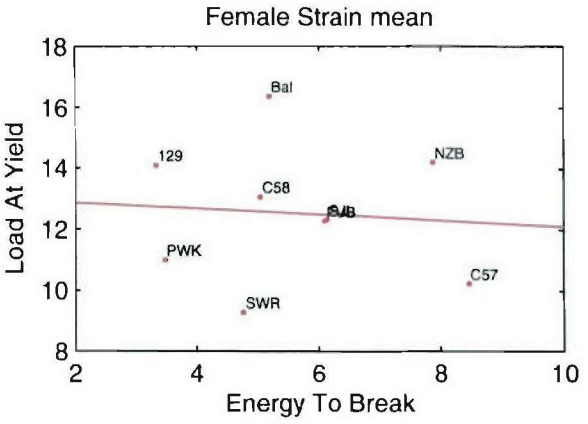
Female Strain mean
Load At Yield
Energy To Break
Bal
129
NZB
C58
PWK
C57
SWR

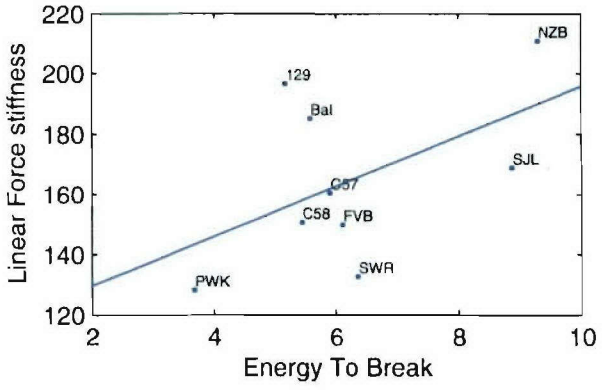
Linear Force stiffness
Energy To Break
NZB
129
Bal
SJL
C57
C58
FVB
PWK
SWR

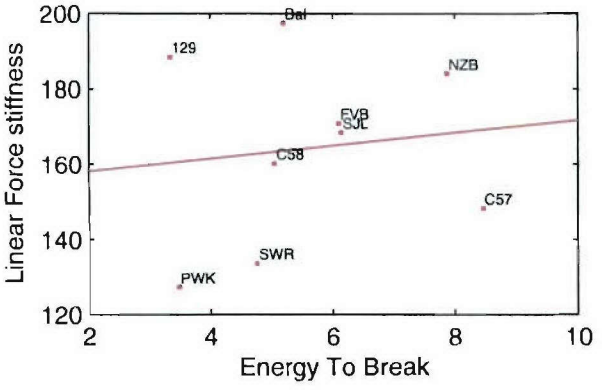
Linear Force stiffness
Energy To Break
Bal
129
NZB
FVB
SJL
C58
C57
SWR
PWK

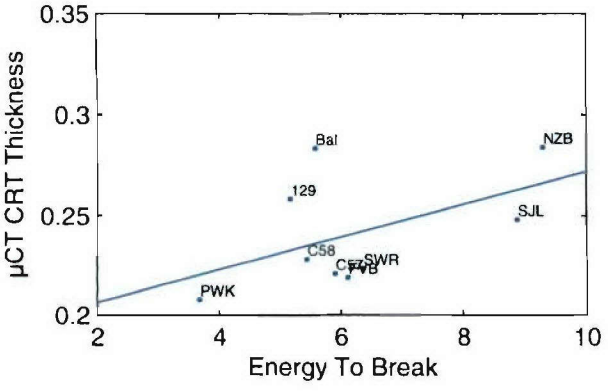
µCT CRT Thickness
Energy To Break
Bal
NZB
129
SJL
C58
SWR
PWK

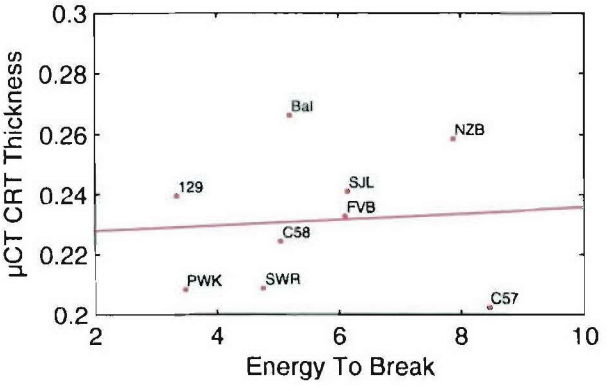
µCT CRT Thickness
Energy To Break
Bal
NZB
129
SJL
FVB
C58
PWK
SWR
C57

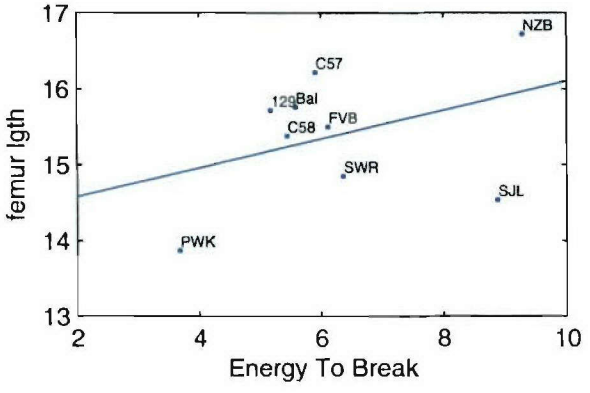
femur lgth
Energy To Break
NZB
C57
Bal
C58
FVB
SWR
SJL
PWK

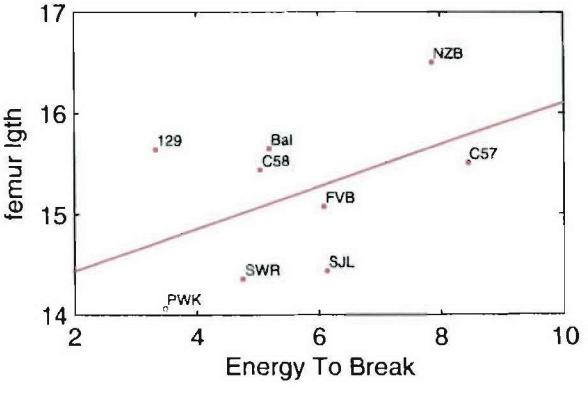
femur lgth
Energy To Break
NZB
129
Bal
C58
C57
FVB
SWR
SJL
PWK

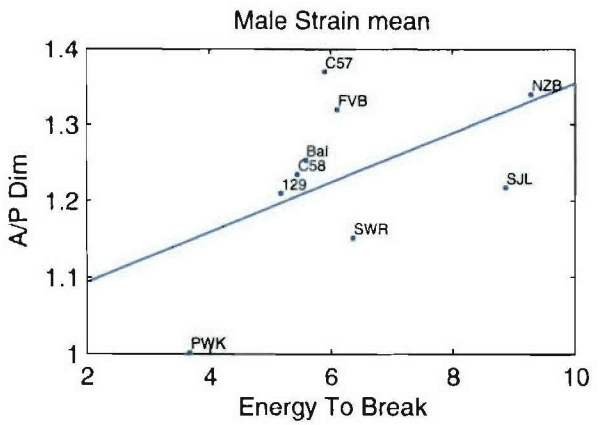
Male Strain mean
A/P Dim
Energy To Break
C57
NZB
FVB
Bal
C58
129
SJL
SWR
PWK

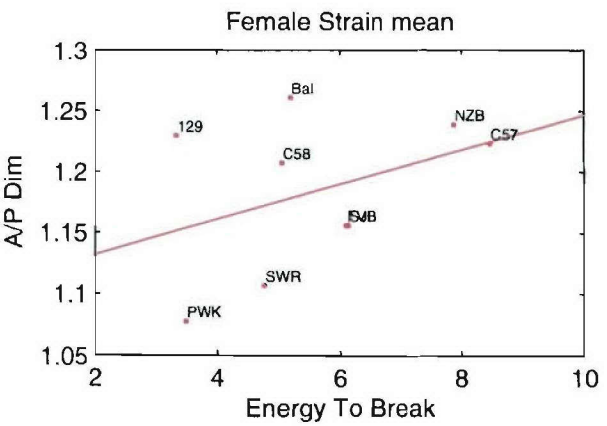
Female Strain mean
A/P Dim
Energy To Break
Bal
129
NZB
C57
C58
SWR
PWK

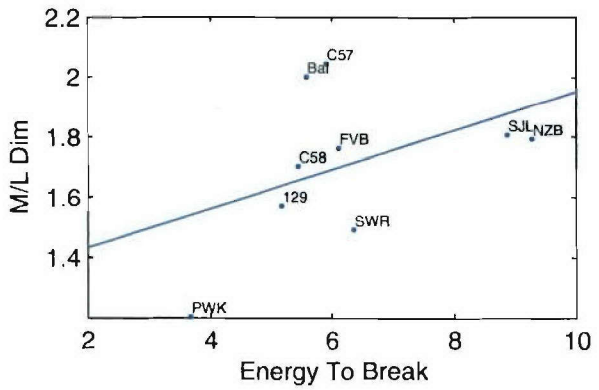
M/L Dim
Energy To Break
C57
Bal
SJL
NZB
FVB
C58
129
SWR
PWK

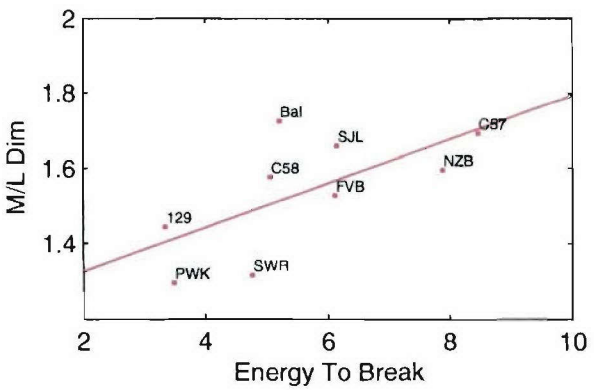
M/L Dim
Energy To Break
Bal
SJL
C57
C58
NZB
FVB
129
PWK
SWR

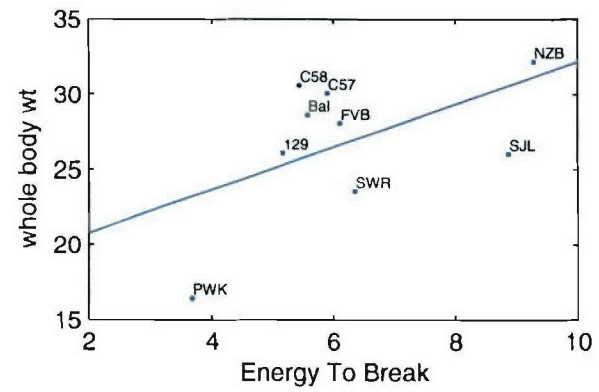
whole body wt
Energy To Break
NZB
C58
C57
Bal
FVB
129
SJL
SWR
PWK

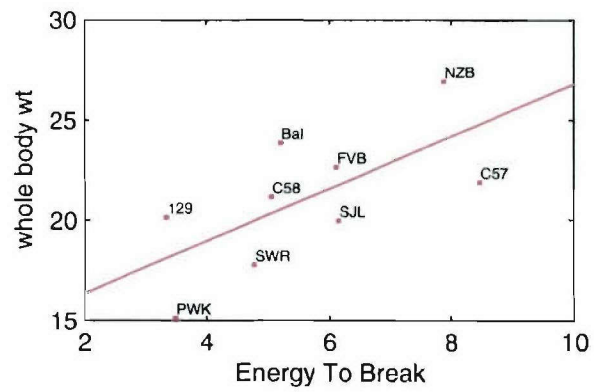
whole body wt
Energy To Break
NZB
Bal
FVB
C57
C58
129
SJL
SWR
PWK

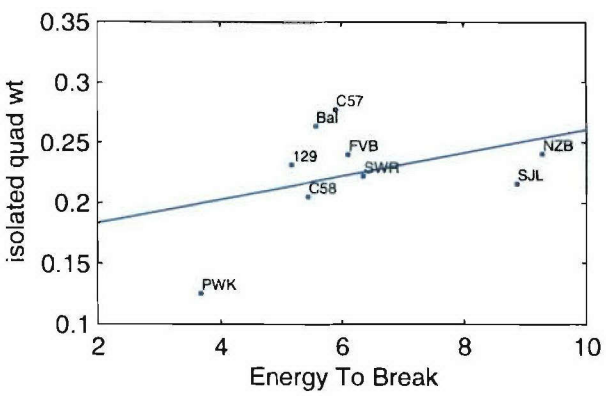
isolated quad wt
Energy To Break
C57
Bal
FVB
NZB
129
SWR
SJL
C58
PWK

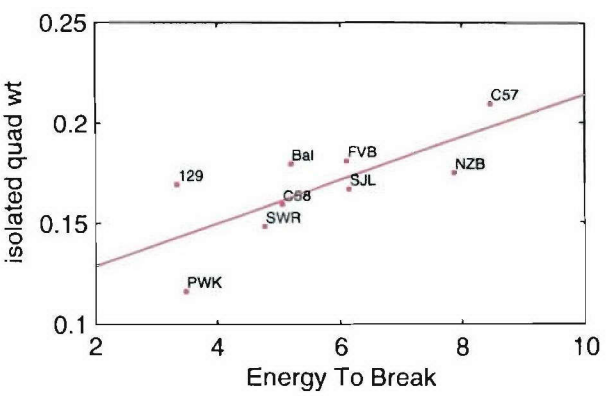
isolated quad wt
Energy To Break
C57
Bal
FVB
129
NZB
SJL
C58
SWR
PWK

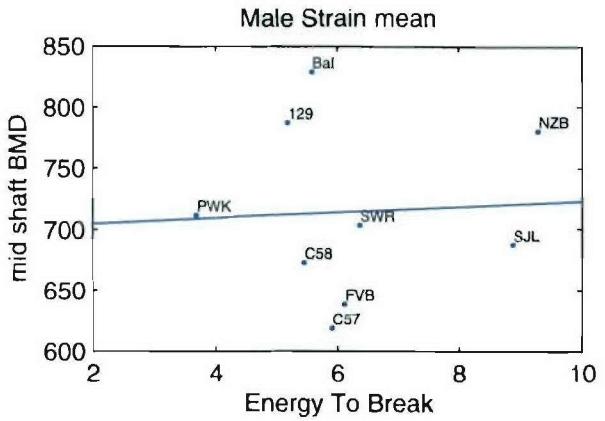
Male Strain mean
mid shaft BMD
Energy To Break
Bal
129
NZB
PWK
SWR
SJL
C58
FVB
C57

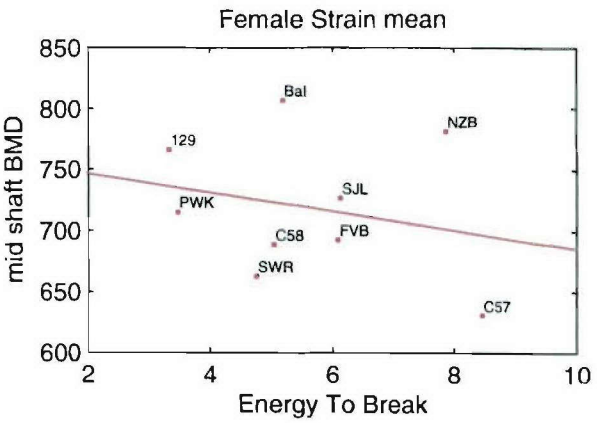
Female Strain mean
mid shaft BMD
Energy To Break
Bal
NZB
129
SJL
PWK
C58
FVB
SWR
C57

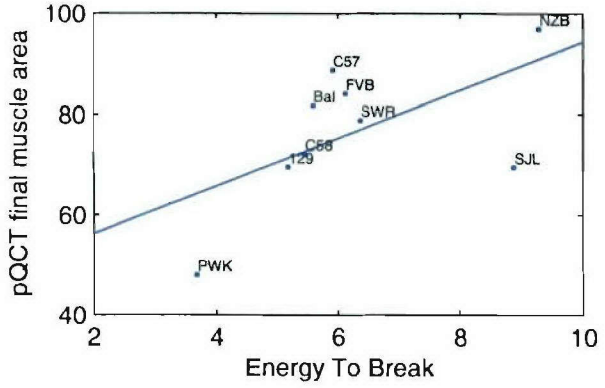
pQCT final muscle area
Energy To Break
NZB
C57
FVB
Bal
SWR
C58
129
SJL
PWK

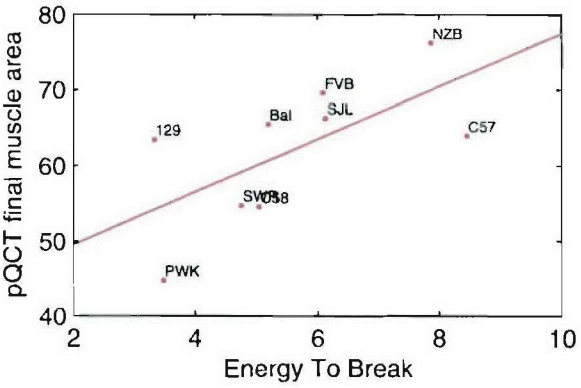
pQCT final muscle area
Energy To Break
NZB
FVB
SJL
Bal
129
C57
PWK

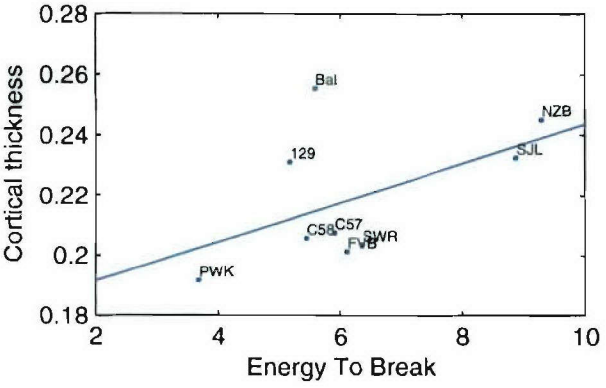
Cortical thickness
Energy To Break
Bal
NZB
129
SJL
C58
C57
SWR
FVB
PWK

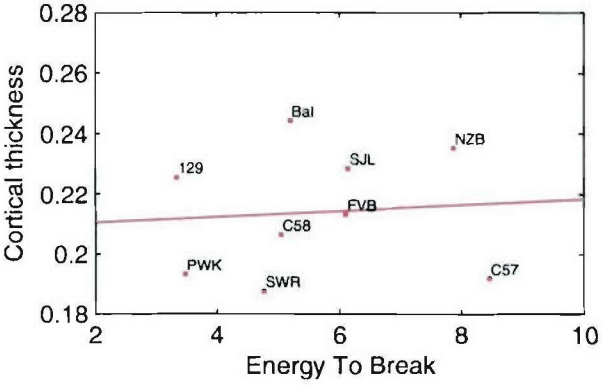
Cortical thickness
Energy To Break
Bal
NZB
129
SJL
FVB
C58
PWK
SWR
C57

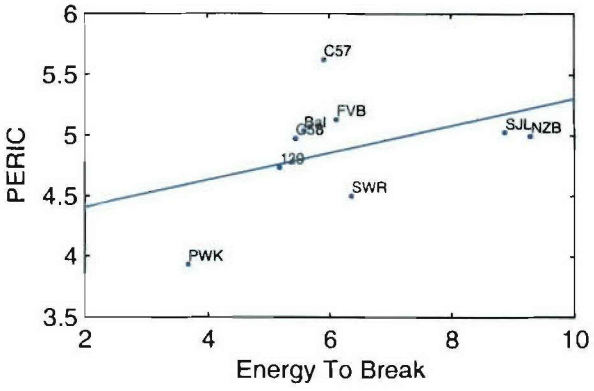
PERIC
Energy To Break
C57
FVB
Bal
SJL
NZB
129
SWR
PWK

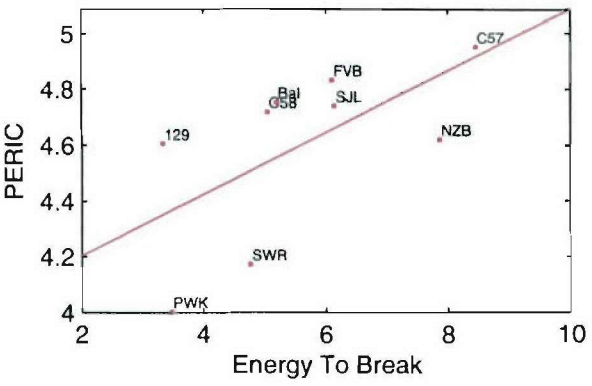
PERIC
Energy To Break
C57
FVB
Bal
SJL
129
NZB
SWR
PWK

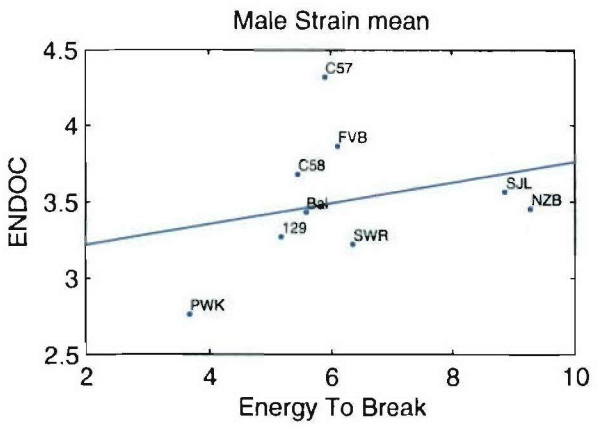
Male Strain mean
ENDOC
Energy To Break
C57
FVB
C58
SJL
Bal
NZB
129
SWR
PWK

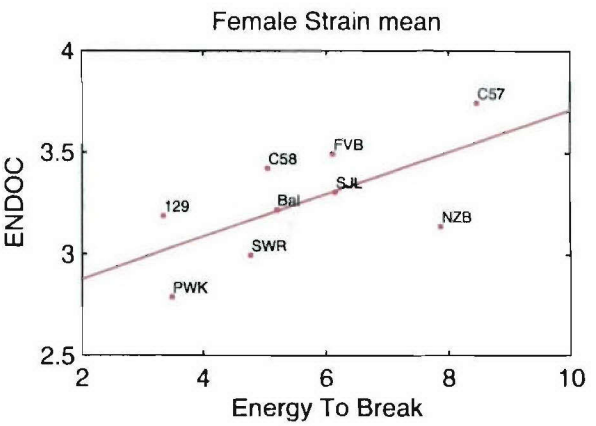
Female Strain mean
ENDOC
Energy To Break
C57
C58
FVB
SJL
129
Bal
NZB
SWR
PWK

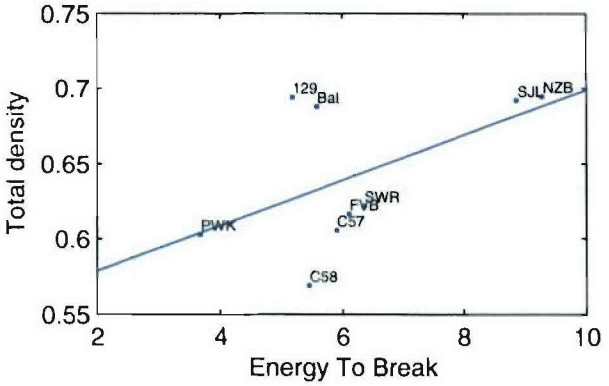
Total density
Energy To Break
129
Bal
SJL
NZB
SWR
FVB
PWK
C57
C58

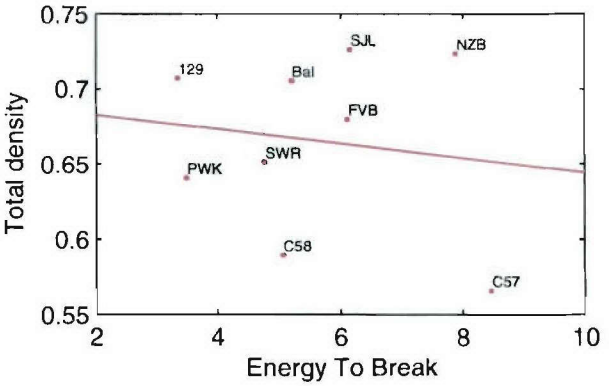
Total density
Energy To Break
SJL
NZB
129
Bal
FVB
SWR
PWK
C58
C57

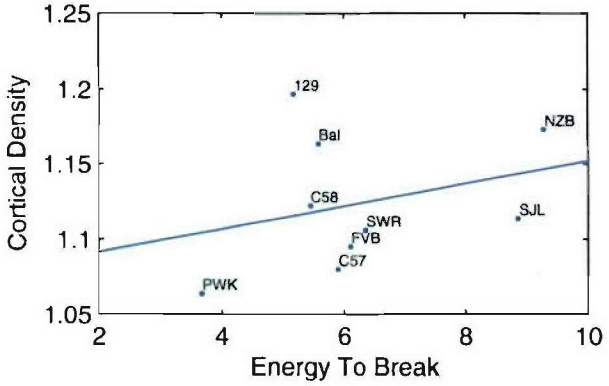
Cortical Density
Energy To Break
129
NZB
Bal
C58
SWR
SJL
FVB
C57
PWK

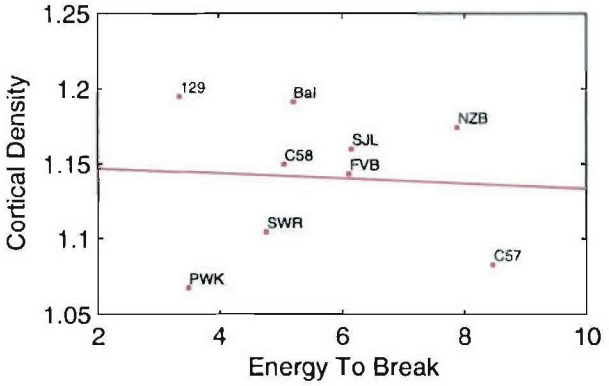
Cortical Density
Energy To Break
129
Bal
NZB
SJL
C58
FVB
SWR
C57
PWK

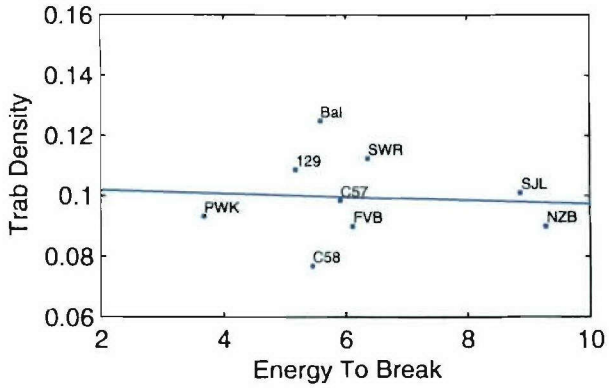
Trab Density
Energy To Break
Bal
SWR
129
SJL
C57
PWK
FVB
NZB
C58

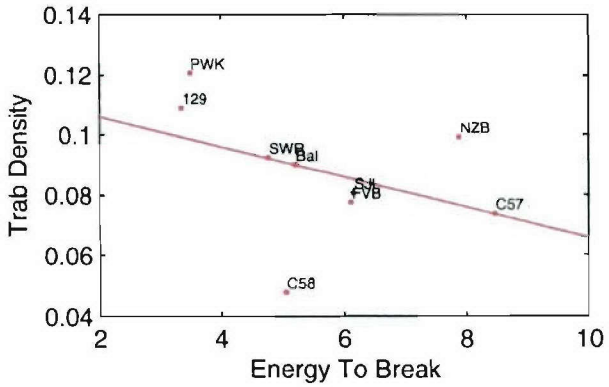
Trab Density
Energy To Break
PWK
129
NZB
SWR
Bal
SJL
FVB
C57
C58

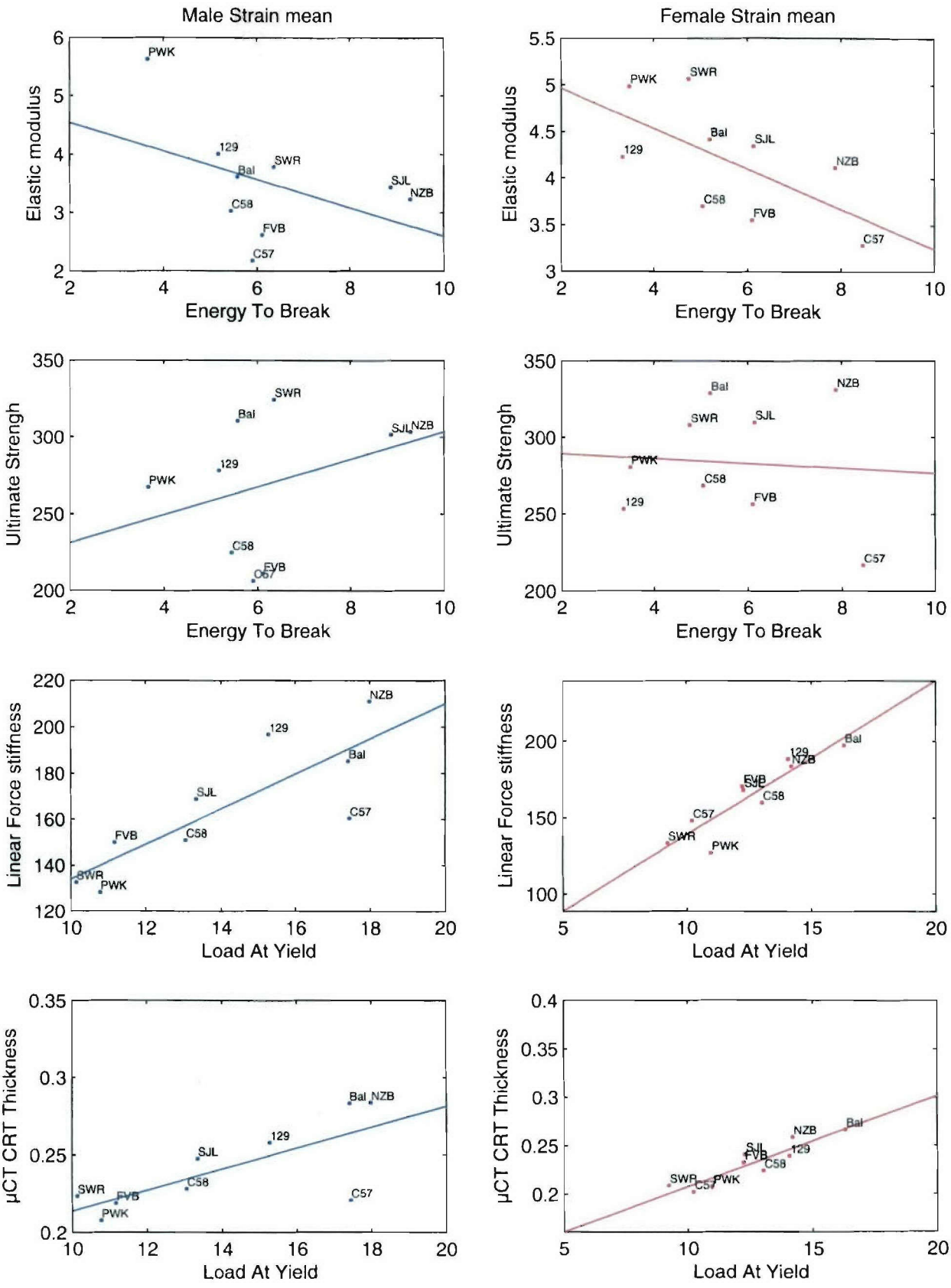
Male Strain mean
Female Strain mean
Elastic modulus
Energy To Break
Ultimate Strengh
Linear Force stiffness
Load At Yield
µCT CRT Thickness
PWK
SWR
129
Bal
SJL
NZB
C58
FVB
C57

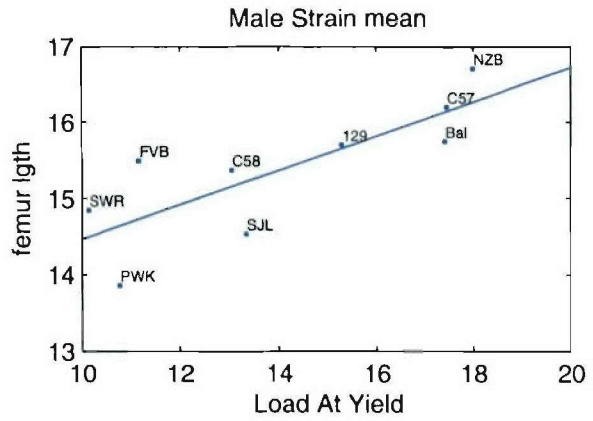
Male Strain mean
femur lgth
Load At Yield
NZB
C57
Bal
129
FVB
C58
SWR
SJL
PWK

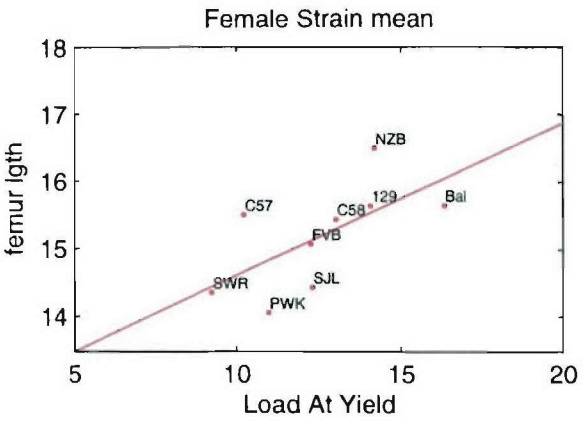
Female Strain mean
femur lgth
Load At Yield
NZB
C57
C58
129
Bal
FVB
SWR
SJL
PWK

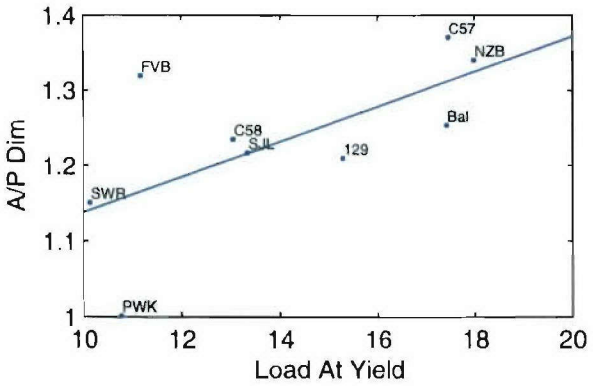
A/P Dim
Load At Yield
C57
NZB
FVB
Bal
C58
SJL
129
SWR
PWK

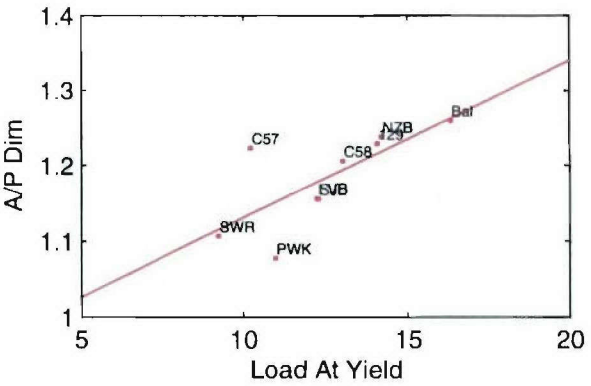
A/P Dim
Load At Yield
Bal
NZB
C57
129
C58
FVB
SWR
PWK

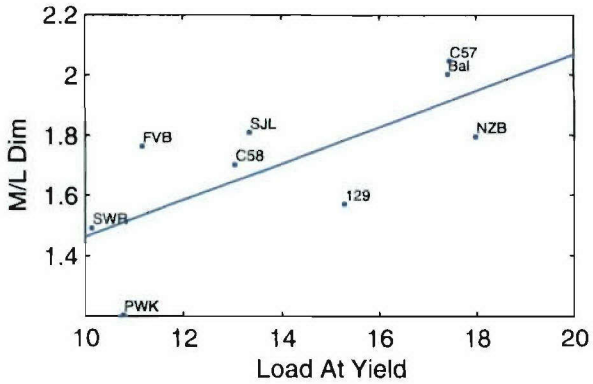
M/L Dim
Load At Yield
C57
Bal
SJL
FVB
NZB
C58
129
SWR
PWK

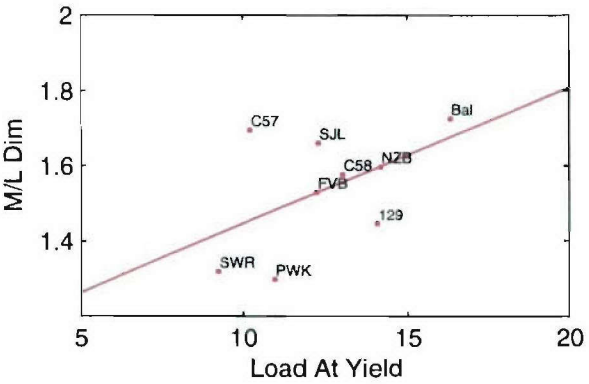
M/L Dim
Load At Yield
Bal
C57
SJL
C58
NZB
FVB
129
SWR
PWK

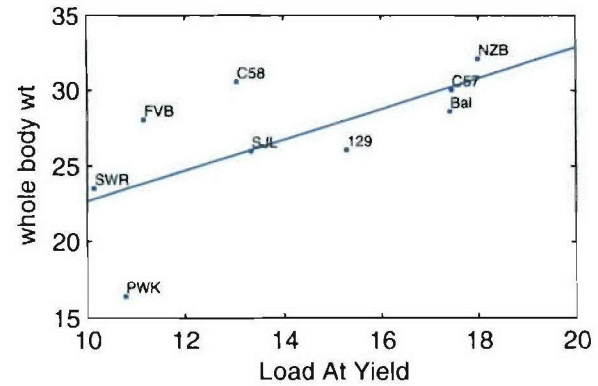
whole body wt
Load At Yield
NZB
C58
C57
FVB
Bal
SJL
129
SWR
PWK

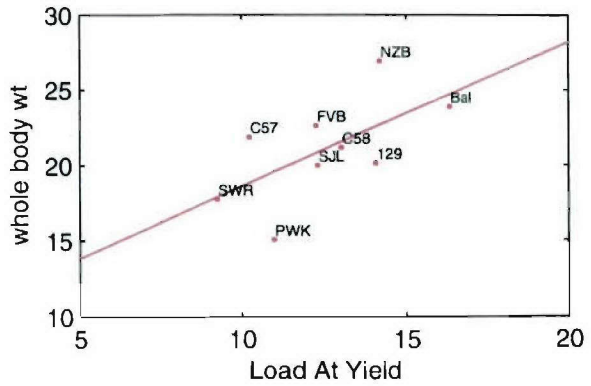
whole body wt
Load At Yield
NZB
Bal
C57
FVB
C58
SJL
129
SWR
PWK

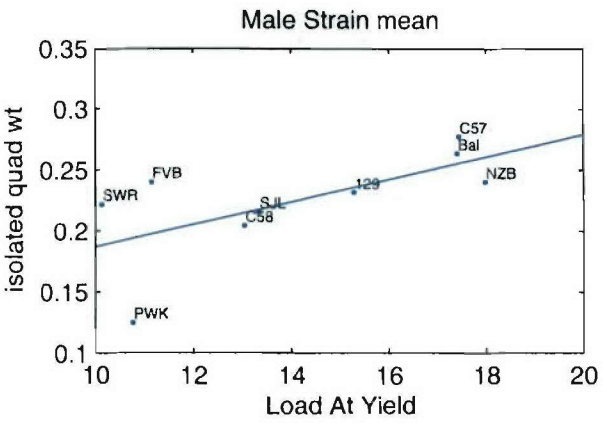
Male Strain mean
isolated quad wt
Load At Yield
C57
Bal
FVB
NZB
SWR
SJL
129
C58
PWK

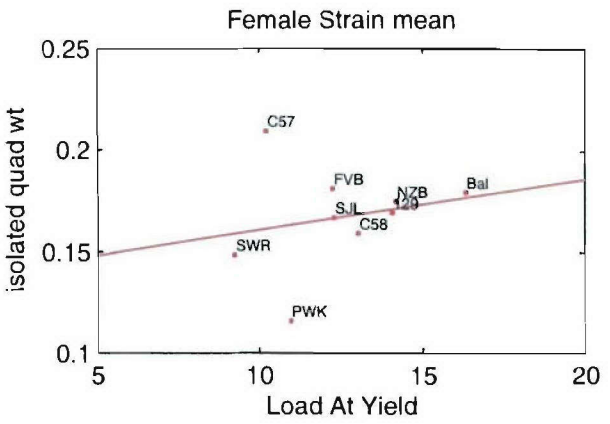
Female Strain mean
isolated quad wt
Load At Yield
C57
FVB
NZB
Bal
SJL
129
C58
SWR
PWK

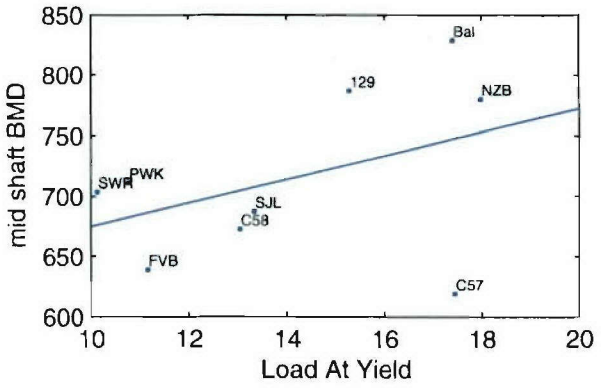
mid shaft BMD
Load At Yield
Bal
129
NZB
SWR
PWK
SJL
C58
FVB
C57

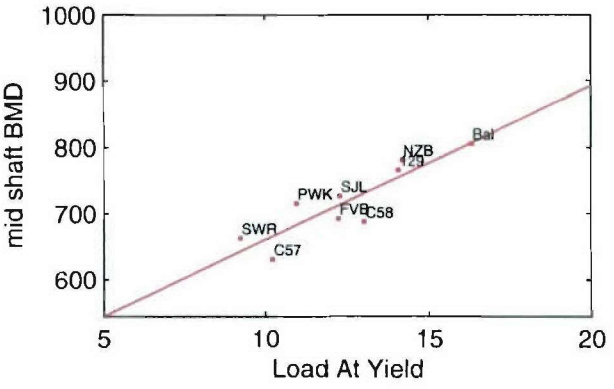
mid shaft BMD
Load At Yield
NZB
Bal
129
PWK
SJL
FVB
C58
SWR
C57

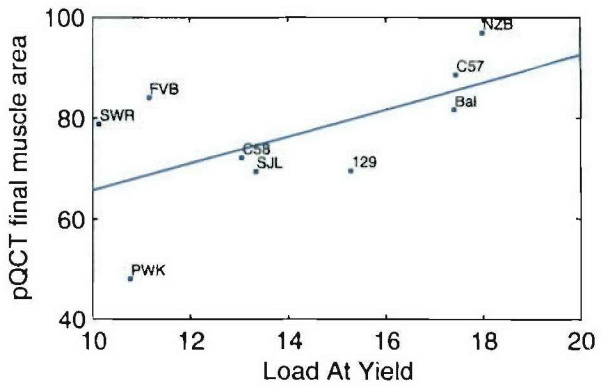
pQCT final muscle area
Load At Yield
NZB
C57
FVB
SWR
Bal
C58
SJL
129
PWK

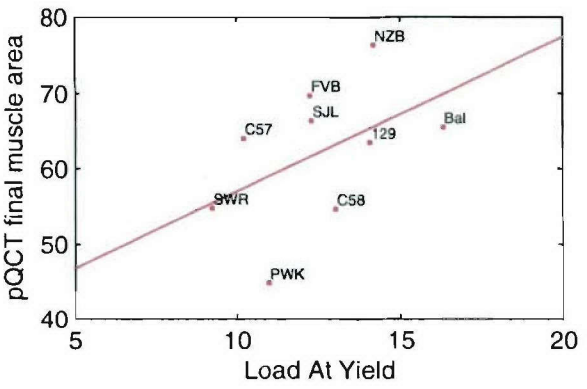
pQCT final muscle area
Load At Yield
NZB
FVB
SJL
C57
Bal
129
SWR
C58
PWK

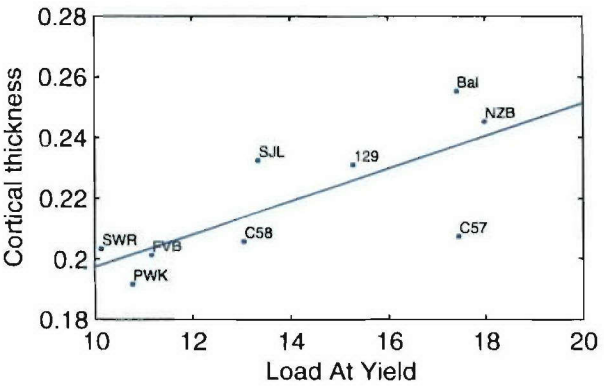
Cortical thickness
Load At Yield
Bal
NZB
SJL
129
SWR
FVB
C58
C57
PWK

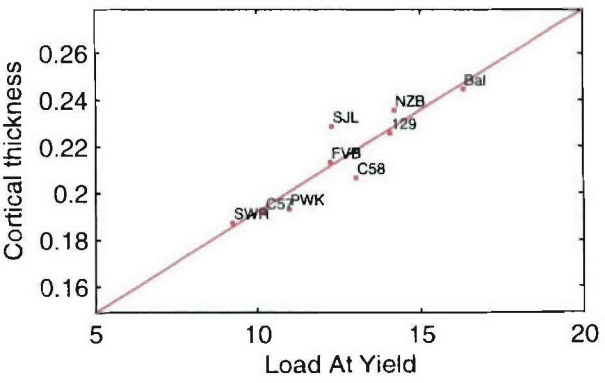
Cortical thickness
Load At Yield
Bal
NZB
SJL
129
FVB
C58
SWR
C57
PWK

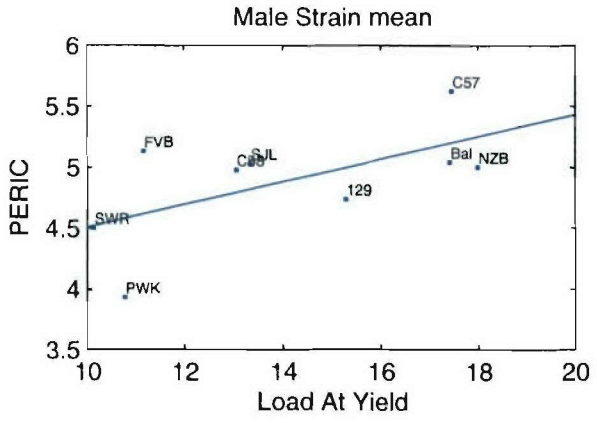
Male Strain mean
PERIC
Load At Yield
C57
FVB
SJL
Bal
NZB
129
SWR
PWK

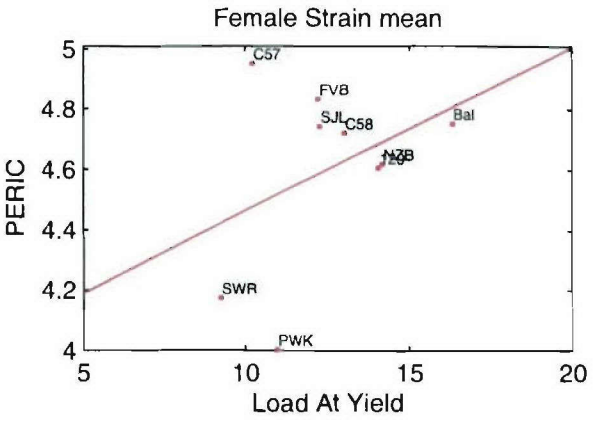
Female Strain mean
PERIC
Load At Yield
C57
FVB
SJL
C58
Bal
NZB
SWR
PWK

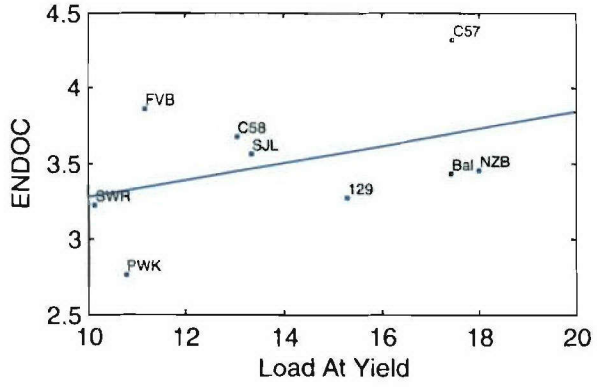
ENDOC
Load At Yield
C57
FVB
C58
SJL
Bal
NZB
129
SWR
PWK

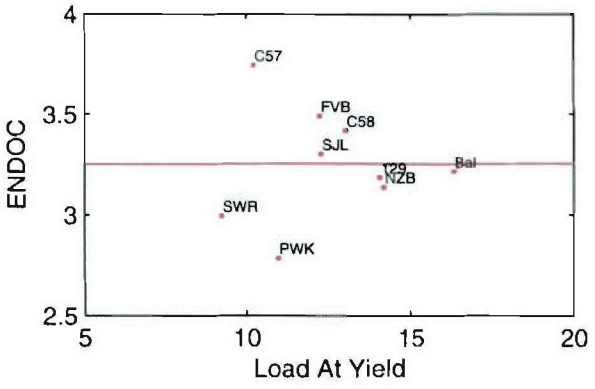
ENDOC
Load At Yield
C57
FVB
C58
SJL
129
Bal
NZB
SWR
PWK

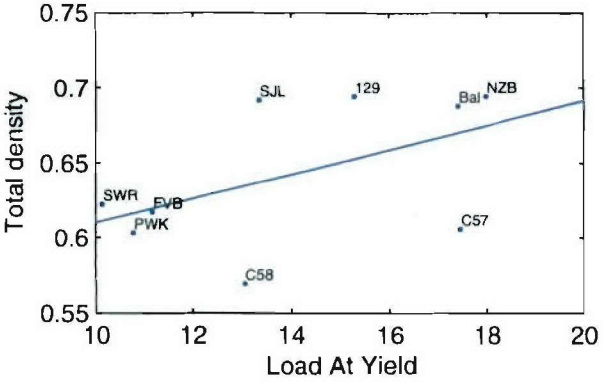
Total density
Load At Yield
SJL
129
Bal
NZB
SWR
FVB
PWK
C57
C58

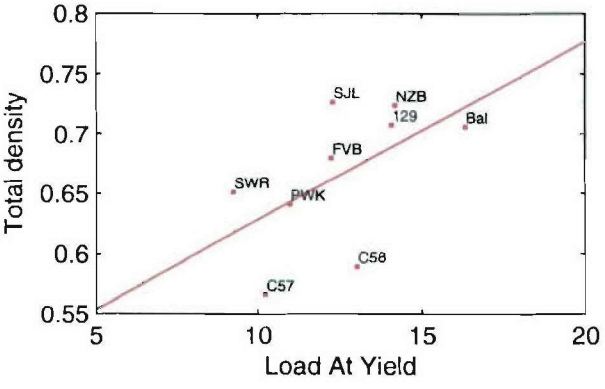
Total density
Load At Yield
SJL
NZB
129
Bal
FVB
SWR
PWK
C58
C57

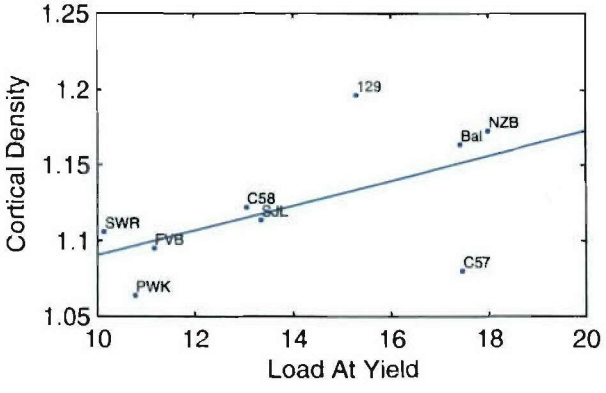
Cortical Density
Load At Yield
129
Bal
NZB
C58
SJL
SWR
FVB
C57
PWK

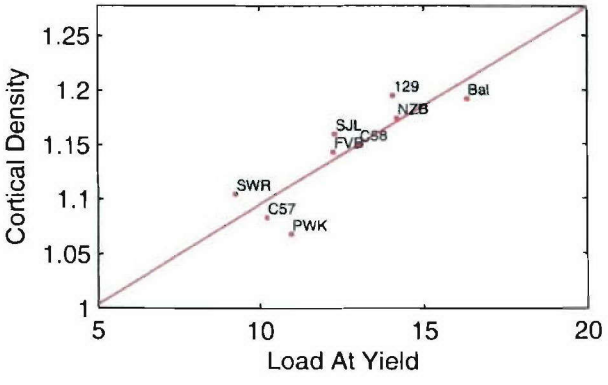
Cortical Density
Load At Yield
129
Bal
NZB
SJL
C58
FVB
SWR
C57
PWK

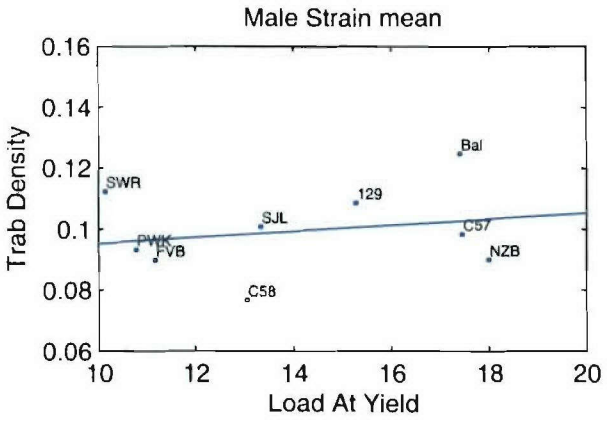
Male Strain mean
Trab Density
Load At Yield
Bal
SWR
129
SJL
C57
PWK
FVB
NZB
C58

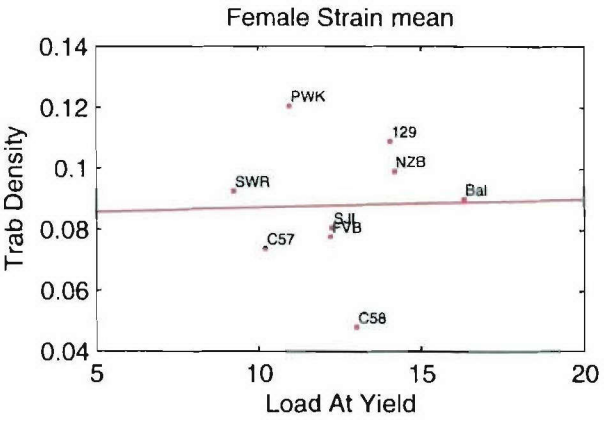
Female Strain mean
Trab Density
Load At Yield
PWK
129
NZB
SWR
Bal
SJL
FVB
C57
C58

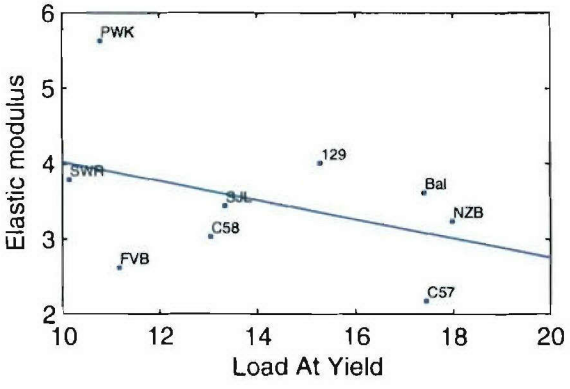
Elastic modulus
Load At Yield
PWK
129
SWR
Bal
SJL
NZB
C58
FVB
C57

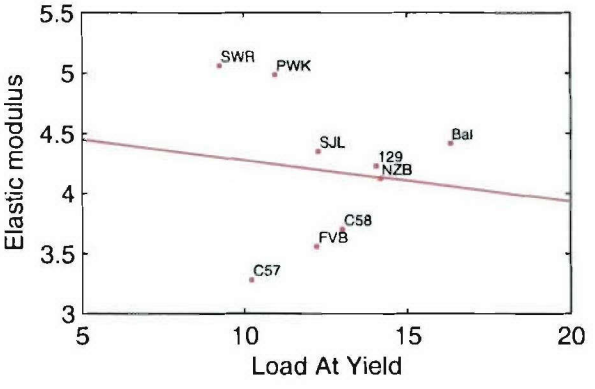
Elastic modulus
Load At Yield
SWR
PWK
SJL
Bal
129
NZB
C58
FVB
C57

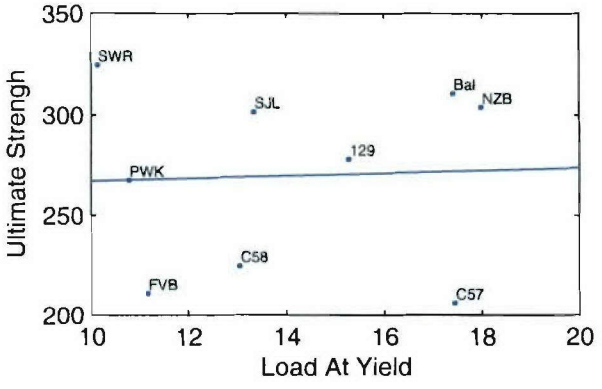
Ultimate Strengh
Load At Yield
SWR
Bal
NZB
SJL
129
PWK
C58
FVB
C57

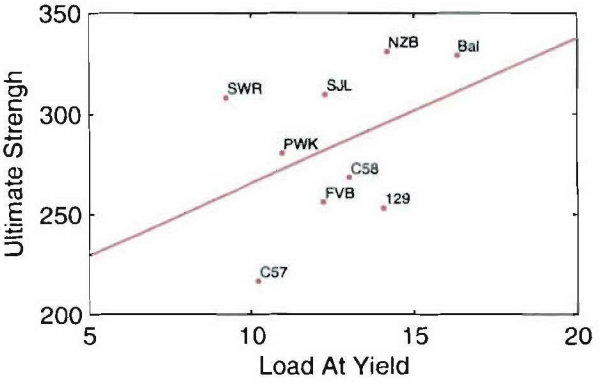
Ultimate Strengh
Load At Yield
NZB
Bal
SWR
SJL
PWK
C58
FVB
129
C57

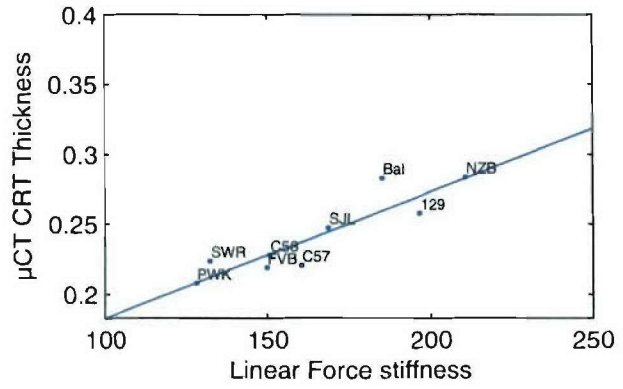
µCT CRT Thickness
Linear Force stiffness
Bal
NZB
129
SJL
SWR
C58
FVB
C57
PWK

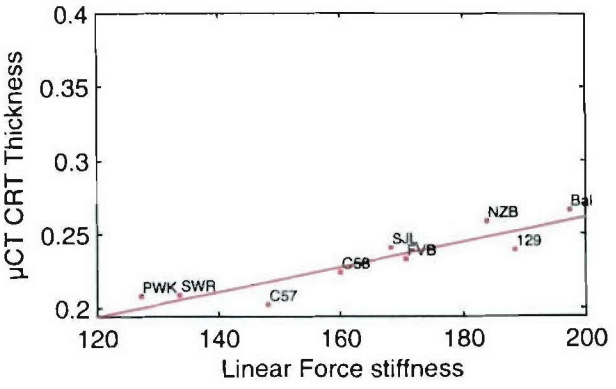
µCT CRT Thickness
Linear Force stiffness
NZB
Bal
SJL
129
FVB
C58
PWK
SWR
C57

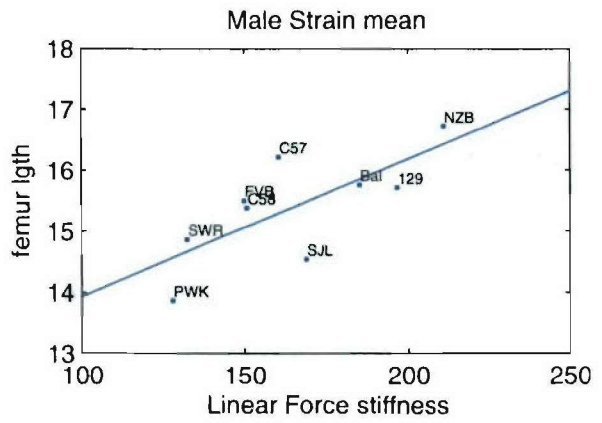
Male Strain mean
femur lgth
Linear Force stiffness
NZB
C57
Bal
129
FVB
C58
SWR
SJL
PWK

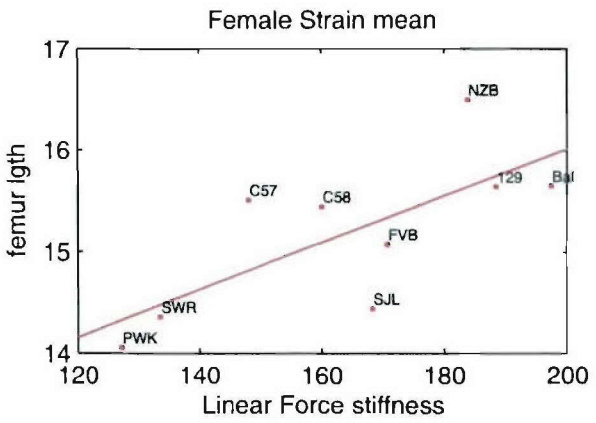
Female Strain mean
femur lgth
Linear Force stiffness
NZB
C57
C58
129
Bal
FVB
SWR
SJL
PWK

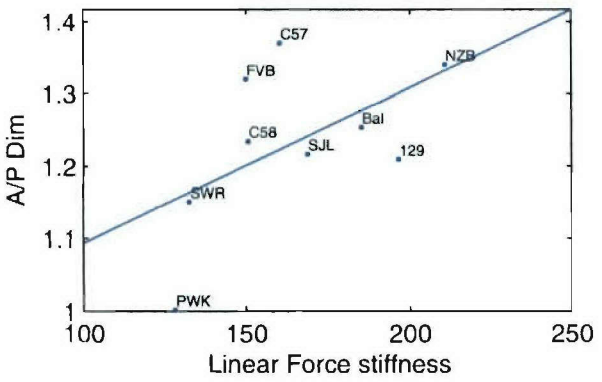
A/P Dim
Linear Force stiffness
C57
NZB
FVB
Bal
C58
SJL
129
SWR
PWK

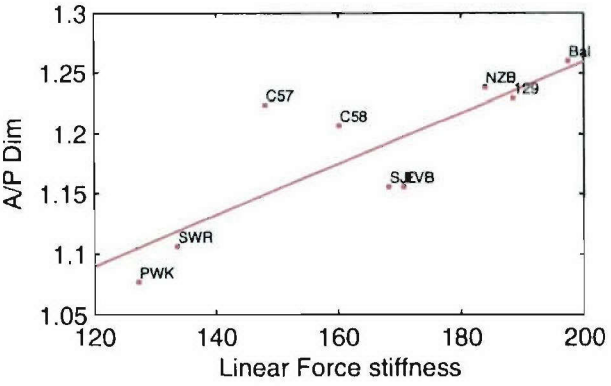
A/P Dim
Linear Force stiffness
Bal
NZB
129
C57
C58
SJL
FVB
SWR
PWK

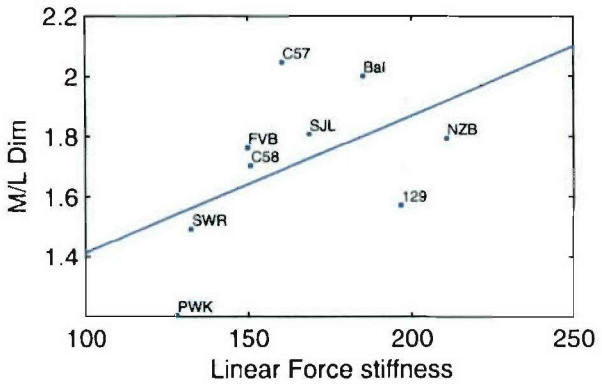
M/L Dim
Linear Force stiffness
C57
Bal
SJL
NZB
FVB
C58
129
SWR
PWK

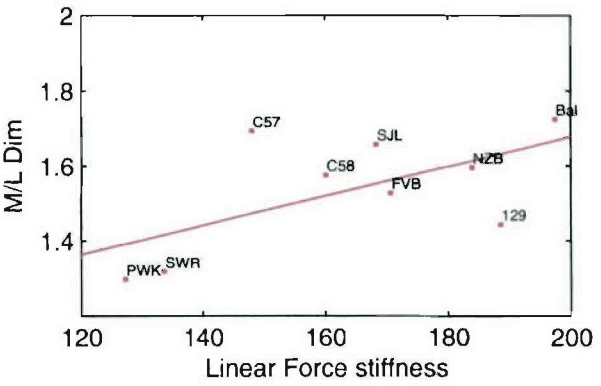
M/L Dim
Linear Force stiffness
C57
SJL
Bal
C58
NZB
FVB
129
PWK
SWR

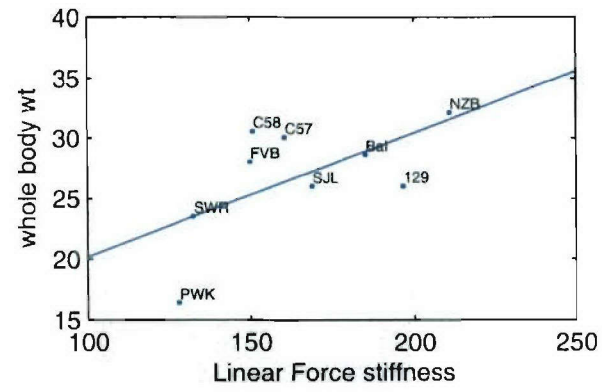
whole body wt
Linear Force stiffness
NZB
C58
C57
FVB
Bal
SJL
129
SWR
PWK

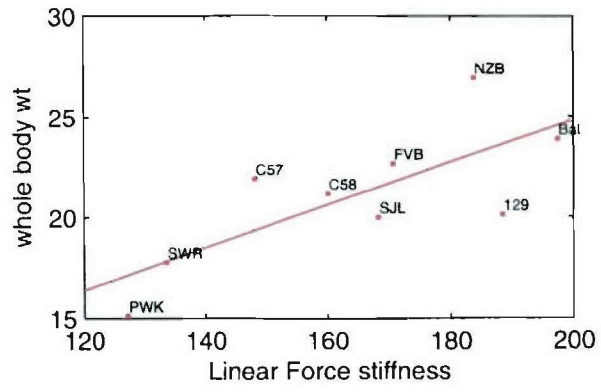
whole body wt
Linear Force stiffness
NZB
Bal
C57
FVB
C58
SJL
129
SWR
PWK

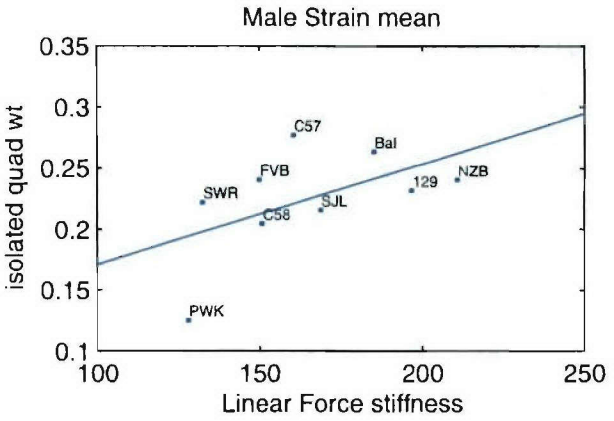
Male Strain mean
isolated quad wt
Linear Force stiffness
C57
Bal
FVB
NZB
SWR
129
SJL
C58
PWK

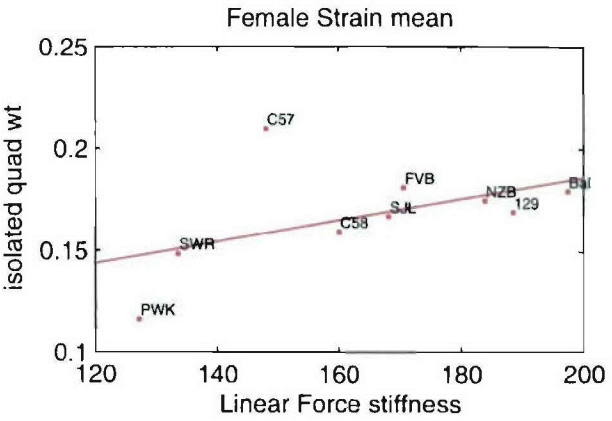
Female Strain mean
isolated quad wt
Linear Force stiffness
C57
FVB
NZB
Bal
SJL
129
C58
SWR
PWK

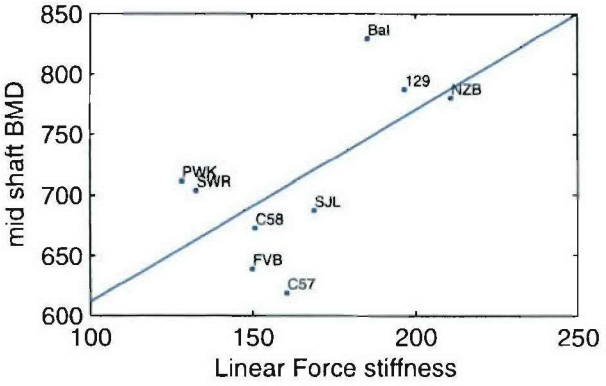
mid shaft BMD
Linear Force stiffness
Bal
129
NZB
PWK
SWR
SJL
C58
FVB
C57

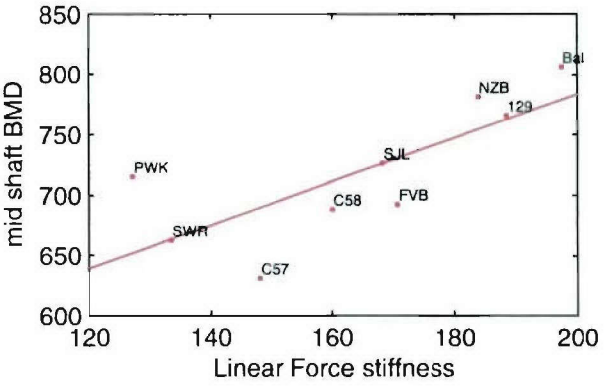
mid shaft BMD
Linear Force stiffness
Bal
NZB
129
SJL
PWK
C58
FVB
SWR
C57

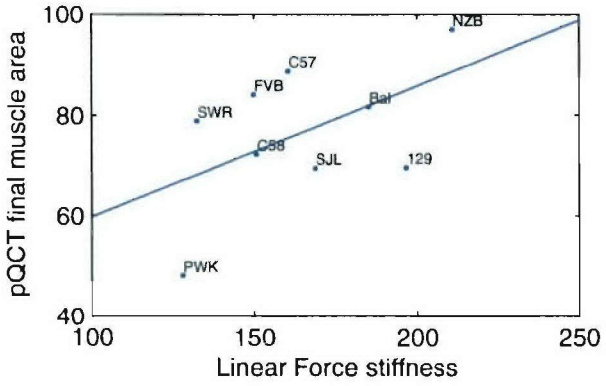
pQCT final muscle area
Linear Force stiffness
NZB
C57
FVB
Bal
SWR
C58
SJL
129
PWK

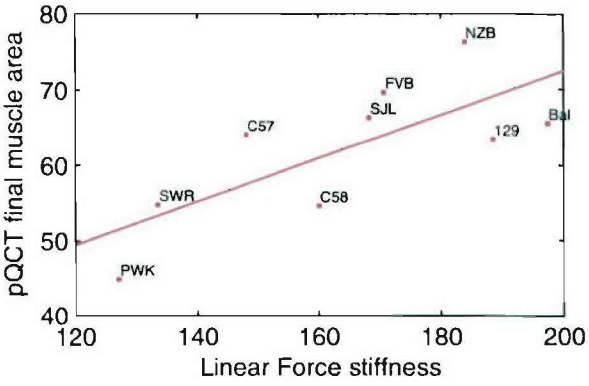
pQCT final muscle area
Linear Force stiffness
NZB
FVB
SJL
C57
Bal
129
SWR
C58
PWK

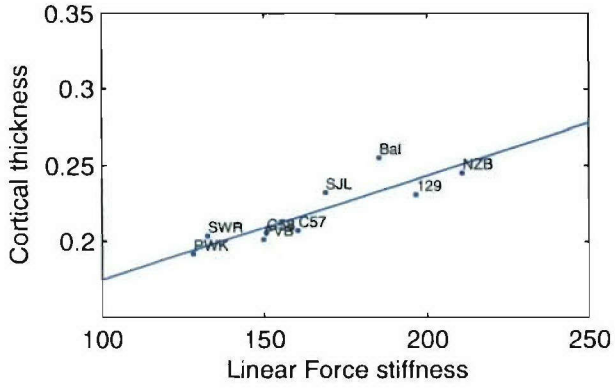
Cortical thickness
Linear Force stiffness
Bal
NZB
SJL
129
SWR
C57
PWK

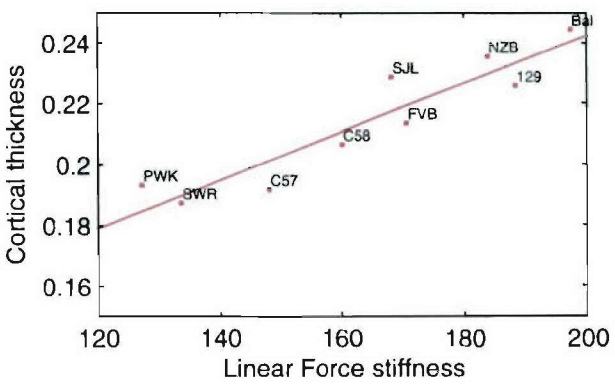
Cortical thickness
Linear Force stiffness
Bal
NZB
SJL
129
FVB
C58
PWK
C57
SWR

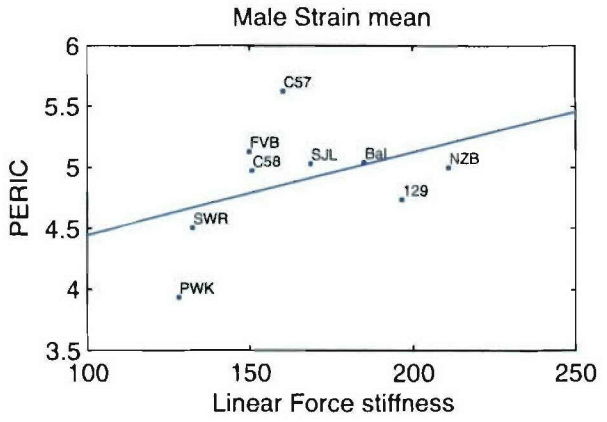
Male Strain mean
PERIC
Linear Force stiffness
C57
FVB
C58
SJL
Bal
NZB
129
SWR
PWK

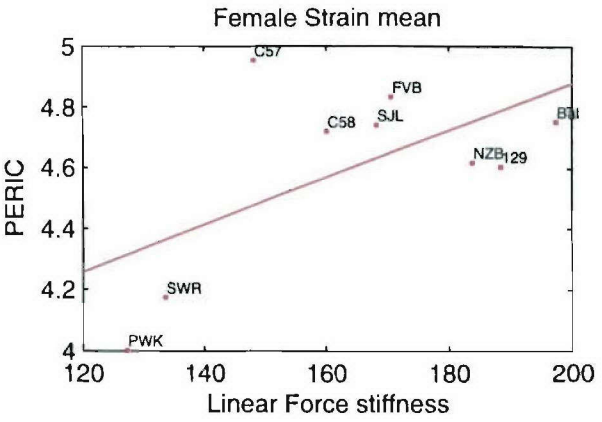
Female Strain mean
PERIC
Linear Force stiffness
C57
FVB
C58
SJL
NZB
129
SWR
PWK

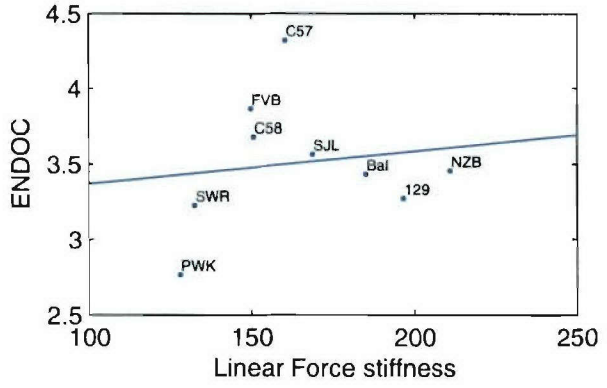
ENDOC
Linear Force stiffness
C57
FVB
C58
SJL
Bal
NZB
129
SWR
PWK

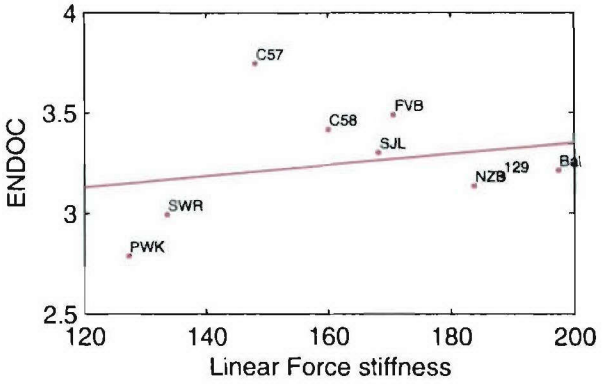
ENDOC
Linear Force stiffness
C57
FVB
C58
SJL
NZB
129
SWR
PWK

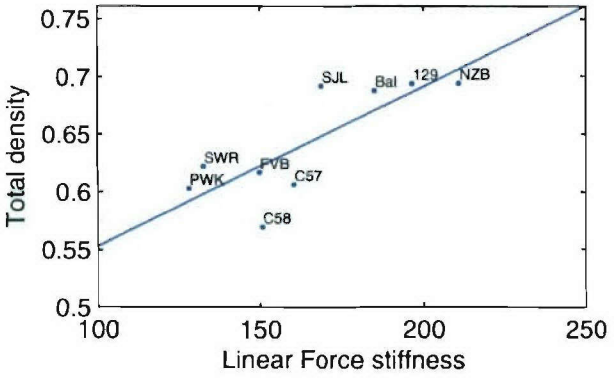
Total density
Linear Force stiffness
SJL
Bal
129
NZB
SWR
FVB
PWK
C57
C58

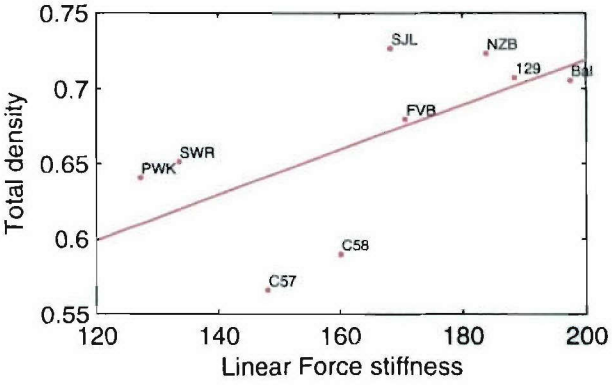
Total density
Linear Force stiffness
SJL
NZB
129
Bal
FVB
SWR
PWK
C58
C57

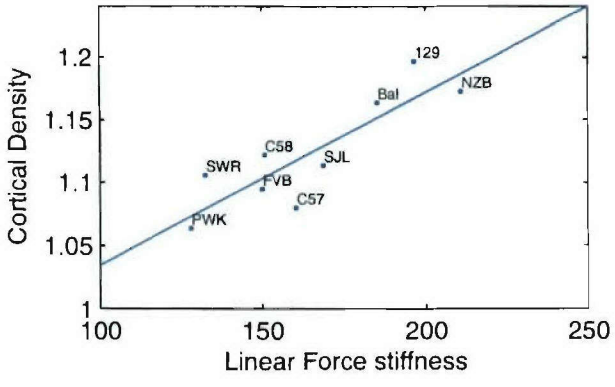
Cortical Density
Linear Force stiffness
129
Bal
NZB
C58
SJL
SWR
FVB
C57
PWK

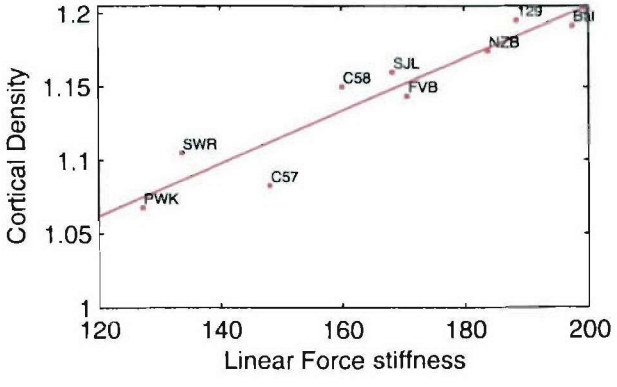
Cortical Density
Linear Force stiffness
129
Bal
NZB
SJL
C58
FVB
SWR
C57
PWK

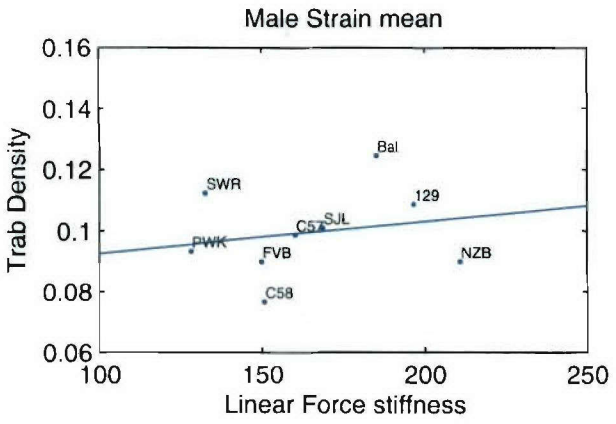
Male Strain mean
Trab Density
Linear Force stiffness
0.16
0.14
0.12
0.1
0.08
0.06
100
150
200
250
Bal
SWR
129
SJL
C57
PWK
FVB
NZB
C58

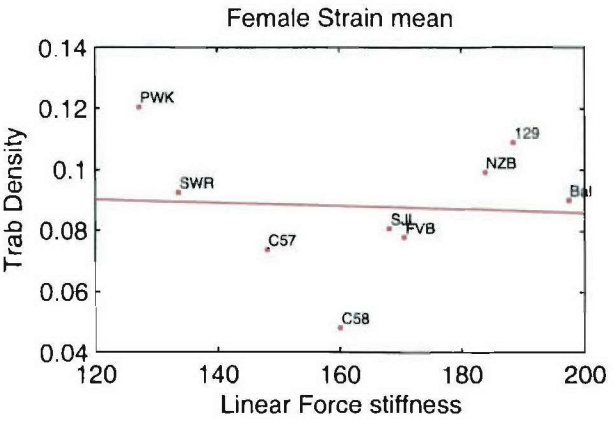
Female Strain mean
Trab Density
Linear Force stiffness
0.14
0.12
0.1
0.08
0.06
0.04
120
140
160
180
200
PWK
129
NZB
SWR
Bal
SJL
FVB
C57
C58

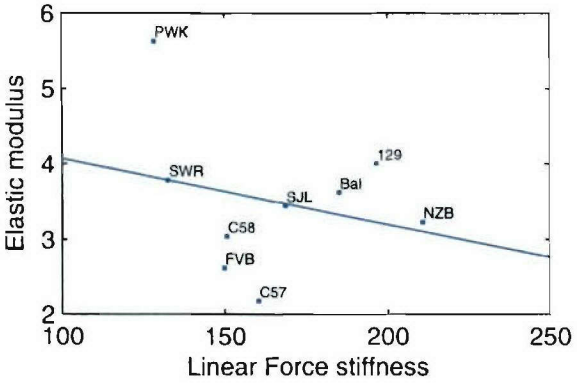
Elastic modulus
Linear Force stiffness
6
5
4
3
2
100
150
200
250
PWK
129
SWR
Bal
SJL
NZB
C58
FVB
C57

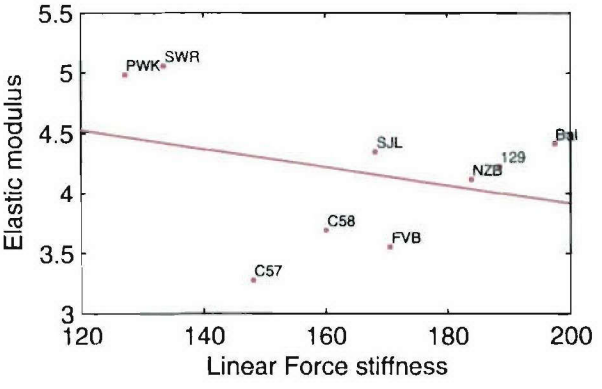
Elastic modulus
Linear Force stiffness
5.5
5
4.5
4
3.5
3
120
140
160
180
200
PWK
SWR
SJL
Bal
129
NZB
C58
FVB
C57

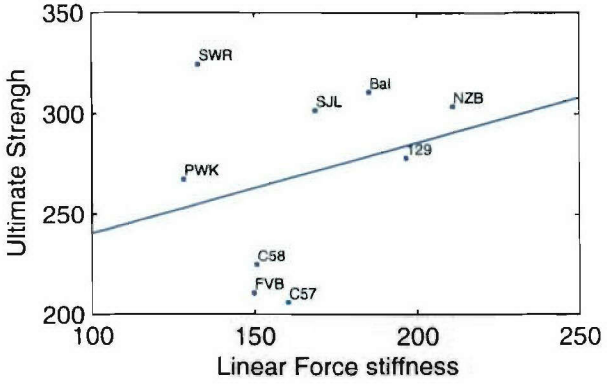
Ultimate Strengh
Linear Force stiffness
350
300
250
200
100
150
200
250
SWR
Bal
SJL
NZB
129
PWK
C58
FVB
C57

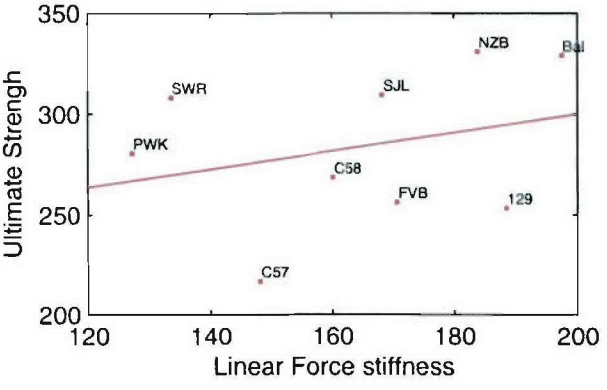
Ultimate Strengh
Linear Force stiffness
350
300
250
200
120
140
160
180
200
NZB
Bal
SWR
SJL
PWK
C58
FVB
129
C57

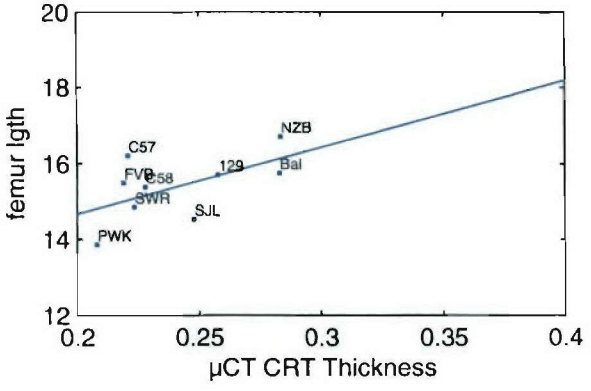
femur lgth
μCT CRT Thickness
20
18
16
14
12
0.2
0.25
0.3
0.35
0.4
C57
NZB
FVB
C58
129
Bal
SWR
SJL
PWK

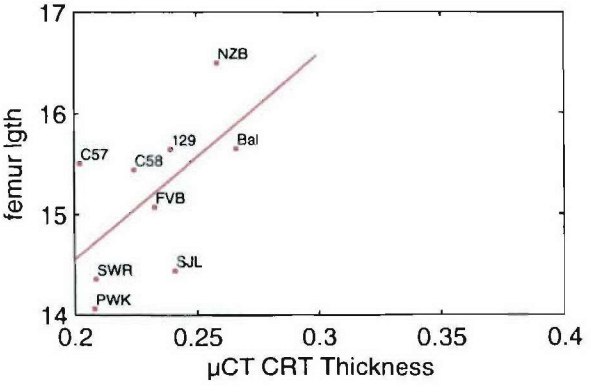
femur lgth
μCT CRT Thickness
17
16
15
14
0.2
0.25
0.3
0.35
0.4
NZB
C57
129
Bal
C58
FVB
SWR
SJL
PWK

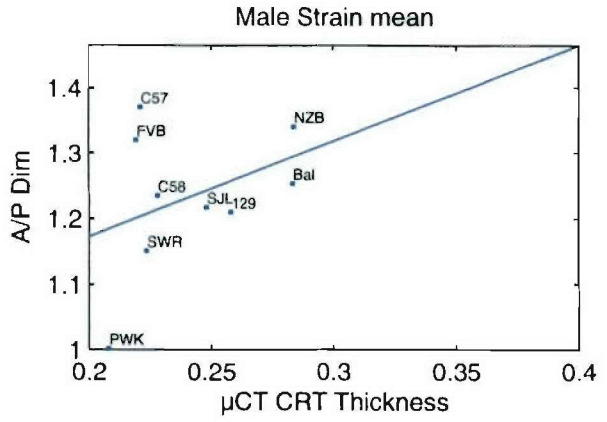
Male Strain mean
A/P Dim
µCT CRT Thickness
C57
FVB
NZB
C58
SJL
129
Bal
SWR
PWK

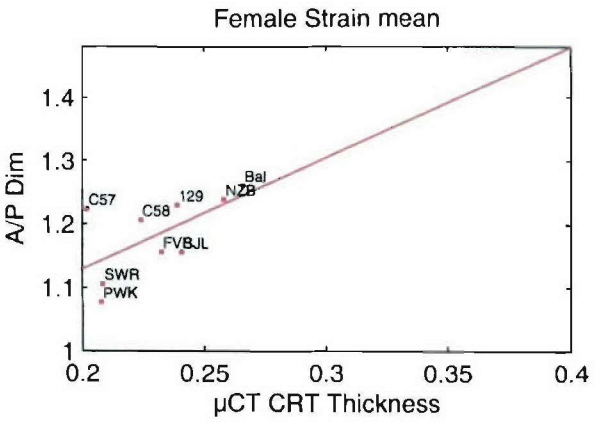
Female Strain mean
A/P Dim
µCT CRT Thickness
C57
C58
129
Bal
NZB
FVB
SJL
SWR
PWK

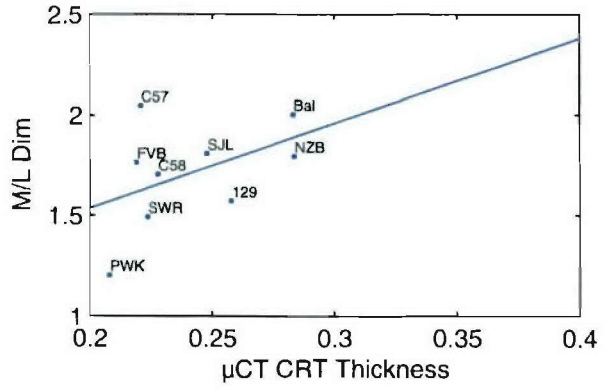
M/L Dim
µCT CRT Thickness
C57
Bal
FVB
SJL
NZB
C58
129
SWR
PWK

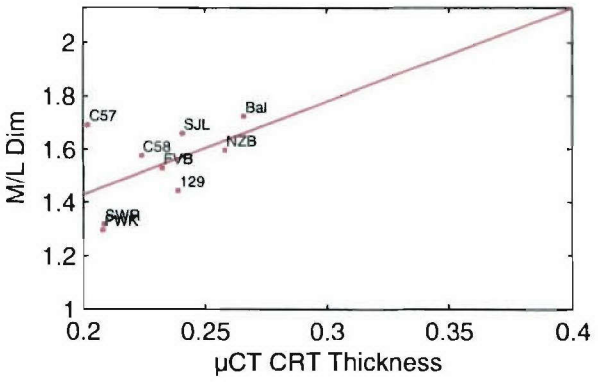
M/L Dim
µCT CRT Thickness
C57
SJL
Bal
C58
NZB
FVB
129
SWR
PWK

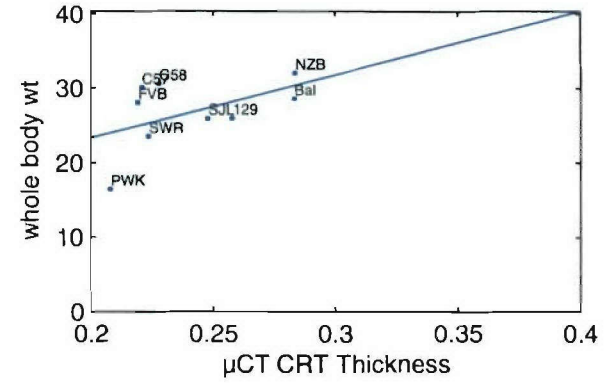
whole body wt
µCT CRT Thickness
NZB
C58
C57
FVB
Bal
SJL
129
SWR
PWK

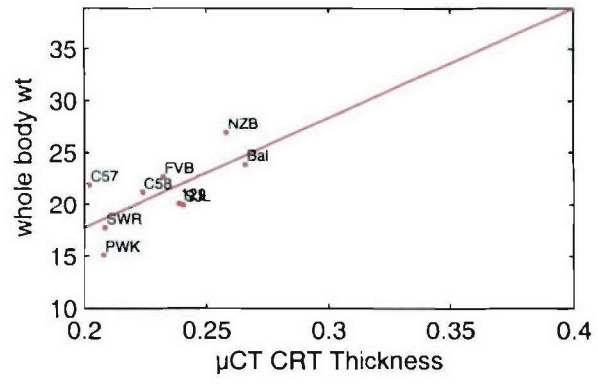
whole body wt
µCT CRT Thickness
NZB
Bal
FVB
C57
C58
SWR
PWK

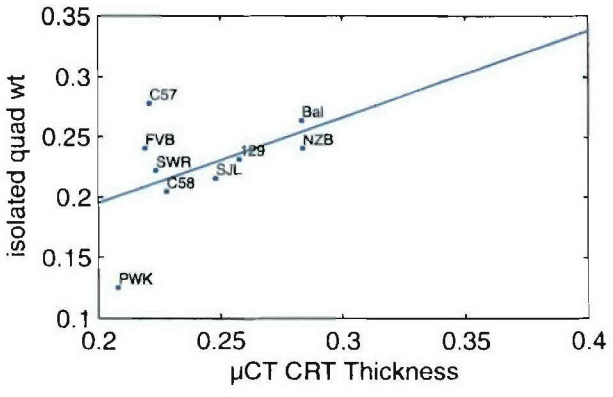
isolated quad wt
µCT CRT Thickness
C57
Bal
FVB
129
NZB
SWR
SJL
C58
PWK

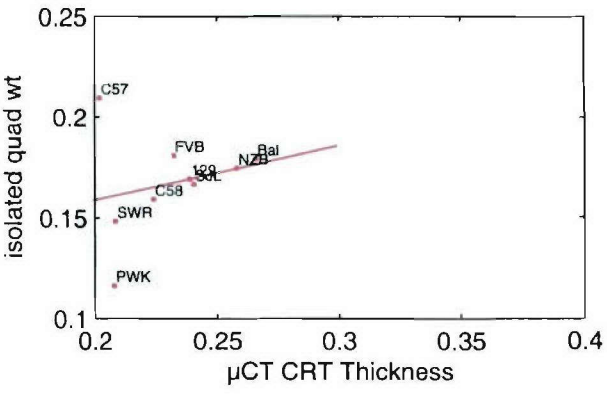
isolated quad wt
µCT CRT Thickness
C57
FVB
Bal
NZB
C58
SWR
PWK

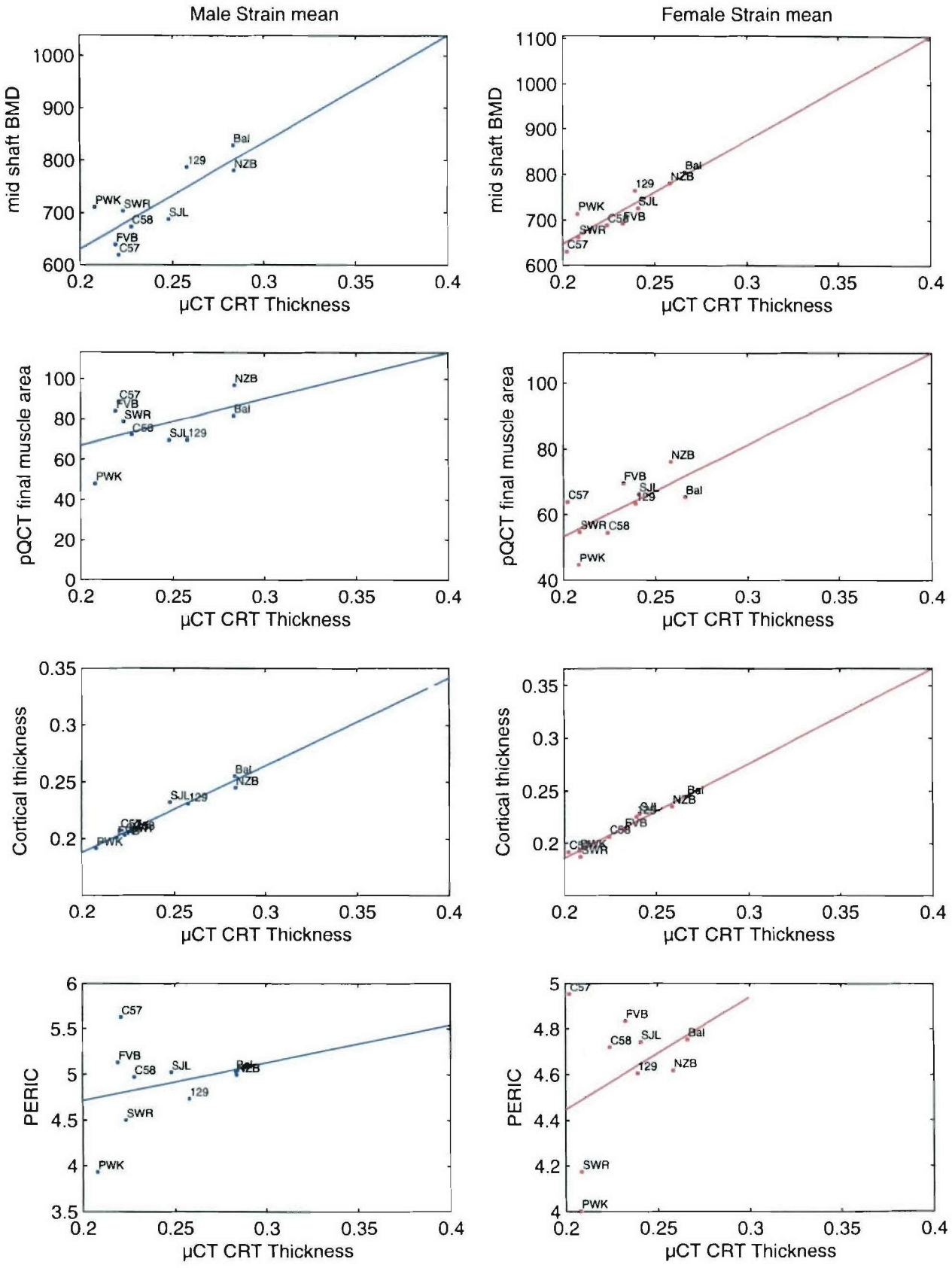
Male Strain mean
Female Strain mean
mid shaft BMD
pQCT final muscle area
Cortical thickness
PERIC
µCT CRT Thickness
PWK
SWR
C58
SJL
FVB
C57
129
NZB
Bal

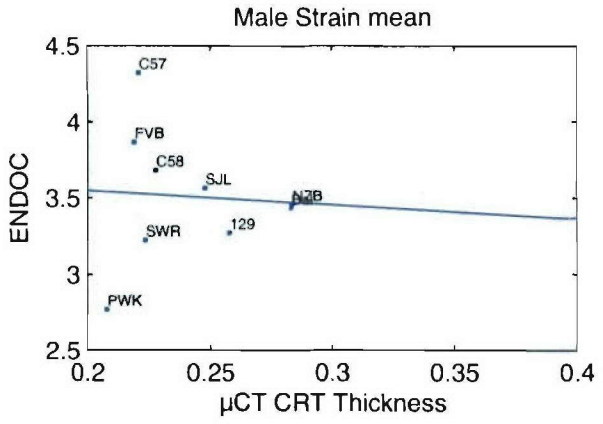
Male Strain mean
ENDOC
µCT CRT Thickness
C57
FVB
C58
SJL
NZB
SWR
129
PWK

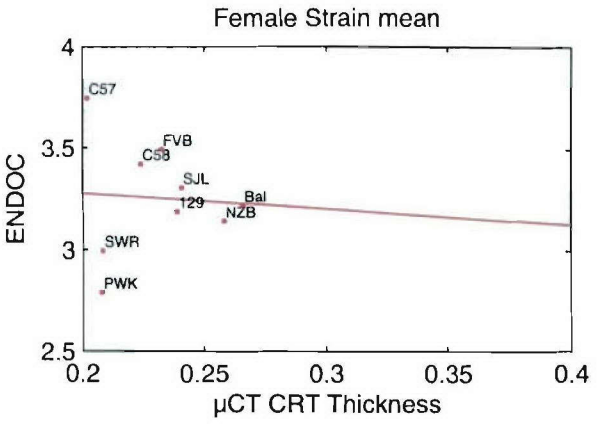
Female Strain mean
ENDOC
µCT CRT Thickness
C57
FVB
C58
SJL
129
Bal
NZB
SWR
PWK

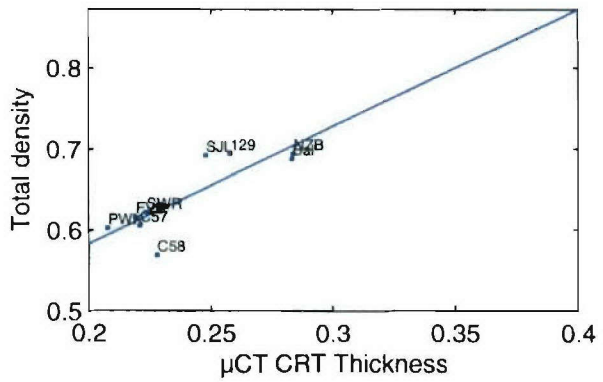
Total density
µCT CRT Thickness
SJL
129
NZB
Bal
SWR
FVB
PWK
C57
C58

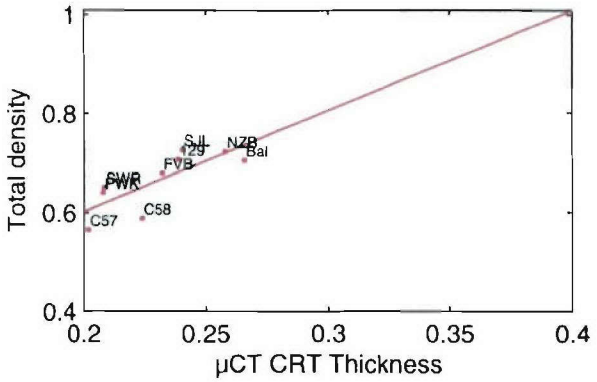
Total density
µCT CRT Thickness
SJL
NZB
129
Bal
FVB
SWR
PWK
C57
C58

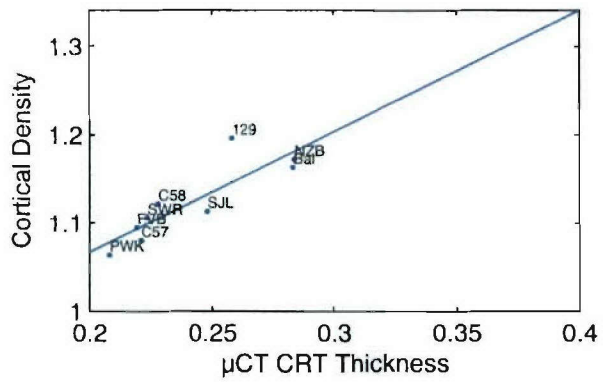
Cortical Density
µCT CRT Thickness
129
NZB
Bal
C58
SWR
SJL
FVB
C57
PWK

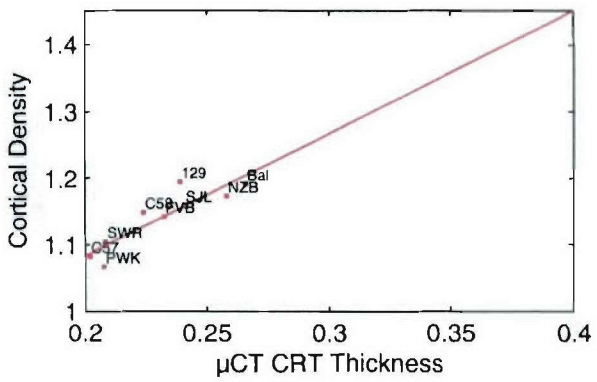
Cortical Density
µCT CRT Thickness
129
Bal
SJL
NZB
C58
FVB
SWR
C57
PWK

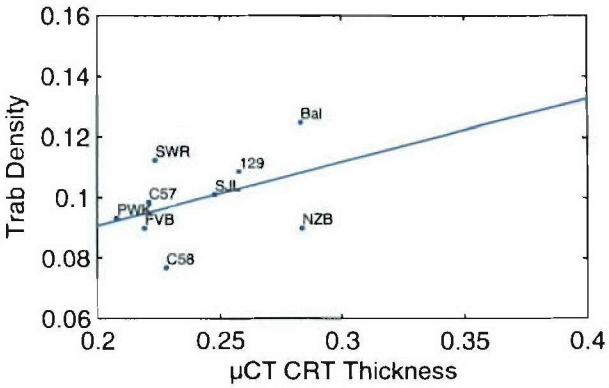
Trab Density
µCT CRT Thickness
Bal
SWR
129
SJL
C57
PWK
FVB
NZB
C58

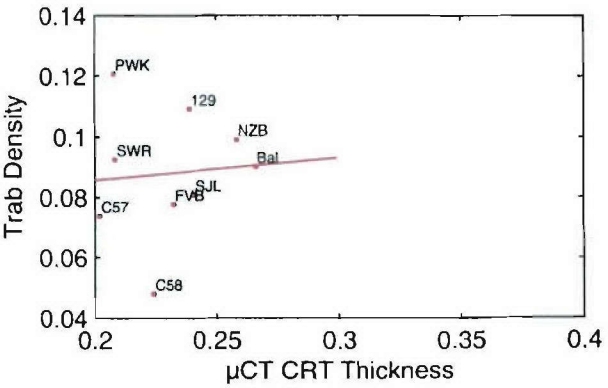
Trab Density
µCT CRT Thickness
PWK
129
NZB
SWR
Bal
SJL
C57
FVB
C58

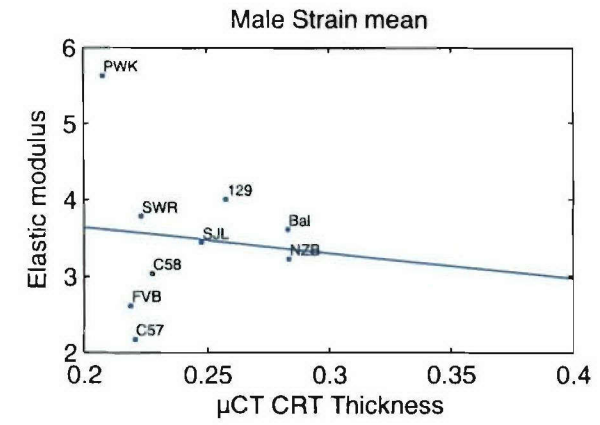
Male Strain mean
Elastic modulus
µCT CRT Thickness
PWK
SWR
129
Bal
SJL
NZB
C58
FVB
C57

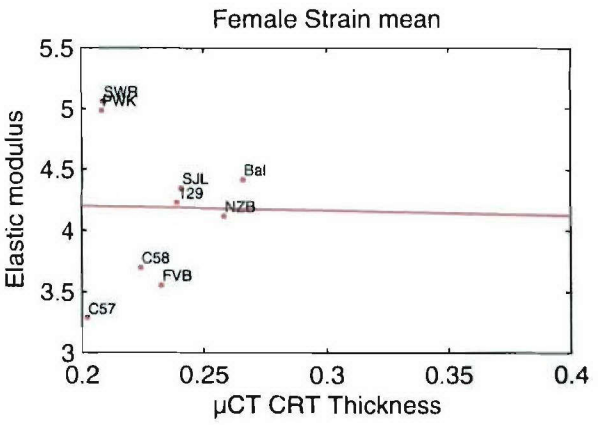
Female Strain mean
Elastic modulus
µCT CRT Thickness
SWR
PWK
SJL
Bal
129
NZB
C58
FVB
C57

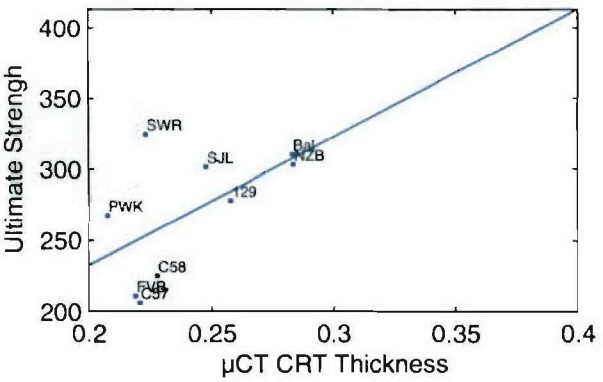
Ultimate Strengh
µCT CRT Thickness
SWR
SJL
Bal
NZB
PWK
129
C58
FVB
C57

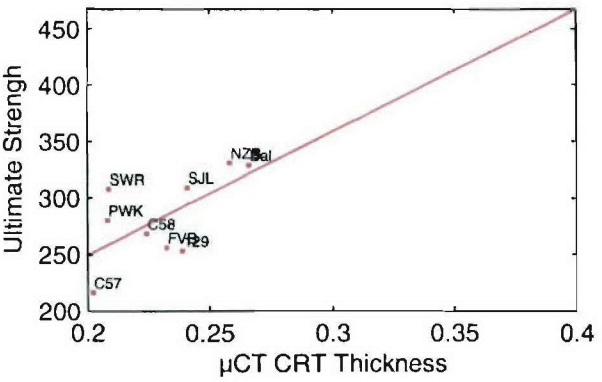
Ultimate Strengh
µCT CRT Thickness
NZB
Bal
SWR
SJL
PWK
C58
FVB
129
C57

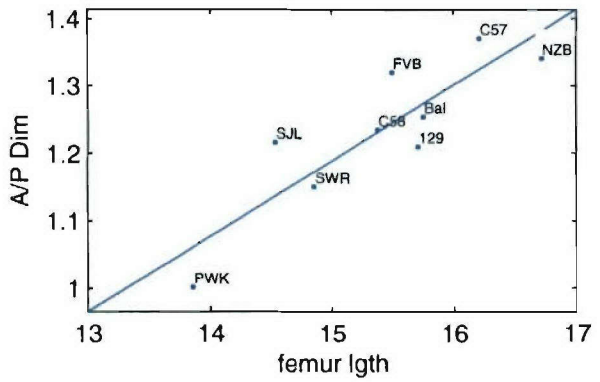
A/P Dim
femur lgth
C57
NZB
FVB
Bal
SJL
C58
129
SWR
PWK

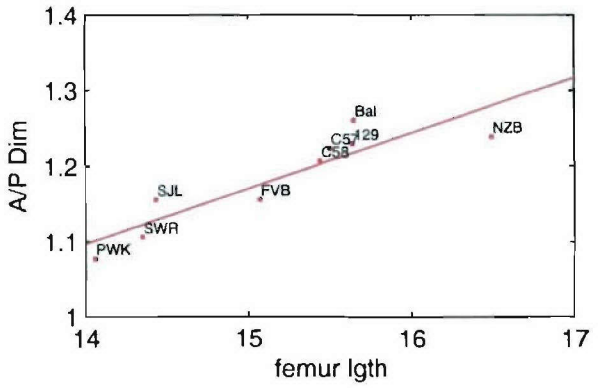
A/P Dim
femur lgth
Bal
C57
129
NZB
C58
SJL
FVB
SWR
PWK

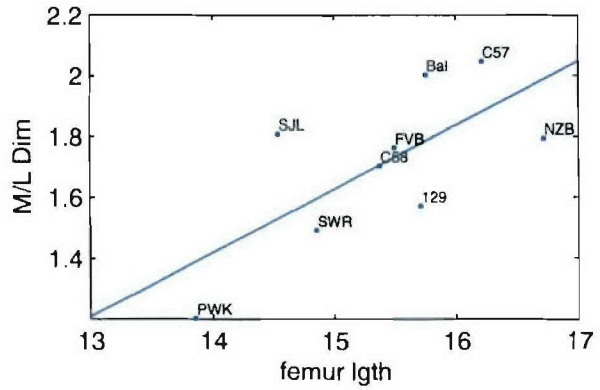
M/L Dim
femur lgth
Bal
C57
SJL
NZB
FVB
C58
129
SWR
PWK

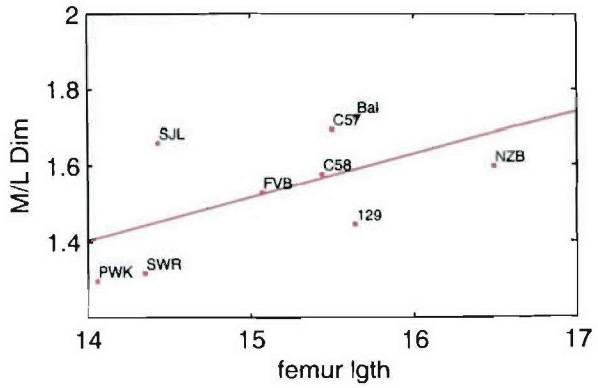
M/L Dim
femur lgth
Bal
SJL
C57
NZB
C58
FVB
129
PWK
SWR

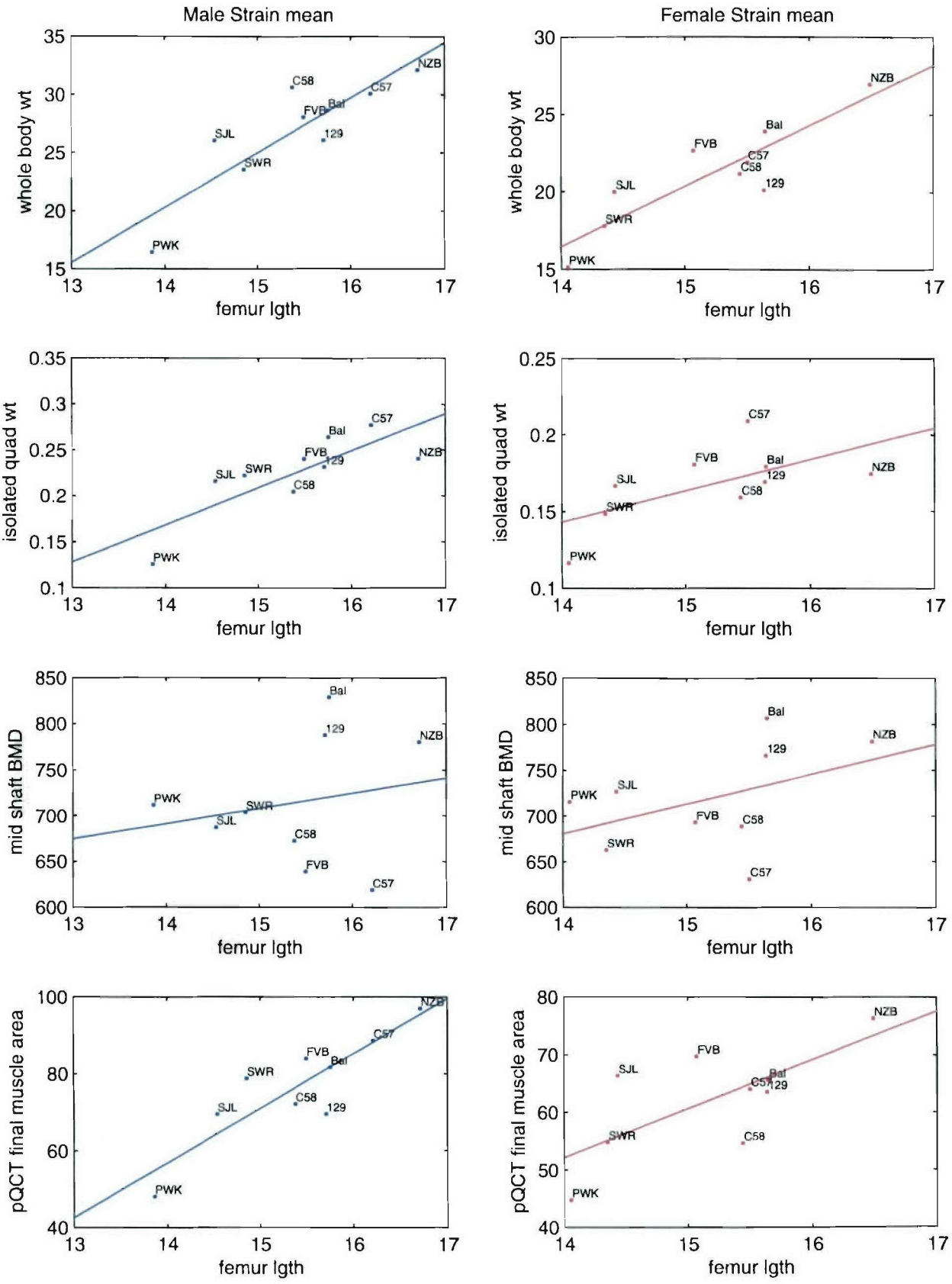
Male Strain mean
Female Strain mean
whole body wt
isolated quad wt
mid shaft BMD
pQCT final muscle area
femur lgth
PWK
SJL
SWR
C58
129
FVB
Bal
C57
NZB

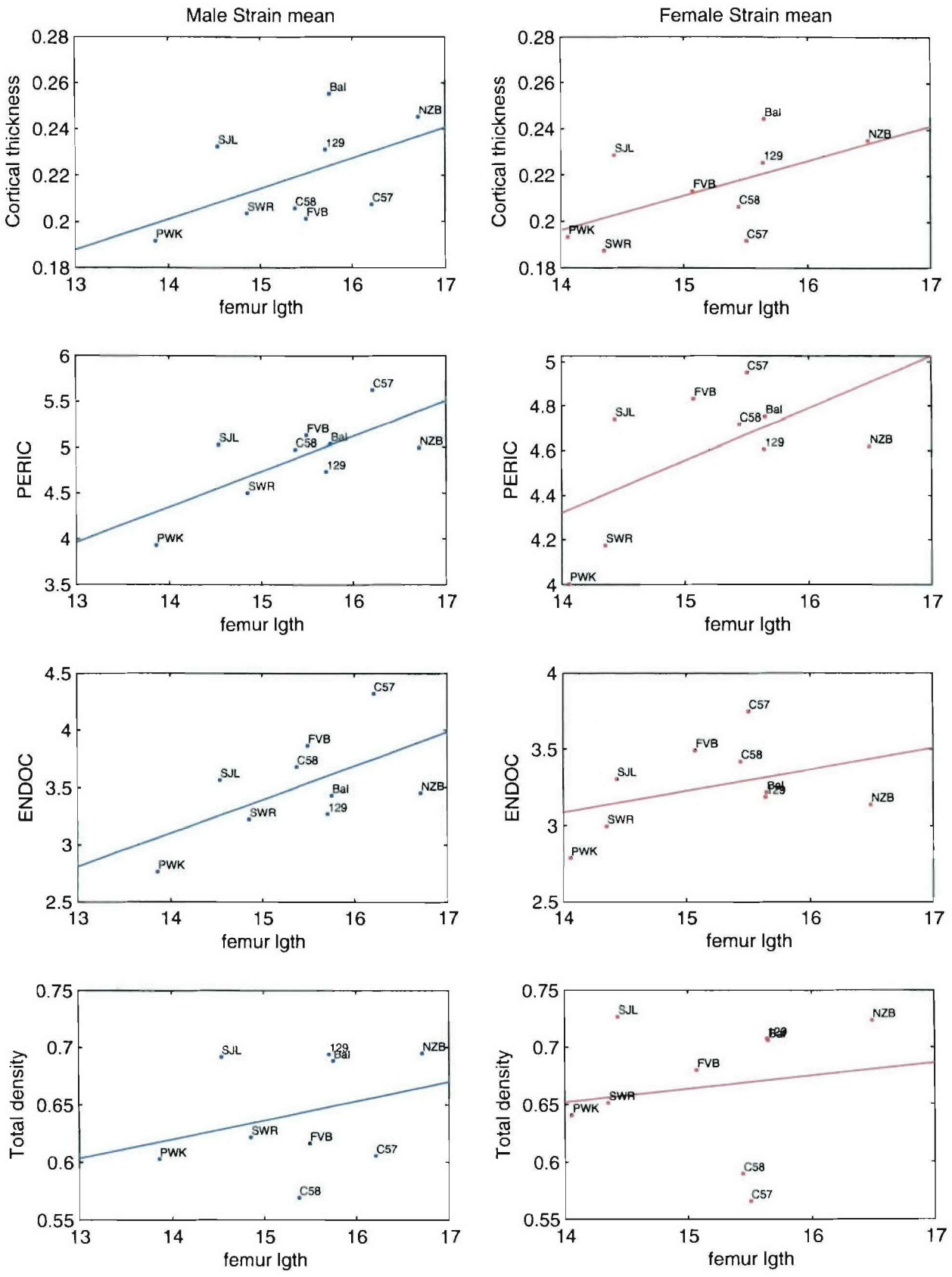
Male Strain mean
Female Strain mean
Cortical thickness
PERIC
ENDOC
Total density
femur lgth
PWK
SWR
SJL
129
Bal
NZB
FVB
C58
C57

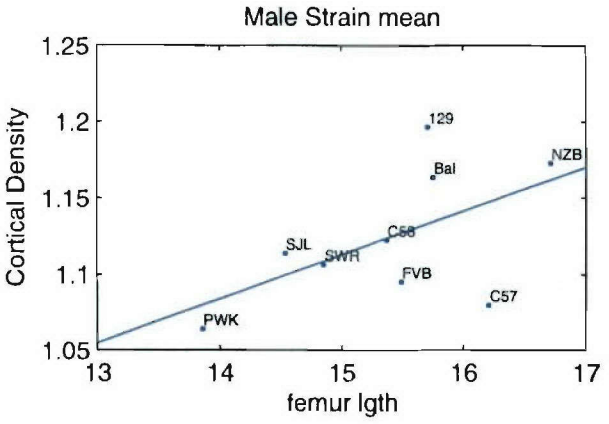
Male Strain mean
Cortical Density
femur lgth
129
Bal
NZB
SJL
SWR
C58
FVB
C57
PWK

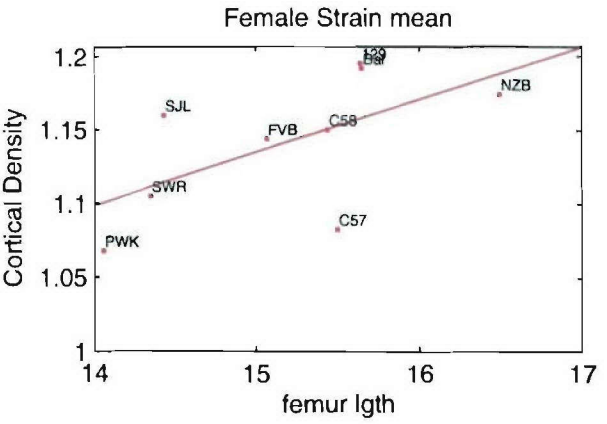
Female Strain mean
Cortical Density
femur lgth
NZB
SJL
FVB
C58
SWR
C57
PWK

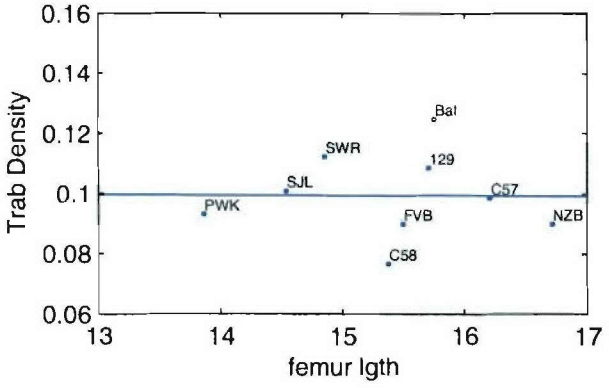
Trab Density
femur lgth
Bal
SWR
129
SJL
C57
PWK
FVB
NZB
C58

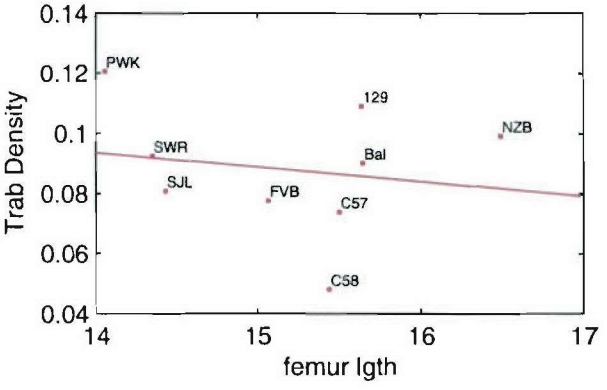
Trab Density
femur lgth
PWK
129
NZB
SWR
Bal
SJL
FVB
C57
C58

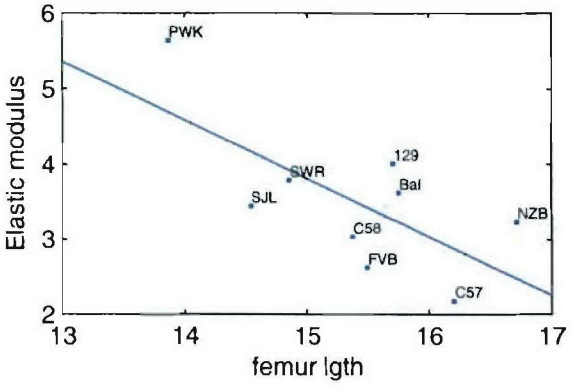
Elastic modulus
femur lgth
PWK
129
SWR
Bal
SJL
NZB
C58
FVB
C57

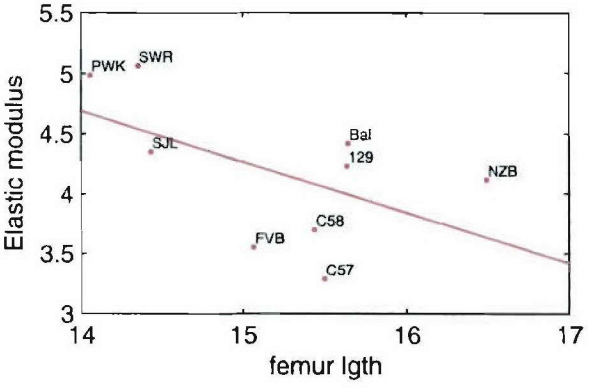
Elastic modulus
femur lgth
PWK
SWR
SJL
Bal
129
NZB
C58
FVB
C57

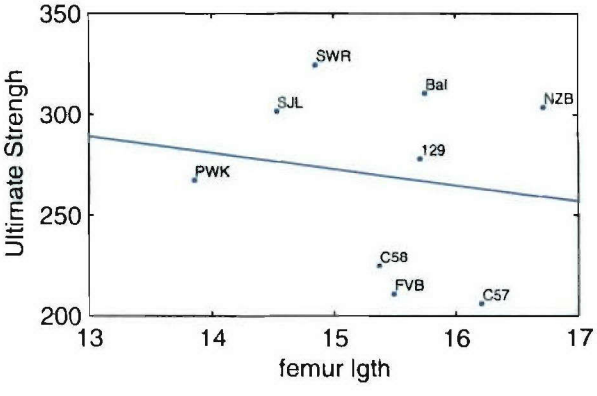
Ultimate Strengh
femur lgth
SWR
Bal
SJL
NZB
129
PWK
C58
FVB
C57

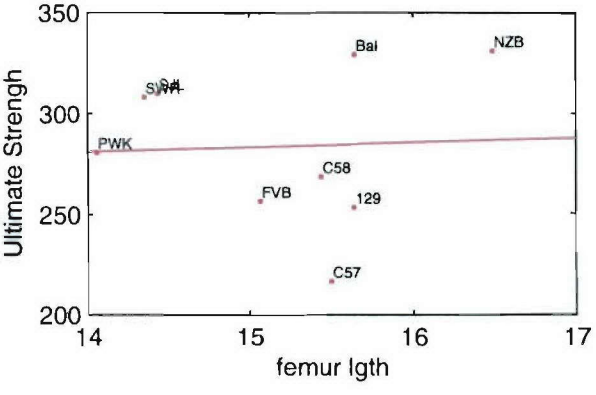
Ultimate Strengh
femur lgth
Bal
NZB
PWK
C58
FVB
129
C57

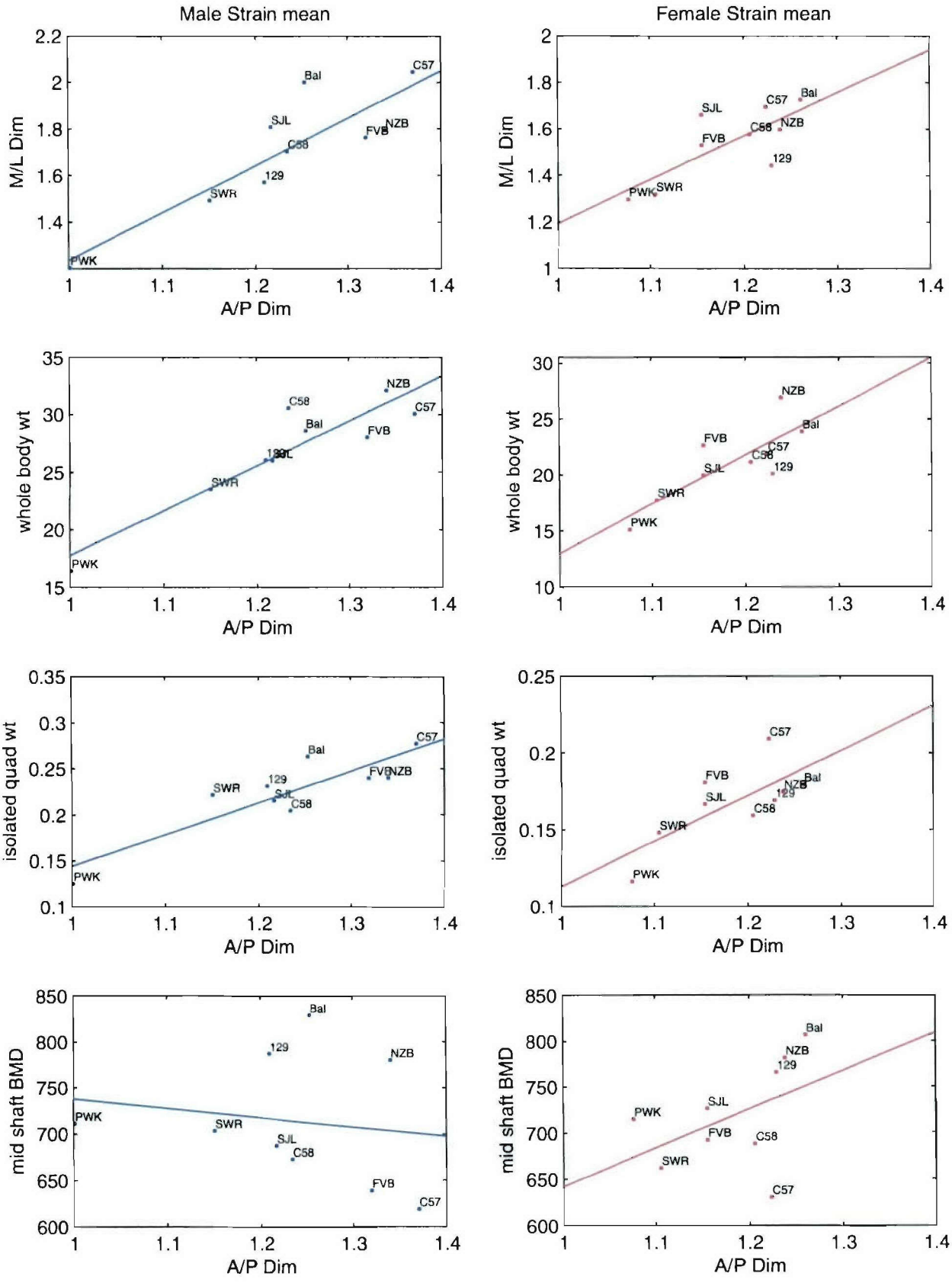
Male Strain mean
Female Strain mean
M/L Dim
A/P Dim
whole body wt
isolated quad wt
mid shaft BMD
PWK
SWR
129
SJL
C58
FVB
NZB
Bal
C57

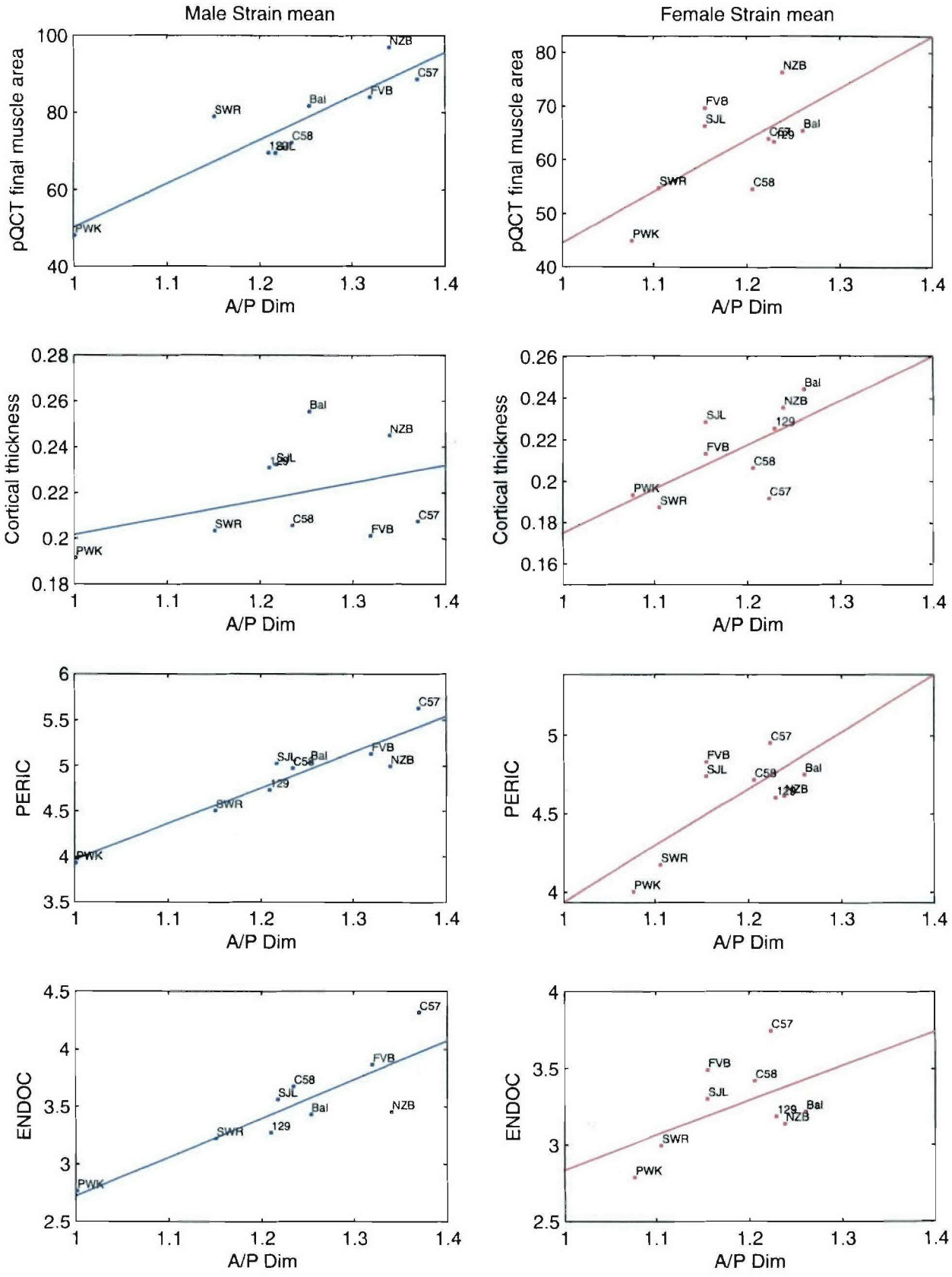
Male Strain mean
Female Strain mean
pQCT final muscle area
Cortical thickness
PERIC
ENDOC
A/P Dim
PWK
SWR
129
SJL
FVB
C57
C58
Bal
NZB

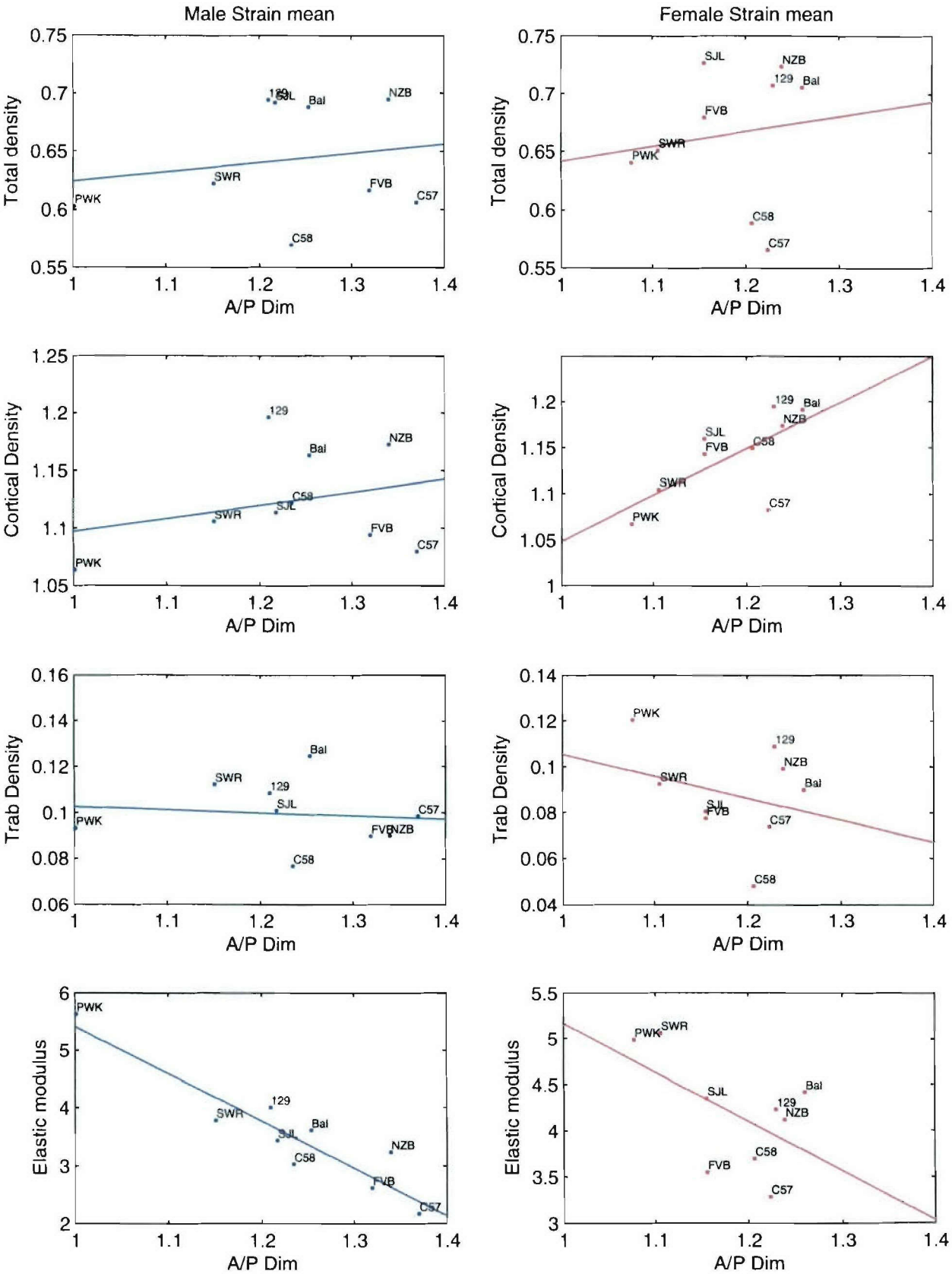
Male Strain mean
Female Strain mean
Total density
Cortical Density
Trab Density
Elastic modulus
A/P Dim
PWK
SWR
129
SJL
Bal
NZB
FVB
C57
C58

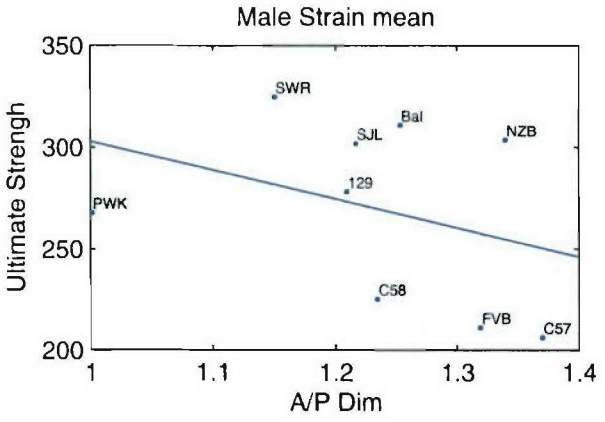
Male Strain mean
Ultimate Strengh
A/P Dim
SWR
Bal
SJL
NZB
129
PWK
C58
FVB
C57

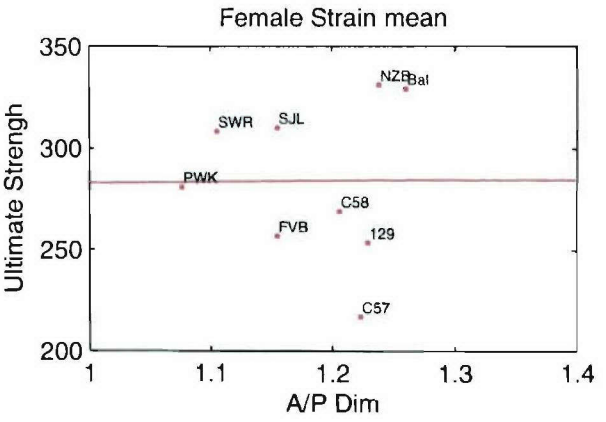
Female Strain mean
Ultimate Strengh
A/P Dim
NZB
Bal
SWR
SJL
PWK
C58
FVB
129
C57

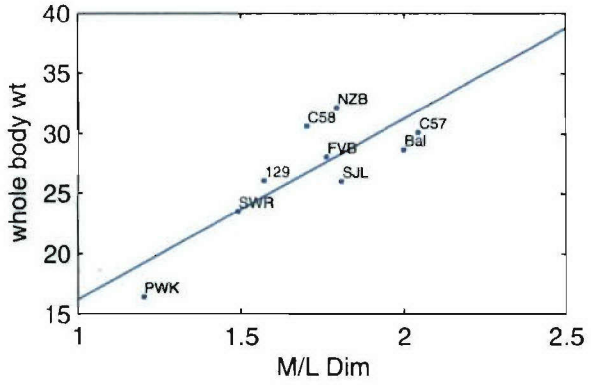
whole body wt
M/L Dim
NZB
C58
C57
FVB
Bal
129
SJL
SWR
PWK

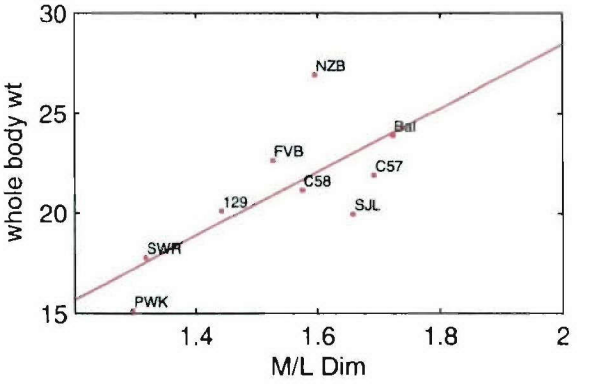
whole body wt
M/L Dim
NZB
Bal
FVB
C57
C58
129
SJL
SWR
PWK

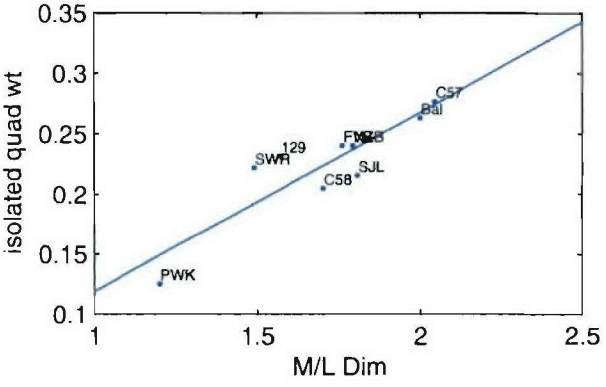
isolated quad wt
M/L Dim
C57
Bal
129
SWR
SJL
C58
PWK

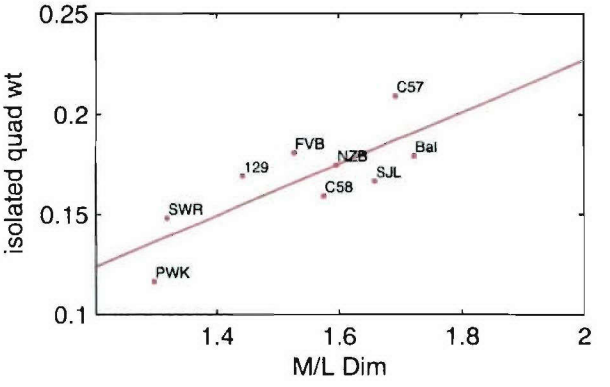
isolated quad wt
M/L Dim
C57
FVB
Bal
NZB
129
SJL
C58
SWR
PWK

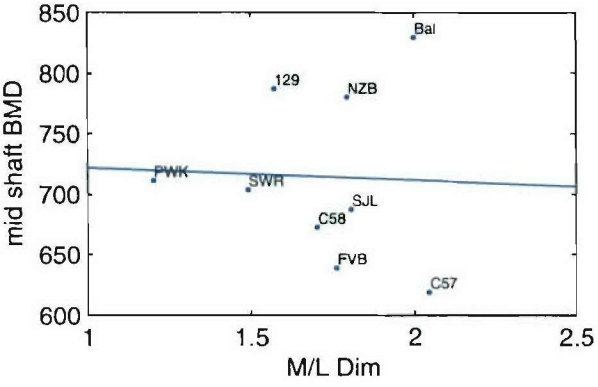
mid shaft BMD
M/L Dim
Bal
129
NZB
PWK
SWR
SJL
C58
FVB
C57

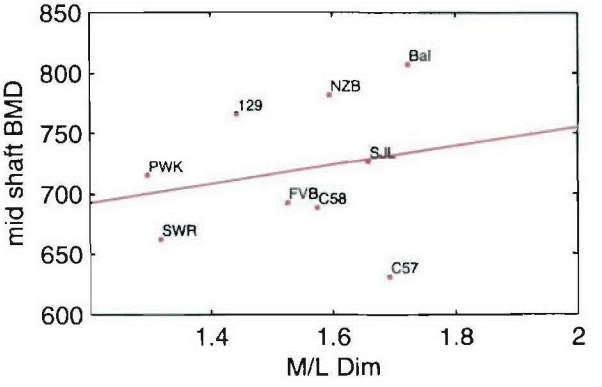
mid shaft BMD
M/L Dim
Bal
NZB
129
SJL
PWK
FVB
C58
SWR
C57

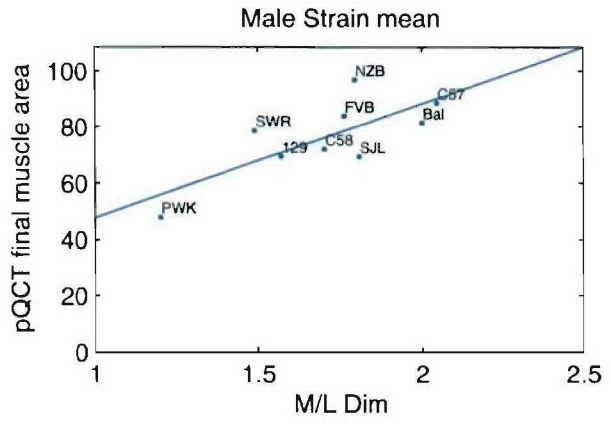
Male Strain mean
pQCT final muscle area
M/L Dim
NZB
C57
FVB
SWR
Bal
129
C58
SJL
PWK

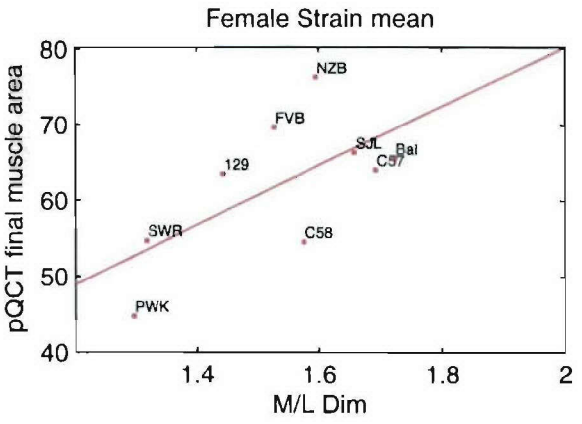
Female Strain mean
pQCT final muscle area
M/L Dim
NZB
FVB
SJL
Bal
C57
129
SWR
C58
PWK

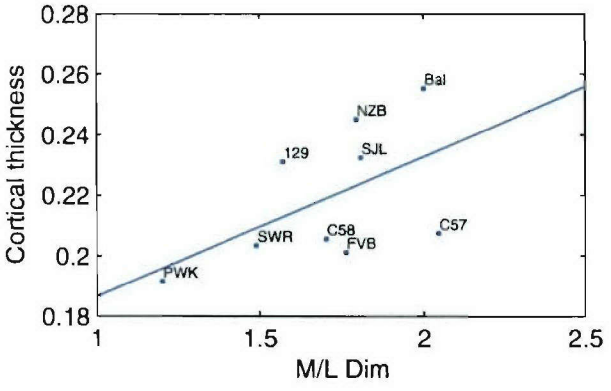
Cortical thickness
M/L Dim
Bal
NZB
129
SJL
C57
SWR
C58
FVB
PWK

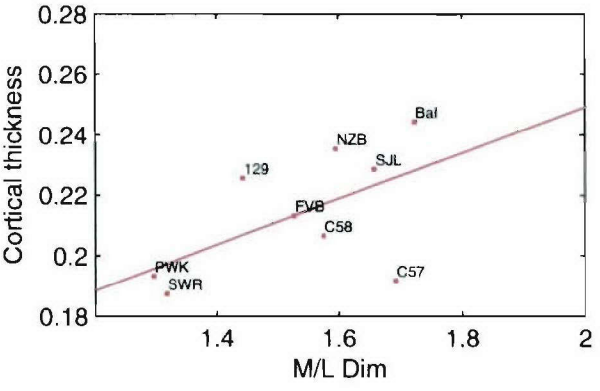
Cortical thickness
M/L Dim
Bal
NZB
SJL
129
FVB
C58
PWK
C57
SWR

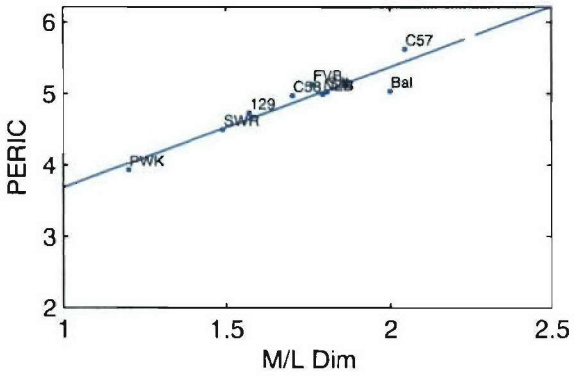
PERIC
M/L Dim
C57
FVB
Bal
129
SWR
PWK

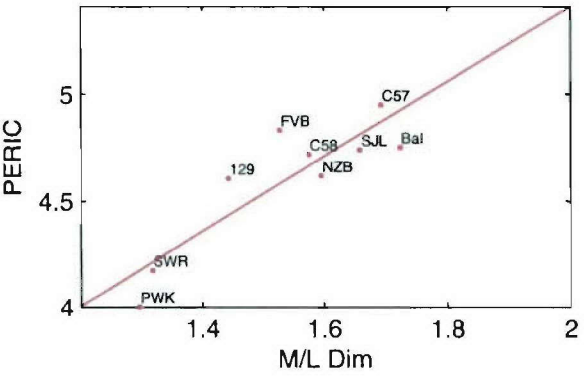
PERIC
M/L Dim
C57
FVB
C58
SJL
Bal
129
NZB
SWR
PWK

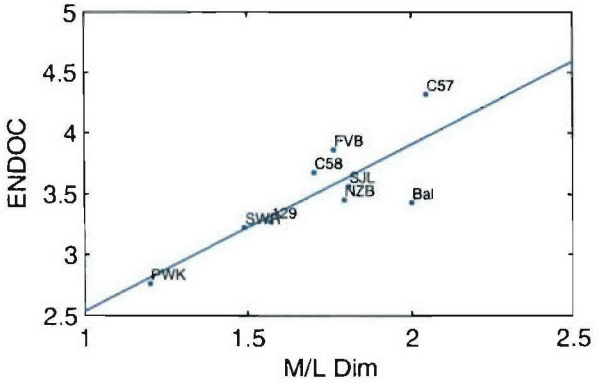
ENDOC
M/L Dim
C57
FVB
C58
SJL
NZB
Bal
SWR
129
PWK

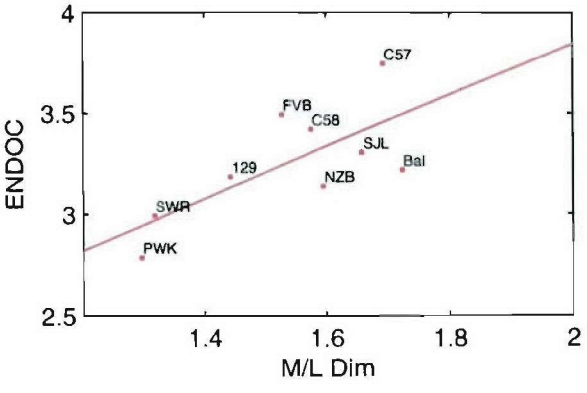
ENDOC
M/L Dim
C57
FVB
C58
SJL
129
Bal
NZB
SWR
PWK

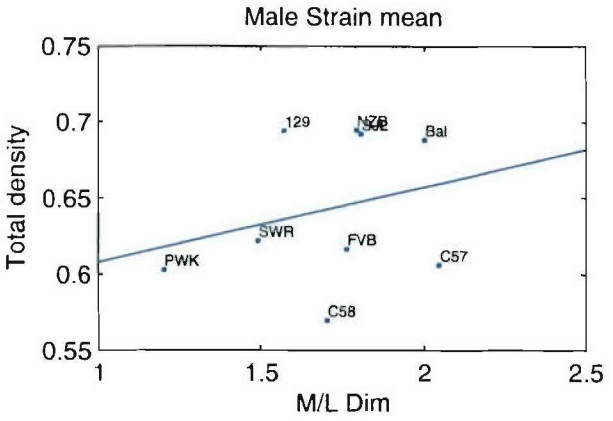
Male Strain mean
Total density
M/L Dim
129
NZB
SJL
Bal
SWR
FVB
PWK
C57
C58

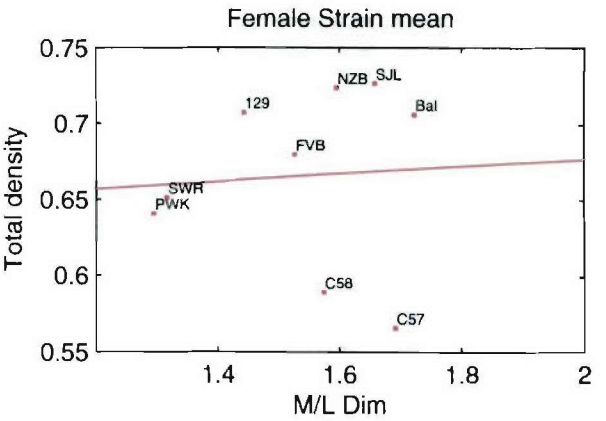
Female Strain mean
Total density
M/L Dim
NZB
SJL
129
Bal
FVB
SWR
PWK
C58
C57

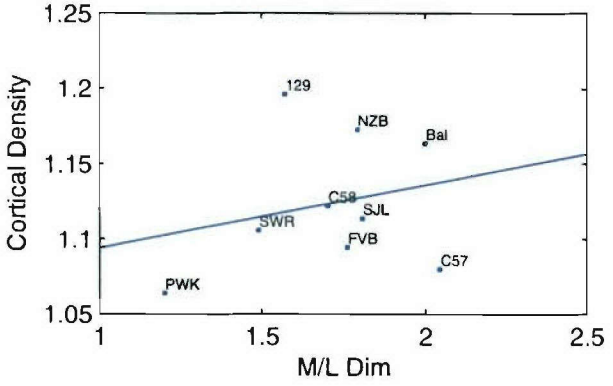
Cortical Density
M/L Dim
129
NZB
Bal
C58
SJL
SWR
FVB
C57
PWK

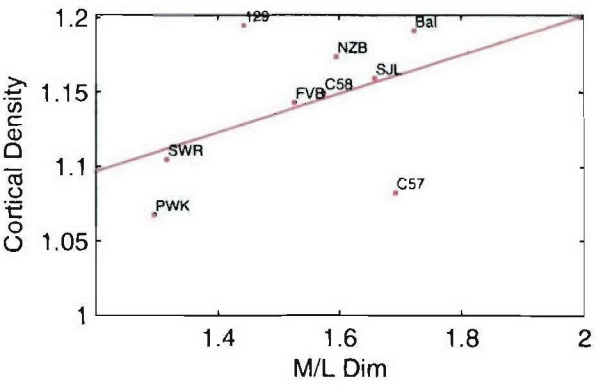
Cortical Density
M/L Dim
129
Bal
NZB
SJL
FVB
C58
SWR
C57
PWK

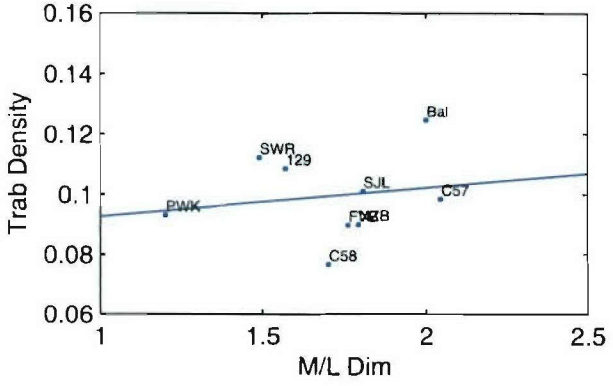
Trab Density
M/L Dim
Bal
SWR
129
SJL
C57
PWK
C58

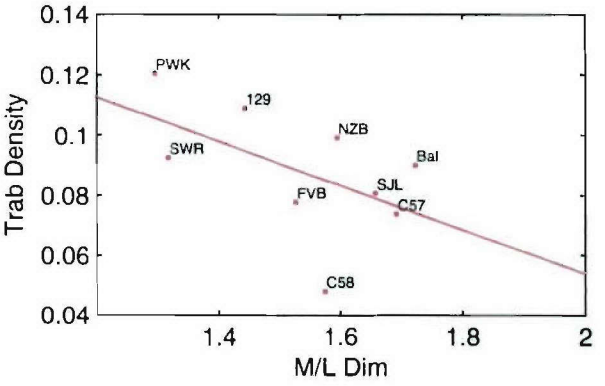
Trab Density
M/L Dim
PWK
129
NZB
SWR
Bal
SJL
FVB
C57
C58

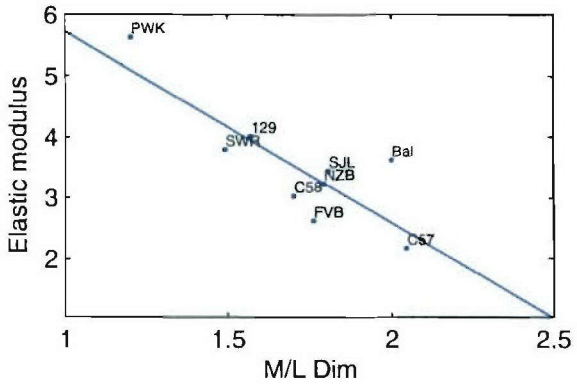
Elastic modulus
M/L Dim
PWK
129
SWR
Bal
SJL
NZB
C58
FVB
C57

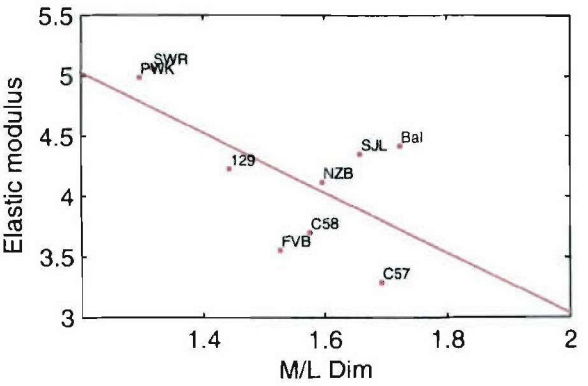
Elastic modulus
M/L Dim
SWR
PWK
SJL
Bal
129
NZB
C58
FVB
C57

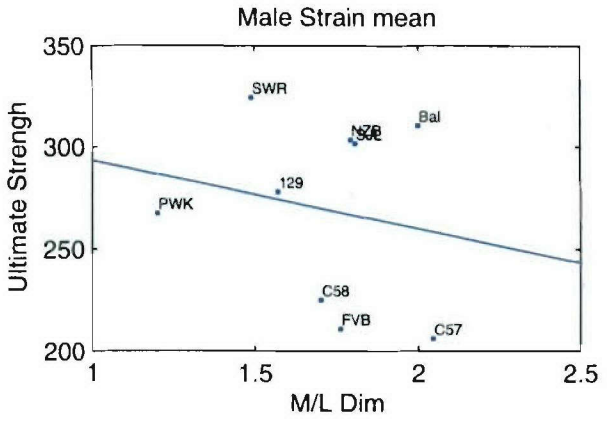
Male Strain mean
Ultimate Strengh
M/L Dim
SWR
Bal
NZB
129
PWK
C58
FVB
C57

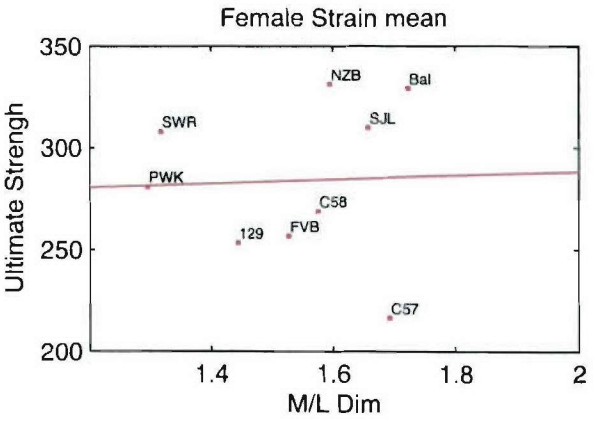
Female Strain mean
Ultimate Strengh
M/L Dim
NZB
Bal
SWR
SJL
PWK
C58
129
FVB
C57

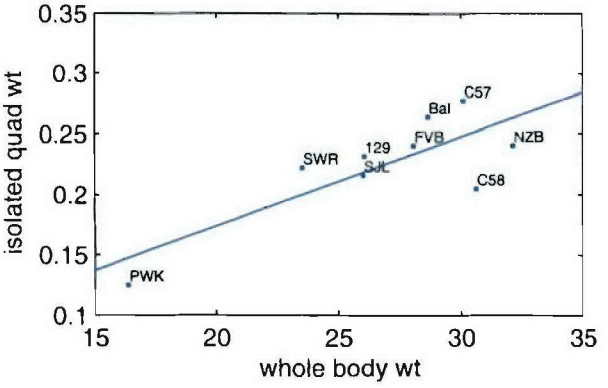
isolated quad wt
whole body wt
C57
Bal
FVB
NZB
SWR
129
SJL
C58
PWK

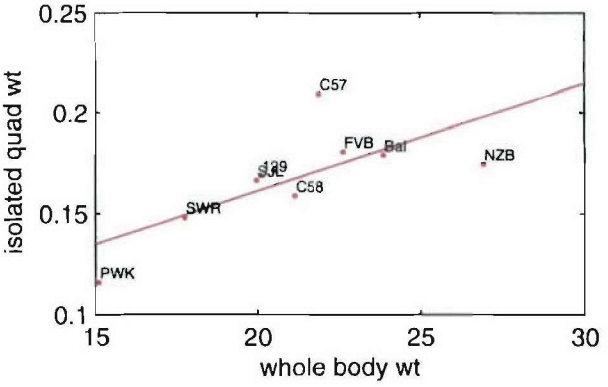
isolated quad wt
whole body wt
C57
FVB
Bal
NZB
SJL
C58
SWR
PWK

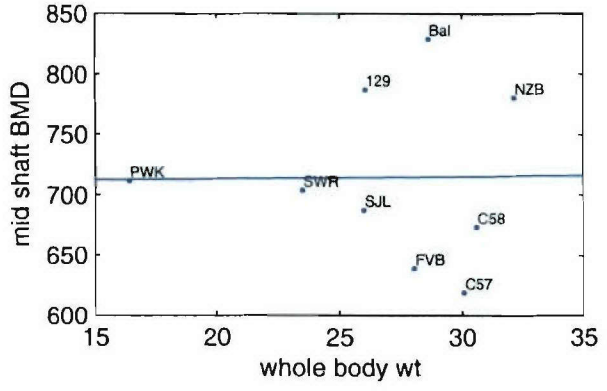
mid shaft BMD
whole body wt
Bal
129
NZB
PWK
SWR
SJL
C58
FVB
C57

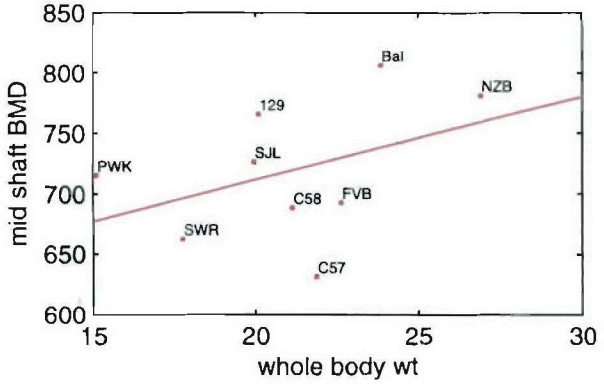
mid shaft BMD
whole body wt
Bal
NZB
129
SJL
PWK
C58
FVB
SWR
C57

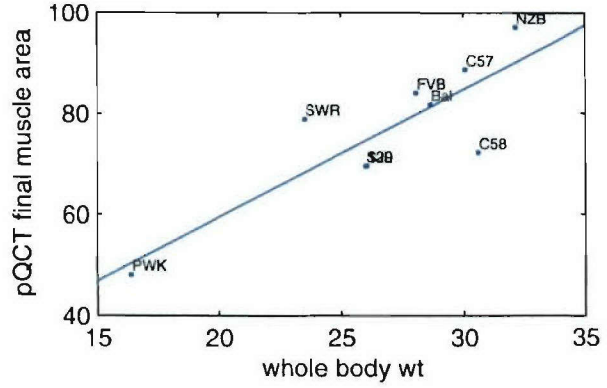
pQCT final muscle area
whole body wt
NZB
C57
FVB
Bal
SWR
C58
PWK

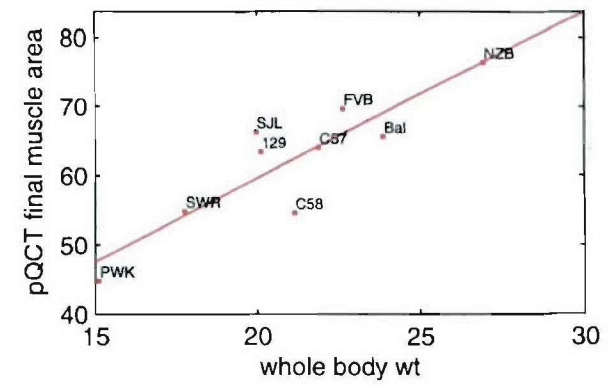
pQCT final muscle area
whole body wt
NZB
FVB
SJL
129
Bal
SWR
C58
PWK

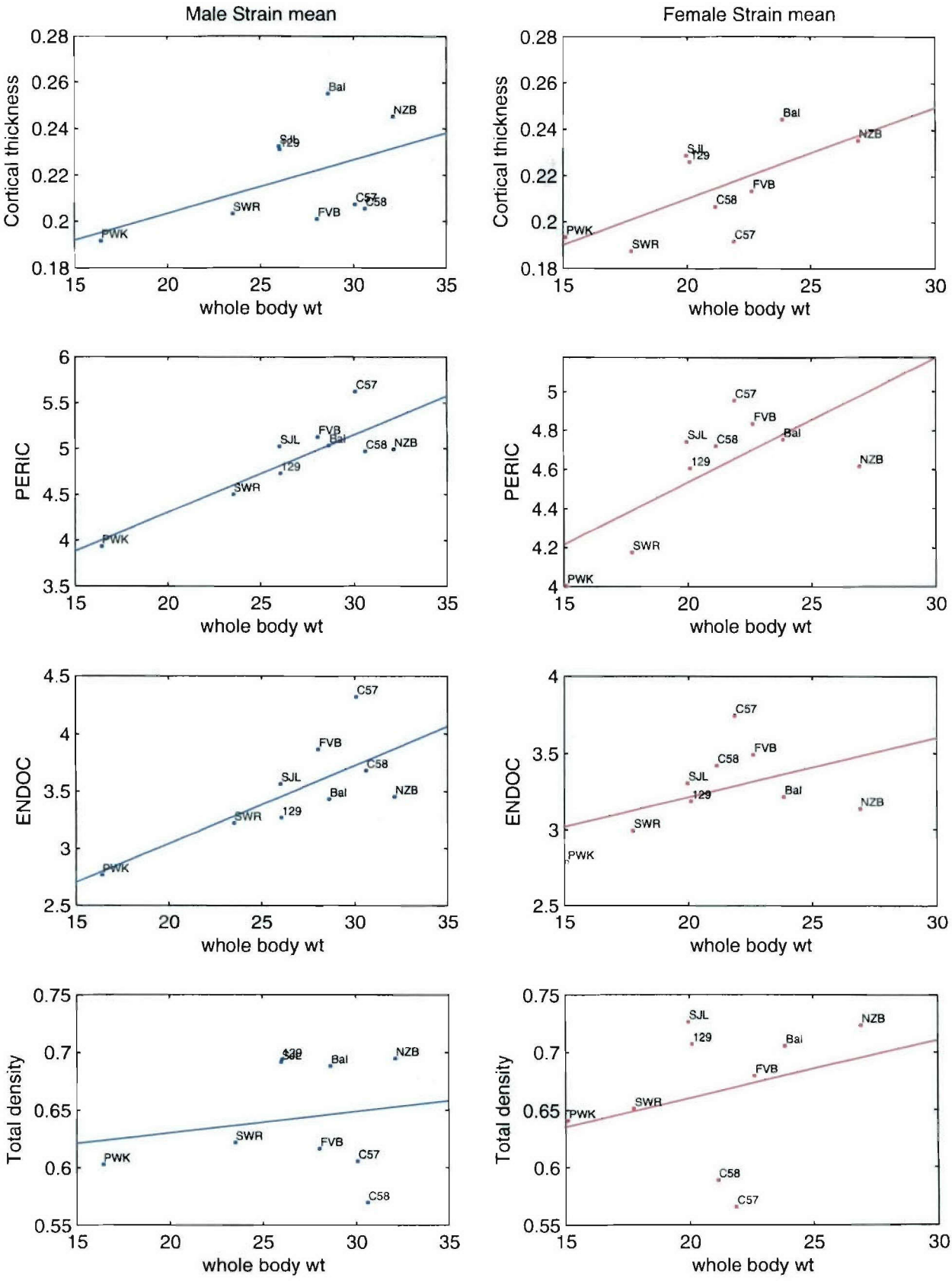
Male Strain mean
Female Strain mean
Cortical thickness
PERIC
ENDOC
Total density
whole body wt
PWK
SWR
FVB
C57
C58
SJL
129
Bal
NZB

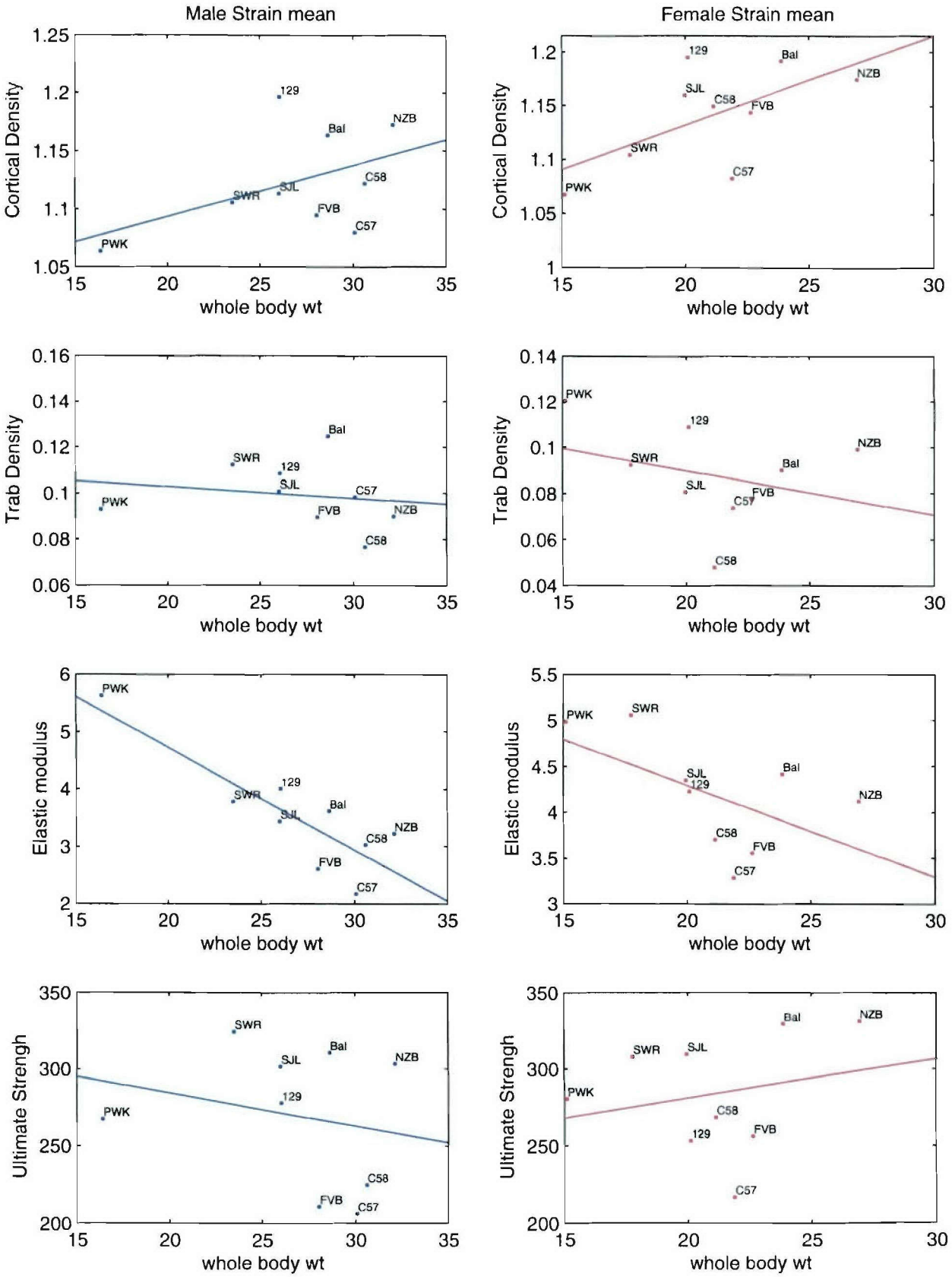
Male Strain mean
Female Strain mean
Cortical Density
Trab Density
Elastic modulus
Ultimate Strengh
whole body wt
PWK
SWR
129
SJL
Bal
C57
C58
FVB
NZB

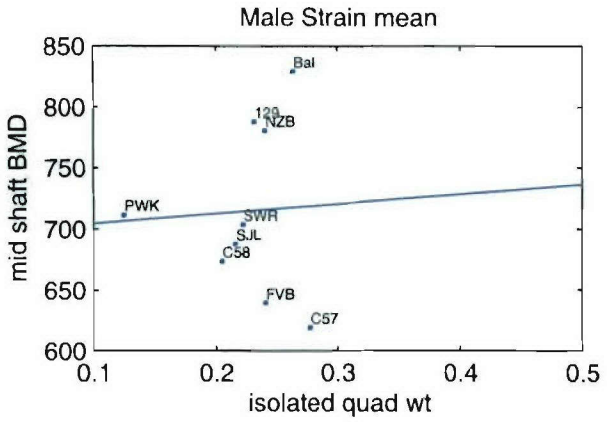
Male Strain mean
mid shaft BMD
isolated quad wt
Bal
129
NZB
PWK
SWR
SJL
C58
FVB
C57

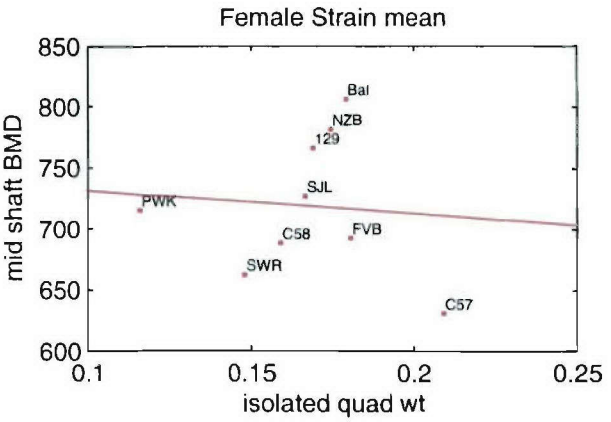
Female Strain mean
mid shaft BMD
isolated quad wt
Bal
NZB
129
SJL
PWK
C58
FVB
SWR
C57

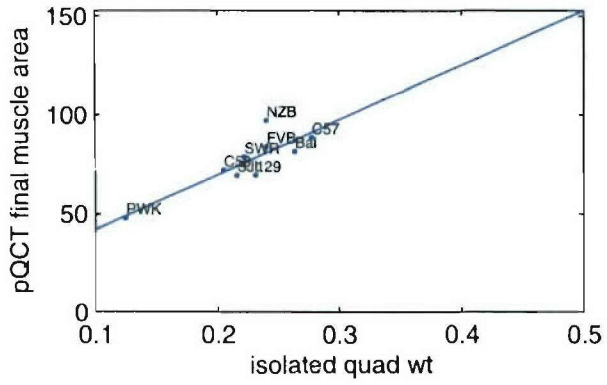
pQCT final muscle area
isolated quad wt
NZB
C57
FVB
Bal
SWR
C58
SJL
129
PWK

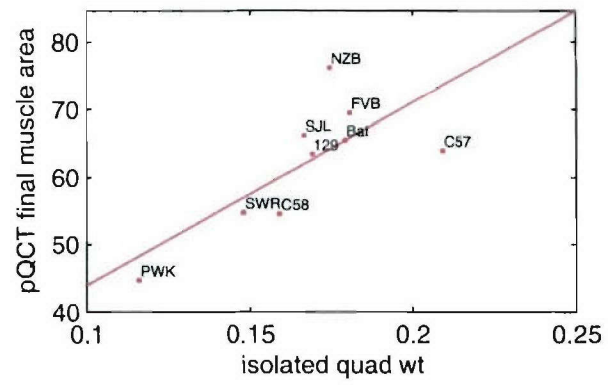
pQCT final muscle area
isolated quad wt
NZB
FVB
SJL
Bal
129
C57
SWR
C58
PWK

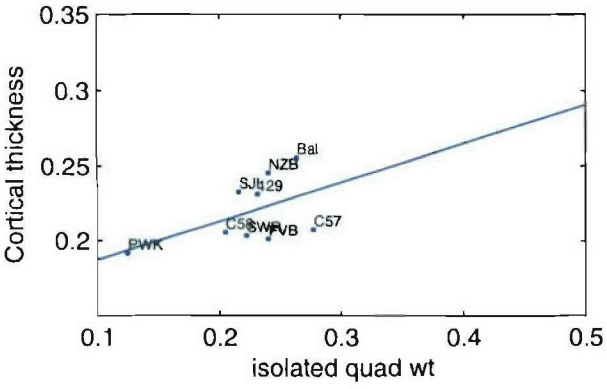
Cortical thickness
isolated quad wt
Bal
NZB
SJL
129
C58
SWR
FVB
C57
PWK

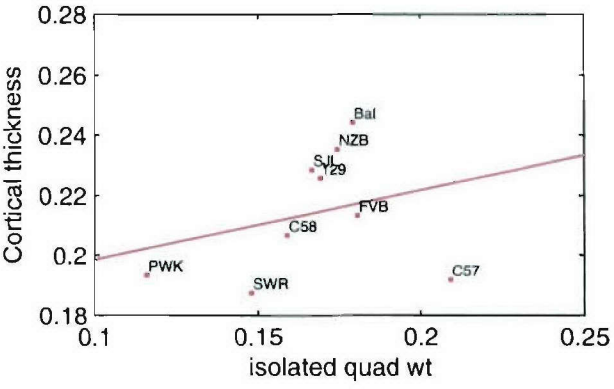
Cortical thickness
isolated quad wt
Bal
NZB
SJL
129
FVB
C58
PWK
C57
SWR

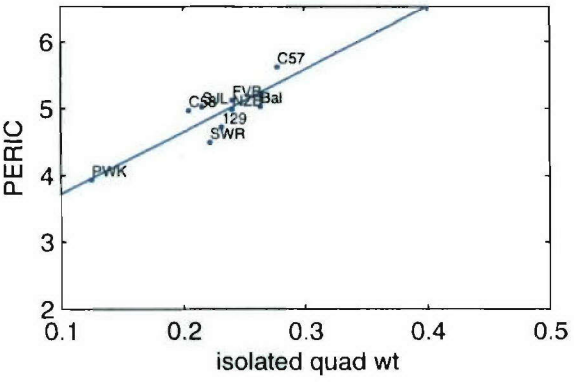
PERIC
isolated quad wt
C57
C58
SJL
FVB
Bal
129
SWR
PWK

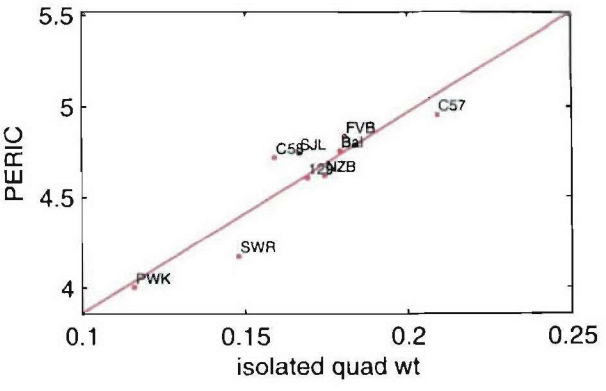
PERIC
isolated quad wt
C57
FVB
C58
SJL
Bal
129
NZB
SWR
PWK

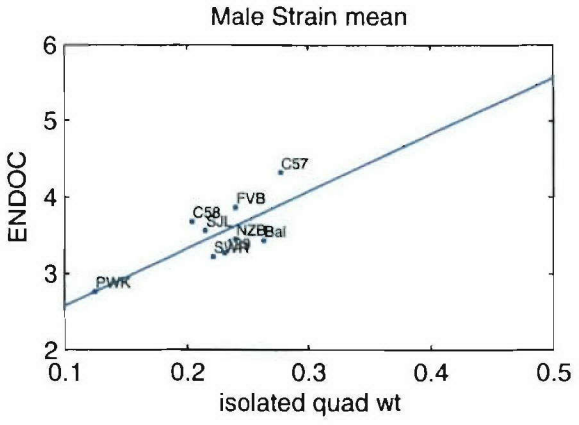
Male Strain mean
ENDOC
isolated quad wt
PWK
C58
C57
FVB
SJL
NZB
Bal
SWR
129

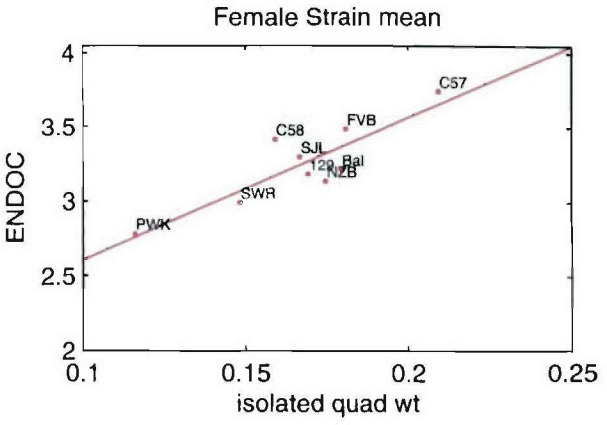
Female Strain mean
ENDOC
isolated quad wt
C57
C58
FVB
SJL
129
Bal
NZB
SWR
PWK

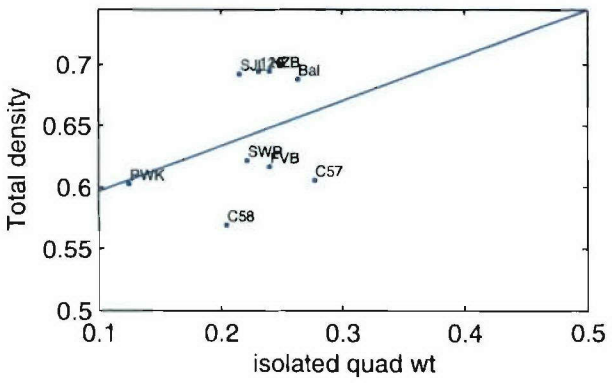
Total density
isolated quad wt
SJL
NZB
Bal
SWR
FVB
PWK
C57
C58

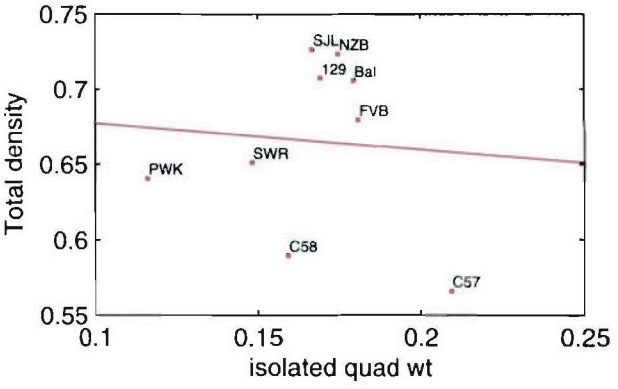
Total density
isolated quad wt
SJL
NZB
129
Bal
FVB
SWR
PWK
C58
C57

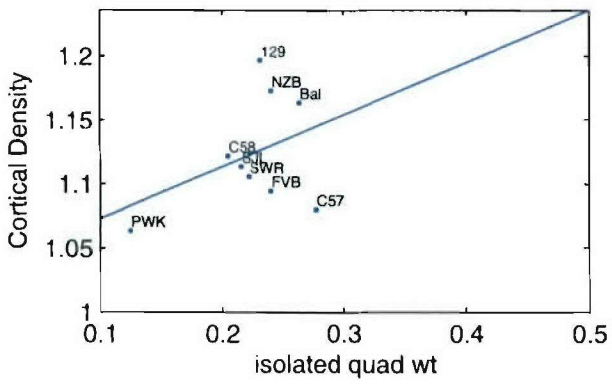
Cortical Density
isolated quad wt
129
NZB
Bal
C58
SJL
SWR
FVB
C57
PWK

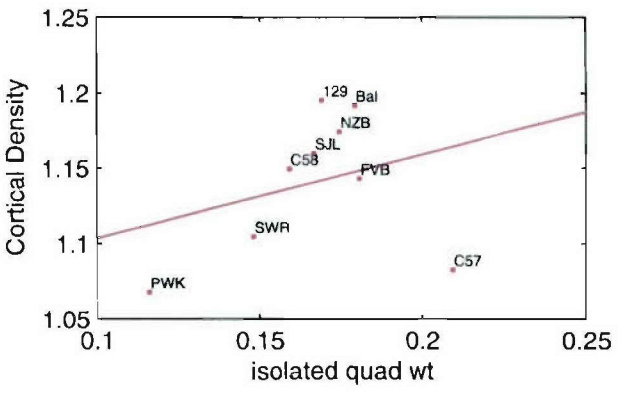
Cortical Density
isolated quad wt
129
Bal
NZB
SJL
C58
FVB
SWR
C57
PWK

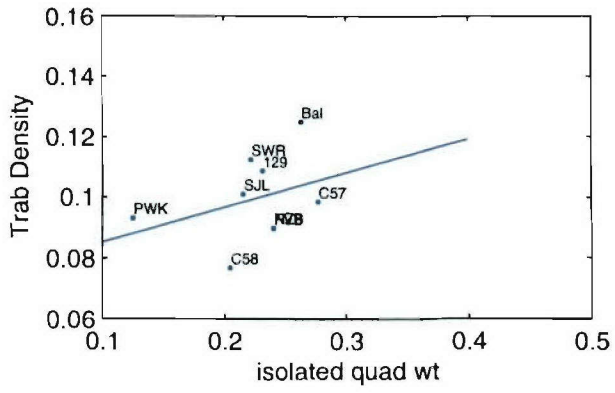
Trab Density
isolated quad wt
Bal
SWR
129
SJL
C57
PWK
NZB
C58

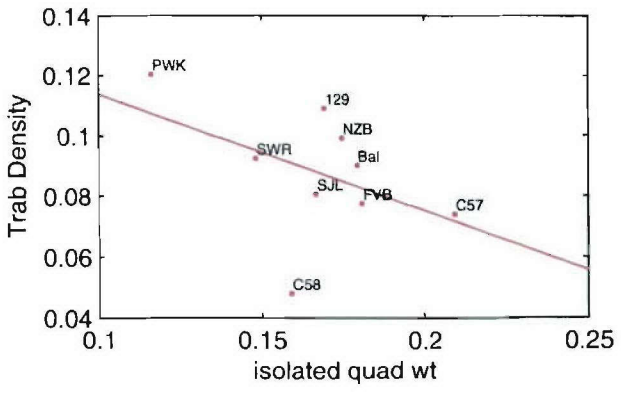
Trab Density
isolated quad wt
PWK
129
NZB
SWR
Bal
SJL
FVB
C57
C58

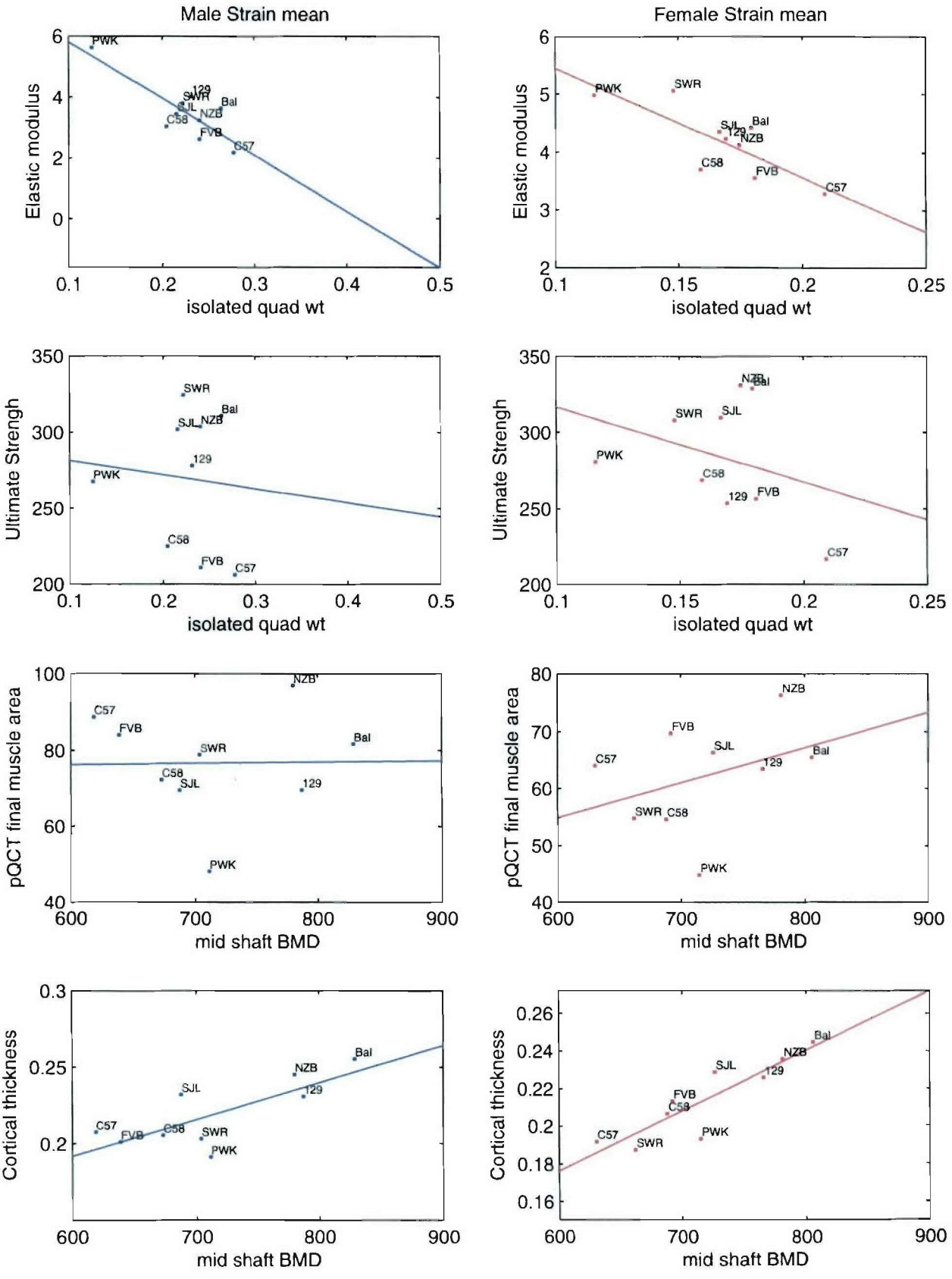
Male Strain mean
Female Strain mean
Elastic modulus
isolated quad wt
Ultimate Strengh
pQCT final muscle area
mid shaft BMD
Cortical thickness
PWK
SWR
129
Bal
SJL
NZB
C58
FVB
C57

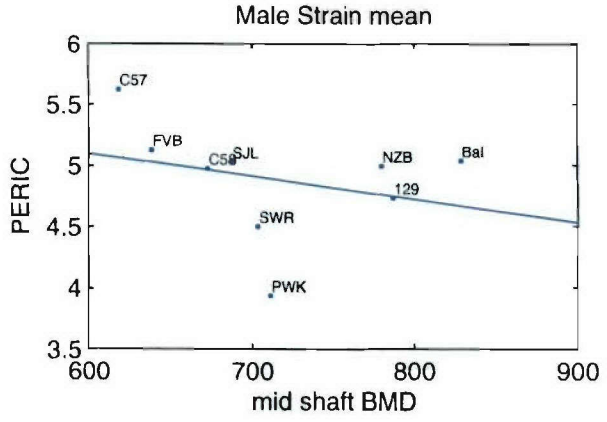
Male Strain mean
PERIC
mid shaft BMD
C57
FVB
C58
SJL
NZB
Bal
129
SWR
PWK

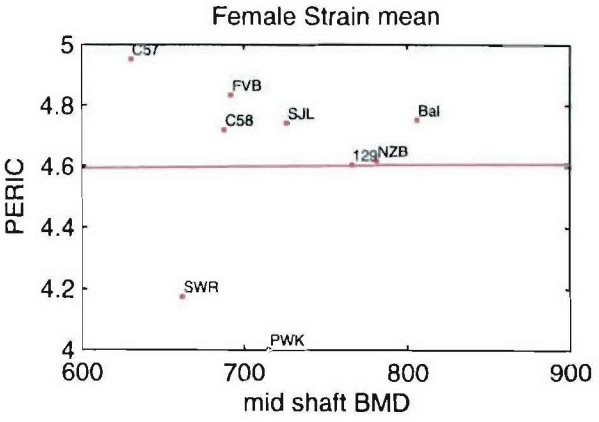
Female Strain mean
PERIC
mid shaft BMD
C57
FVB
C58
SJL
Bal
129
NZB
SWR
PWK

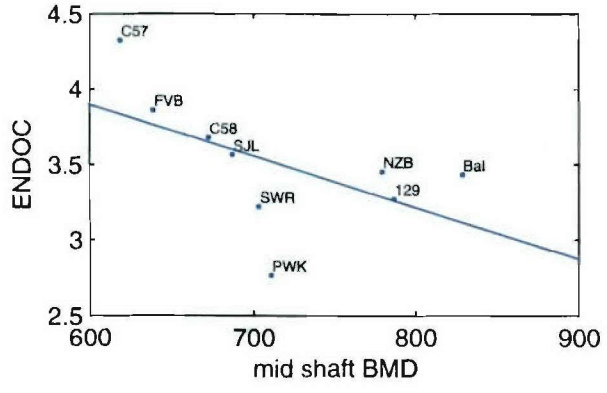
ENDOC
mid shaft BMD
C57
FVB
C58
SJL
NZB
Bal
129
SWR
PWK

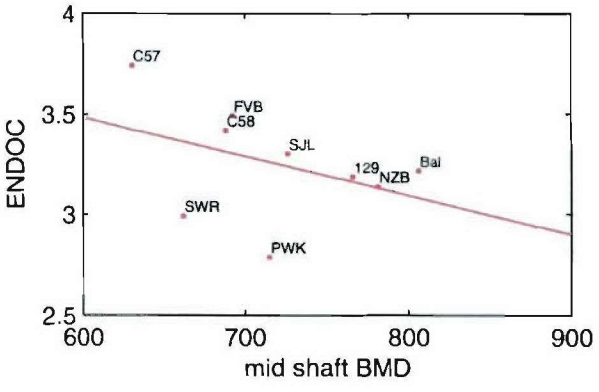
ENDOC
mid shaft BMD
C57
FVB
C58
SJL
129
NZB
Bal
SWR
PWK

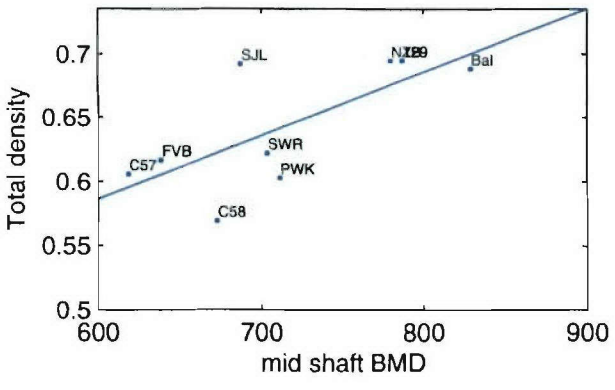
Total density
mid shaft BMD
SJL
NZB
129
Bal
FVB
C57
SWR
PWK
C58

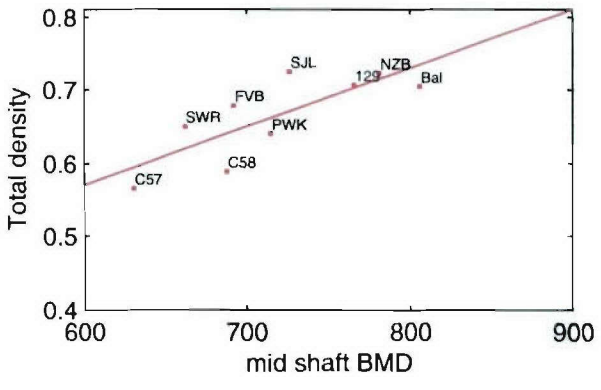
Total density
mid shaft BMD
SJL
NZB
129
Bal
FVB
SWR
PWK
C58
C57

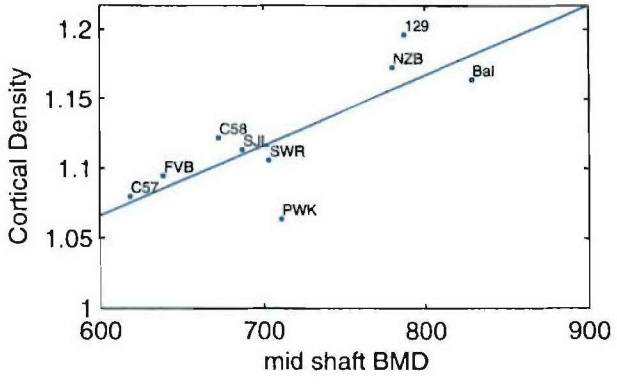
Cortical Density
mid shaft BMD
129
NZB
Bal
C58
SJL
SWR
FVB
C57
PWK

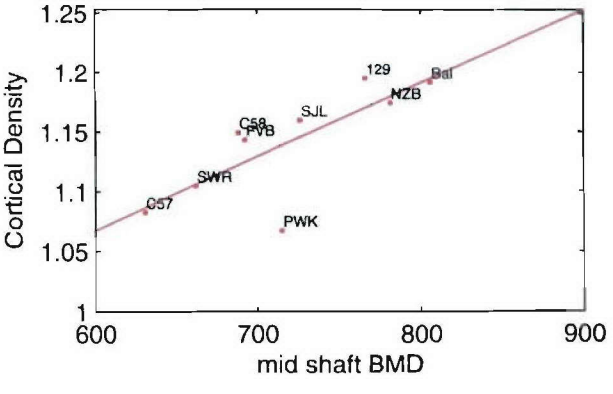
Cortical Density
mid shaft BMD
129
Bal
NZB
SJL
C58
FVB
SWR
C57
PWK

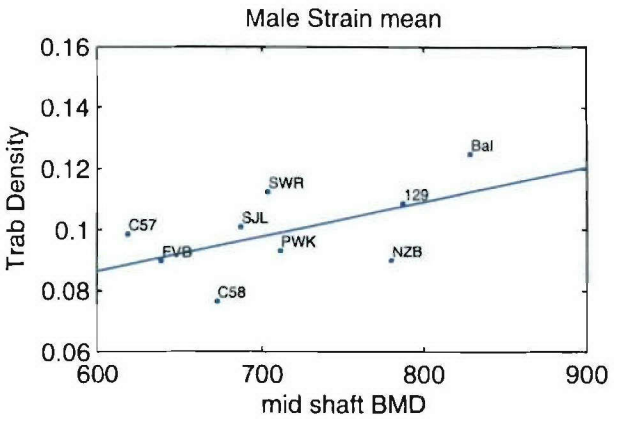
Male Strain mean
Trab Density
mid shaft BMD
0.16
0.14
0.12
0.1
0.08
0.06
600
700
800
900
Bal
SWR
129
C57
SJL
FVB
PWK
NZB
C58

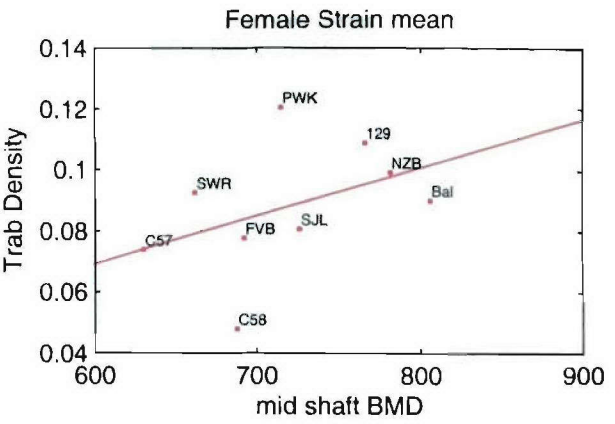
Female Strain mean
Trab Density
mid shaft BMD
0.14
0.12
0.1
0.08
0.06
0.04
600
700
800
900
PWK
129
NZB
SWR
Bal
C57
FVB
SJL
C58

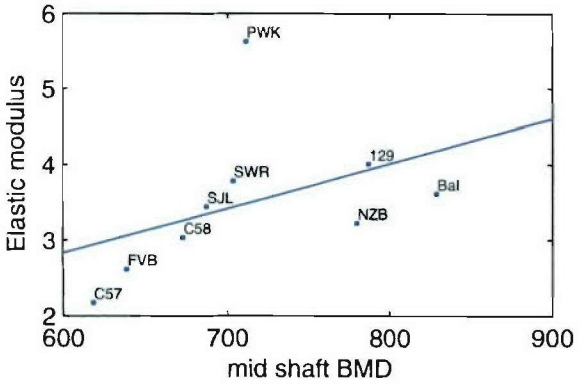
Elastic modulus
mid shaft BMD
6
5
4
3
2
600
700
800
900
PWK
129
SWR
Bal
SJL
NZB
C58
FVB
C57

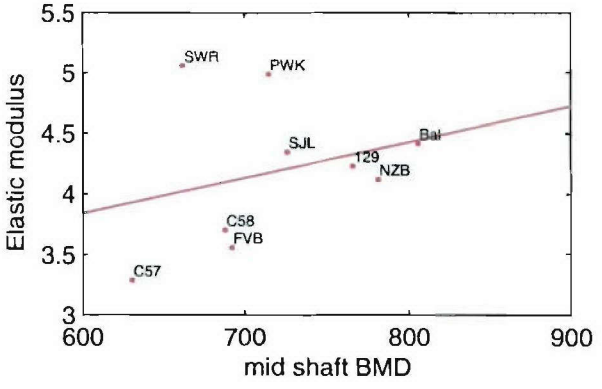
Elastic modulus
mid shaft BMD
5.5
5
4.5
4
3.5
3
600
700
800
900
SWR
PWK
SJL
Bal
129
NZB
C58
FVB
C57

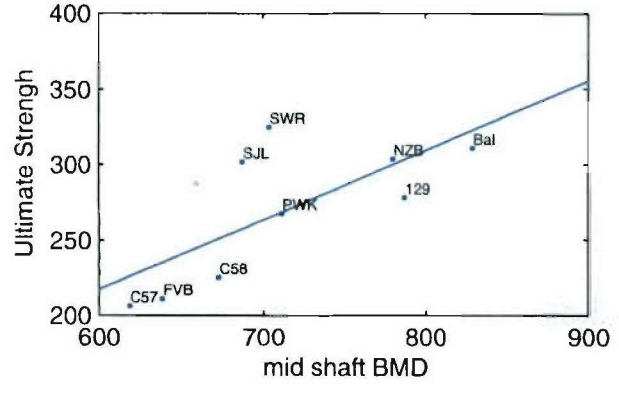
Ultimate Strengh
mid shaft BMD
400
350
300
250
200
600
700
800
900
SWR
SJL
NZB
Bal
PWK
129
C58
C57
FVB

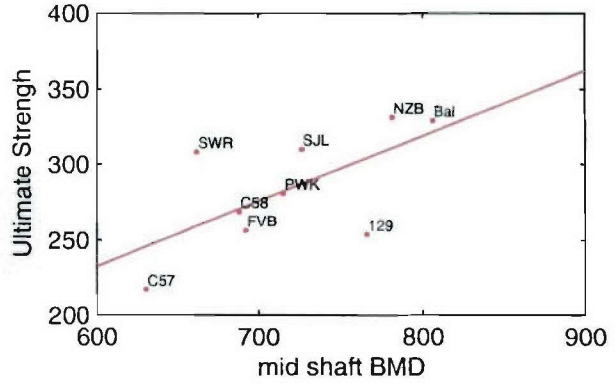
Ultimate Strengh
mid shaft BMD
400
350
300
250
200
600
700
800
900
NZB
Bal
SWR
SJL
PWK
C58
FVB
129
C57

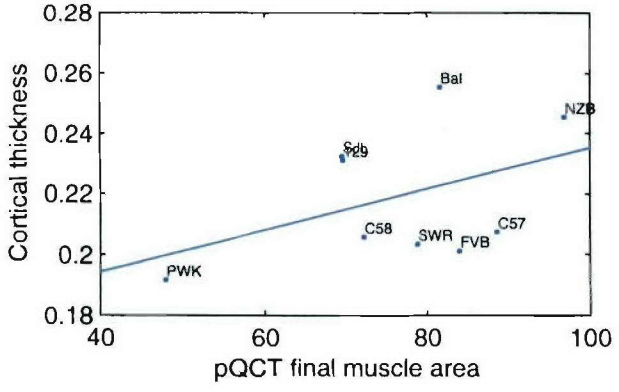
Cortical thickness
pQCT final muscle area
0.28
0.26
0.24
0.22
0.2
0.18
40
60
80
100
Bal
NZB
129
C58
SWR
C57
FVB
PWK

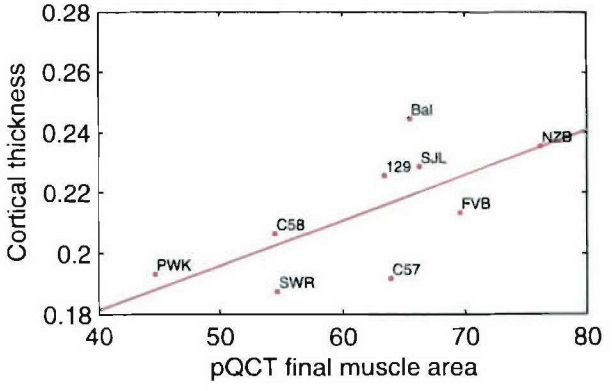
Cortical thickness
pQCT final muscle area
0.28
0.26
0.24
0.22
0.2
0.18
40
50
60
70
80
Bal
NZB
129
SJL
FVB
C58
PWK
C57
SWR

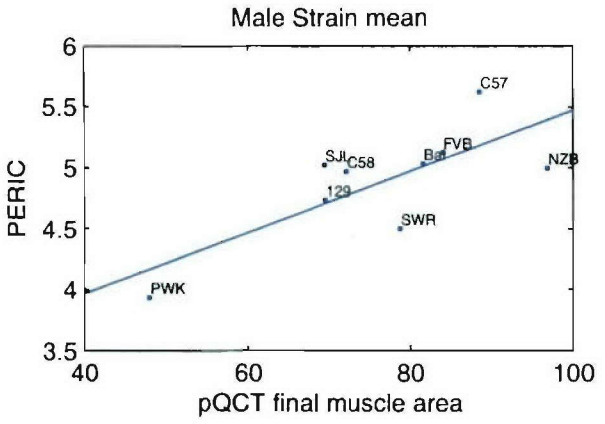
Male Strain mean
PERIC
pQCT final muscle area
C57
SJL
C58
Bal
FVB
NZB
129
SWR
PWK

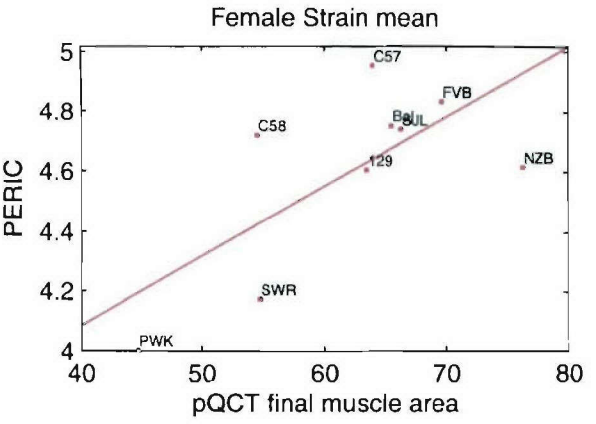
Female Strain mean
PERIC
pQCT final muscle area
C57
FVB
C58
Bal
SJL
129
NZB
SWR
PWK

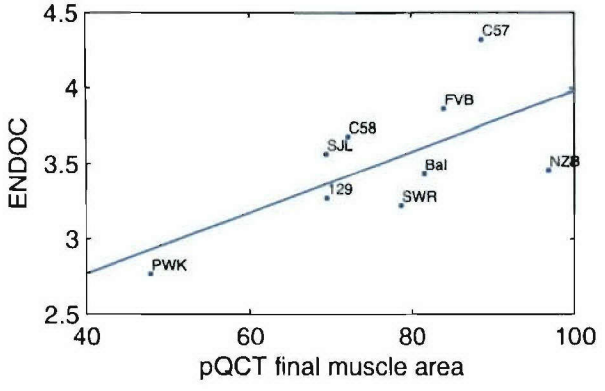
ENDOC
pQCT final muscle area
C57
FVB
C58
SJL
Bal
NZB
129
SWR
PWK

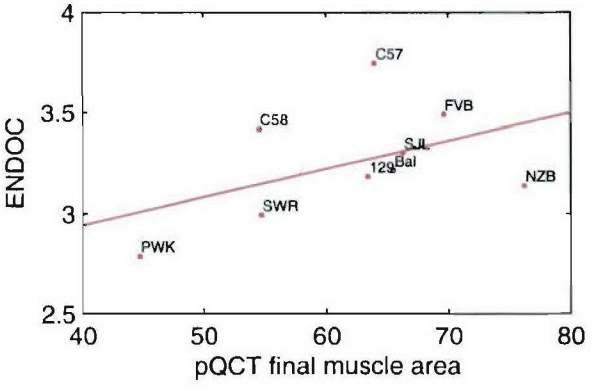
ENDOC
pQCT final muscle area
C57
C58
FVB
SJL
129
Bal
NZB
SWR
PWK

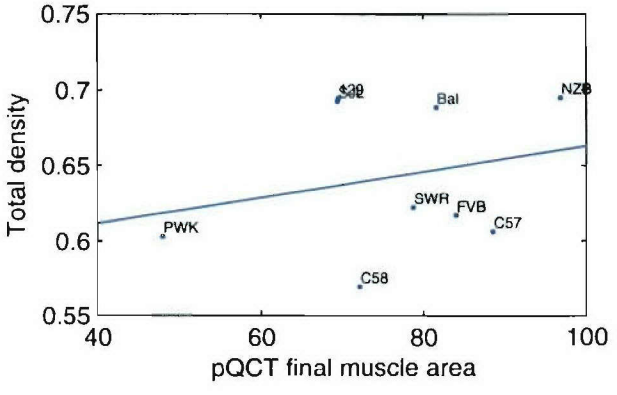
Total density
pQCT final muscle area
Bal
NZB
SWR
FVB
PWK
C57
C58

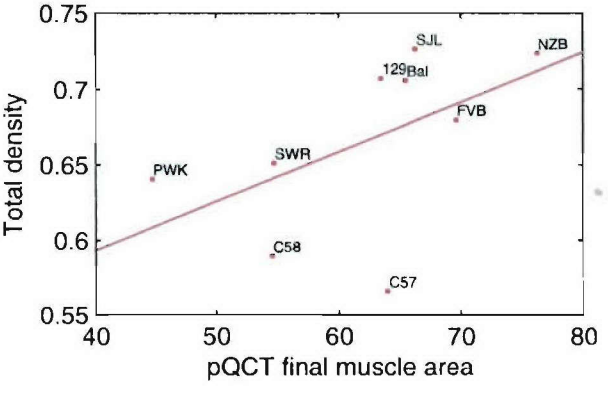
Total density
pQCT final muscle area
SJL
NZB
129
Bal
FVB
SWR
PWK
C58
C57

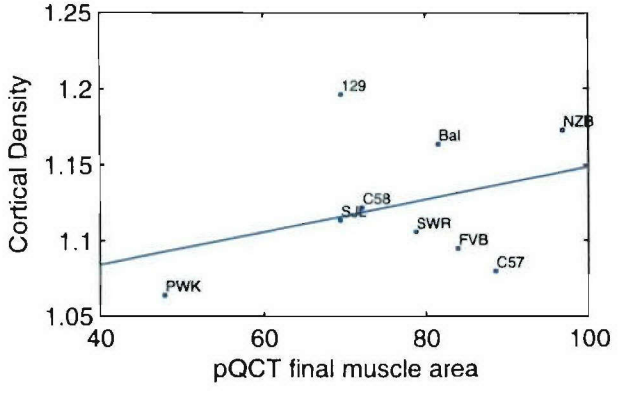
Cortical Density
pQCT final muscle area
129
Bal
NZB
C58
SJL
SWR
FVB
C57
PWK

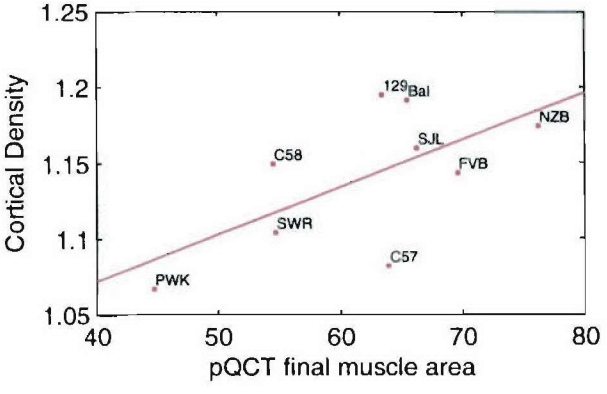
Cortical Density
pQCT final muscle area
129
Bal
NZB
C58
SJL
FVB
SWR
C57
PWK

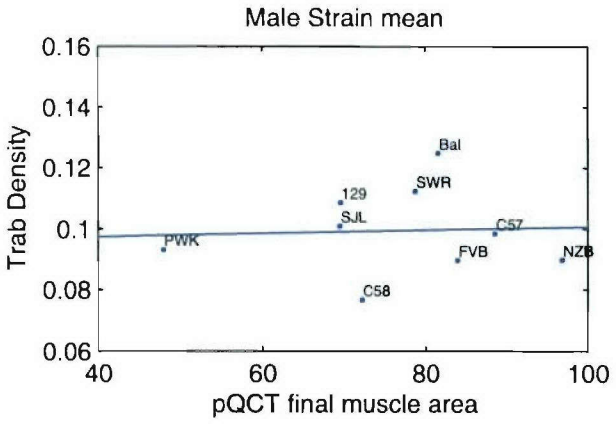
Male Strain mean
Trab Density
pQCT final muscle area
PWK
129
Bal
SWR
SJL
C57
FVB
NZB
C58

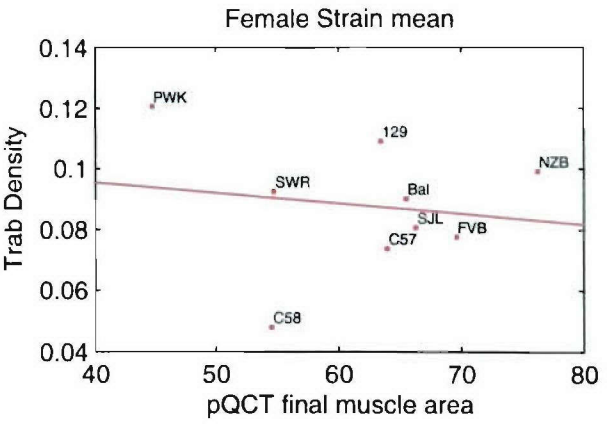
Female Strain mean
Trab Density
pQCT final muscle area
PWK
129
NZB
SWR
Bal
SJL
C57
FVB
C58

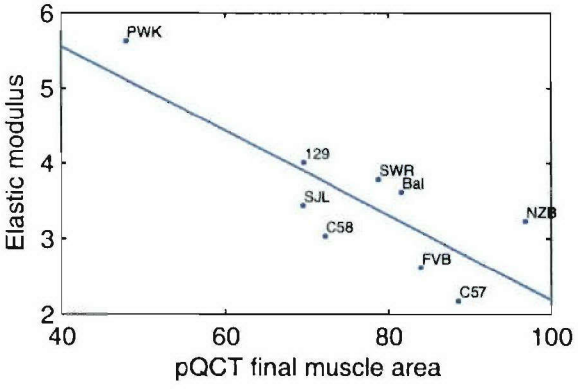
Elastic modulus
pQCT final muscle area
PWK
129
SWR
Bal
SJL
NZB
C58
FVB
C57

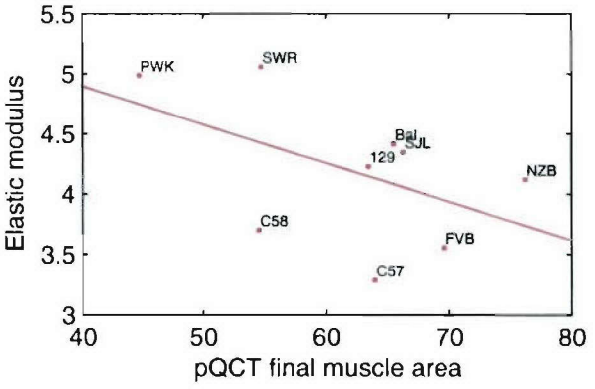
Elastic modulus
pQCT final muscle area
PWK
SWR
Bal
SJL
129
NZB
C58
FVB
C57

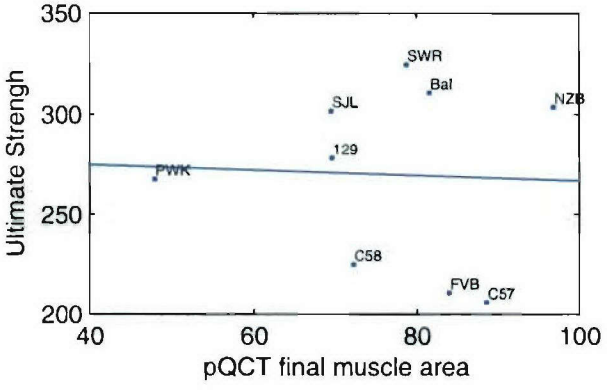
Ultimate Strengh
pQCT final muscle area
SWR
Bal
SJL
NZB
129
PWK
C58
FVB
C57

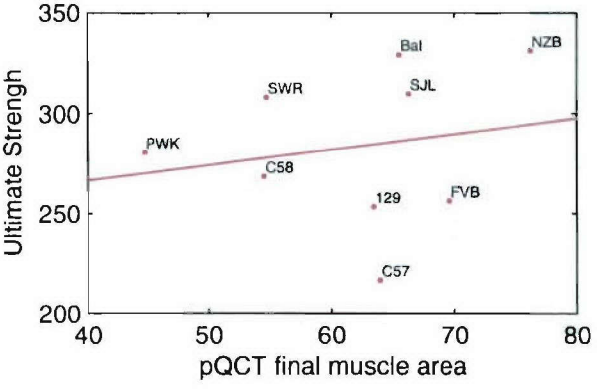
Ultimate Strengh
pQCT final muscle area
Bal
NZB
SWR
SJL
PWK
C58
129
FVB
C57

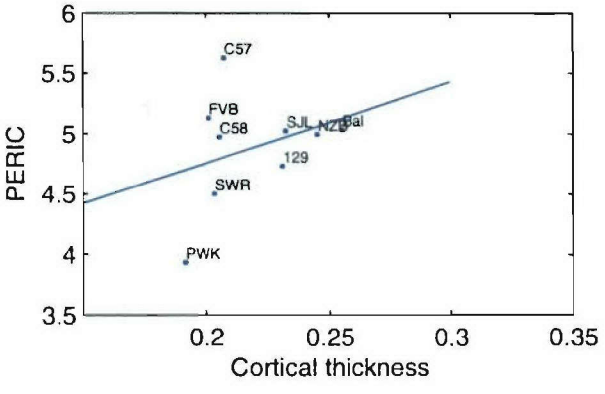
PERIC
Cortical thickness
C57
FVB
C58
SJL
NZB
Bal
129
SWR
PWK

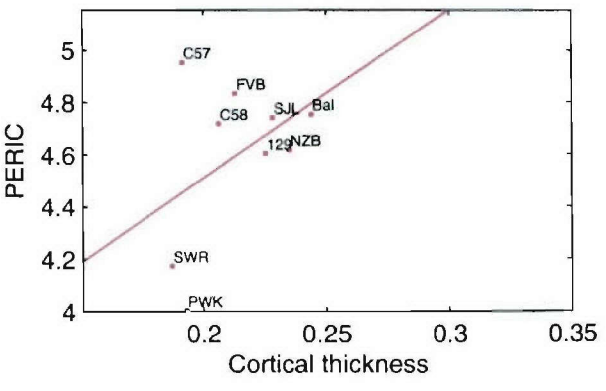
PERIC
Cortical thickness
C57
FVB
C58
SJL
Bal
129
NZB
SWR
PWK

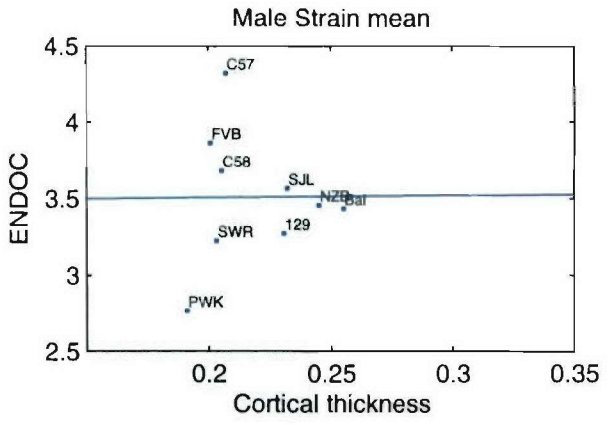
Male Strain mean
ENDOC
Cortical thickness
C57
FVB
C58
SJL
NZB
Bal
SWR
129
PWK

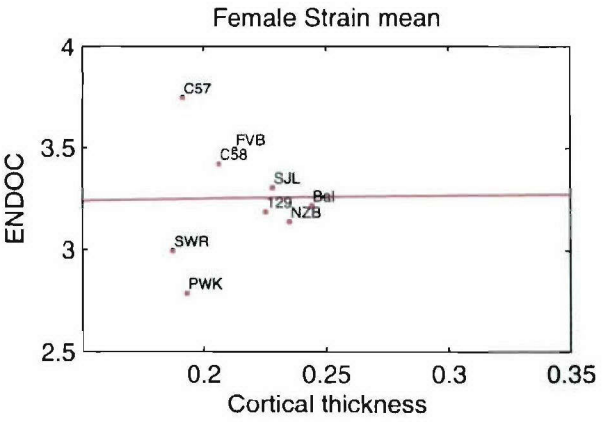
Female Strain mean
ENDOC
Cortical thickness
C57
FVB
C58
SJL
129
Bal
NZB
SWR
PWK

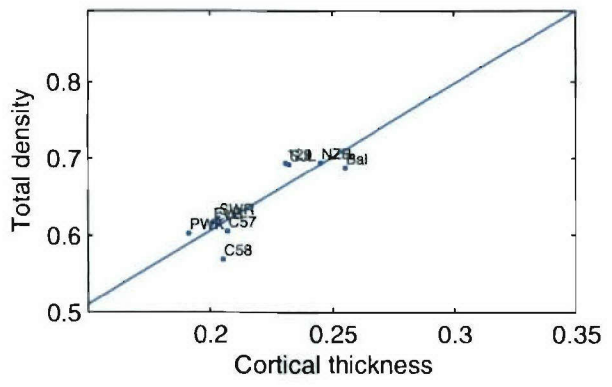
Total density
Cortical thickness
NZB
Bal
PWK
C57
C58

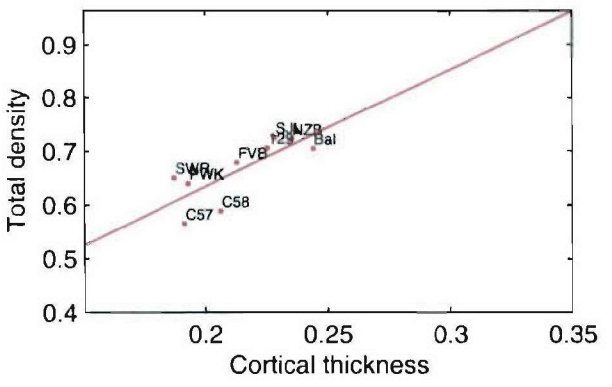
Total density
Cortical thickness
Bal
FVB
SWR
PWK
C58
C57

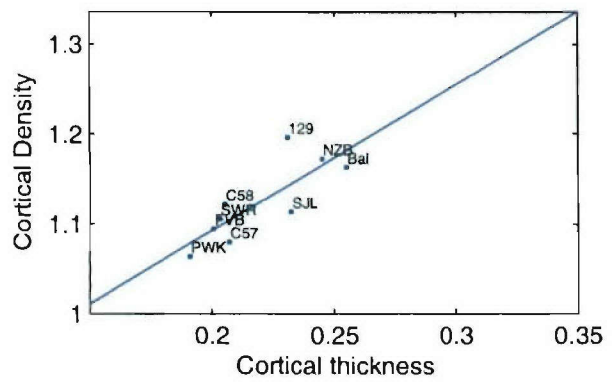
Cortical Density
Cortical thickness
129
NZB
Bal
C58
SWR
SJL
PWK
C57

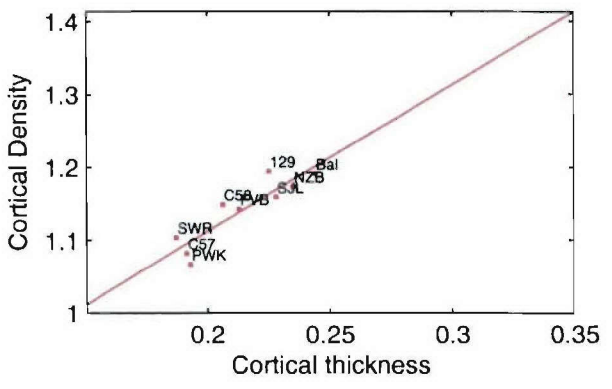
Cortical Density
Cortical thickness
129
Bal
NZB
SJL
SWR
C57
PWK

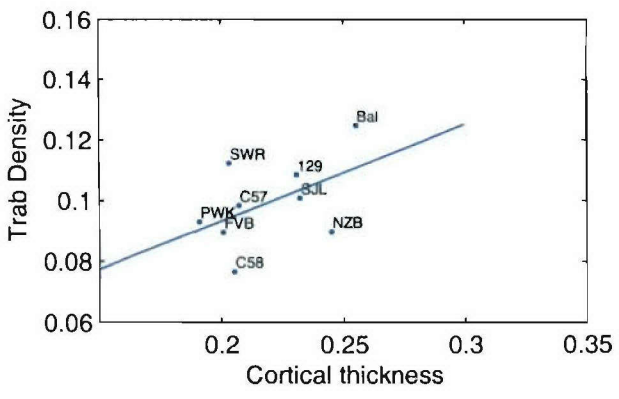
Trab Density
Cortical thickness
Bal
SWR
129
SJL
C57
PWK
FVB
NZB
C58

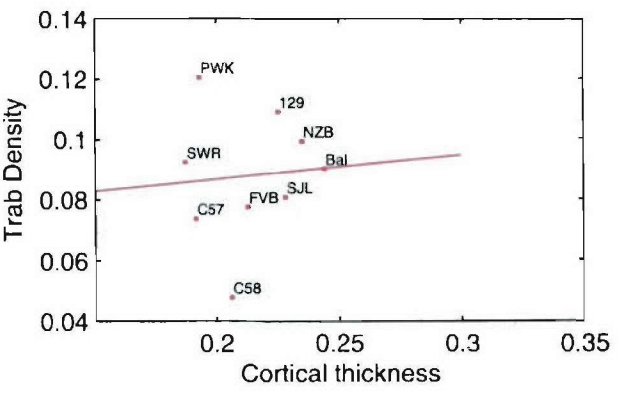
Trab Density
Cortical thickness
PWK
129
NZB
SWR
Bal
SJL
FVB
C57
C58

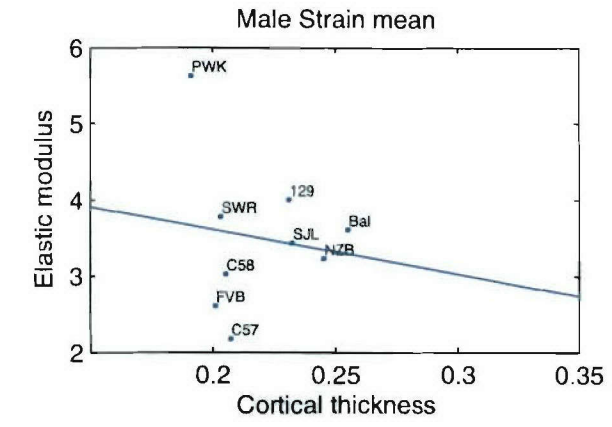
Male Strain mean
Elastic modulus
Cortical thickness
PWK
SWR
129
Bal
SJL
NZB
C58
FVB
C57

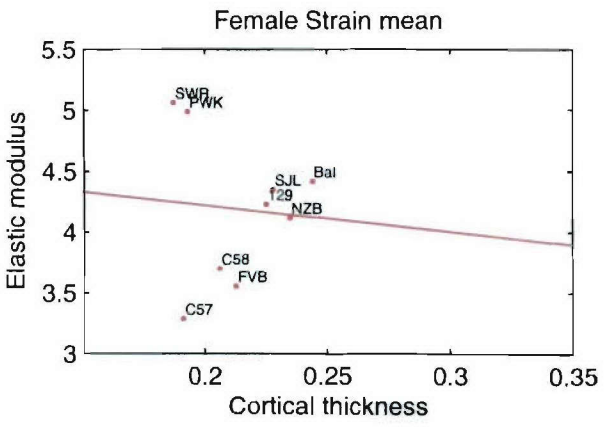
Female Strain mean
Elastic modulus
Cortical thickness
SWR
PWK
SJL
Bal
129
NZB
C58
FVB
C57

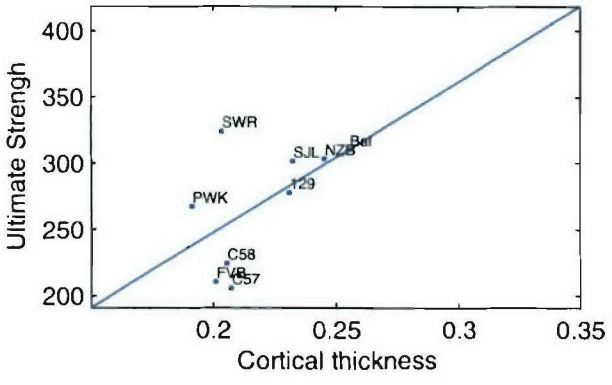
Ultimate Strengh
Cortical thickness
SWR
SJL
NZB
Bal
PWK
129
C58
FVB
C57

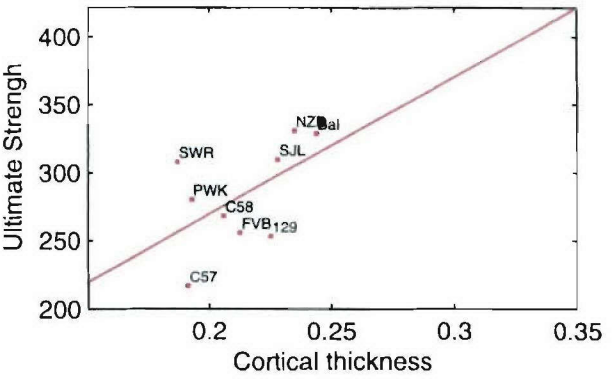
Ultimate Strengh
Cortical thickness
NZB
Bal
SWR
SJL
PWK
C58
FVB
129
C57

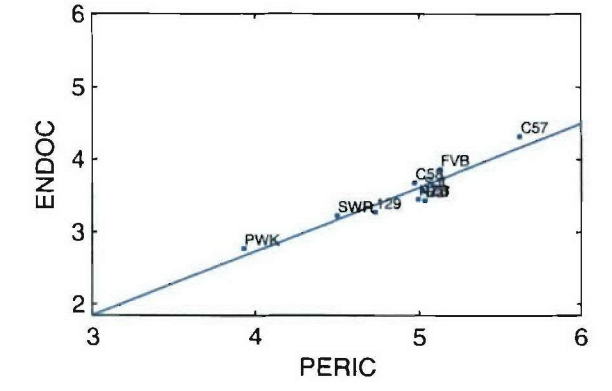
ENDOC
PERIC
C57
FVB
C58
SWR
129
PWK

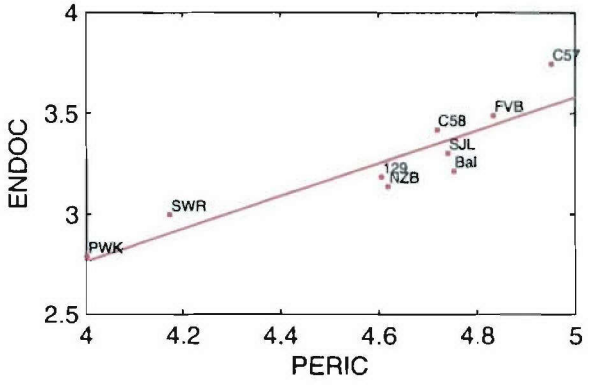
ENDOC
PERIC
C57
FVB
C58
SJL
Bal
129
NZB
SWR
PWK

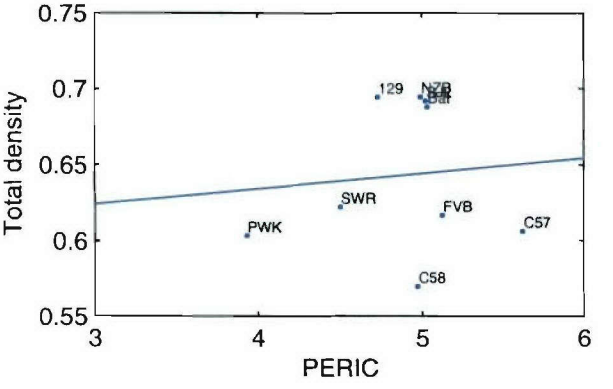
Total density
PERIC
129
NZB
SWR
FVB
PWK
C57
C58

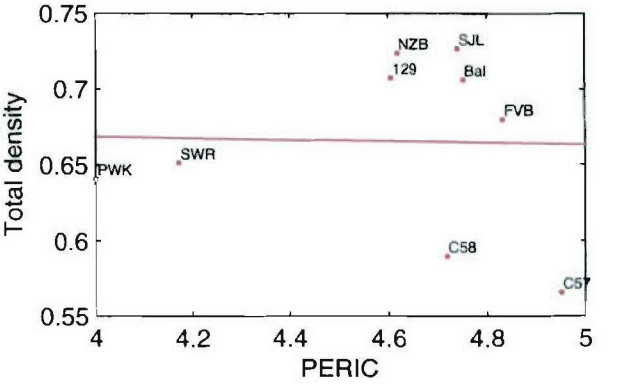
Total density
PERIC
NZB
SJL
129
Bal
FVB
SWR
PWK
C58
C57

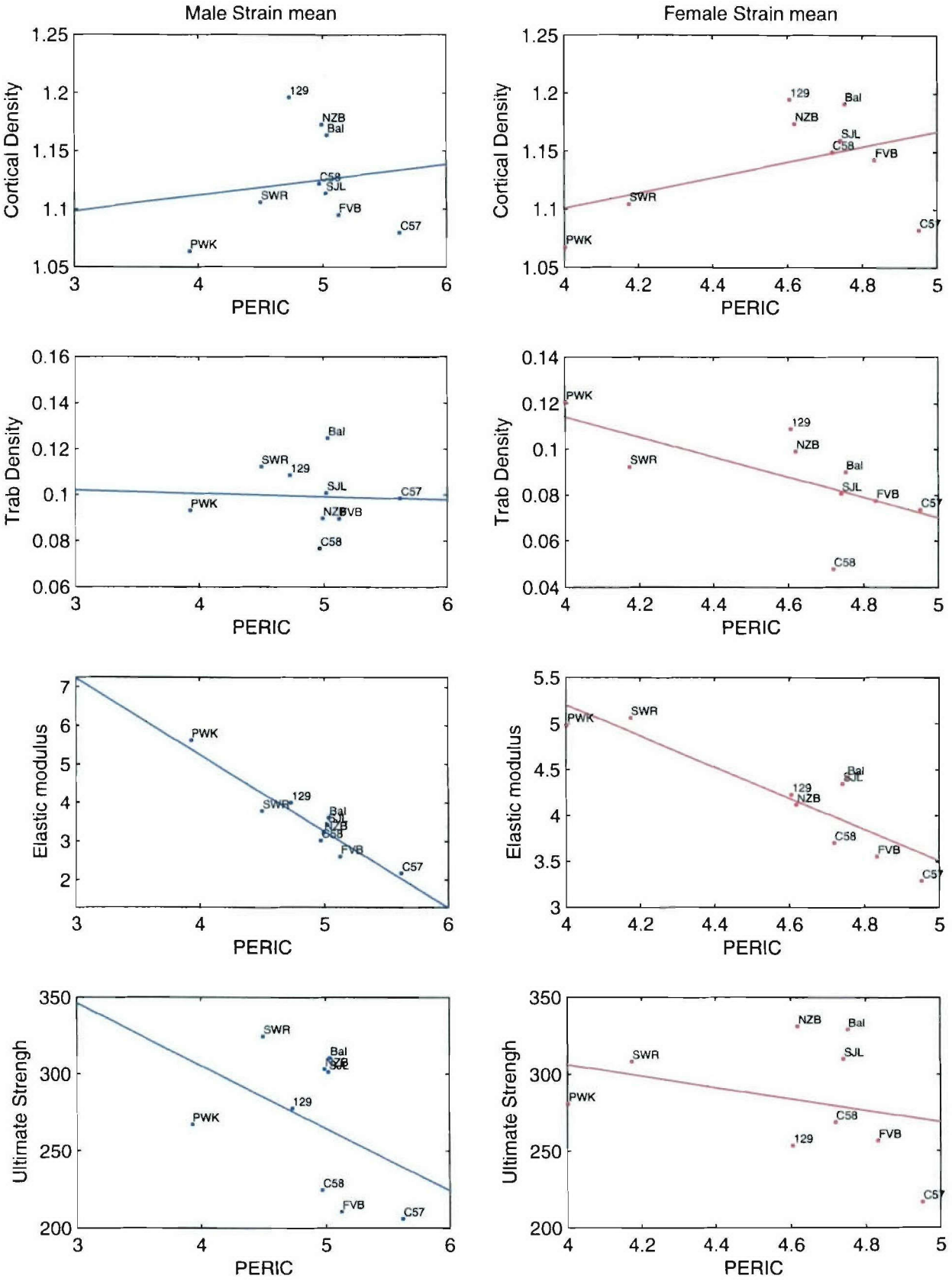
Male Strain mean
Female Strain mean
Cortical Density
Trab Density
Elastic modulus
Ultimate Strengh
PERIC
PWK
SWR
129
NZB
Bal
SJL
C58
FVB
C57

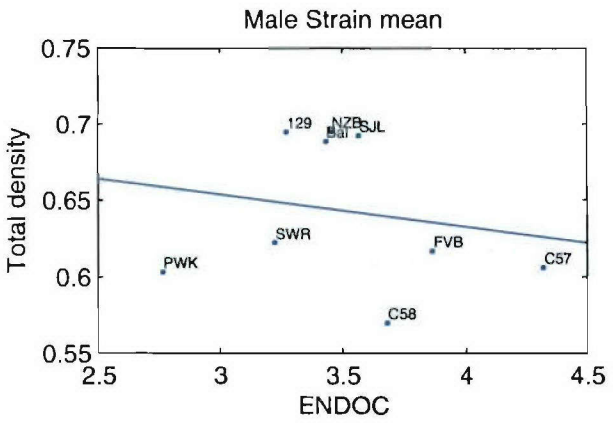
Male Strain mean
Total density
ENDOC
0.75
0.7
0.65
0.6
0.55
2.5
3
3.5
4
4.5
129
NZB
Bal
SJL
SWR
FVB
PWK
C57
C58

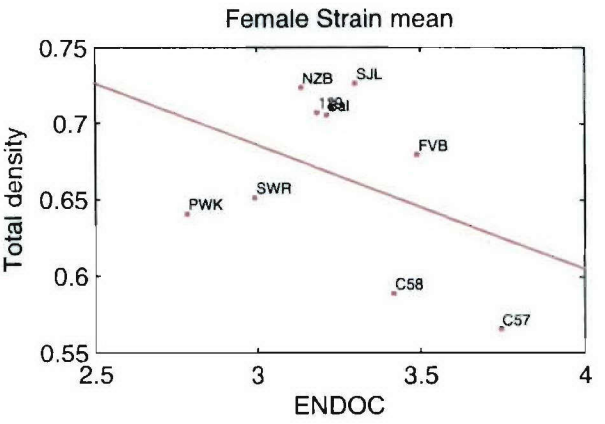
Female Strain mean
Total density
ENDOC
0.75
0.7
0.65
0.6
0.55
2.5
3
3.5
4
NZB
SJL
Bal
FVB
SWR
PWK
C58
C57

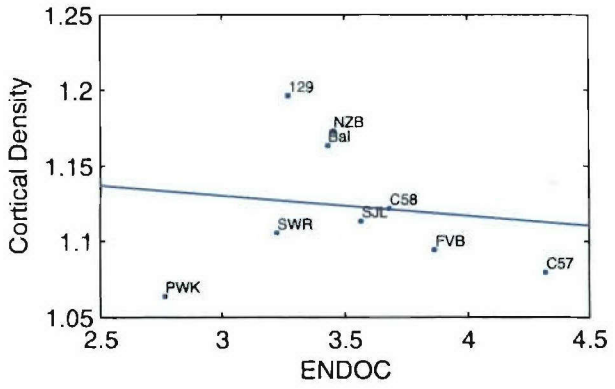
Cortical Density
ENDOC
1.25
1.2
1.15
1.1
1.05
2.5
3
3.5
4
4.5
129
NZB
Bal
C58
SJL
SWR
FVB
C57
PWK

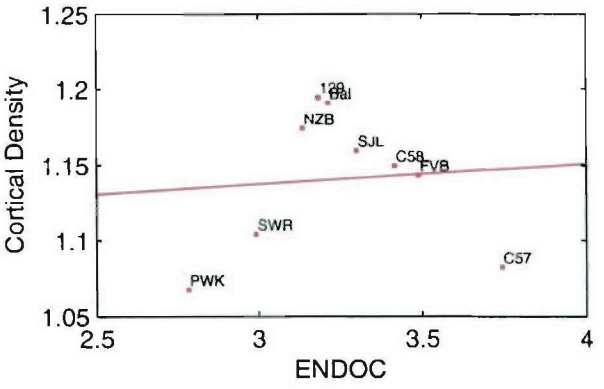
Cortical Density
ENDOC
1.25
1.2
1.15
1.1
1.05
2.5
3
3.5
4
129
Bal
NZB
SJL
C58
FVB
SWR
C57
PWK

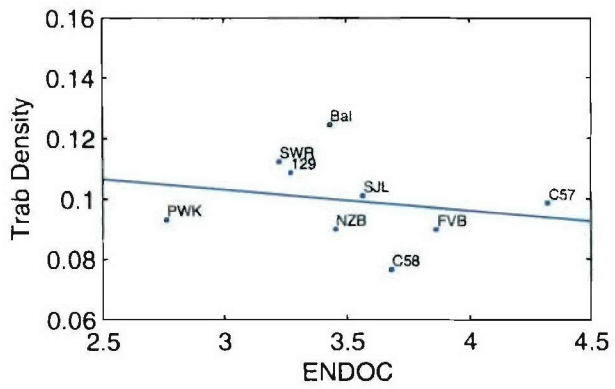
Trab Density
ENDOC
0.16
0.14
0.12
0.1
0.08
0.06
2.5
3
3.5
4
4.5
Bal
SWR
129
SJL
C57
PWK
NZB
FVB
C58

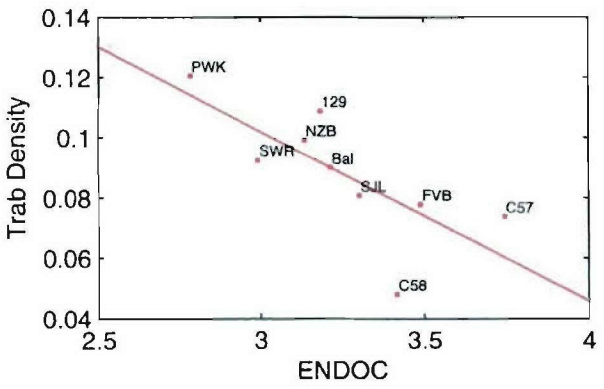
Trab Density
ENDOC
0.14
0.12
0.1
0.08
0.06
0.04
2.5
3
3.5
4
PWK
129
NZB
SWR
Bal
SJL
FVB
C57
C58

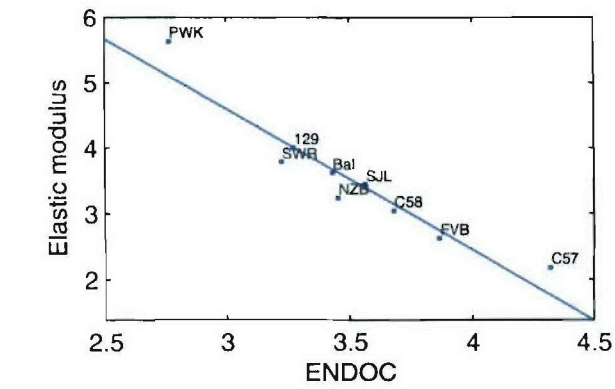
Elastic modulus
ENDOC
6
5
4
3
2
2.5
3
3.5
4
4.5
PWK
129
SWR
Bal
SJL
NZB
C58
FVB
C57

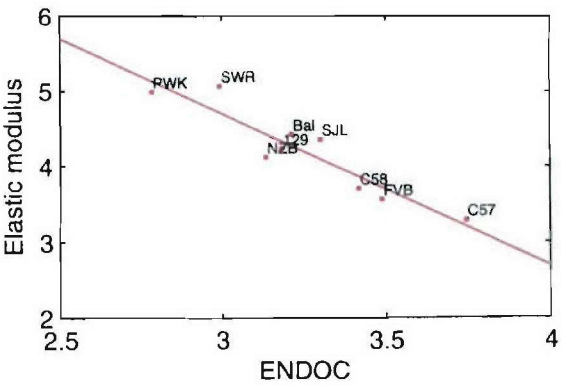
Elastic modulus
ENDOC
6
5
4
3
2
2.5
3
3.5
4
PWK
SWR
Bal
SJL
129
NZB
C58
FVB
C57

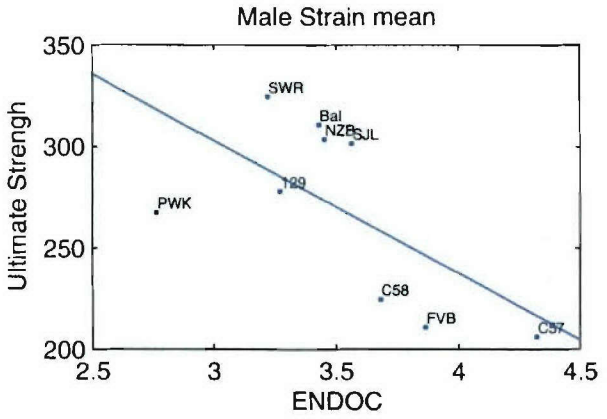
Male Strain mean
Ultimate Strengh
ENDOC
SWR
Bal
NZB
SJL
129
PWK
C58
FVB
C57

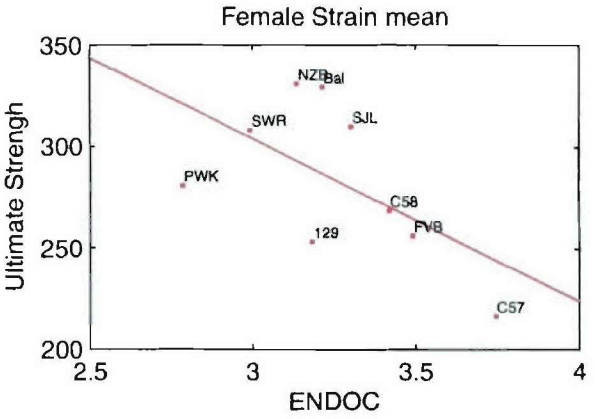
Female Strain mean
Ultimate Strengh
ENDOC
NZB
Bal
SWR
SJL
PWK
C58
129
FVB
C57

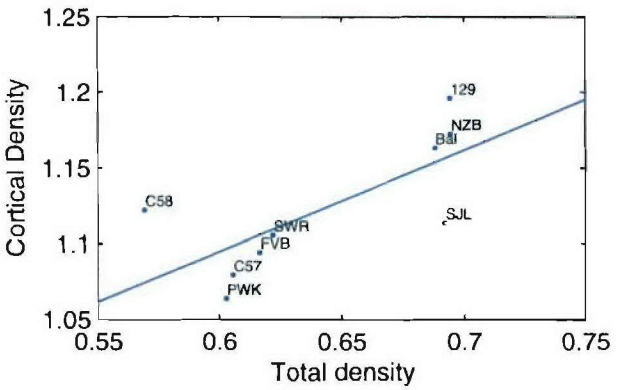
Cortical Density
Total density
129
NZB
Bal
C58
SJL
SWR
FVB
C57
PWK

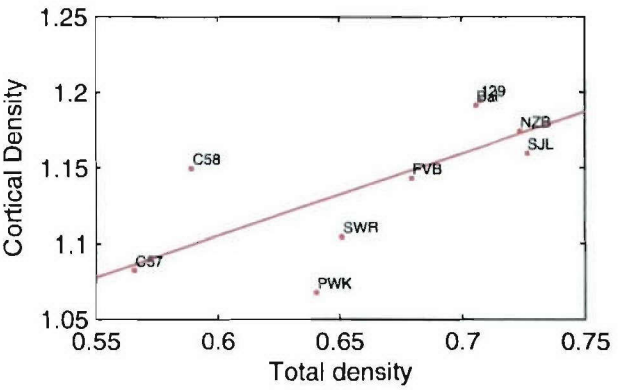
Cortical Density
Total density
129
NZB
SJL
C58
FVB
SWR
C57
PWK

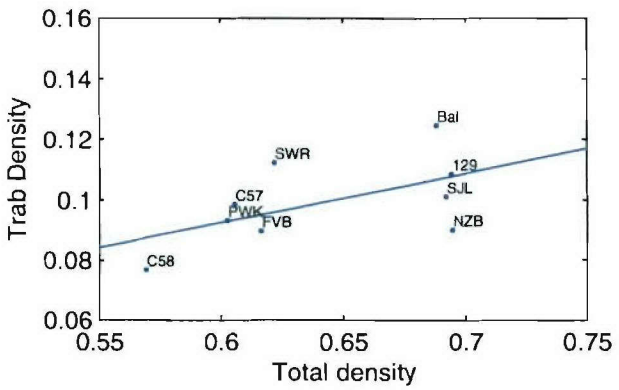
Trab Density
Total density
Bal
SWR
129
SJL
C57
PWK
FVB
NZB
C58

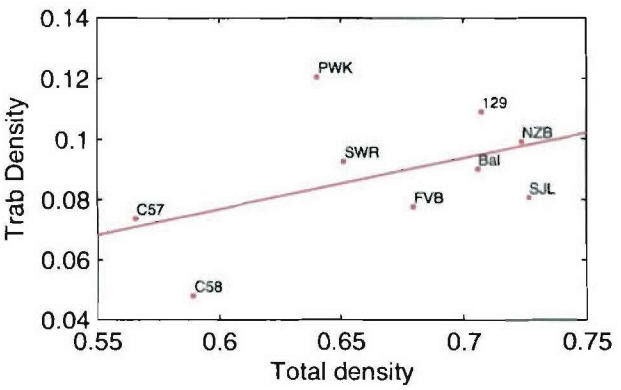
Trab Density
Total density
PWK
129
NZB
SWR
Bal
SJL
FVB
C57
C58

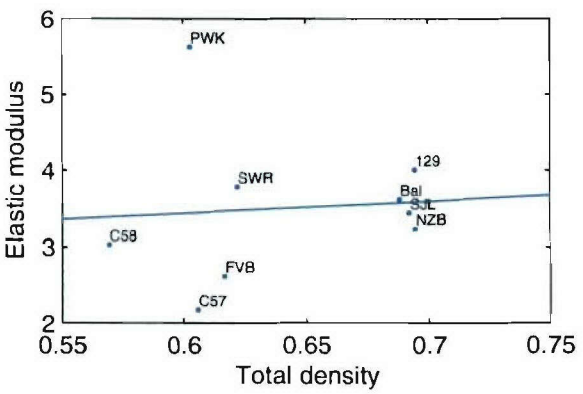
Elastic modulus
Total density
PWK
129
SWR
Bal
SJL
NZB
C58
FVB
C57

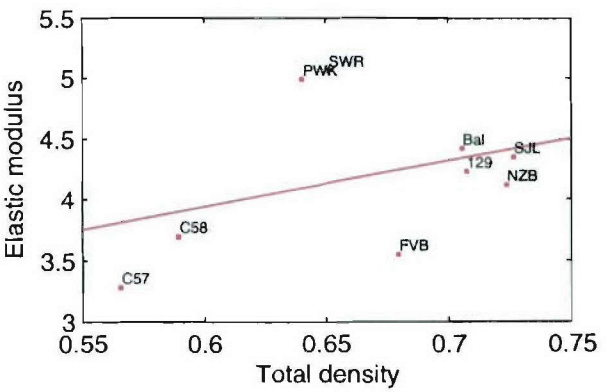
Elastic modulus
Total density
SWR
PWK
Bal
SJL
129
NZB
C58
FVB
C57

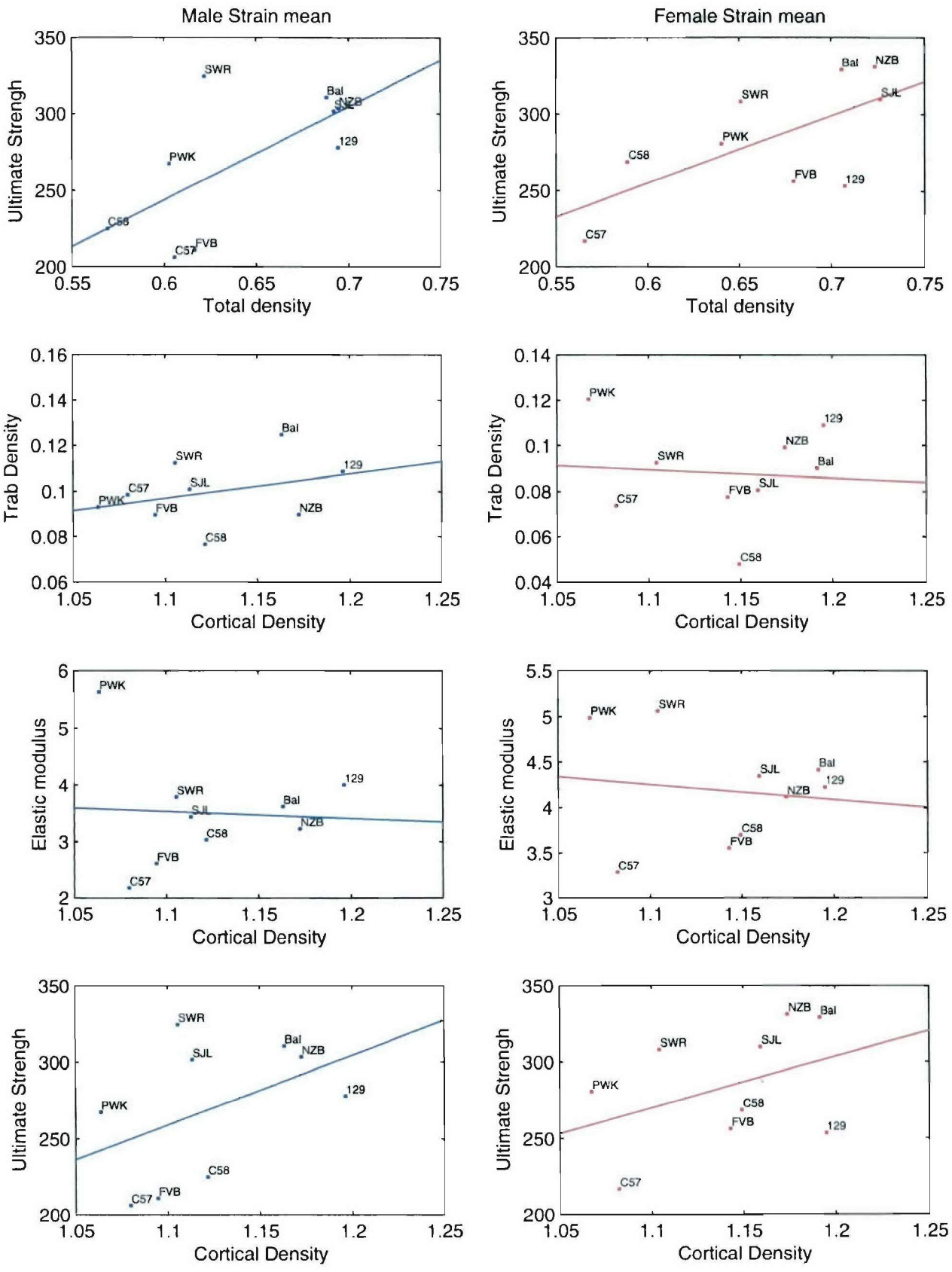
Male Strain mean
Female Strain mean
Ultimate Strength
Total density
Trab Density
Cortical Density
Elastic modulus
SWR
Bal
NZB
SJL
129
PWK
C58
C57
FVB

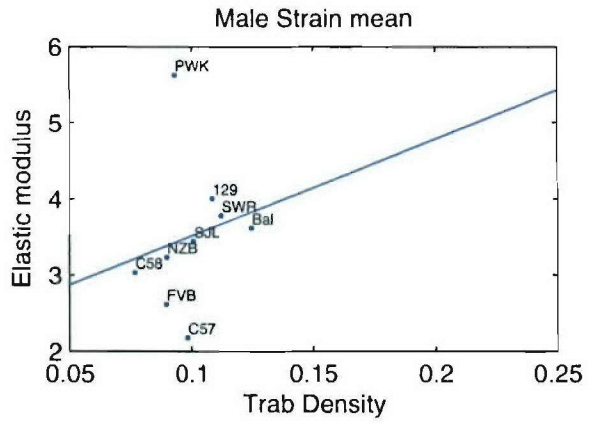
Male Strain mean
Elastic modulus
Trab Density
PWK
129
SWR
Bal
SJL
NZB
C58
FVB
C57

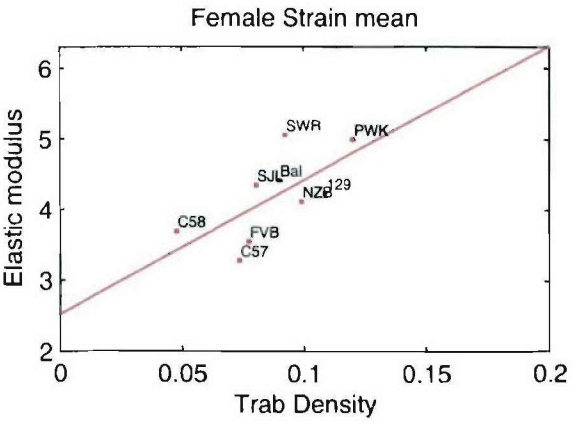
Female Strain mean
Elastic modulus
Trab Density
SWR
PWK
SJL
Bal
NZB
129
C58
FVB
C57

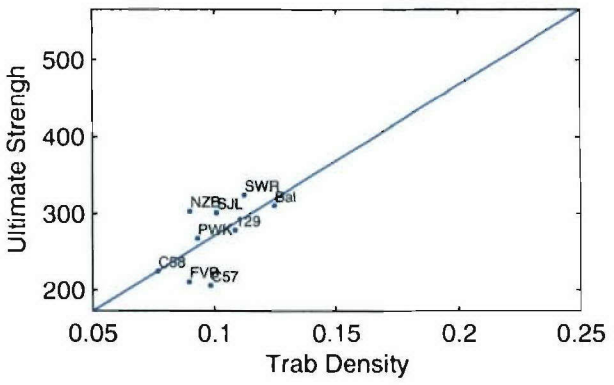
Ultimate Strengh
Trab Density
SWR
NZB
SJL
Bal
PWK
129
C58
FVB
C57

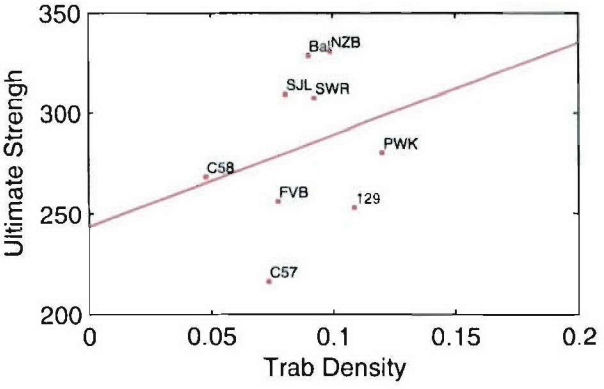
Ultimate Strengh
Trab Density
Bal
NZB
SJL
SWR
PWK
C58
FVB
129
C57

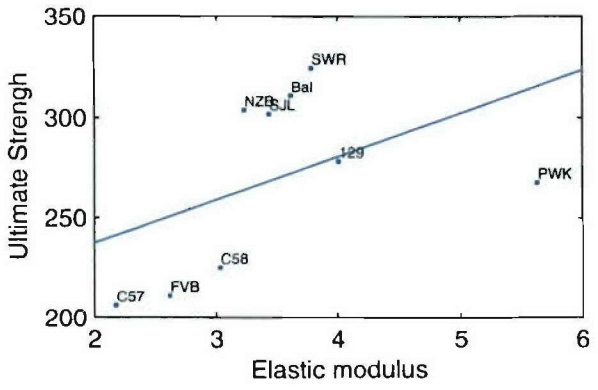
Ultimate Strengh
Elastic modulus
SWR
Bal
NZB
SJL
129
PWK
C58
C57
FVB

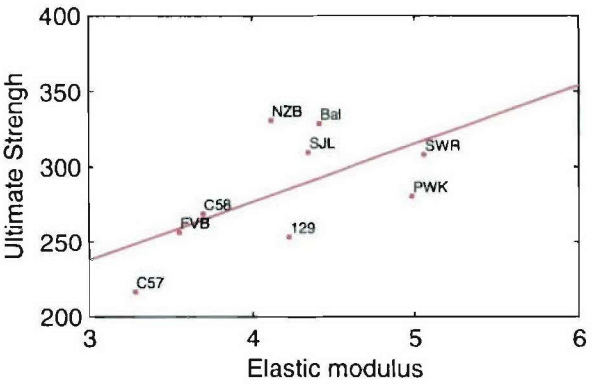
Ultimate Strengh
Elastic modulus
NZB
Bal
SJL
SWR
PWK
C58
FVB
129
C57

Table 6 Strain Means, 28 strains

28 female strains	Body WT (g)			Lean Mass (g)			Fat Mass (g)			Area BMD (g/cm^2)			BMC (g)			SPINE BMD (g/mm^2)			OC (ng/ml)			T4 (ng/ml)			Adj. IGF-1			%Fat			%Lean		
	MEAN	SEM	N	MEAN	SEM	N	MEAN	SEM	N	MEAN	SEM	N	MEAN	SEM	N	MEAN	SEM	N	MEAN	SEM	N	MEAN	SEM	N	MEAN	SEM	N	MEAN	SEM	N	MEAN	SEM	N
129S1/SvImJ	16.30	0.34	10	13.69	0.30	10	2.61	0.09	10	0.049	0.00057	10	0.51	0.012	10	0.094	0.0026	10	84.00	5.74	10	3.88	0.31	10	91.14	2.78	10	16.08	0.48	10	83.98	0.50	10
A/J	18.97	0.60	10	14.72	0.30	10	4.28	0.41	10	0.041	0.00041	10	0.32	0.008	10	0.065	0.0027	10	47.70	1.75	10	4.90	0.20	10	106.44	5.59	10	22.14	1.50	10	77.94	1.50	10
AKR/J	30.32	1.12	10	20.66	0.46	10	9.68	0.79	10	0.053	0.00062	10	0.52	0.011	10	0.090	0.0048	10	40.30	3.45	10	3.55	0.11	10	114.60	4.12	10	31.50	1.49	10	68.55	1.47	10
BALB/cJ	19.50	0.63	10	15.11	0.36	10	4.40	0.37	10	0.046	0.00065	10	0.42	0.011	10	0.074	0.0016	10	51.00	2.88	10	7.92	0.23	10	107.44	2.96	10	22.31	1.22	10	77.74	1.24	10
BTBR T+ tf/tf	23.81	0.64	8	19.96	0.42	8	3.84	0.24	8	0.054	0.00087	8	0.58	0.013	8	0.095	0.0034	8	74.75	2.83	8	4.30	0.15	8	161.71	4.02	8	16.03	0.62	8	83.93	0.68	8
BUB/BnJ	21.93	0.45	10	18.54	0.39	10	3.37	0.18	10	0.048	0.00029	10	0.48	0.006	10	0.075	0.0024	10	40.60	2.67	10	6.64	0.45	10	108.88	3.20	10	15.42	0.70	10	84.56	0.71	10
C3H/HeJ	20.39	0.66	10	15.58	0.34	10	4.78	0.35	10	0.050	0.00047	10	0.47	0.011	10	0.081	0.0016	10	58.00	2.29	10	9.74	0.77	10	127.38	5.49	10	23.26	1.02	10	76.67	1.02	10
C58BL/6J	16.91	0.48	10	14.33	0.38	10	2.60	0.20	10	0.044	0.00047	10	0.38	0.010	10	0.071	0.0013	10	59.40	3.03	10	7.18	0.68	10	83.45	2.07	10	15.24	0.90	10	84.81	0.89	10
C57L/J	18.21	0.31	10	15.34	0.23	10	2.87	0.25	10	0.050	0.00051	10	0.47	0.012	10	0.085	0.0031	10	42.10	1.83	10	5.27	0.24	9	113.26	3.30	10	15.73	1.17	10	84.34	1.17	10
C58/J	19.49	0.80	10	16.80	0.52	10	2.69	0.35	10	0.045	0.00035	10	0.42	0.012	10	0.069	0.0021	10	70.60	4.71	10	5.69	0.27	10	111.09	3.30	10	13.41	1.33	10	86.55	1.31	10
CAST/EiJ	11.66	0.23	10	10.04	0.17	10	1.63	0.09	10	0.040	0.00034	10	0.29	0.007	10	0.054	0.0013	10	57.30	5.64	10	3.59	0.38	10	119.92	4.32	10	13.96	0.57	10	86.17	0.53	10
CZECHII/EiJ	10.49	0.22	12	8.84	0.19	12	1.63	0.11	12	0.039	0.00064	12	0.25	0.011	12	0.059	0.0024	12	69.13	6.66	8	5.51	0.33	7	80.23	4.90	8	15.52	0.89	12	84.32	0.93	12
DBA/2J	19.76	0.57	10	15.25	0.26	10	4.49	0.39	10	0.044	0.00029	10	0.36	0.003	10	0.066	0.0016	10	54.40	2.75	10	6.64	0.40	10	82.87	3.77	10	22.49	1.38	10	77.48	1.39	10
FVB/NJ	19.72	0.43	10	15.58	0.19	10	4.14	0.28	10	0.047	0.00037	10	0.40	0.007	10	0.076	0.0023	10	41.70	2.17	10	3.14	0.18	9	85.75	2.18	10	20.82	0.99	10	79.18	1.01	10
JF1/Ms	13.87	0.38	11	10.83	0.19	11	3.05	0.27	11	0.043	0.00077	11	0.27	0.008	11	0.075	0.0026	11	40.56	2.61	9	5.48	0.30	9	131.29	4.21	9	21.66	1.41	11	78.34	1.43	11
MOLF/EiJ	10.39	0.19	10	9.01	0.17	10	1.37	0.04	10	0.040	0.00047	10	0.27	0.009	10	0.060	0.0023	10	86.70	3.58	10	3.56	0.15	9	101.42	2.91	10	13.20	0.34	10	86.71	0.38	10
MSM/Ms	8.94	0.19	11	7.53	0.21	11	1.40	0.06	11	0.040	0.00085	11	0.27	0.009	11	0.070	0.0013	11	49.63	5.33	8	4.74	0.32	5	95.63	7.60	8	15.90	0.84	11	84.12	0.86	11
NOD/LtJ	20.86	0.32	10	17.95	0.29	10	2.87	0.22	10	0.047	0.00040	10	0.46	0.007	10	0.080	0.0026	10	41.20	4.45	10	4.50	0.48	10	126.56	4.55	10	13.84	1.00	10	86.10	1.03	10
NZB/B1NJ	20.29	0.47	10	16.63	0.31	10	3.63	0.29	10	0.049	0.00058	10	0.47	0.007	10	0.091	0.0030	10	75.40	3.78	10	5.59	0.26	10	110.14	4.05	10	17.82	1.15	10	82.10	1.12	10
NZW/LacJ	24.57	0.66	10	17.57	0.54	10	6.99	0.46	10	0.050	0.00067	10	0.45	0.009	10	0.089	0.0026	10	58.10	3.20	10	4.97	0.27	10	105.11	3.58	10	28.41	1.52	10	71.58	1.56	10
PERA/EiJ	18.12	0.35	10	13.18	0.20	10	4.93	0.25	10	0.044	0.00073	10	0.33	0.013	10	0.057	0.0021	10	49.63	4.61	8	4.38	0.20	8	133.49	3.80	8	27.16	1.00	10	72.85	1.04	10
PL/J	15.97	0.41	10	12.80	0.23	10	3.15	0.25	10	0.044	0.00056	10	0.34	0.007	10	0.069	0.0013	10	52.00	5.02	10	5.43	0.25	10	98.22	3.96	10	19.56	1.07	10	80.33	1.03	10
PWK/PhJ	12.24	0.28	13	10.61	0.27	13	1.65	0.04	13	0.043	0.00070	13	0.34	0.013	13	0.076	0.0027	13	83.00	7.01	7	4.13	0.24	7	120.60	4.07	7	13.60	0.36	13	86.63	0.31	13
SJL/J	16.18	0.39	10	13.30	0.31	10	2.86	0.16	10	0.049	0.00057	10	0.43	0.009	10	0.079	0.0020	10	49.40	3.21	10	3.85	0.25	10	81.51	3.64	10	17.68	0.73	10	82.25	0.72	10
SM/J	15.40	0.44	10	12.03	0.35	10	3.36	0.20	10	0.038	0.00054	10	0.25	0.008	10	0.053	0.0023	10	45.60	4.48	10	--	--	0	54.32	3.59	10	21.84	1.06	10	78.16	1.05	10
SPRET/EiJ	11.37	0.62	10	9.13	0.39	10	2.25	0.25	10	0.047	0.00082	10	0.32	0.010	10	0.089	0.0023	10	34.70	2.54	10	4.03	0.49	8	124.88	5.29	10	19.30	1.03	10	80.68	1.05	10
SWR/J	16.43	0.30	10	13.91	0.24	10	2.52	0.10	10	0.044	0.00021	10	0.36	0.004	10	0.071	0.0011	10	35.67	2.97	9	6.87	0.18	10	105.78	2.88	10	15.30	0.43	10	84.69	0.42	10
WSB/EiJ	11.24	0.23	10	9.71	0.21	10	1.54	0.09	10	0.038	0.00046	10	0.27	0.009	10	0.057	0.0016	10	56.70	3.23	10	2.59	0.12	10	84.01	3.01	10	13.80	0.72	10	86.38	0.70	10

Table 6

28 male strains	Body WT (g)			Lean Mass (g)			Fat Mass (g)			Area BMD (g/cm^2)			BMC (g)			SPINE BMD (g/mm^2)			OC (ng/ml)			T4 (ng/ml)			Adj. IGF-1			%Fat			%Lean		
	MEAN	SEM	N	MEAN	SEM	N	MEAN	SEM	N	MEAN	SEM	N	MEAN	SEM	N	MEAN	SEM	N	MEAN	SEM	N	MEAN	SEM	N	MEAN	SEM	N	MEAN	SEM	N	MEAN	SEM	N
129S1/SvImJ	23.80	0.87	10	18.71	0.57	10	5.07	0.40	10	0.052	0.00070	10	0.53	0.013	10	0.084	0.0022	10	82.89	10.98	9	4.61	0.20	9	109.22	2.90	9	21.15	1.05	10	78.80	1.04	10
A/J	23.23	0.72	10	17.59	0.44	10	5.62	0.40	10	0.041	0.00026	10	0.36	0.006	10	0.061	0.0022	10	46.60	2.68	10	4.36	0.16	10	103.36	3.50	10	24.07	1.13	10	75.91	1.13	10
AKR/J	32.27	0.84	10	22.91	0.33	10	9.38	0.62	10	0.052	0.00062	10	0.52	0.009	10	0.083	0.0036	10	52.50	5.95	4	3.93	0.29	4	68.43	17.12	7	28.78	1.20	10	71.23	1.21	10
BALB/cJ	25.08	0.33	10	20.90	0.26	10	4.19	0.27	10	0.048	0.00033	10	0.47	0.007	10	0.073	0.0026	10	27.80	1.92	10	7.87	0.37	10	118.24	3.52	10	16.65	0.93	10	83.38	0.93	10
BTBR+Tif/tf	27.04	0.84	10	22.78	0.55	10	4.23	0.35	10	0.051	0.00043	10	0.55	0.014	10	0.079	0.0019	10	49.40	3.92	10	5.16	0.17	10	135.69	3.35	10	15.51	0.84	10	84.42	0.82	10
BUB/BnJ	25.13	0.77	10	21.54	0.58	10	3.59	0.34	10	0.049	0.00046	10	0.49	0.007	10	0.068	0.0018	10	33.33	6.94	6	7.50	0.88	6	108.35	6.61	6	14.12	1.12	10	85.88	1.12	10
C3H/HeJ	26.25	0.89	10	20.00	0.53	10	6.25	0.45	10	0.052	0.00049	10	0.50	0.010	10	0.083	0.0026	10	55.50	7.87	10	9.00	0.33	10	122.83	3.16	10	23.60	1.01	10	76.41	1.01	10
C58BL/6J	25.99	0.48	10	21.61	0.23	10	4.38	0.39	10	0.047	0.00033	10	0.46	0.009	10	0.070	0.0025	10	60.30	3.35	10	6.40	0.23	10	87.38	1.22	10	16.66	1.23	10	83.32	1.21	10
C57L/J	25.35	0.52	10	20.36	0.38	10	4.99	0.51	10	0.048	0.00049	10	0.46	0.013	10	0.064	0.0026	10	40.14	7.69	7	5.76	0.23	7	94.74	5.64	8	19.52	1.69	10	80.51	1.67	10
C58/J	25.59	1.08	10	20.07	0.66	10	5.53	0.50	10	0.045	0.00083	10	0.40	0.014	10	0.062	0.0026	10	31.00	3.31	10	3.77	0.14	9	80.30	3.11	10	21.21	1.34	10	78.85	1.34	10
CAST/EiJ	13.51	0.34	10	11.58	0.30	10	1.94	0.09	10	0.039	0.00038	10	0.28	0.006	10	0.057	0.0012	10	61.13	5.46	8	3.08	0.32	8	138.25	4.82	8	14.30	0.57	10	85.72	0.63	10
CZECHII/EiJ	13.39	0.45	12	11.53	0.38	12	1.88	0.12	12	0.040	0.00051	12	0.27	0.009	12	0.056	0.0016	12	39.67	3.57	9	5.91	0.36	8	88.47	1.46	9	13.91	0.60	12	86.11	0.58	12
DBA/2J	25.76	0.86	10	19.51	0.37	10	6.25	0.52	10	0.045	0.00050	10	0.37	0.007	10	0.062	0.0025	10	50.90	5.13	10	5.72	0.38	10	88.44	3.33	10	23.85	1.30	10	76.10	1.32	10
FVB/NJ	23.19	0.47	10	19.80	0.33	10	3.40	0.31	10	0.048	0.00057	10	0.48	0.010	10	0.071	0.0031	10	32.60	3.20	10	2.96	0.19	10	95.13	2.98	10	14.53	1.09	10	85.49	1.11	10
JF1/Ms	20.38	0.56	10	12.95	0.22	10	7.45	0.53	10	0.041	0.00027	10	0.25	0.008	10	0.060	0.0019	10	30.60	1.64	10	3.63	0.33	10	119.41	3.16	10	35.17	2.30	10	63.90	1.76	10
MOLF/EiJ	12.69	0.25	8	10.94	0.26	8	1.74	0.14	8	0.039	0.00046	8	0.26	0.007	8	0.053	0.0024	8	43.13	5.14	8	4.21	0.43	7	93.40	6.68	8	13.76	1.12	8	86.21	1.15	8
MSM/Ms	11.94	0.32	9	10.14	0.22	9	1.82	0.12	9	0.041	0.00072	9	0.27	0.014	9	0.066	0.0023	9	54.14	4.98	7	3.77	0.50	6	110.06	4.52	7	15.12	0.65	9	85.04	0.64	9
NOD/LtJ	25.75	0.70	10	21.94	0.62	10	3.78	0.19	10	0.049	0.00067	10	0.50	0.011	10	0.073	0.0022	10	45.88	5.71	8	3.68	0.56	9	132.63	6.72	9	14.72	0.60	10	85.20	0.60	10
NZB/B1NJ	24.58	0.60	10	20.56	0.59	10	4.00	0.42	10	0.047	0.00031	10	0.45	0.011	10	0.068	0.0020	10	42.90	5.26	10	4.50	0.27	10	107.22	5.77	10	16.26	1.55	10	83.71	1.55	10
NZW/LacJ	26.97	0.88	10	21.99	0.62	10	4.96	0.54	10	0.051	0.00063	10	0.53	0.010	10	0.081	0.0013	10	42.10	2.66	10	4.15	0.25	10	114.72	2.24	10	18.25	1.62	10	81.78	1.59	10
PERA/EiJ	21.30	0.63	10	17.42	0.64	10	3.89	0.12	10	0.048	0.00059	10	0.47	0.012	10	0.072	0.0013	10	44.78	6.70	9	2.61	0.26	9	119.10	6.24	9	18.38	0.79	10	81.65	0.80	10
PL/J	21.32	0.69	11	17.06	0.50	11	4.22	0.25	11	0.044	0.00042	11	0.36	0.009	11	0.072	0.0031	11	53.17	3.32	6	6.40	0.24	6	92.76	7.41	7	19.72	0.67	11	80.14	0.67	11
PWK/PhJ	18.10	0.87	9	14.47	0.44	9	3.62	0.54	9	0.041	0.00053	9	0.30	0.013	9	0.061	0.0016	9	67.33	13.09	9	4.66	0.57	9	122.56	7.88	9	19.44	1.88	9	80.50	1.89	9
SJL/J	22.13	0.47	10	18.57	0.39	10	3.58	0.24	10	0.051	0.00057	10	0.47	0.009	10	0.076	0.0019	10	54.30	4.53	10	3.73	0.52	10	88.53	3.85	10	16.10	0.98	10	83.97	0.99	10
SM/J	23.01	0.53	10	18.37	0.34	10	4.63	0.25	10	0.044	0.00065	10	0.33	0.007	10	0.059	0.0028	10	50.78	7.17	9	--	--	0	60.54	7.44	10	20.06	0.70	10	79.93	0.67	10
SPRET/EiJ	14.47	0.62	10	11.08	0.32	10	3.41	0.34	10	0.043	0.00036	10	0.28	0.007	10	0.072	0.0011	10	39.40	1.78	10	4.17	0.29	7	126.37	4.94	10	23.10	1.45	10	77.04	1.42	10
SWR/J	20.26	0.34	10	17.81	0.25	10	2.45	0.18	10	0.045	0.00029	10	0.44	0.007	10	0.075	0.0017	10	39.78	8.36	9	5.00	0.35	9	94.97	2.69	9	11.95	0.78	10	87.97	0.74	10
WSB/EiJ	13.47	0.30	10	11.47	0.24	10	2.02	0.11	10	0.039	0.00046	10	0.30	0.009	10	0.057	0.0021	10	42.50	5.19	8	2.91	0.31	7	83.44	2.79	8	14.94	0.67	10	85.19	0.68	10

Part II
Table 6

Table 7. P-value of Sex Effect within each strain

28 Inbred Strains	Body WT (g)	Lean Mass (g)	Fat Mass (g)	Area BMD (g/cm²)	BMC (g)	SPINE BMD (g/mm²)	OC (ng/ml)	T4 (ng/ml)	Adj. IGF-1	%Fat	%Lean
129S1/SvImJ	0.0000	0.0000	0.0000	0.0030	0.1390	0.0097	0.9274	0.0726	0.0003	0.0004	0.0003
A/J	0.0003	0.0000	0.0319	0.9514	0.0011	0.2731	0.7351	0.0517	0.6458	0.3174	0.2942
AKR/J	0.1795	0.0009	0.7684	0.8139	0.8566	0.2544	0.0893	0.1531	0.0075	0.1720	0.1770
BALB/cJ	0.0000	0.0000	0.6515	0.0155	0.0019	0.7354	0.0000	0.9098	0.0305	0.0017	0.0018
BTBR T⁺tf/tf	0.0100	0.0014	0.3915	0.0242	0.0715	0.0004	0.0001	0.0021	0.0001	0.6445	0.6641
BUB/BnJ	0.0021	0.0004	0.5766	0.0682	0.1090	0.0392	0.2683	0.3493	0.9364	0.3386	0.3317
C3H/HeJ	0.0000	0.0000	0.0183	0.0565	0.1130	0.5712	0.7640	0.3892	0.4816	0.8157	0.8578
C58BL/6J	0.0000	0.0000	0.0015	0.0181	0.4525	0.0001	0.7749	0.1662	0.0090	0.0812	0.0767
C57L/J	0.0003	0.0011	0.0002	0.8439	0.2827	0.0577	0.0000	0.0000	0.0000	0.0006	0.0007
C58/J	0.0000	0.0000	0.0007	0.0000	0.0000	0.5700	0.8442	0.2889	0.1189	0.3629	0.3350
CAST/EiJ	0.0003	0.0003	0.0241	0.0461	0.4062	0.0009	0.6384	0.3295	0.0120	0.6771	0.5953
CZECHII/EiJ	0.0000	0.0000	0.1327	0.5400	0.0701	0.2487	0.0011	0.4364	0.1105	0.1464	0.1173
DBA/2J	0.0000	0.0000	0.0141	0.0367	0.0583	0.2302	0.5551	0.1115	0.2832	0.4816	0.4828
FVB/NJ	0.0000	0.0000	0.0921	0.4565	0.0000	0.1956	0.0300	0.4955	0.0204	0.0005	0.0005
JF1/Ms	0.0000	0.0000	0.0000	0.0329	0.2883	0.0002	0.0042	0.0007	0.0354	0.0001	0.0000
MOLF/EiJ	0.0000	0.0000	0.0145	0.2816	0.3157	0.0660	0.0000	0.1343	0.2532	0.6024	0.6597
MSM/Ms	0.0000	0.0000	0.0042	0.5095	0.9641	0.0653	0.5502	0.1515	0.1400	0.4910	0.4245
NOD/LtJ	0.0000	0.0000	0.0053	0.0623	0.0049	0.0688	0.5213	0.2783	0.4566	0.4586	0.4625
NZB/B1NJ	0.0000	0.0000	0.4783	0.0164	0.0883	0.0000	0.0001	0.0097	0.6838	0.4284	0.4140
NZW/LacJ	0.0427	0.0000	0.0104	0.0949	0.0000	0.0135	0.0012	0.0401	0.0353	0.0002	0.0002
PERA/EiJ	0.0003	0.0000	0.0015	0.0001	0.0000	0.0000	0.5699	0.0001	0.0758	0.0000	0.0000
PL/J	0.0000	0.0000	0.0066	0.7165	0.0837	0.3543	0.8706	0.0230	0.4922	0.8995	0.8753
PWK/PhJ	0.0000	0.0000	0.0003	0.0917	0.0908	0.0003	0.3487	0.4566	0.8429	0.0016	0.0010
SJL/J	0.0000	0.0000	0.0226	0.0215	0.0081	0.2668	0.3890	0.8372	0.2015	0.2135	0.1773
SM/J	0.0000	0.0000	0.0008	0.0000	0.0000	0.1481	0.5397	--	0.4613	0.1786	0.1733
SPRET/EiJ	0.0023	0.0011	0.0135	0.0003	0.0026	0.0000	0.1476	0.8078	0.8393	0.0462	0.0540
SWR/J	0.0000	0.0000	0.7425	0.0037	0.0000	0.0556	0.7305	0.0002	0.0143	0.0014	0.0011
WSB/EiJ	0.0000	0.0000	0.0038	0.2189	0.0148	0.7967	0.0278	0.2803	0.8931	0.2630	0.2369

p<0.0001

Table 8: Correlation of female strain-mean data, 28 strains

	Body WT (g)	Lean Mass (g)	Fat Mass (g)	Area BMD (g/cm²)	BMC (g)	SPINE BMD (g/mm²)	OC (ng/ml)	T4 (ng/ml)	Adj. IGF-1	%Fat	%Lean
Body WT (g)	1.00	0.97	0.86	0.75	0.80	0.52	-0.19	0.21	0.28	0.57	-0.57
Lean Mass (g)	0.97	1.00	0.70	0.77	0.86	0.54	-0.12	0.24	0.31	0.35	-0.36
Fat Mass (g)	0.86	0.70	1.00	0.57	0.50	0.37	-0.28	0.12	0.17	0.88	-0.88
Area BMD (g/cm²)	0.75	0.77	0.57	1.00	0.94	0.90	-0.06	0.14	0.48	0.31	-0.31
BMC (g)	0.80	0.86	0.50	0.94	1.00	0.81	0.08	0.18	0.40	0.16	-0.16
SPINE BMD (g/mm²)	0.52	0.54	0.37	0.90	0.81	1.00	0.06	0.01	0.46	0.16	-0.16
OC (ng/ml)	-0.19	-0.12	-0.28	-0.06	0.08	0.06	1.00	-0.11	0.03	-0.37	0.37
T4 (ng/ml)	0.21	0.24	0.12	0.14	0.18	0.01	-0.11	1.00	0.04	0.12	-0.13
Adj. IGF-1	0.28	0.31	0.17	0.48	0.40	0.46	0.03	0.04	1.00	0.06	-0.06
%Fat	0.57	0.35	0.88	0.31	0.16	0.16	-0.37	0.12	0.06	1.00	-1.00
%Lean	-0.57	-0.36	-0.88	-0.31	-0.16	-0.16	0.37	-0.13	-0.06	-1.00	1.00

Correlation of male strain-mean data

	Body WT (g)	Lean Mass (g)	Fat Mass (g)	Area BMD (g/cm²)	BMC (g)	SPINE BMD (g/mm²)	OC (ng/ml)	T4 (ng/ml)	Adj. IGF-1	%Fat	%Lean
Body WT (g)	1.00	0.96	0.76	0.82	0.83	0.62	-0.02	0.32	-0.14	0.32	-0.32
Lean Mass (g)	0.96	1.00	0.54	0.84	0.90	0.62	-0.04	0.34	-0.10	0.05	-0.05
Fat Mass (g)	0.76	0.54	1.00	0.49	0.38	0.39	0.03	0.16	-0.19	0.85	-0.84
Area BMD (g/cm²)	0.82	0.84	0.49	1.00	0.95	0.89	0.13	0.27	0.07	0.08	-0.07
BMC (g)	0.83	0.90	0.38	0.95	1.00	0.82	0.08	0.25	0.08	-0.10	0.10
SPINE BMD (g/mm²)	0.62	0.62	0.39	0.89	0.82	1.00	0.23	0.23	0.20	0.10	-0.09
OC (ng/ml)	-0.02	-0.04	0.03	0.13	0.08	0.23	1.00	-0.01	0.08	0.02	-0.02
T4 (ng/ml)	0.32	0.34	0.16	0.27	0.25	0.23	-0.01	1.00	0.02	0.00	0.00
Adj. IGF-1	-0.14	-0.10	-0.19	0.07	0.08	0.20	0.08	0.02	1.00	-0.07	0.06
%Fat	0.32	0.05	0.85	0.08	-0.10	0.10	0.02	0.00	-0.07	1.00	-1.00
%Lean	-0.32	-0.05	-0.84	-0.07	0.10	-0.09	-0.02	0.00	0.06	-1.00	1.00

Part II
Table 8

Using Inbred Mouse Strains to Identify Models for Determining Genetic Regulation of Bone Strength

L.R. Donahue, C.J. Rosen, G.A. Churchill, S-W Tsaih, M.L. Bouxsein, L. Horton, A.R. Sears & W.G. Beamer, The Jackson Laboratory, Bar Harbor, ME

The measurement most often used to predict bone strength is bone mineral density measured by x-ray absorptiometry. Yet other bone traits, including size, shape, architecture and material properties, as well as muscle mass, are important qualitative contributors to bone strength and should be considered when predicting fracture risk. Coupled with this expanded interest in characterizing bone and muscle, is an intense search for genetic determinants of fracture based on these recognized indices of bone strength. Interpretation of these studies is complicated by heterogeneity in human populations and by environmental differences, indicating that genetic regulation of bone strength is complex and that animal models are critical to progress in this field. The purpose of this work was to determine which muscle and bone phenotypes best predict femoral bone strength in inbred strains of mice and to discover models appropriate for further genetic analyses of factors that contribute to bone strength.

We collected skeletal geometry, muscle mass, volumetric BMD (vBMD), and bone strength data from female mice of 9 genetically diverse inbred strains of mice. pQCT (SA Plus,Stratec) was used to measure vBMD, periosteal perimeter (Ps.pm), andmuscle area at the mid diaphysis; digital calipers were used to measure femur length and medio-lateral diameter (M/L) at mid diaphysis; peak load, stiffness, and energy to break (EB) were measured by three point bending (MTS). EB is often used as a measure of the toughness of bone, or the amount of energy required to cause bone to fracture.

We found that peak load and stiffness were both predicted by femur length (p=.002;.001), M/L diameter (p=.009;.029), muscle area (p=.001;.011), and vBMD (p=006;.002). EB was predicted by Ps.pm (p=.044), M/L (p=.037), and muscle area (p=.009), but was independent of vBMD. A strategy to genetically decompose the EB phenotype could be based on crosses between a low EB (low bone size/muscle area) strain and a high EB (plus high bone size/muscle area) strain. Such a combination is present in SWR/J and FVB/NJ, or in 129/SvImJ crossed to C57BL/6J. The F2 generation progeny from either cross would provide mice that could be used to analyze the genetic regulation of EB.

These data show that bone geometry, density and muscle mass are important determinants of femoral strength, and illustrate that bone strength is a complex trait with genetic regulation. We propose a genetic model using inbred strains of mice to discover the genetic regulation bone geometry, muscle mass, and BMD, allowing determination of their relative contributions to overall bone strength.

Skeletal Plasticity…….

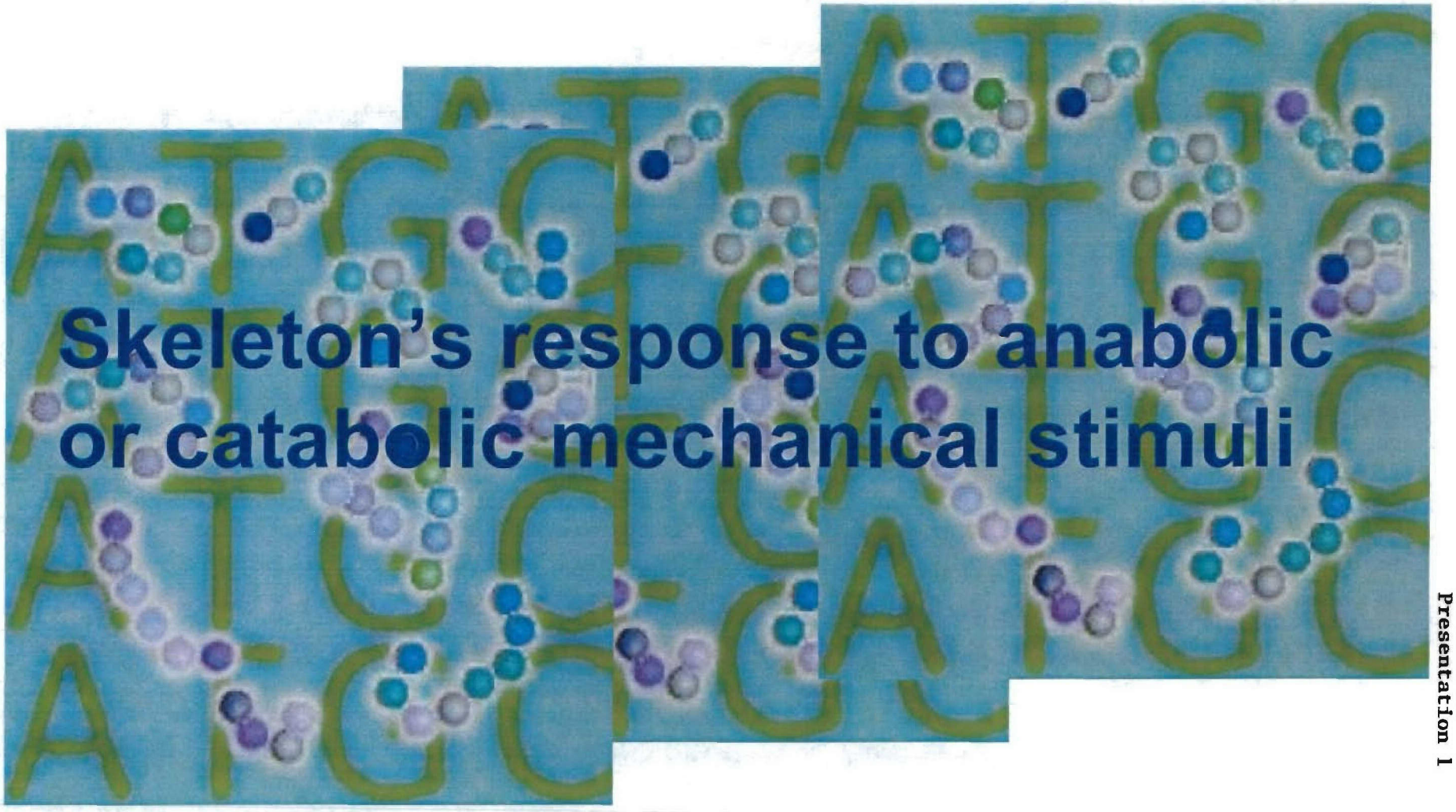

Skeleton's response to anabolic or catabolic mechanical stimuli

bone is a loadbearing structure

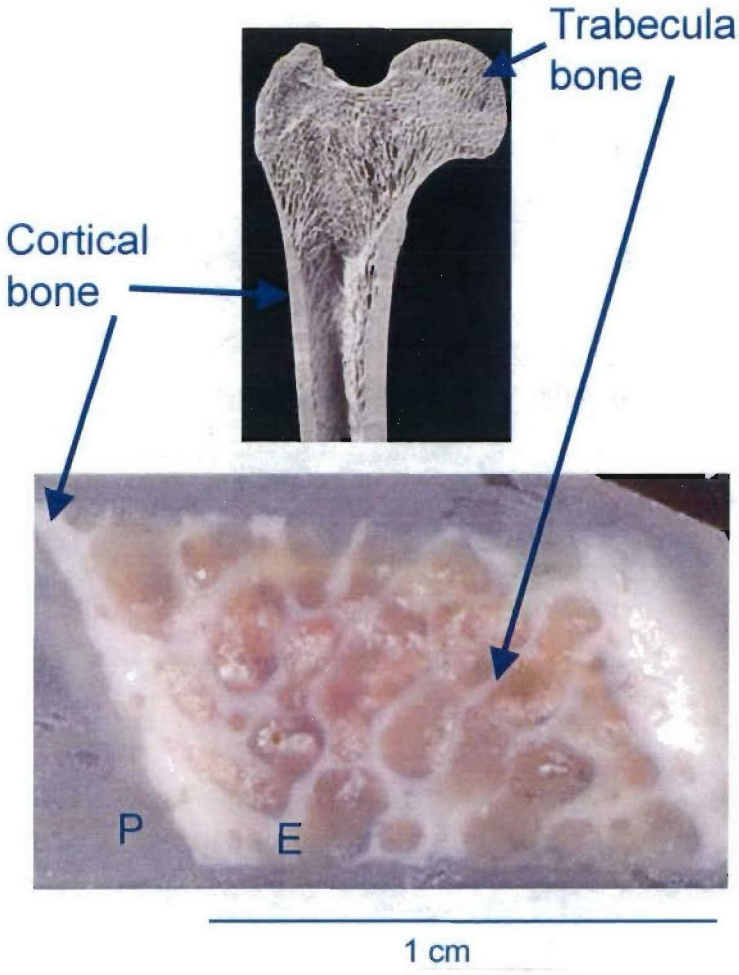

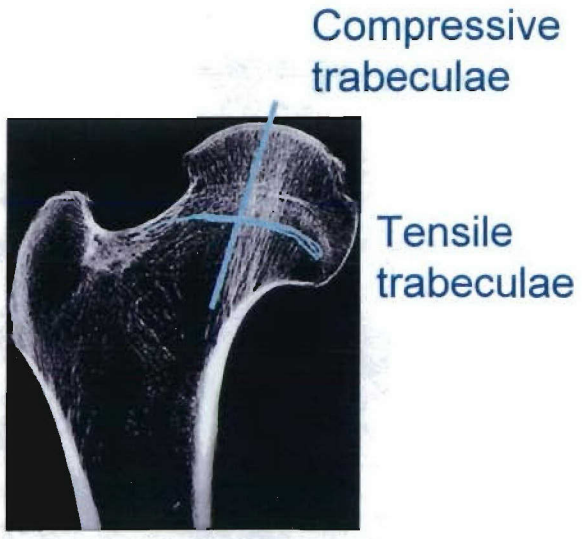

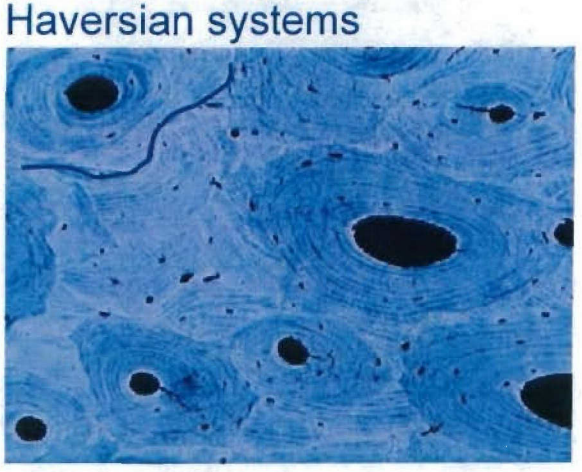

remove mechanical environment

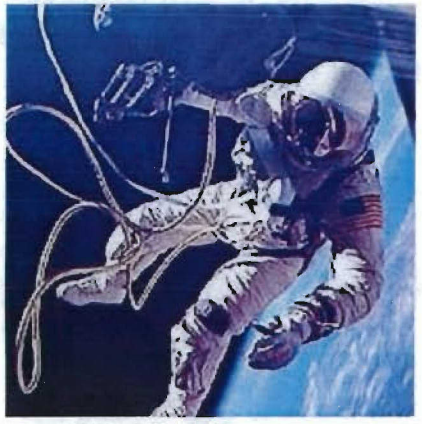

↓ 0-23% trabecular bone
0-4% cortical bone
6 mo in space

↓ BMD 2.3%, 17 wks

Increase in resorption

&

Decrease in formation

↓

Bone loss

Bone remodeling

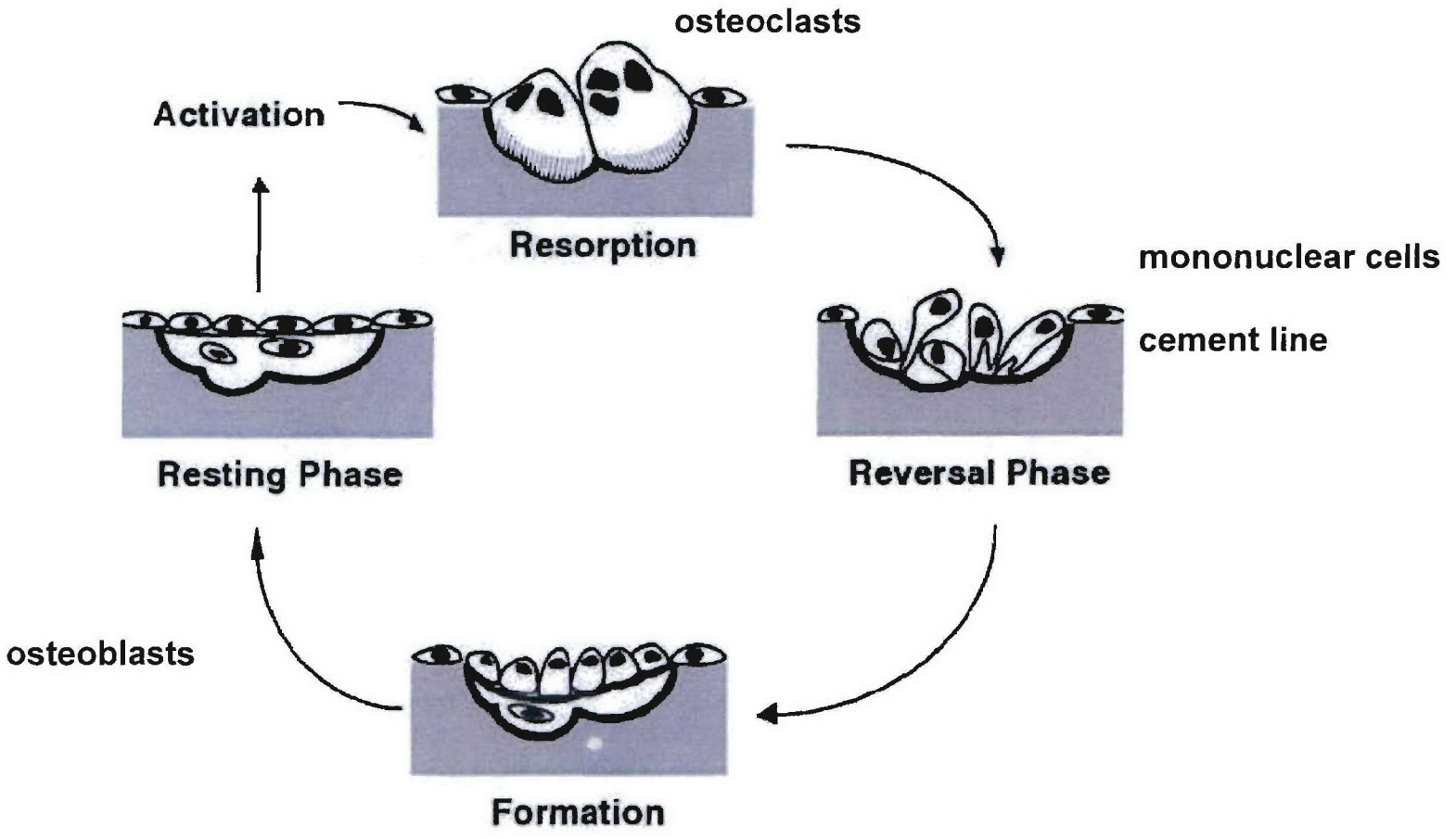

Modified from Roland Baron, 2003

the physics…..
bone stress-strain curve

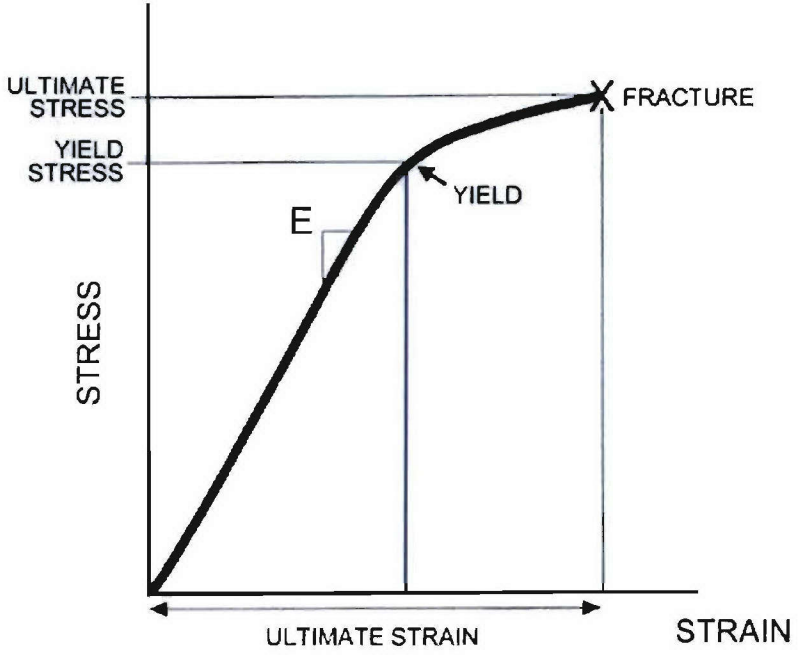

Strain
- compression
- tension
- shear

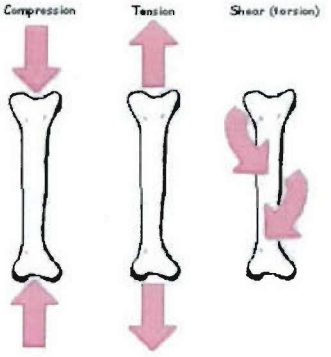

Stress (N, Pa)
- ultimate stress
- yield stress

Elasticity - Stiffness
- Young's modulus (*E*)

Plasticity - Brittleness
- postyield strain

Toughness

How much strain is enough?

~3500 μstrain with vigorous activity

For how long? 26.2 miles? Few minutes?

Limit - bone fails at ~7000 μstrain

Need ≥ 1000 μstrain to be anabolic?

Bone density in athletes

RUNNING

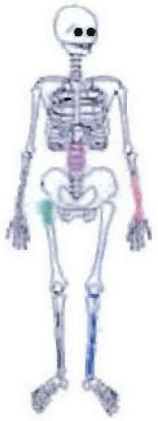

Spine Not different
Hip 10% higher
Arm not different
Leg 10% higher

CYCLING

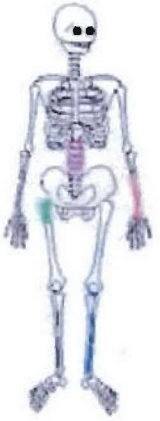

Spine not different
Hip 2% lower
Arm 1% lower
Leg 1% higher

SWIMMING

Spine 3% higher
Hip 3% lower
Arm 1% higher
Leg 3% lower

WEIGHT LIFTING

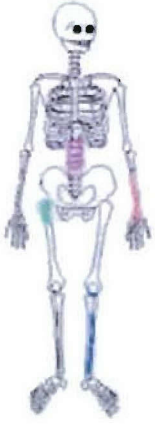

Spine 12% higher
Hip 6% higher
Arm 20% higher
Leg 11% higher

SOCCER

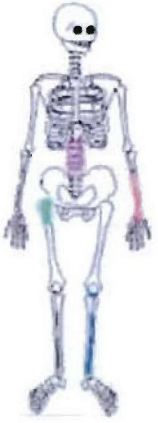

Spine 7% higher
Hip 20% higher
Arm 14% higher
Leg 16% higher

KAYAKING

Spine not different
Hip not different
Arm 10% higher
Leg not different

More ?? than we have answers…

What part does genetic predisposition play in the way that the skeleton responds to mechanical stimulation?

How does the density and quality of bone at the outset affect the response to load or disuse?

Utimately, how can we tailor interventions that will take advantage of genetic tendencies?

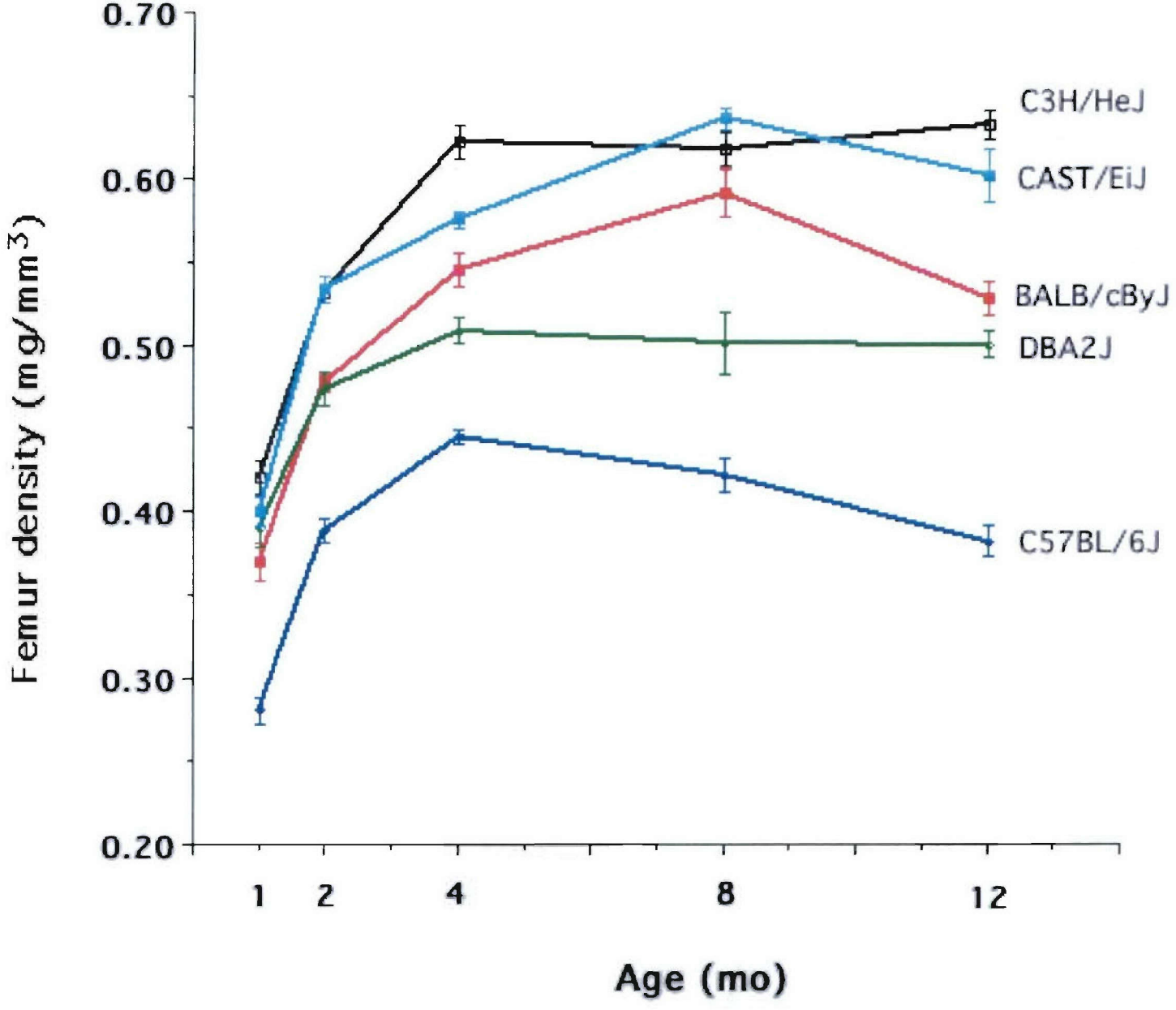
Development of bone density in females of five inbred strains
0.70
0.60
0.50
0.40
0.30
0.20
Femur density (mg/mm3)
1
2
4
8
12
Age (mo)
C3H/HeJ
CAST/EiJ
BALB/cByJ
DBA2J
C57BL/6J

μCT of the distal femur

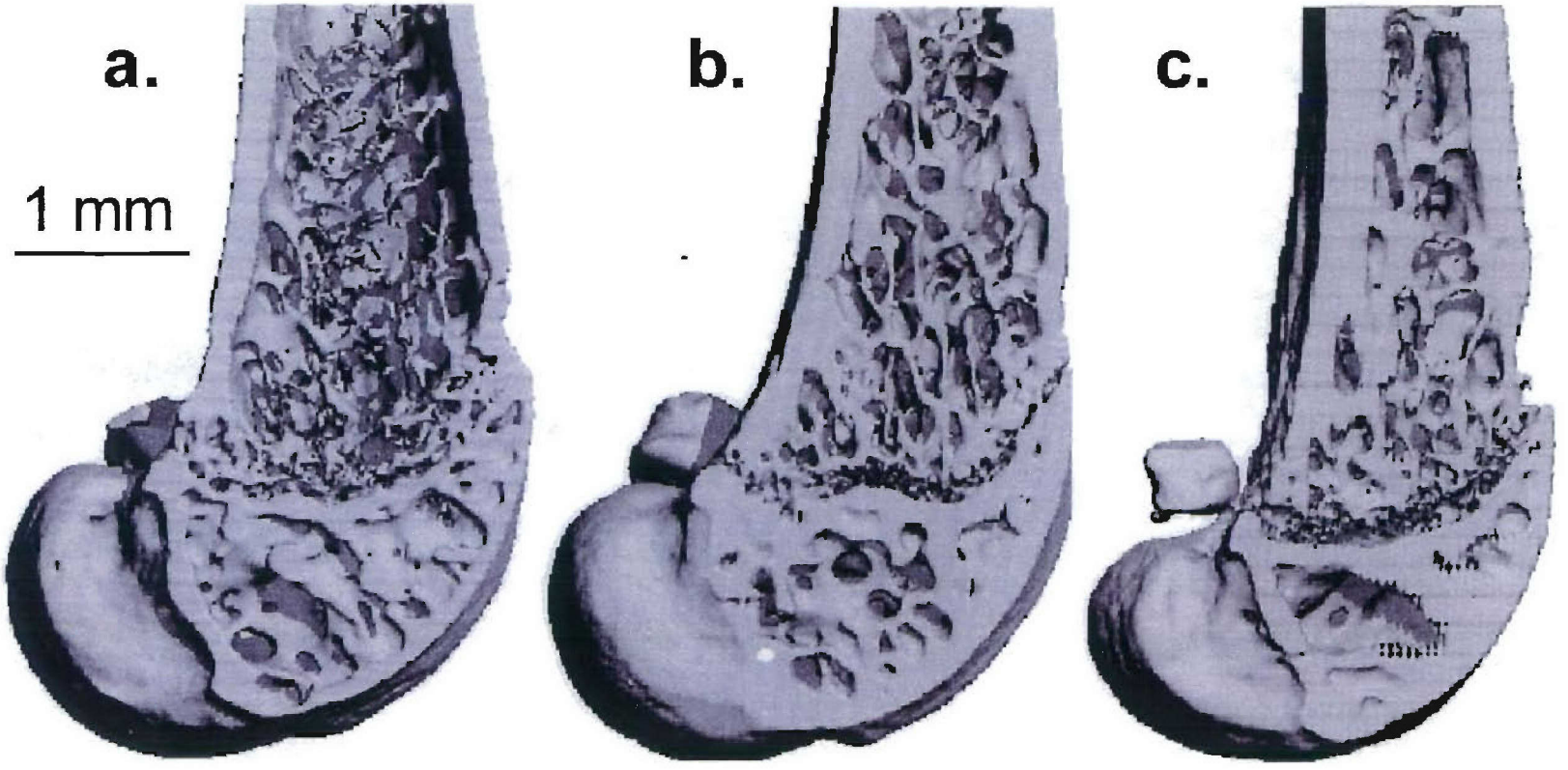

C57BL/6J BALB/cByJ C3H/HeJ

Judex, Donahue, Rubin 2002

metaphysis, epiphysis, middiaphysis of the femur

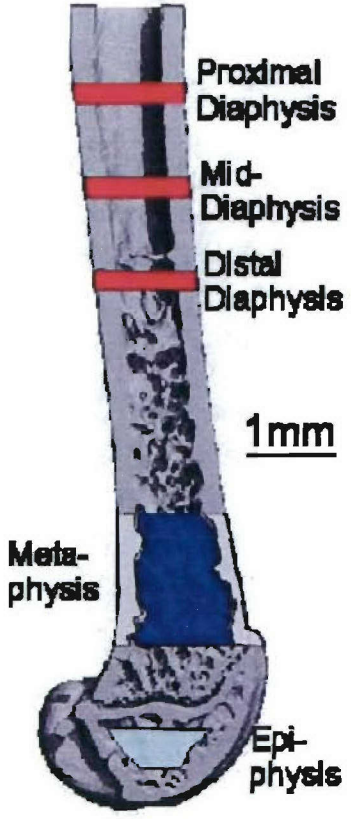

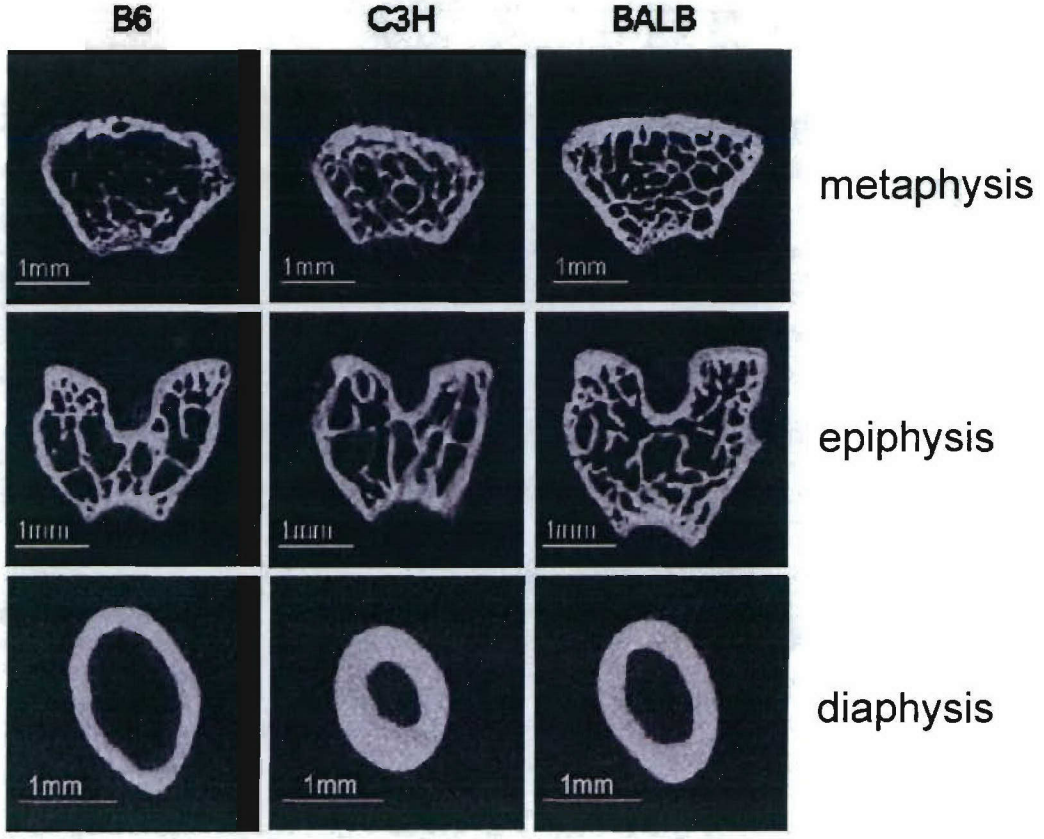

Judex, Garman, Squire, Donahue, Rubin 2004

Strain - orders of magnitude less?

Vibration platform to deliver low load at high frequency

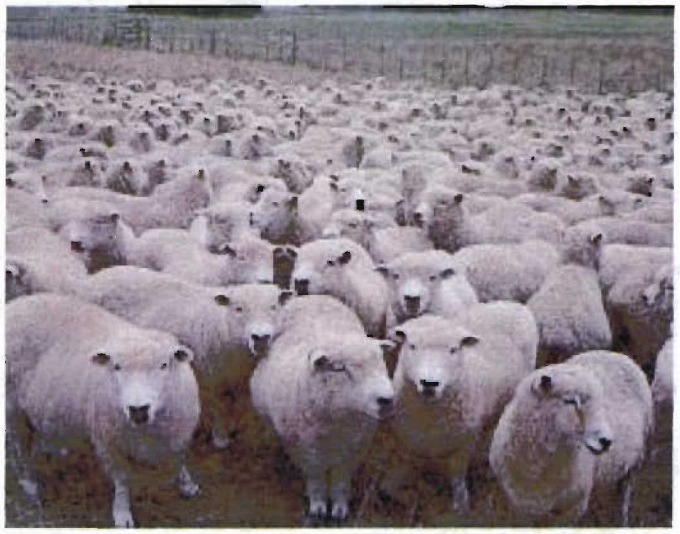

sheep
<5 μstrain at 30Hz
20 min/day 1yr
43% BMD femur
27% strength

Stimulate formation
Enhance BMD
Improve quality
Stiffness & strength

roosters and turkeys
200 μstrain at 30Hz
cortical bone

rats
<10 μstain at 90Hz
10 min/day
Inhibit disuse oseopenia

And, Yes, it works in humans

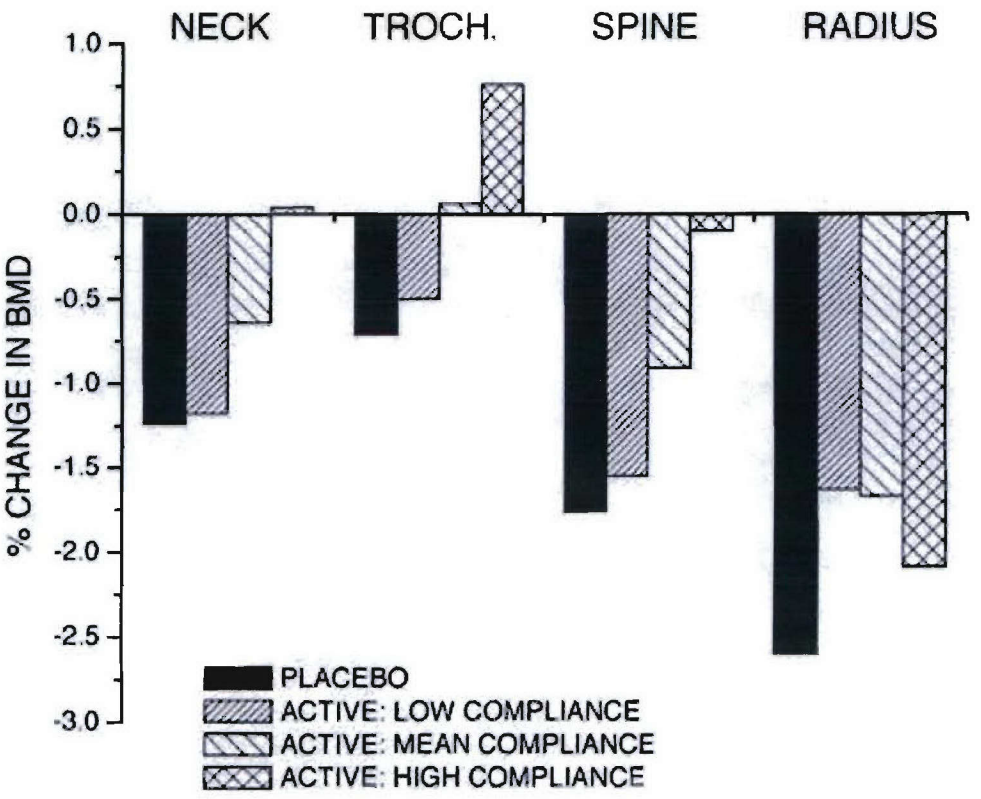

<5 µstrain (~.2g) at 30 Hz
2x10min/day for 1 yr

RUBIN, RECKER, CULLEN, RYABY, MCCABE, MCLEOD, 2004

Experimental Design

B6, BALB, C3H
Females, 16 wks
8-12 mice /group

Histomorphometry

Right proximal tibia

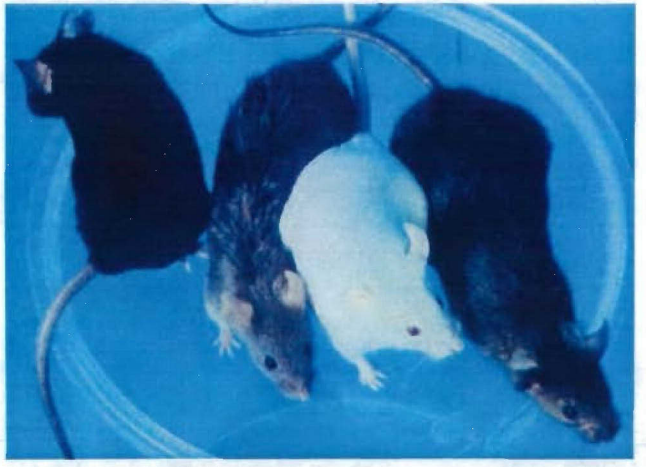

Mechanical Loading

Vibrating plate

- <5 μstrain
- 45 Hz
- 10min/day
- 5 days/wk - 21days

Disuse

- Hind limb suspension
- 21 days

BV/TV trabecular bone, proximal tibia

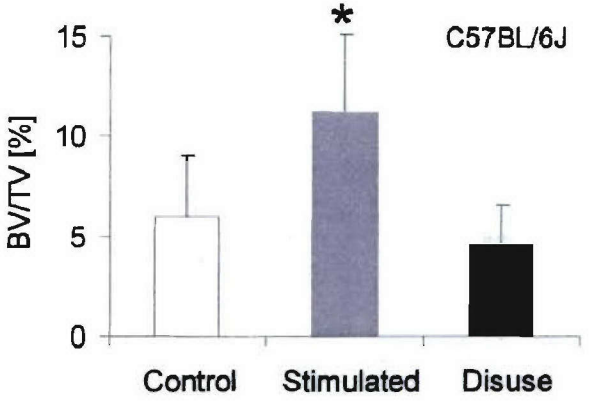

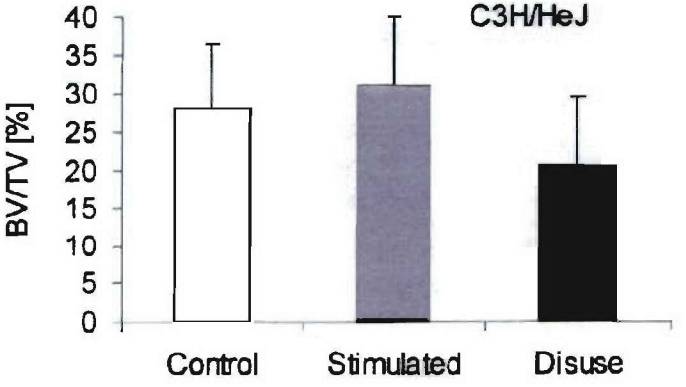

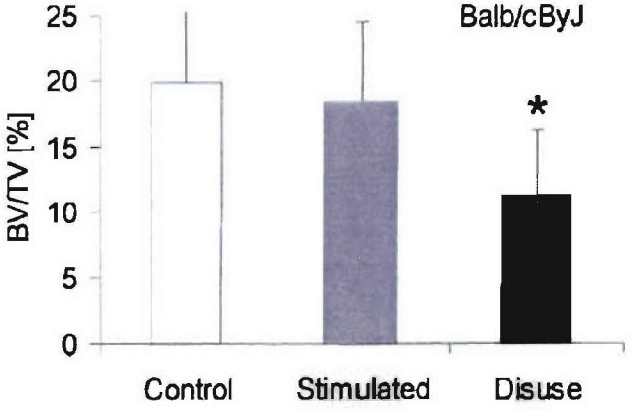

Judex, Donahue, Rubin, 2002

% Difference BFR/TV

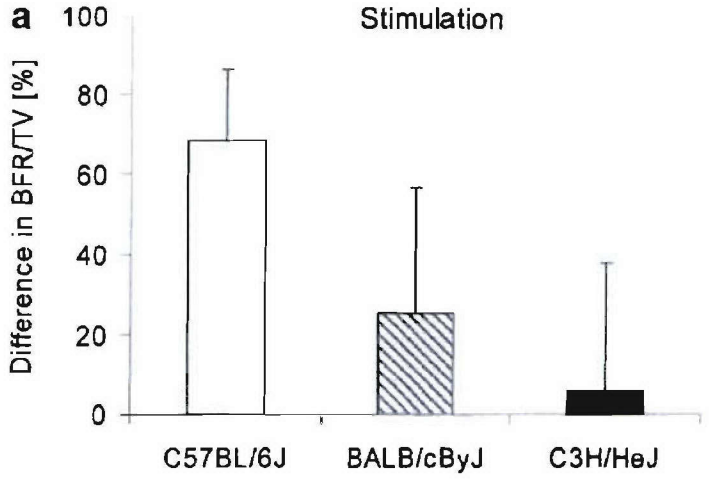

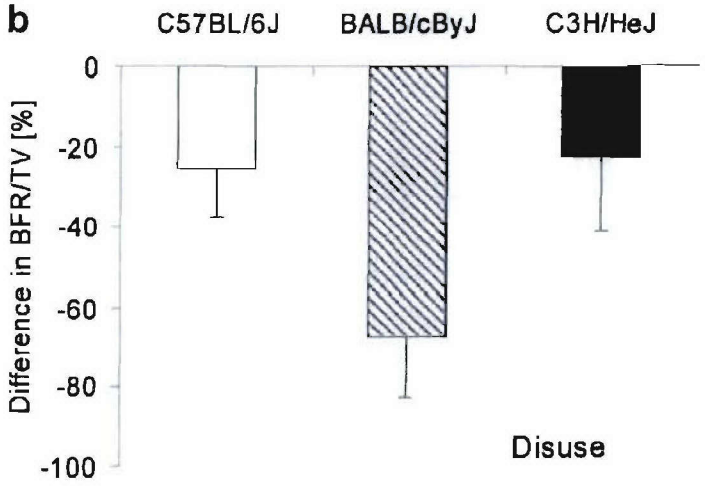

Judex, Donahue, Rubin, 2002

Strain and site specific disuse related changes in females

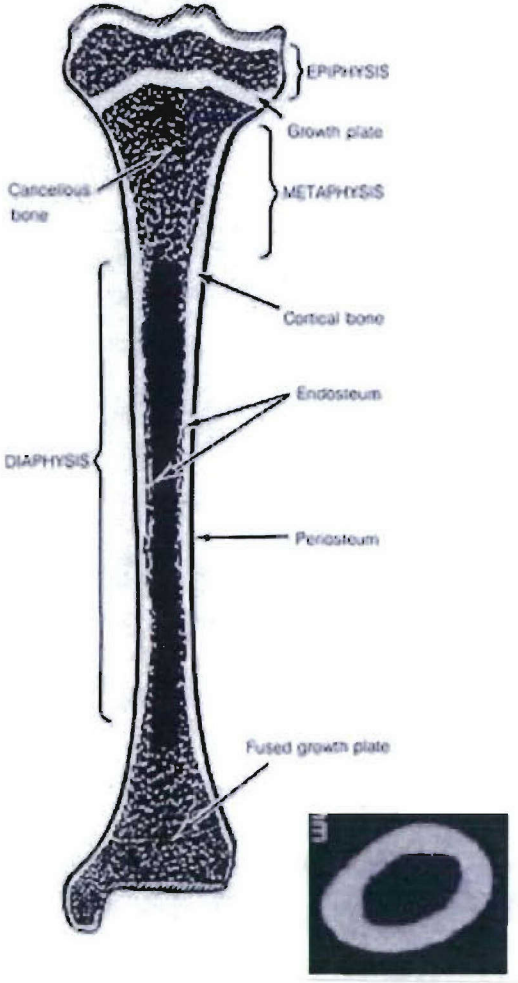

		B6	*C3H*	*BALB*
Metaphysis	BV/TV	↓↓↓	—	↓↓↓↓↓↓
Epiphysis	BV/TV	↓↓↓	—	↓↓↓
Metaphyseal Cortex	Ct.Ar	↓	—	↓↓↓
	Ec.En	↑	↑↑↑	↑↑
	Ps.En	—	↑↑	—
Diaphysis	Ct.Ar	↓↓	—	↓
	Ec.En	—	—	—
	Ps.En	—	—	—

BALB/cBy Female

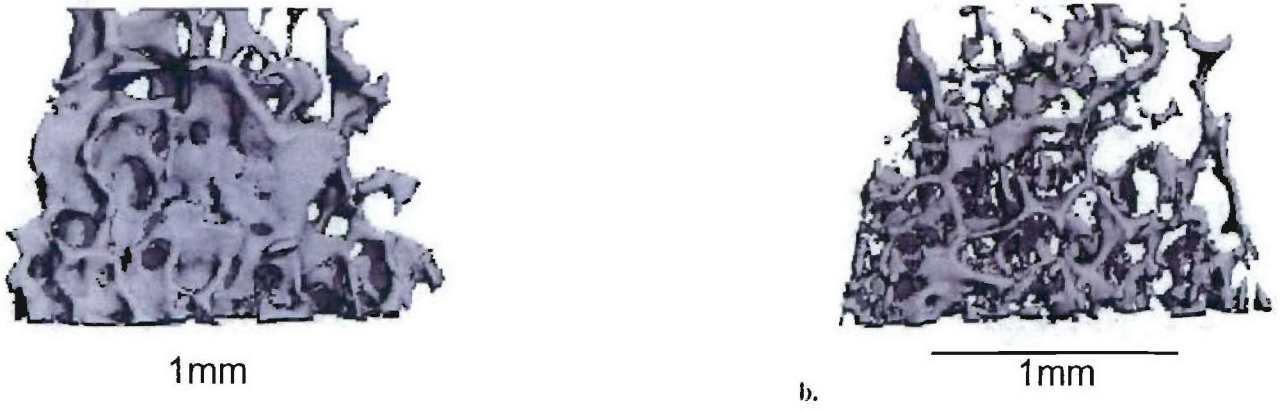

trabecular bone in femur metaphysis

59% loss of bone fractional volume

Judex, Garman, Squire, Busa, Donahue, Rubin, 2004

C57BL/6J female

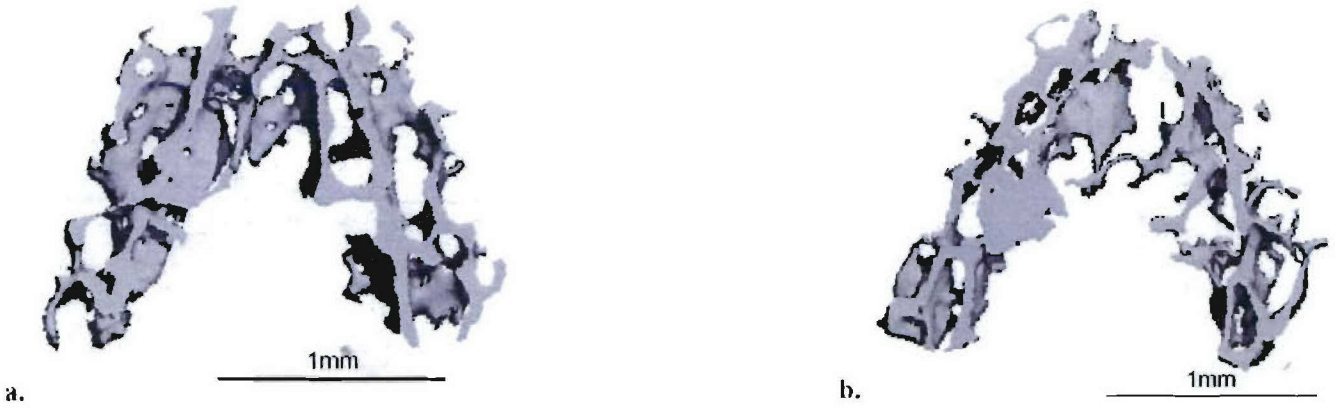

trabecular bone in the femur epiphysis

21% decrease in BV/TV

13% decrease in trabecular thickness

37% loss of connectivity

Judex, Garman, Squire, Busa, Donahue, Rubin, 2004

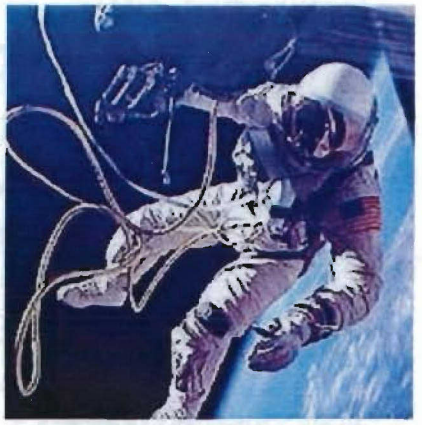

NASA funding:

Sensitivity of the Skeleton to Weightlessness

<u>osteopenia:</u>
1.6% per mo loss of BMD
lower appendicular
skeleton

<u>sarcopenia:</u>
5% per mo loss of
maximum voluntary
muscle contractility

QTL analysis
responders vs non-responders
500 CC3 F2s
males and females

21 days of disuse
in vivo µCT at 0,1,2,3 wks
distal femur & proximal tibia
10 min/mouse, 10micron res.

CC3 F2 females

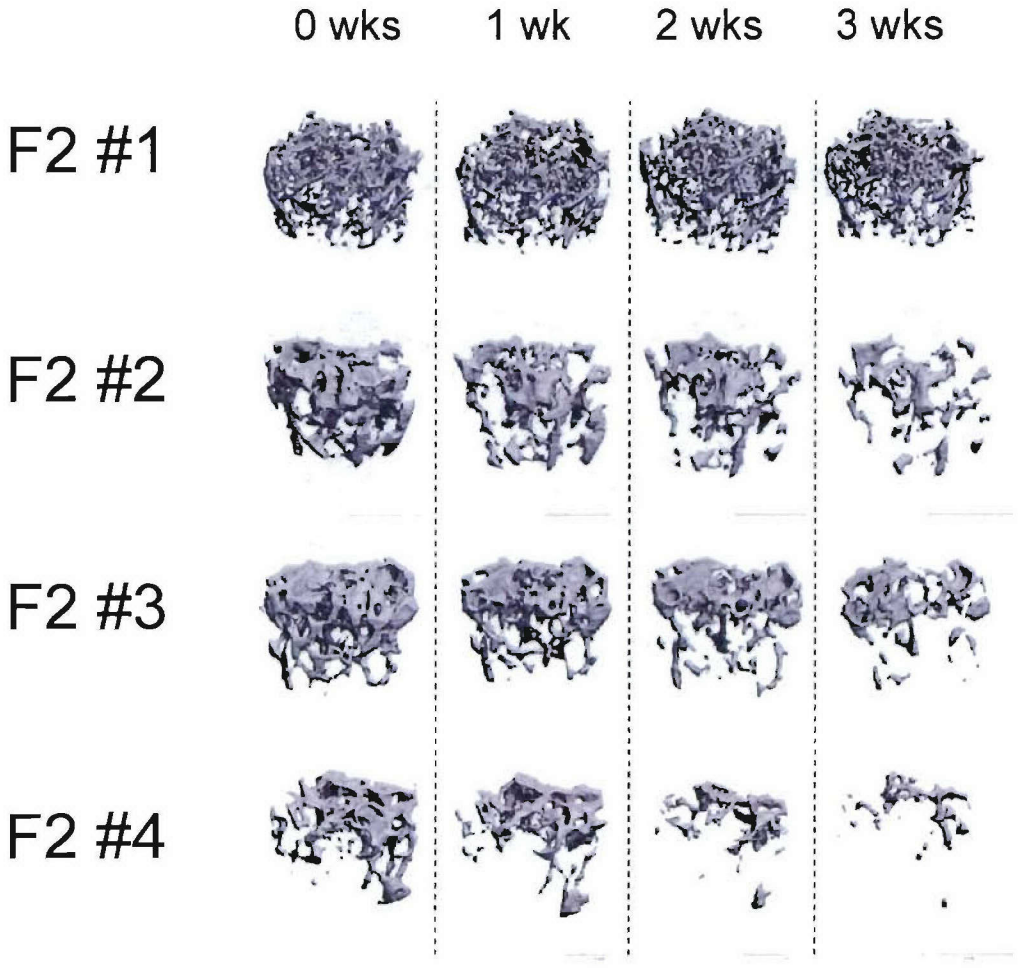

trabecular bone in metaphysis of distal femur

17wks old at start

10-86% bone loss

Genetic model to test skeletal response to loading and unloading

- Bone site specificity [and gender specificity….]
- Bone compartment specificity - differential responses in cortical & trabecular bone at a single site
- Potential to identify genotypes and bone sites that would benefit most from mechanical stimulation
- Genetically driven, non-drug treatments for:
  - disuse osteopenia
  - developmental/nutritional delays in bone formation
  - steroid induced bone loss
  - predisposition to stress fracture
  - age induced osteoporosis

Stefan's lab at its best!

The Extra Strong TJL Duo

Coleen - raising mice and shipping them to Stefan's lab at Stony Brook

Vicki - preparing DNA for SNP typing

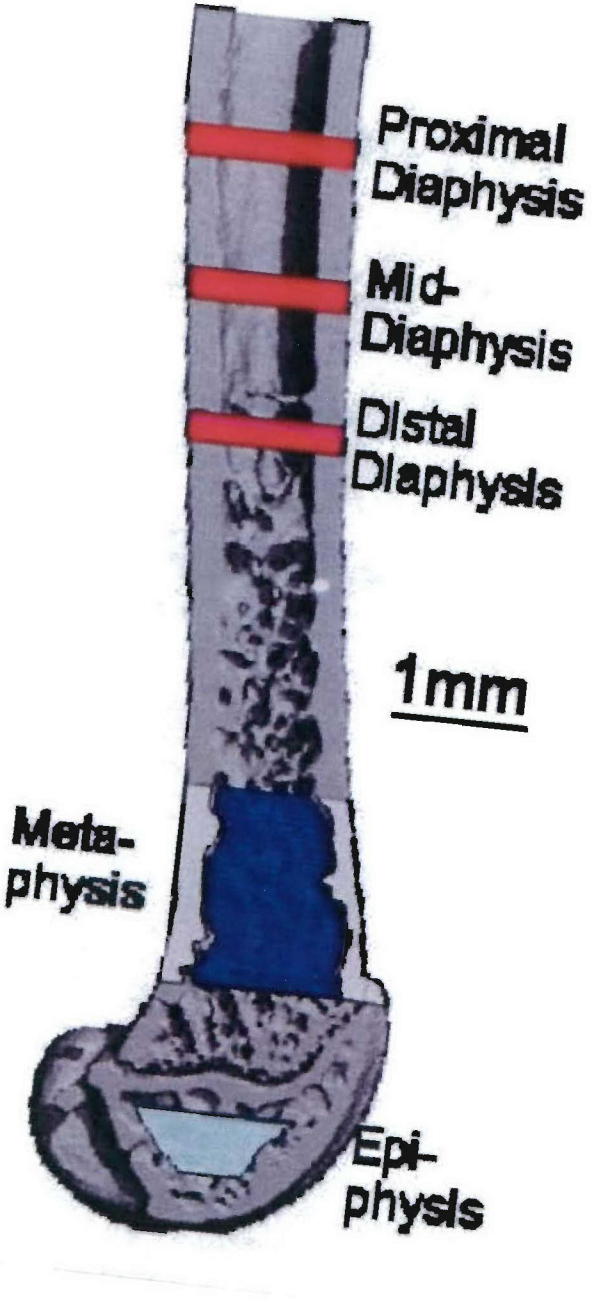
Proximal
Diaphysis
Mid-
Diaphysis
Distal
Diaphysis
1mm
Meta-
physis
Epi-
physis

APPENDIX

Part III: Diallele Cross for Skeletal/Body Composition

Paper submitted to *Mammalian Genome* entitled, "Quantitative Trait Mapping in a Diallel Cross of Recombinant Inbred Lines." Shirng-Wern Tsaih, Lu Lu, David C. Airey, Robert W. Williams, Gary A. Churchill.

Quantitative Trait Mapping in a Diallel Cross of Recombinant Inbred Lines

Shirng-Wern Tsaih[1], Lu Lu[2], David C. Airey[3], Robert W. Williams[2], Gary A. Churchill[1]

Affiliations:

1 The Jackson Laboratory, 600 Maine Street, Bar Harbor, ME 04609

2 University of Tennessee, Center for Neuroscience. 885 Monroe Ave, Memphis, TN 38163

3 Vanderbilt University, Department of Pharmacology, Nashville, TN 37232

Corresponding author:

Gary A. Churchill

The Jackson Laboratory

600 Main Street

Bar Harbor, ME 04609 USA

Email: garyc@jax.org

207-288-6189 (voice)

207-288-6077 (fax)

ABSTRACT

A recombinant inbred intercross (RIX) is created by generating diallel F1 progeny from one or more panels of recombinant inbred (RI) strains. This design was originally introduced to extend the power of small RI panels for the confirmation of quantitative trait loci (QTL) provisionally detected in a parental RI set. For example the set of 13 CXB (C57BL/6ByJ x BALB/cByJ) RI strains can in principle be supplemented with 156 isogenic F1s. We describe and test a method of analysis, based on a linear mixed model, that accounts for the correlation structure of RIX populations. This model suggests a novel permutation algorithm that is needed to obtain appropriate threshold values for genome-wide scans of an RIX population. Despite the combinational multiplication of unique genotypes that can be generated using an RIX design, the effective sample size of the RIX population is limited by the number of progenitor RI genomes that are combined. When using small RI panels such as the CXB there appears to be only modest advantage of the RIX design when compared to the original RI panel for detecting QTLs with additive effects. The RIX however does have an inherent ability to detect dominance effects, and unlike RI strains, the RIX progeny are genetically reproducible but are not fully inbred, providing somewhat more natural genetic context. We suggest a breeding strategy, the balanced partial RIX, that balances the advantage of RI and RIX designs. This involves the use of a partial RIX population derived from a large RI panel in which the available information is maximized by minimizing correlations among RIX progeny.

INTRODUCTION

The construction of a recombinant inbred (RI) strain panel typically begins with an outcross between two-fully inbred progenitor strains. F1 hybrid animals are bred to each other to produce F2 animals, each with a unique genometype. A single pair of F2 animals is chosen and these mice and their progeny are brother-sister mated for greater than 20 generations to create a new inbred strain. This process is repeated starting with several distinct pairs of F2 animals to generate a panel of recombinant inbred strains (Bailey 1971). RI strain panels offer some compelling advantages for mapping complex genetic traits compared to intercross (F2) or backcross (BC) populations, and RI panels have been used to map both Mendelian and quantitative traits in the mouse (Plomin and McClearn 1993; Taylor 1996) and in other organisms (Limami et al. 2002; Nuzhdin et al. 1997; van Swinderen et al. 1997). The accumulation of recombination events during inbreeding results in an average 4-fold increase in recombination in an RI strain compared to a single generation genetic map (Haldane and Waddington 1931). RI strains need to be genotyped only once. Multiple animals with the same genotype can be phenotyped. Thus we can assess phenotypes in multiple environments, measure multiple invasive phenotypes, and can repeat noisy measurements to increase their precision (Belknap 1998; Knapp and Bridges 1990). RI strains are homozygous at essentially all loci, which can increase power for detecting additive quantitative trait loci (QTL) effects compared to F2 populations in which half of animals are heterozygous at any given locus.

There are several drawbacks to working with RI lines as well. RI strains are fully inbred and thus it is not possible to estimate dominance effects using RI strains. Moreover, the natural buffering effects of heterozygosity will be absent in RI strains

(Hartwell 2004). The inbreeding phase of RI strain generation in mice can take 4-5 years, and newly generated strains require dense genotyping. Thus the development of a RI strain panel requires considerable effort and cost. This high initial barrier has restricted the development of mouse RI panels and the resulting small size of most panels limits their usefulness, especially for quantitative trait analysis (Peirce et al. 2004; Taylor 1996; Williams et al. 2004; Williams et al. 2001). The power to detect a QTL increases with increasing number of RI strains (Belknap 1998; Belknap et al. 1996). Thus, the limited number of distinct recombinant genomes is the most serious disadvantage of mapping with RI strain panels compared to other mapping populations that can be rapidly expanded to hundreds or thousands of individuals.

A common feature of any small RI panel is the occurrence of non-syntenic associations in which pairs of loci on different chromosomes have similar or identical strain distribution patterns (SDPs) and therefore appear to be linked. This association can arise either as a result of random fixation of alleles on different chromosomes during the production of RI strains or as a result of selection for particular combinations of alleles on different chromosomes. Unlinked loci showing allelic association can lead to false positive signals when mapping complex traits (Williams et al. 2001). For example, if a QTL is linked to one marker from an associated pair, a high LOD score will also be generated at the other marker. In the case of perfect allelic association, the LOD scores would be identical and there is no analytic approach that can resolve them. In contrast, segregating populations (F2 or BC) can generate a large number of distinct genotypes and, for mapping populations greater than 100 animals, non-syntenic associations of this type are very rare events.

The recombinant inbred intercross (RIX) strategy was first introduced by Threadgill and colleagues (Threadgill et al. 2002) as a means to dramatically increase the number of unique recombinant genomes available using an RI panel. RIX animals are the F1 progeny from a mating between two different RI strains. A panel of n RI strains can generate $n\times(n\text{-}1)$ unique RIX genotypes and furthermore, no additional genotyping is required, as the RIX genotype can be inferred from the parental RI genotypes. RIX animals are reproducible and they share many of the other advantages of an RI panel. RIX animals are heterozygous at one half of all loci which will allow estimation of dominance effects. RIX animals are not fully inbred and thus represent a more realistic genetic constitution. Phenotypic variances within F1 may be lower than for inbred RI animals, due to the buffering capacity of their hemi-heterozygous genome structure.

There are disadvantages to mapping with an RIX cross as well. As we demonstrate here, the combinatorial increase of unique RIX genomes does not overcome the limitation of having a small RI panel. RIX genomes retain the same recombinations as the parental RI strains. There are no new recombinations and moreover, the pattern of non-syntenic association in the RI set will be retained in the RIX cross.

Analysis of the RIX mapping population presents some challenges. RIX progeny are related to one another in different degrees. Widely used statistical methods for mapping quantitative trait loci (QTL) assume that all individuals are equally correlated and thus effectively independent. The correlation structure of RIX progeny violates this assumption. Here we propose a mixed linear model analysis (Littell et al. 1996) and a novel permutation test to account for the correlation among RIX progeny. We present a comparison between the mixed model approach and standard QTL analysis methods

using brain weight phenotype from a CXB (C57BL/6ByJ x BALB/cByJ) derived RIX population. We then use simulations to develop further insights into the statistical nature of the RIX cross. We provide some suggestions for more effectively using the RIX design that are particularly applicable to larger RI panels such as the LXS set (n=77) (Williams et al. 2004), the enlarged BXD set (n=80) (Peirce et al. 2004), or the proposed Collaborative Cross (n=1000) (Churchill, G.A. et al. 2004).

MATERIAL AND METHODS

1. Diallel Cross

An RIX cross has the same genetic structure as a classical diallel cross (Griffing 1956; Hayman 1954a; 1954b) in which the progeny of all pairwise and reciprocal matings are generated from a set of inbred lines. Suppose a set of p inbred lines is chosen and crosses among these lines are made. This procedure gives rise to a maximum of p^2 unique combinations of haploid genomes. This number is doubled when both sexes are considered. Data from such combinations can be set out in a $p \times p$ table in which x_{ii} represents the mean phenotype of the ith parental inbred strain, and x_{ij} represents the mean phenotype of the F_1 hybrid from crossing the ith and jth inbred strains, and x_{ji} represents the mean for the reciprocal cross. A diallel cross is full (or complete) if it includes all the $p(p\text{-}1)$ crosses and p parental lines (table 1A); otherwise, it is partial (or incomplete). A half diallel cross is a partial diallel with only one member of each reciprocal cross pair. The half diallel cross may or may not include the parental lines (table 1B). A balanced partial diallel cross can be formed by selecting a subset of crosses in which each parental strain occurs an equal number of times as both the mother and as

the father (table 1C). For example, a balanced partial diallel of 16 hybrids can be derived from a set of 8 parental lines by choosing each RI line twice as the mother and twice as the father in a set of matings. Progeny families belonging to the same row or column in the diallel array have one parent in common, the progeny families in the same row or column are half-sibs. The relationship among RIX progeny can be divided into three categories: (1) RIX animals that share no common parents, and (2) RIX animals that share exactly one common parent, and (3) reciprocal pairs that share two parents in common.

The simplest statistical model of a diallel cross excludes crosses within parental types (table 1B) and assumes that there are no sex-linked effects and no mitochondrial, cytoplasmic or epigenetic parental effects. The latter assumptions imply that the reciprocal crosses will share the same mean trait value so we could collapse the data to a half diallel (Griffing 1956; Wright 1985). This model for the phenotype of the *k*th offspring of the $i \times j$ mating can be written as

$$y_{ijk} = \mu + g_i + g_j + s_{ij} + e_{ijk} \qquad [1]$$

where μ is the population mean, g_i and g_j are the general combining abilities (GCA) of parents i and j, $s_{ij} = s_{ji}$ is the specific combining abilities (SCA) of $i \times j$ matings, and e_{ijk} is random error associated with *k*th individual within the $i \times j$ progeny. In this model the values of the mother and father effects are tied together as indicated in the notation. In other words, the GCA of a strain is the same regardless of whether the strain was the mother or the father of the F1 progeny. GCA describes the average performance of a parent in hybrid combination with other genotypes. SCA describes the degree to which specific parental combinations lead to deviations in progeny phenotypes from

expectations based on the average parental performance. When the available data are strain averages, the index *k* is dropped and SCA terms are absorbed into the error. Classical diallel analysis does not use genetic marker data or address the problem of mapping the genetic loci responsible for phenotypic variation.

2. A Simple Model

Linear model based analysis of quantitative phenotypes has proven to be a powerful and robust method for QTL mapping in classical populations derived from biparental crosses between inbred lines (Lander and Botstein 1989). The observed phenotype y_i for the *i*th individual with QTL genotype *m(i)* in a sample of size *n* may be described by the linear model

$$y_i = \mu + Q_{m(i)} + \varepsilon_i \qquad [2]$$

where μ is the population mean, $Q_{m(i)}$ is the effect of the *m*th QTL genotype, and ε_i is the residual error, usually assumed to be distributed as N (0, σ_ε^2). Note that $Q_{m(i)}$ may represent a multiple locus genotype. Interaction terms or covariates, such as sex, can also be incorporated in the above model (Ahmadiyeh et al. 2003). We refer to this model as the *simple model*. It assumes that all individuals are equally correlated and thus effectively independent. Therefore, it is suitable for backcross, intercross and unreplicated RI populations. In the case of replicated RI populations, model [2] can be applied to strain averages. However, in the case of RIX populations, model [2] is not appropriate. The strains are related in various degrees and a mixed model analysis is needed to account for their correlation structure.

3. Mixed Model

We have adapted the half diallel model [1] to include the effects of genetic loci in an RIX population. We define a linear mixed model in which the GCA (additive effects) of parents are random effects and the QTL genotypes are fixed effects. The SCA effects are assumed to be negligible here and have been absorbed in the error component. The observed phenotype y_{ijk} of the *k*th individual with mother *i* and father *j* can be written as

$$y_{ijk} = \mu + g_i + g_j + Q_{m(i,j)} + \varepsilon_{ijk} \qquad [3]$$

where μ , g_i, and g_j are as in model [1] and $m(i,j)$ denotes the genotype class at the QTL from progeny of the $i \times j$ cross. By varying the genomic positions of putative QTLs in this model, we can carry out genome scans to map genetic loci using the RIX design. We refer to model [3] as the *half-diallel model* (HD).

An alternative model that does not assume that the mother and father effects are tied together, and allows σ_M^2 and σ_P^2 to be different can be written as

$$y_{ijk} = \mu + M_i + P_j + Q_{m(i,j)} + \varepsilon_{ijk} \qquad [4]$$

where μ and $Q_{m(i,j)}$ are as in model [3]. M_i and P_j are the additive effects of the *i*th mother and *j*th father, respectively. M_i, P_j , and ε_{ijk} are random-effects, distributed as N $(0, \sigma_M^2)$, N $(0, \sigma_P^2)$, and N $(0, \sigma_\varepsilon^2)$, respectively. We refer to model [4] as the *Maternal-Paternal model* (MP model). Both models HD and MP can be applied to strain average data by removing index *k* from the equation.

Further extensions of models [3] and [4] could be considered to include effects that are specific to reciprocal hybrids, such as parent of origin or extranuclear effects by including additional terms as described by Griffing (Griffing 1956). However, one important difference between a standard diallel cross and a RIX is the partitioning of variance generated by Y chromosomes and the mitochondrial genome. These do not produce variance in an RIX. The only difference between 7x2 and 2x7 is in the parental non-genetic, non-mitochondrial contribution. It is also possible to entertain variations on the RIX/diallel design itself. For example, if two different RI panels are available the RIX could include crosses between panels.

3. Implementation

In general, a mixed linear model can be expressed in matrix form as $\mathbf{y} = \mathbf{Xb} + \mathbf{Zu} + \boldsymbol{\varepsilon}$, where $\mathbf{y}$ is the vector of observations, $\mathbf{X}$ and $\mathbf{Z}$ are the known design matrices, $\mathbf{b}$ is the unknown vector of fixed effects and $\mathbf{u}$ is the unknown vector of random effects. In our case the GCA effects and $\boldsymbol{\varepsilon}$ are the random terms and are assumed to be normally distributed with mean $\mathrm{E}\begin{bmatrix} U \\ \varepsilon \end{bmatrix} = \begin{bmatrix} 0 \\ 0 \end{bmatrix}$ and variance $Var\begin{bmatrix} U \\ \varepsilon \end{bmatrix} = \begin{bmatrix} G & 0 \\ 0 & R \end{bmatrix}$. Thus, $\mathrm{E}(\mathbf{y}) = \mathbf{Xb}$ and $\mathrm{var}(\mathbf{y}) = \mathbf{ZGZ}\_ + \mathbf{R}$. In most genetic analyses, we make the additional assumption that $\mathbf{G}$ is a diagonal matrix and $R = \sigma^2 \mathrm{I}_n$. We use this approach to construct a likelihood ratio test statistic for the QTL effects.

For both HD and MP models, the columns of $\mathbf{X}$ (fixed effects) include a mean terms and additional columns representing the QTL genotypes. For the HD model, the $\mathbf{Z}$ matrix (random effects) has one column for each parental strain and for the MP model, $\mathbf{Z}$

has two columns for each parental strain representing different maternal and paternal contributions.

Although standard software is available for fitting linear mixed models, the structure of the HD model requires a special construction for the **Z** matrix. SAS software (SAS Institute, North Carolina) can be used to implement the mixed model for QTL mapping. For example, one could write a SAS macro to fit the HD model in SAS by combining PROC MIXED with PROC IML procedures. Dummy variables can be constructed for each parent using PROC IML as described in the appendix of Xiang and Li 2001 (Xiang and Li 2001). The combined RIX marker data and dummy variables can then be analyzed with PROC MIXED (Littell et al. 1996) with marker data declared as fixed effect in the MODEL statement and dummy variables for parents in multiple RANDOM statements. The option "TYPE=TOEP(1)" must be used to constrain the same variance over dummy variables in half diallel design. Alternatively, one can use the "TYPE=LIN" covariance structure in the RANDOM statement of PROC MIXED to model covariances between different types of relatives in the RIX as linear combinations of unknown. An example of SAS code of how to construct the coefficient matrices data set associated with the TYPE=LIN(q) option for a diallel design has been given in a newly published SAS book (Fry JD 2004).

We have implemented a set of functions in the R computing environment, a freely available statistical package (http://www.r-project.org/), to fit these models and to carry out genome scan analyses. The R functions used for this paper are available at http://www.jax.org/staff/churchill/labsite/index.html under the software link. The R environment provides a variety of tools that can be used for further analysis and

manipulation of the data, including function available in the R/qtl package (Broman et al, 2003).

4. Permutation tests

It is common practice in QTL studies to control type I error for multiple testing due to genome-wide searching using family-wise error rate control (Westfall and Young 1993). Permutation analysis provides a method to compute multiple test-adjusted thresholds or adjusted *p*-values (Churchill, G.A. and Doerge 1994). We typically permute the phenotype data and keep genotype data intact. The maximum logarithm of the odds ratio (LOD) score is recorded on each permutation and percentiles of their distribution provide approximate multiple test adjusted thresholds.

The significance threshold for the likelihood ratio test statistic from the mixed model is based on a unique type of permutation test. Simple shuffling of the RIX progeny phenotypes does not conserve the correlation structure of the mapping population and if this procedure is applied it will result in inappropriately low thresholds. In general, failure to account for positive correlation in data will lead to overly liberal thresholds. In a sense the data have been overly randomized and the effective information content of the permutated data is greater than in the original data. The extremely liberal thresholds obtained by naively permuting RIX data are illustrated in the analysis and simulations below. However, we note that the parental RI genotypes are exchangeable under the null hypothesis and we can construct a permutation of the genotypes by shuffling the "labels" on the parental RI strains and then reconstructing the RIX progeny genotypes based on the shuffled RI strains. For example, consider a panel of RIX progeny derived from a set

of 8 parental RI strains. The original labels of the RI strains are [1, 2, 3, 4, 5, 6, 7, 8]. After permutation, the shuffled labels changed to [4, 1, 2, 8, 6, 7, 3, 5]. The permuted genotype for RIX^*_{2x7} will be reconstructed from RI^*_2 and RI^*_7, which correspond to the RI_1 and RI_3 before shuffling. We run genome scan on the reconstructed RIX genotypes and record the maximum LOD score and use the percentiles of this distribution to establish a genome-wide adjusted significance threshold. This "RIX shuffle" retains the correlation structure of the actual RIX progeny and provides unbiased significance thresholds. In application below we used 1000 shuffles and compute 95th percentile thresholds. However, in simulations we used 200 shuffles and compute 90th percentile thresholds due to the computational demand of permuting within a simulation.

RESULTS

(a) Analysis of the CXB data

The CXB RI panel consists of 13 strains established by Don Bailey and colleagues about 30 years ago at the Jackson Laboratory (Dux et al. 1978). Our CXB RIX mapping population consists of 78 non-reciprocal CXB RIX hybrids, a complete half-diallel cross of the 13 parental CXB RI strains. Twelve mice were generated (roughly 6 male and 6 female) for each RIX hybrid and total brain weight was measured as described (Williams 2000). Significant effects of age, body weight, and sex on brain weight were found in CXB RIX animals. Therefore, individual RIX brain weight was adjusted for these factors prior to computing strain means. After adjustment, the heritability of brain weight in RIX is 38.8%. Mean adjusted-brain weight was used in QTL analysis. With the half diallel design of the CxB RIX population, we cannot directly

confirm that the reciprocal matings will produce the same phenotype distribution. The marginal mean (haplome averages) of brain weight for the RIX hybrids and their 13 parental lines are presented in Table 2. Two-sample t-tests indicate that these are consistent with marginal homogeneity predicted by the HD model. If marginal homogeneity did not hold, the MP model would be a more appropriate choice here. We note that in this half-diallel design, strains do not appear as maternal and paternal contributors to the RIX in equal proportions and two strains (CXB1 and CXB13) contribute to the RIX in only one direction.

CXB RIX genotype data is imputed from parental CXB RI genotypes, which are available at http://www.nervenet.org/papers/bxn.html. The CXB RI genetic map has a cumulative length of approximately 4959 cM, represent roughly 3.6 fold expansion relative to an intercross. A total of 598 markers were typed on CXB RI set and the average resolution spacing is 1-2 cM. There are 374 unique, observed SDPs in the CXB RI marker genotypes. The set of RIX strains has a genotype distribution pattern that resembles an F2 intercross with a 1:2:1 ratio of CC, CB, and BB genotypes at most loci.

We conducted genome-wide scans using the simple, HD and MP models to identify QTL associated with brain weight at 5-cM increments (in RI map units) over the entire genome. Significance thresholds were determined by permutation analysis using simple shuffling and RIX shuffling. Thus we examined a total of six combinations of models and shuffling methods. Results are summarized in Table 3 and in Figure 1.

Results from the CXB RIX data showed that shuffling the RIX progeny phenotype generated inappropriately low threshold values. Using the simple model [2], 13 QTL peaks rise above the significance threshold based on the simple shuffle, whereas

no QTL reached the significance threshold based on the RIX shuffle method (Figure 1A). Both of the mixed models, HD and MP, show a single peak on chromosome 11 that just exceeds the significance threshold based on the RIX permutation method (Figure 1B). In table 3 we show that all 12 additional peaks detected by the simple model (with simple permutation) have a high non-syntenic correlation with the chromosome 11 locus, strongly suggesting that these are false positives generated by spurious association with the chromosome 11 QTL. This occurrence of false positives in the simple model scan is a compelling reason to use the mixed model for RIX analysis.

(b) Analysis of a simulated phenotype on the CXB RIX genotypes

Simulation 1.1: QTL on chromosome 5

We simulated a hypothetical phenotype in the RIX population using the CXB genotype data assuming a QTL with moderate effect on chromosomes 5 is present. The result of genome scans using the simple model and the mixed models are presented in Figure 2. All three models failed to detect a significant peak on chromosome 5 when the RIX shuffle threshold value is used. Failure to detect the simulated QTL on chromosome 5 by either of the mixed model analyses (using the RIX shuffle threshold) is most likely a consequence of the small size of the RI panel used to generate the RIX population resulting in low statistical power. Table 4 summarizes the QTL peaks above the threshold value based on the simple shuffling method. Repeated simulations showed that the simple model had a higher false positive rate than either mixed model, regardless of the shuffling method and that simple shuffling thresholds resulted in an excess of false positive detections for all three models. In the example simulation (table 4), all of the false positive QTLs are highly correlated with the simulated QTL on chromosome 5.

Simulation 1.2: A ghost QTL

When the number of strains in an RI panel is small, the occurrence of non-syntenic association will be high. Mapping with an RIX population generated from a small RI panel presents the same problem. A total of 8 pairs of unlinked loci (typed markers) show perfect association in the CXB RIX genotype data. For example, a typed marker on chromosome 10 has a perfect association with another typed marker on chromosome 3. We simulated a hypothetical phenotype on the RIX population using the CXB genotype data with a QTL on chromosome 10 to illustrate the problem of non-

syntenic association in RIX. A genomescan using the MP model showed a ghost QTL on chromosome 3 with the same LOD score and effect size as the QTL on chromosome 10 (Figure 3). When the allelic association is perfect, as in this example, there is no analytic approach to resolve the ghost QTL that arise by non-syntenic associations. If the non-syntenic association is imperfect it may be possible to identify the causal locus by conditioning on each locus and assessing the conditional LOD at the others. However, this will result in substantial loss of power. Moreover, non-syntenic association can affect many loci and if there are multiple QTLs the cumulative effects can create many spurious LOD peaks. The best solution to non-syntenic association may be to avoid the problem altogether by using a sufficiently large panel of RI strains to establish the RIX or to use a partial RIX.

(c) *Simulation 2: RI simulation*

We conducted simulations to assess the effect of the size of an RI panel on (1) the occurrence of non-syntenic association, (2) the power to detect QTL, and (3) the size and distribution of permutation based threshold values.

Simulation 2.1:

The first simulation demonstrates that non-syntenic association is expected to occur at high frequency in small RI panels and diminishes as the panel size is increased. We simulated RI strain panels of sizes 16, 32, 64, 128, 256, 1000, 5000 and 10000. We repeated each simulation 100 times and recorded the maximum absolute correlation coefficient among unlinked loci. The distribution of maximum correlation is shown in Figure 4A. We conclude that a RI panel of at least 128 strains is needed to ensure that the

maximum correlation between unlinked loci is below 0.4. This simulation can not account for biologically driven non-syntenic associations generated (perhaps) by epistatic interactions that affect fitness, thus 128 is an "idealized" minimum and it is likely that higher strain numbers would be needed to dilute non-syntenic association in real populations.

Simulation 2.2:

The second RI based simulation compares the power for detecting a QTL with additive effects across RI panels with different numbers of strains. We simulated RI panels with 16, 32, 64, 128, and 256 strains. Each RI strain has a phenotype determined by one major QTL on chromosome 5 and three background QTLs on chromosomes 1, 10 and 16. Four possible effect sizes (1.0, 0.5, 0.25, and 0.125) are used for the major QTL and the background QTL effects are fixed at 0.125. We simulated the hypothetical phenotype 4 times and analyzed the strain means. Significance thresholds at the 0.90 adjusted level were determined using 200 permutations within each simulation. We repeated each combination 100 times and recorded the number of times that we detected the major QTLs as well as detection rates for background QTLs and false positives. Results are summarized in Figure 4B. Power to detect the major QTL depends on both the number of RI strains and the effect size of the major QTL relative to the background QTLs. For example, if the effect size of the major QTL is 0.25, a RI panel with 128 strains has 90% power to detect it. Power is reduced to less than 60% if the RI panel is reduced to 64 strains.

The distributions of threshold values obtained from these simulations are shown as box plots in Figure 4C. It is clear that the mean and the variance of the threshold depend on both the size of the RI sets and the effect size of the major QTL. When the number of RI strains is small and when the major QTL effect is large, threshold values are very unstable. This necessitates the use of permutation for each simulation replicate.

(d) Comparison of RIX, RI and F2

Simulation 3: QTL with additive effects

We conducted a set of simulations to compare the power of a RIX mapping population with an RI panel and an F2 using populations of the same size, in total number of animals. We simulated RI panels with N=16, 32 and 64 strains, a balanced partial RIX cross of 64, 128 and 256 hybrids from the RI strains and a F2 cross with 64, 128 and 256 mice. Each RI line occurs 4 times as the mother and 4 times as the father of an RIX hybrid. We simulated one major QTL with additive effect on chromosome 5 and three additive background QTLs on chromosomes 1, 10 and 16. Four effect sizes (1.0, 0.5, 0.25, and 0.125) are used for the major QTL and the background QTL effects are fixed at 0.125. We simulate the phenotype 4 times and ran genome scan on the mean trait value in each RI strain. The RIX and F2 populations were simulated with QTLs in the same locations with the same additive QTL effects as in the RI but individuals were not replicated. In all cases the same total number of individual animals were simulated. We analyzed data using the simple model and the MP mixed model. We repeated the simulations 100 times to compare the power of detecting QTL on chromosome 5 with respect to the size and type of the cross and the effect size of QTLs.

The top panel of Figure 5 (5A to 5C) summarizes the simulation results for an RI panel with 16 strains, and F2 and RIX populations of size 64. The middle panel of Figure 5 (5D to 5F) summarizes the simulation results when the major QTL effect is fixed at 0.5 and the size of RI panel varies from 16 to 64. When the sample size is small and the major QTL has an effect size close to the background QTLs, none of the crosses had sufficient power to detect this additive QTL (Figure 5A). As expected, we observed a higher false positive rate in RI and RIX compared to F2 (Figure 5C). This is because the extent of non-syntenic association is higher in the RI and RIX designs than in F2 design. Consistent with our finding in simulation 2.1, the false positive rate goes down in RI and RIX when the size of the RI panel increases (Figure 5F). Although this simulation shows that RIX has less power to detect an additive QTL than RI and F2, the power of the RIX improves when the size of RI panels increases (Figure 5D). Finally, the results of the ranges of our simulated models indicate that with RIX shuffling method, the simple model is no worse than the MP model at detecting the major QTL on chromosome 5. It also indicate that MP model may have better power in detecting major QTL when the number of parental RI strains is increased.

Simulation 4: QTL with dominant effects

We simulated an RI panel of 16 strains and used it to generate RIX populations with dominant QTL effects using the same strategy as in simulation 3. Results are summarized in the bottom panel of Figure 5 (5G to 5I). When a small panel of RI is used, RIX has limited power to detect the dominant QTL compared to an F2 population of the same size. We also note that the simple model has slightly better power for detecting the

major QTL than MP model. However, the simple model has a higher false positive rate when the effect of the QTL increases and the high rate of false positive detections is a cause for concern.

CONCLUSION

The RIX mapping design was introduced to improve the power of small RI panels for the detection of QTLs. The RIX design shares some of the best and some of the least desirable properties of small parental RI panels. We describe a method of analysis, based on a linear mixed model, and a method of permuting the data to obtain valid thresholds for genome-wide scans of an RIX population. These methods account for the correlation structure of the RIX population. Despite the combinational explosion of unique genotypes that are generated in an RIX design, there appears to be little advantage of the RIX compared to the original RI panel for detecting QTLs with additive effects. The effective sample size of the RIX population is limited by the number of progenitor RI strains used to establish the cross. Nevertheless, there are reasons to consider RIX as a viable genetic mapping design. The ability to study traits in the context of a genetic background with a low formal inbreeding coefficient is one potentially valuable feature of the RIX design. This is difficult to assess with simple simulation studies and awaits further experience with RIX animals. It is clear that large RI sets are needed to achieve reasonable power with the RIX design. Non-syntenic associations arise when regions on different chromosomes show statistically significant positive or negative correlations. A RI panel with at least 128 strains is needed to reduce the maximum absolute correlation among unlinked loci to 0.4. As illustrated in our examples, non-syntenic associations

greater than 0.4 can result in false positive QTL results. Practical constraints on sample sizes will require partial diallel populations like the balanced designs used in our simulations. Another advantage of the partial diallel design is that it decreases the extent of positive correlation among RIX animals and thus the effective sample size approaches the actual sample size.

RI and RIX designs both support studies that incorporate multiple genetic, environmental, and developmental variables into comprehensive models of disease susceptibility. With the combinatorial diversity available in the vast number of potential RIX genomes that can be generated from a large set of RI strains, it will be possible to construct mice to validate statistical models relating genotypes and environments to phenotypic outcomes. With levels of heterozygosity and admixture comparable to human populations, RIX animals represent genetically normal mammals that can be replicated at infinitum.

The mixed model provides the most appropriate statistical description of the RIX population. In our simulations, it did not significantly outperform the simple model in power to detect QTL. However, the mixed model, in combination with the RIX shuffle permutation, substantially reduced the frequency of false positives due to non-syntenic linkage. The mixed model correctly takes into account the correlation structure of the RIX population. The result of this correction is a reduction in the information content (effective sample size) of the RIX population compared to an equivalent number of independently sampled animals. The balanced partial RIX design (Table 1C), in which each parental RI strain is used an equal number of times as mother and as father in generating the RIX progeny, provides a potential solution to the problem of correlation

among the RIX progeny. If the founder RI panel is sufficiently large, a sparse sampling of the RIX population can achieve near independence. Therefore, we recommend the use of partial RIX populations derived from large RI panels for future applications of this breeding design in QTL mapping applications.

ACKNOWLEDGMENTS

This work was support by National Institute of Health (NIH) grants HL55001 and GM070683. The authors thank Dr. David Threadgill for discussion of RIX design.

.

REFERENCES

Ahmadiyeh, N, Churchill, GA, Shimomura, K, Solberg, LC, Takahashi, JS and Redei, EE (2003) X-linked and lineage-dependent inheritance of coping responses to stress. Mamm Genome. 14: 748-57.

Bailey, DW (1971) Recombinant-inbred strains. An aid to finding identity, linkage and function of histocompatibility and other genes. Transplantation 11: 325-327.

Belknap, JK (1998) Effect of within-strain sample size on QTL detection and mapping using recombinant inbred mouse strains. Behav Genet 28(1): 29-38.

Belknap, JK, Mitchell, SR, O'Toole, LA, Helms, ML and Crabbe, JC (1996) Type I and type II error rates for quantitative trait loci (QTL) mapping studies using recombinant inbred mouse strains. Behav Genet 26(2): 149-60.

Broman KW, Wu H, Sen S, Churchill GA. (2003) R/qtl: QTL mapping in experimental crosses. Bioinformatics 19(7):889-890.

Churchill, GA and Doerge, RW (1994) Empirical Threshold Values for Quantitative Trait Mapping. Genetics 138: 963-71.

Churchill, GA, Airey, DC, Allayee, H, Angel, JM, Attie, AD, Beatty, J, et al. (2004) The Collaborative Cross, a community resource for the genetic analysis of complex traits. Nat Genet. 36(11): 1133-7.

Dux, A, Muhlbock, O and Bailey, DW (1978) Genetic analyses of differences in incidence of mammary tumors and reticulum cell neoplasms with the use of recombinant inbred lines of mice. J Natl Cancer Inst 61: 1125-9.

Fry, JD (2004) Estimation of genetic variances and covariances by restricted maximum likelihood using proc mixed. In Genetic Analysis of Complex Traits. A. M. Saxton,eds (Cary, NC, SAS Institute Inc) pp 27-34.

Griffing, B (1956) Concept of general and specific combining ability in relation to diallel crossing systems. Aust. J. Biol. Sci. 9: 463-93.

Haldane, JBS and Waddington, CH (1931) Inbreeding and linkage. Genetics 16: 357-374.

Hartwell, L 2004. Genetics: Robust interactions. Science 303: 774-5.

Hayman, BI (1954a) The analysis of variance of diallel tables. Biometrics 10: 235-244.

Hayman, BI (1954b) The theory and analysis of diallel crosses. I. Genetics 39: 789-809.

Knapp, SJ and Bridges, WC (1990) Using molecular markers to estimate quantitative trait locus parameters: Power and genetic variance for unreplicated and replicated progeny. Genetics 126: 769-777.

Lander, ES and Botstein, D (1989) Mapping Mendelian factors underlying quantitative traits using RFLP linkage maps. Genetics 121(1): 185-99.

Limami, AM, Rouillon, C, Glevarec, G, Gallais, A and Hirel, B 92002) Genetic and physiological analysis of germination efficiency in maize in relation to nitrogen metabolism reveals the importance of cytosolic glutamine synthetase. Physiol Plant. 130(4): 1860-70.

Littell, RC, Milliken, GA, Stroup, WW and Wolfinger, RD (1996) SAS system for mixed models (Cary, NC, SAS Institute Inc)

Nuzhdin, SV, Pasyukova, EG, Dilda, CL, Zeng, ZB and Mackay, TF (1997) Sex-specific quantitative trait loci affecting longevity in Drosophila melanogaster. Proc Natl Acad Sci U S A. 94: 9734-9.

Peirce, JL, Lu, L, Gu, J, Silver, LM and Williams, RW (2004) A new set of BXD recombinant inbred lines from advanced intercross populations in mice. BMC Genet(5): 7.

Plomin, R and McClearn, GE (1993) Quantitative trait loci analysis and alcohol-related behaviors. Behav. Genet. 23: 197-212.

Taylor, B (1996) Recombinant inbred strains. In Genetic Variants and Strains of the Laboratory Mouse. ML Lyon, S Rastan and S. Brown, eds. (Oxford University Press) **3:** 1597-1659.

Threadgill, DW, Hunter, KW and Williams, RW (2002) Genetic dissection of complex and quantitative traits: from fantasy to reality via a community effort. Mamm Genome 13: 175-178.

van Swinderen, B, Shook, DR, Ebert, RH, Cherkasova, VA, Johnson, TE, Shmookler Reis, RJ, et al. (1997) Quantitative trait loci controlling halothane sensitivity in Caenorhabditis elegans. Proc Natl Acad Sci U S A. 94: 8232-7.

Westfall, PH and Young, SS (1993) Re-Sampling Based Multiple Testing. (New York, Wiley)

Williams, RW (2000) Mapping genes that modulate mouse brain development: a quantitative genetic approach. Results Probl Cell Differ. 30: 21-49.

Williams, RW, Gu, J, Qi, S and Lu, L (2001) The genetic structure of recombinant inbred mice: high-resolution consensus maps for complex trait analysis. Genome Biol 2(11): RESEARCH0046.

Williams, RW, Bennett, B, Lu, L, Gu, J, DeFries, JC, Carosone-Link, RJ, et al. (2004) Genetic structure of the LXS panel of recombinant inbred mouse strains: a powerful resource for complex trait analysis. Mamm Genome 15: 637-647.

Wright, AJ (1985) Diallel designs, analyses, and reference populations. Heredity 54: 307-311.

Xiang, B and Li, B (2001) A new mixed analytical method for genetic analysis of diallel data. Can J For Res 31:2252-2259

Table 1A. A full diallel cross from 8 inbred lines

1	1x2	1x3	1x4	1x5	1x6	1x7	1x8
2x1	2	2x3	2x4	2x5	2x6	2x7	2x8
3x1	3x2	3	3x4	3x5	3x6	3x7	3x8
4x1	4x2	4x3	4	4x5	4x6	4x7	4x8
5x1	5x2	5x3	5x4	5	5x6	5x7	5x8
6x1	6x2	6x3	6x4	6x5	6	6x7	6x8
7x1	7x2	7x3	7x4	7x5	7x6	7	7x8
8x1	8x2	8x3	8x4	8x5	7x8	8x8	8

Table 1B. Half diallel cross from 8 inbred lines without selfing

	1x2	1x3	1x4	1x5	1x6	1x7	1x8
		2x3	2x4	2x5	2x6	2x7	2x8
			3x4	3x5	3x6	3x7	3x8
				4x5	4x6	4x7	4x8
					5x6	5x7	5x8
						6x7	6x8
							7x8

Table 1C. Balanced partial diallel cross from 8 inbred lines

	1x2			1x5			
			2x4			2x7	
				3x5			3x8
4x1		4x3					
	5x2				5x6		
6x1							6x8
		7x3			7x6		
			8x4			8x8	

Table 2. Marginal brain weight of RIX hybrids and their parental RI lines

CXB RI Set			CXB RIX Hybrid						
Strain	N	Mean	Maternal RI strain	N	Marginal mean	Paternal RI strain	N	Marginal mean	P-value
1	28	454.17	1	12	489.17	1	0	--	--
2	40	438.86	2	11	467.40	2	1	476.43	--
3	62	475.34	3	10	497.01	3	2	485.05	0.39
4	36	453.63	4	9	489.12	4	3	481.21	0.50
5	27	432.30	5	8	468.56	5	4	479.96	0.18
6	66	460.75	6	7	472.71	6	5	488.27	0.11
7	90	480.68	7	6	485.20	7	6	480.88	0.57
8	43	463.53	8	5	480.18	8	7	483.17	0.77
9	47	473.80	9	4	475.49	9	8	487.52	0.13
10	53	446.83	10	3	465.35	10	9	487.45	0.11
11	52	426.12	11	2	464.01	11	10	463.29	0.95
12	49	458.03	12	1	468.15	12	11	486.49	--
13	62	421.00	13	0	--	13	12	471.42	--

Table 3. Significant QTL peaks in the CXB RIX analyses

Chromosome No.	Lod Scores		Correlation with Chr 11 locus
	Simple model[1]	MP model[2]	
1	5.8	--	0.59
3	9	--	-0.59
5	6.6	--	0.43
8	9.5	--	0.69
9	7.2	--	0.43
10	8.1	--	-0.59
11	10.8	19.3	1.0
12	5.5	--	0.57
13	5.3	--	-0.51
14	6.0	--	-0.51
15	7.9	--	0.59
17	5.3	--	0.43
18	7.4	--	0.59

[1] QTL peaks above significant threshold (LOD score = 4., $p<0.05$) from simple shuffle + simple QTL model. None of the peaks here above the significant threshold (LOD=16.4) based on RIX shuffling method.

[2] QTL peaks above significant threshold (LOD score =19.3, $p<0.05$) from RIX shuffling method + MP QTL model

Table 4. Simulated QTL peak on chromosome 5[1]

Chromosome No.	LOD scores			Correlation with Chromosome 5
	Simple model[2]	MP model[3]	HD model[4]	
2	6.9	--	12.7	-0.63
5	12.3	10.7	14.5	1.00
6	9.0	4.8	5.0	-0.85
9	5.1	--	--	-0.63
10	4.3	--	--	0.68
12	9.0	4.9	8.7	0.84
13	5.3	--	--	-0.54
14	6.9	--	--	0.85
16	4.6	--	--	0.54
19	4.3	--	--	-0.50

[1]QTL peaks exceeding the simple shuffling threshold
[2] Significance thresholds for $p<0.10$ are 3.7 (simple shuffle) and 12.5 (RIX shuffle).
[3] Significance thresholds for $p<0.10$ are 4.2 (simple shuffle) and 10.7 (RIX shuffle).
[4] Significance threshold for $p<0.10$ are 4.3 (simple shuffle) and 16.2 (RIX shuffle)

Figure legends

Figure 1. Genome-wide scan of adjusted mean Brain weight from the CXB RIX population. LOD scores were computed using the simple QTL model (A), the MP model (B), and the HD model (C). Genome-wide significance ($P<0.05$) based on 1000 permutations using the simple shuffle (---), and RIX shuffle (...) methods.

Figure 2. Genome-wide scan of a hypothetical phenotype. Data were simulated based on the CXB genetic marker data with a major QTL (effect size 1.5) on chromosome 5. Normal residual error was simulated with standard deviation 1.0. LOD scores were computed using the simple QTL model (A), the MP model (B) and the HD model (C). Genome-wide significance ($P<0.1$) based on 200 permutations using the simple shuffle (---) and RIX shuffle (...) methods.

Figure 3. Ghost QTL simulation. Data were simulated based on the CXB genetic marker data with a major QTL (effect size 1.5) on chromosome 10 to illustrate the problem of non-syntenic association in RIX. Normal residual error was simulated with standard deviation 1.0. LOD scores were computed using the simple QTL model (A), the MP model (B), and the HD model (C). Genome-wide significance ($P<0.1$) based on 200 permutations using the simple shuffle (---) and RIX shuffle (...) methods.

Figure 4. RI line simulations. Distribution of maximum correlation among unlinked markers from RI panels with different number of strains in 100 simulations (A). Power to detect the major QTL effect across RI panels with different number of strains. Each RI

panel has a phenotype determined by three background QTLs (effect size 0.125) on chromosomes 1, 10 and 16, and one major QTL on chromosome 5 with effect size ranged from 0.125 to 1.0. (B). Distribution of the significance thresholds for LOD scores at the 0.90 genome-wide adjusted level. Threshold values were determined using 200 permutations within each RI simulation (C).

Figure 5. Power comparison of a balanced partial RIX mapping population with an RI panel and an F2 using populations of the same size, in total number of animals. The top panel summarizes the comparison of an RI panel with 16 strains, and F2 and RIX population of size 64 while the major QTL effect size varied from 0.25 to 1.0 on chromosome 5 (A to C). The middle panel summarizes the power comparison of RI, F2 and RIX when major QTL effect size is fixed at 0.5 across different size of the mapping panels (D to F). The bottom panel summarizes the power of detecting dominant QTL effects size ranged from 0.25 to 1 between a partial RIX cross and a F2 populations of size 64. (G to I)